THE SEDIMENTOLOGY AND PETROGRAPHY OF LOWER CARBONIFEROUS LIMESTONES AND DOLOMITES; HOST ROCKS TO THE NAVAN ZINC-LEAD DEPOSIT, IRELAND.

GIANCARLO RIZZI. B.Sc. (London).

THESIS SUBMITTED FOR THE DEGREE OF Ph. D.

UNIVERSITY OF GLASGOW.

DEPARTMENT OF GEOLOGY AND APPLIED GEOLOGY.

DECEMBER 1992.

ProQuest LLC.
789 East Eisenhower Parkway
P.O. Box 1346
Ann Arbor, MI 48106 – 1346

DECLARATION.

I declare this thesis is entirely my own work except where otherwise stated and has not been submitted for a degree at any other institution.

Giancarlo Rizzi.

ABSTRACT.

The Navan Zn-Pb ore deposit is located along the SW margin of the Longford Down Lower Palaeozoic Inlier approximately 40 km NW of Dublin. The orebody is hosted by Lower Carboniferous (Courceyan) limestones which dip gently to the SW.

The folded Lower Palaeozoic basement is overlain unconformably by Red Beds. These are interpreted as reflecting deposition in a fluviatile system. Deposition was not continuous, periodic abandonment of the flood plain led to the formation of caliche. The overlying Laminated Beds reflect alternations of barrier sandstones, lagoonal mudstones and siltstones, and tidal flat sediments. At least 2 episodes of emergence occured, the first is represented by a pedogenic green clay, the second produced nodular anhydrite (reflecting a sabkha environment). The Muddy Limestone which follows is believed to represent a clastic influenced lagoon.

The limestones above, the Pale Beds, host 97% of the ore body and are sub-divided into a lower Micrite Unit and an upper Grainstone Unit. The Micrite Unit consists of approximately 20 metre scale lagoon tidal-flat shallowing-upwards cycles, with oolitic grainstones reflecting periodic incursions of more open marine conditions. Many cycles culminate in emergent surfaces. Three of these surfaces are important because they host high grade mineralization. The lowest is an *in situ* breccia overlain by a pedogenic green clay, the second prominent surface, 10 m above, is also a breccia surface. The youngest surface is a karren type palaeokarst. The upper surface of the Micrite Unit is bounded by a palaeotopography, which includes a NW striking channel.

The Grainstone Unit blankets the Micrite Unit. It reflects a sequence of open marine oolitic and bioclastic sand shoals. Several stratigraphic marker horizons are present within the Grainstone Unit; the Lower Dark, Nodular and Upper Dark Markers. These are believed to represent lagoonal sediments, suggesting alternate regression and transgression. The Grainstone Unit contains several solutionally modified surfaces similar to the palaeokarst surfaces in the Micrite Unit below, suggesting that deposition was again punctuated by subaerial erosion.

The sequence overlying the Pale Beds is Late Courceyan to Arundian in age and consists of Shaley Pale and Argillaceous Bioclastic Limestones and Waulsortian Limestones. Together they reflect continued deepening. These are truncated by an erosion surface which cuts down through the entire sequence at Navan. This is overlain by the Boulder Conglomerate, believed to reflect a submarine debris flow system, perhaps associated with synsedimentary faulting. The overlying Upper Dark Limestones represent basinal turbidites.

Cementation of lime sediment began early and was in part contemporaneous with sedimentation. Features of shallow marine and meteoric cementation are present but both are over-printed by mechanical compaction which is itself over-printed by blocky (burial) calcite cement. The final result was a tightly cemented limestone with low porosity and permeability

Dolomitzation in the Pale Beds is confined to a limited area, having a linear NE-SW trend and an overall plume shaped geometry. Relic fractured grains within dolomite and replacement of both calcite cements and stylolites indicates that dolomitization post dates sediment compaction and calcite cementation. Three stages of dolomitization are recognised, separated by dissolution events. The geometry and distribution of dolomitziation, dolomite rock textures, fluid inclusion homogenization temperatures of 59.7 ^{o}C to 159.3 ^{o}C and oxygen isotope values of $\delta\ ^{18}O$ -6.1 to -10.4 ‰ PDB indicate that dolomitizing solutions were heated.

The most permeable part of the sequence at Navan is the Pale Beds, high porosity and permeability are not pervasive but confined to subaerial erosion surfaces separated by tightly cemented limestones. In addition grainstones have controlled the distribution of

dolomite, which, relative to grainstones, has a high porosity and permeability. The Pale Beds are enclosed in an envelope of low porosity and permeability consisting of the Laminated Beds and the sequence overlying the Pale Beds.

The location of ores in the western mine area is strongly dependent on ground conditions and ores are located along karren type palaeokarst surfaces. This view contrasts with that of Anderson (1990) who believed that the cavities were the result of soft sediment pulling away from the base of dolomite 'crusts' during burial and compaction. Mineralization occured between stages of dolomitization. However, alteration of dolomite by sulphide, replacement of dolomite by sulphide and the occurrence of sulphide filling fractures and brecciation within dolomite indicate that mineralization continued after dolomitization was complete. The linear NE-SW trend of the dolomitization is contiguous with the outline of the orebody at Navan supporting the view that dolomitization and mineralization are genetically related.

At Navan the Red Beds pinch out and the Pale Beds contain evidence of subaerial erosion, both suggest a basin margin position, supporting the geophysical data of Brown & Williams (1985). Apparent lack of alteration of Lower Palaeozoic rocks, leaching of feldspars and mafics in the Red Beds accord with derivation of ore fluids from the basin which underlies the Irish Midland region, following the stratal aquifer model of Lydon (1986) for ore genesis.

CONTENTS.

Chapter 6.

Chapter 7.

LIST OF FIGURES.

LIST OF PLATES.

ACKNOWLEDGEMENTS.

This thesis is the culmination of a great many influences in my life. From apprentice days I would like to thank the men of the British Steel Corporation, South Teesside who taught me my trade, Robert Bishop, James Foster, Walter Teesdale and Johnny Walker whose workmanship impressed me profoundly. My friends back home Peter Atkinson, Stephen Hogg and Mark Cockerill are thanked for their support, encouragement and happy memories. James Russell and Chris Pellant are thanked for guiding me through part time 'A' levels at Kirby College of Further Education, Middlesbrough.

I would like to thank Dr. Roger Anderton for giving me the opportunity to study for my Ph.D. and for introducing me to the Geology of the Irish ore field. Professor Mike Russell is thanked for taking on the role of temporary supervisor during 1989. The Natural Environmental Research Council of Great Britain is thanked for providing a maintenance grant during the tenure of my thesis and for providing funds to attend the Dolomeiu Conference on Carbonate Platforms and Dolomitization in Italy. I would also like to thank Barclays Bank plc and the D.H.S.S for financial support during the closing stages of this thesis and Oxfam for some decent bargains over the last few years.

In Ireland I would like to thank Dr. Kerr Anderson, Freida Baragwanath and Eamonn Brady for inviting me to stay at their homes together with James and Mary Jane Russell of Russells Bed and Breakfast for their kindness, generosity and the wonderful food. I am grateful to Peter Powell, the Chief Mine Geologist at Tara for making the facilities of the Mine Geology Department available to me and for providing financial support on several occasions. I would like thank, Dr. John Ashton, Assistant Chief Geologist at Tara, for his advice and guidance and for ensuring the thesis is technically correct with respect to the mine operation. The staff of the Mine Geology Department at Tara Mines, although extremely busy on many occasions were generous with their time and advice, I owe them a great deal and would particularly like to say thanks to Tom Donoghue, Adrian Black, Eugene Hyland, Mark Holdstock, Jim Geraghty, Padraic Duffy, Dessie O'Brien and Gerry Gough.

I would also like to acknowledge Drs. Brian Bell, Alan Owen, Brian Bluck, J. J (Ben) Doody of the Department of Geology and Applied Geology, Glasgow University whose friendly and supportive attitude over the last few years was greatly appreciated. I am endebted to Douglas Maclean for his photographic advice and for providing the 'nice n contrasting' prints, thanks also go to Murdoch MacLeod and Dougie Turner for help with X.R.D. analysis. I am grateful to Dr George Bowes for assistance and advice with respect to word processing. Thin sections were produced by Andrew Monaghan and many thanks to Roddy Morrison for providing various bits and pieces. At the S.U.R.R.C. I thank Dr. A. E. Fallick for making the facilities of the stable isotope laboratory available to me and for reading over the isotopic sections of the thesis.

I am grateful to the post doctoral community at Glasgow, notably Drs Maggie Cusack and Andrew Mullis for helpful advice. A big thank you to my friends and flat mates at Glasgow for their companionship, advice and opinions, particularly Joseph Crummy, Mark Osborne, Derek (see you on the big day!) Walton, Stephen Penman and Lindsay Ferguson. I am eternally grateful to Susan Waldron for the use of her electric kettle over the last year or so. Special thanks go to Russ Claydon for sharing some treasured Scottish mountain days.

There is one man who above all I am most grateful, my Supervisor, Dr. Colin Braithwaite. Thank you for your support and guidance. To my girlfriend Helen, I would just like to say thank you for your patience and support during the thesis. Without you the long road to submission would have been just that little bit longer.

DEDICATION.

To my mother Eileen and my father Dillo,
and my sisters Bernadette and Maria.

With love and affection always.

Gian.

We shall not cease from exploration and the end of all our exploring will be to arrive where we started and know the place for the first time.

T.S. Elliot.

1.1. INTRODUCTION.

This chapter begins with a short background to carbonate hosted Pb-Zn deposits and a brief introduction to the Irish ore field. This is followed by a summary of the previous work carried out on the host rocks to the Navan ore body with respect to stratigraphy, sedimentology and petrography. Mineralization and the tectonic features at Navan are described in the following section. The Lower Carboniferous palaeogeography of Ireland is then considered, followed by a summary of the data base and the techniques employed during this study. Finally the aims of the thesis are outlined and a brief summary of the thesis structure is given.

1.2. BACKGROUND TO CARBONATE HOSTED Pb-Zn DEPOSITS.

Carbonate hosted Pb-Zn deposits fall into two major categories; Mississippi Valley Type (MVT) and Sedimentary Exhalative (SEDEX). Together these account for 65% of world zinc and 77% of world lead reserves (Sangster, 1990). Mississippi Valley Type deposits are traditionally grouped into districts, although isolated deposits also occur. MVT deposits occur within thick carbonate platform sequences which accumulated in tectonically stable zones. These platforms are located along the periphery of cratonic and intra-cratonic basins (Kyle, 1983; Sangster, 1976, 1990). The classic MVT districts of central North America occur in this setting and include the Southeast Missouri, Upper Mississippi Valley, Tri State and East-Central Tennessee districts. Major Canadian deposits, notably the Pine Point district also occur in this setting. A few MVT deposits are hosted by limestones which accummulated in rift systems. The best known of these is the Alpine Triassic district where deposits occur beneath unconformities which formed along the uplifted margins of rift blocks (Klau & Mostler, 1986).

The host limestones of MVT deposits reflect the whole spectrum of shallow marine carbonate environments. Deposits occur in rocks reflecting evaporitic, intertidal and lagoon environments. The Alpine district of Austria is a notable example where several deposits occur in the "cyclic facies" of the Witterstein Limestone (Bechstadt & Munich, 1975; Bechstadt & Dohler-Hirner, 1983). The Cambrian deposits of SW Sardinia are also hosted by lagoon-tidal flat limestones (Boni, 1986). The Tri-State and Upper Mississippi Valley deposits of central North America are hosted by bioclastic and oolitic grainstones reflecting high energy shallow marine conditions (Hagni, 1976; Sangster, 1976). Many deposits are hosted by reefs and fore-reef breccias, notably in the Devonian Pine Point district of the Canadian North West Territories (Skall, 1975). Lower Ordovician stromatolitic bioherms host several deposits in the Tennessee ore fields (Briskey *et al,* 1986). Finally, a few deposits are hosted by limestone-shale transition sequences interpreted as reflecting a platform margin environment, an example is again seen in the Pine Point district (Sangster, 1990).

Limestones which host MVT deposits are typically modified in two ways; by subaerial exposure and by dolomitization. The typical products of subarial exposure are unconformities, either regional or localized, collapse breccias (tabular or vertically extensive), palaeokarst surfaces and palaeosols (Kyle, 1983; Sangster, 1976, 1990; Bechstadt & Dohler-Hirner, 1983). The open spaces produced by subaerial erosion act as recepticles for lead-zinc ores, thus MVT deposits are typically crosscutting and mineralization occured late, post-dating lithification.

The association between dolomitization and Zn-Pb deposits is widely recognized (Badiozamani, 1973; Sangster, 1976, 1990; Morrow, 1982b; Kyle, 1983). In the Canadian North West territories deposits the entire Pine Point district is encapsulated by a zone of regional dolomitization, the Presqu'ile Facies (Skall, 1975). Dolomite is also a common host rock in the Alpine Pb-Zn district (Klau & Mostler, 1986. Table 1) and the Polish Silesian-Cracow ore district (Bocagz, 1976, Sangster, 1990). In central North America, in the Teneessee Valley district, dolomitiztion is extensive but more localized, surrounding individual deposits (Kyle; 1983; Sangster, 1990). Finally in the Tri-State and Upper Mississippi Valley districts, dolomitization is closely associated with ore deposits and has long been used as a guide to ore zones (Badiozamani, 1973; Hagni, 1976).

In contrast SEDEX deposits occur in basinal settings with basins initiated during extension of passive continental margins (Sangster, 1990). SEDEX deposits may be hosted by either siliciclastic or carbonate sequences. Siliclastic lithologies are varied and consist of shales, siltstones, sandstones turbidites and submarine debris flows. Notable carbonate hosted SEDEX deposits include the Howards Pass body in Canada where the ores are hosted by deep marine argillaceous limestones, and the Duncan deposit in Canada, hosted by pure basinal marine limestones (Sangster, 1990). The Mid Proterozoic Mount Isa deposit, Australia, is hosted by mixed carbonate clastic rocks, with limestones displaying extensive dolomitzation (Hagni, 1976; Sangster, 1990). Ore deposition in SEDEX deposits occured early and was concurrent with sedimentation, and thus, ore bodies are stratiform. The main features of MVT and SEDEX deposits are contrasted in Fig. 1.1.

The published literature suggests that the Irish Zn-Pb deposits do not conform to either the MVT or SEDEX types. Deposits display styles of mineralization common to both MVT and SEDEX and are generally referred to as "Irish Type". They are located along the margins of Lower Palaeozoic inliers and are associated with fault systems (Hitzman & Large, 1986; Lydon, 1986; Anderson, 1990). Most Irish Zn-Pb deposits are hosted by Lower Carboniferous, Courceyan limestones. These limestones form two informal groups; the Argillaceous Bioclastic Calcarenite Group (the ABC Group) which inludes Waulsortian Facies Limestones, and the Navan Group, typically shallow marine limestones. A stratigraphical and sedimentological summary is given in Fig.1.2 and the distribution of Irish Zn-Pb deposits is shown in Fig.1.3. The Navan Zn-Pb deposit is the

	MVT	SEDEX
GEOLOGICAL SETTING	Thick carbonate platform sequences located around the periphery of cratonic and intra-cratonic basins. Some limestones accumulated in tectonically active rift zones.	Basinal and basin margin.
HOST ROCK	**Limestones** only; mudstones wackestones, packstones, grainstones, stromatolitic bioherms, reefs and fore reef breccias.	**Carbonates**; argillaceous limestones and 'pure' basinal limestones. **Siliciclastic**; siltstones, sandstones, turbidites and submarine debris flows.
HOST ROCK DEPOSITIONAL ENVIRONMENT	Tidal flats, lagoons, high energy shallow marine, reefs and platform margin setting.	Deep or shallow marine basinal environment. Basin margin setting.
HOST ROCK ALTERATION	Limestones are typically dolomitized. Extensive modification by subaerial erosion. Regional and local unconformities, karst surfaces, collapse breccias and palaeosols.	Limestones may be dolomitized
TIMING OF MINERALIZATION	LATE; mineralization is post lithification and fills karst cavities.	EARLY; deposition of ores contemporaneous with deposition of sediments.
GEOMETRY OF ORE BODY	Deposits occur in districts. Individual deposits are stratabound and crosscutting with no feeder zone.	Isolated stratiform deposits with "feeder" zones.

Fig. 1.1. Major features of SEDEX and MVT Pb-Zn deposits. Based on Sangster (1976, 1990); Gustafson & Williams (1981); Kyle (1983); Lydon (1986).

Fig. 1.2. Sedimentological and stratigraphic summary of Irish Zn-Pb deposits. Based on papers in *The geology and genesis of mineral deposits in Ireland* (edited by Andrew *et al* 1986). Additional information from [1]Holdstock (1982); [2]Philcox (1984); [3]Harwood &Sulliven (1990); [4]Anderson (1990).

DEPOSIT	Mt	AGE OF HOST ROCK	FORMATION	HOST ROCK	HOST ROCK DEPOSITIONAL ENVIRONMENT	ALTERATION	PUBLISHED INTERPRETATION
[4]NAVAN.	69.9	Courceyan (3% of the ore deposit is hosted by Arundian debris flows).	NAVAN GROUP, Pale Beds.	Micrite, fenestral micrite, oolite, bioclastic calcarenite, debris flows.	Tidal flat, lagoon, shallow high energy marine. Platform margin debris flows with syn-sedimentary tectonism.	Stratal and crosscutting dolomitization.	MVT - SEDEX
[2]SILVERMINES	17.7	Courceyan	ABC GROUP, Waulsortian Limestones; NAVAN GROUP, Ballysteen Limestone, Basal Sandstone and Red Beds.	Waulsortian facies, oolitic limestones, bioclastic limestones, sandstones.	Alluvial plain and marginal marine environments. Lagoons and unspecified shallow water shelf environments. Waulsortian Facies form mudbanks at base of photic zone in waters 200 to 300 m deep.	Dolomitization of host limestones in ore zones, some silicification of host rocks.	SEDEX
[2]TYNAGH	9.4	Courceyan	ABC GROUP Waulsortian Limestones.	Waulsortian Facies	Waulsortian Limestones formed mudbanks in a shelf setting in water depths of 100 to 300 m.	Dolomitized aureoles around mineralized zones. Some Tertiary weathering and karstification.	SEDEX.
LISHEEN--GALMOY	8.0	Courceyan	ABC GROUP, Waulsortian Limestones.	Waulsortian Facies	No data	Regional dolomitization of host rocks.	No data, latest discovery.
[2]KEEL	5.0	Courceyan	NAVAN GROUP, Mixed Beds ABC GROUP. Waulsortian Limestones.	Mineralization is hosted by a fault zone which cuts through sandstones, quartz pebble conglomerate, bioclastic limestone, oolite and micrite.	No data.	Some dolomitization of bioclastic limestones and oolite.	Mineralization is fault controlled.
BALLINALACK	4.0	Courceyan	ABC GROUP, Waulsortian Limestone; NAVAN GROUP Mixed Beds.	Fenestral micrite, bioclastic limestones, oolite, thin sandstones Waulsortian facies micrite and wackestones.	Tidal flats, Waulsortian limestones are believed to represent water depths of 200 to 300 m.	No data	SEDEX
TATESTOWN	1.6	Courceyan	NAVAN GROUP, Pale beds.	Micrites, fenestral micrites, calcarenites, oolite, wackestones. A few shales and thin sandstones also occur.	Inter-supra tidal flats and lagoons. Shallow high energy marine environment with ooid shoals.	Stratal dolostones and subaerial emergence with meteoric cementation.	Syn-diagenetic
OLDCASTLE	3.0	Courceyan	NAVAN GROUP. Pale Beds.	Fenestral micrites, micrites, evaporites silty micrites, siltstones, bioclastic limestones occasional sandstones.	No data	No data.	Epigenetic
ABBEYTOWN	1.1	Chadian to Arundian	ABC GROUP, Ballysodare Formation and Ballyshannon Limestone.	Bioclastic calcarenite with a few sandstones and shales	Shallow marine shelf with barrier sands and lagoons.	Extensive dolomitization of host limestones.	MVT.
[1]HARRERTON BRIDGE	0.5	Courceyan to Arundian	ABC GROUP. Waulsortian Limestones.	Fenestral micrites, calcarenites agillaceous limestones. Waulsortian Facies.	Shelf setting with tidal flats and lagoons. Shallow open marine environment with sand shoals, some deposition below wave base.	Extensive dolomitization of Waulsortian Limestones.	Epigenetic
COURTBROWN	0.25	Courceyan	ABC GROUP, Ballysteen Limestone.	No data	No data	Localized dolomitization.	MVT
[3]MOYVOUGHLY	0.125	Courceyan	NAVAN GROUP, Moyvoughly Beds, equivalent to the Pale Beds at Navan.	Micrites, fenestral micrites, wackestones, oolite and sandstones.	Intertidal-supratidal, high energy shallow marine shelf environment, perhaps a ramp. Syn-sedimentary tectonism.	No data	Epigenetic
NEWTOWN CASHEL	No data	Courceyan	NAVAN GROUP, Mixed Micrite Unit.	Shales, micrite, fenestral micrite sandstones, algal laminated micrite	Intertidal flats, perhaps cut by channels, lagoons, clastic barriers and offshore sand bars.	Extensive dolomitization of host limestone. Several unconformities present, gypsum is present, interpreted as reflecting subaerial exposure.	Newtown cashel Fracture controlled mineralization.
DUNCORMICK	No data	Courceyan	Unspecified limestones	No data	No data	Host rocks contain several dolomitized zones	Epigenetic
CARRIKITTLE	No Data	Courceyan	ABC GROUP, Waulsortian Limestones.	Waulsortian Limestone with crinoids, brachiopods and bryozoans.	No data.	Extensive dolomitization of host limestone.	Epigenetic

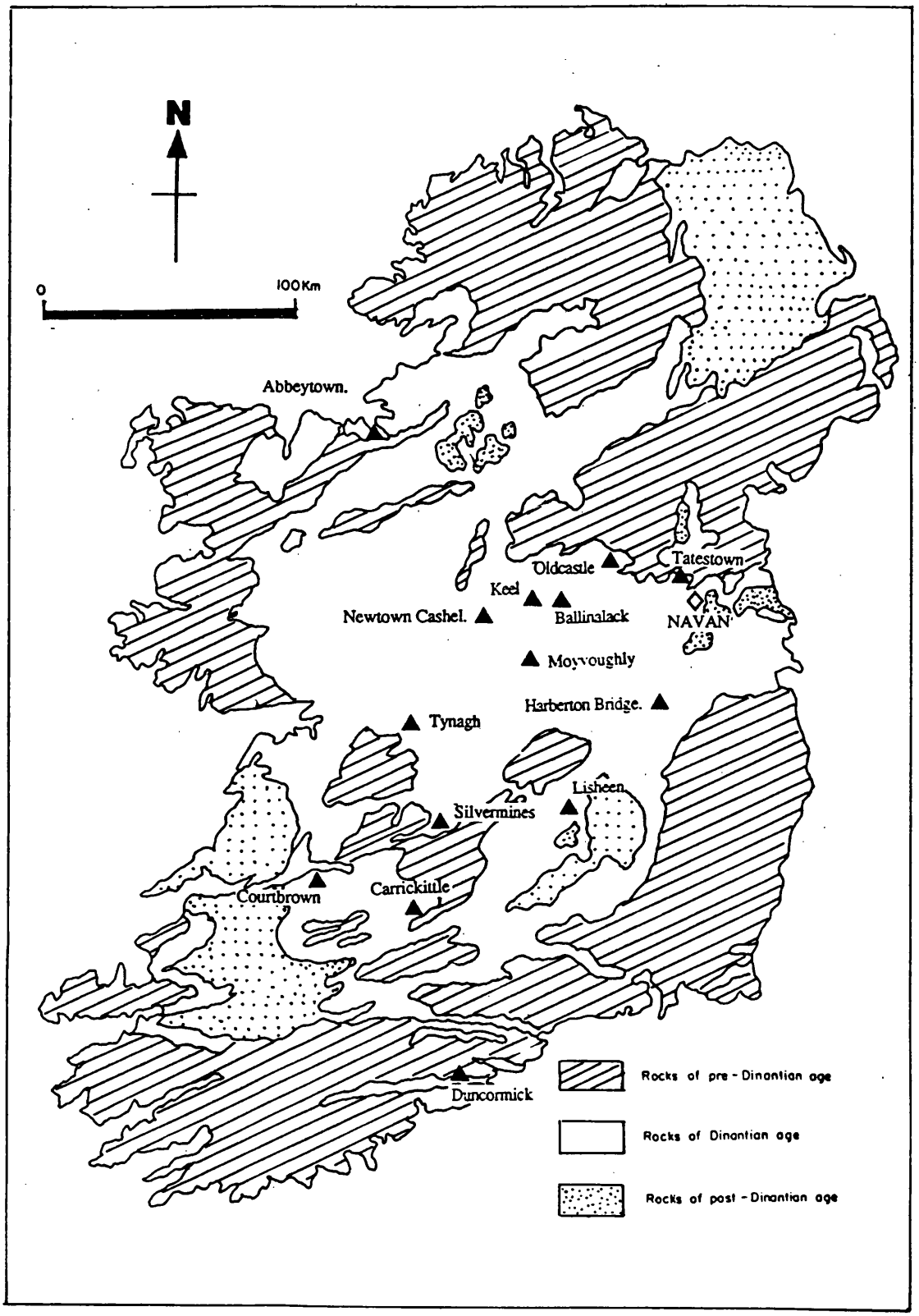

Fig. 1.3. The distribution of Irish Lower Carboniferous Zn-Pb deposits. From Hitzman & Large (1986).

most important so far discovered in Ireland. It is the largest Zn-Pb deposit in Europe and is of world status.

1.3. PREVIOUS WORK.

1.3.i. Introduction.

The Navan Zn-Pb deposit it is located along the SW margin of the Longford Down Lower Palaeozoic Inlier, 1 km west of the town of Navan (Fig. 1.4). It was discovered in 1970 by Tara Prospecting Ltd and production began in 1977. The calculated ore reserve is 70 million tonnes, and 97% of the ore is hosted by Lower Carboniferous, Courceyan, shallow marine limestones, informally known as the Pale Beds. The remainder of the orebody is hosted by Chadian submarine debris flows (Andrew & Ashton, 1985; Ashton *et al,* 1986). Previous studies of the host rocks to the Navan Ore Body have concentrated on stratigraphy. Sedimentology and diagenesis have only been dealt with in a generalised way and no detailed studies are available.

1.3. ii. Stratigraphy and sedimentology.

The oldest known subsurface rocks at Navan are Lower Palaeozoic in age, comprising an unweathered Ordovician sequence consisting of Llanvirn tuffs and tholeiitic lavas which pass upwards to Caradocian calc-alkaline basalts, keratophyres and volcaniclastics and Ashgillian marine sediments, notably mudstones, siltstones and sandstones. Silurian sediments to the north of Navan consist of undifferentiated purple, green and black shales with turbiditic grits. Together these rocks have undergone Caledonian deformation. To the NE of the Navan deposit they have been intruded by a syenite of probable Late Caledonian age (Romano, 1980; Andrew & Ashton, 1985; Ashton *et al,* 1986). This syenite has been extensively altered to chlorite and calcite and has undergone some silicification (thin section from Tara Mines collection). These rocks constitute the Longford Down Lower Palaeozoic inlier which lies within the Iapetus suture zone (Owen pers. comm. 1993).

The Lower Palaeozoic sequence is overlain by clastic Red Bed facies and a Carboniferous sequence of Courceyan to Arundian age. The Courceyan succession is divided into two groups; the Navan Group and the ABC Group. The Navan group is divided into four basic units, these are the Laminated beds, Muddy Limestone, Pale Beds and Shaley Pale Limestones. The overlying ABC Group consists of the Argillaceous Bioclastic Limestone and Waulsortian Limestone facies. An erosion surface cuts down throught the succession and truncates the Navan Group. This is overlain by the Boulder Conglomerate and the Upper Dark Limestone both of which are considered to be Arundian (Ashton *et al,* 1986; Philcox, 1989; Ashton *et al,* 1992 in press). The stratigraphy of the Navan host rocks is summarized in FIG. 1.5.

The Red Beds rest unconformably on the Lower Palaeozoic rocks (Philcox, 1984; Andrew & Ashton, 1985). The Red Beds occur throughout Ireland and generally thicken

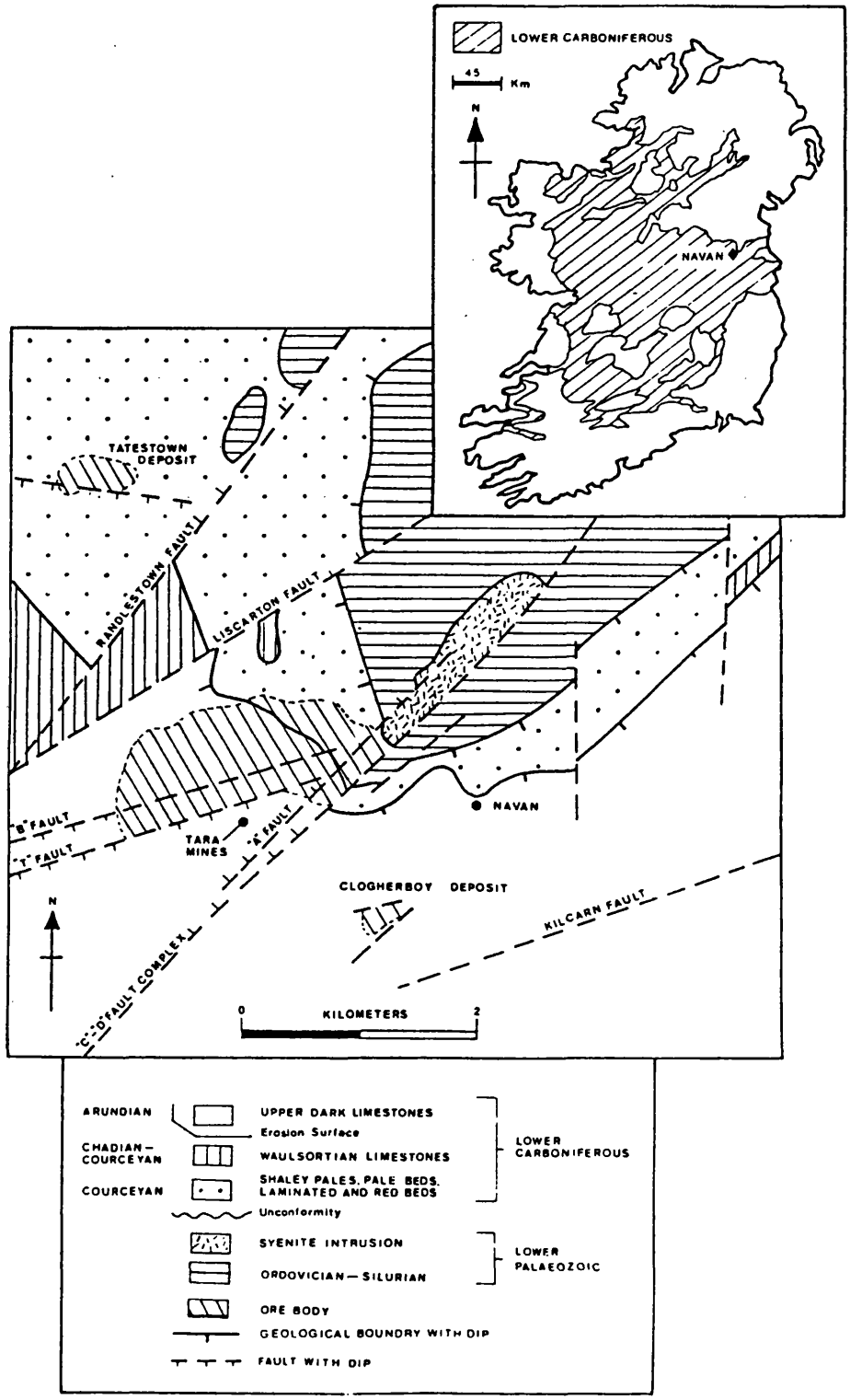

Fig. 1.4. Map showing the surface solid geology of the Navan area and the location of the Navan ore body. From Andrew & Ashton (1985); Ashton *et al,* (1986).

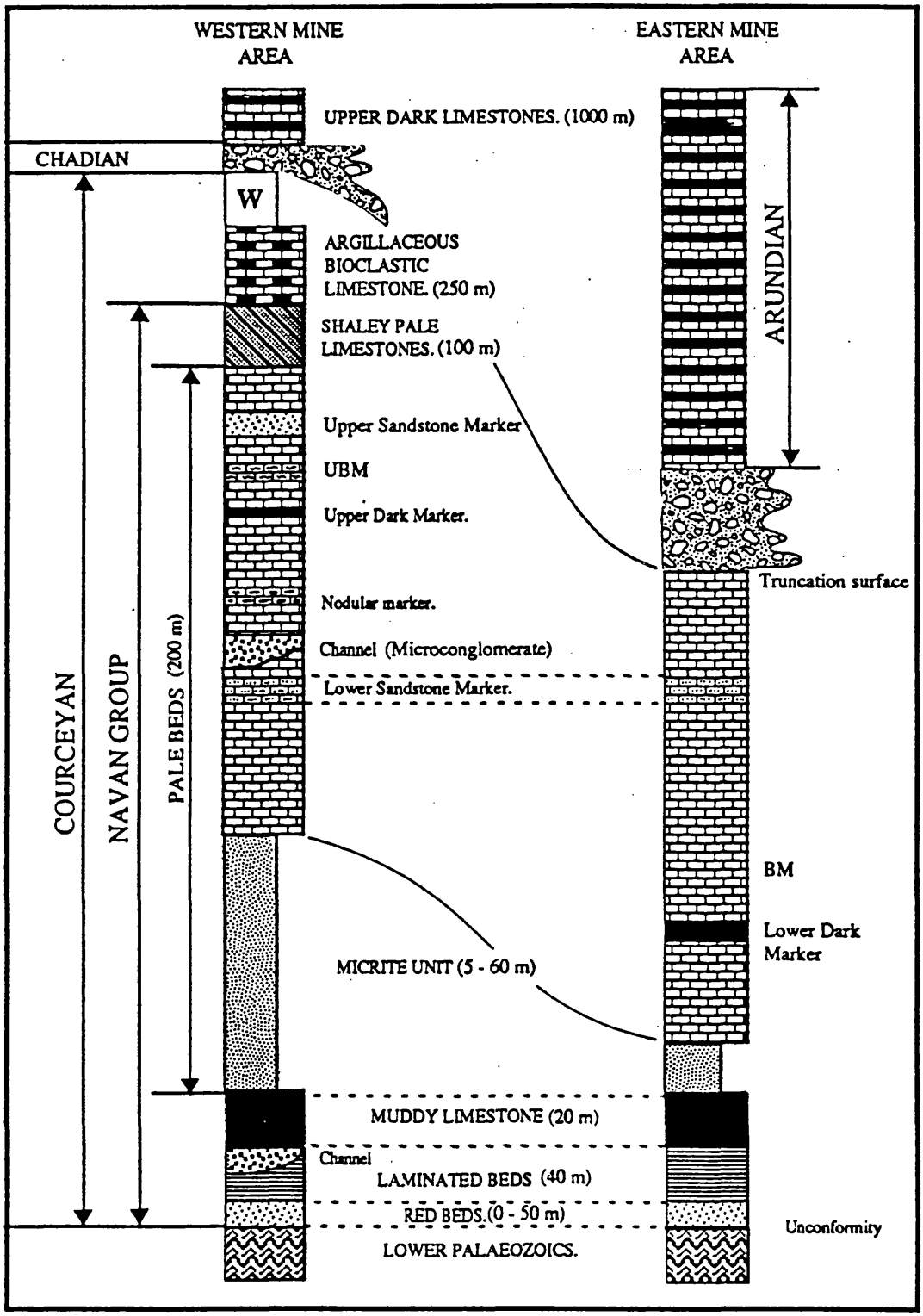

FIG. 1. 5. The stratigraphy of the Navan Mine, based on Ashton *et al*, (1986) and Anderson (1990). Figures in brackets indicate approximate thickness.

Boulder Conglomerate
Limestone turbidites
Sandstones
Lower Paleozoics
Shaley limestones
Crinoid rich shaley limestone
Calcarenite
Argillaceous mudstone -wackestone
Fenestral calcite mudstones - wackestones
Sandstones - shales - calcisiltites -
Granule-small pebble grade calcarenites
W Waulsortian Limestone
BM Brachiopod Marker UBM Upper Bryozoan Marker

southwards, attaining 240 m at Tynagh (Philcox,1984) and culminating in over six kilometres in the South Munster Basin (Phillips & Sevastopolo, 1986). At Navan they attain a maximum thickness of only 50 m but are much thinner locally (Philcox, 1984). The Red Beds consist of conglomerates, sandstones, siltstones, shales and caliche (Philcox, 1984; Andrew & Ashton, 1985; Anderson, 1990 and personal observations). Miospores from Red Beds to the west of Navan suggest a Lower Courceyan age (Andrew & Ashton, 1985, Ashton *et al,* 1986; Anderson, 1990; quoting Keegan, 1981). However, Strogen *et al,* (1990) using palynological data recovered from hole EP 27 at Navan suggested an early late Courceyan age for the Red Beds. The Red Beds have been interpreted as terrestrial sediments deposited in a fluviatile environment (Andrew & Ashton, 1985; Ashton *et al,* 1986; Anderson, 1990). Other interpretations include the suggestion that deposition occurred on a low lying coastal braid plain (Strogen *et al,* 1990) and that of Philcox, (1984) who suggested that rocks might reflect deposition in an alluvial fan.

The Laminated Beds have a gradational relationship with the Red Beds. They consist of 40 m of interbedded silts, shales, sandstones and limestones subdivided by Philcox (1984) into six lithological units referred to as the 'C-G', 'C-F', 'C-E', 'C-D', 'C-C' and 'C-B' units which can be laterally correlated. The Laminated Beds occur throughout the Irish Midlands where they are known as the Mixed Beds. At the base, the 'C-G' unit consists of interbedded sandstones and argillites (Anderson, 1990). The overlying 'C-F' unit is a distinctive light grey sandstone 3 m thick. The 'C-E' unit consists of thin oncolitic limestones, flaser bedded sandstones and calcisiltite (Anderson, 1990). The 'C-D' unit is a uniform calcisiltite overlain by light grey silicified nodules which are believed to have replaced anhydrite (Ashton *et al,* 1986). These nodules are known in the mine area as the **Quartz Marker.** The overlying 'C-C' unit is composed of irregularly interbedded shales and calcite mudstones. Finally the uppermost 'C-B' unit is composed of interbedded packstones and silty packstones. Philcox (1980), Andrew & Ashton (1986) and Anderson (1990) all recognized a channel cutting through the laminated beds as far down as the 'C-E' unit. This is overlain by the **Limestone Conglomerate** (Philcox, 1980) described as a calcrudite by Anderson (1990).

The Laminated Beds mark the initial transgression of the Lower Carboniferous sea over the terrestrial sediments of the Red Beds (Andrew & Ashton, 1985; Philcox, 1984). The lithological association and sedimentary structures of the sequence led Andrew & Ashton (1985); Downing & Ashton (1985) and Anderson, (1990) to interpret them as resulting from deposition in a clastic shallow marine-intertidal environment. The 'C-F' sandstone has been interpreted as representing low sand bars, discontinuous sand barriers, and channel sands (Strogen *et al,* 1990; Anderson, 1990). Strogen *et al,* (1990 Fig. 6.a) identified keystone vugs within the 'C-F' sandstone in hole U4855 and suggested that it had undergone emergence. It was suggested by Strogen *et al,* (1990) that tidal flat heterolithic sands accumulated behind these sand barriers. The lack of

burrowing, preservation of layering in the sandstones, shales and limestones, and the quartz (anhydrite) marker, suggested to Anderson (1990) that salinity was high enough to restrict colonisation by a diversified fauna. Shelly layers within the Laminated beds were interpreted by Anderson (1990) as representing storm or spring tide deposits.

The Laminated beds are overlain by the **The Muddy Limestone.** Originally this was considered to be part of the Laminated beds, the so called 'C-A' unit (Philcox, 1984). It is approximately 20 m thick and described as calcisiltite and argillite by Anderson, (1990). It includes a thin black shale, the so called Fine Silty Unit. Corals present include *Michelinia favosa* and *Syringopora reticulata* (Andrew & Ashton, 1985) which Strogen *et al* (1990) interpreted as Late Courceyan. The Muddy Limestones have been interpreted as lagoonal deposits (Andrew & Ashton, 1985) and were confusingly thought to have been deposited with little or no terrigenous influence (Andrew & Ashton, 1985). It has been suggested that the Muddy Limestones represents the point at which the succession changes from clastic to carbonate sedimentation (Ashton *et al,* 1986).

The overlying **Pale Beds** have been divided into a lower **Micrite Unit** and an overlying unit described by Andrew & Ashton, 1985; Anderson, 1990 as consisting of oolites and calcarenite. The Micrite Unit consists of interbedded mudstones and fenestral mudstones. Other lithologies present include occasional oolites, thin black shales (Anderson, 1990), and a thin green shale, the so called **'Footwall Green Shale'.** Sedimentary structures include bedding, oncolites and burrows. The unit has a maximum thickness of 60 m, but the top is highly irregular having a local relief of 6 m. This irregular surface culminates in a linear zone of thining which strikes NW-SE, along which the Micrite Unit is only a few metres thick (Andrew & Ashton, 1985). The nature of this feature is poorly understood, Andrew & Ashton (1985) suggested that it represents a channel, conversely Anderson (1990) suggested that it reflects a palaeohigh in the Lower Palaeozoic basement. At the Tatestown deposit 3 km to the northwest of Navan the Courceyan conodont, *Polynathus comunis carina* has been recovered from the Micrite Unit, together with *Eoforschia, Tournayella discoidea* and species of *Latiendothyra* which indicate a late Courceyan age (Strogen *et al,* 1990).

Oncolites, fenestrae, calcispheres and rare gypsum were quoted by Andrew & Ashton, (1985) and Anderson (1990) as evidence for deposition of the Micrite Unit in lagoons and supratidal flats. Strogen *et al,* (1990) also noted the occurrence of shallowing up cycles. These begin with subtidal oolites and pass upwards into fenestral supra-intertidal mudstones which were thought to accumulate behind carbonate sand shoal systems. Fissure fills, rootlet structures and alveolar textures described from holes EP27 and N915 at Navan were used by Strogen *et al* (1990) as evidence that the Micrite Unit had undergone emergence.

Overlying the Micrite Unit and filling the "channel" is a 'blanket' oolites and calcc arenites 150 m thick. Conodonts recovered include *Scalognathus.anchoralis* of Courceyan age (Andrew & Ashton, 1985). Seven argillaceous and sandy markers divide

this part of the sequence (Philcox, 1984, Andrew & Ashton, 1985; Ashton *et al,* 1986; Anderson 1990). These are referred to individually, from the lowest upwards, as the **Lower Dark Marker**, the **Sub Lower Sandstone**, the **Lower Sandstone Marker**, the **Nodular Marker**, the **Sub Dark Marker**, the **Upper Dark Marker** and finally the **Upper Sandstone Marker**. In addition two palaeontological markers are present, the **Brachiopod Marker** and the younger **Lower Bryozoan Marker** (see Fig. 1.5). These markers are important for two reasons; they enable correlation of drill cores and thus allow structural interpretations leading to the construction of cross sections.

Strogen *et al* (1990) suggested that the calcarenites and oolite grainstones of the Pale Beds at Navan were deposited on a ramp. Andrew & Ashton (1985) and Downing & Ashton (1985) suggested deposition in a shallow water high enegy shelf environment with sand bars and oolite shoals, while Anderson (1990) suggested formation on a subtidal bank margin. In addition to the clastic markers a variety of 'exotic' clastic grains have been noted within the calcarenties and oolites. These include feldspar, muscovite, tourmaline, illmenite, zircon and glauconite (Andrew & Ashton, 1985). The source of these grains was thought to be in longshore drift fed by a fluviatile system to the west (Philips & Sevastopoulo 1986, Strogen *et al,* 1990) with the Lower Dark Marker interpreted as a "deltaic incursion" by Andrew & Ashton, (1985). The sedimentology of the remaining marker horizons has not been considered. Anderson, (1990) suggested that clastic sediments were sourced from syenite and keratophyric breccias to the northeast of the ore body. Alternatively Andrew & Ashton (1985) suggested that the sediment was aeolian and derived from a low relief hinterland.

The calcarenties and oolites contain a channel sequence in the western Mine area striking NW-SE and cutting down as far as the Lower Sandstone Marker in the western mine area. The channel fill is known as the Microconglomerate and has been described as a calcrudite interbedded with calcisiltite (Anderson, 1990). The microconglomerate was interpreted as being deposited as a series of "pulses" by Anderson (1990).

The **Shaley Pale Limestones** overlie the Pale Beds, they are approximately 100 m thick and comprise a varied succession of interbedded shales, unspecified limestones and sandstones which Philcox (1989) divided into Lower, Middle and Upper Shaley Pales. *Tetraxis Sp.* and *Sc. anchoralis* recovered from the Lower Shaley Pale limestone (Andrew & Ashton, 1985) indicate a Courceyan age. The conodont *Polygnathus mehili* has also been recovered (Strogen *et al,* 1990).

As a whole the Shaley Pale Limestones have been considered to be the deeper water offshore equivalent of the grainstones below, marking a change from shelf to quiet water deposition (Andrew & Ashton, 1985; Anderson, 1990; Strogen, *et al* 1990; Ashton *et al,* 1992 in press). The lack of abraded shells in the lower Shaley Pale Limestone was used by Strogen *et al,* (1990) as evidence for quiet water sedimentation. The Middle Shaley Pale Limestones are also interpreted as reflecting prolonged quiet water subtidal

sedimentation where the rate of sedimentation did not exceed the rate of subsidence. The deposition of the Upper Shaley Pale Limestones was believed to have been interrupted by storm sedimentation and soft sediment deformation which suggested deposition near to the shelf (Strogen *et al*, 1990) although the reasons for this interpretation were not stated.

The **Argillaceous Bioclastic Limestones** are of generally similar lithology to the Shaley Pales but have a higher clastic content and display nodular textures. In the Navan area they are 130 m thick. They contain a conodont assemblage akin to part of the *Sc. anchoralis* zone recovered from the lower and middle parts of the unit and are thus again Courceyan (Andrew & Ashton, 1985). This unit was interpreted by Strogen *et al*, 1990 as representing a continuation of tranquil subtidal shelf sedimentation related to regional deepening of the ocean.

The **Waulsortian Facies Limestones** are poorly represented in the mine area. They occur only to the west and are cut off to the east by a large erosion surface. The limestones are dense, cream coloured, massively bedded calcite mudstones and crinoidal wackestones. Andrew & Ashton, (1985) suggested that the Waulsortian Facies is entirely Chadian in age. However the recovery of *Scaliognathus anchoralis* suggests the lower part is still Courceyan (Philcox, 1984). The precise position of the Courceyan-Chadian boundary in the mine is uncertain (Philcox, 1989; Strogen *et al*, 1990). However, a pale green mudstone within the Waulsortian Limestones present to the north may be related to a wide spread tuff occuring near the Courceyan-Chadian boundary throughout the North Irish Midlands (Philcox, 1984; Andrew & Ashton 1985). The Waulsortian Limestones form stromatactis mudbanks (Andrew & Ashton 1985; Downing & Ashton, 1985). Granular crinoidal facies have been interpreted as mound flank deposits by Andrew & Ashton (1985) and Philcox (1984).

A truncation surface is present which cuts down 700 m southwards through the sequence in the central mine area and has a channel like profile (Boyce *et al* 1983; Andrew & Ashton 1985; Downing & Ashton, 1985; Ashton *et al*, 1986; Strogen *et al*, 1990; Philcox, 1989; Ashton *et al*, in press 1992). This surface was initially interpreted as a subaerial erosion surface (Philcox, 1980, 1984). It was later described as a submarine fault scarp (Boyce *et al*, 1983). Work by Philcox (1989) and Ashton, *et al* (1992 in press) has since suggested that it is composed of a series of low angle syn-sedimentary slump-fault scarps. The slumps are thought to have been initiated by an extensional regime with decollment occurring in the weaker argillaceous layers. Later faulting interrupted and offset the slump scars.

The erosion surface is overlain by the **Boulder Conglomerate** which consists of blocks and boulders of Pale Beds, Shaley Pale limestones and Waulsortian limestone up to 6 m diameter in a dark shale matrix. An Arundian macro fauna has been recovered from the matrix by Philcox (1989). The Boulder Conglomerate was interpreted as a submarine debris flow triggered by the faulting (Boyce *et al*, 1983; Andrew & Ashton, 1985; Downing & Ashton, 1985; Ashton *et al*, 1992 in press). Philcox (1989) has

shown that it consists of a series of flows of varying density interspersed with basinal muds.

The **Upper Dark Limestones** which follow, informally known as the Calp, blanket the Irish Midlands. These are distinctive interbedded limestones and fissile black shales. The basal member, the Thinly Bedded Unit consists of 10 to 30 cm thick alternations of limestone and shale (Philcox, 1989). A microfauna indicates a Chadian age (Philcox, 1989). The Arundian-Chadian boundary is taken at the first appearence of primitive discoidal *Archaeodiscidae* in hole N915 at Navan by Strogen *et al* (1989). Andrew & Ashton (1985) suggested that the Upper Dark Limestone youngs upward into the Holkerian.

The Thinly Bedded Unit overlaps the Boulder Conglomerate and has been interpreted by Philcox (1989) as reflecting "tranquil sedimentation in the basinal environment below wave base". The Upper Dark Limestones as a whole are thought to represent a turbidite sequence (Andrew & Ashton, 1985; Downing & Ashton, 1985; Strogen *et al.* 1990; Anderson, 1990). It is said to have been derived from the north east and deposited in about 500 m of water (Anderson, 1990) parallel to the known palaeoslope (Andrew & Ashton, 1985; Philcox, 1989). Finally Tertiary **basalt dykes** are present within the mine (Turner *et al,* 1971). These dykes are easterly trending and dip from 10^0 to 70^0 to the south. The basalt is altered and friable and limestones adjacent to the dykes have been intensely altered (Hole N725 at depth 343.0 m).

1.3.iii. Petrography

A very generalised diagenetic sequence for the Pale Beds was established by Andrew & Ashton (1985) using samples mostly from the Tatestown deposit 3 km to the NW of Navan plus a limited number from Navan itself. The first stage was confusingly described as micrite rims and said to be developed only where syntaxial overgrowths occur. Deposition of this was said to be followed by unspecified alteration of allochems and by the deposition of vadose rim cements described as an-isopachous pendant bladed spar. The second stage characterised by compaction, was confusingly described as resulting in plastic deformation of ooliths and development of sutured grain contacts. The main event during "stage three" was dolomitization which was thought to have taken place within 50 m of the sediment water interface. It was suggested that mineralisation was contemporaneous with this. Leaching of dolomite and brittle fracturing were the last events during this stage and were followed by succesive stages of fracture fill cementation and mineralization.

More detailed work was carried out by Anderson (1990) who erected a general paragenetic sequence for the Pale Beds. Three stages of calcite cementation were recognised filling primary and some secondary pores. Anderson, (1990) described a bladed non-luminescent calcite followed by well zoned crystals with alternate brown-yellow / bright yellow cathodoluminescent zones, becoming brighter outward toward the

crystal faces. Both bladed and zoned cements were described as forming syntaxial overgrowths and pore fill cements. A blocky ferroan calcite cement with a patchy medium dull (orange?) luminescence was said to overlie these, with the remaining pore space filled by dolomite cement.

No distinction was made between the cement sequences in the Micrite Unit and those in the overlying calcarenites. However, it was noted that internal zonation of cements varied and was in need of more detailed study. The cements were interpreted as marine, forming within 10 m of the sea floor during passage of the sediments through the oxidizing zone into the zone of bacteriogenic reduction. Silicification was noted as taking the form of euhedral overgrowths on detrital clastic grains.

Anderson (1990) recognised three types of dolomitization in the Pale Beds which he described as stratal, pervasive and "partial". The dolomite were generally referred to as "fine grained". Stratal dolomite was described as bedding parallel, locally corresponding to the stratigraphic marker units of the Lower Sandstone and Sub Lower Sandstone.

Anderson (1990) subdivided the stratal dolomite into three stages. Stage one was described as cloudy and inclusion rich with a dull brown-red luminescence and corroded margins. This was overlain by stage two, dark to non-luminescent, and occuring in veins which cut stage one. Stage three was described as a dark-bright red sequence occuring in veins which cut both stages one and two and overlain by blotchy luminescent calcite.

Pervasive dolomite was described as occurring only in the Western Mine area, where it was said to extend vertically over 50 m. Once again, several stages of dolomite were recognised. Stage one dolomite corrresponds to stage one dolomite present in the stratal dolomite. This was followed by a couplet consisting of an inner bright orange-yellow zone and an outer orange-red zone. Non-luminescent ferroan dolomite containing one or two bright red zones was described as forming a cement. This cement was also noted in vugs forming saddle crystals and associated with sulphides These vugs were thought to have been produced by volume reduction concomitant with dolomitization. Pores were partially occluded by brightly luminescent calcite. Partial dolomitization was described as replacing both cements and allochems. It was noted that stylolites cut the dolomite and suggested that the stratal, pervasive and partial dolomite were all formed during shallow burial with the later saddle dolomite forming from fluids of higher temperature.

1.4. MINERALIZATION AND TECTONIC SETTING OF THE NAVAN MINE.

1.4.i.Mineralization.

The Pale Beds Marker horizons have been used to divide the ore body into five 'lenses'. For detailed describtion of these lenses refer to Andrew & Ashton (1982); Andrew & Ashton (1985); Ashton *et al* (1986) and Anderton (1990). The Green Shale occuring in the Micrite Unit is taken as the footwall to mineralization since ores do not

occur below this. The **5 Lens** represents all mineralization below the Lower Dark Marker. The Lower Dark Marker is absent in the western part of the mine, instead a laterally discontinuous dolomite which extends along the base of the grainstones, the **Lower Dark Marker Equivalent** is used to define the top of the Five Lens in this area. All mineralization between the Lower Dark Marker and the Lower Sandstone Marker is referred to as the **4 Lens**. Due to low grades, **lenses 2 and 3** are frequently combined and their upper limit is the base of the Nodular Marker. The **1 Lens** occurs between the Nodular Marker and Upper Dark Marker. These lenses are illustrated diagramatically in Fig. 1.6.

The mineralogy of the ore is simple, it consists of sphalerite and galena, with gangue minerals barite and calcite. Anderson (1990) carried out extensive textural and sulphur isotope studies on the ores. Five main styles of mineralization were identified; massive, sulphide cementation of brecciated zones; vein filling and cavity filling. In addition, some mineralization is believed to have begun before cementation of lime sediment was complete and is referred to as "syndiagenetic". It was noted by Anderson (1990) that the style of mineralization varies systematically. In the eastern part of the mine, mineralization within each lens is vertically continuous, either massive or breccia hosted. To the west, vertical continuity diminishes, and the ores are confined to cavities (refer Fig.1.6). The cavities are laterally extensive and have consistent stratigraphic positions. Up to 3% of mainly pyritic ore is present within the Boulder Conglomerate and is referred to as the Conglomerate Group Ore.

Anderson (1989, 1990) demonstrated that the Pb-Zn ores were characterised by both isotopically heavy sulphur characterised by $\delta^{34}S$ of 19‰ and isotopically light sulphur characterised by $\delta^{34}S$ of -14 to -23‰. The isotopically light sulphur was interpreted as reflecting bacteriogenically reduced seawater with the isotopically heavy sulphur interpreted as being derived from hydrothermal fluids. The occurrence of both heavy and light sulphur in the ores was interpreted as reflecting an *in situ* mixing of bacteriogenically reduced seawater and hydrothermal sulphur at the site of ore deposition. The source of the hydrothermal solutions is unknown (Ashton *et al,* 1992 in press) but Pb isotope studies suggest the lead may have been derived from the Lower Palaeozoic Basement (Mills *et al,* 1987).

1.4.ii. Tectonic setting.

The Lower Carboniferous succession at Navan is dominated by a broad anticline which plunges approximately 20^0 to the south west (Andrew & Ashton, 1985; Ashton *et al,* 1986; Ashton *et al,* 1992 in press). This structure has been displaced by a series of faults; an early ENE trending system and a later NE trending system. (Andrew & Ashton, 1985; Ashton *et al,* 1986; Ashton *et al,* 1992 in press). The distribution is shown in Fig.1.4. The early system consists of faults locally reffered to as the 'B' and 'T' Faults. These dip to the south and have listric profiles with down throw to the south. The

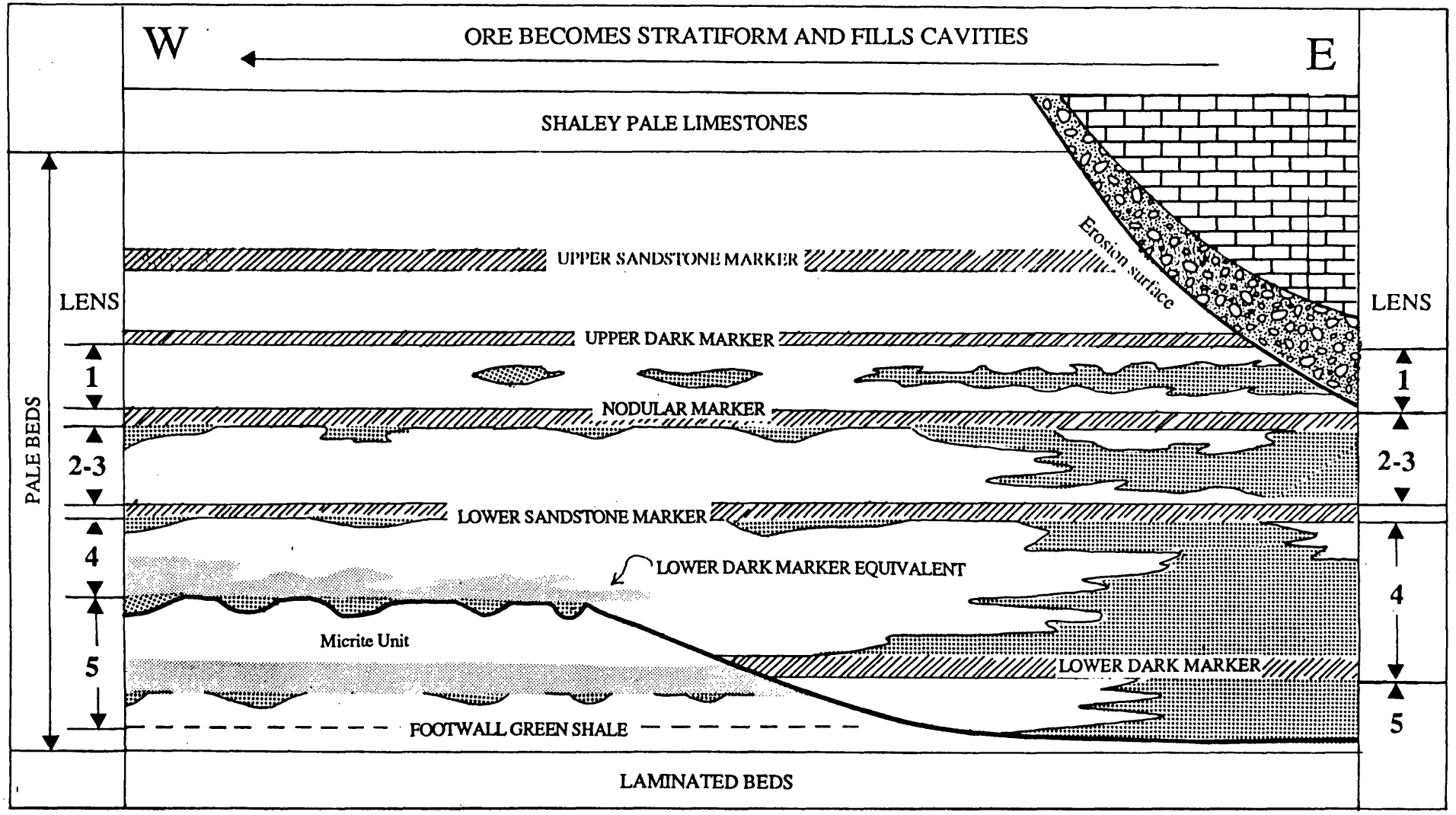

Fig. 1.6. Navan ore lenses defined by Marker horizons. Based on Ashton *et al* (1986); Anderson (1990).

maximum throw on the 'B' Fault is approximately 70 m, that on the 'T' Fault is of 200 m. Both faults are considered to be late Courceyan in age as the 'B' Fault is truncated by the submarine erosion surface and does not penetrate the Upper Dark Limestones. However, the 'T' Fault exhibits several stages of movement, and it displaces the erosion surface by 50 m, suggesting that some movement occured during the Chadian. The 'T' Fault zone, observed in the 1175 mine level and is 30 cm wide and consists of three sub parallel planar faults and associated fault gouge dipping at approximately 45^0. Associated with these faults are swarms of NE trending mineralized fractures which are believed to represent initial zones of weakness prior to faulting.

The NE trending faults, named the 'A', 'C', 'D', Castle and Randlestown Faults are later. The 'A' Fault dislocates the Upper Dark Limestones and is belived to be a dextral strike slip fault with a displacement of 100 m and a reverse component of 80 m. The 'A' fault is present in the 1345 mine level 375 stope where 'splay' faults can be seen associated with it. The 'C' Fault again cuts the Upper Dark Limestones and displays a normal component throw which varies from <100 m to >150 m. The Randlestown and the 'D' fault are wrench faults and are preseumed to be Hercynian in age. The Liscarton and Castle Fault both dip to the NW and are believed to be of similar age to the 'B' and 'T' Faults with the Castle fault undergoing reactivation during the Hercynian. Finally, other Hercynian structures include north trending isoclinal folds a few metres in amplitude, which are confined to the Upper Dark Limestones, and NW trending fractures filled with blocky calcite which locally cut ENE trending faults. The relationship between stratigraphy, mineralization and faulting is illustrated in Fig. 1. 7.

1.5. LOWER CARBONIFEROUS PALAEOGEOGRAPHY OF IRELAND.

During late Devonian to early Carboniferous times the Old Red Sandstone continental facies became influenced by a crustal scale extensional tectonic regime. In NW Europe, in the area which is now the British Isles and Ireland, the extensional tectonics culminated in the formation of a series of blocks and basins (Fig. 1.8).The most southerly block is St. Georges land, which is represented in Ireland by the Leinster massif. To the north several other blocks have been identified; the East Midlands Block, the Askrigg-Alston Block, the Cumbrian-Askrigg block and the Southern Uplands Block, the last represented in Ireland by the Longford Down Massif (Anderton *et al,* 1985; Walkden, 1987; Leeder, 1987)

The Lower Carboniferous of Ireland has been divided into three geological provinces (Philcox, 1984), the South Munster Basin, the Limerick Province and the Midlands province, each defined by its stratigraphic sequence (Fig. 1.9). The contemporaneous evolution of each province has been analysed in terms of four conodont zones the *spicatus, inornatus-siphonodella, carina* and *anchoralis* zones (Varker & Sevastopolo,1985).

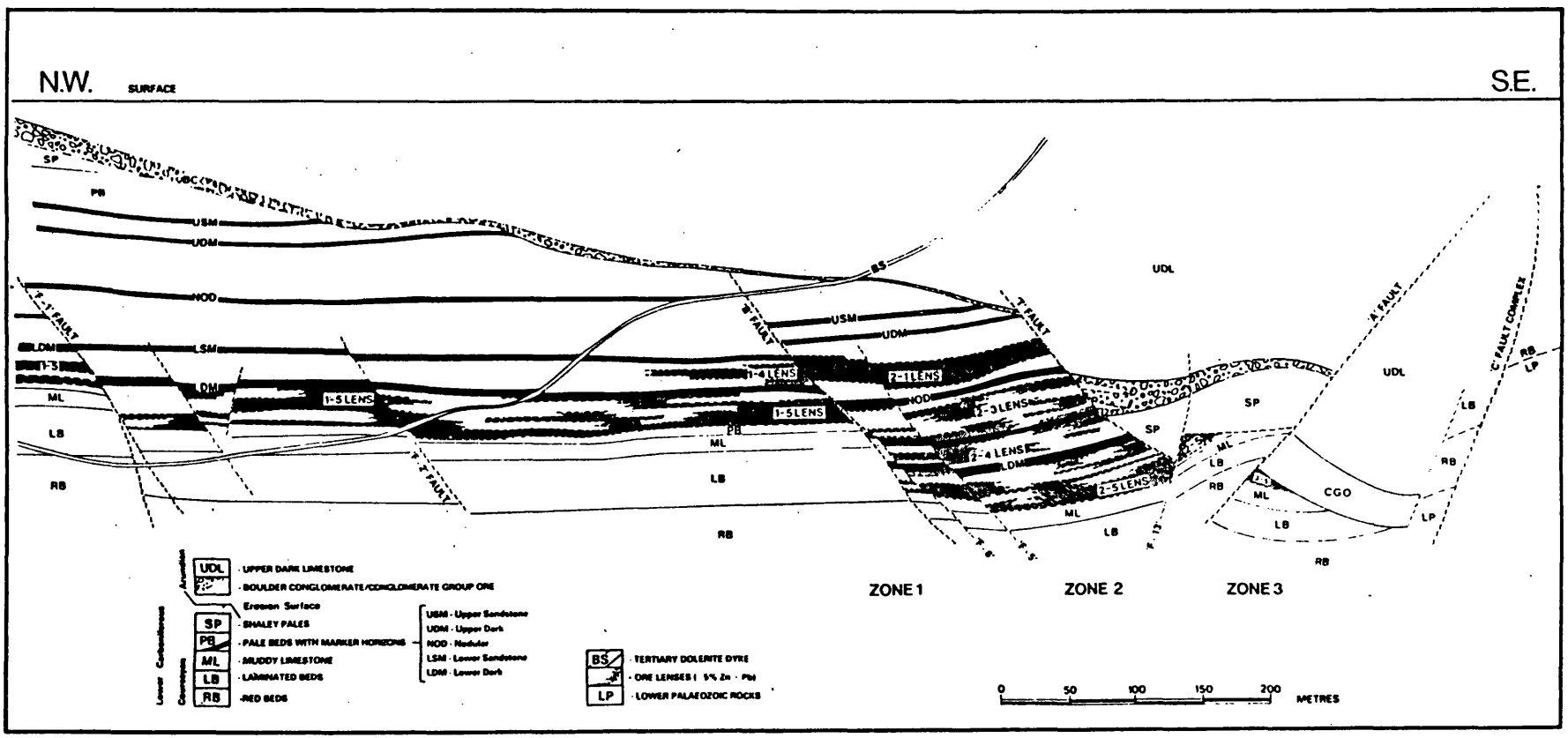

Fig.1.7. NW-SE strike section through the central part of the Navan mine showing the relationship between the host rocks, mineralization and faulting. From Ashton *et al* (1986)

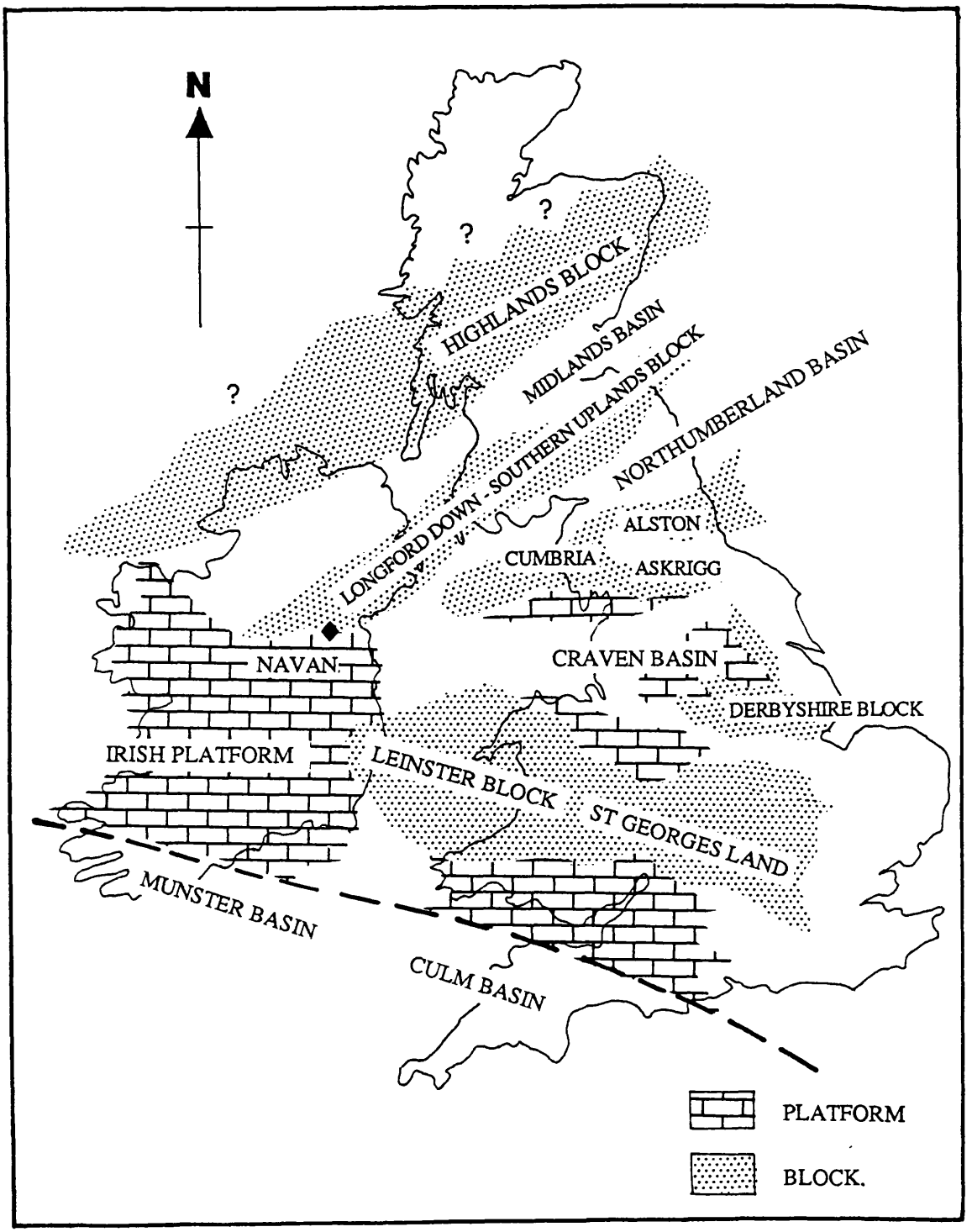

Fig.1.8. Generalized palaeogeography of the British Isles and Ireland. Based on Anderton *et al* (1985); Leeder (1987); Walkden (1987).

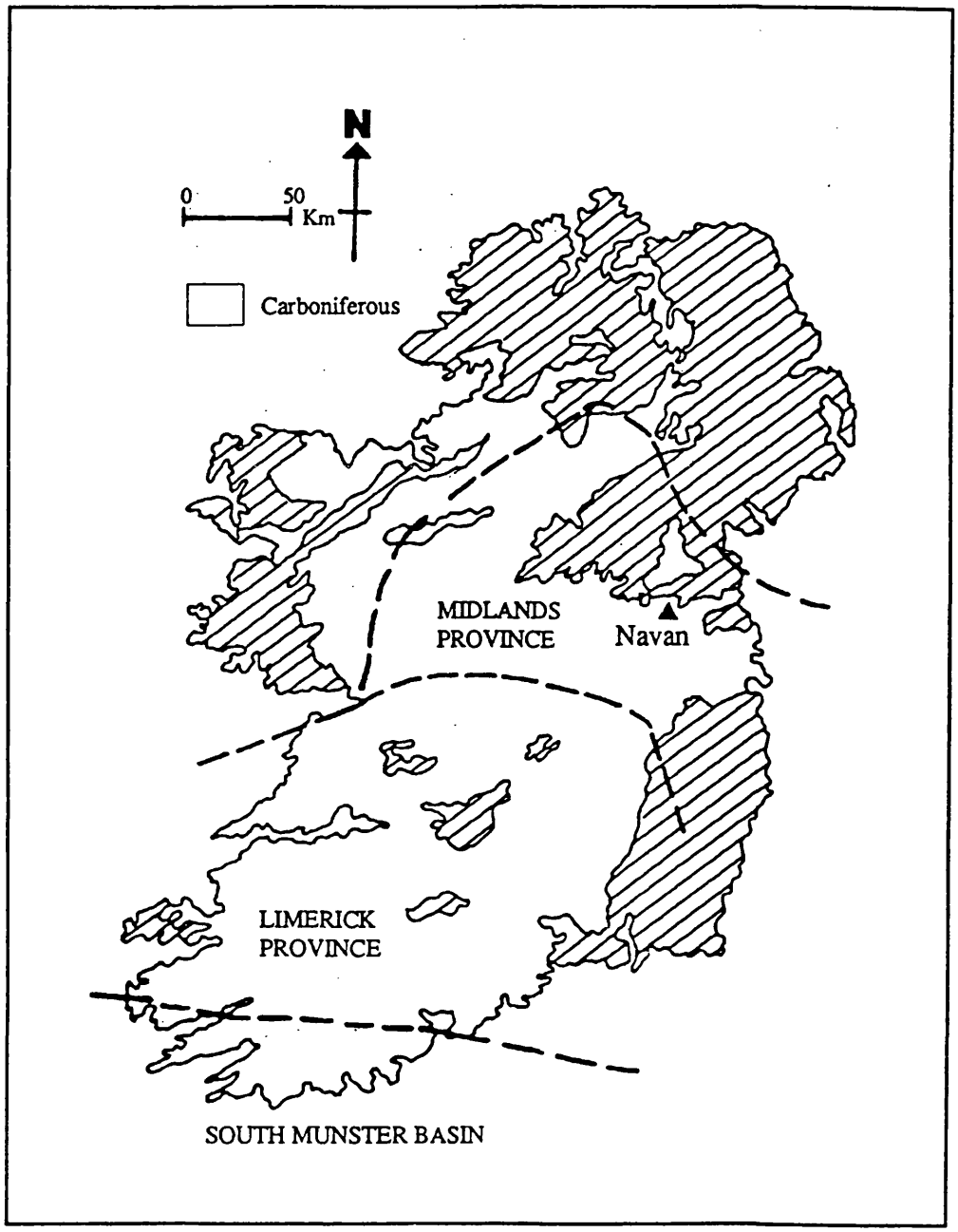

Fig.1.9. Lower Carboniferous palaeogeographic provinces of Ireland. From Philcox (1984); Phillips & Sevastopulo (1986).

During *spicatus* times the sea transgressed northwards over the Old Red Sandstone Continent. Mudrocks and sandstones were deposited in the South Munster Basin (the Kinsale Formation) and these pass northwards into shallow marine clastics and limestones of the southern Limerick Province. The palaeoshoreline at this time is thought to have corresponded to the northern boundary of the Limerick Province and is represented by clastic shallow marine sands (The Mellon House Beds).

During *inornatus-siphonodella* times the sea deepened, resulting in deposition of thick mudrocks in the South Munster Basin (The Courtmacsherry Formation) and the Limerick Province (the Ringmoylan Shales). At the same time, the shoreline migrated northwards into the Midland Province, depositing marginal marine sands which are probably represented at Navan by the Laminated Beds.

During lower *carina* times an open marine shelf covered the Limerick province, resulting in deposition of the Ballymartin Point Formation which passes northward into the Ferbane Mudstone of the southern Midland Province. Further correlation in the Midlands Province is tenuous but marine conditions probably reached Navan and resulted in deposition of the Muddy Limestone (Phillips & Sevastopoulo, 1986).

By late *carina* - *anchoralis* times a carbonate platform convered Ireland. This deepened to the south, culminating in the South Munster Basin but was associated with a number of broad facies belts (Fig. 1.10). The Limerick Province was covered by open marine carbonate sands, known as the Ballysteen Limestones. These host significant mineralization at Silvermines and Tynagh. They are thought to pass laterally into the lagoonal and intertidal sediments of the North Midlands Province, the Pale Beds (Philcox, 1984). At Navan they are represented by the fenestral and non fenestral calcite mudstones of the Micrite Unit.

The Pale Beds pass northwards into evaporitic tidal flats with thin gypsum layers attaining a maximum thickness of 1.5 m. Notable localities include Keel, Granard, Oldcastle and Roscommon, which occur to the west, southwest and northwest of Navan (Philcox, 1984). The Waulsortian mudmound facies first began to develop during early *carina* times along the northern margin of the South Munster Basin and by *anchoralis* times covered the Limerick Province and most of the Midlands Province (Philcox, 1984; Philips & Sevastoupoulo, 1986; MacCarthy & Gardiner, 1987).

During the early Arundian, extensional tectonism affected the British and Irish Lower Carboniferous (Leeder, 1987), this is represented in Ireland by submarine debris flows, represented at Navan by the Boulder Conglomerate which formed the northern margin of the Dublin Basin (Strogen *et al* 1990). Similar debris flows also formed at Silvermines, County Tipperary and Tynagh, County Galway (Boyce *et al,* 1983). This period was also a time of high heat flow, represent in Ireland by sporadic volcanism (Philcox, 1984; Phillips & Sevastoupoulo, 1986). The Dublin Basin became the site of deposition of the

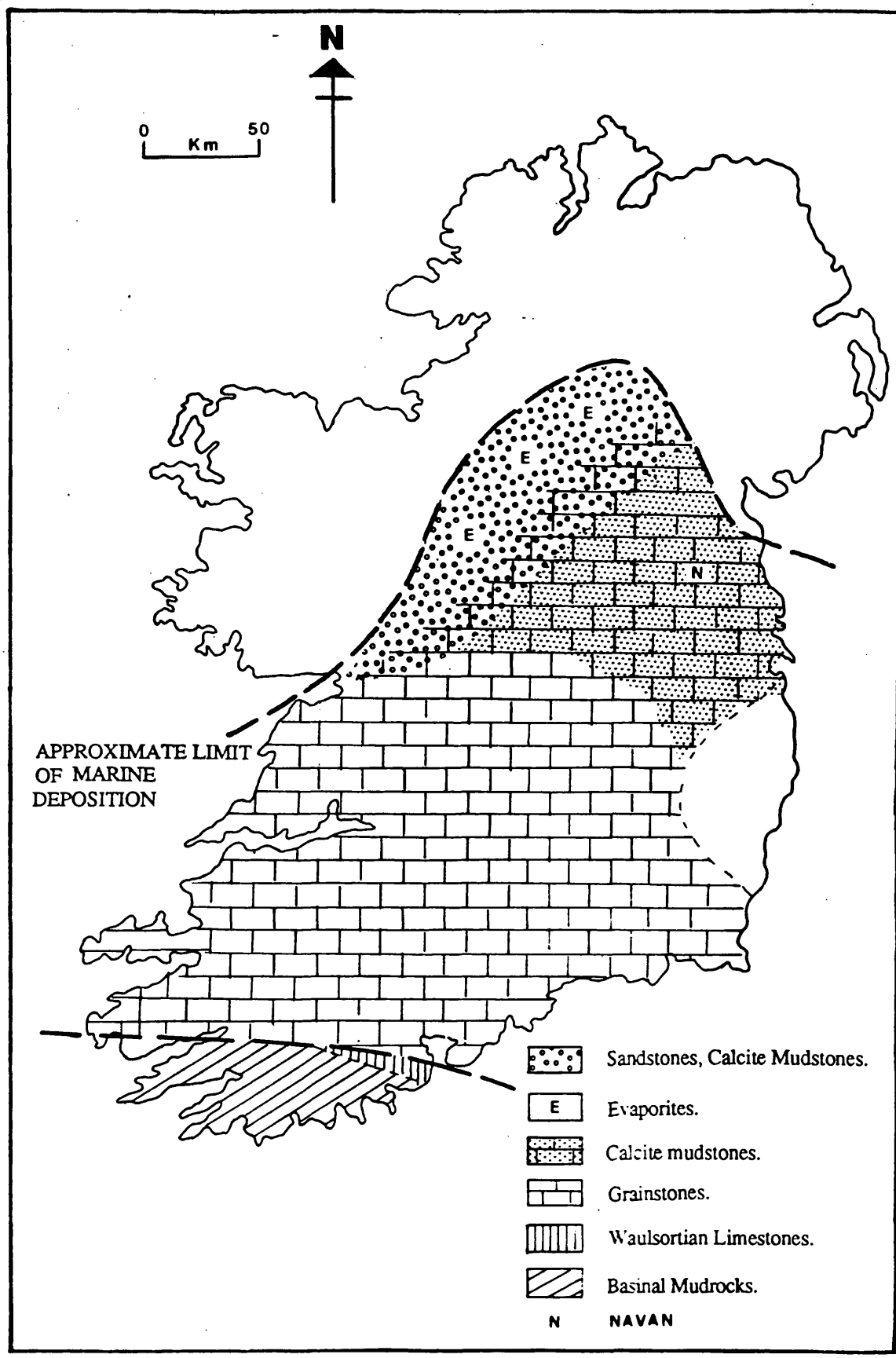

Fig.1.10. Generalized palaeogeography during *carina - anchoralis* times (deposition of Pale Beds at Navan). From Phillips & Sevastopulo (1986).

turbiditic Upper Dark Limestones which eventually blanketed the Irish Midlands. The lithostratigraphy of the Irish Lower Carboniferous is summarized in Fig.1.11.

1.6 DATA BASE AND EQUIPMENT USED.

1.6.i. Drill cores.

The Irish Midlands consist of gently rolling farmland, and there are few exposures of the Navan Ore Body host rocks. All lithological information has to be produced from surface diamond drilling and coring. Over 11.5 km of 3.5 cm diameter (BQ) drill core have been examined and this forms the data base of this study. Over 70 separate drill cores from the Tara Mine Archive of 1100 holes have been logged at 1: 250 scale with logging extending from the Laminated Beds to the upper limit of the Pale Beds. Other cores were examined in order to briefly describe the Lower Palaeozoic rocks, the Red Beds, Shaley Pale Limestones, Boulder Conglomerate and the Upper Dark Limestones. When more detailed work was required, logging was carried using specifically designed log sheets at 1:10 and 1:1 scale. These sheets also facilated the recording of limestone - dolomite relationships and textures.

The study area is approximately 6 km^2, a line striking north-south, through the surface ore storage depot divides the area into 2 zones, the western mine area and eastern mine area (Fig.1.12.). Much of the work in this thesis was carried out in the western mine area where surface diamond drilling is curently taking place. Over 50% of drill cores were chosen from an area extending between the 'T' and Castle Faults. Drill cores were also selected from areas between other major faults. Several widely spaced cores from beyond the mine were also logged so as to provide a sedimentological evelope around the main study area. One dip section 'A-A' and four strike sections 'B-B', 'C-C', 'D-D', and 'E-E' were constructed through the study area to illustrate lateral and vertical facies associations (Fig.1.12). These sections were constructed between approximately vertical drill cores. The locations of cross-sections was chosen on a map provided by the Mine Geology department showing the location of every bore hole. Only cores with little or no faulting were chosen. However, locally the use of faulted drill core was unavoidable and when this occurred restoration was neccessary. This was undertaken by using the Upper Dark Marker as a horizontal datum and then correlating the marker horizons present in the Pale Beds. This method has also been used by Philcox, (1989). The most consistently useful markers are the Lower Dark Marker, Lower Sandstone Marker, Upper Sandstone Marker and the Upper Bryozoan Marker. The constant vertical thicknesses of the units between these markers demonstrates that they formed discrete horizontal layers. Other useful markers include the Nodular Marker and the Five Lens Dolomite. Underground mapping of drift side walls and headings was carried out on standard Mine Geology Department mapping sheets, mine levels visited are shown in Fig. 1.13. Both logging and underground mapping were supplemented by standard field notes and photography.

Fig .1.11. Lower Carboniferous lithostratigraphy of Ireland. Modified from Philcox (1984).

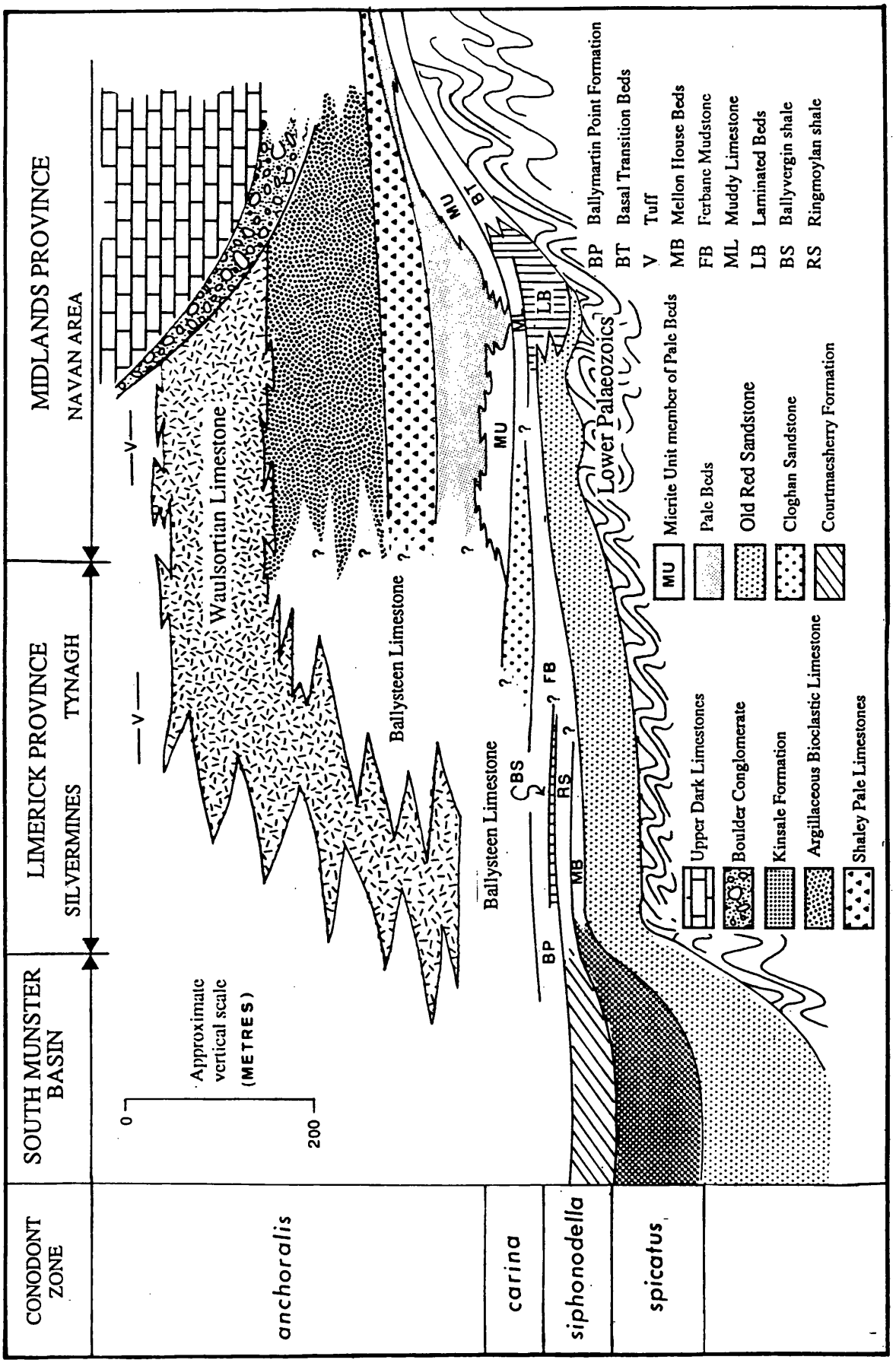

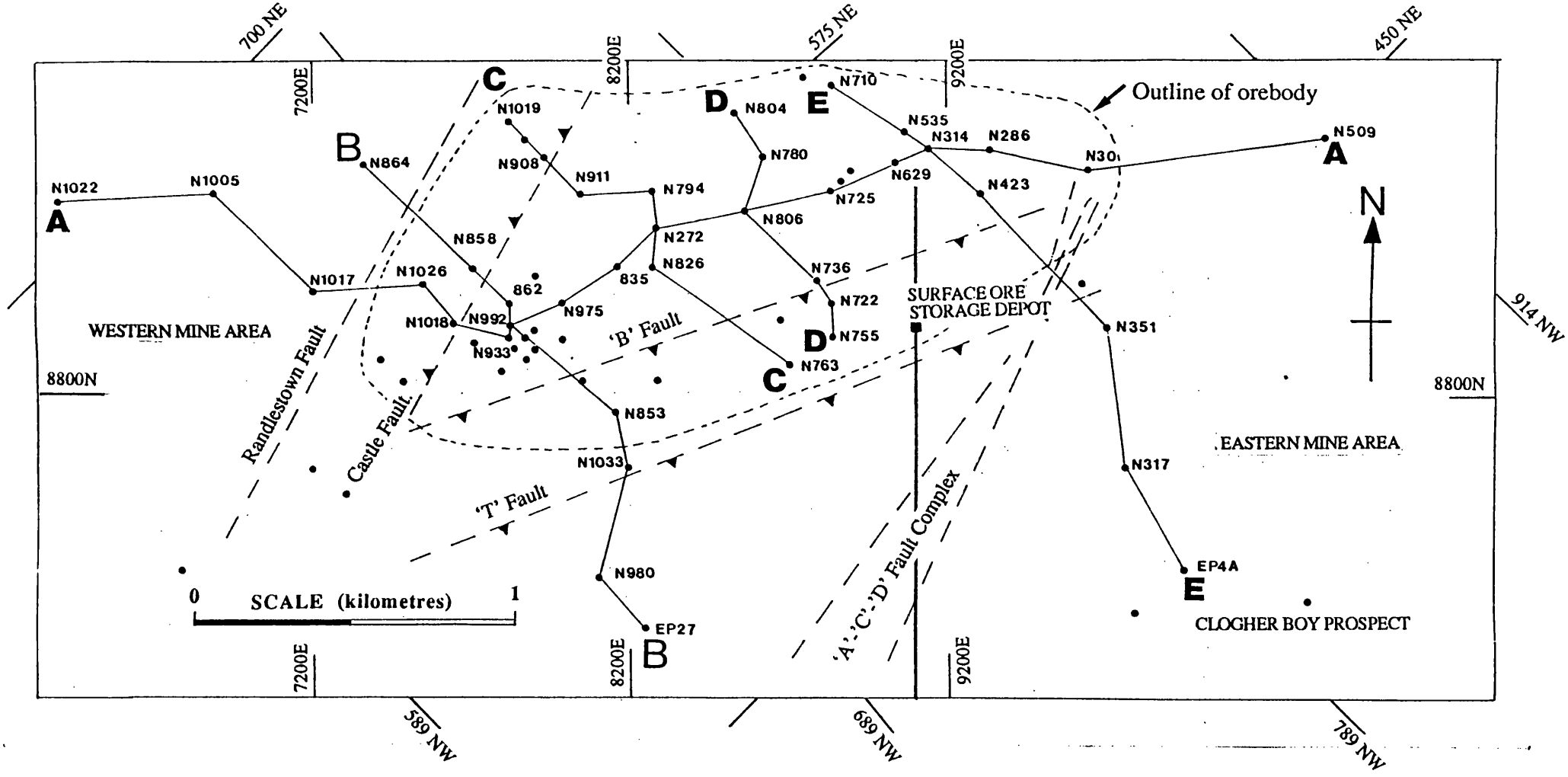

Fig. 1.12. Location of drill cores logged and cross-sections constructed through the Navan orebody. For summary of drill core data refer to Appendix 1.

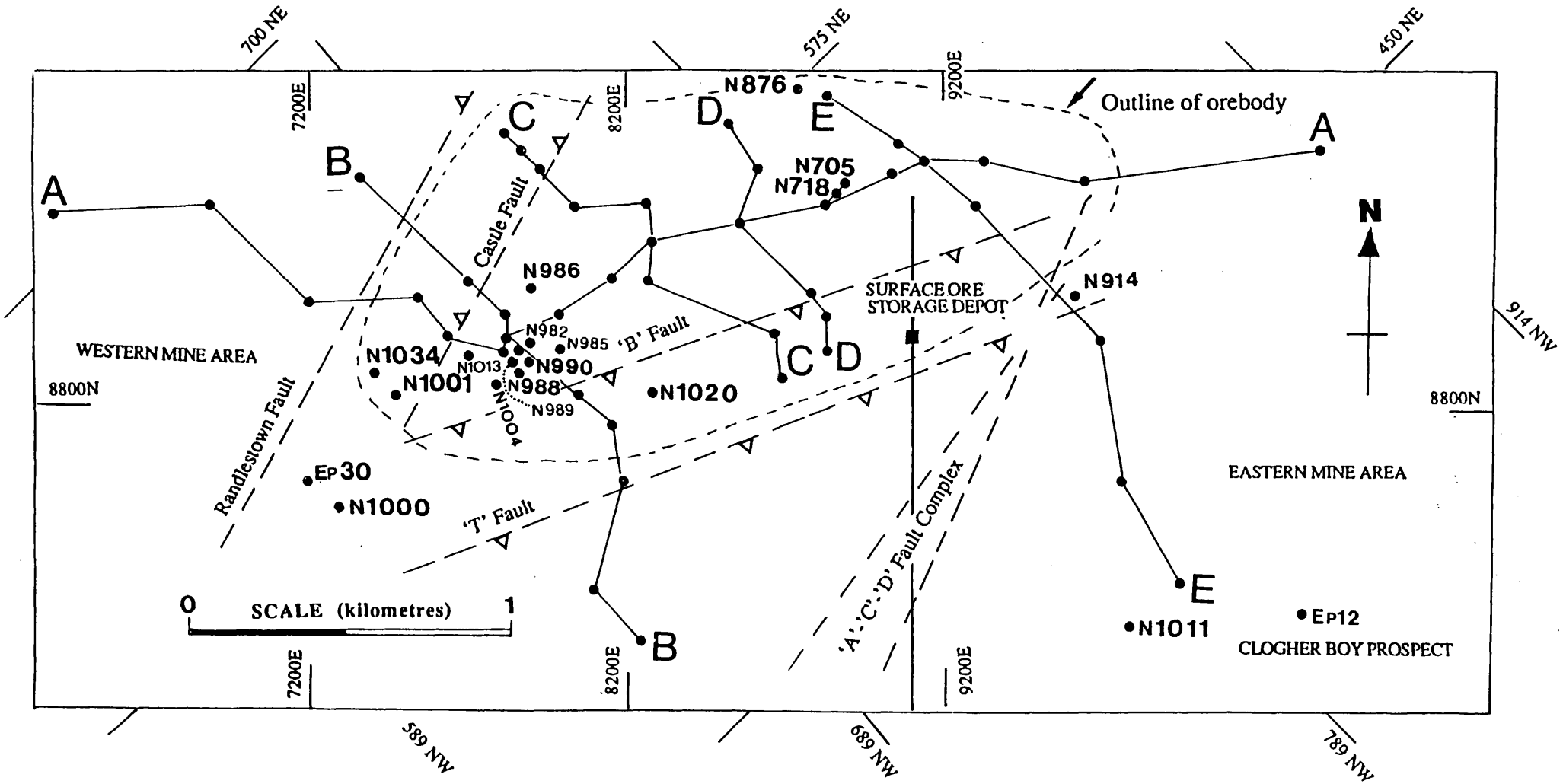

Fig. 1.12 (continued). Location of non cross-section drill cores.

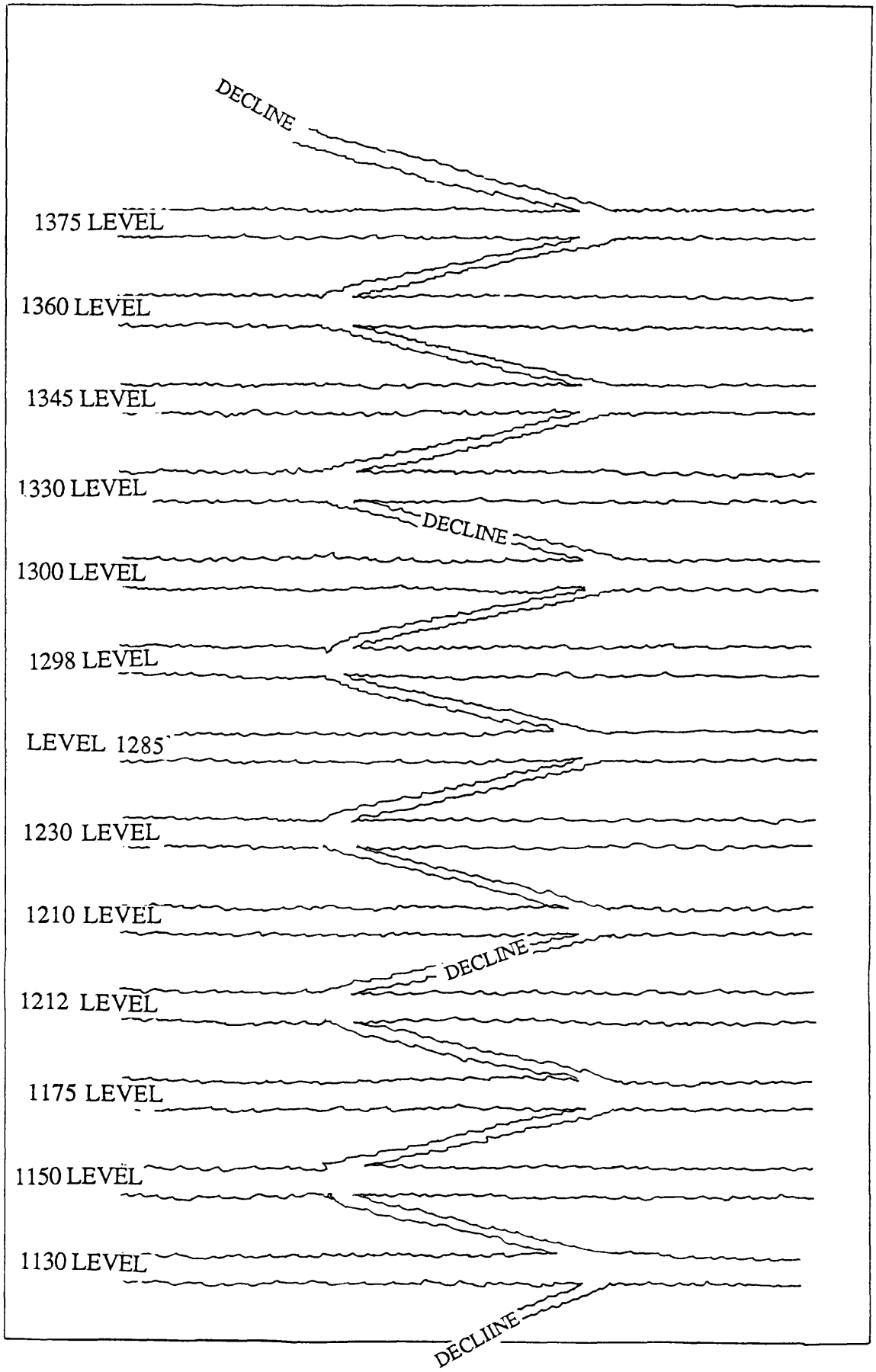

Fig. 1.13. Cartoon showing layout of mine levels visited during this study.

1.6.ii. Petrography

Over 280 large (50mm x 75mm) and small (25mm x 75mm) polished thin sections were produced from samples of drill core and from underground mine headings. Over 150 of these were stained with a mixture of Potassium Ferricyanide and Alzarian Red to elucidate the variation in iron content of both calcite and dolomite (Dickson, 1966). Petrographic textures are classified according to the scheme of Dunham (1962). In addition over 100 hand samples were cut, polished and stained. All thin sections were examined using transmitted light microscopy on a Zeiss Axioplan petrological microscope. Cold cathodoluminescence was carried out using a Technosyn 8200 Mark 2 model. This was normally operated at 20 to 25 Kv with the gun current fixed at 25 Kv using the Technosyn Autohold system. Photomicrographs were taken with a Zeiss MC100 automatic camera. The best results for cathodoluminescence were obtained using Ilford XP2 black and white film, advancing the rating to 800 ASA. Standard transmitted light micrographs were taken using Ilford FP4 film. Fluid inclusion microthermometry and analyses of oxygen and carbon stable isotopes were undertaken. The techniques and data are presented in Appendix 4.

1.7. THESIS AIMS AND THESIS STRUCTURE.

1.7.i. Aims.

The Navan ore body is a good example of an "Irish Type" Zn-Pb deposit apparently having both SEDEX and MVT type styles of mineralization (Anderson, 1990). Research on Irish ore deposits has concentrated on ore genesis and ore textures while little work has been carried out on the sedimentology and diagenetic evolution of the sediments themselves (see Fig.1.). The Navan Zn-Pb deposit has generated over 1100 closely spaced drill cores from an essentially undeformed sequence of limestones. It thus provides and ideal oppotunity to study the sedimentology and diagenetic evolution of an Irish Type ore deposit of world status.

1). The first aim of the thesis is to describe and interpret the sedimentology of the rocks below above and hosting the ore body.

2). The second aim is to describe and interpret the diagenetic evolution of the host rocks and show how this has affected the porosity and permeability of the host rocks and hence their ability is to transmit and trap ore bearing solutions.

3). Anderson (1990) demonstrated that dolomitization has affected the host rocks at Navan. The third aim of the thesis is therfore to describe and interpret the dolomitization at the Navan mine. The closely spaced nature of drill core provides a unique opportunity to characterize the geometry of dolomitization, which is currently believed to be an importatant but elusive criterion for the interpretation of dolomitzation (Hardie, 1987: Wilson *et al.* 1990).

4.) Walkden (1987 p.132) noted that the Lower Carboniferous Irish Platform was "extensive and poorly known". The fourth aim of the thesis is therefore to contribute to the current knowledge of Irish Dinantian palaeogeography and basin analysis.

1.7.ii. Thesis structure.

The first chapter has presented a description of previous sedimentological and petrographic work and an outline of the Lower Carboniferous palaeogeography and stratigraphy of Ireland. Some background information concerning Zn-Pb in the Irish Lower Carboniferous is also presented. The nature of the data base, and the equipment and methods used have also been described. Chapter 2 will consider the sedimentology and petrology of the Red Beds, Laminated Beds and the Muddy Limestones from new observations. Chapter 3 covers the sedimentology and diagenetic evolution of the Micrite Unit while Chapter 4 describes and interprets the sedimentology and petrography of the overlying grainstones. Each chapter begins with a description of the lithologies and sedimentary structures followed by interpretation. This is followed by a description of the petrography and elucidation of the diagenetic evolution. Emphasis has been placed on the Pale Beds since this part of the sequence hosts 97% of the ores and most of the dolomite at Navan.

Chapter 5 presents an analysis of the dolomitization, encompassing, geometry, petrology and origin. Chapter 6 briefly considers the sedimentology of the Shaley Pale Limestones, Argillaceous Bioclastic Limestones, Boulder Conglomerate and Upper Dark Limestones, thus completing the sedimentological envelope to the Navan ore body. Chapter 7 is a disscussion with conclusions. It briefly reviews the deposition and diagenesis of the units, relative changes in sealevel and the factors influencing dolomitization. Porosity and permeability is discussed in the context of ground preparation together with the relationship between mineralization, host limestones and dolomitization. The findings of the thesis are outlined, and discussed with respect to exploration in the Irish ore field. The final section considers further work at the Navan Mine.

Four appendices are presented. Appendix 1 catalogues the drill cores logged during this project, Appendix 2 is a brief review of carbonate diagenetic environments and their products. Appendix 3 is brief review of dolomitzation while Appendix 4 outlines the methods employed during stable isotope analysis and fluid inclusion microthermometry.

Figures in Chapters 1, 2, 6 an 7 and including those occuring in the Appendices are integrated within the text. However, figures in Chapters 3, 4, and 5 are not integrated within the text, they are placed at the back of their respective chapters and are numbered in consectutive order and described in the contents section of the thesis. The term Courceyan is equivalent to the Tournasian and is used by the authour. Similarly, the mine nomenclature, although informal, has also been adopted and used throughout this thesis.

2. INTRODUCTION.

The sequence from the Red Beds to the Laminated Beds and through to the Muddy Limestone is not mineralized. For this reason drilling commonly ceases upon entering this part of the succession, typically within the Laminated Beds. However it is neccessary to consider this succession briefly to better understand the sedimentological evolution of the overlying, ore hosting, Pale Beds.

2.1. RED BEDS.

2.1.i. Introduction.

At Navan the Red Bed facies attains a maximum thickness of 50 m (Philcox, 1984) and rests with sharp unconformity on Lower Palaeozoic rocks. The Lower Palaeozoic rocks at Navan consist of black fissile shales over 10 m thick (holes N1014, N1022) and tuffs in hole EP3, lacking significant fracture porosity. The rocks have a slightly reddened surface (hole N1014) which may extend vertically over several metres (Ashton, pers commn, 1992). The Red Beds overlie this surface and are composed of four lithologies; conglomerates, sandstones, silty mudstones and mudstones. Fining up cycles and sedimentary structures such as cross-bedding and desiccation cracks are common.

Diagenesis of the Red Beds has resulted in compaction, alteration of feldspars and mafic grains, growth of authigenic clay, quartz and feldspar, and calcite cementation. Philcox (1984) demonstrated that the cover of Red Beds is incomplete at Navan suggesting that the Lower Palaeozoic basement had a relief at the time of deposition of the unit.

2.1.ii. Description.

The conglomerates are texturally immature and clast supported with a sandy matrix. Clasts are sub-angular to rounded and attain cobble grade (Plate 2.1.A.). The sandstones have a uniform red brown colour and are texturally mature, with grain size varying from coarse to fine. The mudstones and silty mudstones are red brown and generally structureless with a friable blocky texture. Typically the mudstones and silty mudstones are interbedded with sandstones. The conglomerates and sandstones contain quartz and feldspar grains, rock fragments and mica flakes. Visual estimation of modal composition is hampered by extensive alteration of detrital grains. However, as a general guide the rock consists of approximately 50% quartz, 25% feldspar, 15% rock fragments and 10% mica, hornblende and other grains. They are therefore classified according to the scheme of Pettijohn *et al* (1972) as arkosic arenite.

A variety of quartz grains are present which may be polycrystalline, sheared polycrystalline, strained with undulose extinction, or monocrystalline grains which contain linear inclusion trails. Inclusions may be solid or liquid filled vacuoles. Solid inclusions include needle crystallites and elongate laths (silliminite ?) which displays an olive to dark green pleochroism. Fluid inclusions may be either single or two phase.

Feldspars include orthoclase, microcline and plagioclase and all display some alteration visible in drill core as white speckles on the surfaces of the sandstones. The plagioclase displays albite twinning which in some grains has been deformed while orthoclase commonly displays Carlsbad twinning. Muscovite and biotite flakes are common, while hornblende and jasper grains are rare. Lithoclasts include fragments of igneous rocks, fragments of shale, red sandstone and mudstones, and caliche fragments. Igneous fragments consist of quartz and feldspar, suggesting an acidic composition, further interpretation is hampered by the extensive alteration. The shale lithoclasts contain derived quartz grains which display authigenic overgrowths (Plate 2.1.B).

A variety of sedimentary structures are present in the Red Beds. Bedding varies from thick lamination to more massive units 50 cm thick. Cross bedding and ripples are common in the sandstones and desiccation cracks occur in the mudstones (hole N1014), the latter typically overlain and filled by sand. A channel over 4 m wide is visible in the 1360 mine level (number 3 zone access drift). This forms a trough, cutting down 3 m into horizontally bedded sandstones and mudstones and filled by conglomerate up to cobble grade (Fig. 2.1). The conglomerate passes gradationally upward into sandstone which is overlain in turn by mudstone (Plate 2.1.C.). This is only one of a number of fining up units which have been identified, the thickest of these attaining 2.5 m in hole N1014.

Caliche is very common and forms horizons up to 1.5 m. thick (hole N1022). Nine individual caliche horizons are present in hole N1022. Each is made up of irregular white glaebules and stringers of fine grained carbonate (micrite-microspar) which are more or less vertically elongate (Plate 2.1.D.). Some glaebules are greater than 3.5 cm diameter. Internally they have a clotted-mottled appearance and contain inclusions of the host sediment. Other internal features include faint concentric zonation which is locally centred upon inclusions of host sediment. The caliche may occur in mudstones, sandstones (hole N933) or conglomerates.

2.1.iii. Sedimentology.

Continental Red Bed facies occur throughout the Irish Midlands (Philcox, 1984) and elsewhere in Ireland (Phillips & Sevastopolo, 1986) and typically Devonian Old Red

PLATE 2.1. General features of the Navan Red Beds.

A. General view of polymict conglomerate, note subanglar to rounded clasts. Base of hole N915, depth interval unrecorded. Pencil for scale.

B. Derived quartz grain with authigenic overgrowth (arrow) within shale lithoclast. Note irregular outline of overgrowth. Hole N1022 at depth 610.9 m. Scale bar = 250 microns.

C. General view of fining up unit. Conglomerate (extreme right) passing up to sandstone overlain by dark thinly interbedded sandstones and silty mudstones. Note extensive white alteration of sandstone and caliche nodules (arrow). Hole N915 depth interval unrecorded. Pencil indicates scale and way up.

D. Caliche glaebules, in red mudstones, note vertical elongate nature of glaebules which are inclusion rich and display an internal concentric structure (arrow). Hole N995 at depth 581.5 m, scale in millimetres.

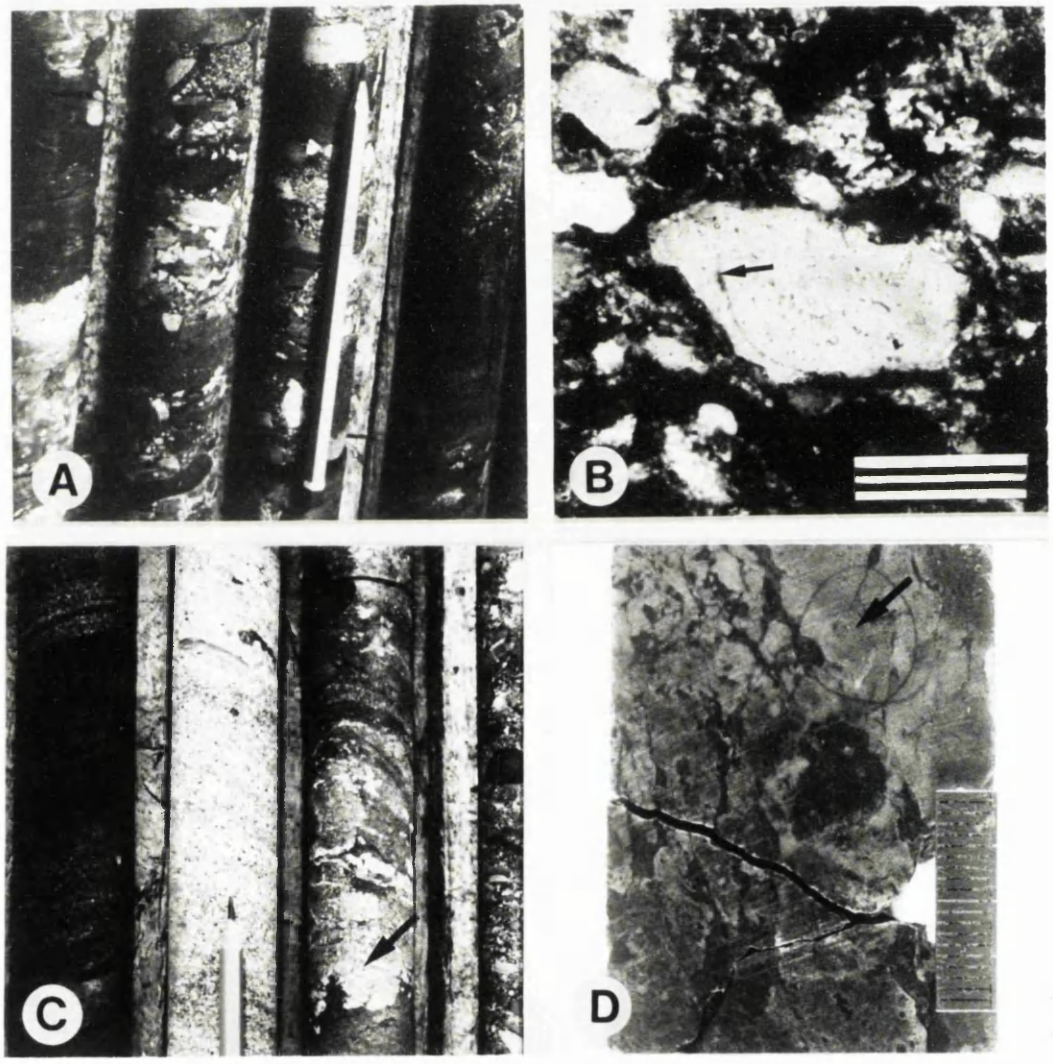
A
B
C
D

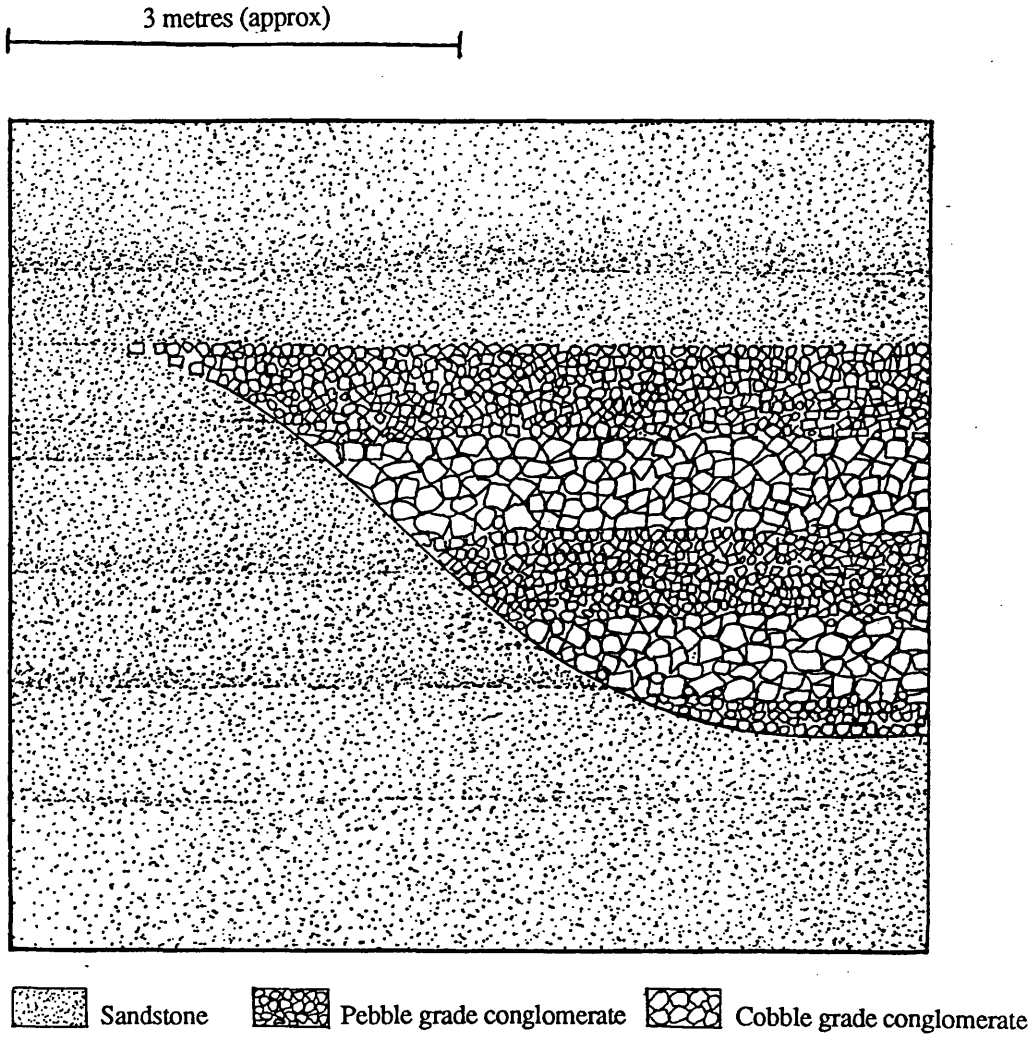

Fig. 2.1. Sketch of channel cutting horizontally bedded sandstones and filled with cobble and pebble grade conglomerates. 1360 mine level (number 3 zone access drift).

Sandstone facies (the ORS). Notable localities include Counties Tipperary and Kilkenney (Colthust, 1978), the Curlew Mountains (Simmon, 1984) and County Waterford (Ori & Penney, 1982). The facies consists of conglomerates, sandstones and mudstones arranged in fining up cycles, and has been widely interpreted as representing either fluviatile or alluvial fan deposition (Clayton *et al*, 1980)

ORS Red Bed facies also occur in Britain where they have also been interpreted as representing fluviatile and alluvial fan deposition (Anderton *et al,* 1985). In particular the ORS facies of the Welsh Borderlands consists of conglomerates, sandstones and mudstones arranged in fining up units which contain cross-bedding, desiccation cracks, and caliche, and is interpreted as representing a meandering river system (Allen, 1970). This sequence, illustrated in Fig. 2.2, is the generally accepted model which represents vertical and laterally accreting meander systems (Walker, 1984. p. 73).

The Red Beds at Navan, consisting of conglomerates, sandstones and mudstones arranged in fining up units, with associated cross-bedding, desiccation cracks, channel structures and caliche, resemble those described for the ORS of the Welsh Borders and the Irish ORS facies. It is likely, therefore, that the Red Beds at Navan also represent deposition within a meandering river system.

Modern caliche is precipitated from alkaline groundwaters (review by Collinson, 1986 p.43), probably over a period of about 10 000 years (Leeder, 1973). It occurs in semi arid climates with 100 to 150 mm of seasonal rainfall and annual temperatures of 16 to 20 ^{0}C (Anderton *et al*, 1985 p.122; Collinson, 1986 p.43) and requires long periods of non deposition or low sediment accumulation rates (Leeder, 1975). As caliche is common at Navan it is probable that sedimentation there took place under a similar climatic regime with part of the fluvial plain periodically inactive.

Grains of plagioclase, orthoclase and microcline feldspar together with quartz in sheared polycrystalline grains, polycrystalline grains, grains showing undulose extinction and monocrystalline grains and rock fragments are similar to those described for other Irish Red Bed (ORS) facies. Such clasts are widely regarded as being sourced from the Dalradian and Moinian rocks of NW Ireland (Clayton, 1980; Anderton *et al*, 1985).

2.1.2.i. Petrography.

Four thin sections from conglomerates and sandstones have been examined. Diagenetic features include compaction, dissolution of quartz, alteration of feldspar, growth of authigenic minerals, and formation of calcite cement. These and associated features are described below.

1). Compaction can be divided into mechanical and chemical. Mechanical compaction has resulted in mica flakes detaching internally along cleavage planes (Plate 2.2.A.).

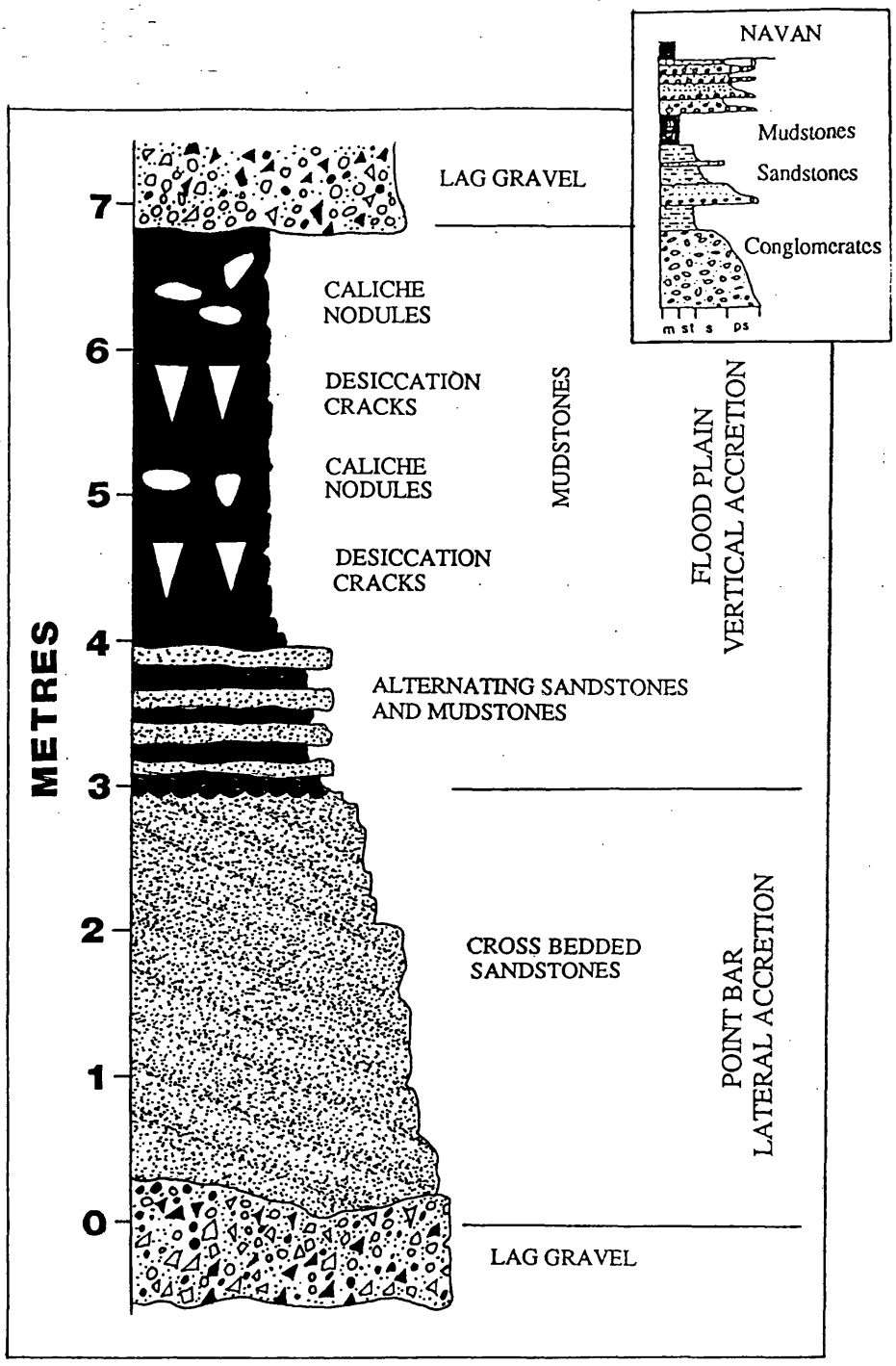

Fig. 2.2. Model for lateral and vertical accretion deposits of a meandering system showing an overall fining upwards trend. After Allen (1970) but modified from Walker (1984 p.73). Inset shows a fining up unit in the Navan Red Beds, Hole U4855 (Strogen *et al* 1990).

Chemical compaction has resulted in pressure dissolution at grain contacts, producing inter-penetration of feldpar and quartz grains and rock fragments (Plate 2.2.B.) with some grains displaying embayed margins (Plate 2.2.C.).

2). Feldspar grains and rock fragments show alteration and dissolution. The alteration is selective, occuring along twin planes, within individual compositional zones, and along surfaces of grains, imparting a ragged pitted appearance. Clays are present as products of alteration, forming 'skins' around quartz and feldspar grains, locally forming a pseudo matrix (Plate 2.2.D.).

3). Micas and other ferrous silicates have been altered to iron oxide. This has a variety of relationships, staining clays and altered feldspar grains and forming particulate coatings on surrounding grains.

4). Rare feldspar grains have developed euhedral syntaxial overgrowths (Plate 2.2.E.).

5). Authigenic quartz is rare but occurs in three forms, as syntaxial overgrowths on grains (Plate 2.2.F), as euhedral quartz crystals (Plate 2.2.G.), and as chalcedony spherules with an internal radiating structure.

6). Pyrite occurs as cubic crystals and as spheroidal clusters of crystals or framboids. Both are finely disseminated throughout the sediment.

7). Secondary pores are filled with two calcite cements, microspar of more or less even thickness and a blocky spar cement. Calcite has replaced feldspars both internally and around the margins of grains (Plate 2.2.H.). Coarse calcite also fills subvertical joints. Staining of the calcite produces a zoned mauve to red colouration demonstrating that the cement varies with respect to its iron content.

8). Reduction of iron oxides has occurred along the contact between the Red Beds and the overlying Laminated Beds. This has produced a bleached surface which extends downward along jointing (1345 level, 347S stope) and along bedding (hole N1014).

9). Brittle fracture has resulted in sub vertical jointing.

2.1.2.ii. Petrographic Interpretation.

Diagenesis began syn-depositionally, with precipitation of caliche. Mechanical infiltration of clays followed, culminating in the development of clay skins with individual platelets orientated parallel to the grain surface. Mechanical compaction followed, resulting in grain fracture and distortion of mica flakes. Compaction continued during burial, culminating in pressure dissolution and suturing of grain contacts. Suturing of grain contacts suggests lack of early cementation, and is generally believed to take place before significant cementation (Harwood, 1989 p.127).

PLATE. 2.2.Photomicrographs (plane light) of Navan Red Bed diagenetic features.

A. Mica flake bent and wrapped around quartz grain as a result of mechanical compaction. Note distortion of clevage planes (arrow) and alteration of mica to iron minerals. Hole N1024 depth 609.0 m. Scale bar = 250 microns.

B. Sutured grain contacts as a result of chemical compaction (arrow). Hole N1022 depth 609.0 m. Sample dye impregnated. Scale bar = 100 microns.

C. Quartz grain with embayed margins resulting from dissolution. Hole N1022 depth 610.9 m. Dye impregnated. Scale bar = microns.

D. General view of clay skins (arrow) developed around grains, note also diagenetic clay matrix. Hole N1022 depth 610.9 m. Scale bar = 250 microns.

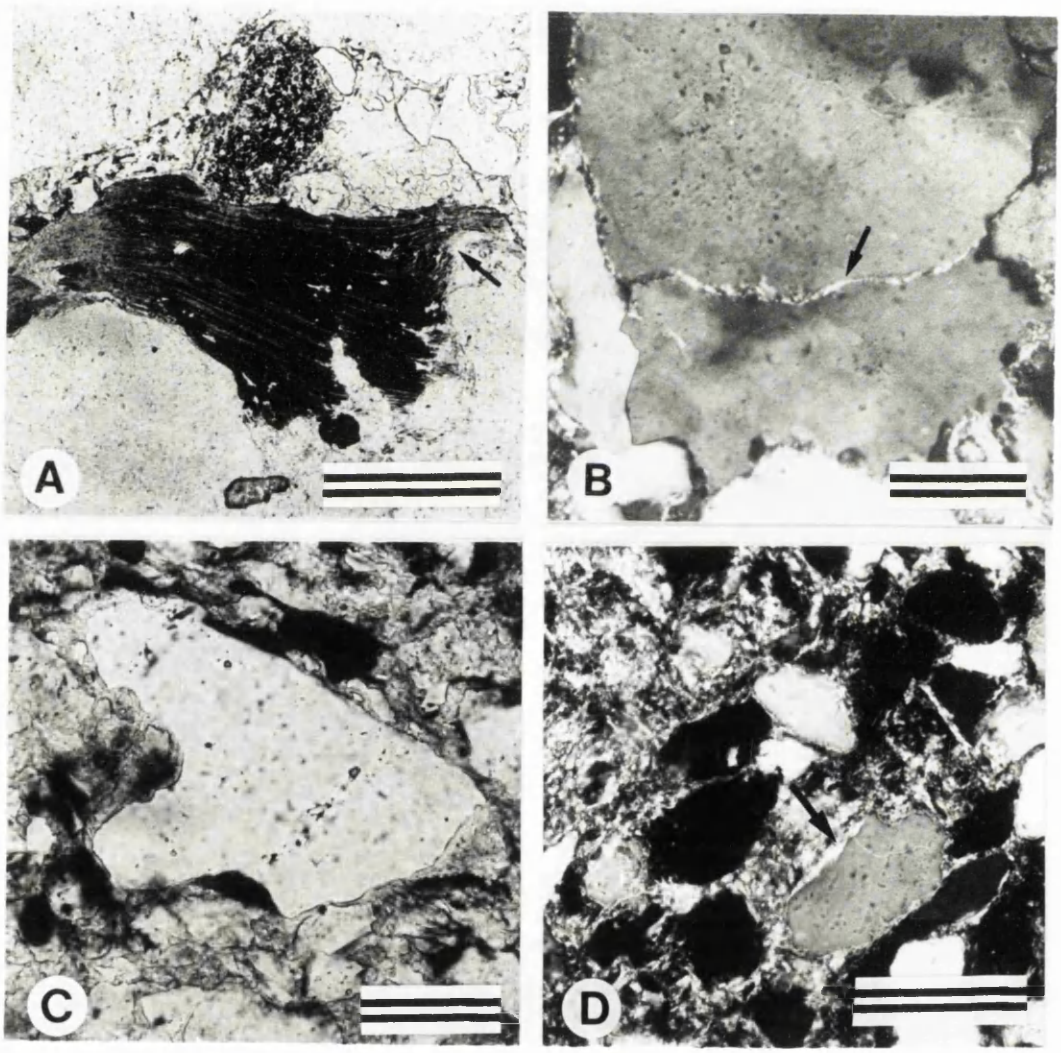
A
B
C
D

PLATE 2.2 (Continued).

E. Euhedral overgrowth (o) developed on altered feldspar grain (F). Note fresh appearence of overgrowth and overlying poikilotopic calcite cement (c). Hole N1022 at depth 610.9 m. Scale bar =250 microns.

F. Authigenic quartz overgrowth (o), note patches of clay occuring along primary grain interface and planar overgrowth crystal face (arrow). Hole N1022 at depth 610.9 m. Scale bar = 100 microns.

G. Euhedral authigenic quartz crystal. Faint inclusion trails (arrows) parallel to crystal margins suggest that this could be an authigenic overgrowth on a clastic grain. Hole N1022 at depth 610.9 m.Scale bar = 250 microns.

H. Altered and dissolved rock fragment filled by calcite (c). Calcite contains 'floating' quartz grains (arrows) displaying undulose extinction. Hole N1022 at depth 610.9 m. Scale bar = 100 microns.

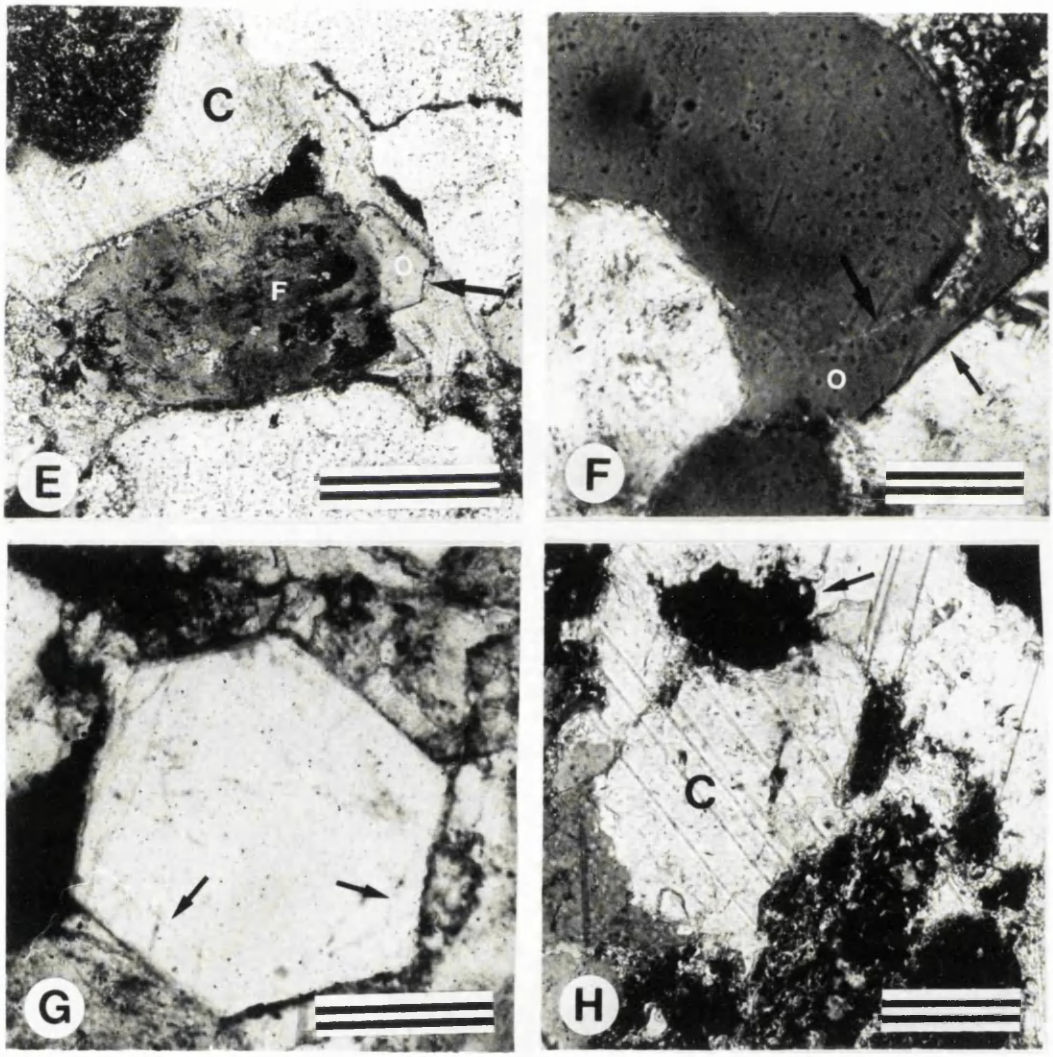
C
F
O
E
O
F
G
C
H

Feldspar grains displaying sutured contacts have a corroded appearance. This suggests that alteration and dissolution of feldspars and growth of the authigenic clays followed compaction, culminating in the formation of a diagenetic clay matrix. Associated with this period are corroded quartz grains with embayed margins filled by clays. The alteration and dissolution of feldspar, growth of authigenic clay and corrosion of quartz most likely followed the same pathway as in other Red Beds, beginning early in the near surface environment and continuing during deeper burial (Walker *et al.* 1978). This alteration resulted from reaction with a variety of fluids which may have included meteoric water, organic acids derived from clay mineral transformations (illite to smectite) or compactional waters containing CO_2 (Bjørlykke, 1985).

Alteration of mica flakes also followed mechanical compaction, beginning along cleavage planes. The staining of adjacent clays and altered feldspars by iron oxides suggests that alteration of ferromagnesian minerals occured during or shortly after the growth of clays. The oxidised Fe^{3+} released from ferrous silicates contributed to the red colour of the sediment. This compares with the observations of Walker (1967) who described this mechanism for the development of red colouration of sediment occurring in moist tropical climates.

Pyrite formation requires a source of decomposable organic matter, reactive detrital iron minerals and anoxic pore waters where anaerobic bacteria can reduce dissloved sulphate (Berner, 1984). The morphology of pyrite has been related to the timing of its formation (Raiswell, 1982), with framboidal pyrite typically forming early via a monosulphide precursor in the near surface environment, while granular euhedral pyrite forms later, relying on import of iron from adjacent areas. This is consistent with framboids in the Red Beds which occur along grain surfaces, suggesting early formation, while euhedral pyrite is associated with clays and altered feldspar grains, suggesting later formation.

Syntaxial feldspar overgrowths are euhedral but have grown upon altered feldspar grains suggesting that authigenic feldspar postdates feldspar alteration. The preservation of euhedral outlines of authigenic quartz crystals and overgrowths demonstrates that these post date dissolution of quartz grains. Highly birefringent minerals occuring along the interfaces between quartz overgrowths and host grains could be either clay skins or authigenic clay. This suggests that the youngest age for the authigenic quartz is post clay formation. The Ca^{2+}, Mg^{2+}, K^{+}, Al^{2+}, Na^{++} and Si^{2+} required for quartz and feldspar overgrowth cements and authigenic minerals may have been released during clay mineral transformations, by alteration and dissolution of detrital quartz and feldspar and by pressure dissolution (McBride, 1989).

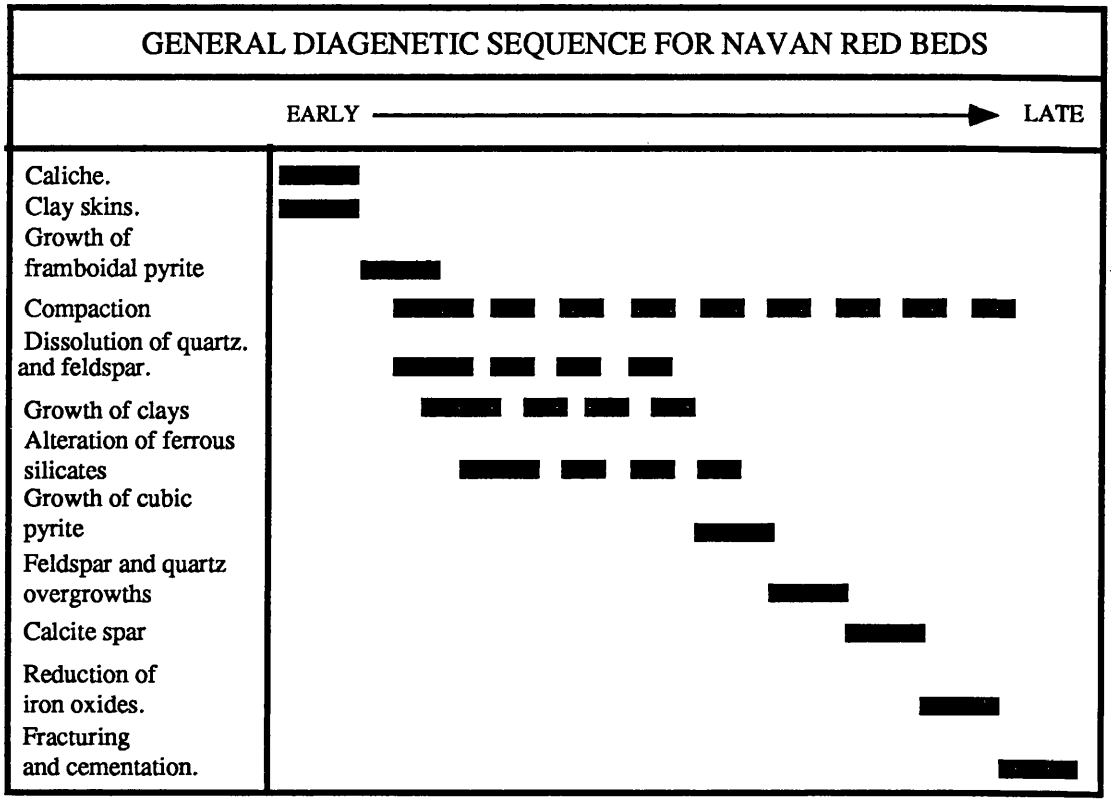

Fig. 2.3. General paragenetic sequence for the Navan Red Beds...

The earliest (non caliche) calcite microspar cement coats the fractured surfaces of grains and is therfore post mechanical compaction. Blocky calcite spar cement overlying this contains inclusions of clays. The "clast-shaped" outline of many areas of cement, and the occurrence of "floating" strained quartz grains within cement, demonstrates that some of the calcite fills pores within altered feldspars and rock fragments. It therefore post dates these alteration and dissolution events. In addition, it overlies overgrowth cements and, when in contact with either quartz or feldspar has replaced them. The replacement of silica by carbonate has been attributed to reaction with an alkaline fluid (Walker, 1962) and is discussed in Appendix 2. The youngest diagenetic events include reduction and removal of iron oxides, brittle fracture and associated fracture fill cementation with calcite.The diagenetic sequence is summarized in Fig. 2.3.

2.2. LAMINATED BEDS.

2.2.1.Introduction.

The Laminated Beds rest conformably on the Red Beds (Plate. 2.3.A.) and have an approximate thickness of 35 m throughout the mine area (Ashton *et al*, 1986). They have been subdivided by Philcox (1984) into six informal units, in ascending stratigraphic order, these are the 'C-G', 'C-F', 'C-E', 'C-D', 'C-C' and 'C-B' units (Fig. 2.4.). These units consist of silty shales, interbedded sandstones and silty shales, sandstones, interbedded calcite mudstones and calcareous siltstones and bioclast grainstones. Green clays, algal laminated calcite mudstones, evaporites and oncolites are also present. These lithologies will be described before considering the general sequence.

2.2.2. DESCRIPTION OF LITHOLOGIES.

2.2.2.i. Silty Shales.

These are generally dark with a maximum thickness of 7 m in hole N763 (Plate 2.3.B) where they form the base of the 'C-G' Unit. They form beds 1 to 2 m thick in holes N971 and N975 higher in the succession, particularly in the 'C-E' and 'C-C' Units. Occasional dark green shales up to 25 cm thick (hole U6230) are present within the silty shales, together with thin light grey very fine grained cross-laminated sandstones and bioclast grainstones. Scattered throughout the shales are solitary bioclasts including crinoid ossicles, shell fragments and fenestrate bryozoans. A few small marcasite nodules are also present. Burrowing is common, individual burrows are elliptical in cross-section, sand filled and contain spreite (hole EP 26). Locally burrowed horizons are 50 cm thick.

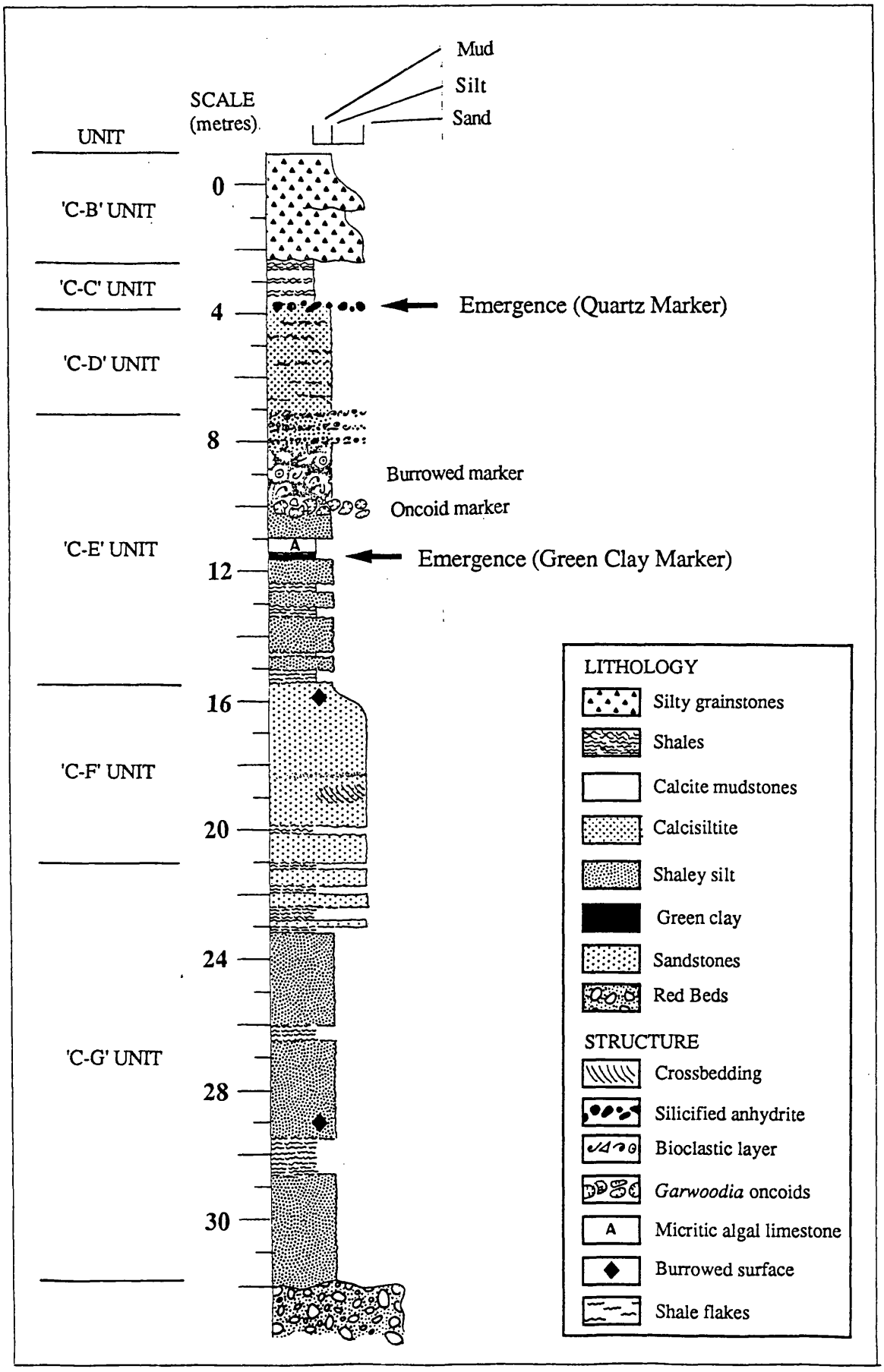

Fig. 2.4. Summary log of the Laminated Beds sequence showing lithological subdivisions of Philcox (1984). Log based on hole U6230, the Navan mine standard 'type section'.

2.2.2.ii. Interbedded sandstones and silty shales.

Interbedded sandstones and silty shales attain a maximum thickness of 7 m where they form the top of the 'C-G' Unit. The sandstones are light grey and generally thin, averaging 1 to 2 cm although beds up to 10 cm thick appear in hole N1034 and 30 cm thick in hole EP27. The shales may be up to 30 cm thick. The upper and lower contacts between sandstones and shales may be either sharp or gradational. Load / scour structures commonly occur along the bases of the sandstones. The layering of the thin bedding is generally planar but some can be classified as lenticular according to the scheme of Reineck & Wunderlich (1968). Most sandstone beds display internal cross laminatation. Burrowed horizons are present, some are over 30 cm thick. Individual burrows are elliptical in cross-section with a maximum diameter of 1.5 cm and are sand filled (Plate 2.3.C.). Bromley (1990), has disscussed the problems of identifiing trace fossils in core. Using Bromley's plates as standards, these burrows most likely belong to the *Skolithos* ichnofacies of Seilacher (1967) variety *Thalassinoides*. The facies relationship between the interbedded sandstones and silty shales is summarized in Fig. 2.5.

2.2.2.iii. Sandstones.

Two sandstone units are present, the lower forming the 'C-F' Unit, and the upper, part of the 'C-E' Unit . Both are generally light grey and fine grained with occasional coarse sand layers, mud flakes, micaceous layers and silty partings. Thin black shales are also present in the 'C-F' Sandstone in hole EP27. The lower ('C-F') sandstone varies from 4 m thick in hole N1014 to 70 cm thick in hole N725 which suggests a lenticular geometry, also noted by Anderson (1990). In hole U6230 the upper 30 cm of the same sandstone is dark green.

The main features of the 'C-F' Sandstone are summarised in Fig. 2.6.B. Beds are typically 50 cm thick. Trough cross-lamination is common (hole N974) and planar low angle cross bedding with foresets dipping 5^0 to 10^0 also occurs (Plate 2.3.D). The base of the sandstone observed in the 1150 mine level (block 19, 1 zone) contains asymmetrical ripples of 75 mm wavelength and 15 mm amplitude. The main features of the upper 'C-E' sandstone are shown in Fig 2.6.A. This sandstone is not extensive and is only present locally (Ashton, pers. commn.1992). The minimum thickness is 70 cm in hole N971 and is up to 5 m thick in hole N975, again suggesting a lenticular geometry. It contains elongate lithoclasts of sandstone up to 2 cm long (hole N975). Planar and trough cross laminae are common (Plate 2.3.E.). Troughs may be either symmetrical or asymmetrical, with an amplitude up to 3 cm (hole N975). Foresets contain thin silty partings. Trough cross-lamination and planar lamination alternate in hole N975, with cross-laminated sections up to 2m thick. Both sandstones have

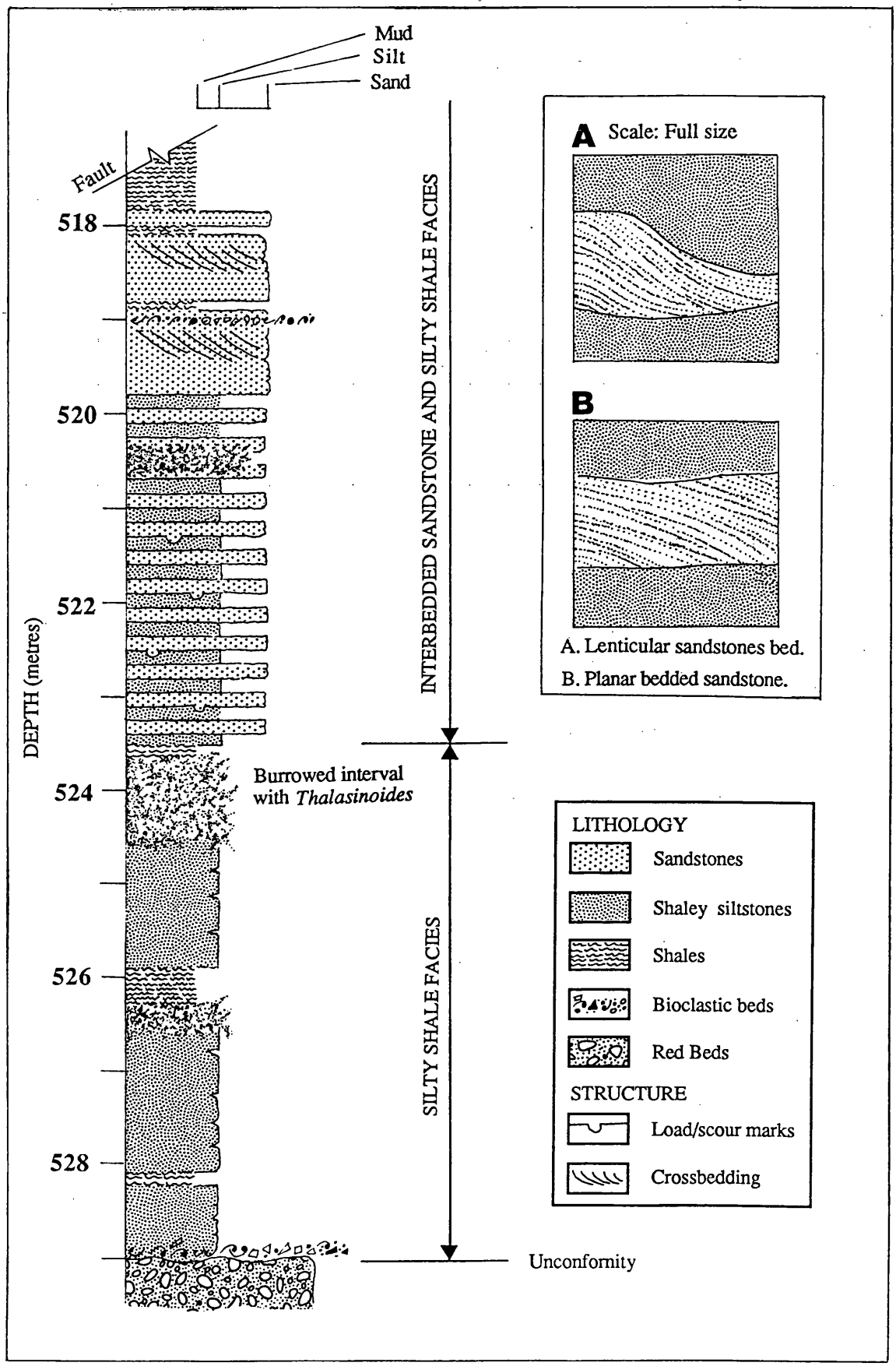

Fig.2.5. Log showing relationship between the silty shales and interbedded sandstones and silty shales, the 'C-G' Unit, hole N978. Inset, detail of sandstone beds.

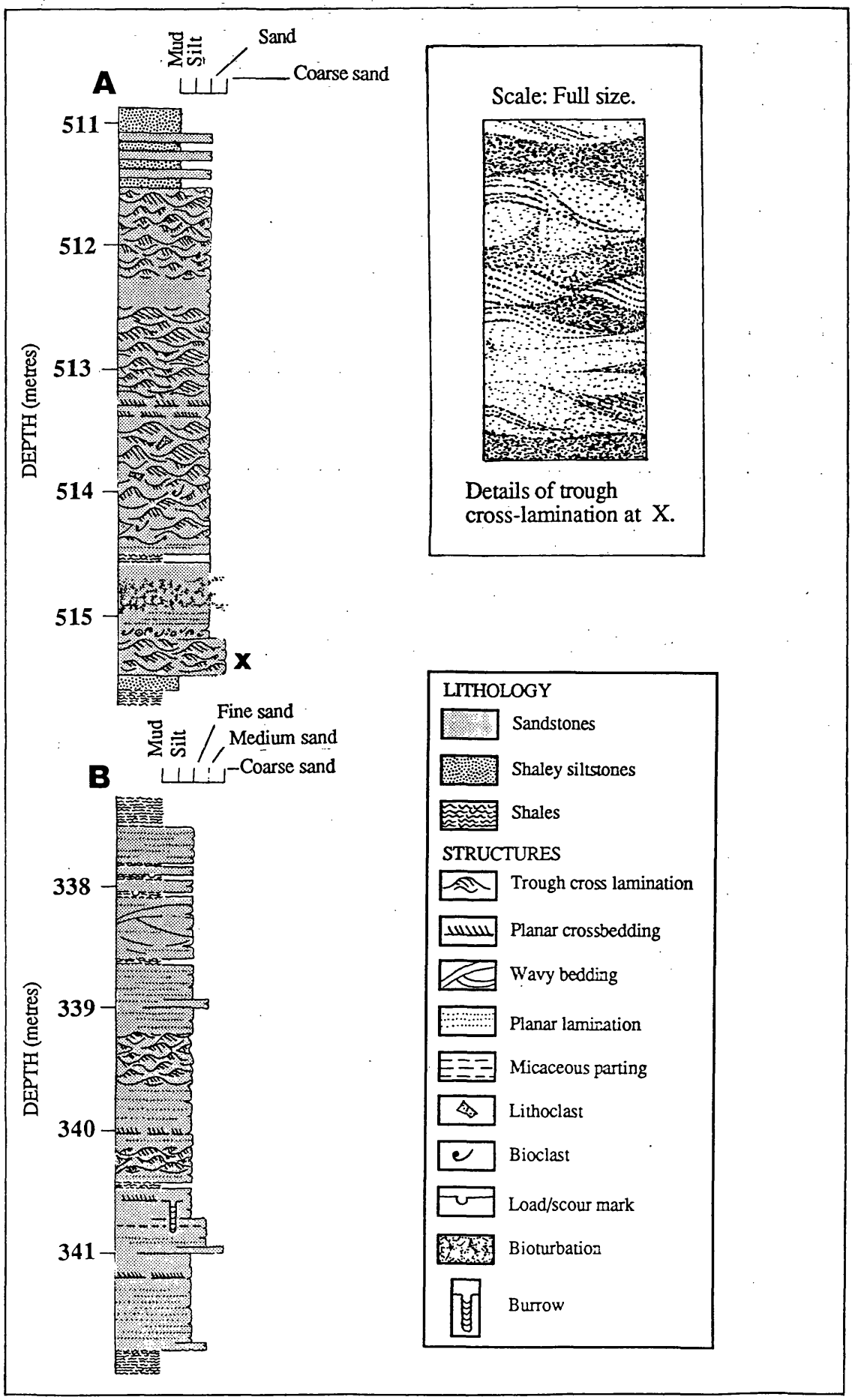

Fig. 2.6. 'A' Trough cross-laminated sandstone occuring within the 'C-E' Unit, hole N975. Inset, detail of trough cross-lamination at depth 515.8 m. 'B' the'C-F' sandstone, hole N725.

PLATE. 2.3. Sedimentological features of the Laminated Beds.

A. Contact between Red Beds and Laminated beds. Note clasts of Red Bed Conglomerate in the Laminated Beds. Sample from underground production drill core, hole U6230. Scale in mm.

B. Vertical facies sequence (a) silty shale, (b) interbedded sandstones and silty shales, (c) sandstone (the C-F Unit). Hole EP. 26, at depth interval 839.0 m to 869.0 m. Pencil for scale and arrow points to way up.

C. Detail of interbedded sandstone and silty shale passing up into sandstone of the 'C-F' Unit, note elliptical burrows (B). Scale in centimetres.

D. Cross-bedding in 'C-F' Sandstone Unit, perhaps reflecting wedge shaped cosets. Hole N1034 at depth 691.5 m. Pencil for scale points to way up.

E. Trough cross-lamination in 'C-E' Unit sandstone at depth 516.0 m, scale in centimetres.

F. Interbedded calcareous siltstones and silty shales (A) hole N864 at depth 552.5 m. (B) calcareous siltstones, note bedding parallel mudflakes, (M) = massive anhydrite bed note truncation surface (arrow). Pencil for scale points to 'way up'.

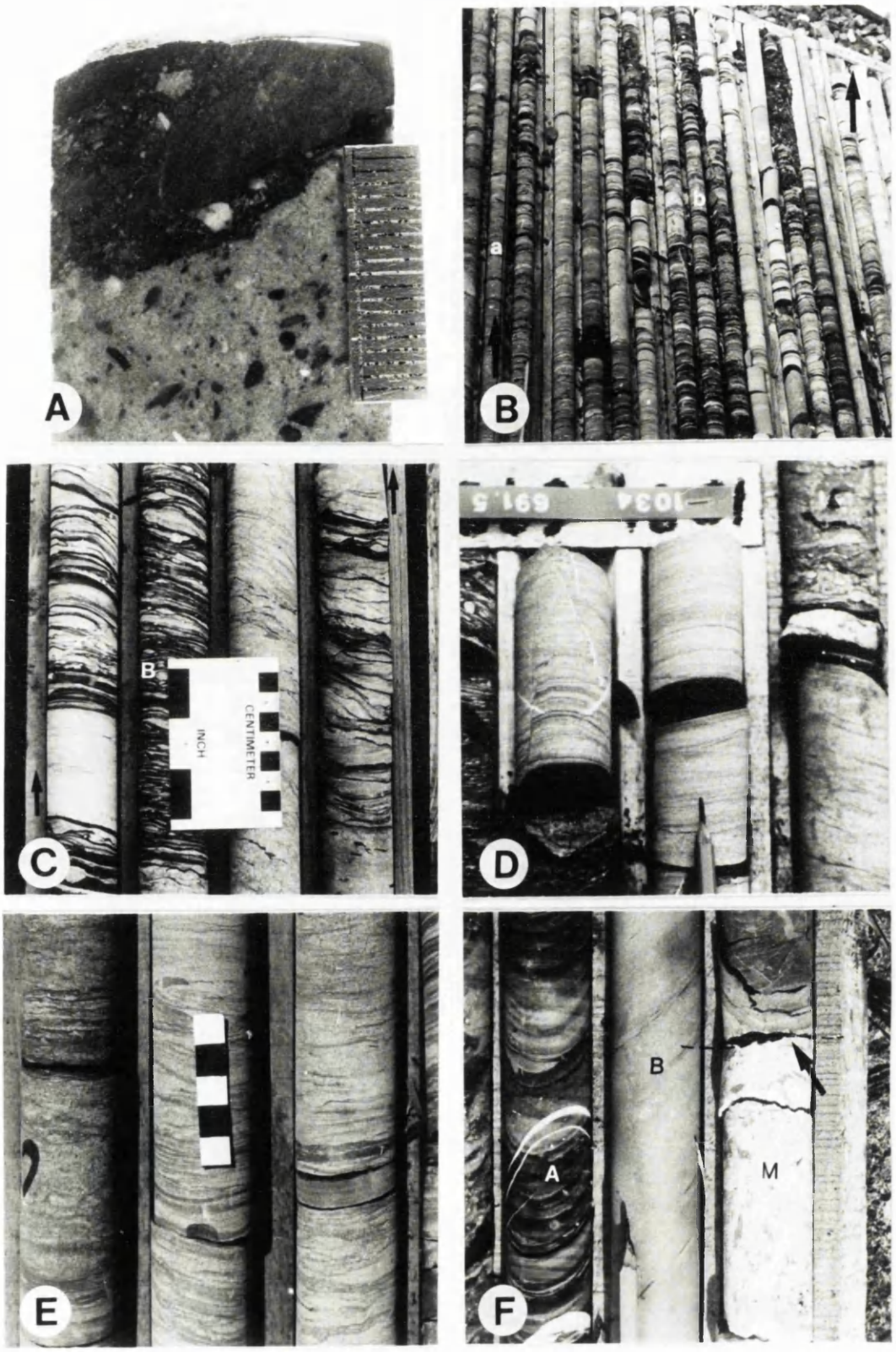
A
B
a
b
C
B
INCH
CENTIMETER
D
E
F
B
A
M

been burrowed with individual burrows arranged horizontally and vertically and containing spreite. Burrows are typically 6 mm diameter in hole N725 at depth 341.0 m.

2.2.2.iv. Interbedded calcareous siltstone and silty shales.

Interbedded calcareous siltstones and silty shales occuring in the 'C-E' Unit have an aggregate thickness 1 to 2 m and consist of dark fissile shales and lighter coloured calcareous siltstones (Plate 2.3.F). Siltstones are thin, averaging 1 to 2 cm containing millimetre scale lamination. Burrows are prominent and disrupt bedding. One unit, 50 cm thick, displays a chaotic ichnofabric and has proven to be a useful marker. Individual burrows within this marker (Plate 2.3.G) can be recognised, these are horizontal and "tear" shaped in cross-section and contain spreite. Using the criteria of Bromley (1990) they are most likely *Rhizocorallium.*

2.2.2.v. Plant material.

Dark carbonaceous plant fossils occur in shaley siltstones in the vicinity of the 'C-F' Sandstone. The plant fossils are fragmental and have no preferred orientation. Stems are over 3 cm wide and are over 50 cm in length and often display branches, internally they display a rib type structure which extends along their entire length (Plate 2.3.H.). These plant fossils are believed to represent ferns (Burton, pers commn, 1992).

2.2.2.vi. Green Clay.

A friable waxy green illitic clay, present near the top of the 'C-E' Unit, has proven to be a useful marker. This reaches a maximum thickness of 10 cm in hole U6230 (Plate 2.3.I.). It contains randomly distributed silt grade siliciclastic grains which include angular and millet seed quartz grains, monocrystalline, polycrystalline and polycrystalline sheared quartz. Plagioclase and microcline feldspar grains and mica also occur. Some grains form circular clusters which resemble burrow linings.

2.2.2.vii. Algal Laminated Limestones.

This facies is approximately 35 cm thick in hole N985 and overlies the Green Clay member of the 'C-E' Unit. The algal laminae are 1 to 2 mm thick (Plate 2.3.J.) and consist of calcite mudstone containing a network of radiating tubules less than 100 microns in diameter (Plate 2.3.K.), and irregular voids. The laminae contain rectangular millimetre scale voids now filled by calcite spar. These are interpreted as moulds of evaporite (gypsum ?) crystals now filled with calcite. Interbedded with and overlying the algal laminae are layers consisting of individual silt grade dolomite crystals and siliciclastic silt. The algal laminae are cut by fissures which extend vertically downwards

from their surfaces and may represent desiccation cracks, locally they have been buckled into domal structures. Associated with these laminae are 1 to 2 mm thick dark siliciclastic-carbonate couplets. The carbonate consists of calcite mudstone, lithoclasts of calcite mudstone and flakes of algal laminae, while the very finely laminated siliciclastic layers contain bedding parallel mica flakes and disseminated pyrite framboids.

2.2.2.viii. Oncolites.

A layer of oncolites up to 30 cm thick in hole N864 near the top of the 'C-E' Unit has proven to be a useful marker (Plate 2.3.L.). Individual oncoids are lenticular in section with a maximum thickness of 8 mm and a maximum length of 2 to 3 cm (hole N746). Each contains a nucleus consisting of a lithoclast or shell fragment, the shape of the nucleus determining the shape of the oncoid so that some are elongate and others spherical. The nucleus is surrounded by up to eight concentric layers of more or less equal thickness. Within these layers and orientated normal to them are branching tubes less than 100 microns in diameter and irregular voids (growth cavities?). Both cavities and tubules are lined with microspar overlain by a coarse equant spar which occludes any remaining porosity (Plate 2.3.M).

In some layers tubules are dense while in others they are scarce. This variation in structure resembles the porostrome texture described by Monty (1981) and believed to have been produced by blue green algae (Cyanobacteria). Similar oncoids have been described from the peritidal Lower Carboniferous Llanelly Formation of South Wales where they have been attributed to the genus *Garwoodia* (Wright, 1983). Associated with algal layers is a fauna consisting of ostracods, forams, and thin shelled brachiopods. The facies association of Green Clay, algal laminated limestone, and oncolites is summarized in Fig. 2.7.

2.2.2.ix. Calcareous Siltstones.

This distinctive lithology forms the entire 3 m thick 'C-D' Unit. It has a uniform light grey colour and beds are thinly laminated. Dark silty partings and thin shale partings up to 2 cm. thick are present, with bedding parallel mud wisps up to 3 cm long (Plate. 2.3.F.). Within the upper part of the calcareous siltstones is a distinctive white to light grey coarse silica layer 15 cm thick. This occurs as a massive layer (hole N864), as discreet nodules (hole EP27), and as finely disseminated crystals. The nodules are irregular and up to 6 cm diameter, locally coalescing and distorting against each other to from a nodular mosaic separated by inclusions of host sediment (Plate 2.3.N.). The nodular layer has been sharply truncated by an erosion surface with a few centimetres of relief (refer Plate 2.3.F.). Blue-grey finely crystalline anhydrite is present in some

PLATE 2.3 (continued)

G. Burrowed marker, *Rhizocorallium* burrow indicated by arrow. Pencil for scale.

H. Fossil ferns; note internal structure 1285 mine level magazine. Scale in millimetres.

I Green clay marker (c) hole N975 at depth 508.6 m, also detail of trough cross-lamination (T) within 'C-E' sandstone. Scale in centimetres.

J. Algal lamination in micritic limestones occuring in the 'C-E' Unit. Hole N975 at depth 509.8 m. Scale in millimetres.

K. Photomicrograph (plane light) of algal lamination. Note radiating tubules of former cyanobacteria and silt grade dolomite, quartz and feldspar between laminae. Hole N975 at depth 580.4 m. Inset shows evaporite (gypsum ?) mold now filled by calcite. Scale bar = 1 mm.

L. Oncolite marker, pencil for scale points to oncolite

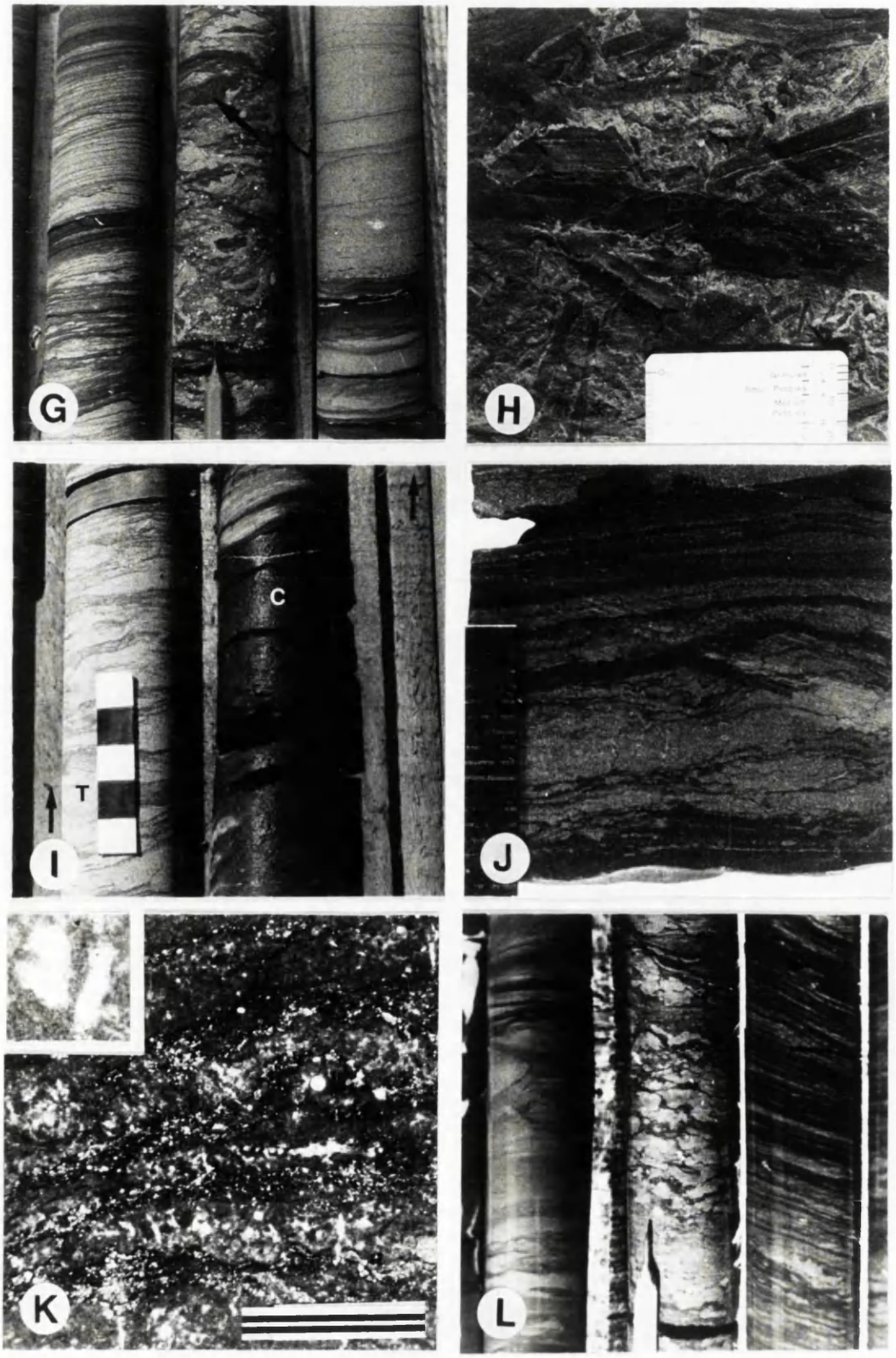
G
H
C
T
I
J
K
L

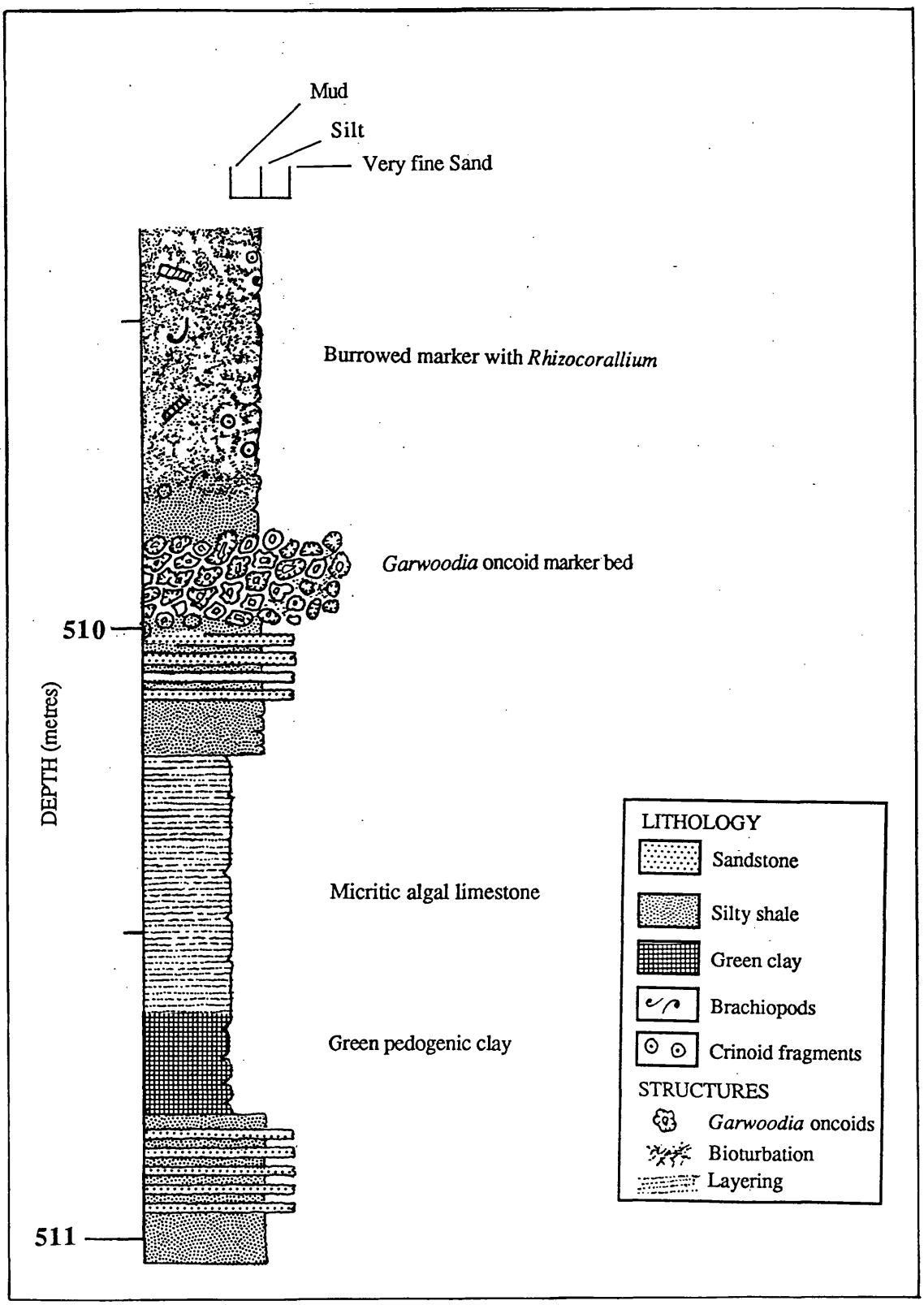

Fig. 2.7. Log showing relationship between green clay, micritic algal laminated limestone and *Garwoodia* oncoid marker bed, hole N985.

nodules. In others it has been dissolved to leave nodule shaped moulds which remain open. However most anhydrite has been replaced by "cauliflower chalcedony" (Ashton *et al,* 1986). This silicified evaporite layer is known informally as the **Quartz Marker.**

2.2.2.x. Calcite mudstones and calcareous siltstones.

This facies forms the 'C-C' unit and is 2.5 m thick in hole N971. It consists of dark calcareous siltstones which contain irregular beds of calcite mudstone (Plate. 2.3.O). Both lithologies form beds up to 30 cm thick but the calcite mudstones are typically only 10 cm thick. Contacts are generally sharp. Fenestrae were recorded in these mudstones in holes N971, at depth 457.0 m and N725, at depth 327.0 m. and in hole N866. Thin beds of silicified evaporite have also been noted from this facies, 1 to 2 m above the base (Ashton pers commn, 1992).

2.2.2.xi. Bioclast grainstones.

Bioclast grainstones form the 'C-B' Unit and are up to 4 m thick in hole N718. They are of fine to medium sand grade but also contain coarser bioclastic layers up to 40 cm thick and dark silty layers. Sedimentary structures include graded bedding, thin bedding and burrows (Fig.2.8.). Burrowed units are over 50 cm thick and occur in hole N974. Thin bioclast packstones also occur within the silty shale facies of the 'C-G' and 'C-E' Units (Plate 2.3.P.). These are laminated and up to 20 cm thick in hole N975 at depth 516.0 m. They contain crinoid ossicles, echinoid spines and plates with mud filled stereome, impuncate and punctate brachiopod shell fragments, brachiopod spines, bryozoan, ostracod, and oncoid fragments. Siliciclastic grains form 25% of the sediment and include sheared and polycrystalline quartz, plagioclase and microcline, muscovite and rock fragment. Both feldspars display some alteration.

2.2.3. VERTICAL FACIES SEQUENCE OF THE LAMINATED BEDS.

The overall trend in this sequence is towards a gradual disappearance of siliciclastic sand. Above the green shale the sequence consists of algal laminated limestone, interbedded calcite mudstones and silty shales, calcareous siltstones, bioclast packstones and silty shales together with silicified evaporites and oncolites. The lithological sequence and its relationship to the stratigraphic units of Philcox (1984) are described below and summarized in Fig. 2.4. The sequence begins with silty shales which conformably overlie Red Bed facies in the 1345 level 347S. These pass upwards into interbedded sandstone and silty shale facies and together these constitute the 'C-G' Unit. A sandstone, the 'C-F' Unit, above, is followed by 1 to 2 m of silty shale facies containing thin bioclast packstones. A second sandstone with extensive trough cross lamination

PLATE 2.3 (continued).

M. *Garwoodia* oncoid showing concentric growth and radiating spar filled tubes at depth. Hole N1019 at depth 580.4m.Scale bar = 1 mm.

N. Detail of anhydrite showing nodular mosaic texture. Hole EP 26 at depth 834.7 m. Scale in millimetres

O. Interbedded silty shale and calcite mudstones, pencil for scale, hole N1034 at depth 679.2 m.

P. Bioclast grainstone in 'C-E' Unit, hole N975 at depth 516.0 m. Scale in centimetres


M

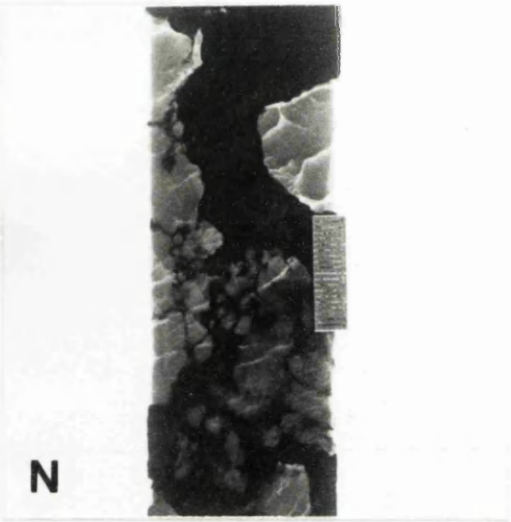
N

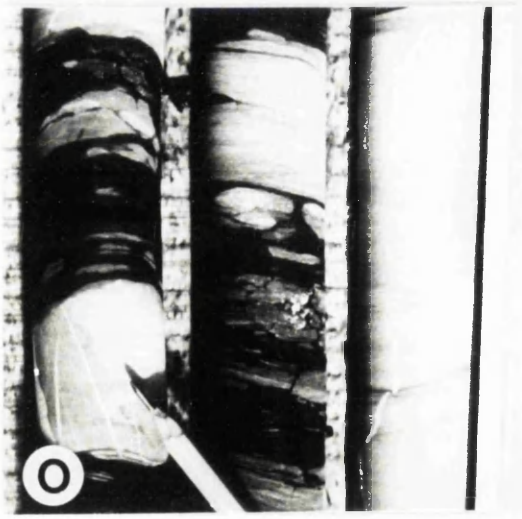
O

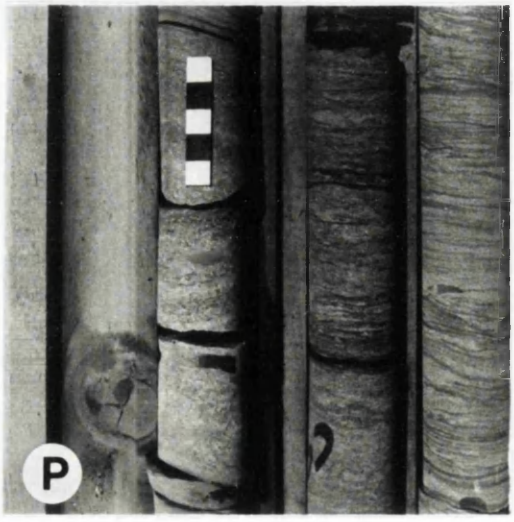
P

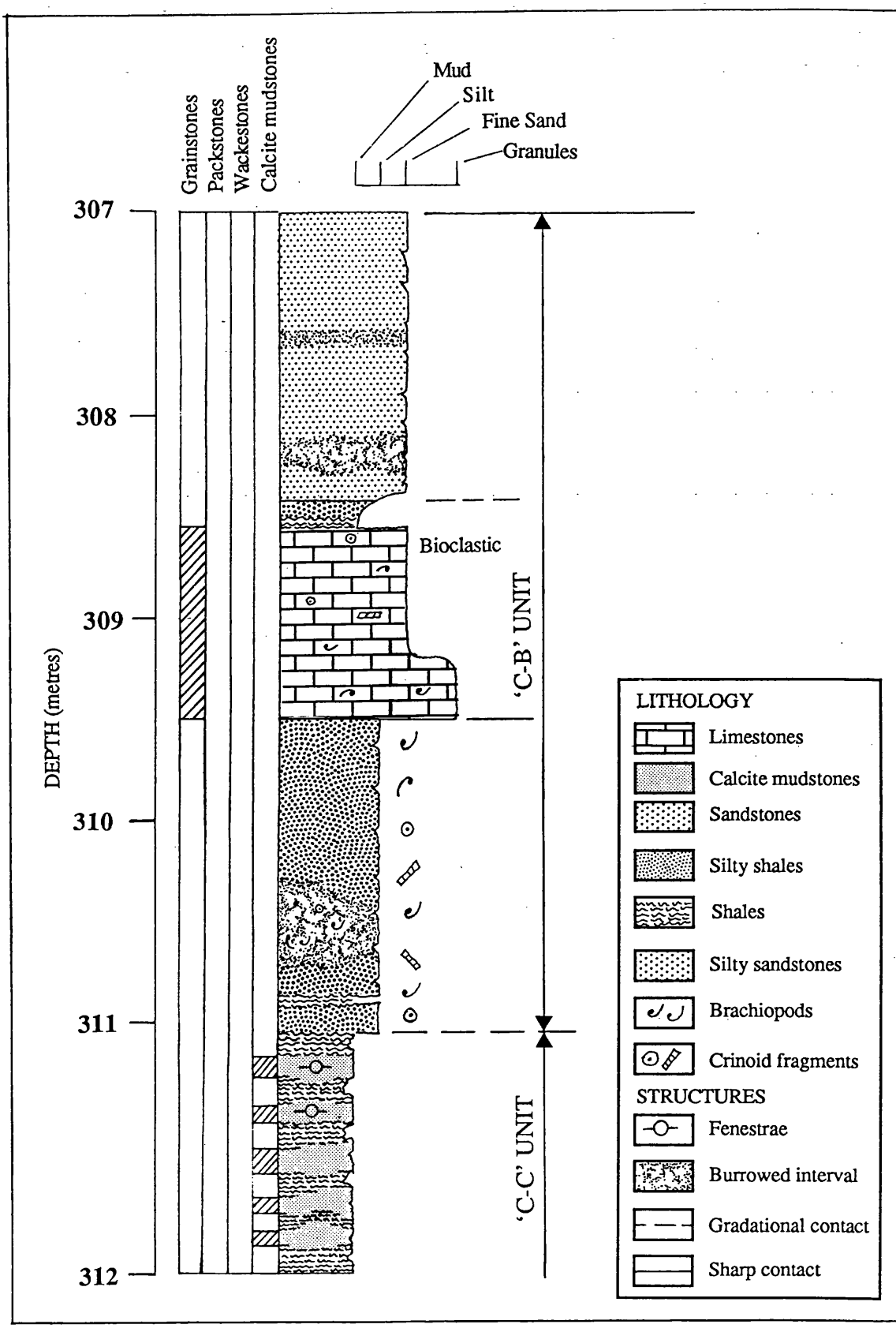

Fig. 2.8. Log showing the relationship between the interbedded silty shale and calcite mudstone facies consitituting the 'C-C' Unit and the overlying bioclastic grainstones, silty shales and sandstones of the 'C-B' Unit. Hole N705.

(present locally) is followed by 1 to 2 m of interbedded calcareous siltstones and shales, also containing occasional bioclast packstones, capped by the green clay.

The succession above this begins with algal laminated limestones followed by interbedded calcareous siltstones and silty shales containing oncolites and the burrowed marker. This assembly, from the top of the 'C-F' Sandstone Unit is known collectively as the 'C-E' Unit. It is overlain by calcareous siltstone and the silicified anhydrite which forms the 'C-D' Unit. This is followed by interbedded silty shales and calcite mudstones of the 'C-C' Unit capped by the bioclast packstones of the 'C-B' Unit.

2.2.4. PETROGRAPHY OF THE LAMINATED BEDS LITHOLOGIES

2.2.4.i. Introduction.

Petrographic analysis is based on six thin sections from sandstones, silty shales, green clay and bioclast grainstones occuring in the 'C-E' unit (hole 975). These lithologies are similar to those in other units and are considered to be representative of the Laminated Beds as a whole. Calcareous siltstone and the silicified anhydrite of the quartz marker from the 'C-D' Unit have also been examined.

2.2.4.ii. Sandstones.

The visually estimated modal composition is 50% quartz, 20% feldspar, 20% allochems and 10% mica and these are thus, according to Pettijohn *et al* (1972) arkosic arenites. Angular quartz grains may be mono or polycrystalline. Microcline and plagioclase both display some alteration. Both biotite and muscovite are present. Lithoclasts are typically fragments of calcite mudstone and bioclasts include crinoid ossicles and shell fragments.

Mechanical compaction has resulted in the distortion of mica flakes around grains and pressure dissolution at grain contacts, giving elongate, sutured grain boundaries. (Plate 2.4.A). Finely disseminated pyrite framboids are common. A blocky ferroan calcite cement (stains purple with alizarin red and potassium ferricyanide) fills pores. Scattered rhomb crystals occurring between grains have anhedral inclusion rich cores and up to four clear zones (plate. 2.4.B.). Some display the sweeping extinction characteristic of saddle dolomite (Radkhe & Mathis, 1980). Keystone vugs with geopetal crystal silts have been reported by Strogen *et al,* (1990, Fig. 6.a.) from hole EP30 (depth 779.8 m).

The petrogenesis began with mechanical compaction and growth of pyrite framboids. Compaction continued, culminating in suturing of grain interfaces. This was followed by deposition of ferroan calcite spar. Finally, dolomite has selectively and partially replaced calcite.

2.2.4.iii.Silty shales.

The silty shales have a similar grain composition to the sandstones, containing bedding parallel muscovite flakes and some bioclasts, typically crinoid ossicles and brachiopod shell fragments. Finely disseminated pyrite framboids and dolomite rhombs are scattered evenly throughout (Plate 2.4.C.).

2.2.4.iv. Bioclast grainstones.

Within the bioclast grainstones shell fragments have been fractured following compaction. Syntaxial overgrowths have developed on pelmatozoan fragments. Dolomitization was generally matrix selective (Plate. 2.4.D.) but some echinoderm fragments have also been partially replaced. Individual dolomite crystals have cloudy anhedral cores surrounded by up to four clear zones. Typically they display the sweeping extinction characteristic of saddle dolomite (Radkhe & Mathis, 1980). Some bioclasts contain microdolomite rhombs (identified by staining). Euhedral authigenic quartz crystals are present, together with finely disseminated pyrite framboids. Sutured seam stylolites. Elucidation of the paragenetic sequence is hampered by dolomitization. It probably began with the growth of pyrite framboids. The timing of grain fracture is problematical, but most likey occured early before significant cementation (compare Harwood, 1989). Deposition of syntaxial calcite followed. This been replaced by dolomite which is itself replaced by authigenic quartz crystals. Compaction continued during these events, culminating in development of the sutured seam stylolites.

2.2.4.v. Calcareous siltstone.

The visually estimated modal composition is 50% quartz, 20% feldspar (commonly plagioclase), 20% calcite mudstone lithoclasts, 10% muscovite, and scattered grains of heavy minerals. At least two heavy minerals are present, a cubic isotropic mineral, probably magnetite or pyrite, and an unknown mineral forming colourless elongate grains with dark outlines (Plate 2.4.E.). Both heavy mineral grains and muscovite are concentrated in thin laminae. Mica flakes are bent around rigid clastic grains. Granular calcite cement fills pores between clastic grains. This is locally replaced by dolomite. Individual rhombs have cloudy anhedral cores surrounded by clear rims but some contain inclusions of calcite. Following compaction, culminating in the distortion of micas, calcite cement formed in primary pores. Finally dolomite locally replaced the calcite.

PLATE 2. 4 Photomicrographs (plane light) of diagenetic features of Laminated Beds.

A. General view of sandstones. Hole N975, depth 512.0 m.Scale bar = 1 mm.

B. Sandstone with calcite cement (c) replaced by dolomite (D), note "clear" zones are inclusion free. Hole N975, depth 512.0 m. Scale bar = 50 microns.

C. Shaley siltstone. Hole N975 at depth 512.0 m. Scale bar = 1 mm.

D. Grainstone showing syntaxial overgrowths (O) partially replaced by matrix selective dolomitization. Note authigenic quartz crystal (Q) replacing dolomite. Hole N975, depth 516 .0 m. Scale bar = 250 microns.

E. Calcareous siltstone with layer of heavy minerals, note different varieties. Inset, dolomite rhomb within cement. Sample from underground, 1285-1300 decline. Scale bar = 250 microns

F. Silica replacing anhydrite represented by inclusions. Sample from 1298-1300 decline. Scale bar = 1 mm.

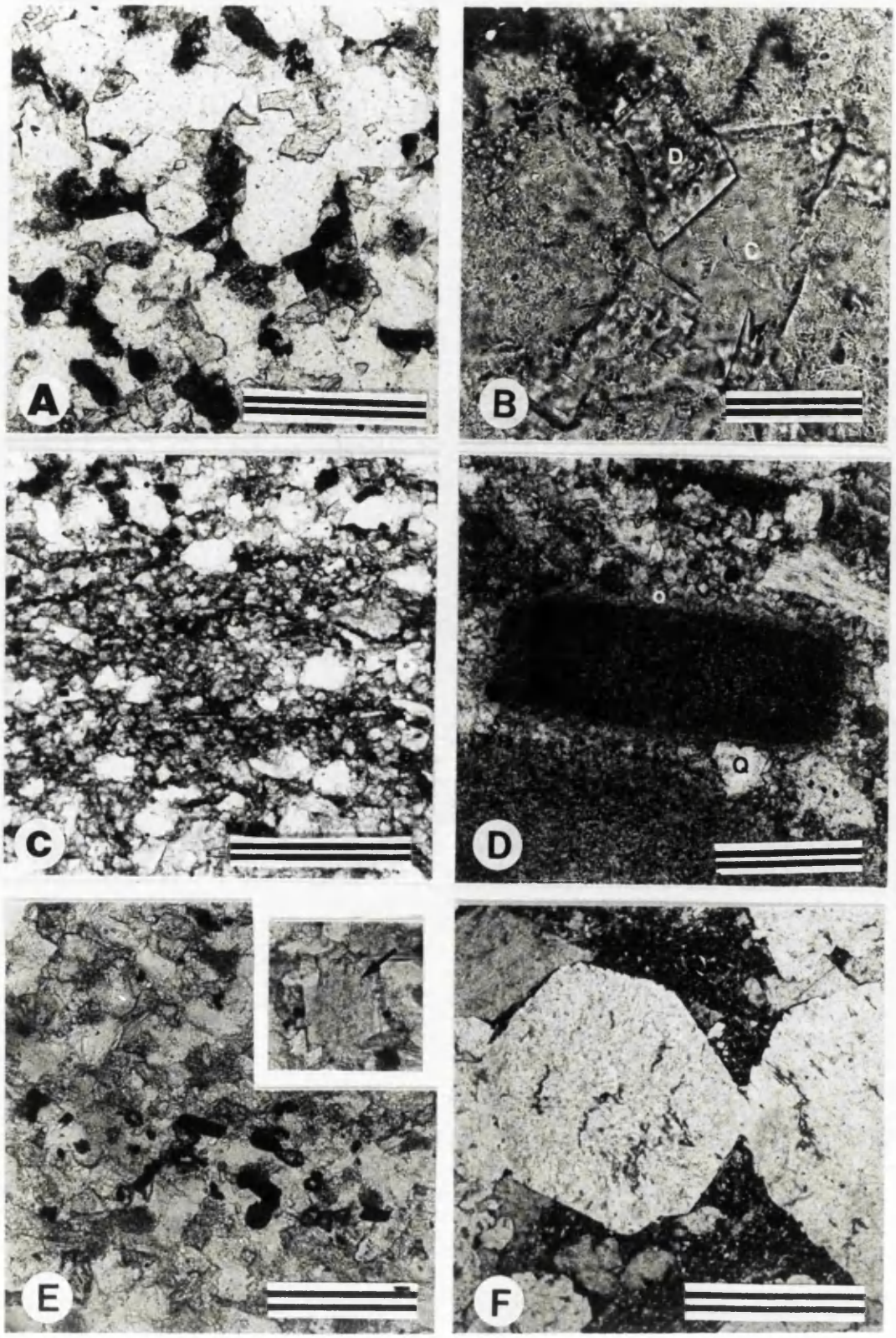
A
B
D
D
C
D
Q
Q
E
F

PLATE 2.4 (continued).

G. Radiating quartz crystals lining inside of evaporite mould, the Quartz marker 1298-1300 decline. Scale bar = 1 mm.

H. Photomicrograph (plane light) of sepic plasmic fabric in green clay hole. Note crude rectilinear fabric. N975 at depth 509.8 m. Scale bar = 250 microns.

I. Photomicrograph (plane light) of clay cutan (C) in green clay. Hole N975 at depth 509.8 m. Scale bar = 100 microns.

J. Photomicrograph (plane light) of pyrite faecal pellets in green clay. Hole N975 at depth 509.8 m.Scale bar = 100 microns.

K. Photomicrograph (plane light) of calcite crystallaria (C) in green clay hole N975 at depth 509.8 m.Scale bar = 100 microns.

L. Photomicrograph (plane light) of calcite filled fissure (F) within siliciate grain Hole N975 at depth 509.8 m. Scale bar = 100 microns.

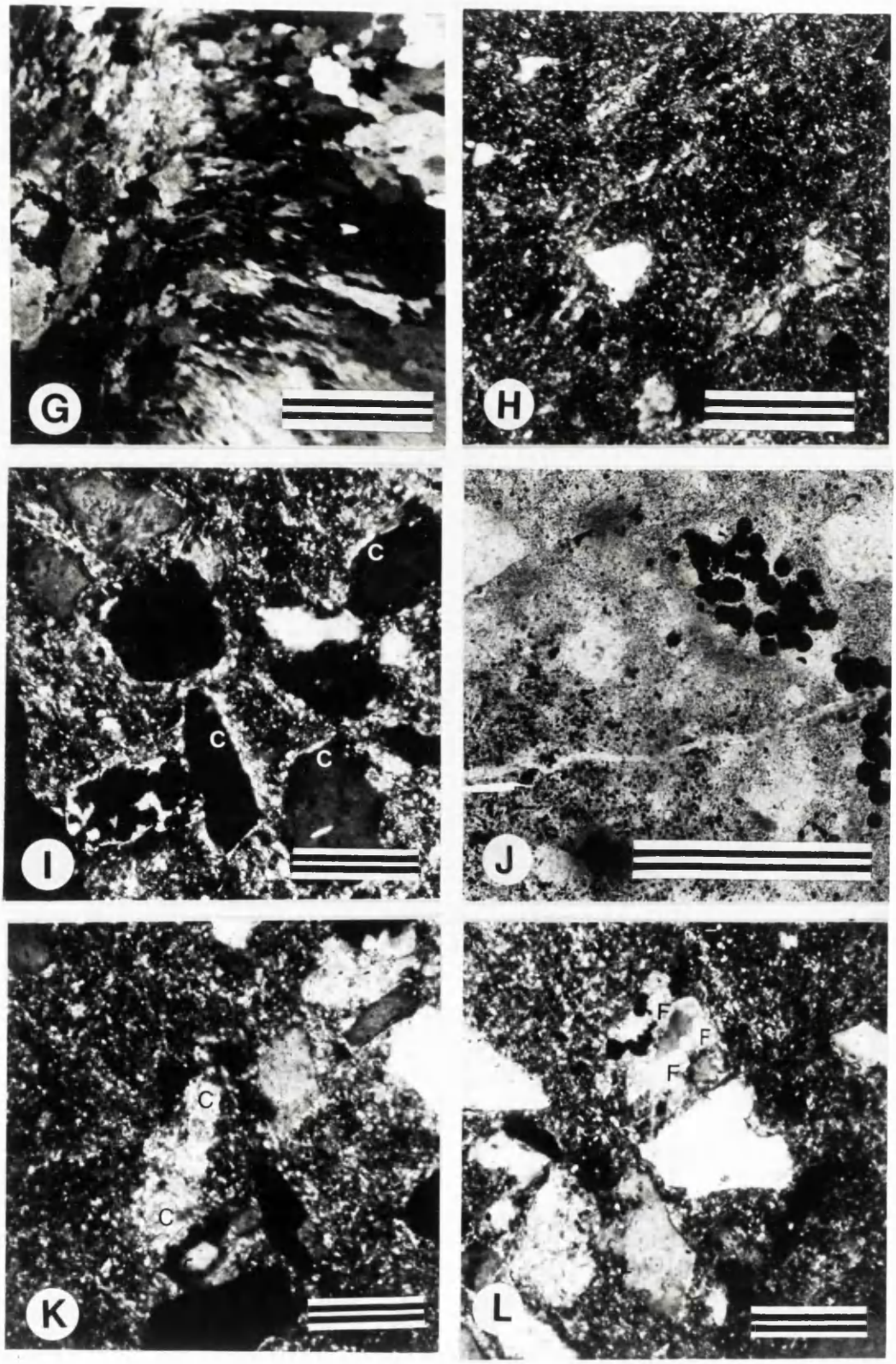
G
H
C
C
C
I
J
C
C
K
F
F
F
L

2.2.4.vi. Quartz Marker.

The anhydrite displays a very finely crystalline texture. This has been extensively replaced by quartz. Two styles of replacement occur, quartz has replaced whole nodules of anhydrite, displaying a uniform internal structure with uniform extinction (Plate 2.4.F). This contains numerous inclusions, some of which form arcuate trails. The inclusions have a high birefringence and are interpreted as relic anhydrite. In the second style of replacement thin bladed-fibrous crystals line former nodules, overlain in the nodule interior by larger anhedral crystals (Plate 2.4.G.). This style of replacement is very common in the Lower Carboniferous of Tennessee (Chowns & Elkins, 1974; Milliken, 1979) and has been termed the "silica evaporite syndrome" (Milliken, 1979).

2.2.4.vii. Green Clay.

The Green Clay is predominantly illitic in composition. In thin section it displays a distinctive fabric consisting of short discontinuous plasma separations (Brewer, 1964) crudely orientated at 90^0 to each other (Plate 2.4.H.). This is very similar to the Sepic Plasmic fabric of Brewer (1964) suggesting that the clay has undergone pedogenic processes. The siliclastic grains are randomly distributed (skeletal grains of Brewer, 1964). Some of these display cutans, another common pedogenic feature (Plate 2.4.I.). Pores which are circular in section are lined with spheres of pyritic material (Plate 2.4.J.). They are interpreted as pyritized faecal pellets which have filled burrows. Some voids have been filled by anhedral microcrystalline calcite comparable to the crystallaria of Brewer (1964) (Plate 2.4.K) another common pedogenic structure. Calcite has also replaced the margins of some siliclastic grains, a feature recorded from calcrete occuring in the Old Red Sandstone of the Welsh Borders (Allen, 1986) and has extended along internal fissures (Plate 2.4.L.)

2.2.5. SEDIMENTOLOGICAL INTERPRETATION OF THE LAMINATED BEDS.

The vertical facies transition, in ascending order, consisting of silty shale, to interbedded sandstones and silty shales and finally to sandstones at the base of the Laminated Beds is similar to the facies sequence of a prograding barrier beach described by Selley, (1985 p.158), they are compared in Fig. 2.9. It also compares to the vertical facies changes of modern barrier beaches such as Galveston Island, Texas and the Oxnard-Ventura barrier sytem of California (McCubbin, 1982 p. 257-258). Similar sequences in the geological record include the Cretaceous Gallup Sandstone of New Mexico (McCubbin, 1982 p.260). In all these examples, silty shales deposited offshore,

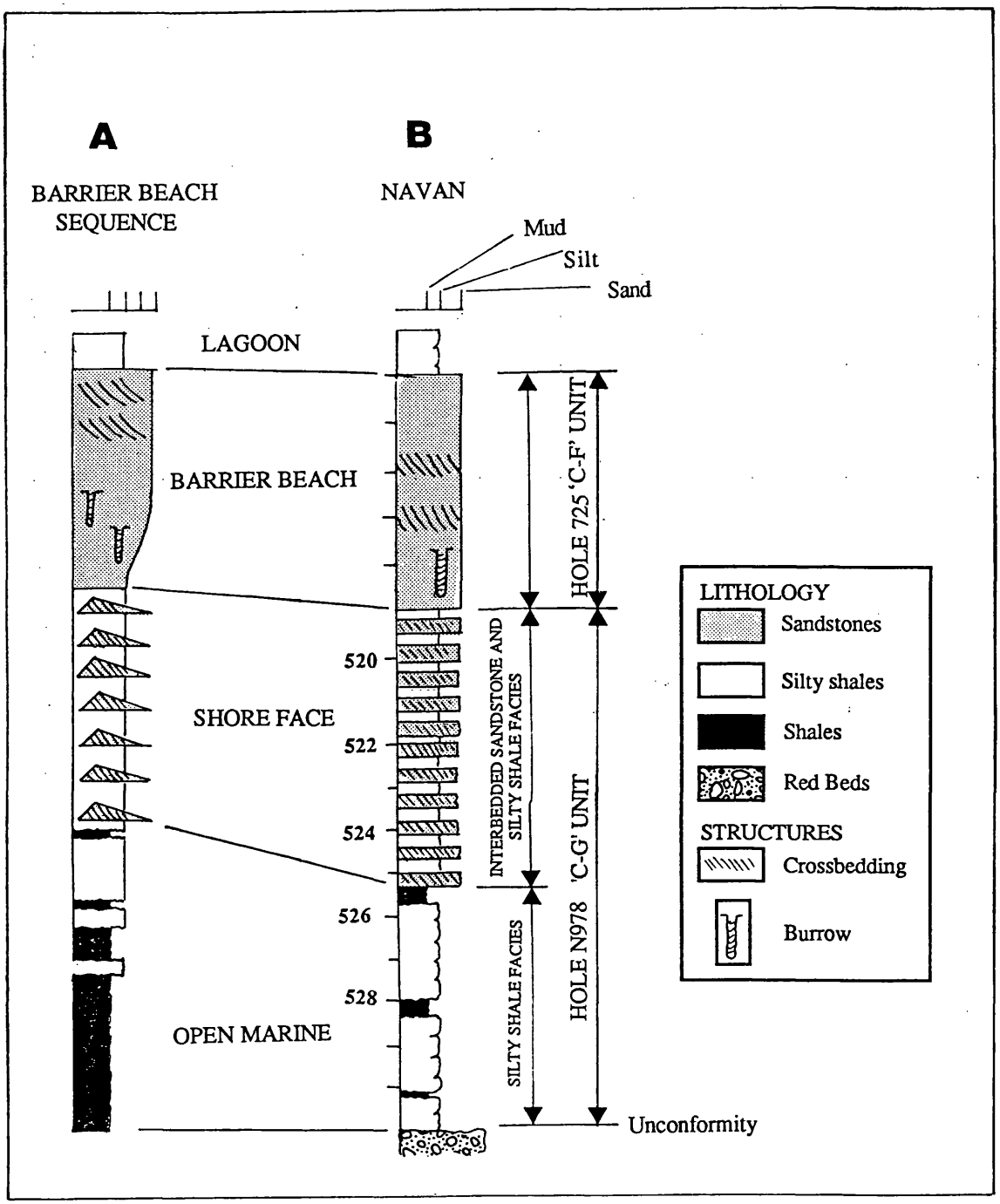

Fig. 2.9. 'A'. Ideal barrier beach sequence, from Selley (1985) p.158. compared with 'B', the sequence at Navan consisting of silty shales, interbedded sandstones and silty shales and sandstones.

are overlain by interbedded sands and silty muds of the shoreface, and finally by sandstones of the barrier itself.

The Navan silty shale has a contact which varies from gradational to sharp. Interbeds of Red Bed conglomerates and silty shale in holes U6230 and N780 at 327.0 m depth show that Red Bed deposition was extending into the marine environment, indicating marine transgression began before depostion of the Red Beds had ceased. The silty shale was deposited from suspension under low energy conditions and the crinoids, brachiopods and fenestrate bryozoans indicate a marine environment. Together, these features suggest offshore deposition below fair weather wave base (Elliot, 1986). Occasional thin sandstones and bioclast grainstones within the silty shale may reflect periodic deposition by storms.

The interbedded cross laminated sandstones and muddy silts with burrowed surfaces are consistent with a shoreface environment encompassing lower, middle and upper zones (Walker, 1984 p.122; McCubbin, 1982 p.255). This is supported by the occurence of *Thalassinoides* at Navan, common in shoreface environments (Frey & Pemberton, 1984). Similar associations have been recorded from the Oxnard-Ventura coast of California where interbedding results from wave generated wash and backwash processes overprinted by storm activity (Howard & Reineck, 1979). The 'C-F' Sandstone is fine-medium grained and well sorted. Structures include planar cross bedding dipping 10^0 to 20^0, plane bedding, trough cross bedding and ripples, typical of barrier sands (Selley, 1985 p.148; Elliot, 1986 p.170) and their associated beach face environment (Reinson, 1984; McCubbin, 1982). The keystone vugs, noted in the 'C-F' Sandstone by Strogen *et al* (1990) were interpreted as reflecting emergence. Thus, the Navan succession of silty shales, interbedded sandstones and silty shales and sandstones is interpreted as a storm and wave influenced barrier beach system and similar to that proposed by Hayes, (1979). This view is supported by the independent observations at Navan by Anderson (1990) and Strogen *et al* (1990) who also suggested that the sequence represented a barrier beach system.

The sandstone is overlain by silty shales 1 to 2 m thick. In other areas such sediments overlying barrier sandstones are interpreted as back barrier lagoon deposits. (Selley 1985, p.149; Reinson, 1986). Support for this interpretation is provided by plant fossils which have been recovered from this part of the sequence. Such fossils within this type of facies sequence are believed to reflect lagoonal environments. (Selley, 1985; Reinson, 1986 p.130; Elliot, 1986 p.167). The occurrence of plant fragments suggests the presence of an adjacent flood plain at this time (Burton, pers commn, 1992). The suggested facies model for this part of the succession is shown in Fig. 2.10. The second sandstone occurs within the silty shales. Insufficient data are

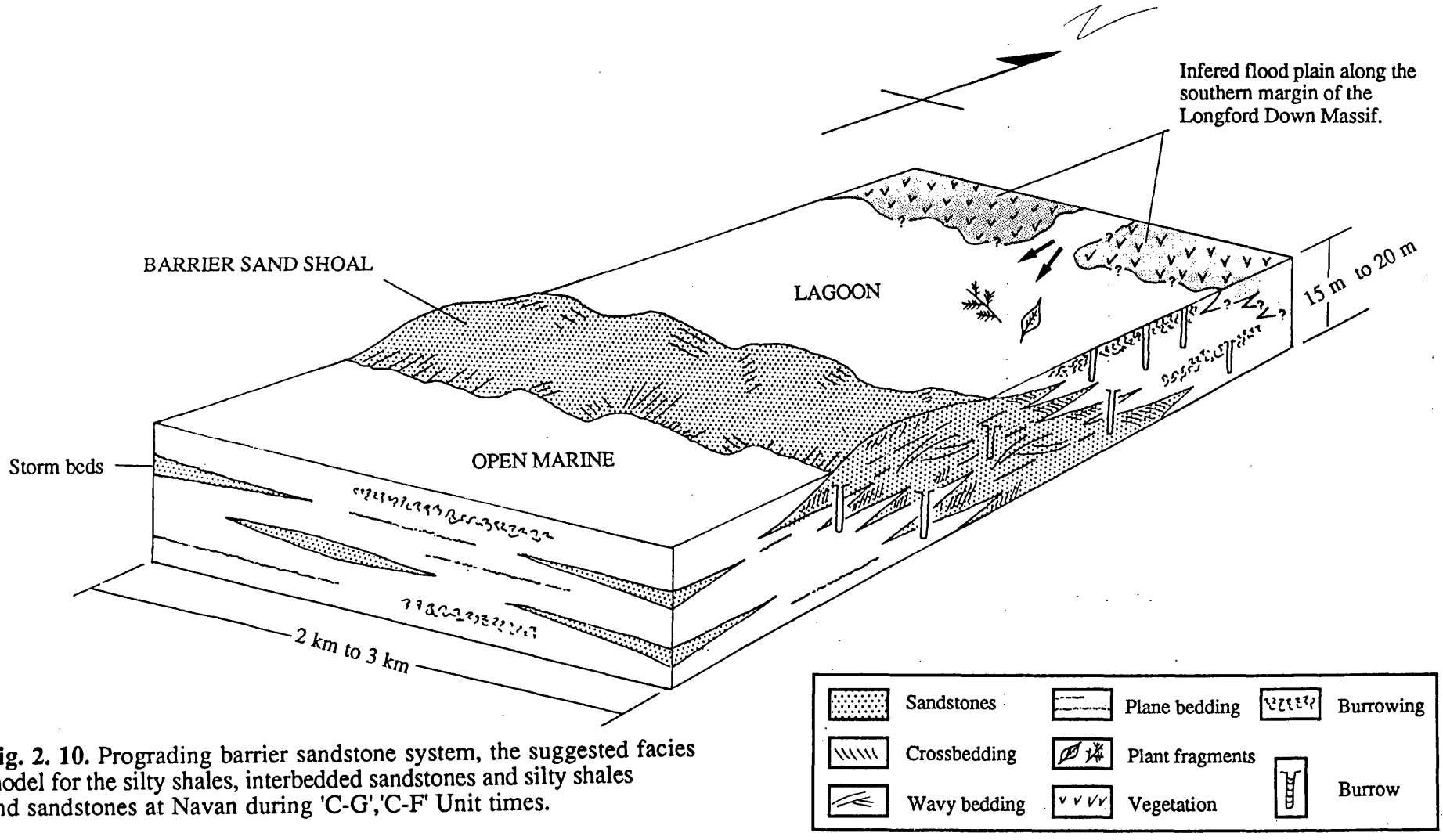

Fig. 2. 10. Prograding barrier sandstone system, the suggested facies model for the silty shales, interbedded sandstones and silty shales and sandstones at Navan during 'C-G','C-F' Unit times.

currently available on this lithology, however the lenticular geometry, localised occurrence and cross lamination suggest it reflects either a channel, barrier bar sandstone. However since it occurs within 'lagoonal' sediment, it could be an overwash sand.

This sandstone is overlain by 1 to 2 m of interbedded calcareous siltstones and silty shales with prominant burrowed surfaces. The green clay which caps this part of the sucession contains a number of structures interpreted as pedogenic in origin. The millet seed quartz grains in it suggests possible aeolian derivation. Thus it seems likely that the the green clay at Navan represent an emersion surface on which a soil was established.

The algal limestone above the green clay compares with algal mats on the present intertidal flats of the Trucial coast. These form a belt over 2 km wide (Kendall & Skipwith, 1968) in an area hostile to grazing cerithiid gastropds. The Trucial coast mats form accumulations up to 1 m thick consisting of alternating carbonate and clastic laminae 1 to 2 mm thick containing gypsum crystals. They include coatings of wind blown silt size quartz, feldspar and dolomite. Typically mats have been disrupted by desiccation, by growth of evaporites, and by compaction. During storms and flood tides mats are reworked and re-deposited as conglomerates (Park, 1977). The Navan laminated limestones include 1). algal lamination, alternating siliciclastic and carbonate laminae, 2). reworked algal laminated layers 3). pseudomorphs of gypsum crystals. Based on these similarities it is likely that the Navan algal laminated limestone represents a thin arid tidal flat sequence.

Overlying the algal limestone is a 1 to 2 m thick sequence of silty shales and calcareous siltstones. This facies is typical of a lagoonal environment (Reinson, 1984 p.129; Elliot, 1986 p.167). The interbedded silty shale and calcareous siltstones at this locality contain the marker horizon consisting of *Garwoodia* oncoids. Since cyanobacteria absorb the blue end of the light spectrum they indicate water depths of less than 10 m (Park, 1977). The concentric to slighlty asymmetric lamination of the *Garwoodia* oncoids shows that gentle (tidal ?) rolling occured during growth with minor periods of stillstand (Wright, 1983). The burrowed marker with *Rhizocorallium* also presents a lithology typical of quiet water-low energy environments (Frey & Pemberton, 1984). Thin laterally persistent bioturbated horizons have been interpreted as reflecting significant non deposition, often preceeding a facies change (Walker, 1984). The suggested facies model incorporating the pedogenic clay, algal laminated limestones and interbedded calcareous siltstones and silty shales is shown in Fig 2.11.

The calcareous siltstone facies of the 'C-D' Unit also implies lagoonal conditions. The preservation of millimetre scale lamination consisting of mica flakes, heavy minerals, siltstones and thin mudstones, and the lack of current generated structures indicate quiet water deposition. The absence of bioclasts and burrows suggests an abnormal

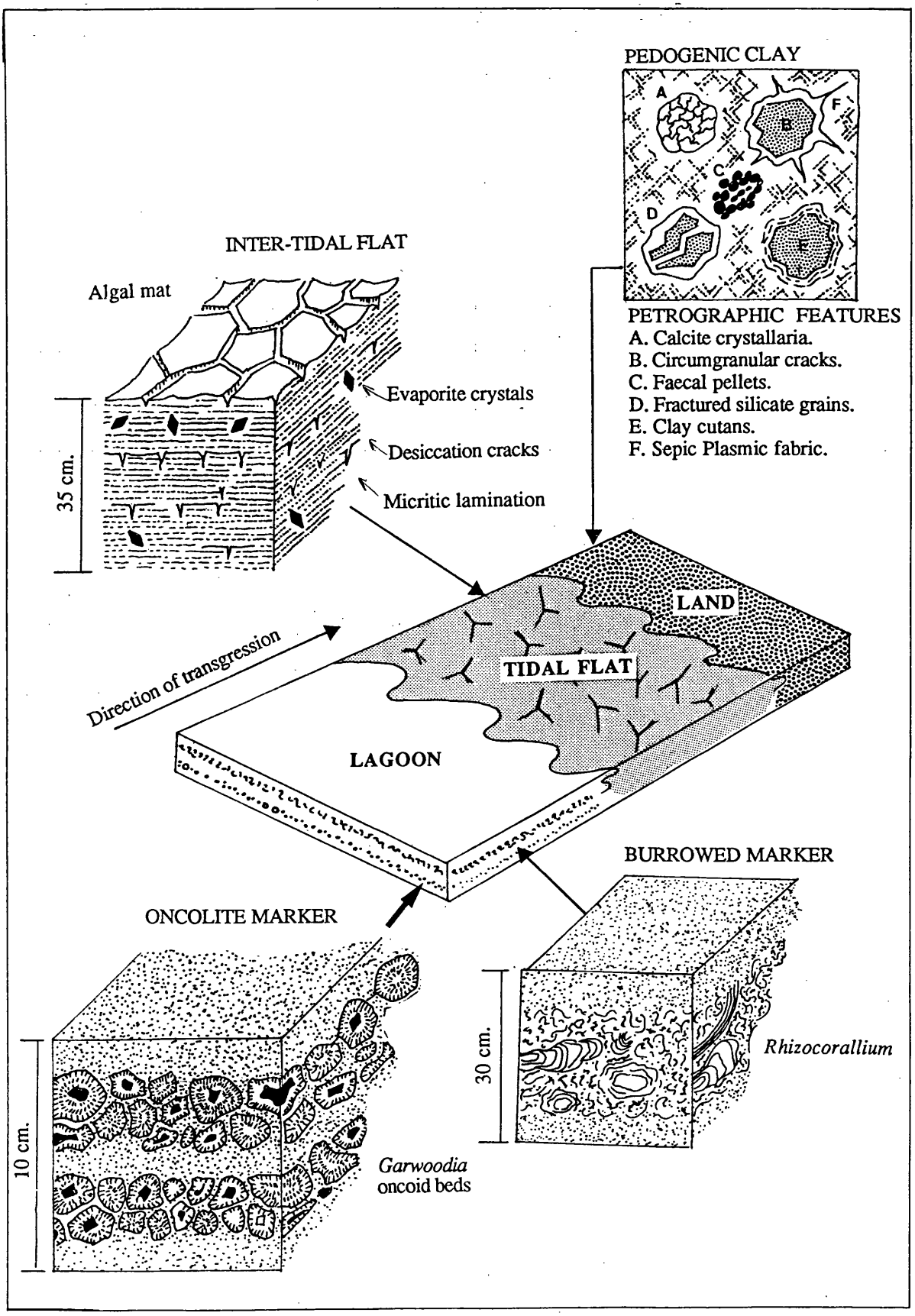

Fig. 1.11. Suggested facies model during 'C-E' Unit times at Navan. Lagoon and micritic tidal flats transgress over adjacent land area represented by pedogenic clay.

environment while the silicified anhydrite in the upper 30 cm of the facies indicates transition to hypersaline conditions.

The calcareous siltstones with nodular evaporite are similar to an ideal sabkha cycle; they are compared in Fig. 2.12. Nodular mosaic anhydrite is currently forming in the sabkhas of the Trucial coast (Kendall, 1984) and similar deposits in the geological record have been interpreted as reflecting formation in a supratidal-sabkha environment (Schreiber *et al.* 1986). The growth of anhydrite on the Abu Dhabi sabkha occurs both by displacement and by replacement of the unconsolidated sediment. Such disruption may contort lamination, eventually destroying the sedimentary fabric (James, 1984 p.221). The nodules at Navan have distorted against each other and inclusions of host sediment occur as partings between nodules, showing that this evaporite grew in a similar manner to the Recent sabkha evaporites of the Trucial coast.

The evaporites at Navan have been cut by a truncation surface. James (1984) has described the formation of such surfaces from the Abu Dhabi sabkhas, following *in situ* growth of evaporite and upward displacment of sediment. Since the water table does not accompany this vertical movement the sediment and evaporite are subject to deflation, producing an erosion surface. The occurrence of such truncation surfaces at Navan suggest a similar proccess has operated here. The association of calcareous siltstone and nodular and massive anhydrite, and single crystals formerly of sulphate together with associated truncation surfaces, compare with the ideal vertical sabkha sequence of Kendall (1984).

The Silty shales and calcite mudstones suggest deposition from suspension. Calcite mudstones occur in Recent lagoons and tidal flats of the Bahamas (Shinn *et al,* 1969) and the Trucial coast. They were apparently common in similar environments in the geological record (Wilson, 1975; Flugel, 1982). The occurrence of millimetre scale spar filled cavities in some calcite mudstones, interpreted as fenestrae, suggest that they represent tidal flats deposits. The absence of bioclasts and burrows and the presence of beds of silicified evaporite demonstrate that elevated salinities were continuing

The assemblage of crinoids, brachiopods and echinoderm fragments in the grainstones at the top of the Laminated Beds are typical of stenhohaline conditions and indicate that shallow marine environments existed nearby. However, the fragmental and abraded nature of bioclasts indicates current transport. The graded beds show that deposition occurred rapidly from decelerating currents. The dark silty layers indicate that carbonate production was punctuated by periodic influxes of clastic material.

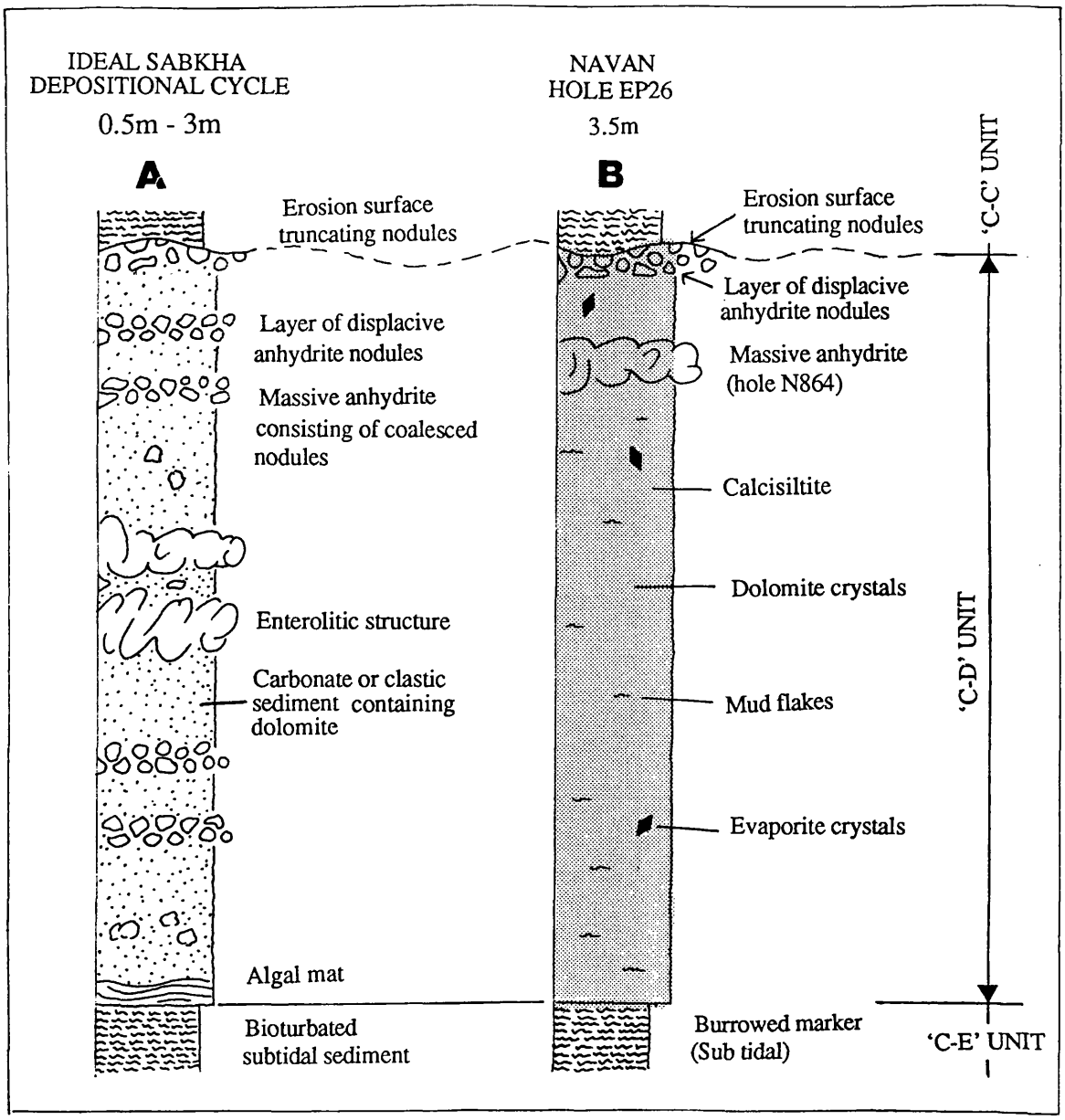

Fig. 1.12. 'A'. Ideal sabkha cycle (Shearman, 1978) but modified from Schreiber (1986) p. 205 and Kendall (1986) p. 269. This is compared with 'B' the 'C-D' Unit at Navan.

2.3. LINEAR EROSIVE FEATURE.

2.3.i. Introduction.

In the western mine area a prominent linear erosive feature cuts down through the Laminated Beds to just above the algal laminated limestones. The total relative depth of the feature was recorded from drill core using the top of the Laminated Beds as a datum and these data contoured.

The contour map (Fig. 2.13.) indicates that the linear feature has a maximum width of 500 m narrowing to 100 m to the SE and about 20 m deep. The linearment strikes NW to SE for at least 2 km and extends beyond the study area in both directions. It is symmetric in section and the floor apparently had no measurable gradient.

2.3.ii. Interpretation.

The linearment is consistent with a channel. Channels are common in recent carbonate environments, including the Bahamas (Shinn, 1983), the Persian Gulf (Shinn, 1973) and Florida (Jindrich, 1969) where they are orientated more or less normal to the shoreline. Such channels cut through tidal flat, lagoonal and barrier island deposits, often extending out into the shallow marine environment. They seem to have been cut by diurnal tidal activity over several thousand years. In Recent examples, depth is controlled by the underlying Pleistocene bed rock which acts as a physical barrier, thus present day channels are around 4 m deep.

Blue Fish channel north of Key West, Florida (Jindrich, 1969) is a linear channel, cut by strong diurnal currents, is over 10 km long, more than 200 m wide, and 3.3 m deep. It has cut across a muddy lagoonal area and dissected a tidal barrier, extending into the shallow marine environment. The cross-section varies along the length of the channel and may be either asymmetrical or symmetrical. The Navan example has similar characteristics. Similar channels occur in the geological record. The Miocene of the Sirte Basin of Libya has been interpreted as a mixed carbonate-siliclastic shoreline sequence consisting of lagoonal and barriers island deposits cut by a sequence of channels 300 m wide x 10 m deep (Selley, 1967). Once again these features are comparable with the Navan example.

2.4. THE LIMESTONE CONGLOMERATE.

2.4.i. Introduction.

Lining the floor of the channel is a poorly sorted grainstone. The boundary of the channel floor is sharp (Plate. 2.5.A.) but in hole N1039 the surface has been burrowed

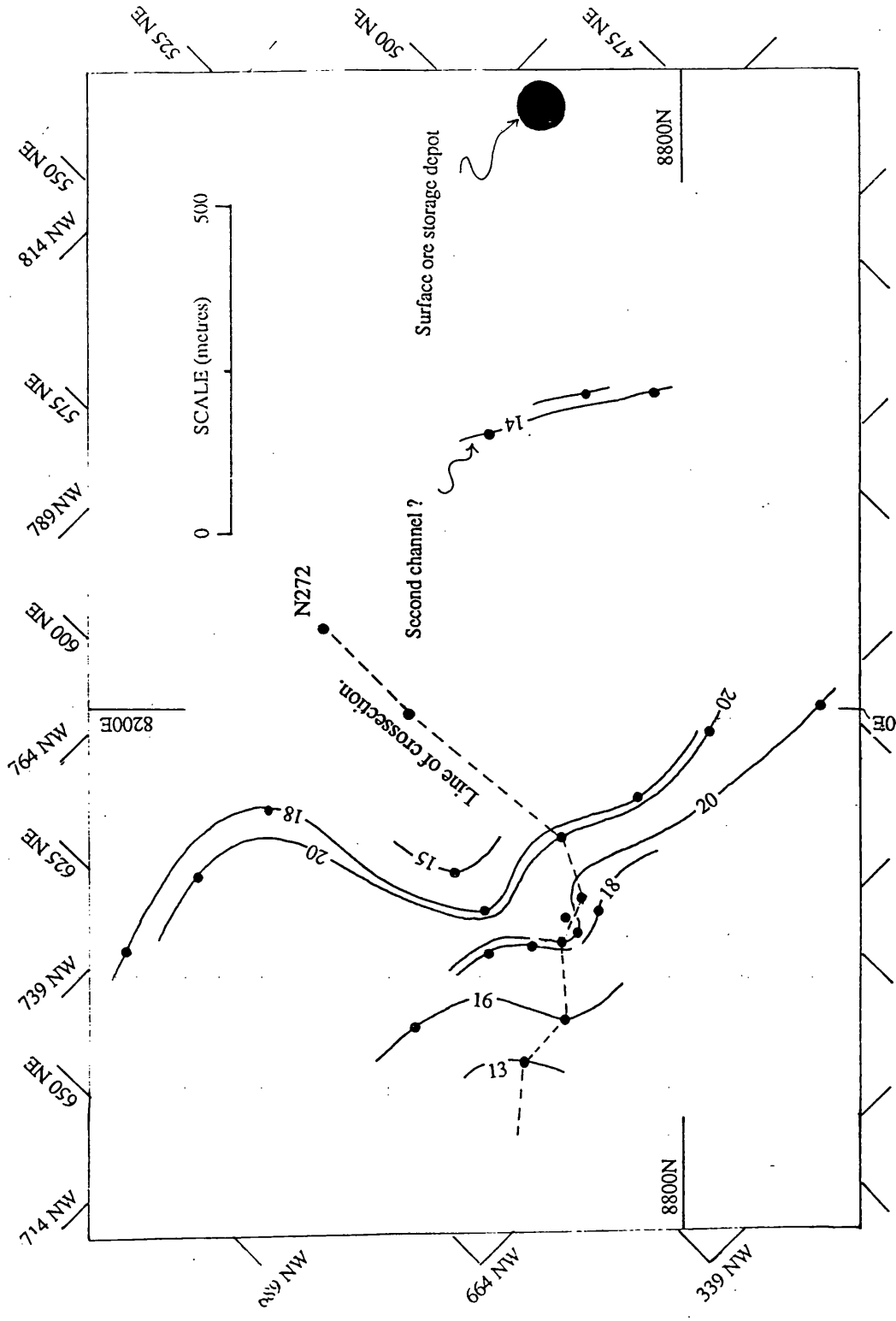

Fig. 2.13. Channel cutting Laminated Beds, top of Muddy Limestone as datum, depth in metres.

(Plate 2.5.B). The unit was first recorded by Philcox (1980) who referred to it as the "Limestone Conglomerate".

2.4.ii. Description.

The Limestone Conglomerate reaches 15 m thick in hole N853 and ranges from fine sand to poorly sorted granule or small pebble grade grainstone. The contacts between lithologies are typically gradational but are sharp where coarse grainstones overlie sand grade grainstones. Some thin grainstone laminae are dark and silty. Black shales 3 to 7 cm thick are present within the sequence in hole N1033. Thick and thin bedding and lamination are present (Plate 2.5.C.). Some layers are homogeneous while others show normal or reverse grading. Cross bedding is present in some holes with foresets dipping 10^0 to 20^0 (hole N975) and sets reaching thicknesses up to 50 cm. Horizontal and vertical sinuous burrows are present in the finer grained material and may be up to 8 mm in diameter, filled with dark mud and containing spreite. Fining-up units up to 1.5 m thickness are common. The main features are summarized in Fig. 2.14.

2.4.iii. Composition.

The Limestone Conglomerate consists of lithoclasts, bioclasts and siliciclastic grains. The dominant lithoclasts are of light grey **calcite mudstone**. The largest are over 3 cm maximum diameter and crudely rectangular in section. They are fossiliferous in hole N835 and some have been bored (hole N1019). Importantly many contain angular fragments of pale mudstone and sandstone up to 2 cm diameter or of dark mudstone in a pale mudstone matrix (Plate 2.5.D). Others are internally laminated (Plate 2.5.E) and some contain angular silt grade quartz and feldspar grains.

A conspicuous group of dark mudstone lithoclasts up to 1.5 cm long and 1 cm deep also occur. These have a mottled-glaebular texture and contain a variety of features. These include former pores, circular in section and 0.25 mm in diameter, lined with micrite and filled by calcite spar. Irregular linear cracks radiate away from these pores. These lithoclasts are stained black, probably by iron oxides (Plate 2.5.F). Circular pores, irregular cracks, micrite coatings and glaebular-clotted fabrics are typical pedogenic features (Brewer, 1964). Similar blackened pebbles with micrite coatings, circular pores and irregular cracks containing calcite spar are described from palaeosols occuring in the Upper Jurrassic Purbeck Beds of Southern England (Francis, 1986). The occurrence of pedogenic features indicates that these lithoclasts are fragments of **Palaeosols.** Angular fragments of **oolitic grainstone** contain radial concentric ooliths with elongate planar contacts. Pore spaces in these contain an isopachous acicular calcite cement overlain by blocky calcite (Plate 2.5.G).

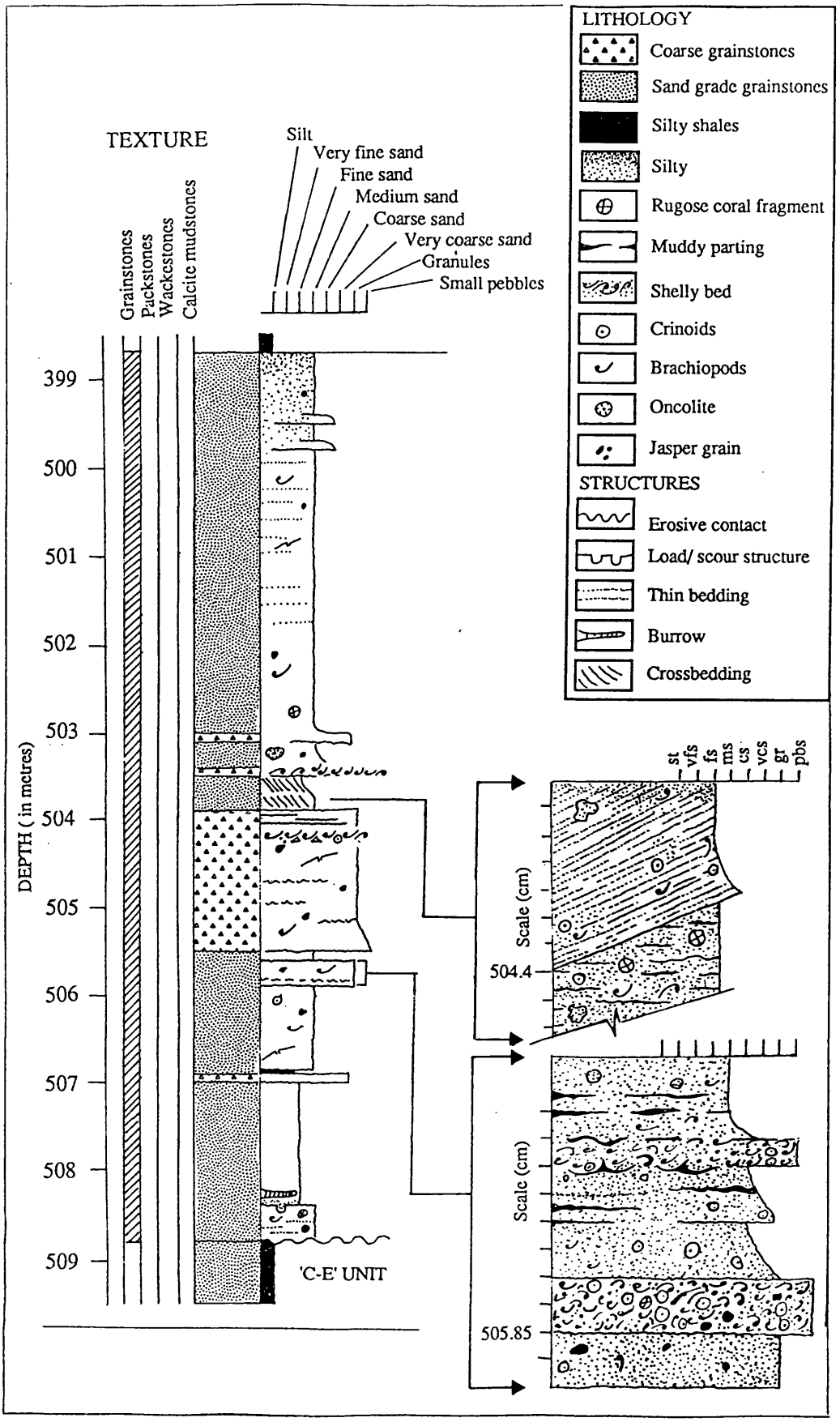

Fig. 2.14. Summary log of Limestone conglomerate, note fining-up units, crossbedding and jasper grains. Hole N975.

PLATE 2.5 General features of the Limestone conglomerate.

A. Contact between Limestone Conglomerate and Laminated Beds. Limestone Conglomerate has cut down as far as the algal laminated limestones. The contact is sharp. Note micrite clasts (M) containing bioclasts and fragments of sandstone (S). Hole N835 at depth 343.0 m. Scale in centimetres.

B. Burrowed contact (arrow) between Limestone Conglomerate and Laminated Beds. Pencil for scale. Hole N1039 at depth 495.7 m.

C. Thinly bedded Limestone Conglomerate, note silty layer containing calcite mudstone lithoclast, pencil for scale points to way up..

D. Photomicrograph (plane light) of calcite mudstone lithoclast containing clasts of calcite mudstone. N1020 at depth 599.1 m. Clast is approximately 2 mm in length.

E. Photomicrograph (plane light) of laminated calcite mudstone lithoclast. Hole N1020, depth 599.1 m. Clast is approximately 3 mm in length.

F. Photomicrograph (plane light) showing detail of palaeosol lithoclast, note black staining and circular section void lined by micrite. Hole N1019 at depth 579.4 m. Scale bar = 1mm.

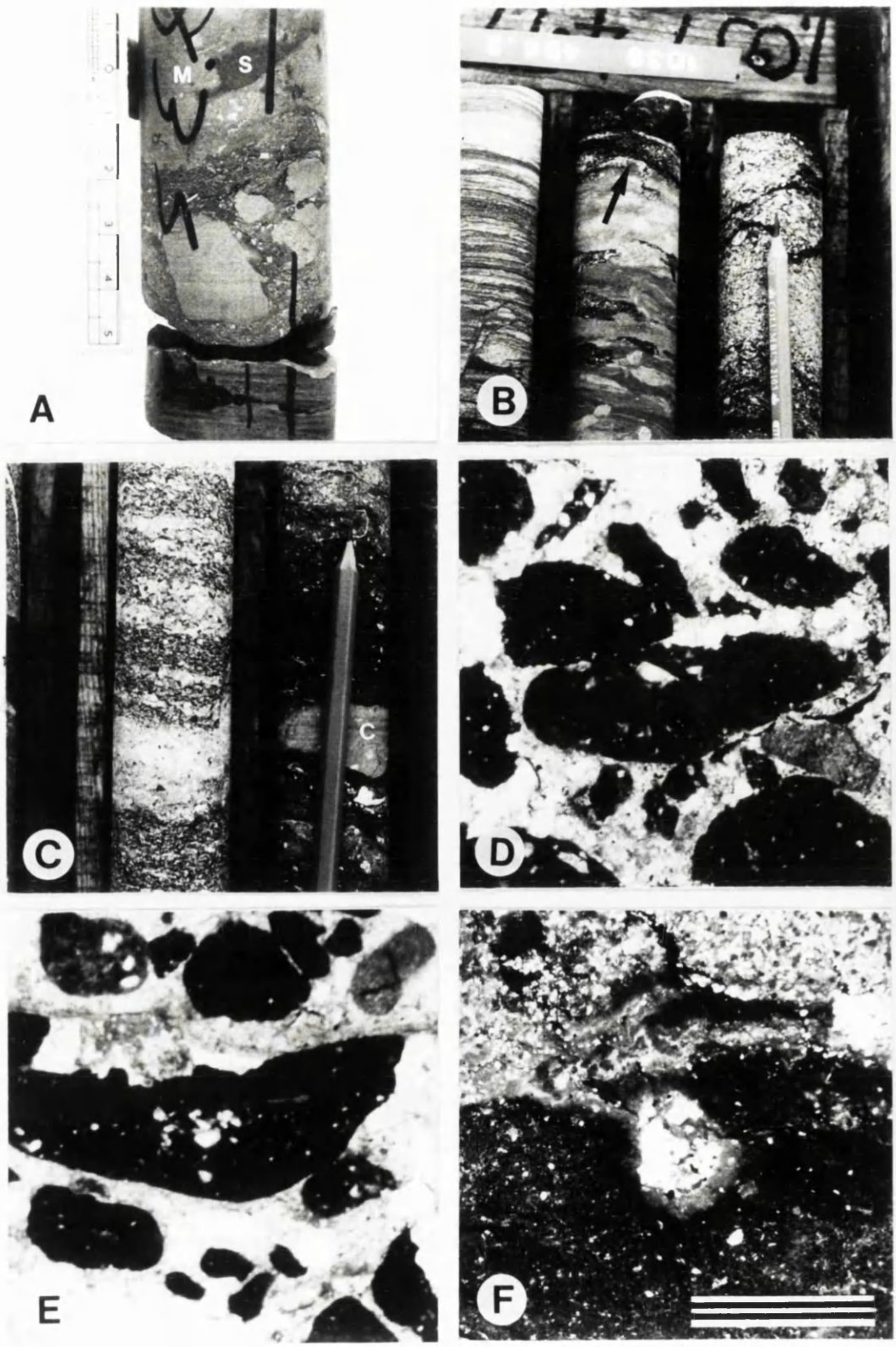
M
S
A
B
C
C
D
E
F

A variety of calcite **cement fragments** have been identified using cathodoluminescence microscopy (CL).One cement fragment consists of a dark orange luminescent zone which is truncated by an irregular dissolution surface. This is overlain by a sequence of six conformable zones, a bright orange zone, a thick dull orange zone and a second bright orange zone are followed by a non luminescent zone, a dull orange zone and a thick non luminescent zone (Plate. 2.5.H.). One cement fragment consists of a thick non luminescent zone followed by eight couplets, each consisting of inner dull and outer bright orange zones (Plate 2.5.H. inset). A third clast consists entirely of cloudy inclusion rich columnar crystals with intersecting cleavage traces (Plate 2.5.I.). These features are consistant with radiaxial calcite. Finally one clast consists of clear equant blocky crystals (Plate 2.5.J.). The zonal sequences in cement lithoclasts differ from that in the Limestone Conglomerate itself, demonstrating that they are indeed fragments of cement and not *in situ* void fill.

Bioclasts include crinoid ossicles, echinoid plates, and fragments of rugose corals, oncoids, gastropods, brachiopods, brachiopod spines, bryozoans, ostracods, trilobites and foraminifera. **Non skeletal grains** include peloids and ooliths and oncoids.

Non-carbonate lithoclasts include elongate very finely laminated fragments of shale up to 25 mm long and 8 mm thick containing silt grade quartz and feldspar grains (Plate 2.5.K.). Small angular fragments of red mudstone (Plate 2.5.L) and elongate fragments of green clay (Plate 2.5.M) are also present. Angular **siliciclastic grains**, account for 25 to 30% of the sediment. Four types of angular quartz are present, grains with undulose extinction, polycrystalline, polycrystalline sheared and monocrystalline grains containing vacuole trails including both single and two phase fluid inclusions. Conspicuous grains of red jasper are also present (Plate 2.5.N). Scattered altered feldspars and micas are also present.

2.4.iv. Provenance of the Limestone Conglomerate.

Calcite mudstones are common in Recent carbonate environments, occurring in the sheltered bays and lagoons of the Trucial coast, Florida Shelf and in the Bahamas (Shinn *et al*, 1969). They are also very commonly interpreted as representing lagoonal sequences in the geological record (Wilson, 1975; Flugel, 1982). The calcite mudstone clasts at Navan may have been fed directly into the channel from nearby lagoonal or tidal flat environments or sourced from lithified calcite mudstones. The angular nature of the clasts and the horizontal undistorted bedding within some of them show they were consolodated prior to erosion. Angular clasts of mudstone and sandstone within other mudstone lithoclasts reflect repeated reworking. The assemblage of brachiopods, crinoid ossicles,

PLATE 2.5 (continued)

G. Photomicrograph (plane light) of oolitic grainstone lithoclast, hole N1019 at depth 579.4 m. Clast is approximately 3 mm in diameter. Inset also shows cement fragment.

H. Photomicrograph (CL) of calcite spar cement fragments, note truncation of zonal sequence by clast margins. Hole N1020 at depth 599.1m. Scale bar = 1mm.

I. Photomicrograph (plane light) of radiaxial fibrous calcite cement fragment. Hole N1020 at depth 599.1 m. Clast is approximately 3 mm in length..

J. Photomicrograph (plane light) of calcite spar cement.fragment. Hole N1020 at depth 599.1 m. Scale bar = 250 microns.

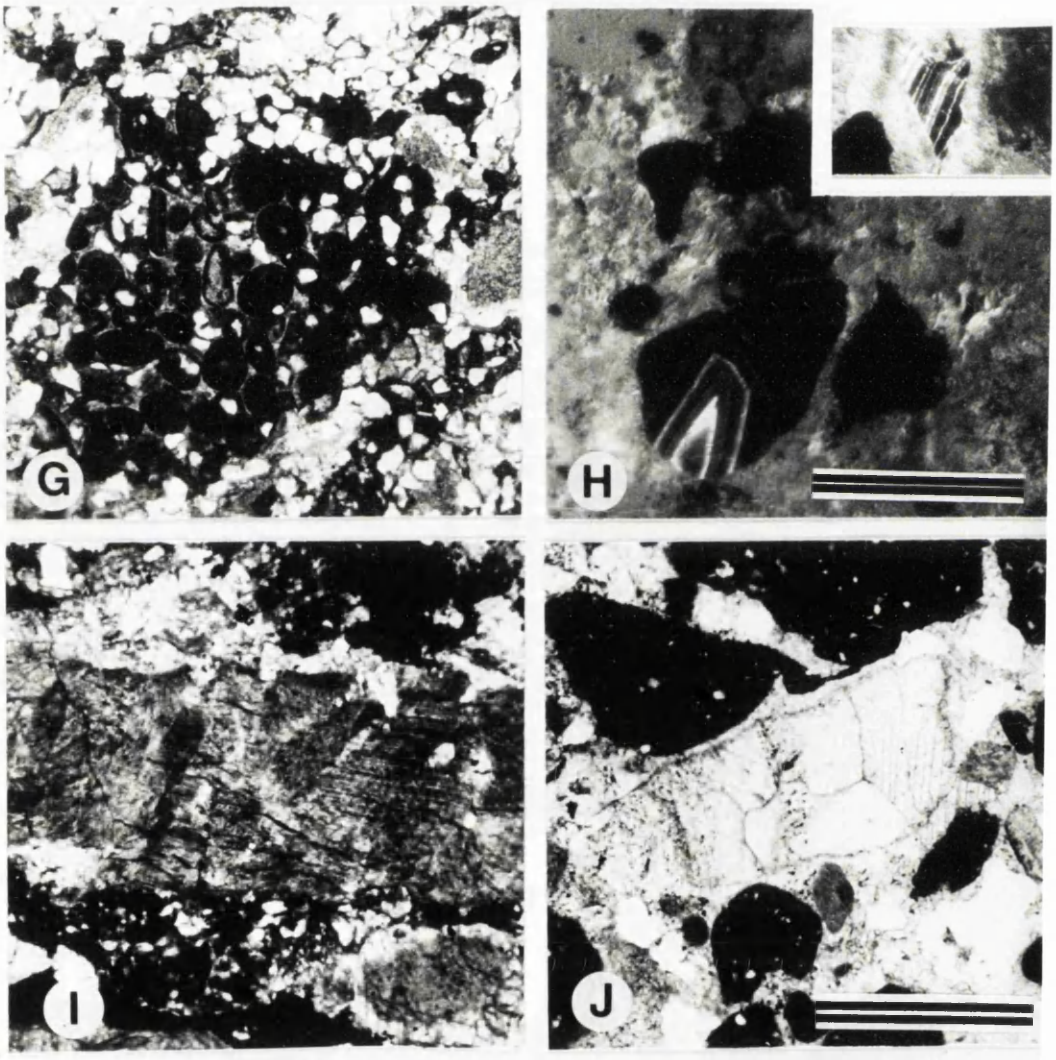
G
H
I
J

PLATE 2.5 (continued)

K. Photomicrograph (plane light) of shale lithoclast. Hole N1019, depth 579.4 m.Clast is approximately 4 mm thick.

L. Photomicrograph (plane light) of red mudstone lithoclast. Hole N1019 depth 579.4 m. Clast is approximately 1 mm in diameter.

M. Green clay lithoclast (arrow). Hole N975 depth 501.1 m. Scale in millimetres.

N. Limestone Conglomerate showing granular and sand grade textures. Jasperoid grain also present indicated by arrow. Hole N975. Scale in centimetres.

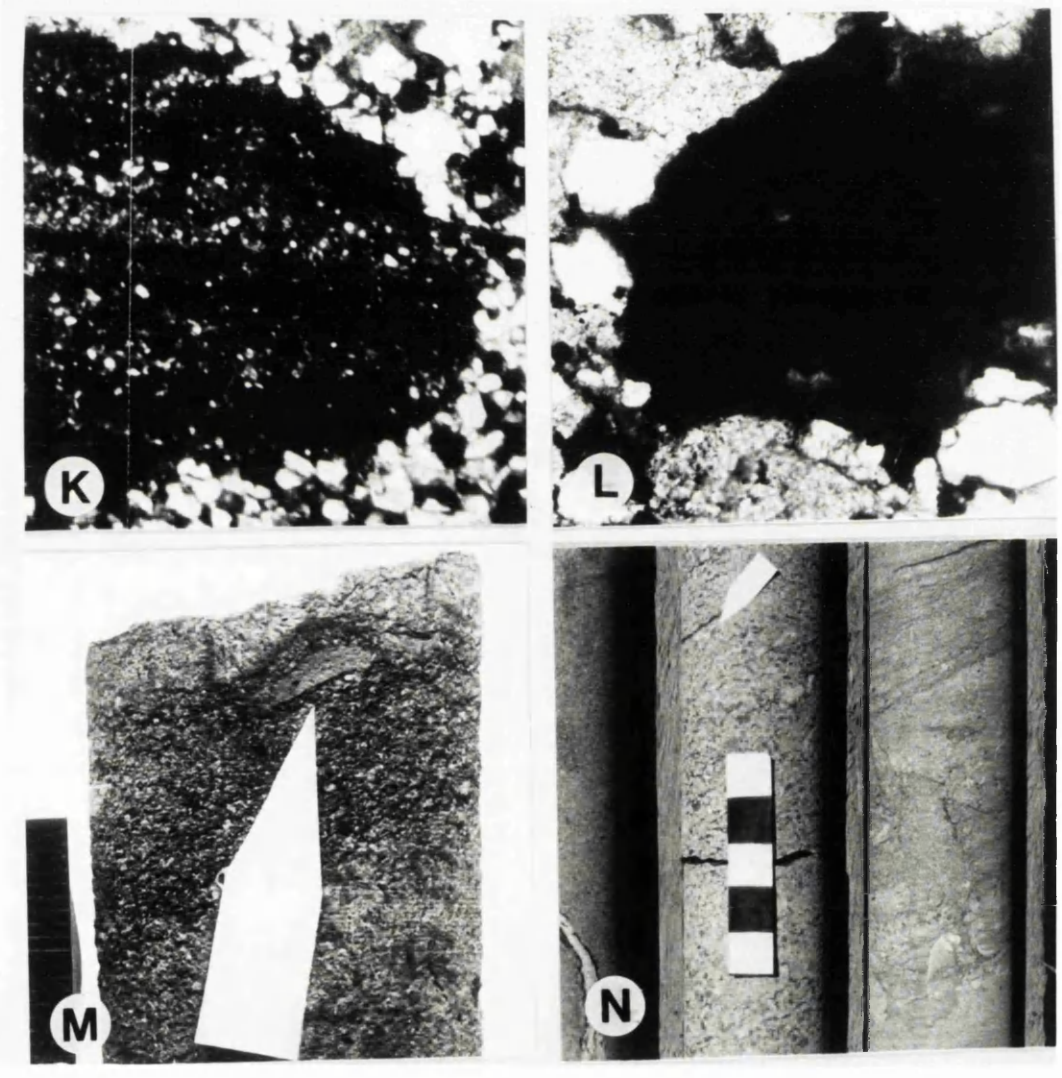
K
L
M
N

echinoids and rugose corals is stenohaline and indicates that normal marine conditions existed nearby (Wilson & Jordan, 1983 p.301). Oncolites indicate very shallow water.

Oolites are also common in Recent shallow marine carbonate environments such as the Persian Gulf and the Bahamas where they form large sand bodies (Wilson & Jordan, 1983 p.314 to 315). Oolites in the geological record are believed to reflect similar conditions (Flugel, 1982). The ooliths within the Limestone Conglomerate therefore indicate that shallow oolite shoals were supplying sediment at this time. However the elongate contacts between individual ooliths within fragments of oolite grainstone and their associated cements show that these had undergone a long and diverse diagenesis prior to erosion (Braithwaite pers. commn. 1991). Such provenance is supported independently by fragments of blocky calcite cements. Harwood (1989), Harris, *et al* (1985) and Moore (1989) suggest that blocky calcite is representative of burial cementation. Radiaxial calcite has been described forming speleothems (Harwood pers. commn. 1993). However it is widely believed to represent a marine phreatic cement. (Kendall, 1985). The occurrence of these cements indicates derivation from lithified limestones which had undergone differing sequences of diagenesis.

Shale lithoclasts could have been derived from the underlying Laminated Beds where such lithologies are common, or from older rocks outside the study area. The elongate undistorted outlines indicate they were cohesive prior to deposition. Clasts of red mudstones and jasper indicate derivation from continental Red Beds suggesting that this type of facies was exposed to the north of the study area at this time. Such Red Bed facies lie beneath the Laminated Beds. Fragments of green clay could have been sourced from rocks deposited in a low energy marine environment or perhaps from palaeokarst surfaces (Walkden, 1974; Davies, 1991; Riding & Wright, 1981; Bechstadt & Dohler-Hirner, 1983). The fragments could also have been derived from the Laminated Beds where a green clay has been identified and interperted as representing an emersion (palaeosol) surface.

It is clear that the Limestone Conglomeate had a varied provenance consising of limestones, sediment derived from contemporaneous shallow marine environments, igneous and high-medium grade metamorphic rocks and Red Beds. The limestone terrain consisted of lithified oolitic grainstones and mudstones. Fragments of palaeosols and perhaps, lithoclasts of green mudstone, indicate that palaeokarst surfaces were nearby at this time.

The age of the oolites and cement fragments is problematical.They could be;

i. Pre Carboniferous limestones of Ordovician, Silurian or Cambrian age that clearly have undergone a long and varied sequence of diagenesis, alternatively, they could be;

ii. Lower Carboniferous.

The Limestone conglomerate fills channels cut into the basal Lower Carboniferous. It is unikely that this sequence, in this area or beyond, had been buried to sufficient depths to allow burial cementation (Braithwaite pers commn 1991). This suggests that these clast were derived from Cambrian, Silurian or Ordovician limestones exposed during the Late Devonian-Lower Carboniferous transgression. However, Ashton (pers commn 1992) suggested that such limestones are as yet unknown in the area, suggesting the cement fragments are 'exotic'. Owen (pers. commn. 1993) noted that Upper Ordovician outcrop at Kildare and similar clasts have been recorded from the basal Carboniferous of the Clair Basin and are believed to have been derived from the Cambrian Durness Limestone (Blackbourne, 1987).

2.4.v. Sedimentology of the Limestone Conglomerate.

The Limestone Conglomerate fills and is confined by the channel forms described in section 2.3. Recent tidal channels are also filled by sediment ranging from gravel to sand grade, often arranged in fining up units. Sedimentary structures of Recent channels include graded bedding, mega ripples and sand waves. Bluefish channel (Jindrich, 1969), is filled by pebbly-medium grade carbonate sand. This consists of forams, molluscs, fragments of supratidal mudstones and Pleistocene bedrock sourced along the entire length of the channel. The major bed forms present are plane bedding and straight crested mega ripples up to 35 cm high with internal crossbedding. The Limestone Conglomerate is comparable to the channel fill sediment of Bluefish channel, specifically in terms of grain size, texures and sedimentary structures and is interpreted as reflecting a similar channel fill deposit.

Sedimentary structures of the Limestone Conglomerate provide an insight into depositional procceses. Graded beds and fining up units demonstrate that deposition occured abruptly by decelerating currents (Hjulstrom, 1939). Sharp contacts indicate that some fining up units were trucated by erosion surfaces. Thin black shales show that deposition of carbonate sediment was occasionally overcome by siliciclastic sedimentation from suspension. Cross bedding is a common feature of migrating sands (Selley, 1985) and suggestes that the Limestone Conglomerate was arranged into large ripples or wave like structures up to 50 cm in height.

The Limestone conglomerate was sourced by a hinterland consisting of lithified limestones, Red Beds and igneous and high grade metamorphic rocks. Oolites and bioclasts indicate that the open marine environment was also supplying sediment to the channel. The in-channel mixing of land derived sediment with material from the adjacent marine environment suggests alternate shoreline and seaward directed current activity. Such activity could be satisfied in an area of strong tidal currents. Similar channel fill

sediments in the Miocene of the Sirte basin (Selley, 1967) also contain mixed marine and terrigenous sediment, interpreted as reflecting tidal activity.

2.4.vi. Petrography.

Fourteen thin sections of the Limestone Conglomerate have been examined using transmitted light microscopy and cathodoluminescence (CL). The coarse grain size and small diameter of the drill cores demanded caution to ensure that indigenous diagenetic features, and not those occuring within clasts were described. Petrographic features include calcite and dolomite cements, compaction, dissolution and silicification.

1. Surfaces of some allochems have been bored by endolithic algae and borings filled with microspar to produce dark micrite envelopes.

2. Four types of calcite cement are present, granular isopachous, granular, syntaxial overgrowths and blocky. i. The isopachous cements are cloudy and contain inclusions. They typically show dull brown-orange luminescence. ii Granular cement crystals are scalenohedral with few inclusions. They display a dull orange luminescence with a thin light orange outer zone (Plate 2.6.A). iii. Syntaxial overgrowths display cloudy inclusion rich pinnacled inner zones and thick clear outer zones. Under CL these inner zones show the same luminescence as the granular cements (Plate 2.6. B).

3. Blocky calcite crystals increase in size away from the substrate. They are clear but contain floating fragments of micrite envelope with attached cements. Under CL they are generally dull but there are a number of centripetal zones (Plate 2.6. C). A dark brown orange zone is followed by a thin bright sequence consisting of orange and light orange zones. A second dark brown orange zone is overlain by three couplets consisting of a brown orange inner zone grading into a dark brown outer zone. This is sequence is followed by a light orange zone which forms a useful marker. This zonal sequence also forms the clear outer fraction of the syntaxial overgrowths.

3. The zonal sequence occurring in the blocky calcite has been locally truncated by an irregular surface indicating a dissolution event. This surface is overlain by coarse euhedral dolomite cement which displays the curved crystal faces and sweeping extinction, typical of saddle dolomite (Radkhe & Mathis, 1980). The cores of such crystals are non-luminescent while margins have a thin bright red rim containing faint darker zones (Plate 2.6.D.). Matrix selective dolomite also replaces calcite cement with individual crystals displaying the same luminescent characteristics as the saddle dolomite.

6. Mechanical and chemical compaction have taken place. Mechanical compaction has resulted in fracture of elongate grains (refer Plate 2.6.A). Fracture surfaces do not display granular cements indicating that grain failure post dates granular cementation. Chemical

compaction has resulted in grain penetration and the formation of dissolution seams (Wanless, 1979), typically sutured seam stylolites with associated insoluble residue.
7. Dissolution of unstable presumably aragonite bioclasts occurred leaving micrite envelopes. Locally these have collapsed.
8. Authigenic quartz occurs as overgrowths on detrital grains and partially replacing allochems. Crystals are typically euhedral but contain numerous carbonate inclusions (Plate 2.6.E.).
9. Subvertical fractures are filled with either equant blocky calcite cement or micritic internal sediment overlain by calcite cement (Plate 2.6.F.).

4.2.vii. Paragenetic sequence.

Using data from Scholle (1978) the lithoclasts and bioclasts constituting the cement substrate were of varied composition. Former high magnesium calcite is represented by crinoids and echinoids grains, aragonite is inferred from shell shaped moulds, and low magnesium calcite is represented by mudstone lithoclasts and some bioclasts, typically brachiopods. Porosity was primary interparticle with some intra-skeletal pores, typically the zooeica of bryozoan fronds.

Diagenesis began on the sea floor with boring of some bioclasts by endolithic algae. Holes were filled to produce micrite envelopes. Aragonite is more soluble than calcite and undergoes dissolution in the presence of acidic meteoric water (Bathurst, 1964). Shell shaped moulds outlined by micrite envelopes show that through flow of meteoric water and dissolution of aragonite has taken place with congruent generation of mouldic porosity.

Pores are lined with the cloudy isopachous calcite which is overlain by the granular cements. Cloudy cements have been interpreted as forming in meteoric-phreatic conditions (Harris *et al,* 1985; Moore, 1989; Harwood, 1989). Very similar cements occur in the Pleistocene Belmont formation of Bermuda (Land, 1970).

The earliest portions of syntaxial crystals are also cloudy and share the CL sequence as the cloudy cements indicating that the growth of the two types of crystal began contemporaneously. Syntaxial cements grow in optical continuity with their host (Evamy & Shearman, 1965) and growth is accompanied by conversion of the grain from high to low magnesium. calcite. This place takes place by incongruent dissolution in which Mg^{2+} is exported as $MgCO_3$ without destruction of the crystal lattice.

The lack of granular cements on fracture surfaces within bioclasts indicates that mechanical compaction was the next event. In some sections extensive chemical dissolution has taken place with much grain interpenetration. This implies that pre-compaction cementation was not pervasive.

PLATE 2.6. Limestone Conglomerate diagenetic features.

A. Photomicrograph (CL) of granular cement trucated by fracture (F) cutting across bioclast. Hole N986 at depth 486.4 m. Scale bar = 500 microns.

B. Photomicrograph (CL) of syntaxial overgrowths (O) and circumgranular calcite cements developed on (E) echinoderm grains and overlain by blocky calcite cement (C). Hole N763, at depth 512.2 m. Scale bar = 500 microns.

C. Photomicrograph showing CL sequence of blocky calcite. Hole N763 at depth 512.2 m. Scale bar = 500 microns.

D. Photomicrograph (CL) of intraskeletal pore filled by saddle dolomite, note dissolution surface (arrow). Hole N763 at depth 512.2 m. Scale bar = 500 microns.

E. Photomicrograph (plane light) of authigenic silica replacing trilobite fragment (arrow). Note inclusion of dolomite (arrow). Hole N986 at depth 486.4 m. Scale bar = 250 microns.

F. Photomicrograph (plane light) of fissure filled by cement overlain by micritic sediment reflecting repeated dilation. Hole N985 at depth 507.3 m. Scale bar = 500 microns.

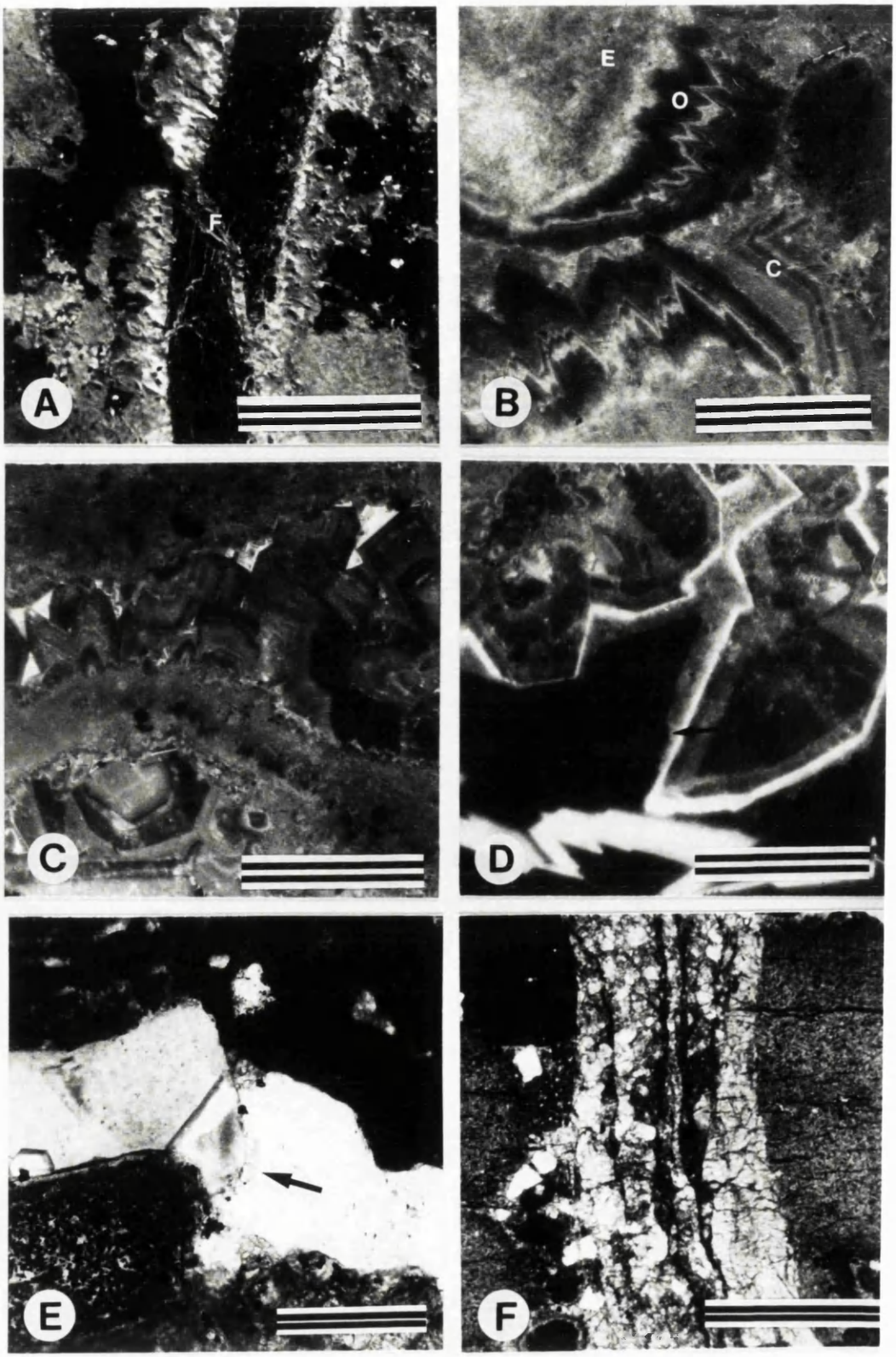
F
A
E
O
C
B
C
D
E
F

The blocky calcite is the youngest calcite cement; it overlies isopachous, granular and and syntaxial cements. In addition the blocky cement overlies fracture surfaces within bioclasts and includes fragments of micrite envelopes indicating that it post dated collapse events. The late timing, dull luminescence and blocky textures suggest that it formed during burial. Reviews by Harwood (1989), Tucker (1990a), Harris *et al* (1985) and Moore (1989) interpret blocky, ferroan and dully luminescent calcite as reflecting burial cementation. Growth of the burial cements was interupted by a dissolution event which truncated the sequence and redefined pores. The overlying saddle dolomite is widely believed to precipitate from saline fluids at in a temperature field of 60^0C to 150^0C (Radkhe & Mathis, 1980). The replacive dolomite has the same CL characteristics as the Saddle dolomite suggesting that the two were contemporaneous. Authigenic quartz replaces allochems and calcite spar and contains dolomite rhombs. This indicates that it must post date dolomitization and is therefore a burial phenomenon.

Brittle fractures postdate all these events. Fractures are filled with blocky dully luminescent calcite spar. In some fractures this cement is overlain by micritic internal sediment indicating continued dilation and downward infiltration of sediment and suggesting proximity to the surface. These fractures can be thought of as a type of neptunian dyke (Smart *et al*, 1988).

2.5. THE MUDDY LIMESTONE.

2.5.i. Introduction.

The Limestone Conglomerate and Laminated Beds are overlain by the Muddy Limestone. This was formerly referred to as the 'C-A' Unit and considered as part of the Laminated Beds by Philcox (1984). The boundary is seen in hole N286 where the Muddy Limestone is approximately 12 m thick.

4.5.ii.Description.

The Muddy Limestone is a dark, locally silty, bioclast mudstone-wackestone. The silty units are generally darker and silt may be either finely disseminated or form beds up to 1 to 2 cm thick (Plate 2.7.A). Rare light grey fine sand grade bioclast packstones up to 1.3 m thick are present in hole N994. These also contain thin dark silty partings. Fossiliferous black calcareous shales, known as the **Fine Silty Unit,** occur in the sequence and are up to 1 to 2 m thick in hole N998. They contain anastomosing silty laminae and, locally irregular sandy layers 1 to 2 cm thick (Plate 2.7.B.). In several holes, N999 (459.4 m), N997 (462.1 m) and N1020 calcite mudstones up to 8 cm thick, occur at the base of the Muddy Limestone. Thin bioclastic layers 1 to 2 cm thick are also

present. The contacts between these different lithologies are generally gradational and are often obscured by burrowing. Approximately two metres above the base of the Muddy Limestone and again four metres above this, prominent coral bearing beds occur containing *Syringopora reticulata* (Andrew & Ashton, 1985). Corallites are upward and outward branching (Plate 2.7.C.). Both layers can be correllated over wide areas but they are locally absent, indicating that they are laterally discontinuous. The coral *Michelina favosa* has also been reported (Andrew & Ashton, 1985). The main features of the Muddy Limestone are summarised in Fig. 2.15.

Bioclasts within the muddy limestones have diameters up to 1 to 2 mm. Fragments of endo and impunctate brachiopods are common with spiriferids attaining over 3 cm width, some filled with light grey calcite mudstone. Two varieties of brachiopod spine are present, one consisting of concentric zones, the other of an inner concentric and an outer prismatic zone. Echinoid fragments with mud filled stereome occur. Other bioclasts include echinoid spines, crinoid ossicles, ostracods, fenestrate bryozoan fragments, miliolid foraminiferids, trilobite cuticles, fragments of solitary rugose corals up to 1.5 cm diameter and filamentous algal lumps. Non-skeletal allochems include lithoclasts of calcite mudstone, occasional ooliths and shale flakes.

Visual estimation suggests that siliciclastic components form 30% of the sediment. Grains are angular and three types of quartz grain are present, monocrystalline, grains showing undulose extinction and polycrystalline grains. Plagioclase, orthoclase and microcline feldspar are present, all show some alteration. Other grains include muscovite flakes and altered rock fragments.

The Muddy Limestone is exposed in the 1230 level and is thinly bedded in units 2 to 3 cm thick. Beds contain laminae, some of which anastomose. Many beds have been extensively burrowed and vertical and horizontal burrows 2 to 3 mm diameter are filled with silt containing spreite. The mixing by bioturbation of argillaceous layers and non argillaceous layers gives the rock a mottled appearence.

The Muddy Limestone contains a channel system which is spatially related to the channel in the Laminated Beds A cross-section was constructed through the channel system (see Fig. 2.13) which indicates the channels are 'stacked' with younger channels cutting down into older (Fig. 2.16). The cross-section shows that individual channels are symetrical and up to 300 m wide and 15 m deep. The base of the channel system is sharp with channels filled by Limestone Conglomerate (Plate 2.7.D). Part of the channel system is exposed in 1 Zone, block 19, 1150 level where it truncates bedding and extends laterally for over 15 m (Fig. 2.17).

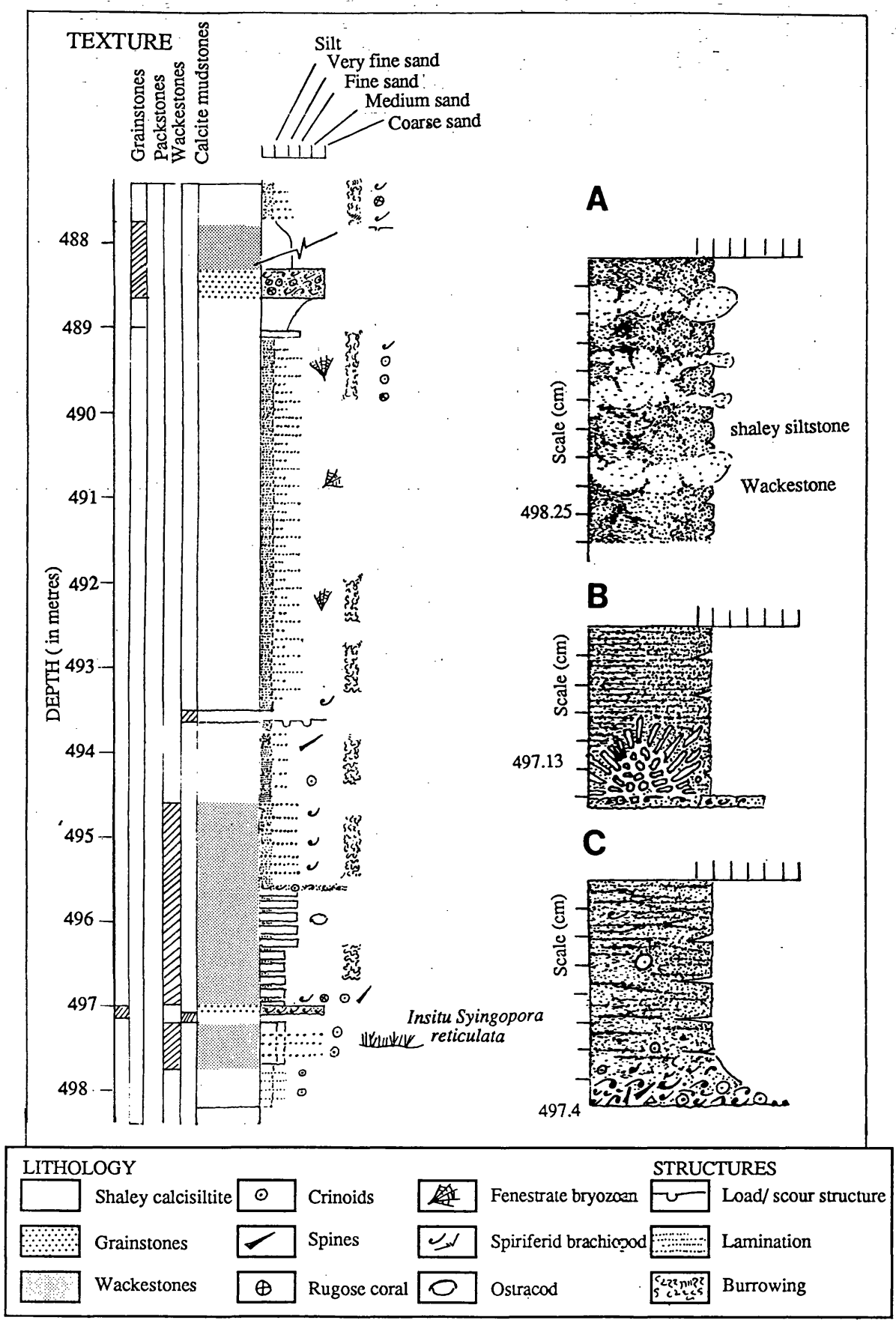

Fig. 2.15. Summary log of Muddy Limestone, hole N975. 'A' detail of wackestones - shaley siltstone interbeds. 'B' detail of *Syingopora reticulata*. 'C' detail of contact with Limestone Conglomerte showing anastomosing laminations.

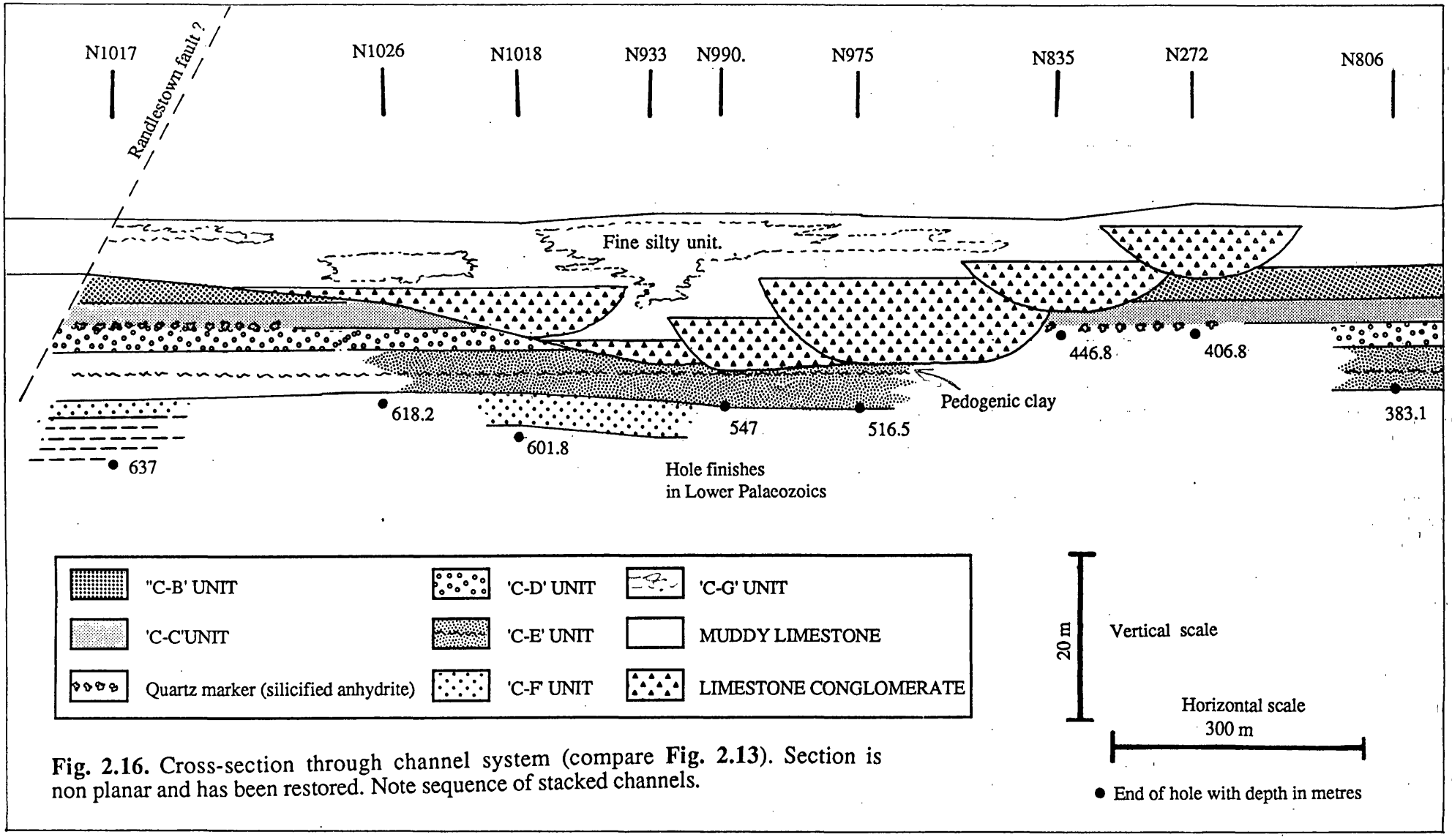

Fig. 2.16. Cross-section through channel system (compare **Fig. 2.13**). Section is non planar and has been restored. Note sequence of stacked channels.

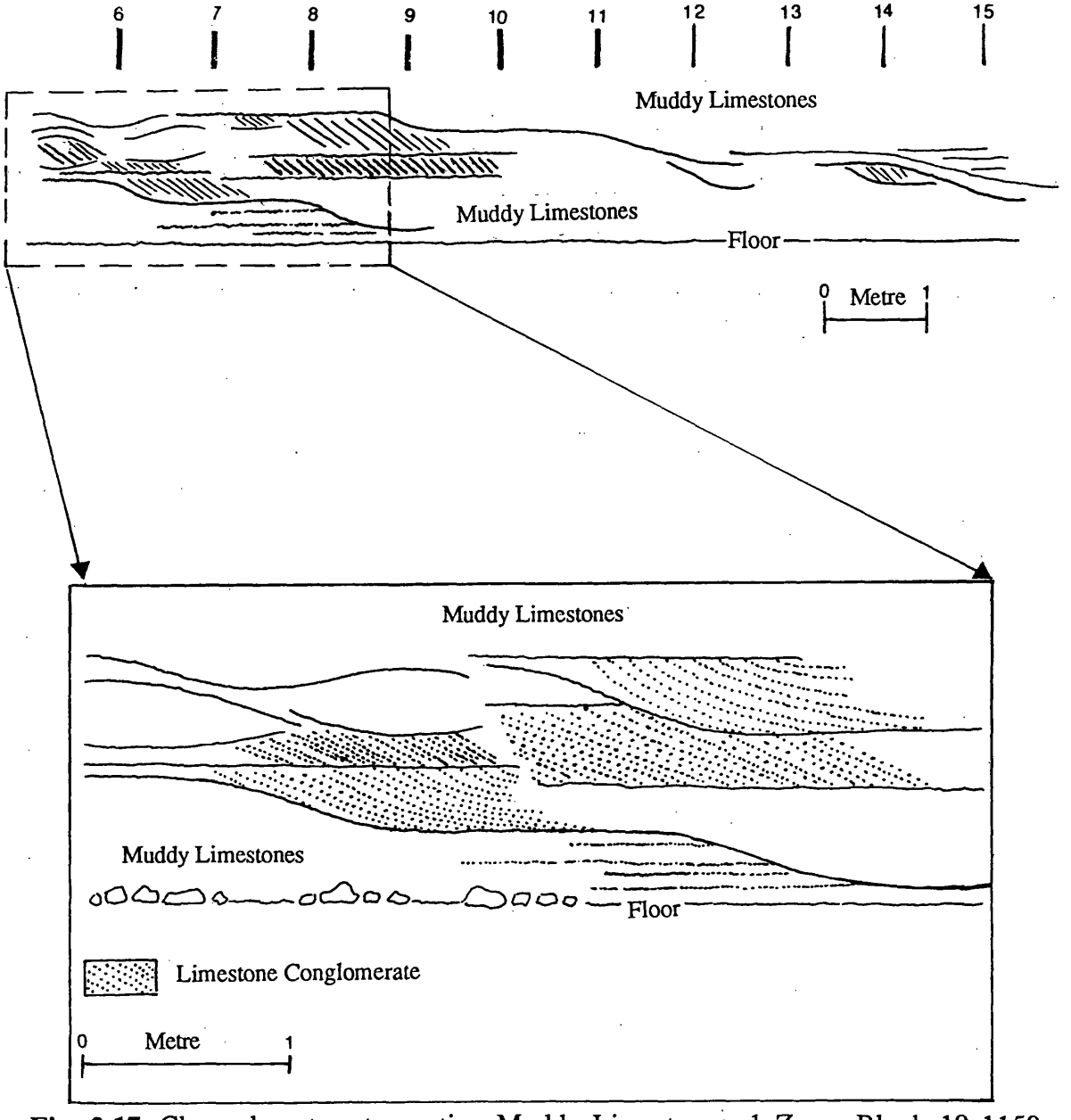

Fig. 2.17. Channel system truncating Muddy Limestones. 1 Zone, Block 19 1150 mine level. Note extensive cross-bedding in channel fill Limestone Conglomerate with young channels truncating old channels.

PLATE 2.7. Sedimentological features of the Muddy Limestone.

A. General view of silty mudstone-wackestone, note brachiopod filled by clean calcite mudstone (arrow). Hole N975. Scale in centimetres.

B. Black fossiliferous shale of the Fine Silty Unit. Hole N998 depth unrecorded.Scale in centimetres.

C. *In situ Syringopora reticulata,* note upward and outward growth of corallites. Hole N1021. Scale in centimetres.

D. Muddy Limestone overlain abruptly by Limestone conglomerate. Hole N1035 depth 634.6 m. Scale in centimetres.

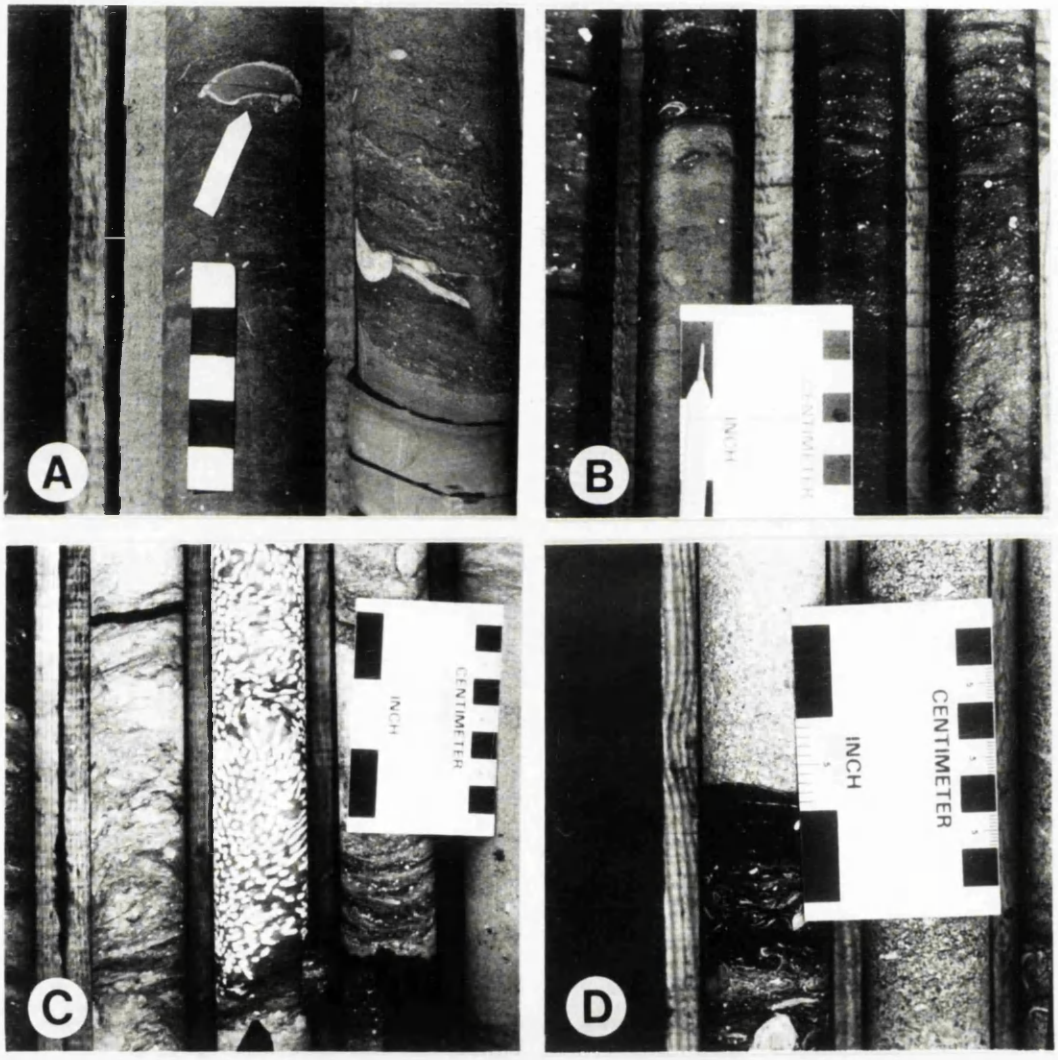
A
B
INCH
CENTIMETER
C
CENTIMETER
INCH
D
CENTIMETER
INCH

2.5.iii.Sedimentology.

Wackestones-packstones are common in Recent carbonate environments occurring in sheltered bays and lagoons of the Trucial coast and the Florida shelf (Tucker, 1990b p. 87 to 96) and the Bahamas (Shinn, 1983 p.172). They are also very common in the geological record (Flugel, 1982). Burrowed horizons in the Muddy Limestone show that substrates were soft and sedimentation rates slow enough to allow colonisation by burrowing fauna. *In situ Syringopora reticulata* shows that the lagoon floor was periodically colonised by corals.

The bioclast assemblage, consisting of spiriferid brachiopods, rugose corals, *Syringopora reticulata*, fenestrate bryozoa and crinoids is stenohaline and indicates an environment of normal marine salinity (Wilson & Jordan, 1983 p.301) with water depths of around 10 to 15 m or less where carbonate production is currently at its highest (review by Tucker, 1990b p.33).

Thin bioclast layers suggest winnowing by surface currents perhaps generated by tidal activity. Similar lag gravels in the English Channel are also believed to reflect winnowing by tides and waves (Larsonner *et al*, 1982). Spiriferid brachiopods, filled by clean light grey calcite mudstone indicate they were derived, perhaps from adjacent lagoonal environments. Layers of shale and dark silty mudstone-wackestones show that there were periodic influxes of siliciclastic muds. Mixed carbonate-siliciclastic lagoons are common in Recent carbonate environments. Around the coast of Puerto Rico, lagoons floored by calcite muds are being filled by both terrigenuous muds and silts and marine carbonate sand (Pilkey & Bush, 1988). The seaward margin of the Belize shelf is rimmed by reefal carbonates (Sellwood, 1986, p.311). These pass landward into a narrow lagoon varying from 6 to 60 m depth. This is floored by carbonate mud, a product of carbonate breakdown. Rivers supply terrigenous material which is deposited on the lagoon floor with 50 to 85% carbonate mud during periods of low current activity. Bioclasts present include miliolid forams, molluscs and ostracods derived from nearby sand shoals during storms.

The muddy limestone contains a channel sequence. Like the channels cut into the Laminated Beds these channels are filled by Limestone Conglomerate. Figure 2.17 shows the channel cut into the Laminated Beds plus the channels formed during the deposition of the Muddy Limestones. The proximity of these channels to the channel cut into the Laminated Beds indicates the same onshore source and suggests these channels were also tidally generated. A similar sequence occurs in the Miocene of the Sirte basin of Libya (Selley, 1968). Here a mixed carbonate clastic shoreline sequence consisting of lagoonal and barrier deposits is cut by a sequence of channels up to 300 m wide x 10 m deep, floored with conglomerate (lag gravels). These pass up into calcareous sandstones

containing calcite mudstone pebbles, some with borings. Graded bedding and trough cross bedding in sets up to 50 cm are common.

2.5.iv. Petrography.

The petrographic features relate to only one thin section of bioclast wackestone. The main features include calcite cement, dolomite, silicifcation and compaction.

1. Calcite cement lining pores is prismatic, cloudy and full of inclusions. Crystals show intersecting cleavage and sweeping extinction. These features are consistent with radiaxial fibrous calcite (Kendal & Tucker, 1973). Staining reveals that these crystals have relatively iron rich outer rims (Plate 2.8.A). Under CL they display dark orange cores and lighter rims.
2. Micrite internal sediment is present partially filling intraskeletal cavities.
3. Mechanical compaction has resulted in crushing of brachiopod spines and ostracod valves (Plate 2.8.B.).
4. Single inclusion rich euhedral crystals of dolomite are present in the matrix, in cements, and in allochems (Plate 2.8.C.). Staining reveals some blue zones which under CL are non luminescent. Some display sweeping extinction, consistent with saddle dolomite (Radkhe & Mathis, 1980). Micro rhombic crystals are common in echinoderm and crinoid fragments. These do not stain and under CL they display dark brown cores surrounded by brighter outer zones. They are interpreted as microdolomites.
5. Some shell fragments have been replaced by patchy chalcedonic silica or euhedral authigenic quartz (Plate 2.8.D.).

2.5.v. Petrographic interpretation.

Only a few large pores were present before the onset of cementation. Typically these were intraskeletal and confined to ostracod valvesand the lumen of brachiopod spines. Radiaxial fibrous calcite has lined these pores, locally occluding them. This type of cement is believed to reflect diagenesis in a marine phreatic environment (Kendall, 1985). This was followed by deposition of micritic internal sediment. Mechanical compaction, resulting in crushing of ostracod tests, suggests that cementation was not pervasive. Cementation is often accompanied by conversion of high magnesium to low magnesium calcite. This proccess has been termed incongruent dissolution (Land, 1967; Bathurst, 1974) since magnesium is lost without disruption of the carbonate lattice, and balanced by import of Ca^{2+}. However microdolomite in the echinoderm tests shows that some magnesium was used to form dolomite (Leutlhoff & Myers, 1984).

Dolomite has also replaced the muddy matrix. The precise timing of this in relation to earlier diagenetic events is unclear, but the saddle texture indicates a burial origin. The

PLATE 2.8. Photomicrographs (plane light) of Muddy Limestone diagenetic features.

A. Radiaxial calcite cement filling intraskeletal pore and overlain by internal sediment (s). Hole N975, depth 495.3m. Stained thin section. Scale bar = 250 microns.

B. Crushed ostracod in muddy siltstone. Hole N975, depth 495.3 m. Scale bar = 250 microns.

C. Authigenic dolomite in muddy siltstone. Hole N975, depth 495.3 m stained thin section.Scale bar = 100 microns.

D.Silicified brachiopod shell in hole N975 at depth 495.3 m.Scale bar = 250 microns.

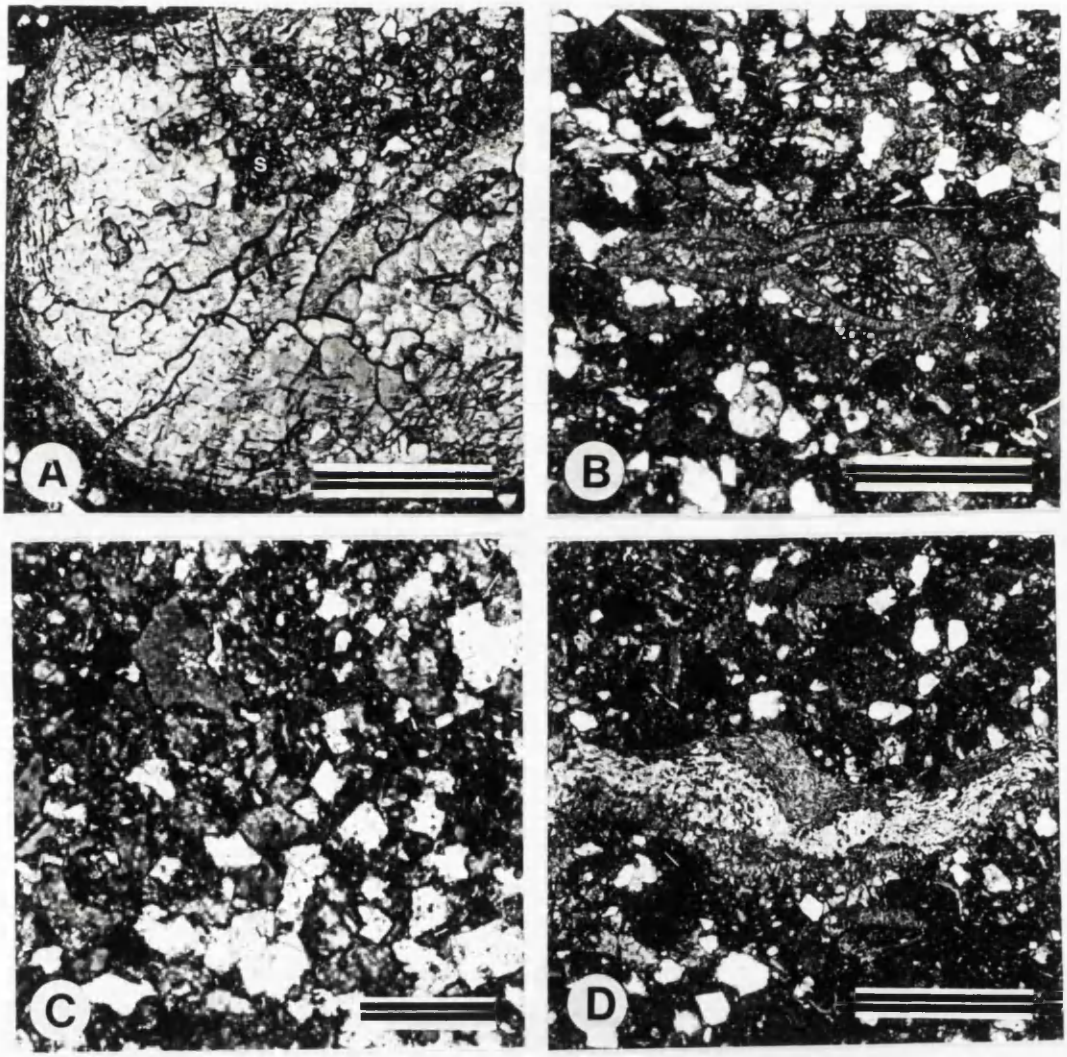
A
B
C
D

timing of silicification is also problematical. but in the adjacent Limestone conglomerate it is obviously post burial dolomitization. The final diagenetic events were pressure dissolution and the formation of sutured seam stylolites, and the formation of joints filled by calcite cements.

2.6. SEDIMENTOLOGICAL SYNTHESIS OF SEQUENCE RED BEDS-MUDDY LIMESTONE.

The Lower Carboniferous marine transgression was reflected at Navan by a change from continental Red Bed fluviatile sediments to shallow marine deposits represented by the silty shales of the 'C-G' Unit of the Laminated Beds. These were overlain by a prograding barrier sandstone sequence represented by the 'C-F' Unit which is in turn overlain by back barrier lagoonal silty shales. Plant fragments within this part of the sequence indicate a transition from an arid climate during deposition of the Red Beds to a more humid climate during C-F to C-E Unit times. Pedogenic structures in the overlying green clay show that emergence followed, culminating in the formation of a palaeosol. Above the green clay carbonates appear for the first time.

The sequence overlying the green clay is transgressive. It begins with reworked algal laminated limestones interpreted as reflecting an arid tidal flat. The algal limestones are overlain by lagoonal burrowed sediments which contain oncoids. The lagoon was filled by calcareous silt of the 'C-D' Unit, forming a shallowed up sequence culminating in hypersaline conditions and precipitation of sabkha anhydrite, suggesting a return to a more arid climate. This is represented by the silicified nodular mosaic anhydrite of the quartz marker. Truncation of the evaporite by an erosion surface indicates a second period of emergence. As will be shown in chapters 3 and 4, emergence became common during deposition of the Pale Beds.

The evaporites are overlain by the interbedded silty shales and calcite mudstones of the 'C-C' Unit. These are again interpreted as lagoonal, but perhaps containing thin prograding tidal flat deposits. The bioclast packstones of the 'C-B' Unit indicate a relative rise in sea level and a return to shallow marine conditions.

The whole sequence is trucated by large tidal channels which must have extended into the shallow marine environment. These are filled by Limestone Conglomerate sourced from an adjacent landmass composed of limestone, Red Beds and igneous and high grade metamorphic rocks. The Muddy Limestone blanketing this sequence is interpreted as representing a mixed carbonate siliciclastic lagoon which was again dissected by tidal channels. The Muddy Limestone passes gradationally up in to the Micrite Unit which forms the subject of the next chapter.

3.1. INTRODUCTION.

The Micrite Unit is up to 60 m thick and consists of four principle lithologies, mudstones, wackestones, packstones and grainstones, together with thin black shales and minor green clay. The sequence is shown Fig. 3.1. Characteristic sedimentary structures include fenestral horizons, cryptalgal lamination and oncoids together with brecciated and dissolution surfaces. Lithologies and structures are grouped to form approximately twenty sedimentary cycles. Petrographic features incude microstalactitic, acicular isopachous and blocky calcite cements together with crystal silts, dissolution of aragonite and features of compaction.

3.2. LITHOLOGIES.

3.2.i. Muddy lithologies.

Calcite mudstones are dark brown when fresh and structureless, breaking with a conchoidal fracture. In thin section, irregular patches of microspar are present which under CL, show a dull orange luminescence. A few silt and sand grade allochems include bioclasts and calcispheres together with finely disseminated opaque grains which are probably organic material. Bioclastic wackestones and packstones consist of fragments of brachiopods, brachiopod spines, bivalves, gastropods, corals, miliolid and fusilinid foraminifera *(Ammodiscus?)*, ostracods, and phylloid algae. Other grains include, ooliths and pellets. The matrix is a dark brown calcite mudstone (Plate 3.1. A.B). Significant sections of mudstones and wackestone are homogeneous with no visible structures. This suggests that the sediment has been thoroughly bioturbated.

Coated grains occur in both mudstones and wackestones. They are up to 3 cm diameter and form laterally discontinuous beds up to 1 m thick extending laterally up to 350 m. Each coated grain contains a nucleus of either a bioclast or lithoclast, the shape of the grain reflecting the shape of the nucleus (Plate 3.1.C.). The grain cortices consist of concentric overlapping micrite laminae and contain a radially branching network of tubules oriented normal to the lamina surfaces. Tubules are approximately 100 microns in diameter and filled with microspar, the pattern is consistent with a porostromate texture described by Monty (1981). The grains are interpreted as oncoids. Similar oncoids have been described from the Lower Carboniferous Llanelly formation of South Wales by Wright, (1983) who attributed them to the genus *Garwoodia* (Garwood, 1931). Tabular lithoclasts of oolite and mudstone (Plate 3.1.E-F) occur within the mudstones. Wedge shaped cracks extend 90^0 from one surface and are 1 mm wide at the surface and taper inwards. The clasts are interpreted as desiccation fragments containing desiccation cracks. The lilthoclasts differ lithologically from the underlying calcite mudstones indicating they cannot be diagenetic nodules.

The muddy lithologies contain abundant spar filled cavities with diameters greater than intergranular pores and are classified, according to Tebbut (1965), as fenestrae. Logan, (1974) defined three types of fenestrae, laminoid, irregular and tubular, each subdivided according to size as fine, medium or large (Fig. 3.2). All three types occur in the Micrite Unit. Approximately 20 fenestral horizons occur within the Micrite Unit. These are up to 5 m thick and can be traced laterally for 750 m to 1000 m. These horizons contain all three types of fenestrae. Laminoid fenestrae are from fine to medium and occur within and between individual laminae which are typically 1 to 2 mm thick. They may be planar or gently undulose. Irregular fenestrae range from fine to coarse and occasionally define a crude stratification (Plate 3.1.F). Tubular fenestrae associated with them are subvertical and slightly sinuous, with a maximum diameter of 2 mm and a length in section of up to 15 mm. Laminoid and irregular fenestrae form distinct alternating horizons best seen in holes N1014 and N1037 at depths 556 m and 472.5 m (Fig.3.3).

Bedding is best developed in association with laminoid and irregular fenestrae. It is exposed underground in the 1130 drainage drift and the 1902 mine level. Beds are tabular and contain millimetre scale lamination and range in thickness from 5 to 30 cm (Fig. 3.4.) Layers of cryptalgal lamination (Aitken, 1967) occur in holes N351 (at depth 98.1m) and N864. Individual micritic laminae are 1 to 2 mm thick and form laterally linked columns of up to thirteen laminae which increase in width upwards (Plate 3.1.G.). In hole N864 at depth 499.8 m they form a layer 3 cm thick (Fig. 3.5). The uppermost layer of this sequence is dark and microspar fills spaces between individual columns. Fissures cutting vertically through the layers are interpreted as desiccation cracks.

3.2.ii. Grainstones.

A few grainstones occur within the muddy lithologies. These are up to 1 m thick in hole N975 and may be oolitic, pelletal or bioclastic. Where they are pelletal individual pellets are elliptical and structureless with a maximum diameter of 0.25 mm. Pelletal grainstones form beds up to 50 cm thick in hole EP27. Matrix supported shell layers 2 to 3 cm thick also occur within the mudstones. These consist of intact and disarticulated brachiopod tests filled with mudstone and beds can be traced laterally for up to 500 m (Plate 3.1. H.). Grainstones, wackestones, packstones and mudstones often form graded beds. The bases consist of either a grainstone or packstone passing up to wackestone then mudstone. Typically graded beds are up to 40 cm thick (Fig. 3.6.a.). Four thick lithologically distinct grainstones have been identified as having consistent stratigraphic positions. In stratigraphic order these grainstones are: oncoidal

PLATE. 3. 1. Features of the Micrite Unit.

A. Photomicrograph (plane light) of wackestone texture. Hole N975 at depth 440.7 m. Scale bar = 1 mm.

B. Photomicrograph (plane light) of packstone texture. Scale bar = 1 mm.

C. Oncolites in argillaceous calcite mudstones. Note shape of nulcei controlling the shape of individual oncoids. Hole N975 at depth 439.9 m. Width of drill core 3.5 cm.

D. Oolitic grainstone lithoclast. Hole N975 at depth 461.3 m. Scale bar = 1 cm.

E. Calcite mudstone lithoclast. Note 'v' shape fissures extending from upper surfaces (arrows). Hole N975 at depth 489.0 m. Scale in centimetres.

F. Irregular and laminoid fenestrae in calcite mudstone. Note planar bedding bounding upper surface of specimen. 1130 mine level, drainage drift, 2 zone. Scale in centimetres.

G. Photomicrograph (plane light) of cryptalgal lamination in calcite mudstones. The laminae display a sharp contact with the underlying calcite mudstones. Individual laminae consist of laterally linked columns which themselves consist of micritic laminae. Note general increase in column width vertically. Hole N351 at depth 98.1 m. Scale bar = 2 mm.

H. Layer of brachipods (?) shell fragments. The shell are dissarticulated, broken and abraded. Note faint mottling of calcite mudstones suggesting burrowing. Hole N975 at depth 440.6 m. Width of drill core 3.5 cm.

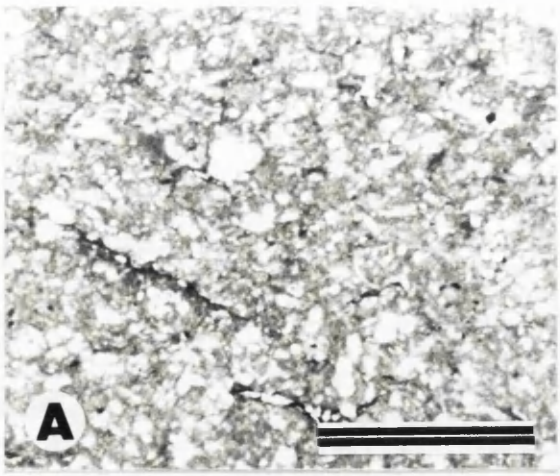
A

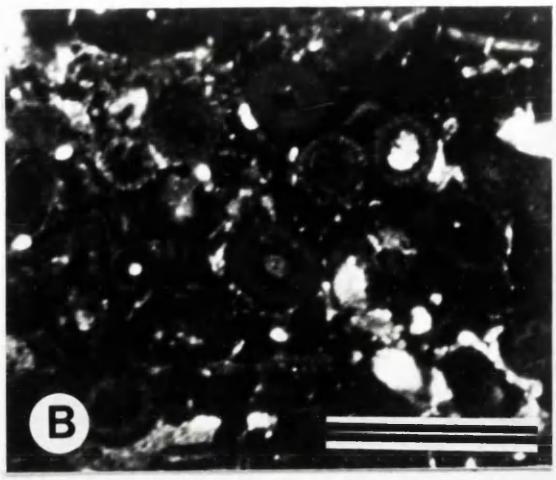
B


C

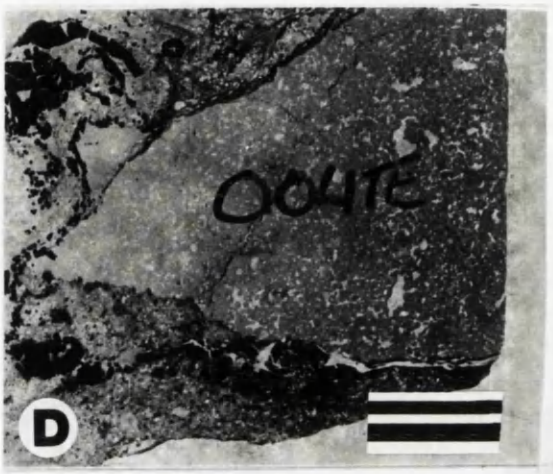
OOLITE
D

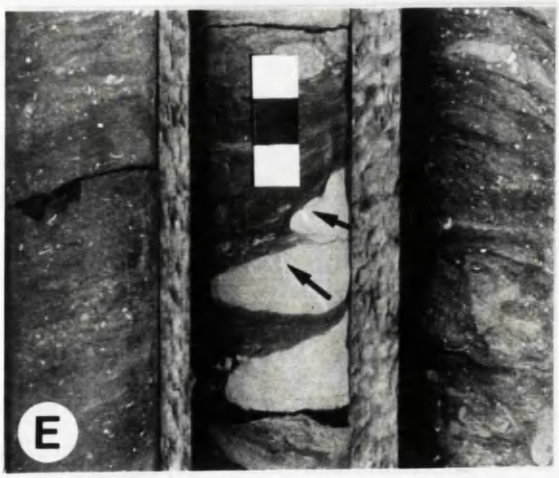
E

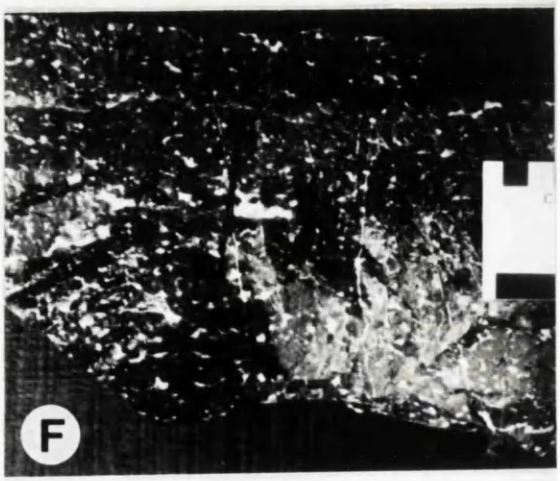
F

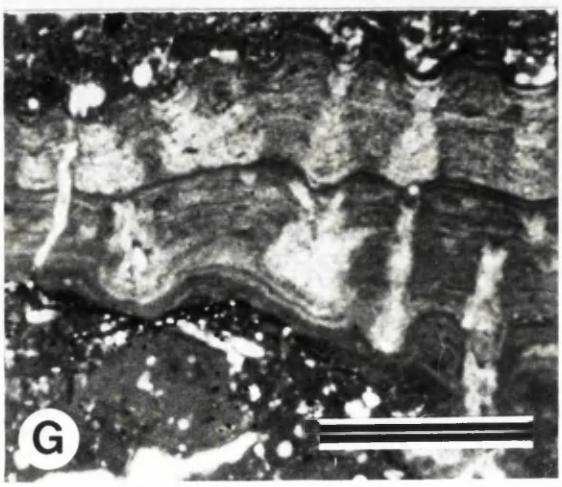
G


H

grainstones, calcite mudstone lithoclast grainstones, oolitic lithoclast grainstones and oolitic grainstones.

Oncoid grainstones form a 20 cm thick laterally discontinuous layer at the base of the Micrite Unit. The oncoids are "bun shaped" with flat bases (Plate 3.2.A). Laminae are asymmetric, increasing in thickness at the top and consist of overlapping and discontinuous concentric layers of micrite. Within these layers ooliths and bioclasts have accreted to the surface. Laminae are generally less than 0.25 mm thick and are separated by thinner layers of microspar presumed to represent a pore fill cement. Many oncoids are disorientated or inverted. Brachiopods and brachiopod shell fragments, gastropods, crinoid ossicles, and broken oncoids also occur.

Calcite mudstone lithoclast grainstones are also laterally discontinuous resting directly on the footwall green clay (see below). The average thickness is 30 cm with a maximum thickness of 1 m in hole N858. They appear to form lenses over 200 m in diameter. They are composed of angular mudstone lithoclasts, with some bioclasts and ooliths but include up to 25% angular silt grade quartz and feldspar grains (Plate 3.2.B). The unit consists of 2 cm thick graded laminae. The bases of the graded units consists of granule-coarse sands which pass up into fine sands (Fig. 3.6.b.).

Oolite lithoclast grainstones occur about 10 to 12 m above the base of the Micrite Unit and are up to 4 m thick and apparently laterally discontinuous. They are composed of irregular oolitic grainstone lithoclasts which are of coarse sand grade (Plate 3.2.C), and both grains and cement have been extensively dolomitized. Lithoclasts have been coated with up to three layers of micrite giving them a smooth rounded outline. Other grains include gastropod, crinoid and brachiopod fragments.

Oolitic grainstones are white-light grey and form a prominent marker approximately 12 m thick near the middle of the Micrite Unit (Fig. 3.7.). They have been extensively dolomitized and are then referred to as the **Five Lens Dolomite.** The processes and products of dolomitization will be discussed in chapter 5. The grainstones consist of ooliths and bioclasts ranging from very fine to very coarse. Ooliths are spherical to subspherical and radially concentric with well developed nuclei and cortices. The nuclei may be either detrital quartz grains or bioclasts, typically echinoderm or foraminiferan fragments (Plate 3.2.D). Surficial ooliths are also present. The fact that some bioclasts have dissolved while ooliths are unaffected points to an original calcitic mineralogy.

Bioclasts are diverse and include echinoderm plates, echinoid spines, crinoid ossicles and arm plates, bivalve and gastropod fragments, punctate and endopunctate brachiopods, brachiopod spines, algal lumps, and chambered foraminiferids (*Ammodiscus?)* and large fragments of *Syringopora reticulata.* Non skeletal grains

include pelloids and micritic intraclasts. Black shales 1 to 2 cm thick occur within these grainstones and are well developed in hole N975 where they occur every 1.5 to 2 m.

Structures in the oolitic grainstones include tabular bedding, exposed underground in the 1130 drainage drift where it ranges from 10 cm to 60 cm thick. Internal structures include planar lamination. Layering is often inclined, indicating the grainstones are cross-bedded in sets up to 50 cm thick (Plate 3.2.E). Foresets are gently curving, dipping at 15° to 20° from the horizontal. Ripple cross lamination occurs along the tops of bedding planes (Plate 3.2.F) in the 1130 drainage drift (Fig. 3.8.). Horizontal and vertical burrows approximately 1 cm in diameter and more than 15 cm long disrupt lamination. These are consistent with the *Skolithos* ichnofacies (Plate 3.2.G). Horizontal sinuous borings occur in the grainstones They are over 3 cm long with sharp margins which truncate both grains and cement and are filled with geopetal muddy sediment containing fragments of ooliths and intraclasts (Plate 3.2.H).

The subsurface distribution of the oolitic grainstones is shown in Fig. 3.9 (refer also Appendix 1). The lithosome extends to the western and southern mine area, to the present limits of exploration drilling. Similar lithologies also appear in the Clogherboy deposit approximately 3 km to the southeast. The oolites are about 30 m thick at Clogherboy (bore holes EP4A and N1011) thinning to less than 9 m at the northwestern limit of the Navan licence. Oolites are absent in boreholes N1005 and N864 suggesting the NW limit of the grainstone body. However thinning is not uniform, contours indicate two parallel ridges striking NW-SE and approximately 700 m apart.

3.2.iii. Siliciclastics.

The muddy lithologies and grainstones commonly contain up to 5 to 10% angular silt-sand grade siliciclastic grains. Four types of quartz grain occur, polycrystalline, polycrystalline sheared, strained grains displaying undulose extinction, and monocrystalline grains, together with grains of plagioclase feldspar and flakes of muscovite. In addition to these, however, thin siliciclastic beds occur at a number of intervals. These are predominantly fine grained but are lithologically distinct, a few occupy precise positions in the sedimentary sequence.

Black calcareous fissile shales occur within mudstones, wackestones and packstones. These are typically a maximum of 10 cm thick and overlie and fill brecciated surfaces where the shale locally forms coatings around clasts. Irregularly sculptured erosion surfaces, described in section 3.3, are overlain by up to 0.5 m of dark friable, siliciclastic sediments first recognised by Anderson (1990). These are structureless silty clays containing angular lithoclasts of calcite mudstones-wackestones up to 2 cm in diameter (Fig 3.10.). These are locally so numerous as to be grain supported. The margins of some clasts have been micritized (Plate 3.3.A). Discrete silty

PLATE. 3. 1. Features of the Micrite Unit.

A. Photomicrograph (plane light) of wackestone texture. Hole N975 at depth 440.7 m. Scale bar = 1 mm.

B. Photomicrograph (plane light) of packstone texture. Scale bar = 1 mm.

C. Oncolites in argillaceous calcite mudstones. Note shape of nulcei controlling the shape of individual oncoids. Hole N975 at depth 439.9 m. Width of drill core 3.5 cm.

D. Oolitic grainstone lithoclast. Hole N975 at depth 461.3 m. Scale bar = 1 cm.

E. Calcite mudstone lithoclast. Note 'v' shape fissures extending from upper surfaces (arrows). Hole N975 at depth 489.0 m. Scale in centimetres.

F. Irregular and laminoid fenestrae in calcite mudstone. Note planar bedding bounding upper surface of specimen. 1130 mine level, drainage drift, 2 zone. Scale in centimetres.

G. Photomicrograph (plane light) of cryptalgal lamination in calcite mudstones. The laminae display a sharp contact with the underlying calcite mudstones. Individual laminae consist of laterally linked columns which themselves consist of micritic laminae. Note general increase in column width vertically. Hole N351 at depth 98.1 m. Scale bar = 2 mm.

H. Layer of brachipods shell fragments. The shells are disarticulated, broken and abraded. Note faint mottling of calcite mudstones suggesting burrowing. Hole N975 at depth 440.6 m. Width of drill core 3.5 cm.

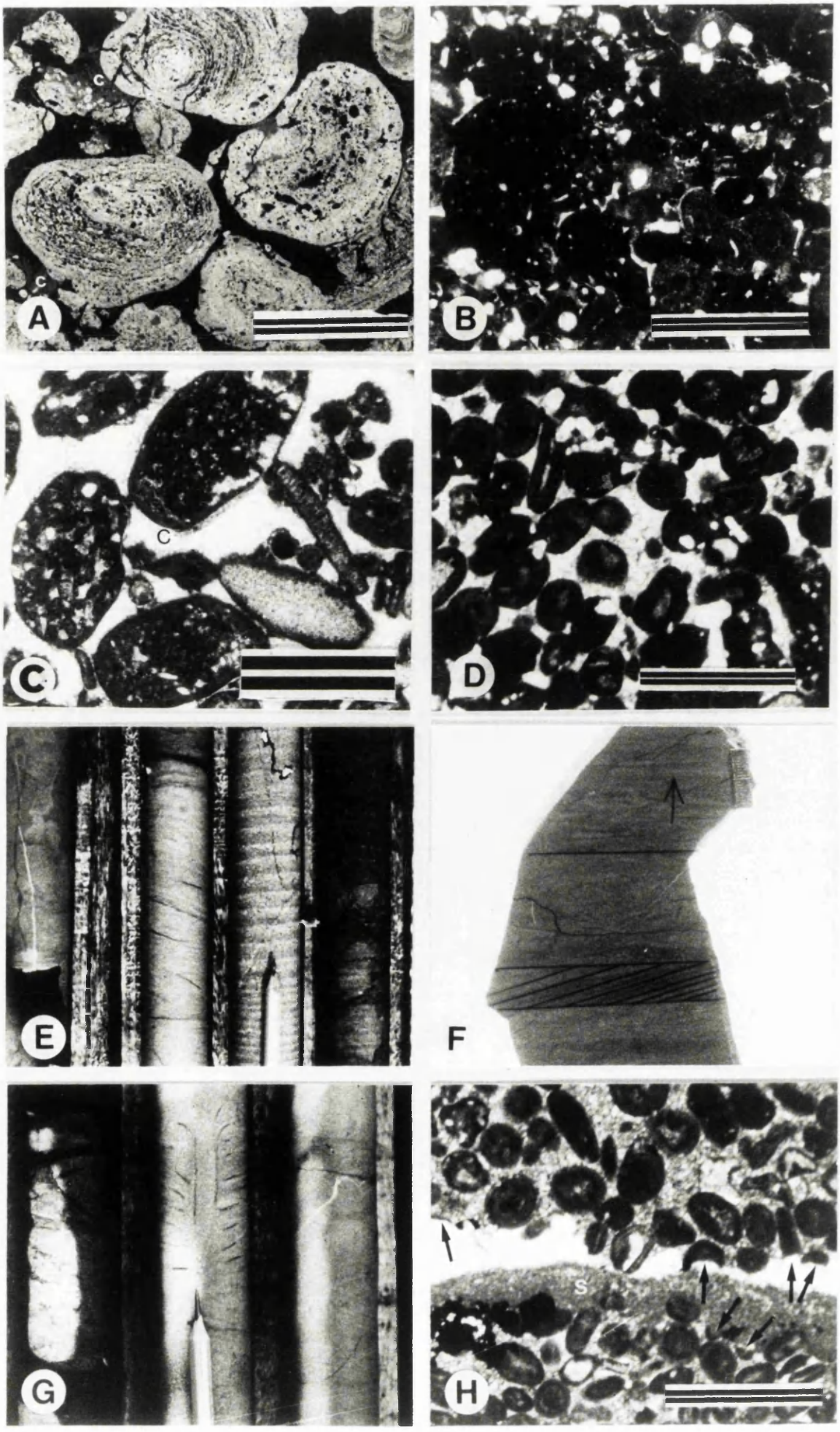
A
C
C
B
C
C
D
E
F
G
H
S

shales also occur. Generally basal contacts are sharp while upper contacts are gradational. Several burrowed silty shales referred to as the **Muddy Limestone Transition** occur in the basal 7 m of the Micrite Unit (Fig. 3.11).

A layer of illitic green clay overlies and fills a brecciated surface approximately 10 m above the base of the Micrite Unit (Fig. 3.12). It reaches a maximum thickness of 50 cm in hole N1039. The clay marks the footwall to mineralization (**the Footwall Green shale**). It is structureless and friable with a waxy lustre and contains angular fragments of blackened calcite mudstone and a few pyrite crystals. The Green Clay forms cutans (Brewer, 1964) which coat the walls of former cavities (Plate 3.3.B) and individual grains and lines the insides of shells (Plate 3.3.C). The clay penetrates between breccia fragments and host rock along irregular hair width cracks. Cutans are monomineralic and made up of overlapping discontinuous laminae. They are associated with micrite coatings on former cavity walls (Plate 3.3.D).

Cutans and micritic coatings are overlain by and alternate with crude layers of dolomitic crystal silt and green clay. Mudstone lithoclasts and cement fragments are included in these sediments. In hole N1034 at depth 656.7 m densely packed lithoclasts have dark oxide coatings and scalloped margins with delicate pinnacles, indicating that dissolution has taken place (Plate 3.3.E). Some lithoclasts have micrite coatings and a few micritized grains are also present (Plate 3.3.F). Cement lithoclasts include zoned calcite cement and on one grain, an attached non luminescent fibrous stalactitic (Plate 3.3.G) cement. The Green Clay locally contains anastomosing subparallel planar spar filled cracks. Cracks have also developed around lithoclasts. (Plate 3.3.H). The subsurface distribution of the Green Clay is shown in Fig. 3.13. (see also Appendix 1).

3.2.iv. Dolomite.

The Micrite Unit contains up to 11 beds of dolomite (hole N985) with beds up to 50 cm thick and extending laterally for up to 250 m (1375 mine level, 1 Zone 128N stope). Basal and upper contacts of these dolomite beds are either sharp or gradational (Plate 3.4.A). There is apparently no control on the location of dolomite in the muddy cycles, they occur within wackestones, packstones and mudstones and within fenestral and oncoidal beds. Dolomite within muddy cycles is brown-pink and is unimodal and individual crystals are subhedral. Individual rhombs are only a few microns in diameter and are rich in inclusions. The dolomite contains a few relic patches of calcite mudstones which appear red when stained with Alizarin Red and Potassium Ferricyanide. Locally the dolomite fabric is selective, replacing the matrix in wackestones, packstones and oncoidal beds (Plate 3.4.B). Under CL the cores of dolomite crystals are light crimson brown, overlain by a non-luminescent zone and finally by an orange rim.

PLATE 3.2. Features of Micrite Unit grainstones.

A. Negative print from thin section of oncoidal grainstone. Individual oncoids are 'bun shaped' having flat bases with laminae increasing in thickness vertically. Oncoid are now inverted. Note calcite crystal silt at grain contacts (c). Hole N286 at depth 172 .2 m. Scale bar = 3 mm

B. Photomicrograph of calcite mudstone lithoclast grainstone. Individual grains display concavo-convex contacts. Note siliciclastic grains and ooliths. Hole N988 at depth 497.1 m. Scale bar = 1 mm.

C. Negative print from thin section of oolitic lithoclast grainstone. Each lithoclast is well rounded and displays a coating. Note microstalactitic cements (c) and skeletal moulds defined by micrite envelopes. Hole N351 at depth 104.1 m. Scale bar = 2 mm.

D. Photomicrograph (plane light) of oolitic grainstone. Hole N1020 at depth 553.6 m. Scale bar = 1 mm.

E. Relic cross-bedding in dolomitized oolitic grainstone (the Five Lens Dolomite). The cross beds have different angles. Note also sharp base to cross-bedded unit. Detail enhanced for clarity using pencil lines. Pencil for scale points to 'way up'.

F. Underground sample of relic cross-lamination along bedding surface within dolomitized oolitic grainstone. Scale in millimetres.

G. Relic *Skolithos* burrow in dolomitized oolitic grainstone (the Five Lens Dolomite). Detail enhanced for clarity using pencil lines. Pencil for scale points to 'way up'.

H. Horizontal boring in oolitic grainstone; note floor of bore overlain by sediment (s) and truncation of grains along margin of bore (arrow). Hole N317 at depth 315 m. Scale bar = 1 mm.

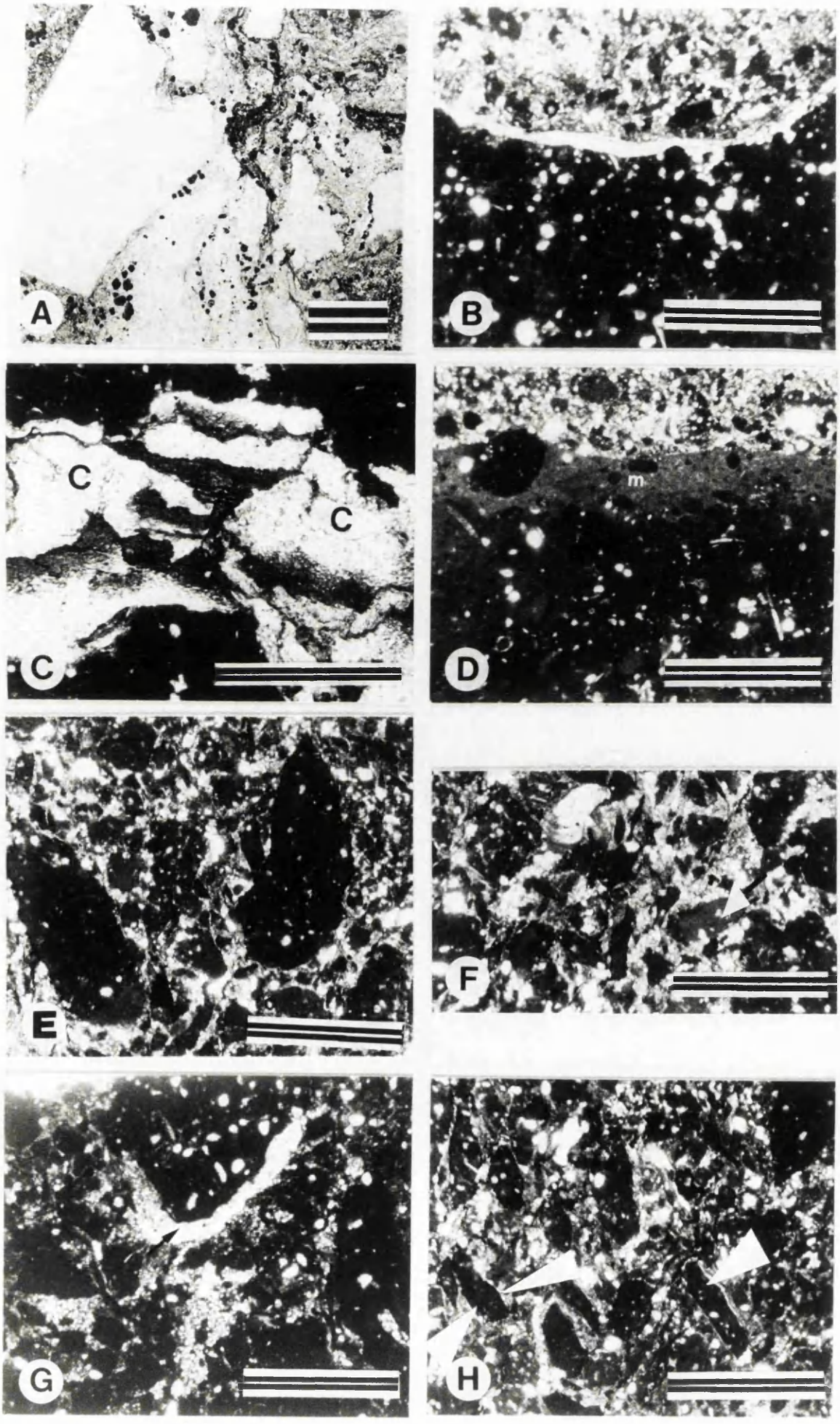
A
B
C
C
C
m
D
E
F
G
H

3.2.v. Former evaporites.

Lath shaped areas filled with calcite are common, occuring throughout the fenestral horizons, with good examples in holes N1036 at depth 625.0 m (Plate 3.4.C). Areas are 1 to 3 mm wide and 7 to 8 mm long with pointed terminations and are six sided or rectangular in sections parallel to the long axis. The geometry resembles that of monoclinic crystals. The spar areas are interpreted as former evaporite (gypsum ?) crystals which have been pseudomorphed by calcite, either by replacement or by dissolution with moulds filled by calcite.

Approximately 20 m above the base of the Micrite Unit, roughly spherical white nodules 1 to 2 cm diameter occur in the 1375 mine level, 1 Zone 128N stope. These consist of anhydrite rosettes, which, unlike the nodules in the 'C-D' Unit, are free of silicification. Some anhydrite also fills wedge shaped fissures cut into dolomitized mudstones. The nodules form laterally discontinuous clusters of up to ten individuals along the top of a 30 cm thick dolomite horizon. Some nodules are closely packed with only a thin layer of calcite mudstone between them forming a nodular mosaic texture (Plate 3.4.D).

3.3. IRREGULAR SCULPTURED SURFACES.

A number of irregular bedding surfaces punctuate the sequence of depositional cycles. These surfaces have been subdivided into four morphologies: small scale shaley breccia surfaces, flute and pinnacle surfaces, larger scale hummocky truncation topography and elongate funnel shaped cavities.

3.3.i. Shaley brecciated surfaces.

Brecciated surfaces are common, occuring in oncolitic, fenestral and non fenestral mudstones, wackestones and packstones and along the bounding surface of the oolitic grainstone. All have a vertical profile which begins with unmodified mudstones. These pass up into mudstone-wackestones cut by irregular vertical fissures up to 1 cm wide. The sequence is capped by breccias consisting of angular blocks of fenestral and non fenestral calcite mudstones. Individual clasts are up to 10 cm in diameter and some display a "Jigsaw" fit such that bedding can be traced from one to another, pointing to an *in situ* brecciation. Elsewhere irregular centimetre scale cavities occur between blocks.

The breccias are normally overlain by dark silty clays which have eluviated downward through the profile, surrounding clasts and filling fissures. These clays contain angular clasts of limestone and also bioclasts which may display a coating of silty clay. Echinoderm fragments in a rubble breccia from hole N975 between 489.3 m

PLATE 3.4. Dolomite and evaporites.

A.Subsurface photo of dolomite bed (D) overlying fenestral calcite mudstones (M). Note anhydrite along the upper surface of the dolomite. 1375 mine level, 1 Zone, 128N stope. Marker pen for scale.

B. Photomicrograph of dolomite within calcite mudstones. The dolomite is unimodal with individual crystals having subhedral outlines. Scale bar = 250 microns.

C. Gypsum (?) crystal in calcite mudstones now pseudomorped by blocky calcite cement. Note crystal has pointed terminations. Hole N1036 at depth 625 m. Scale in centimetres.

D. Detail of anhydrite nodules, note nodules have a fitted fabric sugesting they display nodular mosaic type texture. Vein contains calcite cement. 1375 mine level, 1 Zone, 128N stope. Scale in millimetres.

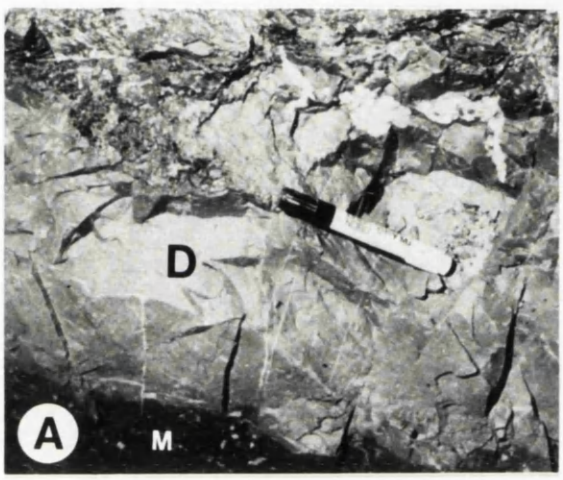
D
A
M

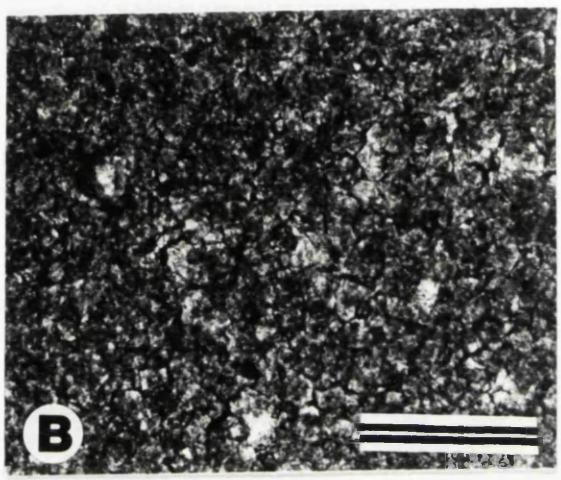
B

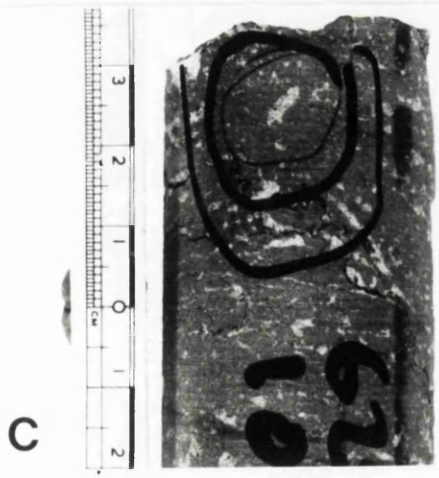
C

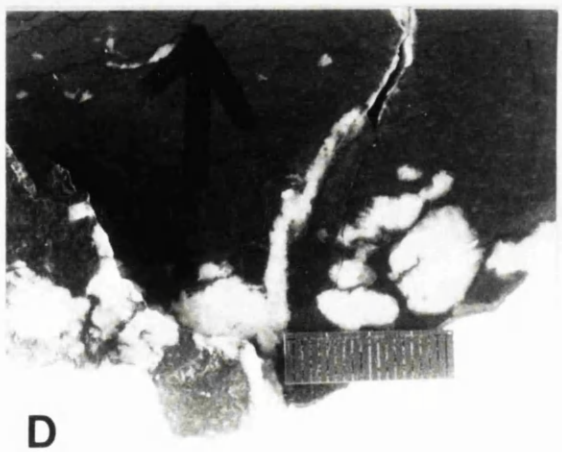
D

and 487.8 m carry syntaxial overgrowths, but these overgrowths have been extensively cut back by dissolution (Plate 3.5.A). They are not associated with stylolites and it is suggested that bioclasts are derived lithoclasts (Fig. 3.14).

Breccia surfaces occur every few metres in hole N975 and elsewhere over the entire interval of the Micrite Unit (refer Fig. 3.1). In hole N1022 between 555.0 and 547.5 m there are three rubble breccias about 1.5 m apart (Plate 3.5.B). Rubble breccias have also been identified underground in the1360 mine level. Two prominant breccias have been correlated laterally, the lower lies approximately 9 m above the base of the Micrite Unit and is overlain and filled by green clay (described in section 3.2.iii.) and exposed in the 1190 footwall drift, 2 Zone (Fig. 3.15.). In hole N1034 at depth 656.7 m fenestral pores in clasts contain microstalagtitic cements and crystal silts (Plate 3.5.C). Rubble Breccias also occur in the oolitic grainstones. In hole N1011 the oolitic grainstone contains several brecciated surfaces (Plate 3.5.D) with the upper surface marked by 0.6 m of brecciation (Fig. 3.16.). The same surface can also be seen in ten other drill cores.

3.3.ii. Flute and pinnacle surfaces.

Small scale dissolution surfaces are present in the 1210 mine level, 1902 stope (Plate 3.6), and in holes N509 and N1036. In hole N509 the surface has a relief of at least 15 cm and cuts horizontal fenestral and non fenestral mudstones and wackestones. Elevations on the surface bear vertical flutes and pinnacles whose terminals are either sharp, blunt or planar. The pinnacles and flutes vary in width, displaying undercut and overhanging side walls. Irregular cavities up to 3 cm in diameter occur in the pinnacles, and some bedding parallel cavities undercut the bases of the pinnacles (Plate 3.7). Some dissolution surfaces are cut by fractures which are not present in the overlying sediment, indicating that movement occurred shortly after deposition and lithification (Plate 3.8). The limestones forming these surfaces contain meteoric diagenetic textures (section 3.7.).

3.3.iii. Hummocky truncation topography.

A hummocky truncation surface occurs 30 m above the base of the Micrite Unit. This was first recognised by Anderson (1990, Fig. 5.23 and 5.30) and described from the Block 6 footwall contour drift . The distribution is shown in Fig. 3.17 (refer to Appendix 1 for summary of data) and in sections 'A-A', 'B-B', 'C-C' and 'D-D'. This type of surface is exposed in the 1230 mine level 126 west stope. Here it extends laterally for over 40 m and cuts down 3 m into muddy depositional cycles (Fig. 3.18).

In detail the surface consists of laterally linked bowl and funnel shaped pits and cavities. Bowls are rounded in section but can have planar bases. The funnel shaped

PLATE. 3.5. Breccia type emersion surfaces inthe Micrite Unit.

A. Photomicrograph of 'floating' echinoderm plate (e) within silty shale which fills a brecciated surface. The echinoderm plate carries a syntaxial calcite cement (c) which has been cut back by dissolution producing an anhedral outline. Hole N975 at depth 487.8 m. Scale bar = 1 mm.

B. Breccia surfaces within calcite mudstones. The surfaces occur every 1.5 m. Each surface dispays a distinct profile. (a) Unmodified calcite mudstone (b) Fissured calcite mudstone (c) *In situ* breccited calcite mudstone. (d) Silty shale, this has eluviated down throught the profile. Hole N1022 at depth interval 550.5 m to 555.0 m. Pencil for scale points to 'way up'.

C. Photomicrograph of microstalactitic cement (arrow) within fenestral cavity within breccia surface ovelain by the pedogenic green clay. Hole N1034 at depth 656 .7 m. Scale bar = 1 mm.

D. Brecciated surface within oolitc grainstone. Note former voids between breccia surfaces now filled with 'exotic' yellow dolomitic clay (D). Hole N975 at depth 558.1 m. Scale in centimetres.

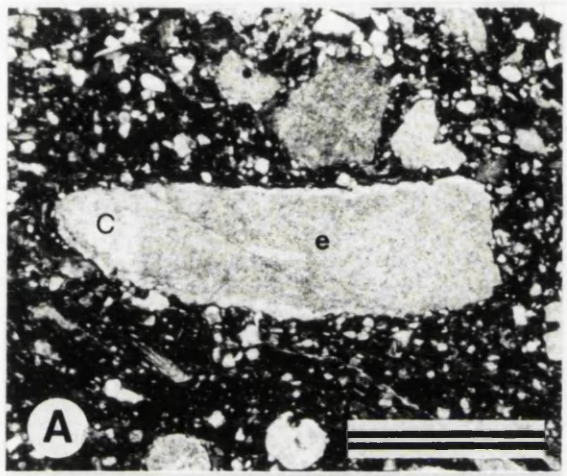
C
e
A


d
c
b
a
B

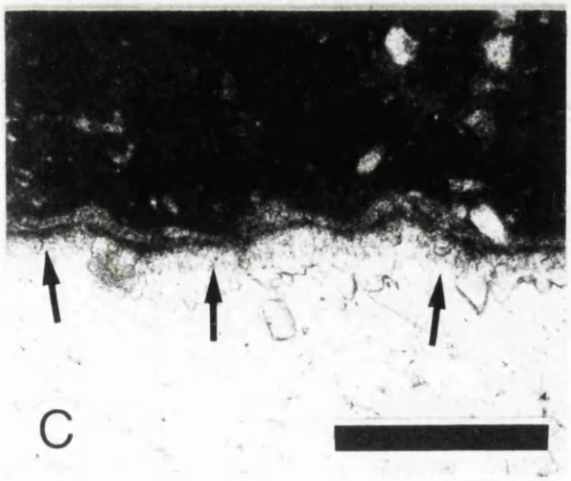
C

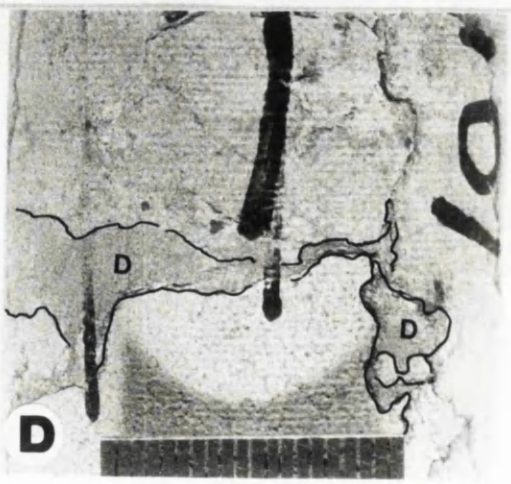
D
D
D

PLATE 3.6. Flute and pinnacle dissolution surface.

Negative print from thin section showing elevation through a flute and pinnalce type dissolution surfae. (A) Relic horizontal surface, (B) Former hole now filled with blocky calcite cement. (C) Multilayered fibrous calcite cement lining voids, this cement is microstalactitic below cavities within adjacent specimens (compare with Plate 3.11. A.). Note truncation of allochems at margins (D) and dissolution of skeletal aragonite. 1375 mine level Zone 2. Scale bar = 4 mm.

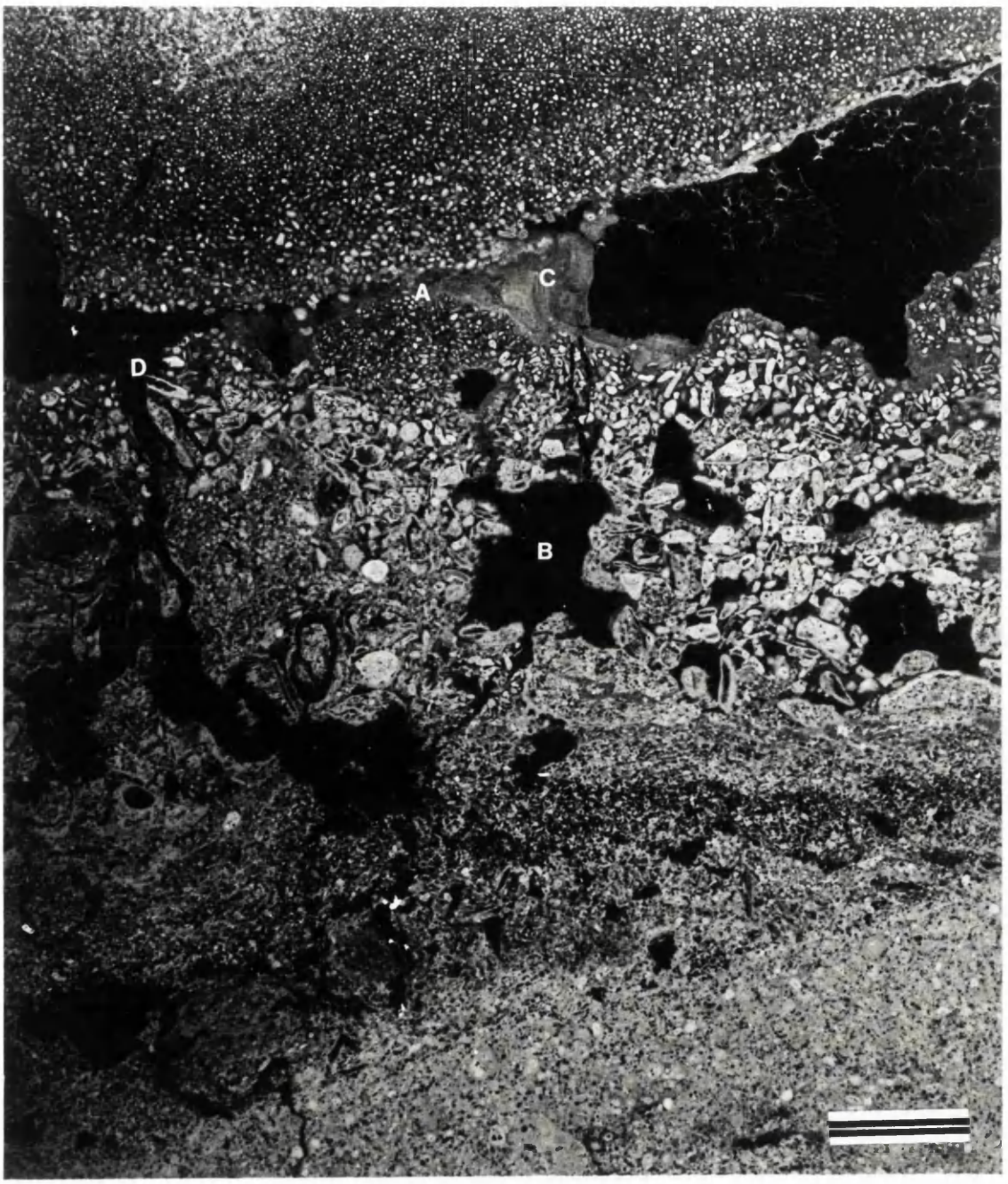
A
C
D
B

PLATE 3.7. Flute and pinnacle dissolution surface with features of meteoric diagenesis.

A negative print from thin section of flute and pinnacle dissolution surface. (A) Relic horizontal surface (B) Pinnacle with overhanging walls, note pinnacle is undercut along the base, (C) Flutes contain former hole (H). Petrographic features include (a) Graded geopetal calcite crystal silt (b) Micritized grains and surfaces.Hole N509 at depth 56. 6 m. Scale bar = 7 mm.


A
A
A
A
B
H
a
b
B
B
b
C

PLATE 3.8. Dissolution surface with stalactitic cements.

Negative print from thin section of dissolution surface. (A) truncation of sedimentary layering. Surface is cut by vertical fissure (F) which dies out in the overlyng dolomitic clay (G), indicating movement occured after deposition of the clay, scale bar = 6 mm. Note pisolites in ovelying sediment. Inset detail at 'x'of pisolith in overlying sediment and microstalactic cement. Hole N509 at depth 45.5 m. Scale bar = 2 mm.

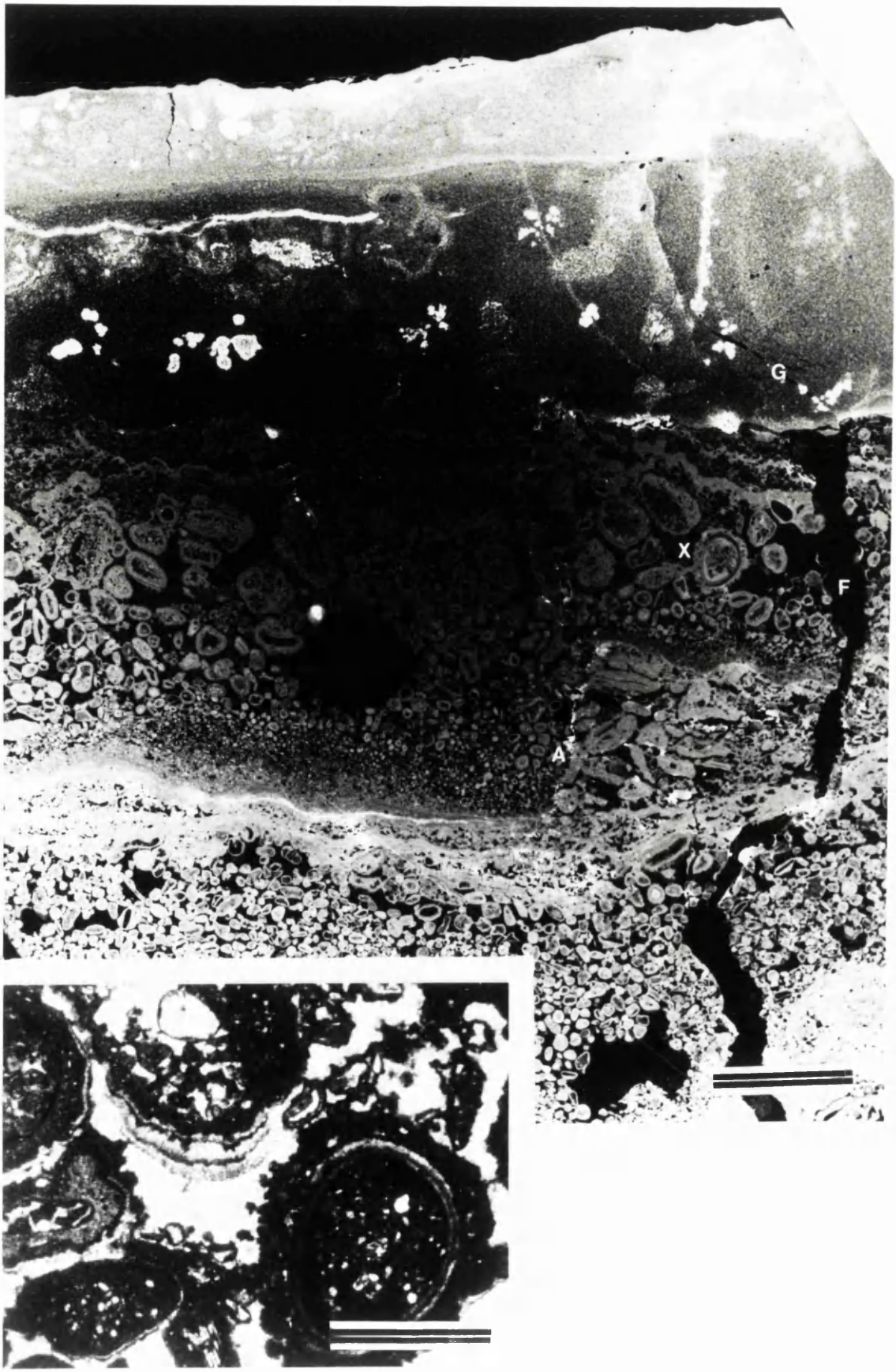
G
X
F
A

pits and bowls are separated by blunt pinnacles and ridges. The funnel shaped pits are triangular in section with a rounded apex. The margins of each pit are "knife" sharp, truncating allochems. Metre scale blocks of mudstone are apparently suspended above the surface. These contain horizontal fenestral layers which correspond with those in adjacent limestones and blocks are interpreted as *in situ* residual wall rock. Lead-Zinc ores have filled these surfaces and surrounded the *in situ* blocks. The hummocky truncation surface also carries funnel shaped depressions. In the 1130 drainage drift these are up to 1.5 m wide, narrowing downwards over 3 m to about 10 cm. Cavites can be traced across mine drifts indicating that they are elongate with a minimum length of at least 4 m (Fig 3.19.). Cavities contain blocks of fenestral and non fenestral mudstone wackestone, which are interpreted as representing *in situ* blocks of wall rock. The margins of cavities are again sharp and are themeselves sculpted by flute and pinnacle topography. Cavities also truncate beds in the muddy lithologies which are bounded by flute and pinnacle surfaces. The surface can be recognised in drill cores and beds directly below it contain meteoric diagenetic features (section 3.7).

3.3.iv.Other discontinuity surfaces.

Bowl shaped pits 1 m in diameter and 30 cm deep occur in the 1375 mine level, 1 Zone 128N stope truncating layers of dolomite and fenestral and non fenestral mudstones, wackestones and packstones (Plate. 3.9.A). In hole N1011 steeply inclined surfaces over 40 cm long truncate layering in the oolitic grainstones occuring 5 m below the brecciated upper surface (Plate 3.9.B). These steeply inclined surfaces are interpreted as cavity margins. A yellow ochre horizontally bedded dolomite silt fills the cavities. This contains a series of circular, matrix supported structures lined by coarser dolomite crystals. Lenticular bedding parallel dissolution cavities up to 5 mm high were noted in the 1210 mine level, 1905 stope. They can extend along bedding for up to 3 m, microstalagmitic cements are present along their roofs (Fig. 3.20.)

3.4. SEDIMENTOLOGY.

3.4.i. Introduction.

A cycle may be defined as "a series of rock types which follow each other in a predictable pattern" (Schwarzacher, 1975). Fenestral and non fenestral muddy lithologies at Navan alternate with each other, and are threrefore cyclic. Up to twenty cycles are present, each cycle is laterally dis-continuous having a maximum width of up to 1000 m. A stylized cycle, based on an example from hole N975, is shown in Fig. 3.21. The sequence begins with non fenestral mudstones which pass upward to

fenestral mudstones terminated by either a shaley rubble breccia, or more rarely, flute and pinnacle topography.

This sequence is a shallowing up cycle comparable to those described by James, 1984 (Fig 3.22). In a typical "James" muddy cycle the base consists of a thin lithoclast grainstone, representing the lag gravel deposited during the initial marine transgression. This is followed by bioturbated mudstones or grainstones representing a lagoon or more open marine environment. The overlying fenestral mudstones, containing cryptalgal lamination and desiccation features represents the tidal flat. The sequence is capped by a thin subaerial erosion deposit consisting of either a breccia which may be overlain by a black shale, soil or caliche. Not all cycles are complete and the palaeokarst surface is commonly missing.

3.4.ii. Sedimentology of a Navan muddy cycle.

Navan calcite mudstones are structureless but are volumetrically important. Muds are common in Recent carbonate environments, occurring in the protected parts of platforms typically in lagoons in waters up to 8 m deep. In such areas wave and current activity is weak with no cross platform currents. These low energy conditions facilitate the accumulation and preservation of muddy sediments.

A lagoon of this type occurs west of Andros Island in the Bahamas. Waters here are up to 4 m deep and are floored by muds. The lime muds and pelletal muds on the Bahamas Platform are homogeneous due to extensive burrowing and consist of aragonite needles 1 to 4 microns long. The pellets are soft, structureless and elliptical, averaging 20 to 50 microns in length. They are produced by a diverse fauna including polychaete worms and cerithid gastropods. (Shinn *et al*, 1969; Shinn, 1983; Hardie, 1977). Other lagoons floored by lime muds occur along the inner Florida shelf (Enos, 1977) and along the Trucial coast of the Arabian Gulf where a tidal barrier system shelters the The Khor Al Bazam lagoon (Schreiber *et al.* 1986).

Lagoons commonly contain a sandy component, particularly where they are only semi restricted, allowing open circulation. Sand deposition occurs along seaward margins where overspill from adjacent shallow marine sand bodies takes place. Storm activity can result in the deposition of some sandy sediment. These storm beds form thin graded layers floored by skeletal lags (Wanless, 1981). Sands are then redistributed by burrowing producing packstone and wackestone textures. Muds *sensu stricto* are restricted to the most protected parts of the lagoon.

The origin of lime muds varies with locality. Kinsman & Holland (1969) showed that the strontium content of the aragonite in the Khor Al Bazam lagoon is around 9400 ppm, close to the expected value for both seawater and inorganically precipitated ooliths, suggesting that it is an inorganic precipitate. Stockman *et al.* (1967) suggested

that most of the aragonite mud of the Florida Bays is produced by the disintegration of calcareous algae such as *Penecillius*. However, Loreau, (1982) showed that only 25 to 40% of crystals in codiacean algae consist of needles, while Bahamian muds contain up to 90% needles, suggesting some inorganic precipitation. This is supported by geochemical analysis of Florida and Bahamian muds: the Sr/Mg ratio of algal aragonite is less than 2, but is more than 4 in inorganic aragonite. Some lagoonal mud can also be produced by general skeletal abrasion (Scholle & King, 1972).

The Navan muddy lithologies probably reflect deposition in a lagoon, with gastropods and ostracods, a common lagoonal fauna (Shinn *et al,* 1969; Walkden, 1987). It is likely that the Navan mudstones originated in a similar manner to modern lagoon muds, from inorganic and organic precipitation together with degradation of skeletal grains. The homogeneous nature of these lithologies suggests exstensive burrowing and pellets are probably faecal. The sandy component reflected in the packstones, wackestones and grainstones points to a semi restricted lagoon with open circulation of seawater. This is supported by the bioclast assemblage of crinoid ossicles, echinoderm plates, brachiopods and corals which are all stenohaline, indicating derivation from a near-by open marine environment. Occasional graded beds and skeletal lags suggest some storm deposition with mudstones accumulating in the more protected shoreward areas. Porostromate oncoids, formed by blue-green cyanobacteria adsorb only the blue light end of the spectrum indicating water depths of only 15 m (Park, 1977).

The accumulation of oncoids in laterally discontinuous layers is interpreted as reflecting gentle tidal activity, concentrating them into thin sheets. The overlapping micrite laminae of the oncoids are interpreted as reflecting gentle rolling during growth with "bun" shaped oncoids indicating less frequent movement, reflected by their flat bases and laminae which thicken upwards (Wright, 1983). Lithoclasts of calcite mudstone and oolitic grainstone within mudstones, point to contemporaneous cementation of tidal flats and adjacent shallow marine environments. Siliciclastic grains and black shales indicate that production of carbonate mud at Navan was punctuated by influx of siliciclastic detritus from an adjacent landmass. This floored the lagoon, producing thin shales. Influx of this siliciclastic material suggests a slight relative fall in sea level. Fig. 3.23. illustrates the facies model for the early Carboniferous lagoon at Navan.

Irregular, laminoid and tubular fenestrae with cryptalgal lamination and desiccation features are common in Navan shallowing up cycles. These features are believed to be reliable indicators of tidal flat environments (Shinn *et al*, 1969; Hardie *et al*, 1977; Shinn, 1983; and summary by Wright, 1990a). The tidal flats adjacent to modern carbonate lagoons typically consist of pelleted and non pelleted lime muds containing a

variety of features including irregular laminoid and tubular fenestrae, algal lamination and desiccation cracks. In these, sedimentation takes place during flood tides and storm events. At such times sediment in the lagoon is stirred into suspension and transported along tidal channels to be deposited on the tidal flats as laminations and thin sand blankets. (Shinn *et al,* 1969; Shinn, 1983).

A well documented 7 km wide tidal flat occurs on the western side of Andros Island in the Bahamas. It can be subdivided into an intertidal zone and a supratidal zone (Shinn *et al,* 1969; Shinn, 1983). Sedimentary structures vary with position. The lower intertidal zone is often homogenised by burrowing organisms, typically annelid worms and gastropods. In the upper intertidal zone irregular and tubular fenestrae are present together with algal mats associated with laminoid fenestrae. Fenestrae are produced by expanding gas resulting from decay of cyanobacterial mats (Shinn, 1968a). Irregular, laminoid fenestrae and cyanobacterial mats are most common in the supratidal zone since grazing organisms are absent. This is also a zone of active cementation, a prerequisite for preservation of fenestrae (Shinn, 1968a). Mud cracks are also common here and tabular intraclasts can be generated from these by storm activity. (Shinn, 1983). A similar zonation occurs along the tidal flats of the Trucial coast. Here tidal flats are up to 30 km wide. Along their outer margins structures are similar to those on Bahamian tidal flats but cyanobacterial mats can be subdivided into smooth, pustular, and cinder mats, the last in the highest (most shoreward) position (Kinsman & Park, 1976). The very wide supratidal zone is represented by the sabkha, an area of active evaporite formation (Shinn, 1983).

Ginsburg *et al* (1977) assigned an Exposure Index to modern tidal flat structures. This is defined as the *"mean annual percent of time that point is exposed"*. Flat lamination indicates 98 to 100% exposure and a maximum height of 50 to 25 cm above sea level. Fenestral pores indicate 60% to 100% exposure and a maximum height of 40 cm above sea level while cryptalgal lamination indicates 85 to 100% exposure and a minimum height of 40 cm above sea level. The Navan tidal flat was zoned, with sparse irregular fenestrae in the lower intertidal zone and irregular and laminoid fenestrae in upper and supratidal zones. Cryptalgal lamination provides evidence that the supratidal flats were colonised by cyanobacterial mats. The fenestral horizons are laterally discontinuous. This may indicate that the shoreline consisted of shallow embayments separated by fenestral tidal flats or perhaps small islands surrounded by shallow semi restricted lagoons. Bedding within these features demonstrates a lack of bioturbation, probably due to elevated salinities. Tabular clasts with wedge shaped cracks suggest desiccation. No tidal creek facies have been observed.

Gypsum crystals are rare on modern humid tidal flats, forming only during the dry season around ponds on Andros Island. They are more common on the arid supratidal

flats of the Trucial coast. The occurrence at Navan of pseudomorphes after gypsum crystals among fenestrae indicates that pore waters were sufficiently saline for evaporite formation. Evidence of more widespresd evaporite formation is provided by the occurrence of nodules of anydrite. The nodular mosaic texture is interpreted as reflecting growth subsurface within soft sediment in the supratidal zone.

The tabular character of the dolomite layers in the muddy cycles compares with the predicted geometry of tidal flat dolomite (refer to Appendix 3). Sedimentary features within muddy cycles include fenestral layers and cryptalgal lamination support this interpretation. Gypsum crystals together with anhydrite nodules along the top of dolomite beds in the 1375 mine level, 128N stope suggest that pore waters which precipitated these evaporites perhaps played a role in dolomitzation. Magnesium may have been delivered to the tidal flat in the manner described by Mckenzie *et al* (1980) with some some evaporitic or tidal pumping.

Using the Exposure Index of Ginsburg (1977), the Navan tidal flats were exposed between 60 to 100% of the time with a maximum height of 40 cm above sea level, a favourable environment for subaerial erosion and karst formation. The facies model of the Navan tidal flat is shown in Fig. 3.24.

The sequence of lagoonal-supratidal shallowing up cycles contains four grainstones (described in section 3.2). Grainstones are believed to reflect a shallow shelf environment and high energy conditions (Halley *et al,* 1983; Wilson, 1975; Sellwood, 1986). The occurrence of these grainstones at Navan indicates that these conditions extended over the prevailing tidal areas and therefore reflect a relative transgression. The sedimentology of the Navan grainstones will now be discussed.

At present most oolites form extensive sand bodies along the windward margins of platforms. Such features act as foci for factors which promote sand body formation. They cause onshore ocean swells to impinge on the sea bed, moving sediment and also concentrate strong tidal currents. The orientation of bank margins with respect to dominant wind, wave, tide and storm activity has a significant effect on sand body shape (Halley *et al* , 1983). Ball (1967) recognised three types of sandbodies, Tidal Bar and Marine Sand Belts and Platform Interior Sand Blankets. Before considering the sedimentology of the Navan oolitic grainstone, a brief review of some modern oolitic sand bodies will be undertaken.

The Schooner keys area, north of Exuma sound, Bahamas is a good example of a tidal bar belt. It runs parallel to the bank margin for up to 100 km. Individual tidal bars, oriented normal to the slope break, are 12 to 20 km long, 0.5 to 1.5 km wide and up to 9 m amplitude with a symmetrical crossection. They are separated by 1 to 3 km wide depressions up to 9 m deep. Lilybank Oolite shoal is a marine sand belt (Hine, 1977). It

parallels a windward bank margin for 25 km and is 2 to 4 km wide, locally dissected by tidal channels. The seaward margin of the shoal terminates in 30 to 50 m of water (Halley *et al,* 1983). The sand body is wedge shaped with its maximum thickness along the shoreward margin. Currently it is prograding into the adjacent lagoon, principally during storms. Some sand bodies are composite, the Joulters Key oolite shoal was originally a marine sand belt. Tidal channels have cut through it and ooliths have been transported into the platform interior and mixed with lime muds. They have been deposited in lobe shaped fans at the heads of tidal channels, forming extensive sand flats (Harris, 1983) and can be thought of as equivalent to a platform interior sandblanket (Ball, 1967).

The surfaces of modern oolitic sand bodies are covered by a hierachy of bed forms (Hine, 1977) which include sand waves, (greater than 6 m high), mega ripples, (less than or equal to 60 cm high) and ripples, (less than 60 cm high). All three structures are generally asymmetrical, reflecting prevailing currents, migrating only during storms. Internally all are cross-bedded with foresets dipping 10 to 20^0. Vertical escape burrows may also be also present.

Modern shelves which have been influenced by Quaternary sea level fluctuation. During the Devensian glaciation (120 000 to 10 000 BP) a solutional unconformity consisting of rocky ridges and channels was produced in pre-Holocene limestone. This surface has controlled the distribution of modern unconsolidated carbonate sands deposited during the ensuing Holocene transgression. Higher areas on the karst surface concentrated tide and wave activity producing conditions favourable to oolitic sand body formation. A Pleistocene palaeohigh, a submerged extension of Andros island, has controlled the distribution of the Cat Key oolite shoal (Harris, 1984). A similar situation occurs on the Honduras peninsula where the distribution of sands and reefs was controlled by the pre-Pleistocene Unconformity (Purdy, 1974). Similar relations occur in Florida, the Persian Gulf and Western Australia (Sellwood, 1986).

As will be shown, the oolitic grainstones at Navan overlie a hummocky palaeokarst surface which has truncated muddy cycles, therefore reflecting a relative marine transgression with the palaeokarst surface perhaps controlling the distribution of the oolitic grainstone (compare Figs 3.9. and 3.17.). Cross-bedding in the oolitic grainstones at Navan indicates that they were deposited as mega ripples of 50 cm amplitude. Cross-lamination indicates that smaller scale ripples occured on the crests and flanks of these mega ripples. Both sets of structures were presumably aligned according to the prevailing tidal currents and wave activity. Vertical *Skolithus* burrows are believed to represent escape structures formed in response to rapid deposition and vertical accumulation of sediment (Frey & Pemberton, 1984). In modern mobile sandbodies burrows are typically located in the troughs between mega ripples but are

absent on crests where currents are strongest. The tabular intraclasts of oolitic grainstone in the muddy lithologies provide evidence of contemporaneous cementation and hardground formation, a feature of many modern carbonate sandbodies (Dravis, 1979). Further evidence of cementation is provided by borings which are also features of modern hardgrounds.

The Navan oolitic grainstones are interpreted as representing a shallow marine sandbody. The general distribution and isopachs of the upper surface suggest a geometry analagous to that of modern marine sand belts. The thin black shales within the oolitic grainstones point to breaks in the production and accumulation of sand, possibly reflecting slight relative falls in sealevel, allowing influx of muddy siliciclastics onto the shelf from the adjacent landscape. The suggested facies model is shown in Fig. 25.

The oncoidal grainstone suggests reworking of shallow water sediments containing stationary oncoids (asymmetric growth profile). Similar oncoidal grainstones occur throughout the geological record and are interpreted as reflecting shallow water high energy conditions (Wilson, 1975). The occurence of this grainstone at the very base of a shallowing up cycle suggests that it was a lag gravel representing a new marine transgression. The calcite mudstone lithoclast grainstones occurs at the base of a shallowing up cycle suggesting that it is a also lag gravel. The grain composition indicates that it was derived from lagoonal and tidal flat mudstones. The texture reflects a moderate to high energy environment with graded beds indicating deposition from rapidly decelerating currents, perhaps in storms. The coated oolite lithoclast grainstones are believed to reflect slow accumulation in a zone of winnowing (Wilson, 1975).

3.4.iii. Interpretation of Navan cycle caps.

The shaley breccia surfaces and flute and pinnacle type topography occuring within the Navan muddy cycles and along the top of the oolitic grainstone are subaerial erosion features like those of the ideal cycle of James, (1984). Meyers, (1988) described similar subaerial surfaces from the Lower Carboniferous of New Mexico and interpreted them as representing regolith weathering. The shaley breccia profiles consist of unmodified limestone passing up into fissured limestone and *in situ* limestone breccias. The profiles are overlain by silty clays which fill spaces between clasts and fissures. The clays contains detrital echinoderm grains with syntaxial overgrowths which have been intensely corroded. These are believed to result from dissolution of the surrounding limestone by vadose meteoric water with the rubble breccia forming by "dissolution fragmentation". Meyers (1988) suggested that the silty clay consists of eluviated sediment, possibly derived by chemical disintegration of the host limestone in

the rubble and fissure zone, and from remobilization of deposited muds by pedogenic illuvation processes.

The profiles of the Navan rubble breccias are compared with those in the Lower Carboniferous of New Mexico (Fig. 3.26.) The similarity and the occurrence of detrital echinoderm grains with corroded syntaxial cements suggests that the Navan profiles also represent regolith profiles. They also indicate a relative fall in sealevel culminating in subaerial erosion. Independent evidence for emergence is provided by meteoric diagenetic textures within the muddy depositional cycles (section 3.7.).

One rubble breccia surface is overlain and filled by the Green Clay. This contains cutans, circumgranular cracks and micritized grains which are typical pedogenic structures (Brewer, 1964). The Gilwern-Llanelly oolite in the Lower Carboniferous of south Wales also contains a rubbly breccia. Like the Navan example, this is filled by an illitic green clay containing pedogenic structures interpreted as a subaerial regolith developing beneath a palaeosol (Riding & Wright, 1983; Wright, 1988).

The hummocky trucation surface with funnel shaped cavities has truncated shallowing up cycles. The smooth sculpted surface points to subaerial dissolution as the main agent of erosion and is therefore a palaeokarst surface (Fig. 3.27). The different types of subareial erosion surfaces are collectively known as karren. The different varieties of karren type palaeokarst are discussed in Appendix 2. The hummocky truncation surface is predominantly rundkarren with funnel shaped cavities comparable to kluftkarren. Petrographic evidence of meteoric textures within the limestones trucated by the karst surface (section 3.7) provides independent evidence of emergence and also important criteria in the elucidation of subaerial exposure (Esteban & Klappa, 1983; James & Choquette, 1984, 1988).

Karren surfaces are common in the geological record. The Lower Carboniferous of Derbyshire contains hummocky surfaces and cylindrical shaped pits up to 1 m deep and 1 m diameter separated by blunt pinnacles. (Walkden, 1974). Dissolution features also occur in the Lower Carboniferous of Anglesey where pits at the top of metre scale shallowing up cycles are up to 2 m deep and separated by irregular scalloped ridges. Like the examples from Derbyshire they are again interpreted as palaeokarst (Davies, 1991). The Lower Carboniferous Gully Oolite of south Wales contains emersion surfaces dissected by dissolution pits up to 1 m deep (Wright, 1988). Similar pits are recorded from the tops of shallowing up cycles in the Lower Carboniferous of north Wales (Somerville, 1979).

Similar features occur in the Pleistocence of Kenya (Braithwaite, 1984) and Bermuda (Land & Gould, 1967), the Triassic of Austria (Bechstadt & Dohler-Hirner, 1983, Bechstadt, 1975) and the Cretaceous El Abra formation of Mexico (Minero, 1988). The hummocky surfaces in the Witterstein limestone are particulary important since they

act as a locus for the deposition of high grade zinc-lead mineralization (Bechstadt & Dohler-Hirner, 1983; Bechstadt, 1975).

The hummocky dissolution and breccia surfaces at Navan are overlain and filled by rubbly siliciclastics. The homogeneous texture of some of these suggests that primary lamination was disrupted by burrowing or dewatering or did not occur at all. Similar subaerial surfaces in the Lower Carboniferous of Angelsey have also been filled by siliciclastic sediment. Such sediment may reflect a further fall in base level with siliciclastic sediment transported basinwards across the exposed shelf, through and over subaerial surfaces (Walkden & Davies, 1983).

3.5.NAVAN CYCLE SEQUENCES.

The cycles at Navan have a maximum lateral expression of 1000 m, indicating that no one cycle is developed throughout the mine area. However, the cycles can be grouped into several "packages" in the western mine area. These cycle packages are described in the following section and summarized in Fig. 3.28.

Cycle sequence 1 is shown on cross-sections 'A-A', 'B-B', 'C-C' and 'E-E' and forms the basal 15 m of the Micrite Unit. The sequence consists of up to four shallowing up cycles. The basal cycle begins locally with the oncoidal grainstone. This "package" of cycles culminates in a breccia surface. This breccia is overlain by the Green Clay which contains micritized grains, circumgranular cracks and cutans which suggest that it is a palaeosol.

Cycle sequence 2 consists of four shallowing up cycles which overlie the Green Clay forming a "package" approximately 15 m thick. The calcite mudstone lithoclast grainstone which rests directly on the green clay occasionally forms the base of the sequence, and is interpreted as a transgressive lag gravel. The oolitic lithoclast grainstone occurs within this package of cycles indicating lagoonal-supratidal cyclicity was punctuated by a phase of shallow water high energy conditions. The fourth cycle is truncated by a breccia recognised on cross-sections 'A-A', 'B-B', 'C-C' and 'D-D' and interpreted as a subaerial erosion surface.

Cycle sequence 3 consists of six shallowing up cycles overlies the breccia. This package is approximately 13 m thick. The hummocky subaerial erosion surface with funnel shaped cavities forming the upper boundry is overlain by dark silty siliciclastics.

Cycle sequence 4 consists entirely of the oolitic grainstones resting on the silty shale on top of the hummocky subaerial erosion surface. The grainstone contains occasional black shales. In hole N1011, brecciated and steeply inclinded surfaces suggest that grainstones are cyclic with cycles culminating in subareial exposure (compare James, 1984, p. 218 Fig. 9). The upper surface of this grainstone packet is again a breccia interpreted as reflecting subaerial erosion.

Cycle sequence 5, the final sediment packet in the Micrite Unit, is at least 20 m thick. It consists of six lagoon-supratidal shallowing up cycles. Like those of the lower packages each cycle is 2 to 3 m thick. The upper boundary of the packet and surface of the Micrite Unit is highly irregular. This surface is the subject of the next section.

3.6. UPPER SURFACE OF THE MICRITE UNIT.

The thickness of the Micrite Unit has been measured in over 70 drill cores and the data contoured. There are substantial variations in thickness. Elevations through the Micrite Unit were constructed using stratigraphic markers within the Micrite Unit and markers occuring higher in the stratigraphic succession, notably the Nodular and Upper Dark Markers. These indicate that the upper surface rather than the lower is irregular, a feature noted by Andrew & Ashton (1985). Truncations of muddy cycles near the top of the Micrite Unit provide further support for this interpretation.

3.6.i. Description.

The upper surface of the Micrite Unit is marked by depressions up to 25 m deep defining several palaeohighs with gradients around 5^0. In addition it has been cut by an erosive linearment, over 2 km wide and 60 m deep (Fig. 3.29 and Appendix 1). Similar linearments have been recognized at Clogherboy and at Tatestown suggesting the same linearment may extend NW-SE for over 6 km (Andrew & Ashton, 1985). 2 km to the east of the channel, beyond the study area, the micrite Unit in hole EP20 thins again to 18 m. This may reflect a second erosive linearment, but remains speculative. The Micrite Unit in the most southerly hole examined, EP 21 is 58 m thick.

In detail the the upper surface of the Micrite Unit hosts several notable features. In holes N1022 and N1036 the surface is marked by flute and pinnacle topography (Fig. 3.30.). Some pinnacles are overhanging and undercut at their bases and perforated by irregular holes. Flutes are up to 10 cm deep and 1.5 cm wide. In addition the upper surface of the Micrite Unit is not planar, several drill cores notably N272, N835 and N826 display steeply inclined surfaces interpreted as former cavity margins. Shaley breccias are also common.

The margin of the linearment is shown in Fig. 3.31. The floor is exposed in seven holes N30, N286, N314, N535, N629, N804 and N710. In hole N710 the contact is sharp but in the remaining holes it consists of brecciated calcite mudstones (Plate 3.9.D). In hole N629 steeply inclined surfaces are present which truncate layering and oncoids (Fig. 3.32.) and are interpreted as the margins of a cavity (Plate 3.9.C). This cavity is followed by a chaotic sequence of calcite mudstone breccia. The entire upper surface of the Micrite Unit, including the floor of the erosive linearment, is mantled by thin dark muddy siliciclastics.

3.6.ii. Interpretation.

The upper surface of the Micrite Unit is not depositional, the rocks forming the Micrite Unit are interpreted as reflecting a lagoon-tidal flat sedimentary system. Such environments have negligible relief and sedimenary structures within the muddy depositional cycles at Navan suggest the maximum height above sea level was 40 cm.

The surface is believed to reflect palaeotopography (Fig. 3.33). It bears flute and pinnacle type topography, brecciated surfaces and cavities which in earlier sections have been interpreted as palaeokarst. This indicates that the palaeotopography was generated by subaerial exposure. The linear erosive feature is believed to represent a subaerial channel, cavities and blocks of calcite mudstone occuring at the base of the channel are also interpreted as being subaerial in origin. The rubble breccias consisting of clayey siltstones containing angular clasts of calcite mudstones and wackestones apparently follow the topography. The shaley breccia surfaces are common features of palaeotoporaphy and are interpreted as representing weathering profiles or protosols (Meyers, 1988; Craig, 1988; Musman *et al*, 1988 and Knight *et al*, 1991).

3.6.iii. Comparison with other examples.

Palaeotopography generated by subaerial erosion is common in the geological record (Purdy, 1974). In the Honduras peninsula the English Cay Channel was cut into Pleistocene limestones during subaerial exposure and compares with the Navan channel. It is 60 m deep, over 2 km, wide and over 10 km long Purdey (1974). A comparable ancient example is provided by the Lower Aptian carbonates of the French Jura. Here a regional channel network is present with individual channels over 10 km long, 1 km wide and 30 m deep (Arnaud-Vannaeu & Arnaud, 1990). Knight *et al*, (1988) have shown that the surface of the Ordovician St. George Group of Newfoundland (consisting of lagoon - intertidal shallowing up cycles) was a hummocky coastal plain cut by valleys forming part of a regional unconformity. Similarly the Knox unconformity (Ordovician) of the Appalacians forms a palaeotopography. The last has up to 100 m relief and also cuts peritidal shallowing up

PLATE 3.9. Dissolution surfaces within the Micrite Unit.

A. Elevation through bowl shaped pit. 1375 mine level, 1 Zone, 128N zone. Marker pen for scale.

B. Steeply inclined surface within oolitc grainstone overlain by exotic yellow dolomitic clay. Arrow points to 'way up'. Hole N1011 at depth 560.3 m. Scale in centimetres.

C. Detail of cavity margin at the base of the channel. Note truncation of sedimentary layering and oncoid. Scale in millimetres.

D. Brecciated calcite mudstone at the base of the channel. Blocks of mudstone display brecciated upper surfaces. Note argillite overlying blocks contain abundant clasts of calcite mudstone. Hole N629 at depth interval 356.5 m to 354.5 m. Pencil for scale points to way up.

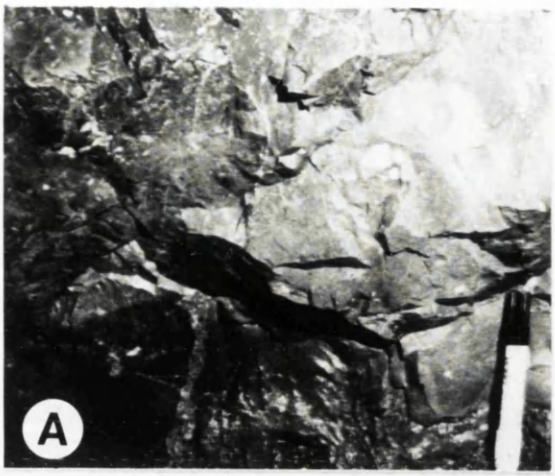
A

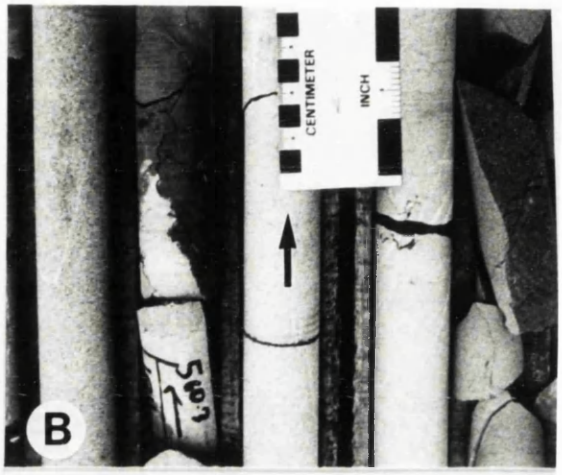
CENTIMETER
INCH
B


C


D

cycles. The last two palaeotopographies are important because they act as loci for the deposition of high grade lead-zinc ores. The limiting surface of the Permian Yates Formation of Texas has up to 60 m of relief believed to represent low lying hills and valleys. (Craig *et al,* 1988). The contours of this palaeotopography compare closely with those of the Navan surface (Fig 3. 34.).

The channels present in these examples were cut as shelves were undergoing drainage during rapid falls in sealevel. Channel formation under such conditions is reviewed by Purdy (1974), Pomar (1991) and Ford & Williams (1989) and has been reproduced experimentally by Purdy (1974). Two other hypotheses have been suggested to explain the Navan channel, these are discussed in chapter 7.

3.7. PETROGRAPHY OF THE MICRITE UNIT.

3.7.i. Introduction.

The sediments of the Micrite Unit are characterized by cyclicity with deposition punctuated by the formation subaerial erosion surfaces. Walkden (1987) and Wright (1982) have suggested that Lower Carboniferous subaerial erosion represents periods of emergence of between a few thousand and several thousand years. These periods allow for the formation of palaeokarst. It is thus to be expected that, apart from surficial indicators of emergence, the rocks themselves should show clear evidence of meteoric diagenesis.

Thirty five thin sections from the muddy lithologies have been examined, of which 28 contained cement. In addition, twelve thin sections of oolitic grainstones, two bioclastic grainstones, and one each from oncoidal, calcite mudstone and oolitic lithoclast grainstones have also been examined. Using data from Scholle, (1978) as a control, the original grains forming the sediment and constituting the cement substrate consisted of high magnesium calcite, represented by pelmatozoan fragments, low magnesium calcite represented by brachiopods and ostracods and probably aragonite, now represented by shell shaped bioclast moulds contained within micrite envelopes.

Porosity has been classified according to the scheme of Choquette & Pray, (1970). In the muddy lithologies it included fenestral porosity and, where the mudstones are pelletal some interparticle porosity, confined to laterally discontinuous horizons. In the grainstones porosity included interparticle and some shelter porosity. Intraskeletal and secondary moldic porosity were common to both lithologies

3.7.ii. Cement types.

Six distinctive cement morphologies are recognised:

1). Microstalactitic calcite cement occurs in grainstones and in the muddy lithologies (Plate 3.10.A). Cements are typically fibrous and contain up to three faint internal layers. Fibres stain red and are non-ferroan and non-luminescent. They do not display any corrosion features or microdolomite rhombs and are interpreted as primarily consisting of low magnesium calcite.

2). Acicular calcite crystals less than 10 microns wide form isopachous crusts. These crusts line pores, locally filling them and displaying polygonal sutures. Crystals have blunt ended terminations and are cloudy and full of inclusions (Plate 3.11.A). They stain red and are non ferroan and under CL are non luminescent. The isopachous crusts have been corroded, with holes up to 30 microns in diameter cutting across individual crystals and filled by bright orange luminescent calcite cement. Crystals appear to be pseudomorphs and the blunt terminations suggests an original aragonite composition (Folk & Assereto, 1976).

3). Micritic cement is locally peloidal but has also has formed at grain contacts (in grainstones) and in discontinuous layers which line intraskeletal and intergranular pores (Plate 3.11.B). Such cements are, however, rare and are recorded from only one muddy cycle and two grainstones

4). Blocky calcite fills remaining pores with crystals which are generally inclusion free and increasing in size away from the substrate.

i. Early crystals are generally equidimensional and line pores (Plate 3.11. C-D). In grainstones these granular crystals form meniscus cements at grain contacts (Plate 3.11.E). Terminations are euhedral but may be either scalenohedral or rhombohedral. Crystals stain red and are non-ferroan. They are generally non-luminescent but may contain up to four bright orange sub-zones up to 10 microns wide and carry a thin bright orange rim.

These early cements also form syntaxial overgrowths on echinoderm fragments which are locally poikilotopic (Plate 3.11.F). These cements are best developed in the grainstones and zones are of the form described by Walkden & Berry, (1984) as "contouring". The overgrowths from muddy lithologies are generally non-luminescent but may include one bright zone and a bright orange rim. In the grainstones early zones are inclusion rich. These are also non luminescent with up to three bright orange subzones and a thin bright orange rim but may contain faint internal sub zones. In hole N806 zones in syntaxial overgrowths are laterally discontinuous and "ragged" (Plate 3.11.G). Rare inter zonal dissolution surfaces occur within some overgrowths (Plate.3.11. H)

PLATE. 3.10.Stalactitic cements in the Micrite Unit.

A. Negative print from thin section of fibrous microstalactitic cement (s) Lining roof of former cavity (c) now filled by blocky calcite, Note layering in the stalactitic cement. 1210 mine level, 1902 stope. Scale bar = 7 mm

B. Photomicrograph (CL) of microstalatitic cement within oolitic lithoclast grainstone. Hole N351 at depth 104.1 m. Scale bar = 500 microns.

C. Photomicrograph (plane light) of microstalactitic cement (arrow) in grainstone of a muddy depositional cycle. Hole N1019 at depth 552.6 m. Scale bar = 2 mm.

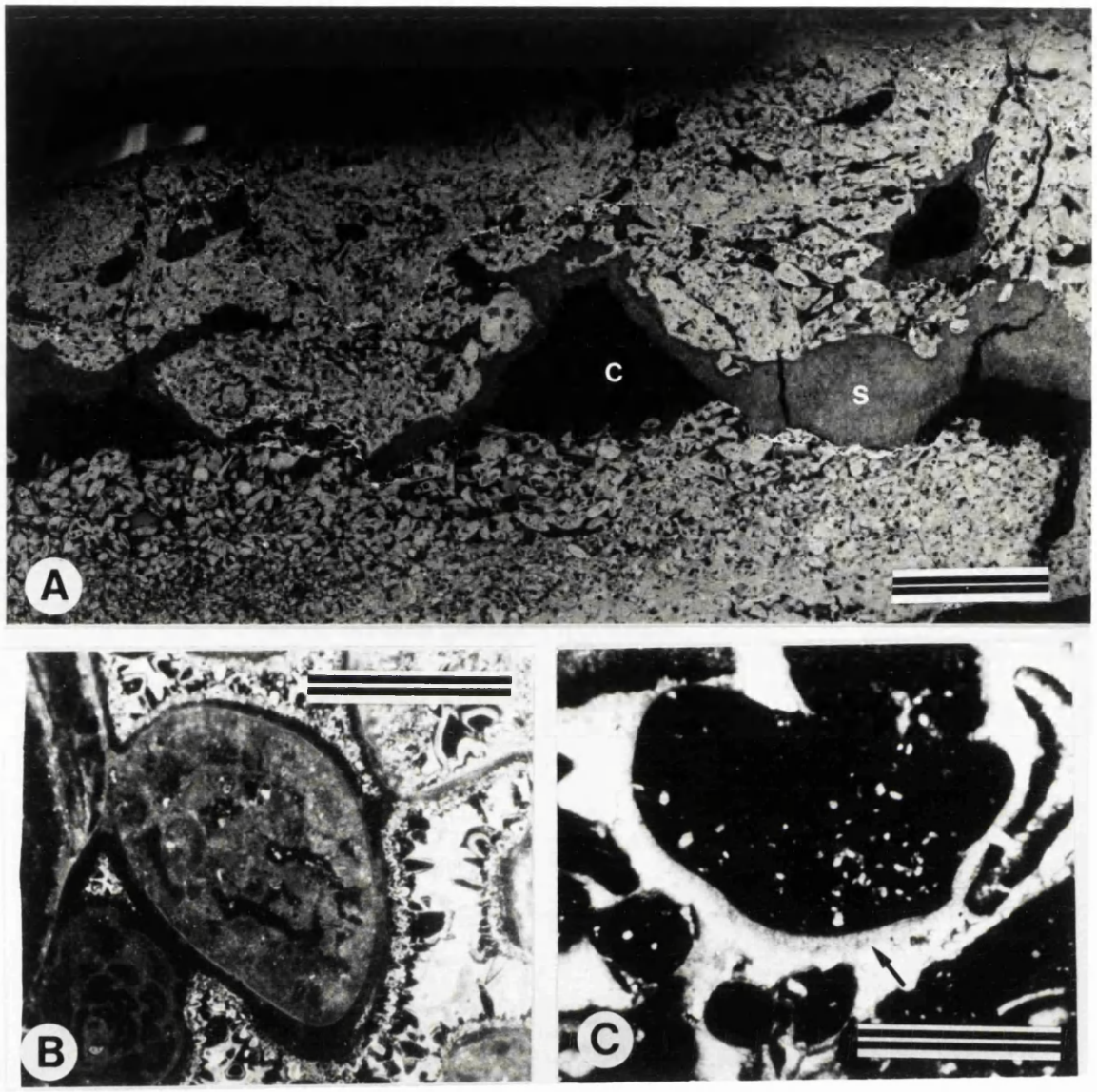
C
S
A
B
C

PLATE 3.11. Photomicrographs of Micrite Unit diagenetic features.

A. Photomicrograph (plane light) of acicular cement within grainstone from muddy cycle. Individual crystals have square to blunt terminations (arrow) suggesting a former aragonite composition. Hole N1019 at depth 552.9 m. Scale bar = 1 mm.

B. Photomicrograph (plane light) of micritic cement occuring at grain contacts overlain by acicular cement. Note bioclast mold defined by micritic envelope of uneven width. Hole N1019 at depth 552.9 m. Scale bar = 1 mm.

C. Photomicrograph (CL) of blocky non-luminescent cement lining fenestral pore in calcite mudstone. Each non-luminescent crystal contains several brighly luminescent zones. Hole N982 at depth 442.3 m. Scale bar = 500 microns.

D. Photomicrograph (CL) of blocky non luminescent cement lining pores in grainstone. Cement occludes pore at (a) and is mensicate at (b). Hole N1019 at depth 554.4. Scale bar = 500 microns.

E. Photomicrograph (plane light) of meniscus non-luminescent cement. Hole N1019 at depth 552.6 m. Scale bar = 250 microns.

F. Photomicrograph of poikilotopic syntaxial calcite cement. The syntaxial calcite has an inclusion rich inner zone (arrow) with later zone containing fragments of collapsed micrite envelope (arrow). Scale bar = 500 microns.

G. Photomicrograph (CL) of non luminescent syntaxial calcite in calcite mudstone. Note bright zone. Hole N982 at depth 441.4 m. Scale bar = 250 microns. Inset, photomicrograph (CL) of nonluminesent syntaxial calcite cement in grainstone. Note internal bright zones which have been locally affected by dissolution. Hole EP4A at depth 555. 8 m. Scale bars = 250 microns.

H. Photomicrograph (CL) of non-luminescent syntaxial calcite cement containing internal dissolution surface. Hole N1011 at depth 569.2 m. Scale bar = 250 microns.

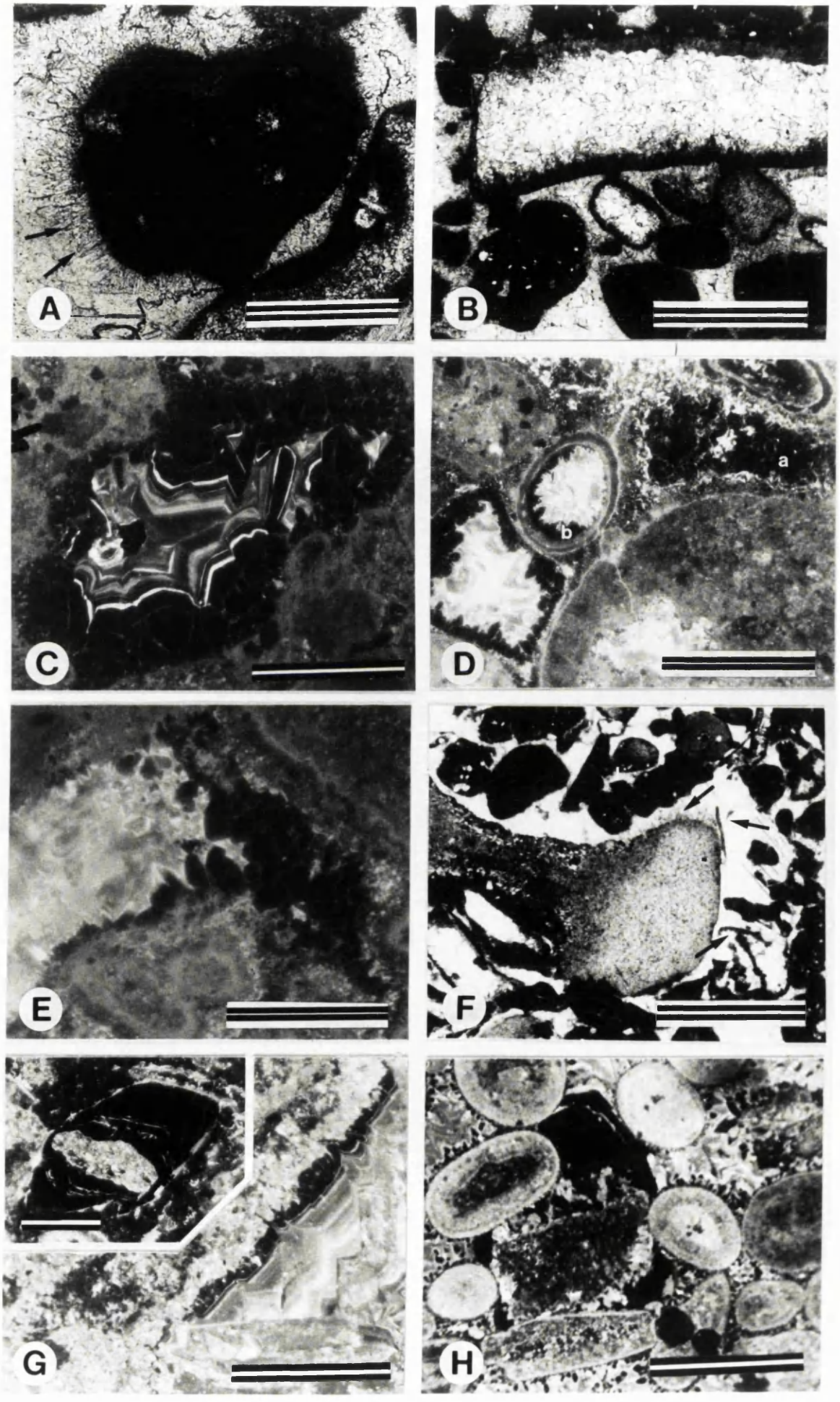
A
B
C
D
a
b
E
F
G
H

ii. Later crystals are larger and grew syntaxially upon the earlier blocky and syntaxial cements. Staining reveals prominent zones which vary from purple to mauve through to bluish. Under CL crystals generally luminesce dull orange but contain up to eight zones ranging from bright orange to dark brown (Plate 3.12.A). They also contain occasional interzonal dissolution surfaces (Plate 3.12. B). Terminations are euhedral but in hole N982 at depth 442.3 m they have been cut back by dissolution.

This association of blocky non-luminescent cement overgrown by dully luminescent cement has been widely recognised in shallow marine limestones. It has been described as the Older Banded Calcite (OBC) and Younger Ferroan Calcite (YFC) sequence (Meyers, 1991) and occurs widely through-out the British Lower Carboniferous (Walkden, 1987).

5). Saddle dolomite occurs in both mudstones - wackestones and grainstones. It consists of euhedral rhombs with curved crystal faces and a sweeping extinction. Staining produces a blue colour indicating that the crystals are ferroan. Locally non luminescent cores within crystals contains up to three dark crimson brown CL zones, the younger of these overlie a corroded surface. Core are overlain by a bright red zone with faint dull sub zones followed by a second non luminescent zone (Plate 3.12.C).

3.7.iii. Other petrographic features.

1). Some bioclasts have been bored by endolithic algae with holes truncating internal structures and filled with micrite. Some micrite filled holes have coalesced to produce micrite envelopes of uneven width (Bathurst, 1964).

2). Calcite crystal silt geopetally lines or occludes pores. Crystal silt is generally structureless but some reverse grading has been observed. Individual crystals are a few microns in diameter and are rhombic and non-luminescent in CL. In hole N806 at depth 362.8 m the crystal silts fill irregular cavities up to 10 mm in width imparting a light coloured "mottling" to the calcite mudstones consistent with dis-micrite fabric (Folk, 1962) (Plate 3.12.D). Muddy internal sediments are common in fenestral pores which they may geopetally line or occlude, some internal sediment is laminated Plate 3.12.E). Shell shaped moulds with micrite envelopes indicate dissolution of skeletal aragonite (Bathurst, 1964) (Plate 3.12.F)

3). Coated grains over 2 mm in diameter are recorded only from hole N509 where they have formed around bioclasts. Coats consist of up to six dark irregular structureless concentric micrite layers (refer Plate 3.8). The outer surfaces are irregular and these are too large to be ooliths and they are therfore classified as pisoliths.

4). Neomorphism has selectively affected bioclasts at points of maximum curvature, typically the apices and troughs of rib structures, extending laterally along internal laminae (Plate 3.12. G). Some bioclasts contain relic structure and dark (organic?) inclusions, indicating complete neomorphic calcitization (James, 1974) (refer plate 3.11.B).

5). Both mechanical and chemical compaction have occured. Allochems in the grainstones and bioclast layers in the mudstone - wackestones have undergone mechanical compaction (Plate 2.12.H). Oolith cortices have spalled, circumgranular and micritic cements have detached from their host grains (Plate 3.13.A) and broken, and micritic envelopes have collapsed, either completely or locally by indentataion of adjacent grains (Plate 3.13.B).

5a. Clasts in calcite lithoclast grainstones are bounded by concavo-convex sutures. In addition, pressure dissolution seams are present which can be classified according to the scheme of Wanless, (1979) as sutured-seam stylolites. Some of these have amplitudes of over 3 cm and have coalesed, producing an interweaving stylolite pattern. Stylolites contain a clay rich insoluble residue, up to 2 mm thick, and also a few clastic grains.

5b. At least two stages of brittle fracture have affected the rocks (Plate 3.13.C-D). Fractures in grainstones are locally controlled by the diagenetic fabric and have refracted around ooliths and syntaxial quartz overgowths.

3.7.iv. Distribution of cements.

1). Microstalactitic cement is recorded from three grainstones and two muddy units. It occurs in a bioclastic grainstone in hole N1019 at depth 552.6 m, and in oolitic lithoclast grainstones in hole N351, at depth 104.1 m and hole N509 at 56.4 m. It forms coatings on all grains but is pendulous beneath only a few grains. In the 1210 mine level, 1902 stope it has formed along the roofs of bedding parallel dissolution cavities within muddy lithologies. The rubble breccia filled by the Green Clay contains fenestral clasts with microstalactitic cement along the roofs of pores.

2). Acicular calcite cement occurs in only eleven thin sections from muddy lithologies, where it lines fenestral pores. This suggests that it was not pervasive. Of four thin sections from hole N982 taken over an interval of 1.3 m only two contain acicular cement, indicating that distribution changes rapidly over a short vertical intervals. Within the 12 m thick oolitic grainstone acicular cement also has a limited lateral and vertical distribution. It is absent from oncoidal, calcite mudstone lithoclast and bioclast grainstones.

PLATE. 3.12. Diagenetic features of the Micrite Unit (continued).

A. Photomicrograph (CL) of dully luminescent blocky cement filling fenestral pore in calcite mudstone. Hole N982 at depth 441.8 m. Scale bar = 250 microns.

B. Photomicrograph (CL) of blocky dully luminescent cement containing interzonal dissolution surface (arrow). Hole N982 at depth 441.0 m. Scale bar = 500 microns.

C.Photomicrograph (CL) of saddle dolomite filling fenestral pore in calcite mudstone. Note dissolution suface separating saddle dolomite from dully luminescent blocky calcite cement. Hole N982 at depth 441.8 m = 500 microns.

D. Photomicrograph (plane light) of calcite crystal silt filling dissolution hole giving dismicrite fabric. Hole N806 at depth 362.8 m. Scale bar = 1 mm.

E.Photomicrograph (plane light) of muddy internal sediment (s) lining floor of fenestral cavity (c) in calcite mudstone (m). This is overlain by reversely graded calcite crystal silt (cs). Hole N1022 at depth 550.7 m. Scale bar = 250 microns.

F. Photomicrograph (plane light) of shell mould (m) defined by micrite envelope. Note former shelter porosity (p) below the bioclast. Hole N982 at depth 441.8 m. Scale bar = 1 mm.

G. Photomicrograph (CL) of shell fragment displaying neomorphism indicated by brightly luminescent calcite. The neomorphism is located at the points of maximum curvature of the shell. Hole EP4A at depth 567.3 m. Scale bar = 250 microns.

H. Photomicrograph (CL) of shell fragment that has fractured. Granular cement is absent on broken surface and shell is surrounded by later blocky dully luminescent calcite cement. hole N1019 at depth 552.6 m. Scale bar = 250 microns.

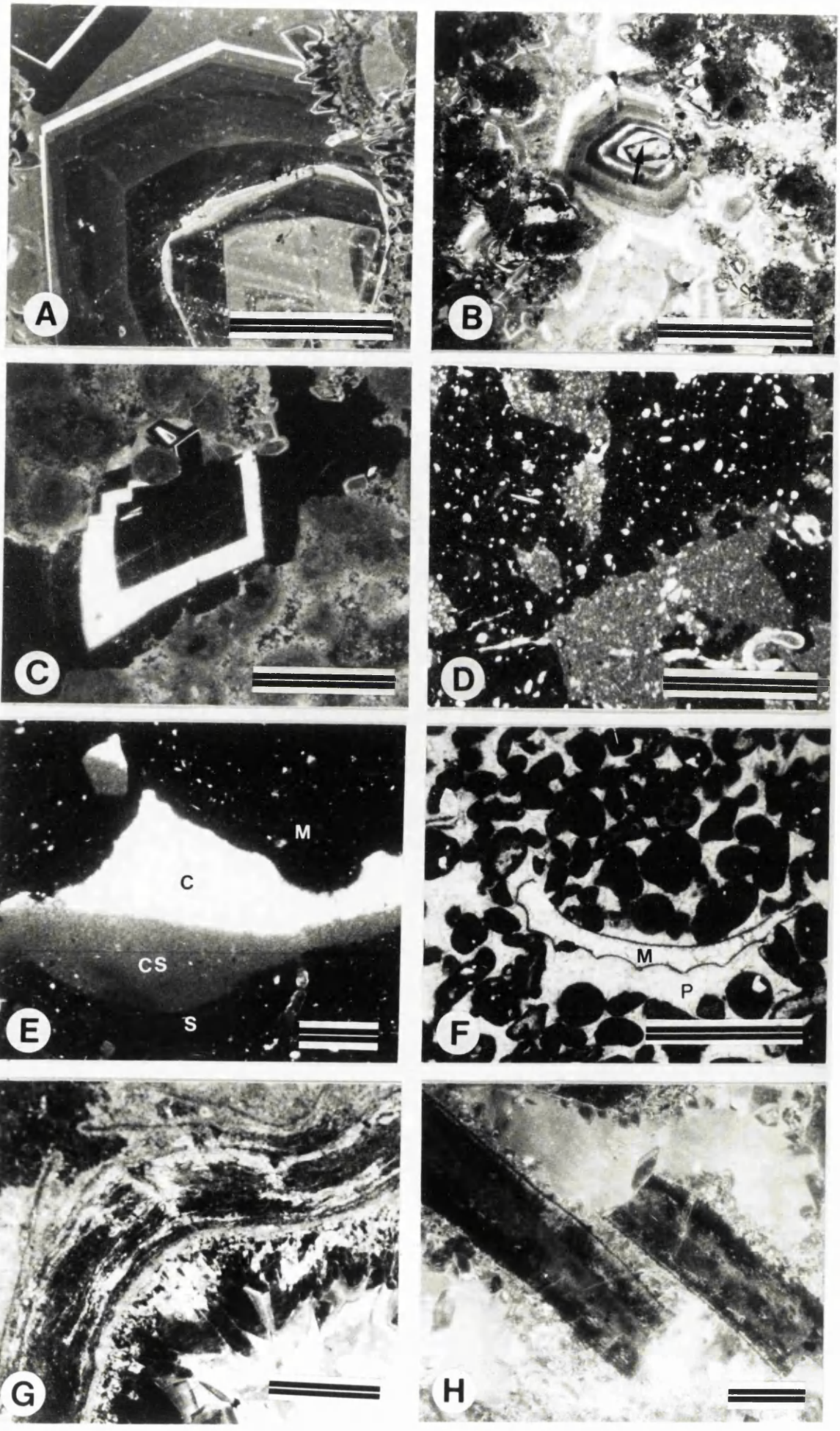
A
B
C
D
M
C
CS
S
E
M
P
F
G
H

PLATE 3.13. Diagenetic features of the Micrite Unit (continued).

A. Photomicrograph (plane light) of micritized ooliths with detached circumgranular cements (arrow). Hole N317 at depth 318.3 m. Scale bar = 500 microns.

B. Photomicrograph of collapsed micritic envelopes with attached cement 'floating', within blocky calcite cement. Scale bar = 1 mm.

C. Photomicrograph (CL) of fracture cutting through oolitic grainstone. The fracture is now filled by with zoned dully luminescent calcite cement (c). Hole N1012 at depth 535 m. Scale bar = 1 mm.

D. Photomicrograph (CL) of fracture (1) cutting oolitic grainstone. This has been cut by a later fracture (2) which has locally refracted around the margins of grains (arrow) Hole N317 at depth 315 m. Scale bar = 250 microns.

E. Photomicrograph (CL) of extensively corroded acicular (?) cement lining fenestral pore. This is overlain by blocky non-luminescent cement which is followed by dully luminescent blocky calcite cement (d). Hole N982 at depth 441.8 m. Scale bar =

F. Photomicrograph (CL) of the same sequence as (E) but in oolitic grainstone. Hole N1011 at depth 569.2 m. Scale bar = 500 microns.

G. Photomicrograph (CL) of non-luminescent cement overlain by dully luminescent blocky calcite. This is followed by a second cycle of non-luminescent cement which is again overlain by dully luminescent blocky calcite cement.Scale bar = 250 microns.

H. Photomicrograph (CL) of fenestral pore in calcite mudstone (m) lined with dully luminescent blocky calcite cement (c) which has incompletely filled the pore leaving relic fenestral porosity (p). Hole N806 at depth 231.8 m. Scale bar = 1 mm.

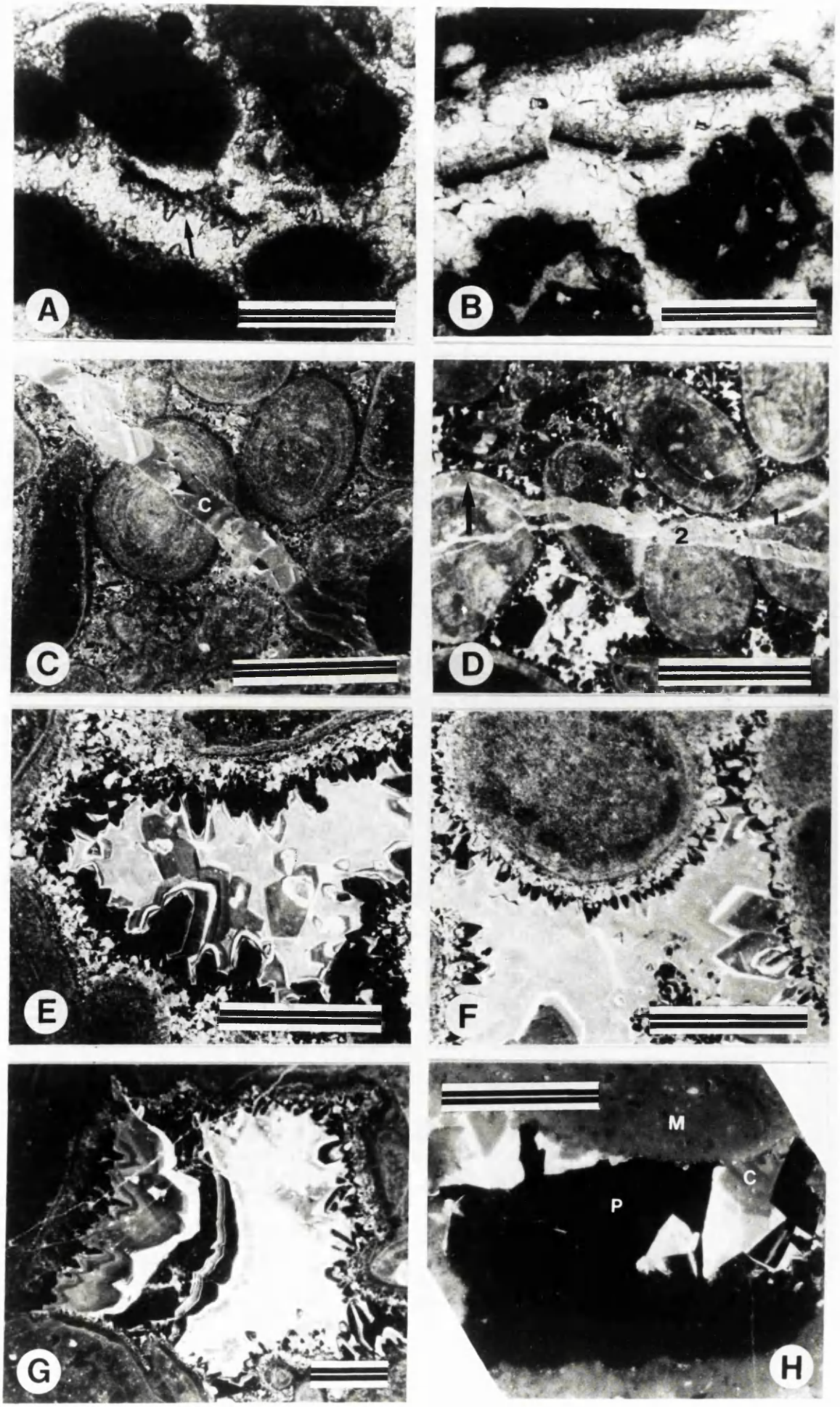
A
B
C
c
D
2
1
E
F
G
H
M
C
P

3). The early non luminescent granular cement occurs in 22 of the 28 samples from the muddy lithologies where it lines fenestral pores. However, the number of bright zones varies rapidly over short distances. This can be seen in 4 thin sections from hole N982, taken over a vertical interval of 1.3 m directly below the subaerial erosion surface bounding cycle sequence number 3. In the lowest sample the early calcite includes up to five thin bright orange zones. Fifty centimetres above, the same cement contains only three bright zones while above this early cements are absent (Fig 3.35.).

However, the early cement is common in the grainstones and is only absent in 3 thin sections where pores have been filled by acicular cement. In oolitc grainstones from hole N1011 and N317 early granular cement extend vertically 3 to 9 m.

4). The later blocky calcite cement is pervasive and volumetrically significant in both muddy lithologies and grainstones. It is absent only where acicular or early blocky cements have occluded pores. The CL zones within the later cement vary over the entire 60 m vertical interval of the Micrite Unit. In addition, zone sequences vary rapidly over short distaces.

5). Sylolites, brittle fracture, neomorphism, dissolution of aragonite and stabilization of skeletal high magnesium calcite are pervasive and occur in both muddy lithologies and grainstones, extending throughout the Micrite Unit. However grain fracture is confined to the grainstones. Other non pervasive petrographic features include crystal silts, recorded from eight samples from muddy lithologies and two from grainstones.

3.8. CEMENT STRATIGRAPHY.

Two cement stratigraphies have been identified which can be referred to as type A and type B. Both types contain crystal silts and skeletal grains which have been affected by neomorphism, dissolution and micritization. Both sequences have been affected by compaction and have been overprinted by later blocky cements. The sequences occur in both muddy depositional cycles and grainstones.

3.8.i.a. Type A .

The type A cement sequence begins with alteration of the grain surface. Begining with the formation of micritie envelopes, this includes later conversion of skeletal high magnesium to low magnesium calcite and dissolution of skeletal aragonite. The dissolution created moldic pores, and increased porosity. Some bioclasts in grainstones display relic internal strucures indicating that calcitization of aragonite also occured.

James and Choquette (1984) discussed the relative timing of skeletal alteration. It was suggested that in a sediment consisting of a mixed carbonate mineralogy, skeletal high magnesium converts to low magnesium calcite, with dissolution and calcitization of aragonite occuring more or less contemporaneously with stabilization of skeletal magnesium calcite. It is likely that the lath shaped evaporite crystals, occuring in muddy lithologies also dissolved at this time as a result of their (inferred) high solubility.

The occurence of palaeokarst suggests that there was also wholesale surficial dissolution of the muddy lithologies. As in other karren, this dissolution most likely began along surficial joints and bedding planes. The evolution of palaeokarst has been reviewed by Ford & Williams (1989) and James & Choquette (1984) and is discussed in Appendix 2.

Calcite crystal silts rest directly on grain surfaces, collecting geopetally at contacts (in hole N286 at depth 172.2 m in the oncoidal grainstone) indicating that they were deposited before cementation. In muddy lithologies they have geopetally filled moldic and fenestral pores and rest directly on muddy internal sediment. They have also filled irregular millimetre scale solution cavities producing dismicrite fabrics. The crystal silts are not pervsasive indicating deposition was punctuated.

Micritic cement is the earliest cement in this sequence forming at grain contacts. This is overlain by fibrous cement which is microstalactitic below a few grains where pores were large enough for water droplets to form. Microstalacmitic cement also occurs along the roofs of moldic pores indicating that it post dates dissolution of skeletal aragonite. Microstalactitic cement also forms along the roofs of bedding dissolution cavitites supporting the view that dissolution of muddy lithologies occured early.

Early blocky non luminescent cements have lined moldic and primary pores and overlie fibrous microstalagtitic cements and crystal silts. In grainstones some early blocky cement forms meniscus layers at grain contacts. Similar cements form syntaxial overgrowths. The precise age relationship between overgrowths and early blocky cement is problematical. However both cements have formed early and the CL characteristics of the early blocky and syntaxial cements from both muddy lithologies and grainstones is the same, suggesting that they were precipitated from pore-waters of the same chemical composition and thus, probably at the same time. The sequence is summarized in Fig. 3.36.

3.8.i.b. Interpretation.

The type A sequence includes:

1. Stabilization of skeletal high magnesium calcite, and dissolution and calcitization of skeletal aragonite, and dissolution of calcite mudstones.

2. Deposition of calcite crystal silt and formation of dismicrite fabrics.
3. Nucleation and growth of meniscus, micrite, microstalacmitic, early granular and syntaxial cements.

These features are widely believed to reflect a diagenetic system dominated by meteoric pore waters (Folk, 1962; Longmann, 1980; James & Choquette, 1984; Walkden, 1987; Horbury & Adams, 1989; Emery & Dickson, 1989; Meyers, 1991 and many review articles). Dissolution and alteration of skeletal high magnesium calcite and aragonite, deposition of crystal sitls and formation of microstalactitic and meniscus cements are typical products of the meteoric vadose zone. If the fluid flux is large enough and pore water strongly undersaturated with respect to aragonite total dissolution will occur. If however, fluid flux is slow and pore waters only slightly undersaturated withe respect to aragonite then cacitization of aragonite will take place (James, 1974). The multilayering present in microstalagtitic cement has been interpreted as representing punctuated vadose drainage (Longmann, 1980). Calcite crystal silt indicates pores were filled with meteoric water and is believed to be a "cryptic" indicator of subarial erosion surfaces (Dunham, 1969; Folk, 1962), with the localized distirbution of crystal silts perhaps, again, reflecting punctuated vadose drainage.

The early non luminescent and syntaxial cements are believed to reflect deposition from meteoric phreatic porewaters (Longmann, 1980; James & Choquette, 1984, Walkden, 1987, Emery and Dickson, 1989; Horbury & Adams, 1989; Meyers, 1991). It is suggested that the sediments displaying these cements underwent contemporaneous vadose and phreatic cementation. The relationship of phreatic cements to vadose features is similar to that in the meteoric cement sequences described by Longman, (1980). In these the phreatic cements which overlie vadose cements are explained as resulting from a rise in the water table generated by a rise in sealevel. The appearence of similar sequences at Navan indicating that the reactive zones were dynamic and moving vertically.

3.8.ii.a.Type B.

The type B cement sequence illustrated in Plate 3.13.E and was recorded from seventeen muddy sequences and six grainstones. The earliest diagenetic event recorded was the deposition of up to two layers of internal sediment. These rest directly along the floors of fenestral pores and do not overlie cement. Micritic cements are the earliest in this sequence lining intraskeletal and intergranular pores.

Nucleation and growth of acicular cement followed, forming isopachous crusts which line fenestral, intraskeletal and interparticle pores in the muddy lithologies and grainstones and overlie micritic cements. The acicular cement is itself locally heavily corroded with irregular holes appearing in isopachous crusts suggesting dissolution

followed the growth of this cement. These holes were then filled by brightly luminescent calcite. The acicular cement is overlain and mouldic pores are lined or filled by blocky calcite similar to that in the type A sequence (Plate 3.13 E-F). This cement is generally non luminescent but has up to three bright orange zones and a bright rim. The early cements apparently have the same luminescence as the neomorphic calcite replacing bioclasts, suggesting that the two were more or less contemporaneous. The sequence is summarized in Fig. 3.37.

3.8.ii.b. Interpretation.

The type B sequence includes (In stratigraphic order):

1. Internal muddy sediment
2. Micritic cement.
3. Isopachous acicular calcite cement.
4. Early blocky cement.

Acicular and micritic cements are widely believed to reflect shallow marine conditions (Longmann, 1980). Modern shallow marine cements form hardgrounds These surficial crusts occur on the crests and flanks of some modern carbonate sandbodies. Crusts can be several centimetres thick and laterally continuous over tens of metres (Dravis, 1979). Where acicular cements fill pores they typically form polygonal sutures (Shinn, 1969). Hardgrounds have been recorded from Jurassic grainstones in France (Purser, 1969).

Like modern acicular cements, the Navan examples have limited lateral and vertical distribution and, where they have filled pores, display polygonal sutures. They are interpreted as marine cements which formed hardgrounds. Borings present in the oolitic grainstone in hole N351 provide further evidence of hardground formation since borings are common in modern and ancient hardgrounds, and provide unequivocal evidence of lithification.

Deposition of acicular cements was followed by dissolution and corrosion of skeletal aragonite and acicular cement. These events were followed by deposition of blocky calcite similar to that in the type A seqence indicating a change to meteoric influenced conditions.

3.8.ii.c. Significance of intra crystal (concentric) CL zones.

In addition to porescale variation in cement, intra-crystal variation is present in blocky and syntaxial cements occuring in both muddy depositional cycles and grainstones. Broad non-luminescent zones contain up to four thin bright orange sub zones. Non-luminescent cements with bright orange subzones have been widely recognised in ancient shallow marine limestones (Meyers, 1991). Cements with these

CL characteristics have been correlated by some workers over large regions and through tens to hundreds of metres of section. However others have shown that similar sequences can die out over very small distances and thicknesses (Walkden, 1987; Horbury & Adams, 1989) The time significance of zones and subzones varies .

1. Packets of subzones forming distinctive sequences may be precipitated synchronously throughout the studied region and throughout the stratigraphic thickness of the host formation. The non-luminescent zones reflect the oxic portions of meteoric palaeo-groundwater systems in water bodies mainly established below post formational subaerial unconformities.

2. Distinctive zonal sequences of cement may be precipitated in a systematically changing environment . Where the environment migrates, as in a rising water table driven by a rising sea level zones are diachronous with those stratigraphically lower in the formation significantly older than those at the top. The distribution in this case reflects the successive development of relatively small oxic meteorc lenses beneath succesive subaerial exposure surfaces.

Early non-luminescent cements with bright orange subzones are common throughout the British Lower Carboniferous occuring in the (Asbian) of the Askrigg and Derbyshire platform, Cumbria, North and South Wales and the Mendips (Walkden, 1987), in the southern Lake District (Horbury & Adams, 1989) and in the Brigantian of Anglesey and Derbyshire (Walkden & Davies, 1983). The Upper Jurassic oolitic Lincolnshire limestone contains cements consisting of non luminescent-bright orange zones whose distribution is also interpreted as reflecting a palaeo-phreatic lens (Emery & Dickson, 1989).

The main feature of the Lower Carboniferous successions is cyclicity, with cycles punctuated by intraformational palaeokarst surfaces. From this Walkden, (1987) suggested that this style of cementation is characteristic of sequences containing sedimentary cycles and palaeokarst. The repeated emergence in these successions allows widespread development of shallow meteoric cements (Walkden, 1987). The non-luminescent to bright orange oscillations are interpreted as reflecting alternating porewater conditions. Non luminescent intervals are believed to reflect the downward penetration of a well oxygenated meteoric water during the subaerial stage while bright orange zones form during relative stagnation related to marine transgression at the surface. The relative thickness of the zones is interpreted as reflecting the duration of the generating event (Walkden, 1987). Walkden (1987) was able to demonstrate the appearence of progressively younger sub zones at higher stratigraphic levels so that his entire sequence was diachronous.

The early syntaxial and blocky calcites in the Micrite Unit are interpreted as reflecting meteoric phreatic conditions. They are non-luminescent and contain bright

orange subzones similar to those in other early phreatic cements in the British Lower Carboniferous. They probably reflect a downwards penetrating phreatic lens formed during a subaerial stage. The thin bright zones indicate stagnation concurrent with a higher sea level. The repetition of the dark bright sequence up to four times indicates sealevel oscillation. Some corrosion of bright cement occured before deposition of non luminescent cement. The strong depositional cyclicity of the Micrite Unit at Navan, punctuated by subaerial surfaces at closely spaced intevals, suggests that the zonal sequences are probably vertically diachronous. However, proof of this would require correlation of the bright subzones beyond that possible with available data.

Like other Lower Carboniferous examples it is not possible to relate individual zonal oscillations to specific subaerial surfaces at Navan. However, the disappearence of the early granular cements over 1.3 m below the palaeokarst surface at the top of the third cycle sequence is interpreted as reflecting the top of a phreatic water lens.

3.8.iii.a.Later Sequences.

The A and B sequences share a common later history. Compaction was accompanied by mechanical fracture, best represented in the grainstones. Oolith cortices were spalled, early blocky cements detached from host grains and some micritic envelopes collapsed. The broken surfaces of these grains do not carry either acicular or early blocky cements, indicating grain fracture post dated formation of these features. Later blocky dully luminescent cement grew syntaxially on early cements. However, on grains broken by compaction, the later cement overlies the fracture surface and renucleates. The later dully luminescent cement also contains fragments of collapsed micrite envelopes and circumgranular cements. It lines all remaining pores in mudstones and grainstones irrespective of cycles, suggesting that that it formed following burial of the Micrite Unit. However, in hole N806 between 330.0 m and 332.0 m and also between 343.0 m and 346.0 m the later blocky cement has not filled the pores, indicating some relic fenestral porosity occurs.

The late blocky dully luminescent cement has been affected by at least two dissoluion events. These are seen in hole N982 at depth 441.0 m where the earliest zone has been cut back and overgrown by a later dull cement during new nucleation. In hole N351 the earliest dully luminescent zone has been cut back and forms an irregular surface. This was then overgrown by non luminescent calcite which contains up to five thin bright zones, overgrown syntaxially by dully luminescent calcite (Plate 3.13. G). The sequence is summarized in Fig. 3.38.

3.8.iii.b. Interpretation.

The early cements prevented destruction of pore space, maintaining fenestral, moldic and primary pores and allowing flow of late cement-forming fluids. As stated in section 3.12, late dully luminescent blocky calcite cement are very common in shallow marine limestones forming 25 to 100% of the cements (Meyers, 1991, Meyers, 1978, Dorobek, 1987, Grover & Read, 1983). Like the Navan examples these cements post date grain compaction, fill fractures and therefore post date the sedimentary cyclicity (Goldstein, 1988; Kaufman *et al,* 1988; Meyers, 1978).

Dully luminescent blocky cements are interpreted as reflecting precipitation in a burial environment from hundreds of metres to several kilometres depth, and involving fluids ranging from slightly modified seawater to highly evolved subsurface brines (Meyers, 1991). The non luminescent zones in the Navan examples suggest downward penetration of well oxygenated porewaters, indicating that growth of the cements was not beyond the influence of surface derived fluids. Meyers (1991) drew attention to the fact that the source and flow directions of fluids forming these late cements cannot be determined from the cement stratigraphy because of the complex and rapidly changing sequence of zones.

Compaction continued after growth of burial cements with the development of sutured seam stylolites and the accumulation of stylocumulate. Siliciclastic grains in these dissolution seams have corroded against the stylolite margins. Where cements were absent grains developed concavo-convex contacts. Some stylolites contain fibrous calcite oritentated normal to their walls pointing to late dilation.

Two stages of brittle fracture have occured, the first set of fractures is filled with bright luminescent calcite cement. The second set cuts across these but is locally controlled by the diagenetic fabrics. In the grainstones they have refracted around ooliths and syntaxial overgowths. These later fractures are filled with dully luminescent blocky calcite. However, some crystals have dark cores followed by a bright orange zone (with faint dark zones) a second dull orange zone (again with faint dark zones) and finally by a faint dark zone. Occasionally this blocky cement failed to fill the pores completely leaving relic fenestral porosity (Plate 3.13. H)

3.9. SEDIMENTOLOGICAL AND PETROGRAPHIC SYNTHESIS OF THE MICRITE UNIT.

The characteristic feature of the Micrite Unit is cyclicity. Cycles record deposition which began in a semi restricted lagoon and which evolved upwards into tidal flats and sometimes subaerial erosion surfaces. There are shallowing up cycles. Four prominent grainstones are persistent within this sequence and reflect temporary incursions of more open marine conditions. Minor cycles can be grouped into three large scale sequences capped by erosion surfaces. The most prominent of these are a regolith filled by green illitic clay which contains pedogenic structures, a palaeokarst surface. These "cycle packets" suggests a second order of cyclicity in addition to high frequency 5th order (Milankovich) cyclicity was also operating.

The base of the Micrite Unit is flat. The upper surface is irregular, and displays steeply inclined surfaces, flute amd pinnacle surfaces, former cavities and is mantled by silty shales. These are key criteria in the elucidation of sub-surface palaeotopography (Esteban, 1991), thus the upper surface of the Micrite Unit is bounded by palaetopography. As will be shown in chapter 7, these erosion surfaces, have been critical in controlling the location of high grade zinc-lead ores.

Two cement sequence are present, one recording meteoric diagenesis the other shallow marine cementation which has been overprinted by meteoric cement. In addition to pore scale variation, concentric zoning records repeated penetration of meteoric water during the subaerial stages with bright zones related to higher sea levels. Overprinting both sequences is a dully luminescent burial cement which postdates the depositional cyclicity.

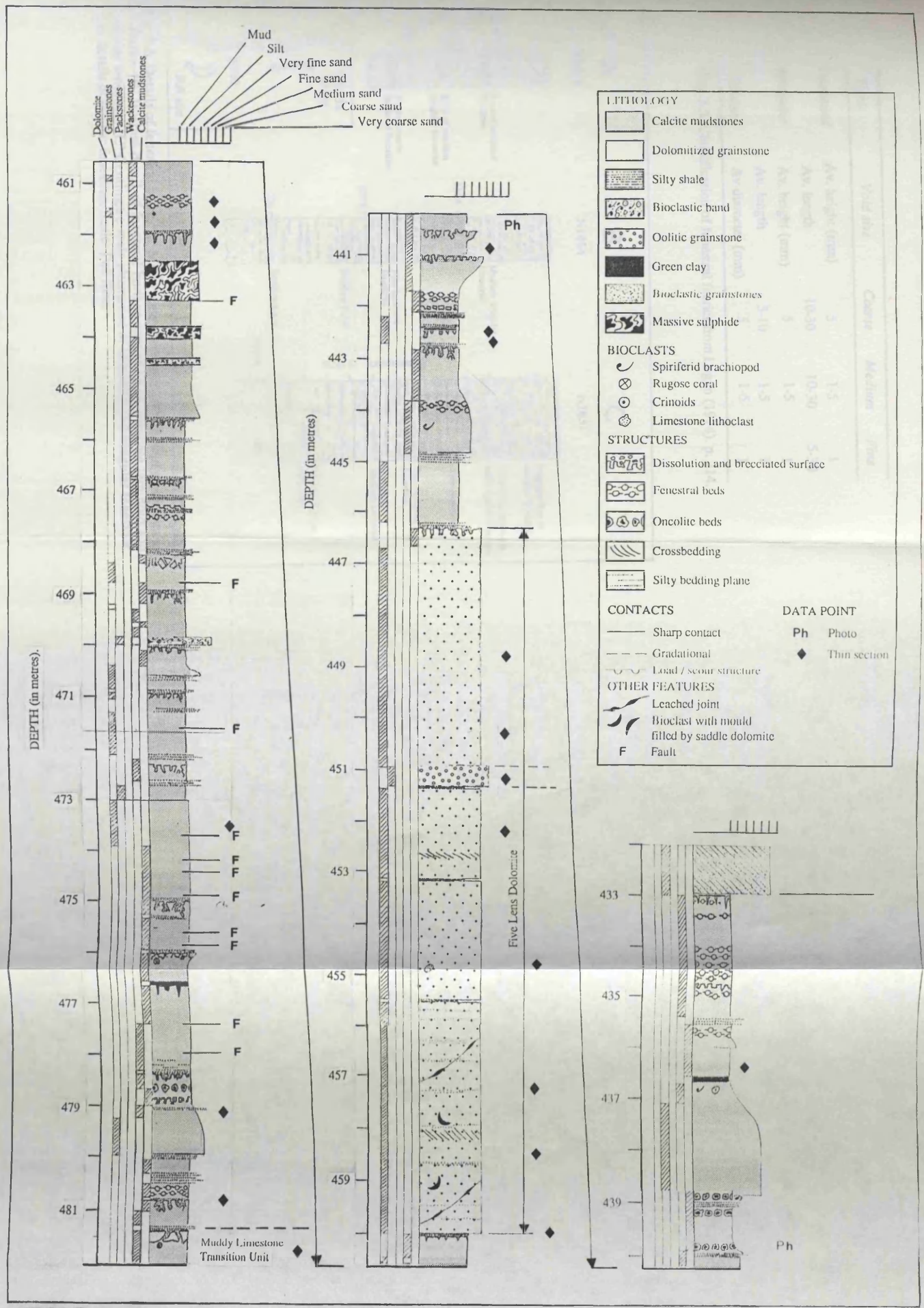

Fig. 3.1. Summary log of the Micrite Unit, western mine area, note shaley brecciated surfaces occuring every few metres.

Type	*Void size*	*Coarse*	*Medium*	*Fine*
Laminoid	Av. height (mm)	5	1-5	1
	Av. length	10-30	10-30	5-30
Irregular	Av. height (mm)	5	1-5	1
	Av. length	5-10	1-5	1
Tubular	Av diameter (mm)	5	1-5	1

Fig. 3.2. Classification of fenestral fabrics from Logan (1974). p. 214.

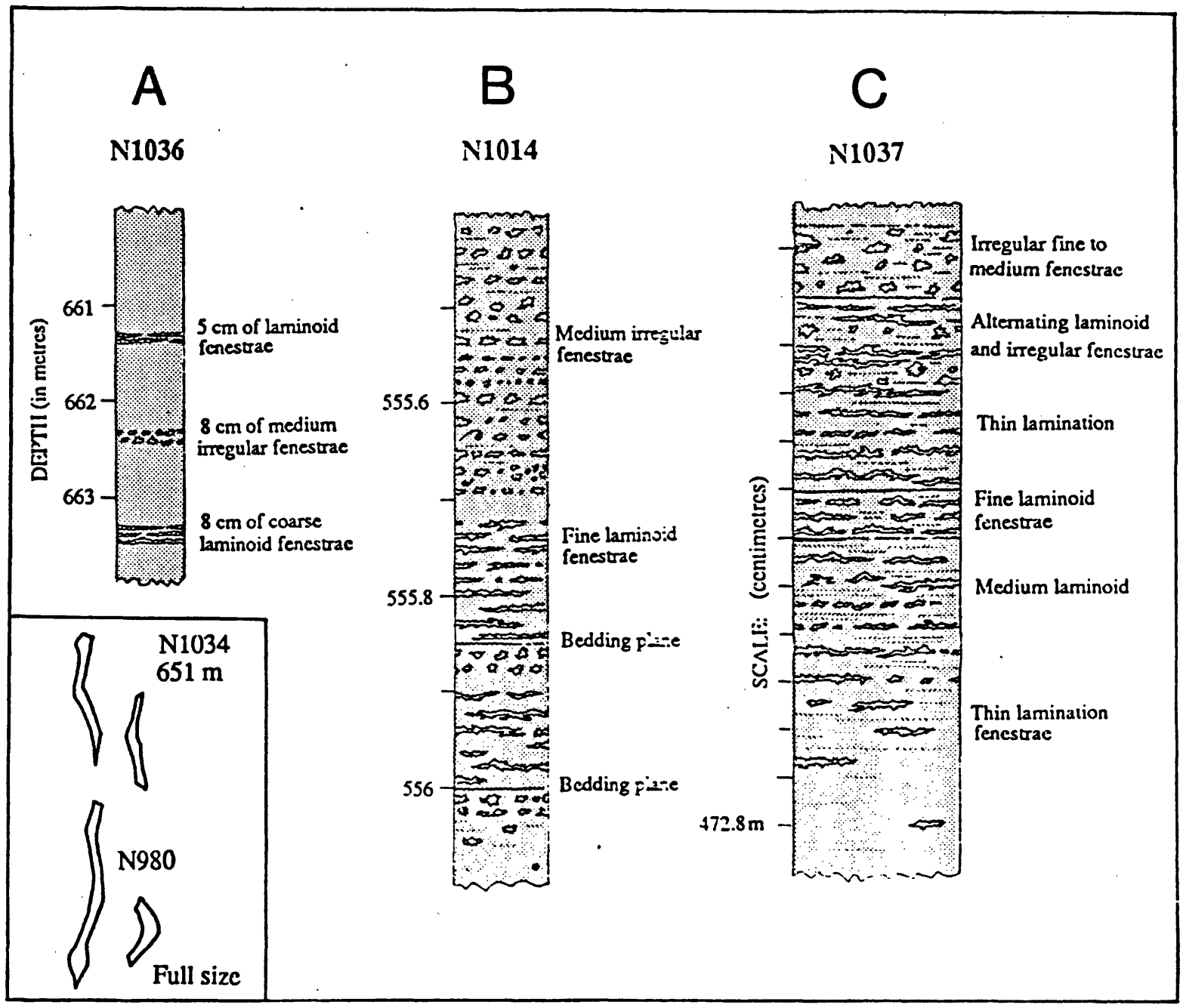

Fig. 3.3. Details of fenestral beds. **'A'** Metre scale alternation of laminoid and irregular fenestrae. **'B'** Internal detail of fenestral horizon consisting of alternate laminoid and irregular fenestrae. **'C'** Centimetre scale alternation of laminoid and irregular fenestrae. Inset details of tubular fenestrae, Scale: Full Size.

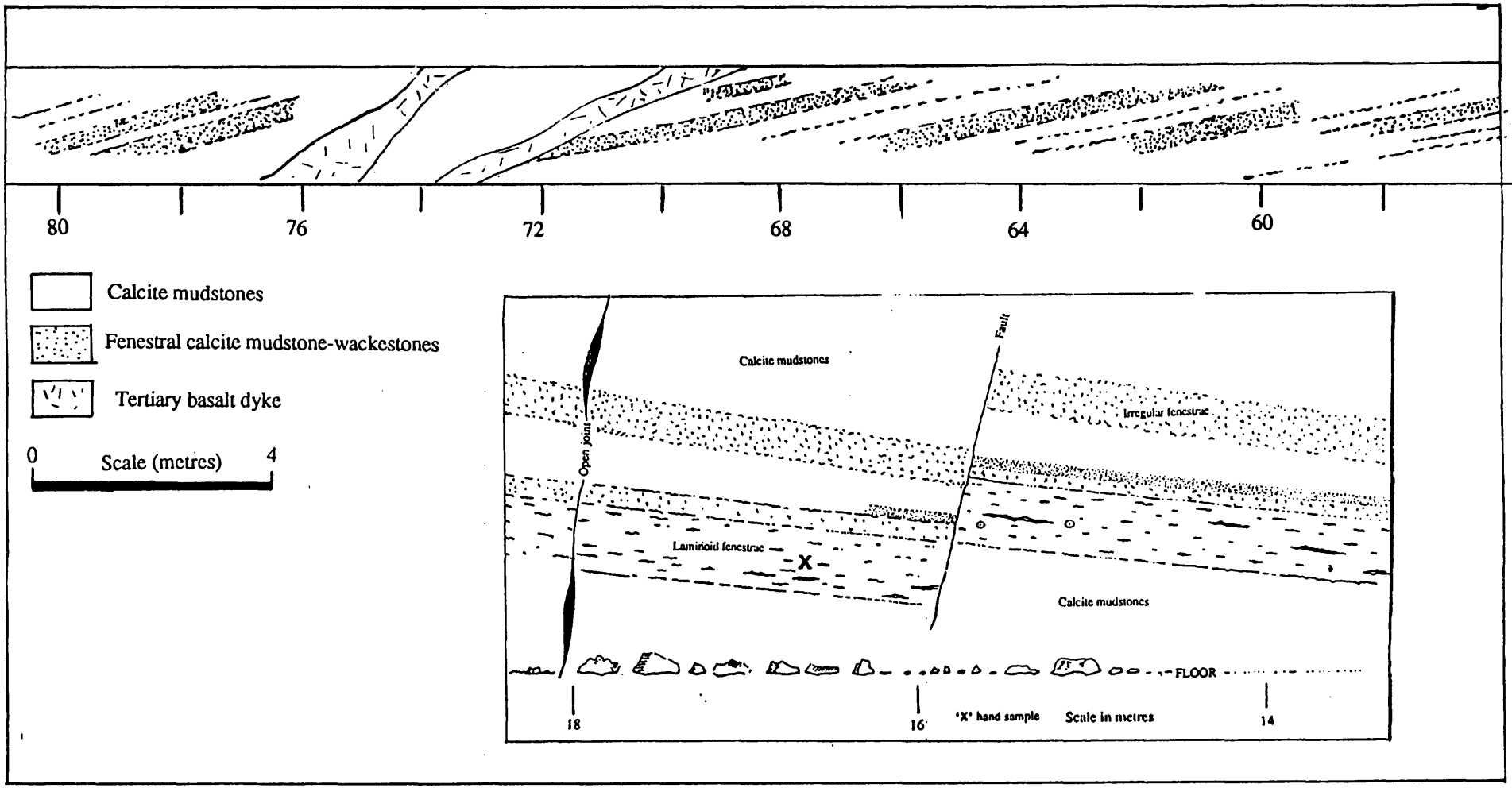

Fig. 3.4. Cyclic alternation of fenestral and non fenestral beds exposed in mine drift, 1130 drainage drift, 2 Zone. Inset, detail of bedding in calcite mudstones, note fenestral horizons and thin sandy beds. 1130 mine level drainage drift, 2 Zone.

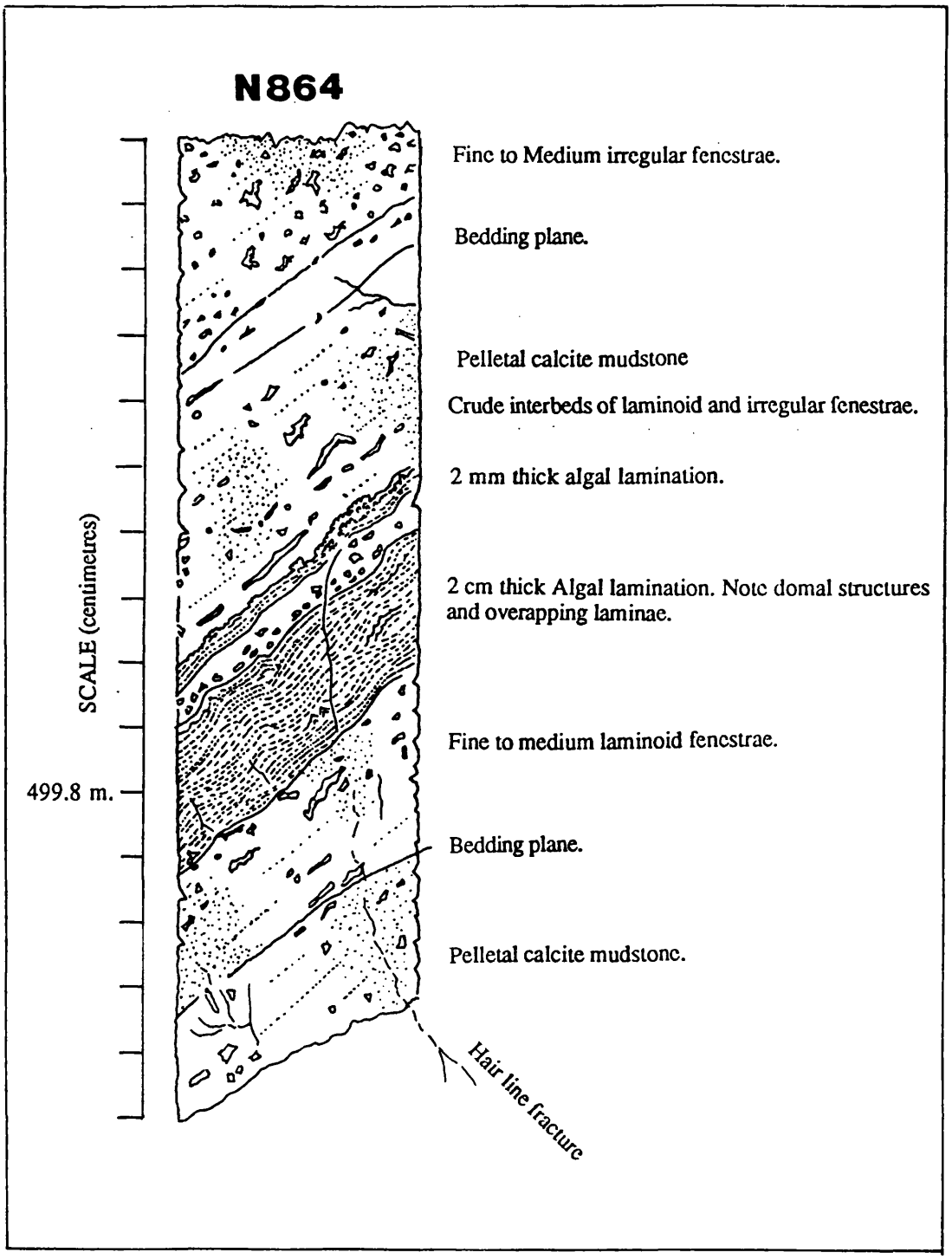

Fig. 3.5. Cryptalgal lamination in calcite mudstone, note domal structures and overlapping lamination. The algal lamination is closely associated with laminoid and irregular fenestrae and thin bedding. Hole N864, Scale: Full Size.

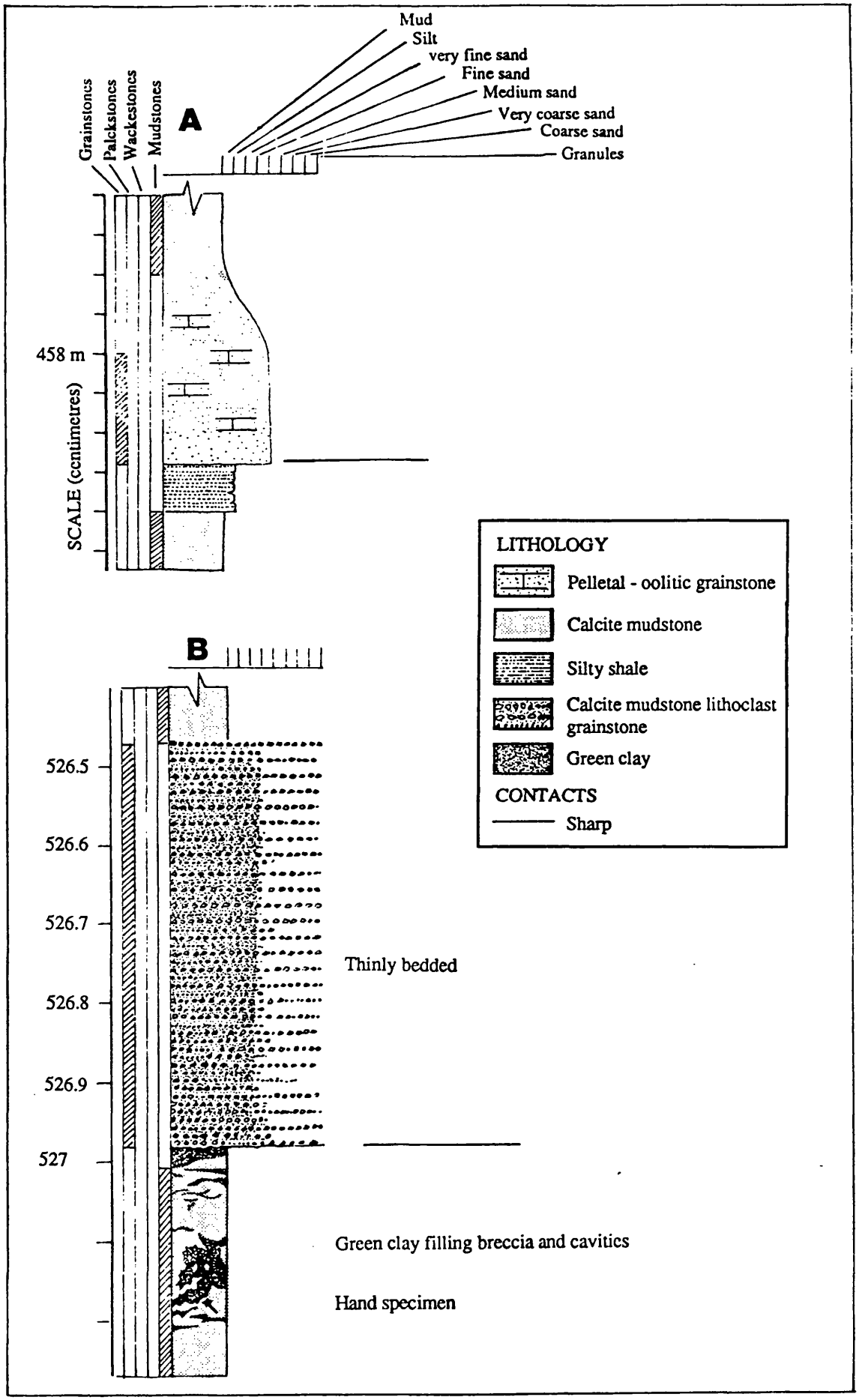

Fig. 3.6. 'A' Log of graded bed in calcite mudstones, note sharp base, hole N987. 'B' Log of calcite mudstone lithoclast grainstone overlying green clay.

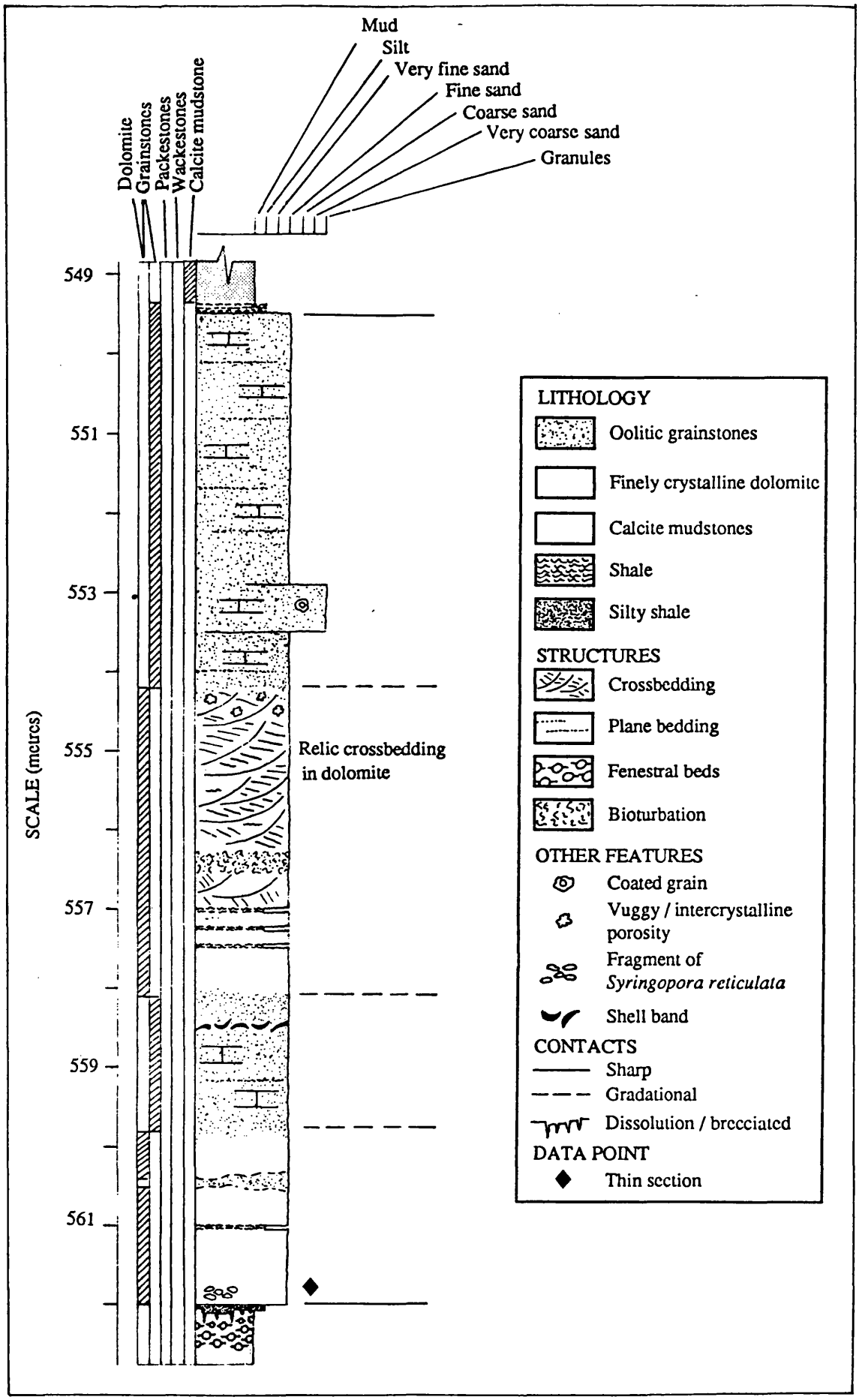

Fig. 3.7. Summary log of oolitic grainstone. Note fenestral calcite mudstones with shaley brecciated surface directly below.

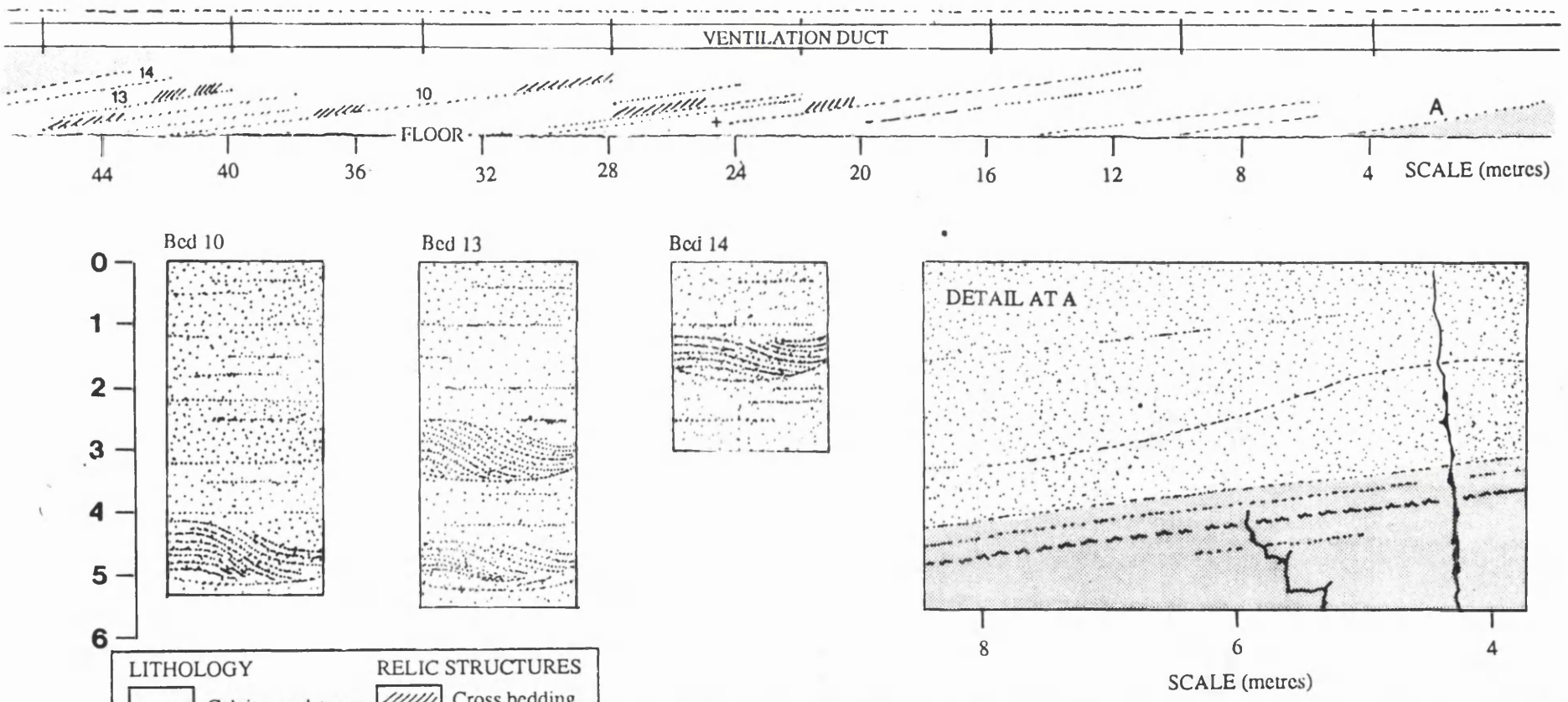

Fig. 3.8. Underground exposure of oolitic grainstone, now extensively dolomitized (the Five Lens Dolomite). Note extensive relic layering and cross-bedding. 1130 mine level drainage drift, 2 Zone.

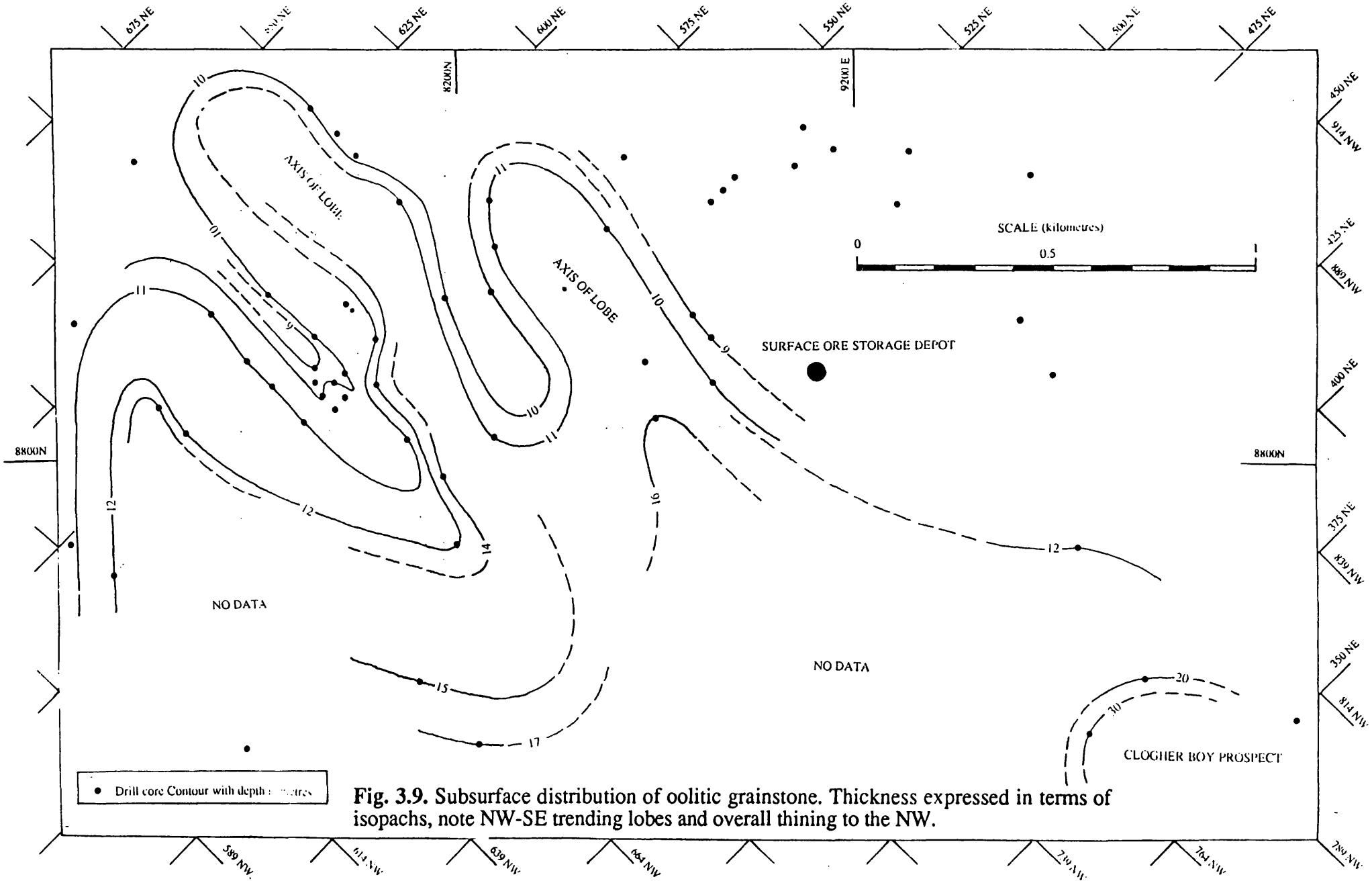

Fig. 3.9. Subsurface distribution of oolitic grainstone. Thickness expressed in terms of isopachs, note NW-SE trending lobes and overall thining to the NW.

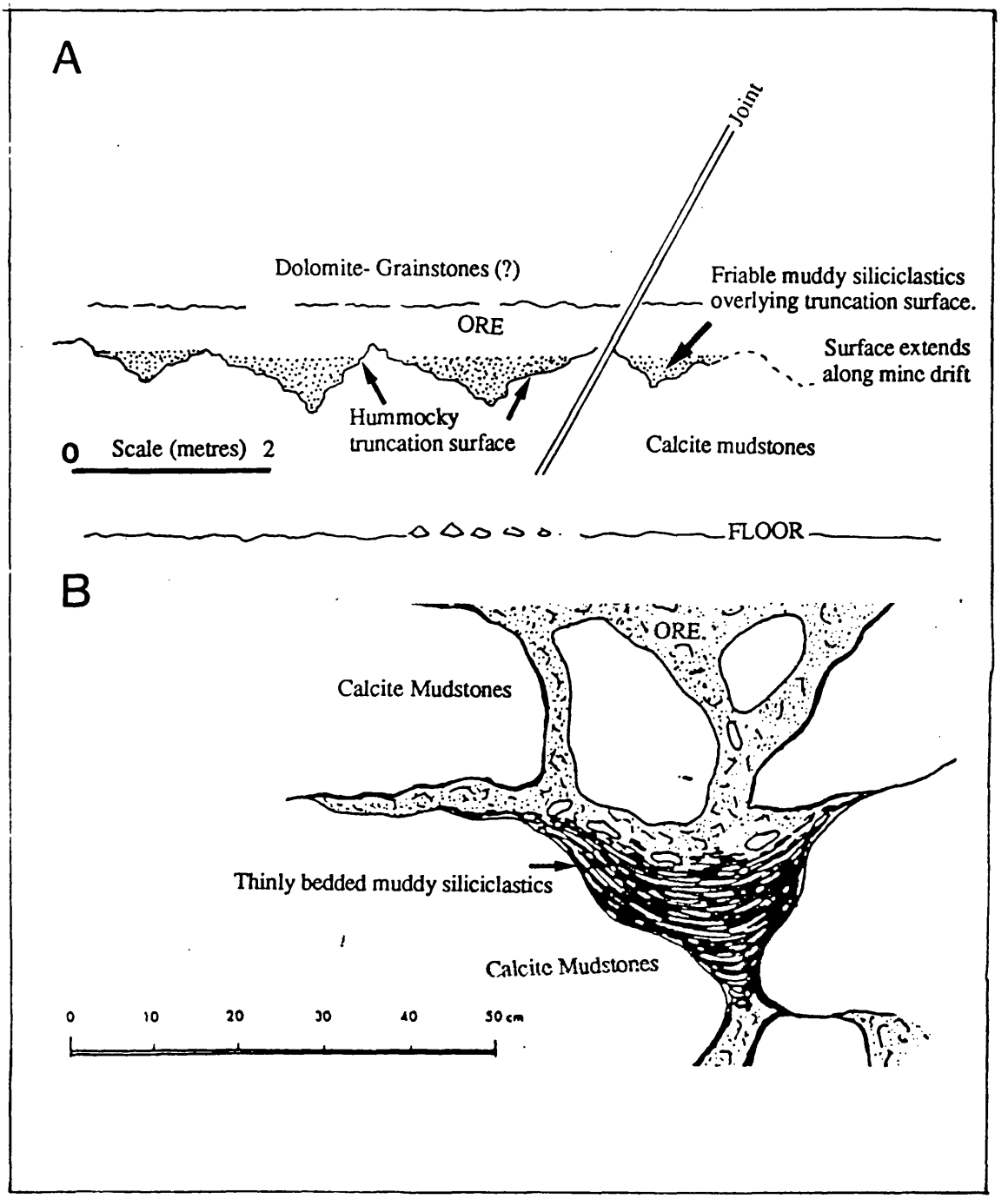

Fig. 3.10. **'A'** Thinly bedded siliciclastics overlying hummocky truncation surface, 1150 mine level, 1905 stope. **'B'** Detail of thinly bedded siliciclastics filling cavity in calcite mudstones, from Anderson, (1990) Fig. 5.26.

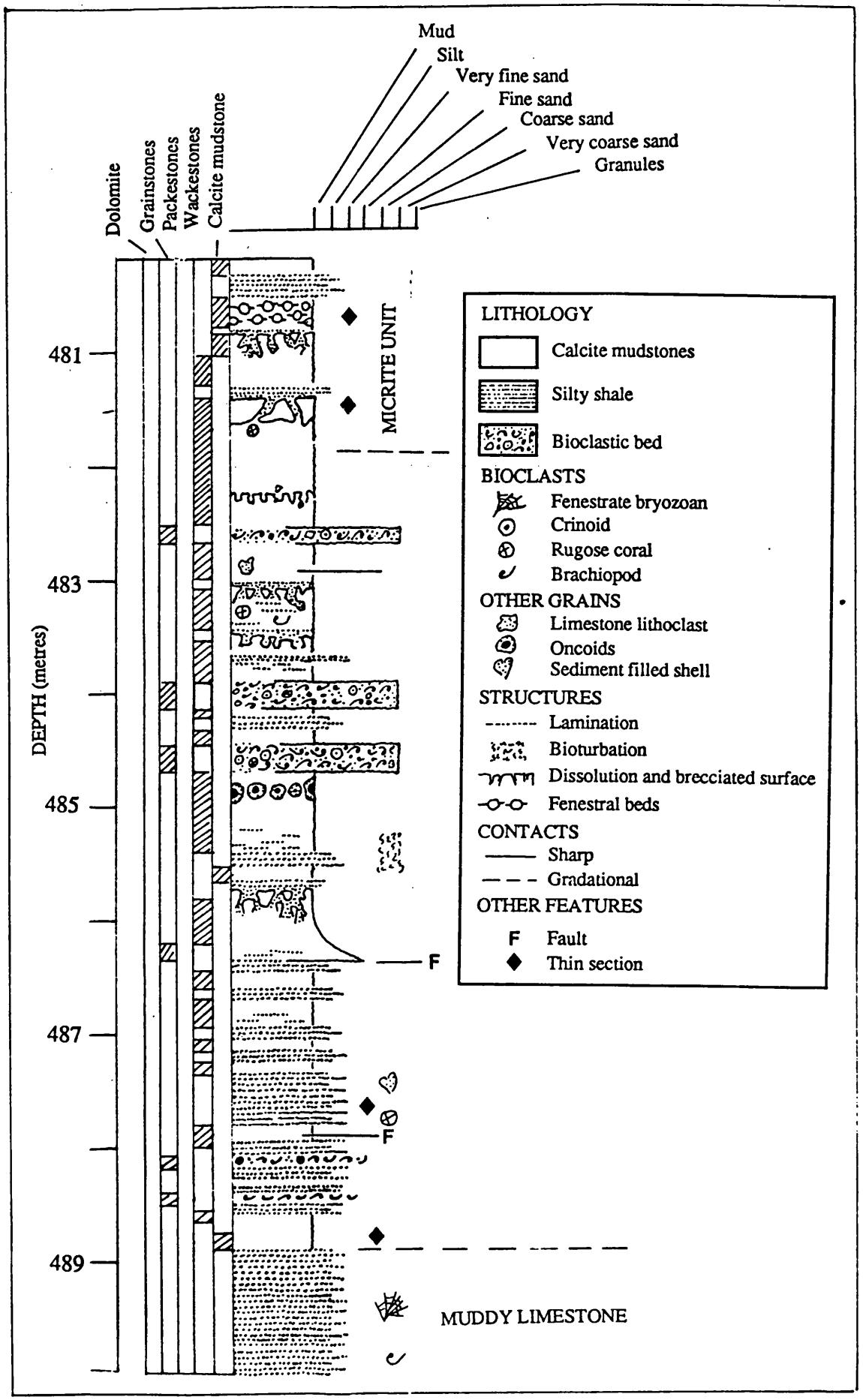

Fig. 3.11. Summary log of the Muddy Limestone Transition Unit, note shaley brecciated surfaces every few metres, hole N975.

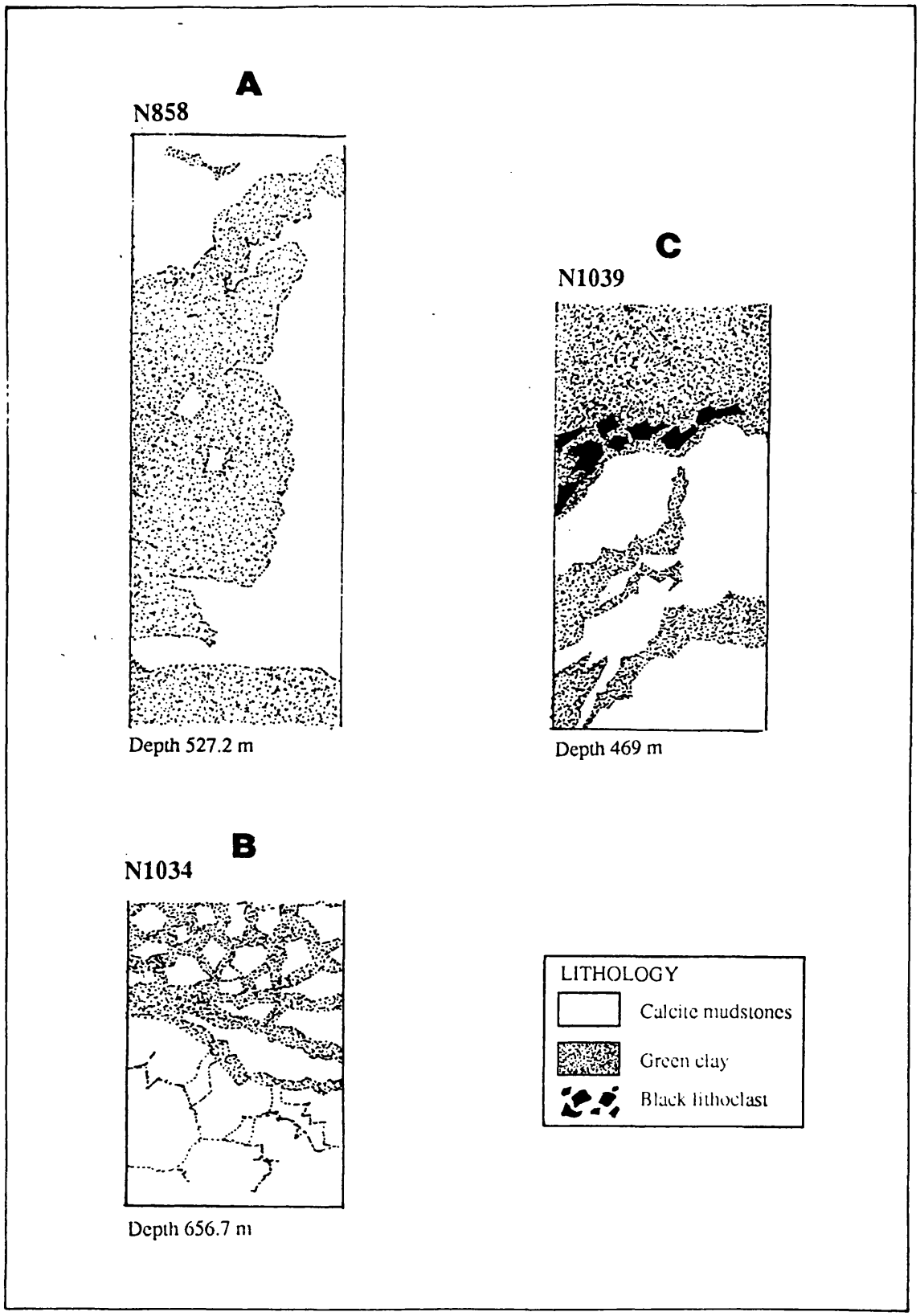

Fig. 3.12. Detail of green clay filling brecciated surfaces.'**A**' green clay filling former cavity. '**B**' *Insitu* breciation of calcite mudstones with green clay extending along fissures. '**C**' Blackened clasts of calcite mudstonewithin green clay. Scale : Full Size.

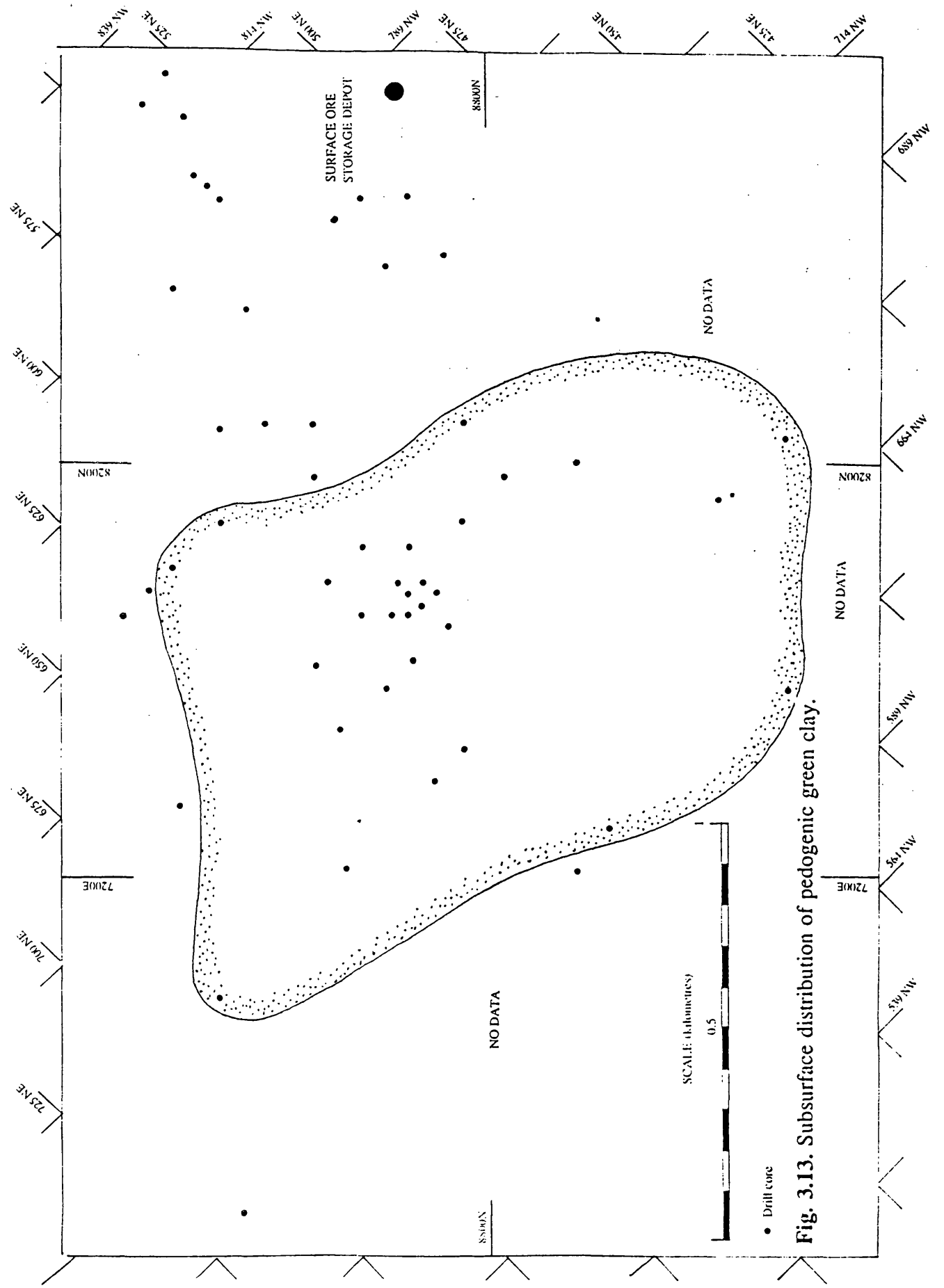

Fig. 3.13. Subsurface distribution of pedogenic green clay.

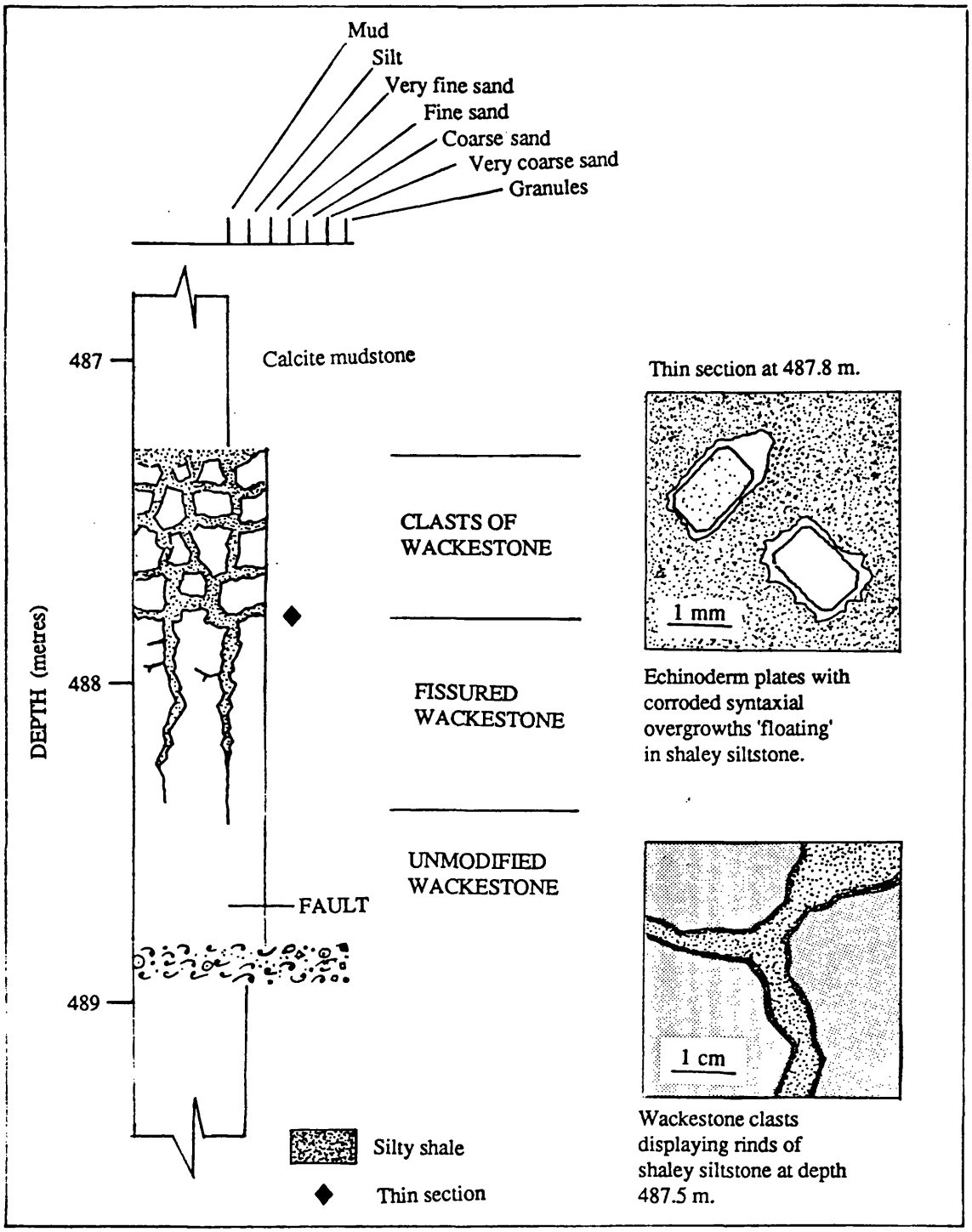

Fig. 3.14. Detail of brecciated surface, note profile. Inset 'A' Crinoid ossicles with heavily corroded syntaxial cements 'floating' in silty clay. Inset 'B' silty clay forming coating around clacite mudstone clasts. Hole N975.

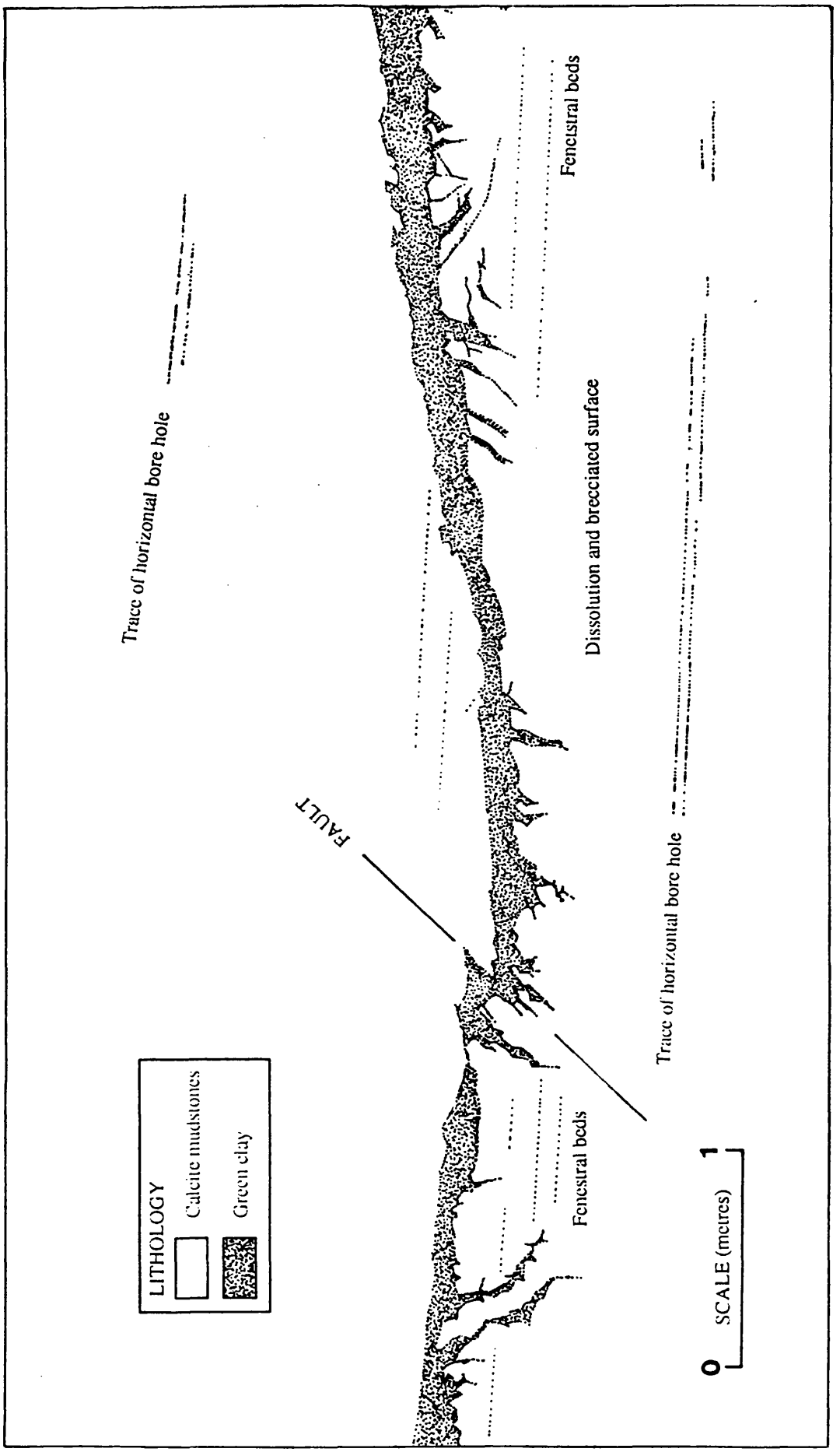

Fig. 3.15. Brecciated surface overlain by the pedogenic green clay. Note truncation of fenestral beds. Tracing from photomontage. 1175 mine level, 274W stope.

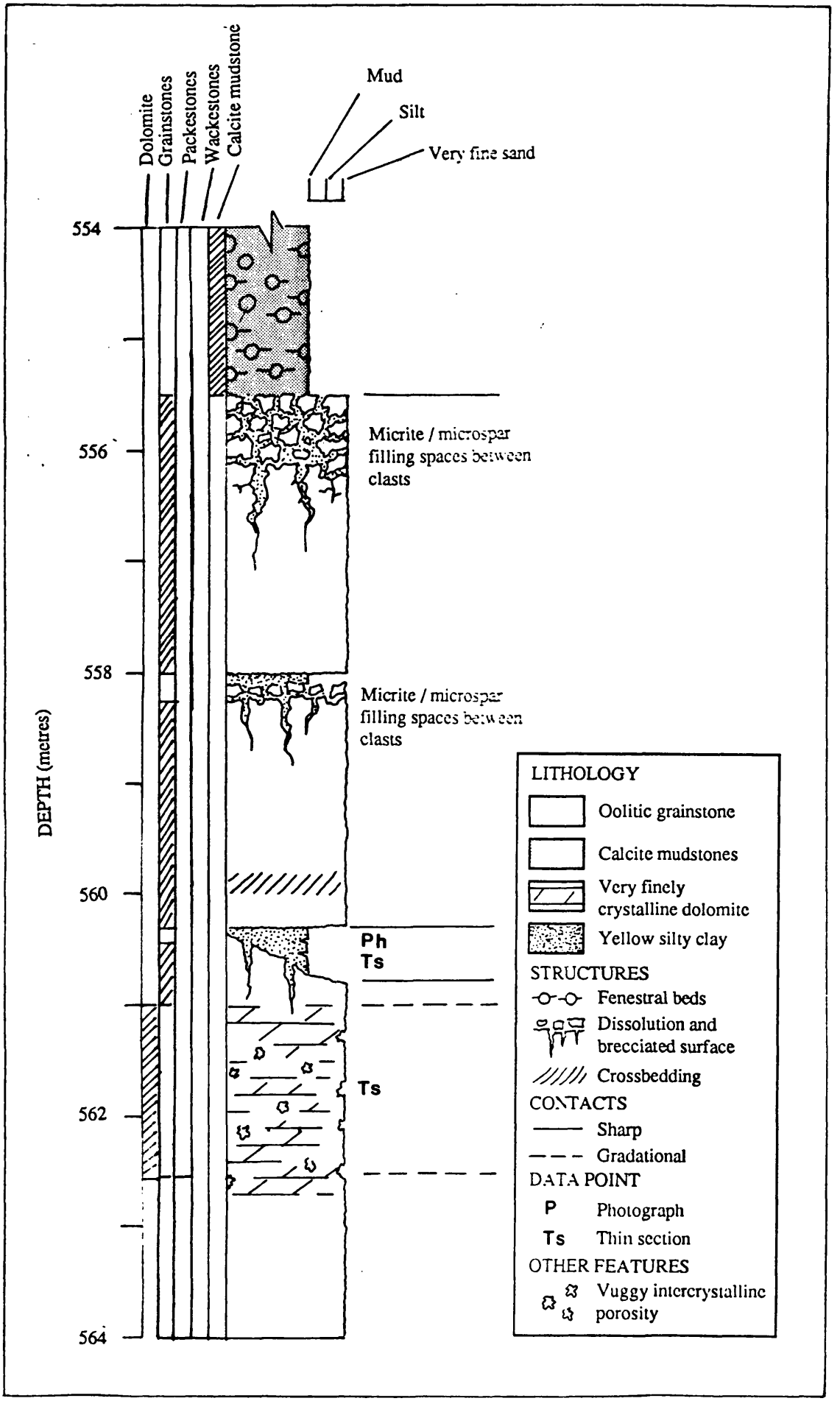

Fig. 3.16. Summary log showing 'grainy' cycles in oolitic grainstone, each cycle culminates in a brecciated surface or cavity margin. Note also brecciated upper surface. Hole N1011.

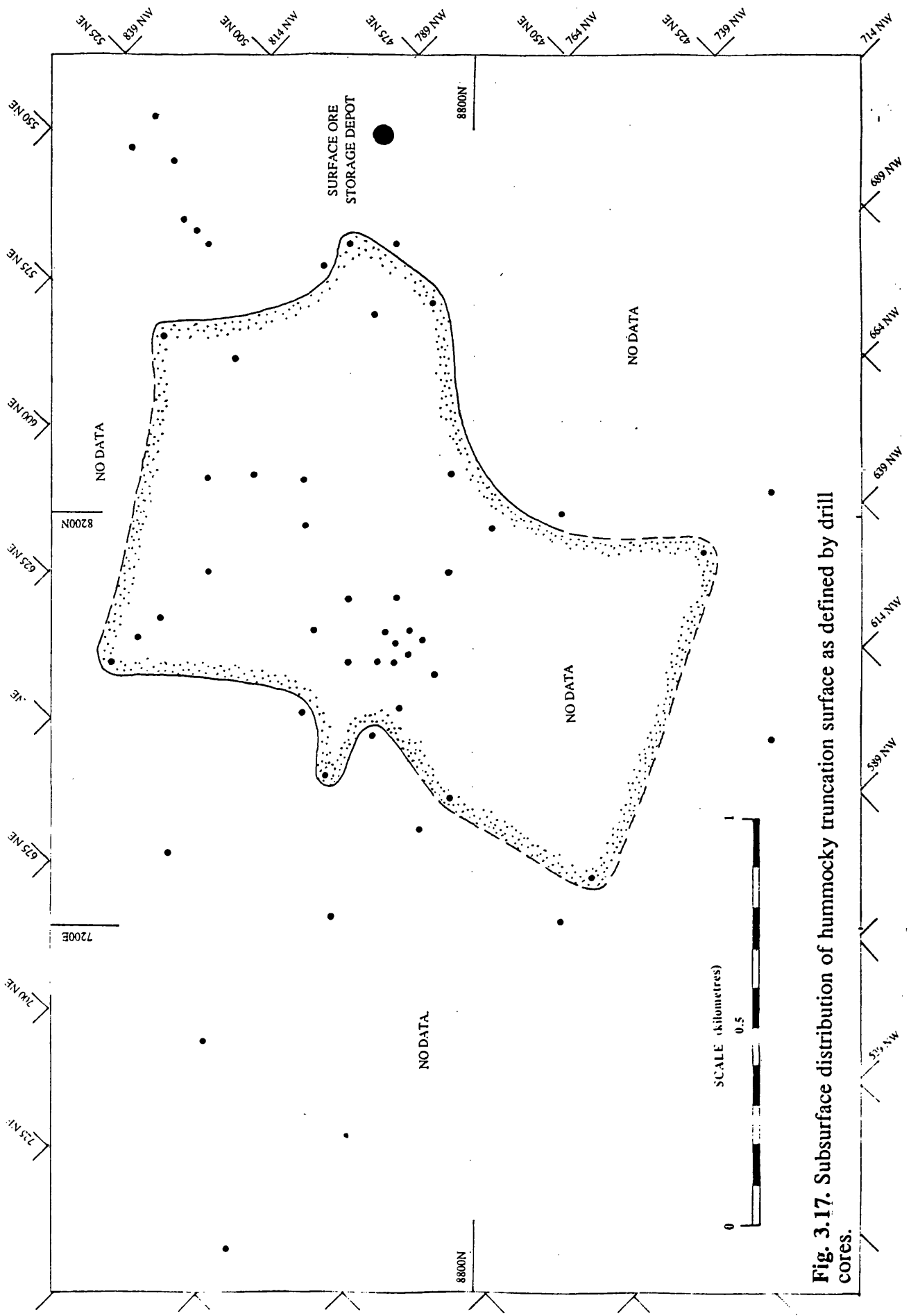

Fig. 3.17. Subsurface distribution of hummocky truncation surface as defined by drill cores.

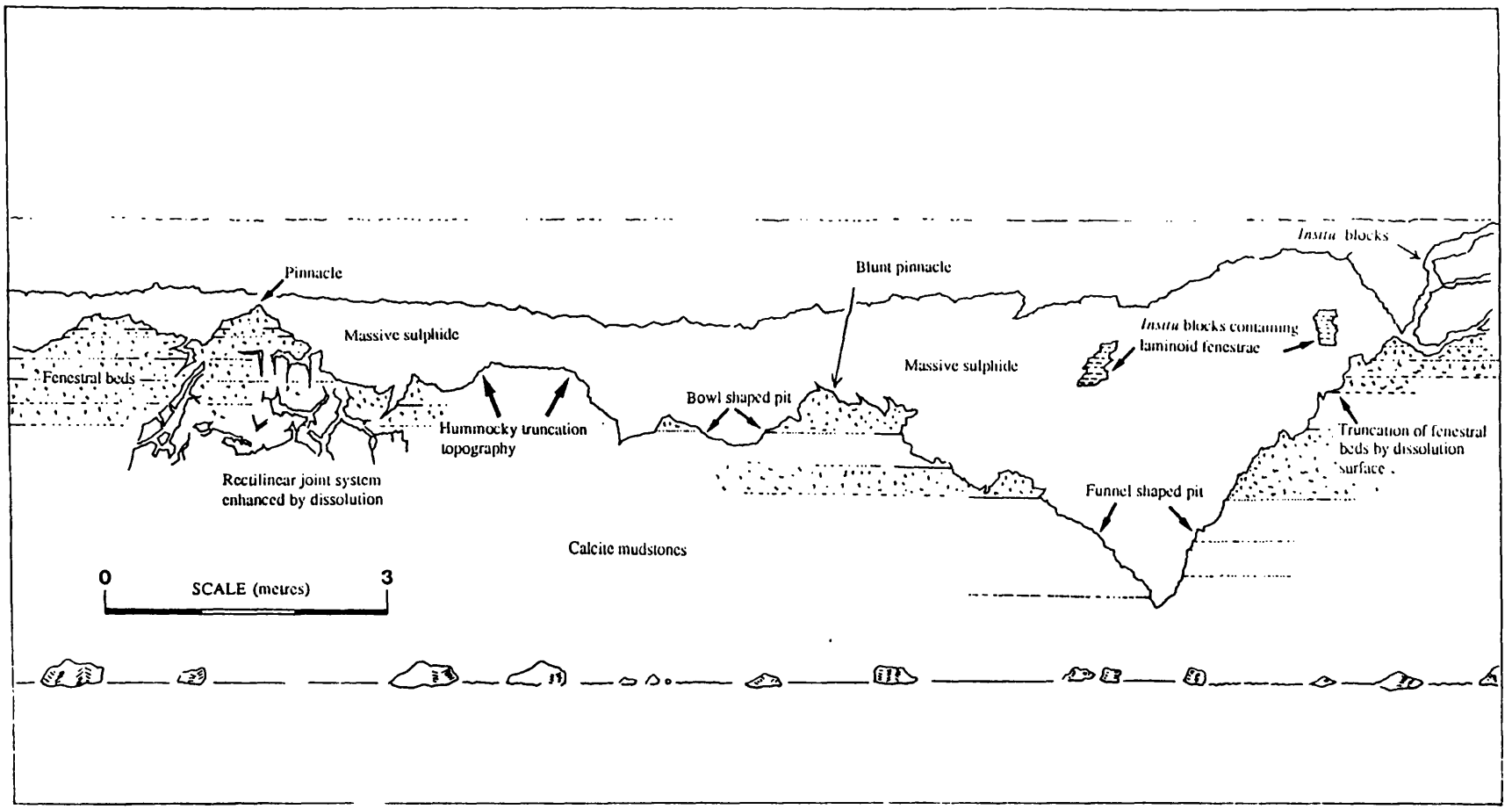

Fig. 3.18. Hummocky surface consisting of bowl and funnel shaped pits separated by pinnacles. The margins are 'knife' sharp and have truncated fenestral horizons. Note solutionaly enlarged joint surfaces and *in situ* blocks above the surface. Tracing from photomontage with additional data from field notes. 1230 mine level, 126W.

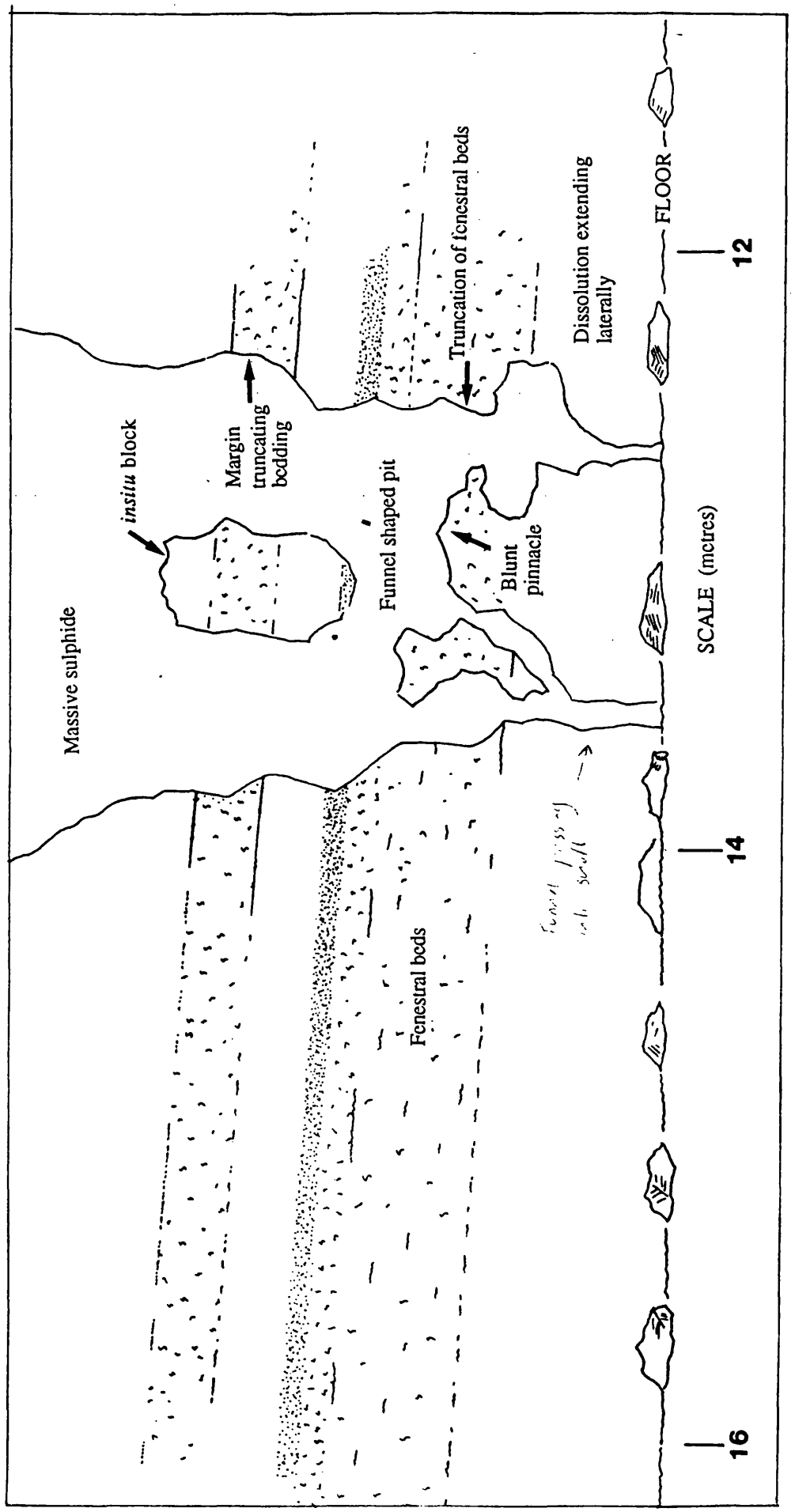

Fig. 3.19. Funnel shaped cavities truncating fenestral horizons. Cavity contains *insitu* blocks of calcite mudstone and passes vertically downward into shafts which are separated by a pinnacles. Note dissolution extending along bedding. The cavity can be traced to the opposite side wall suggesting the cavity is elongate. 1130 mine level drainage drift, 2 Zone

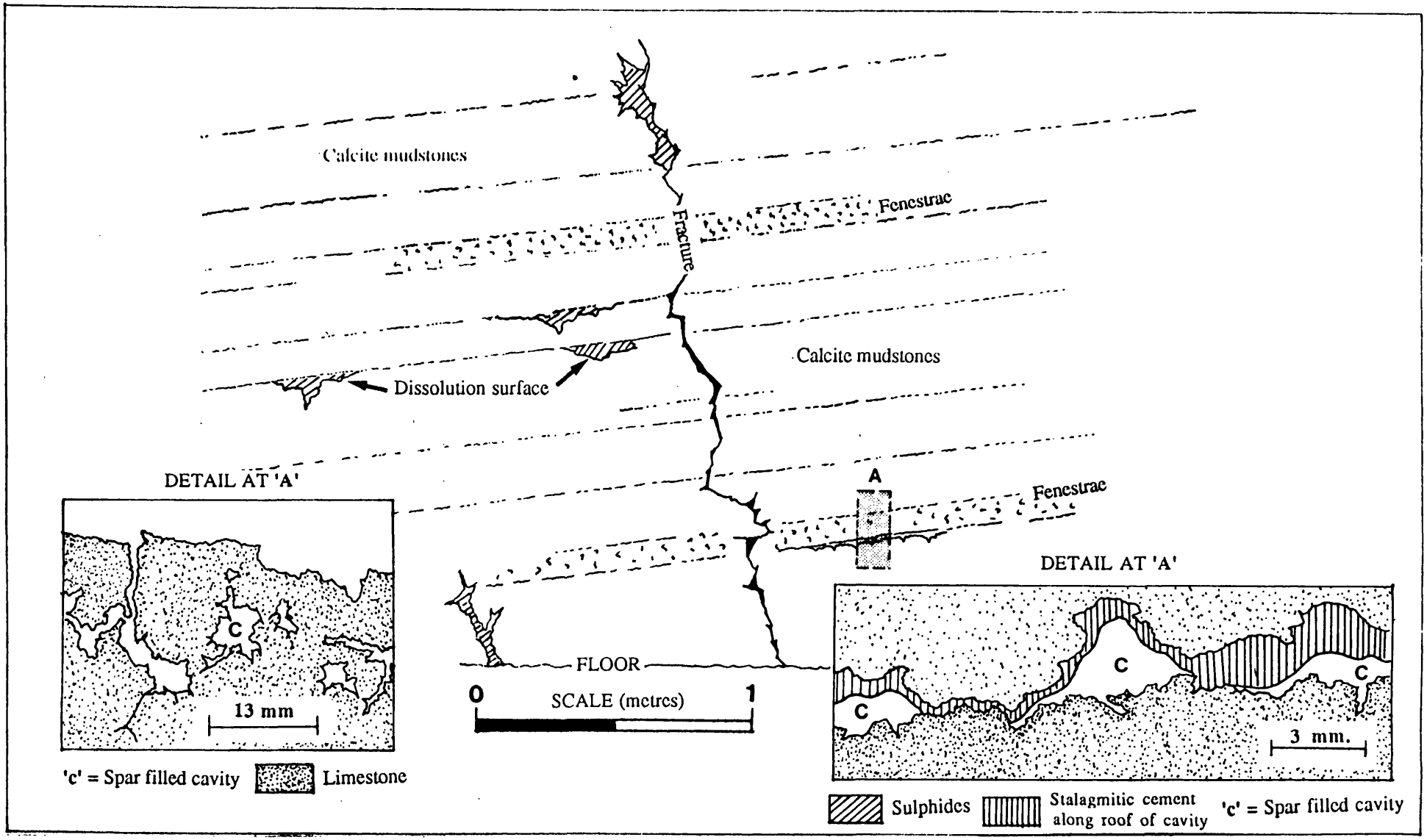

Fig. 3.20. Bedding in calcite mudstones containing bedding parallel dissolution surfaces and cavities, note stalactitic cement along roof of bedding parallel cavity at 'A'. 1210 mine level,1902 stope.

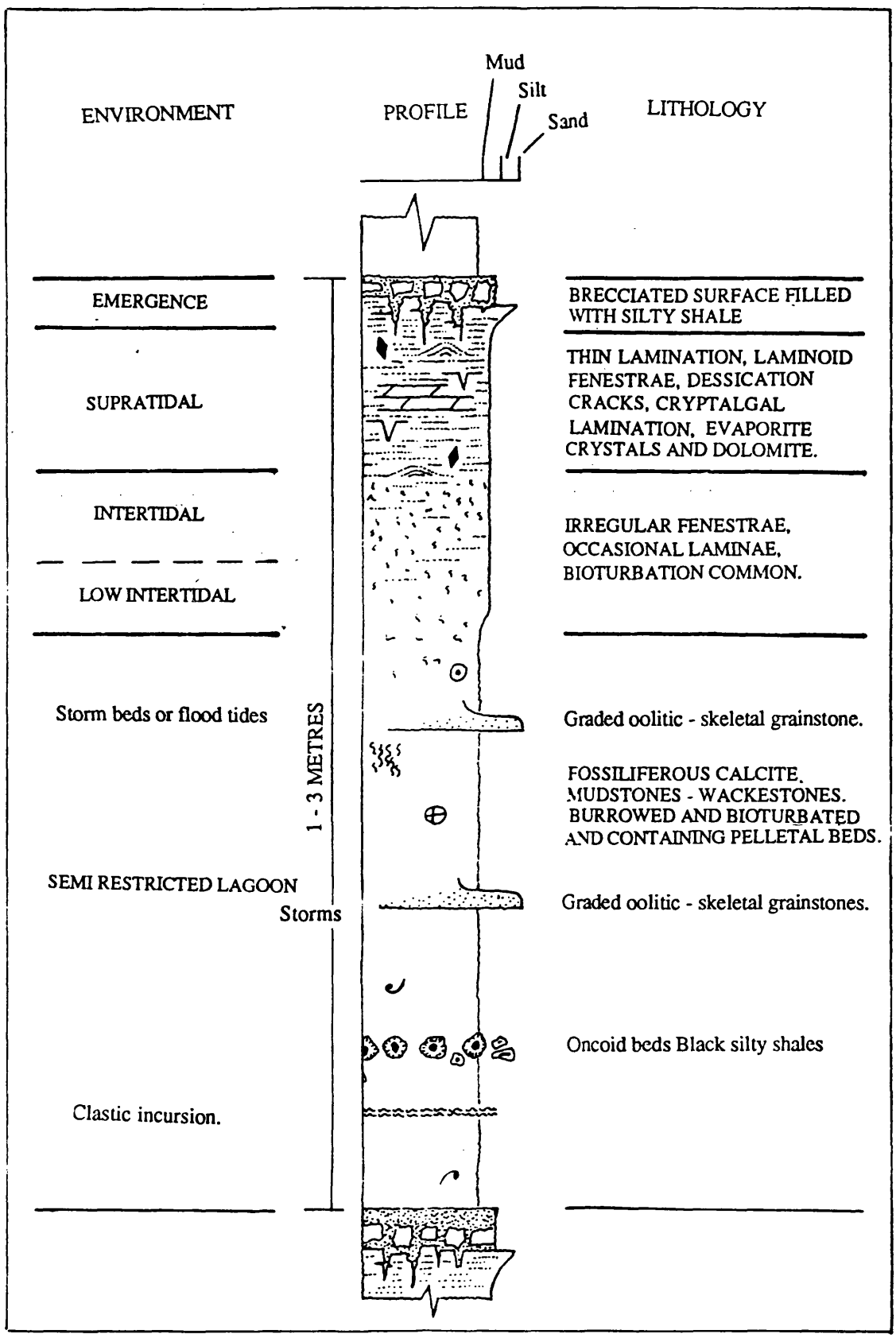

Fig. 3.21. Ideal Navan Muddy shallowing up cycle, based on data from over 70 drill cores.

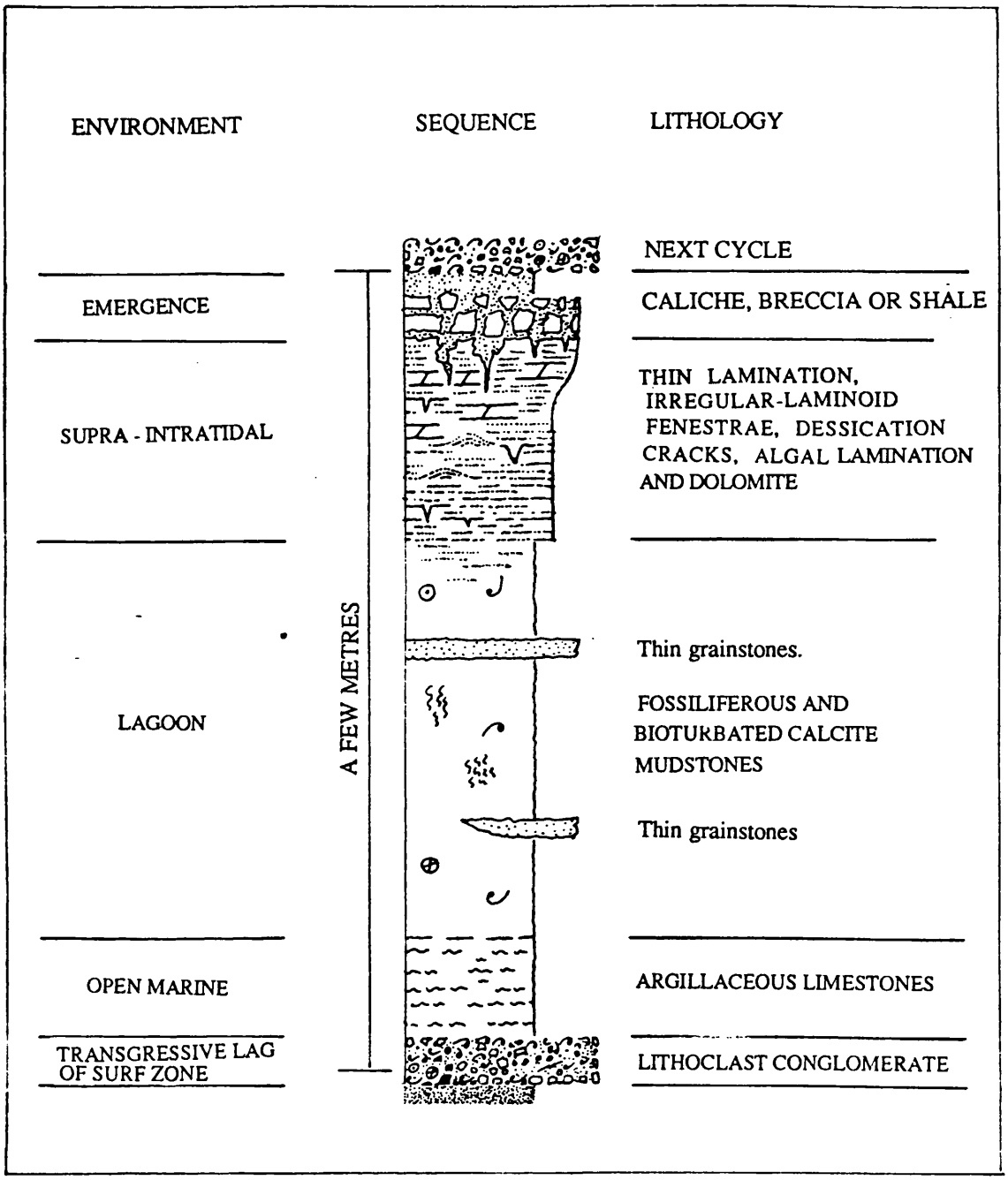

Fig. 3.22. Muddy shallowing up cycle modified from James (1984) Fig. 2, p.214.

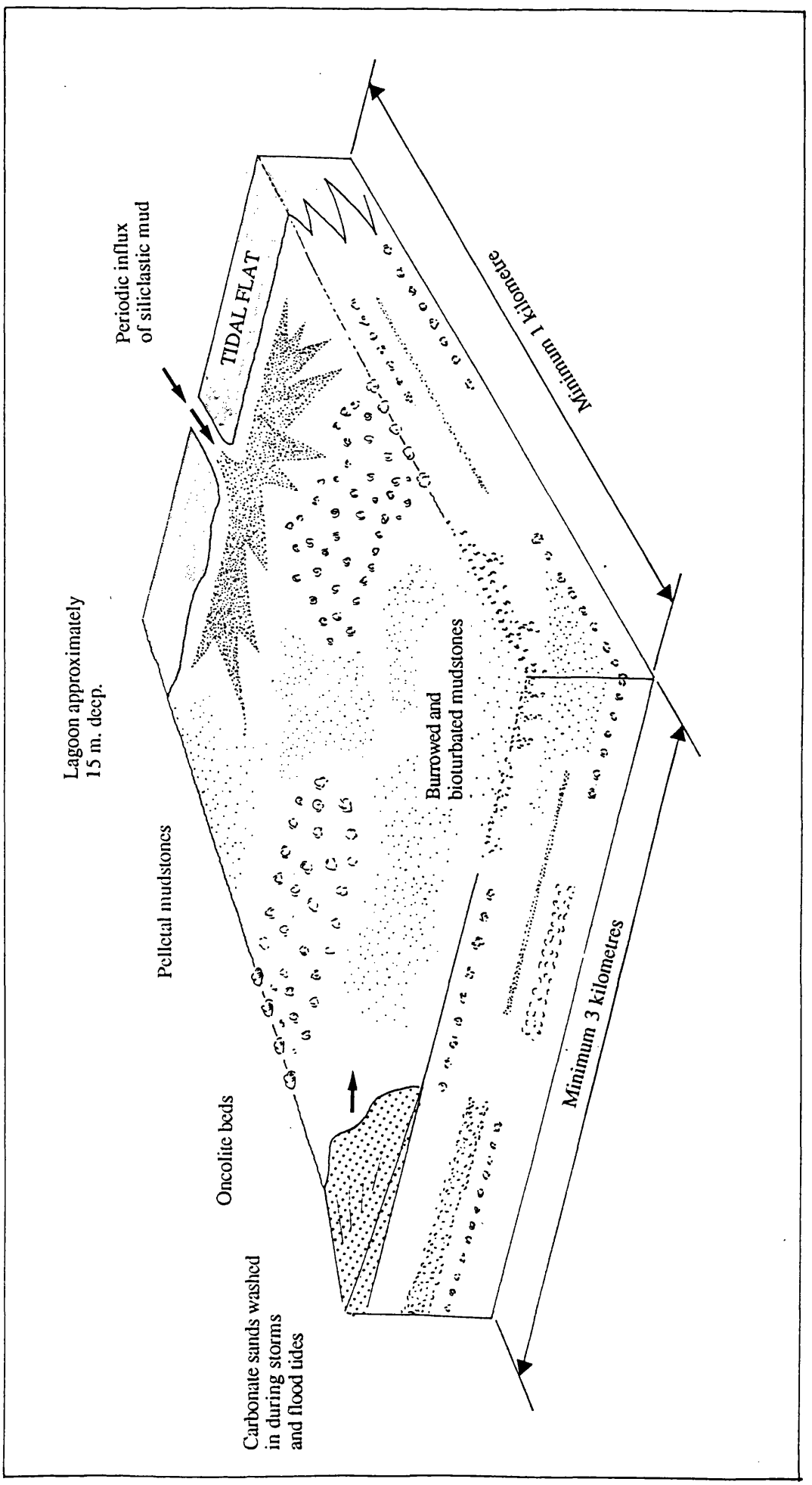

Fig. 3.23. Suggested facies model for the early Carboniferous lagoon at Navan during deposition of the Micrite Unit.

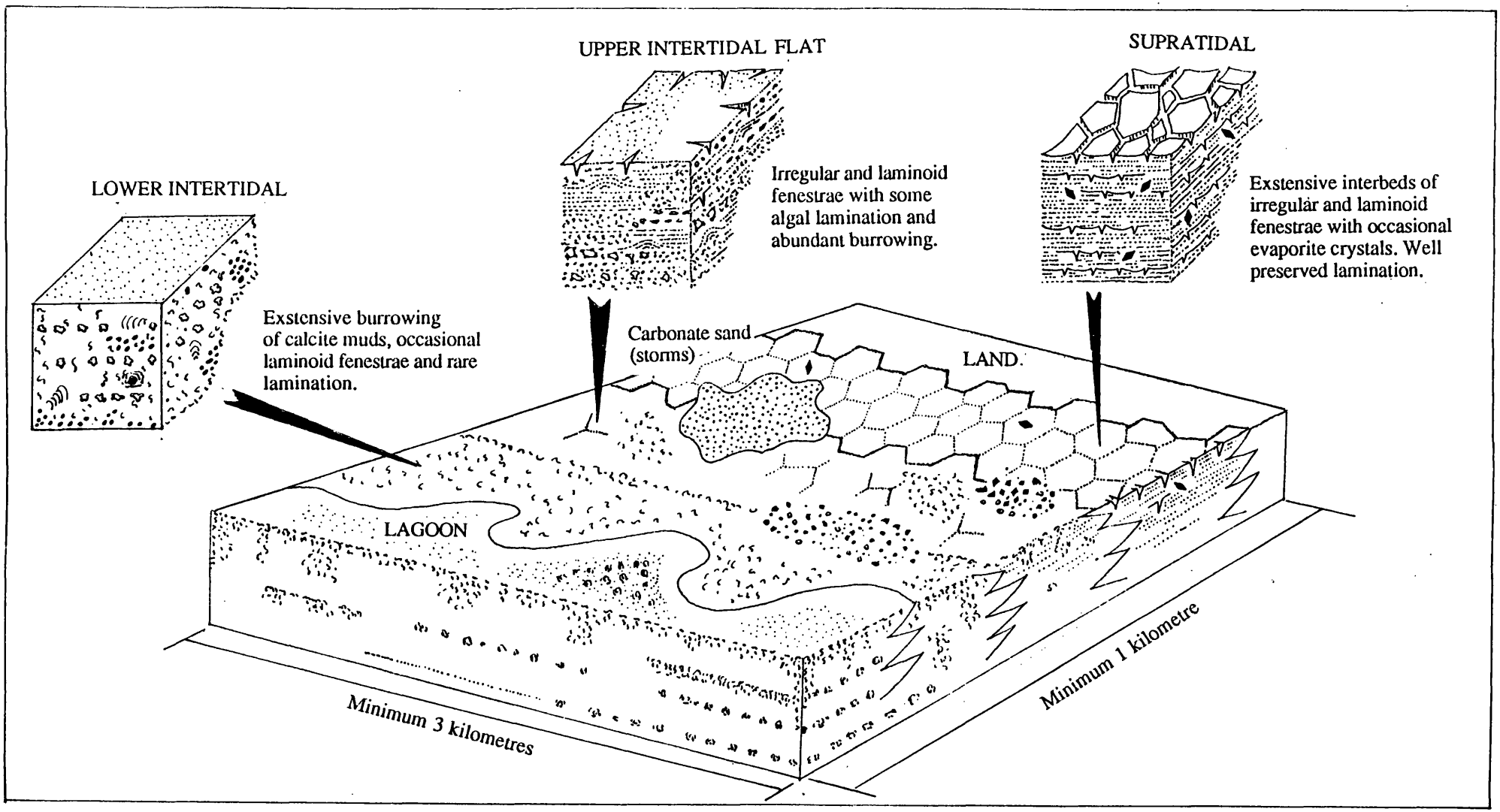

Fig. 3.24. Suggested facies model for the early Carboniferous tidal flat at Navan during deposition of the Micrite Unit.

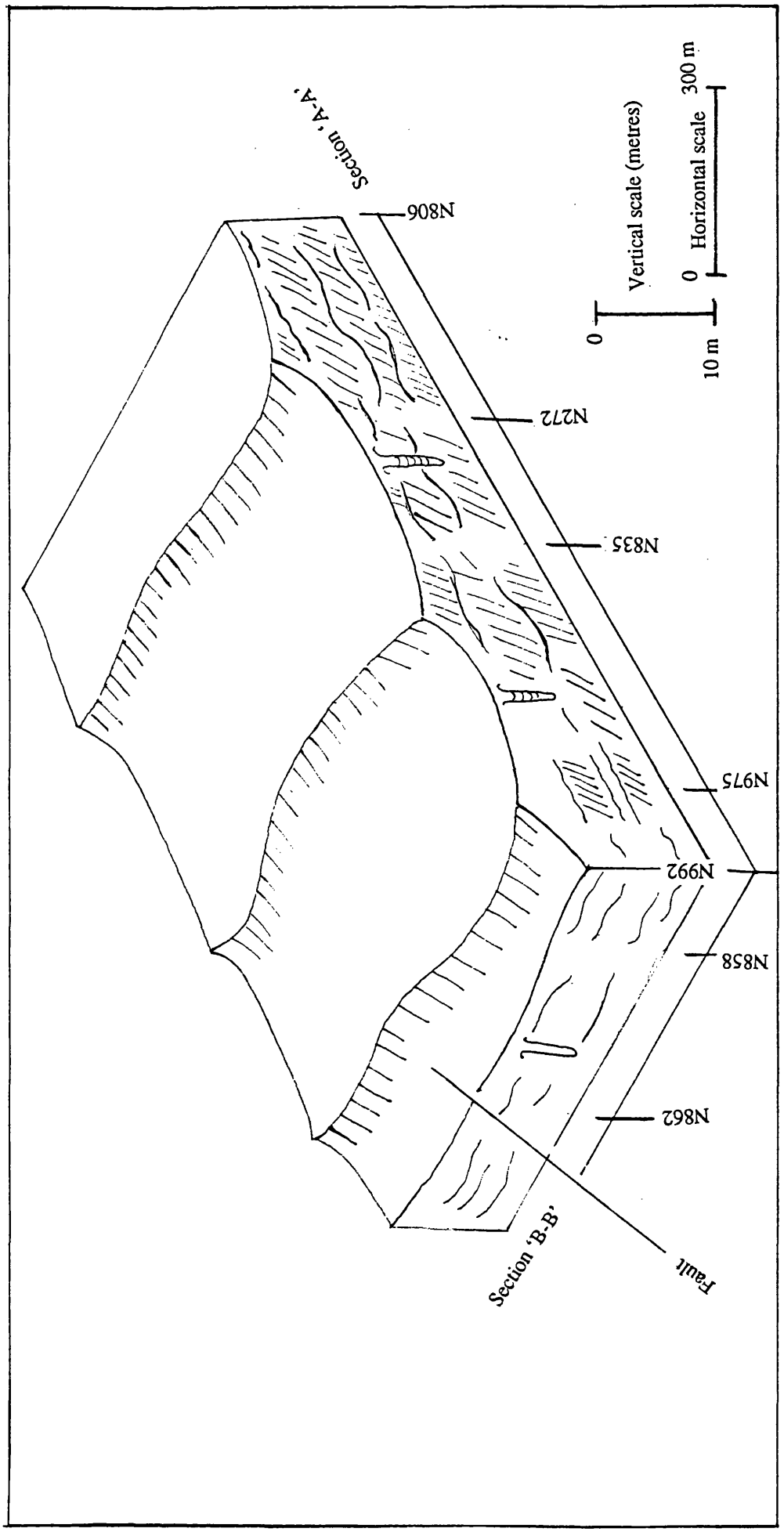

Fig. 3.25. Suggested facies model for the oolitic sand shoal at Navan during deposition of the Micrite Unit.

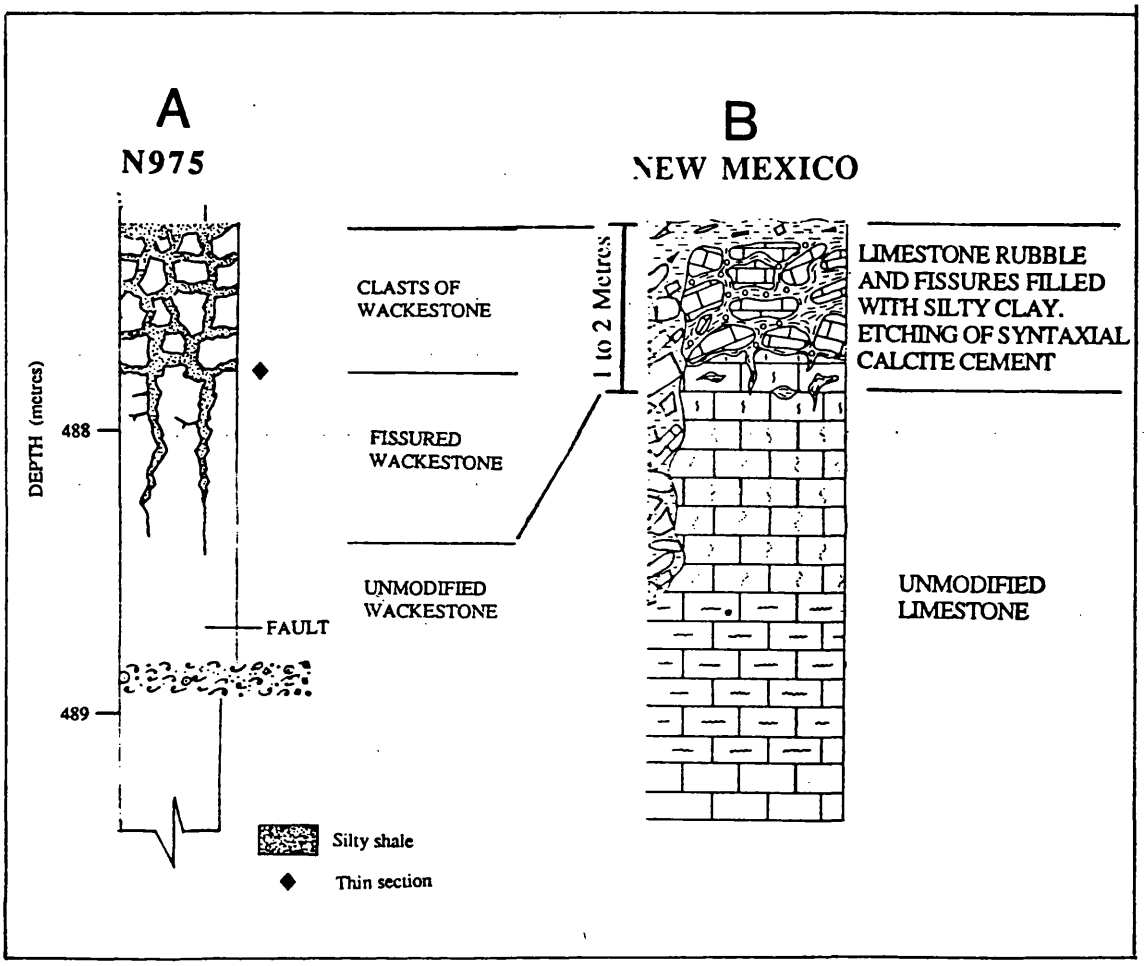

Fig. 3.26. **'A'** Navan shaley brecciated palaeokarst surface compared with **'B'** Breccited palaeokarst surface from Mississippian limestones of New Mexico, from Meyers (1988, Fig 14.4).

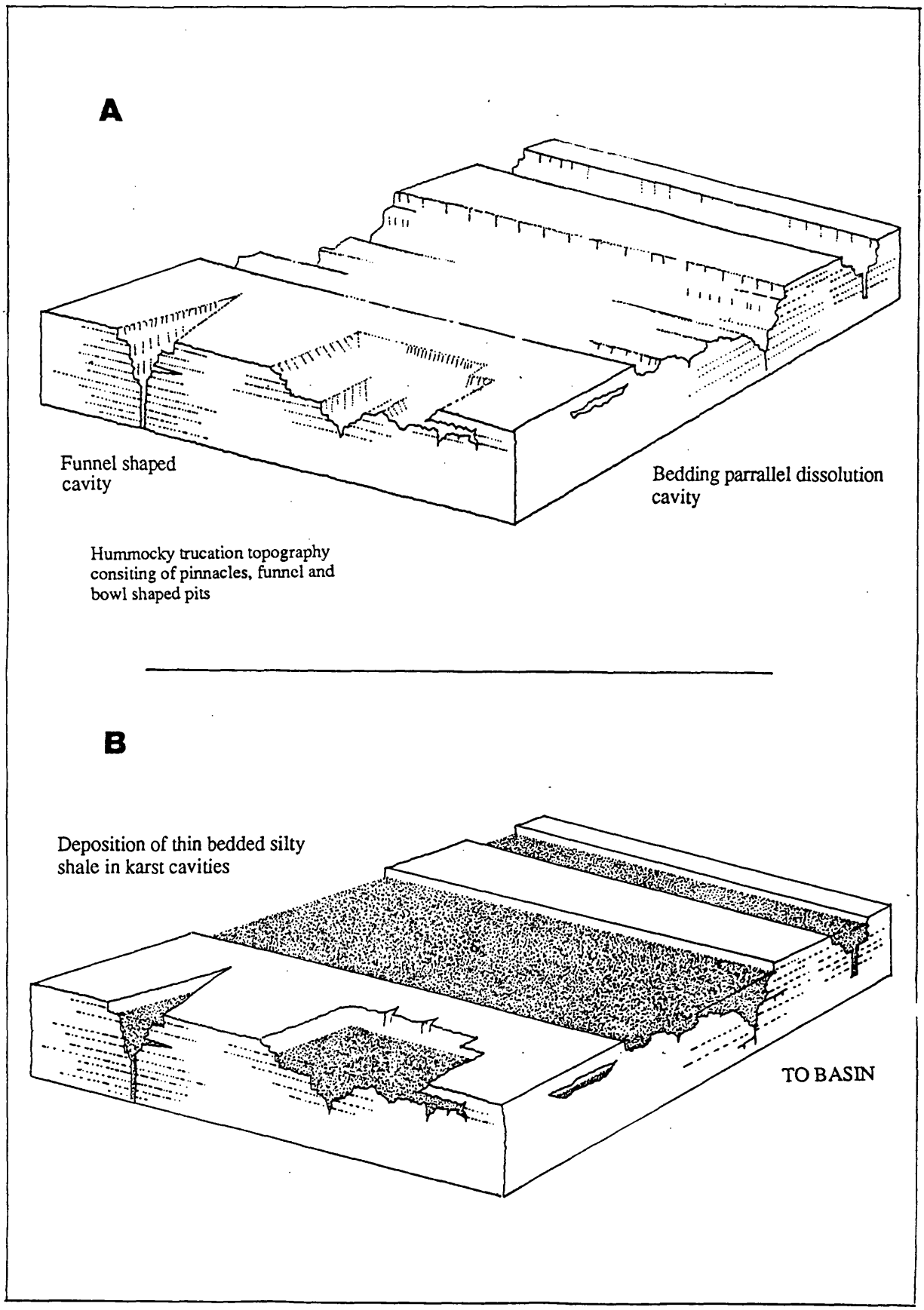

Fig. 3.27. 'A' Early Carboniferous palaeokarst surface at Navan during deposition of the Micrite Unit. Note funnel shape cavities and hummocky truncation surfaces.'B' The same palaeokarst surface following deposition of silty shales over and along the palaeokarst cavities.

Fig. 3.28. Navan cycle sequences in the western mine area. **'A'** Cycle sequence 1 capped by pedogenic green clay. **'B'** Cycle sequence 2 capped by a brecciated surface. **'C'** Cycle sequence 3 capped by the hummocky trucation surface. **'D'** Cycle sequence 4, the oolitic grainstone. **'E'** Cycle sequence 5 capped by surface displaying flute and pinnacle topography, shaley breccia surfaces and cavities.

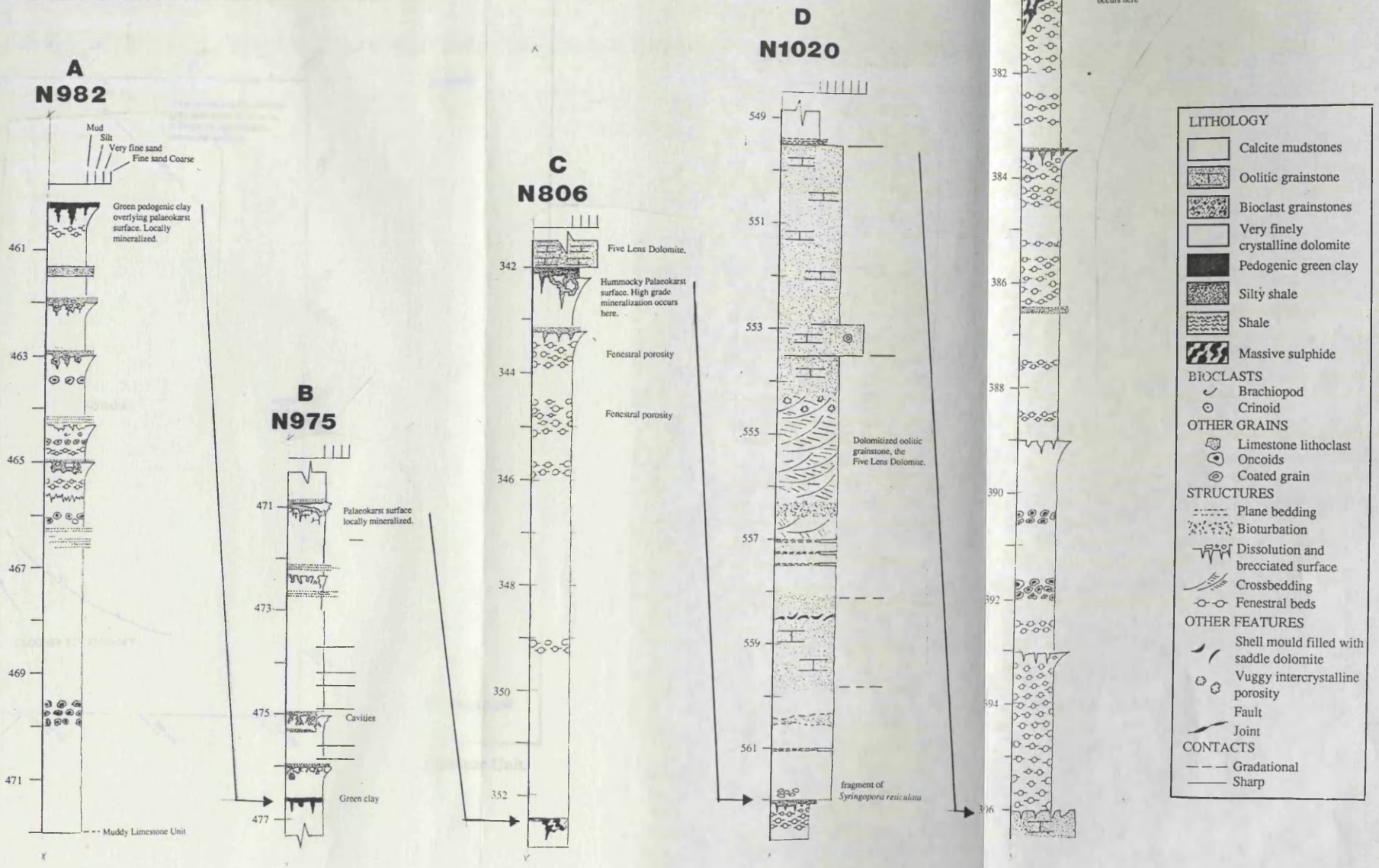

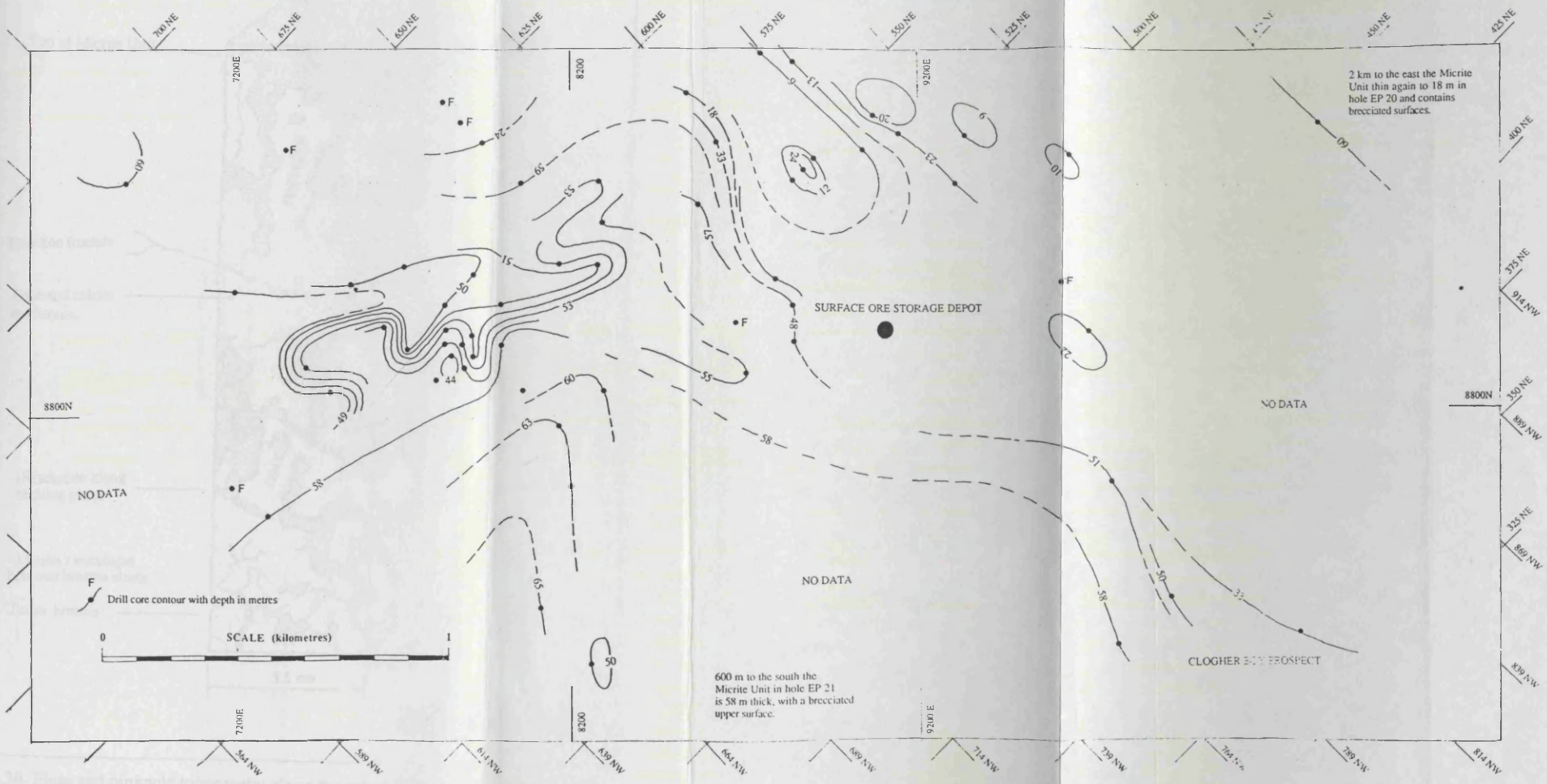

Fig. 3.29. Variation in thickness of the Micrite Unit culminating in a NW-SE striking channel. Expressed in terms of isopach interval from the base to the top of the Micrite Unit.

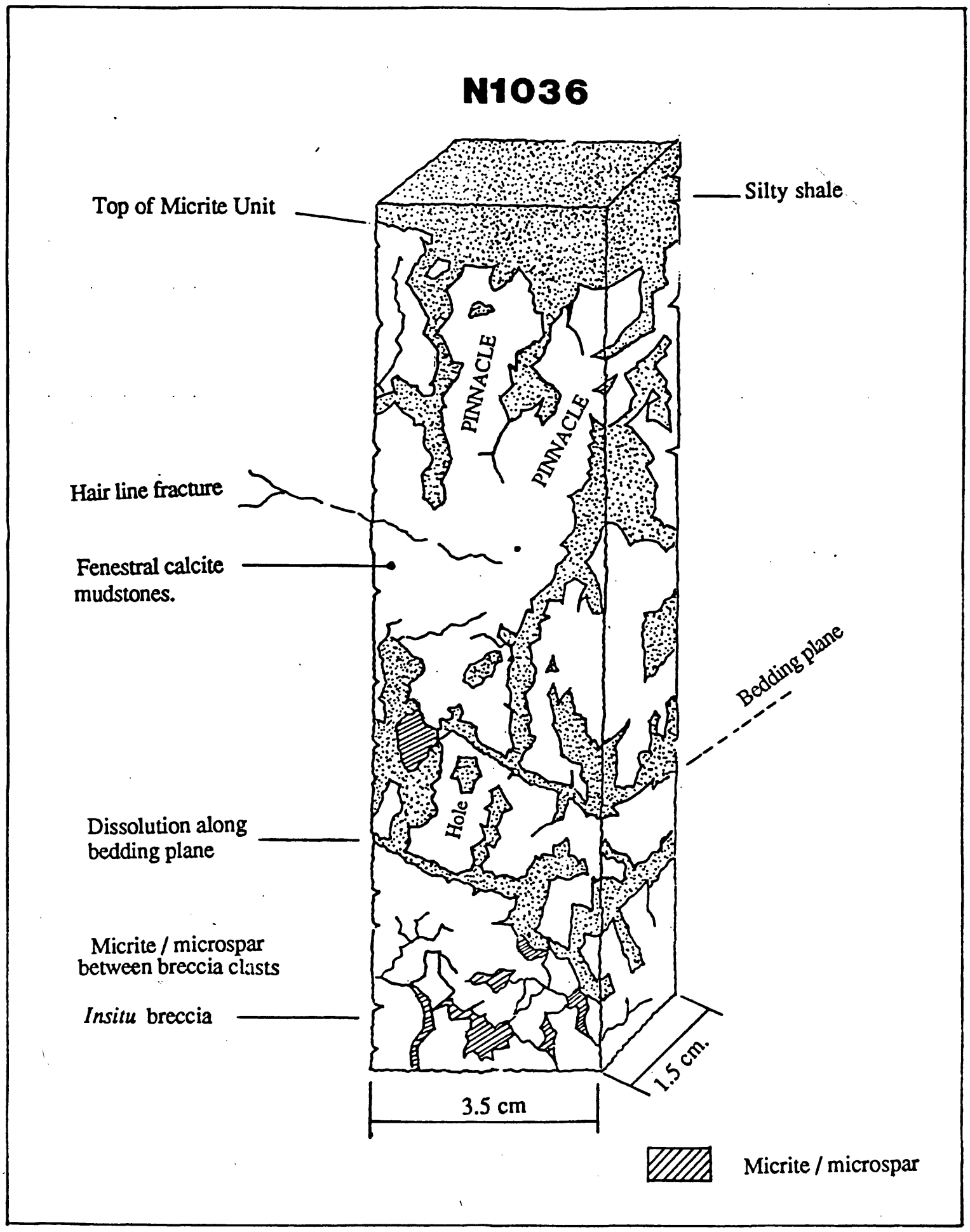

Fig 3.30. Flute and pinnacle topography along the upper surface of the Micrite Unit.

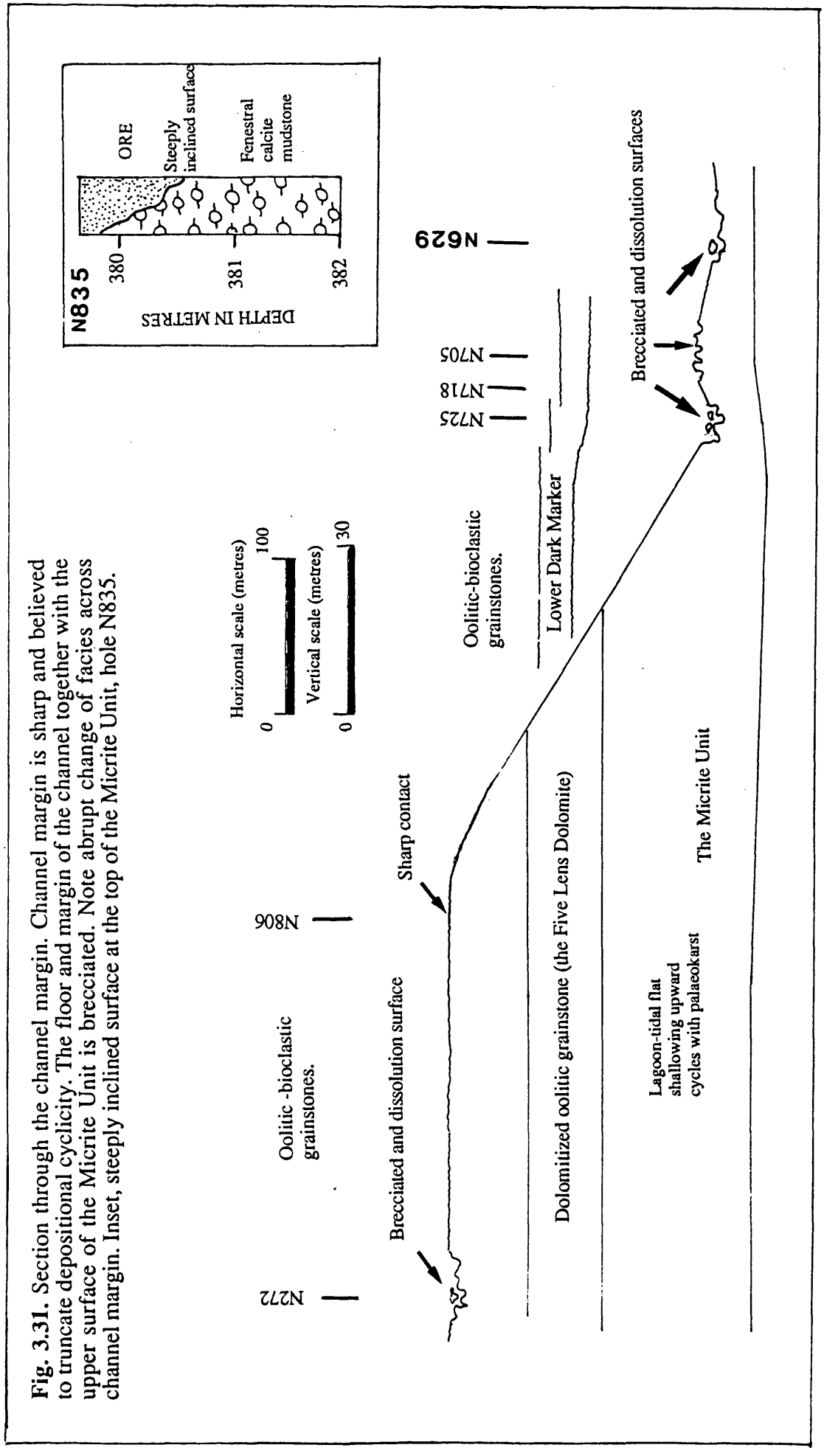

Fig. 3.31. Section through the channel margin. Channel margin is sharp and believed to truncate depositional cyclicity. The floor and margin of the channel together with the upper surface of the Micrite Unit is brecciated. Note abrupt change of facies across channel margin. Inset, steeply inclined surface at the top of the Micrite Unit, hole N835.

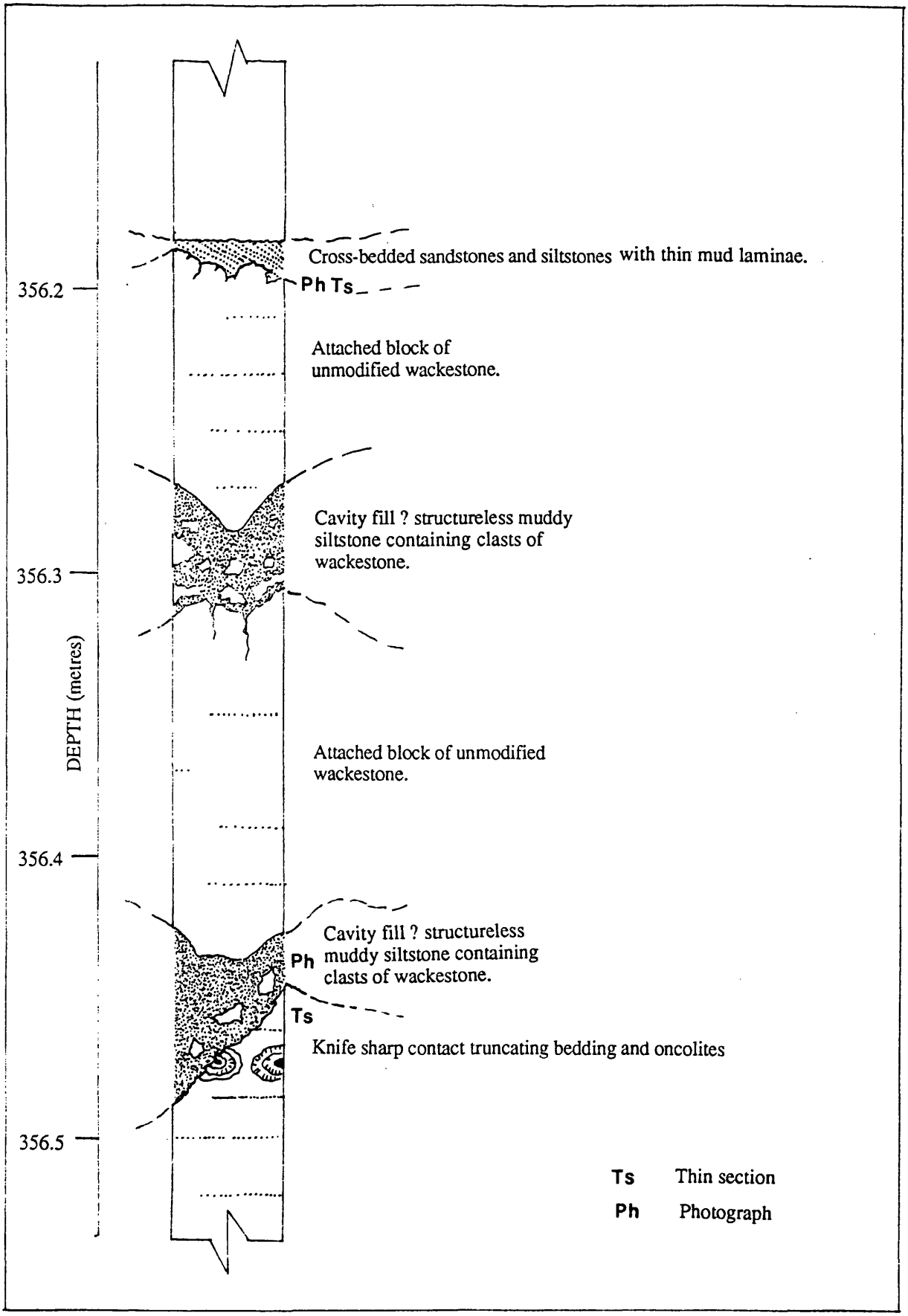

Fig. 3.32. Log of calcite mudstones at the base of the channel. Note sharp truncation of oncoidal beds and layering. The calcite mudstones have irregular, brecciated and steeply inclined contacts with silty shale, they are interpreted as attached blocks.

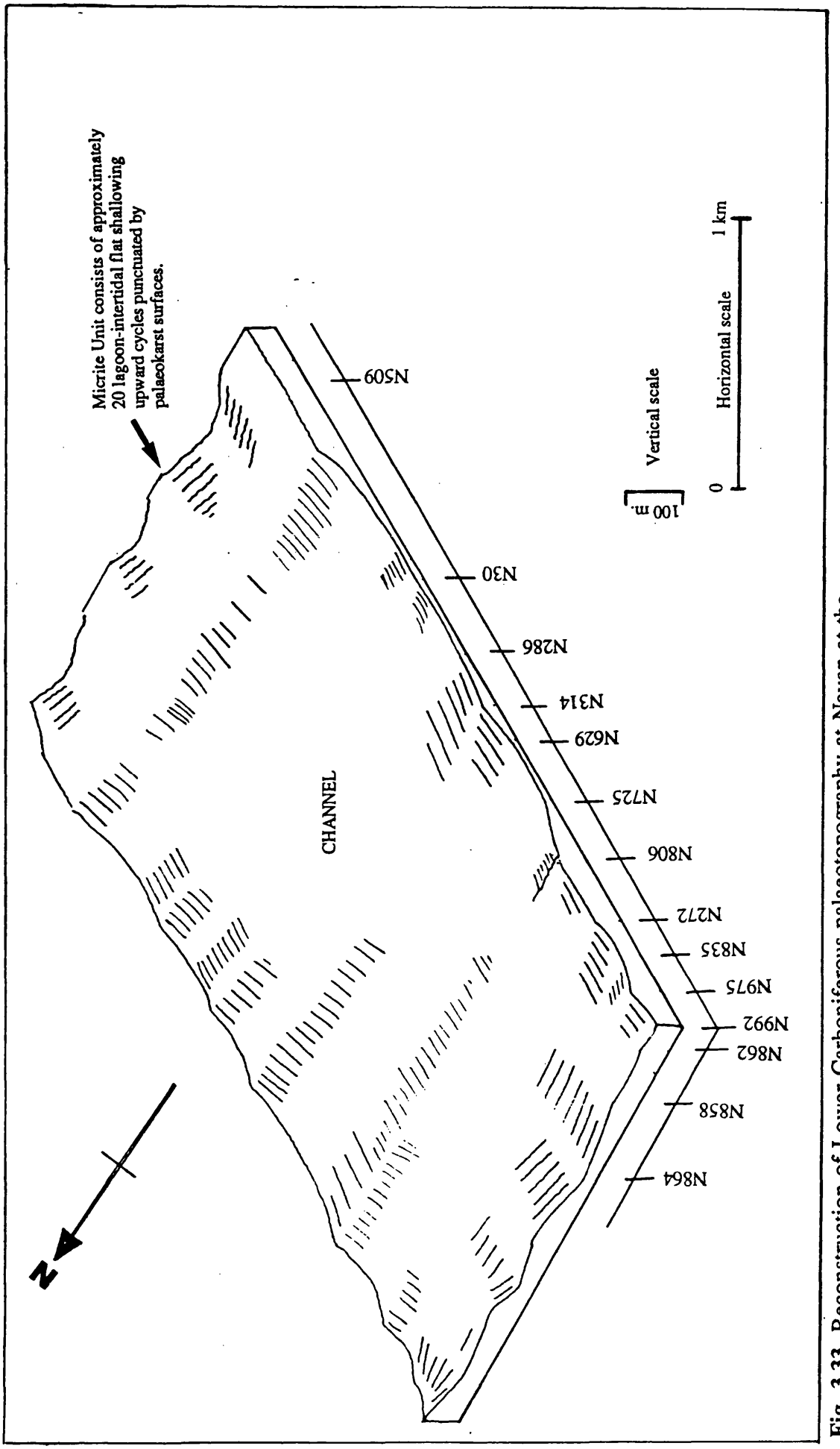

Fig. 3.33. Reconstruction of Lower Carboniferous palaeotopography at Navan at the end of Micrite Unit times.

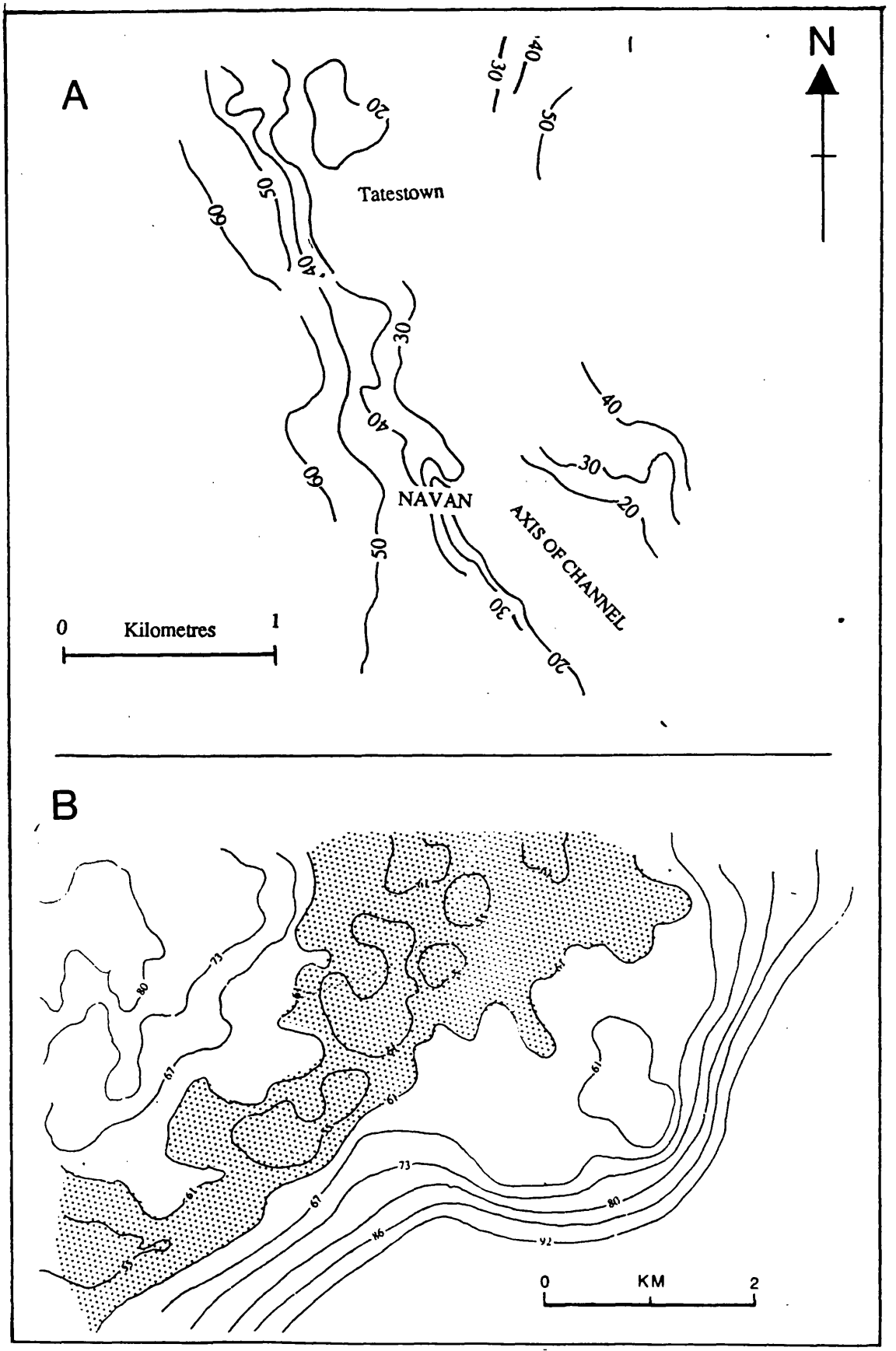

Fig. 3. 34. 'A' Navan palaeotopography bounding the Upper surface of the Micrite Unit and culminating in a channel, from Andrew & Ashton (1985).This is compared with **'B'** the palaeotopography in the Permian San Andreas Dolomite, Yates oil field, West Texas. Note channel defined by 61 m contour. modified from Craig (1988), Fig. 16.11. Both topographies display approximately 50 m of relief.

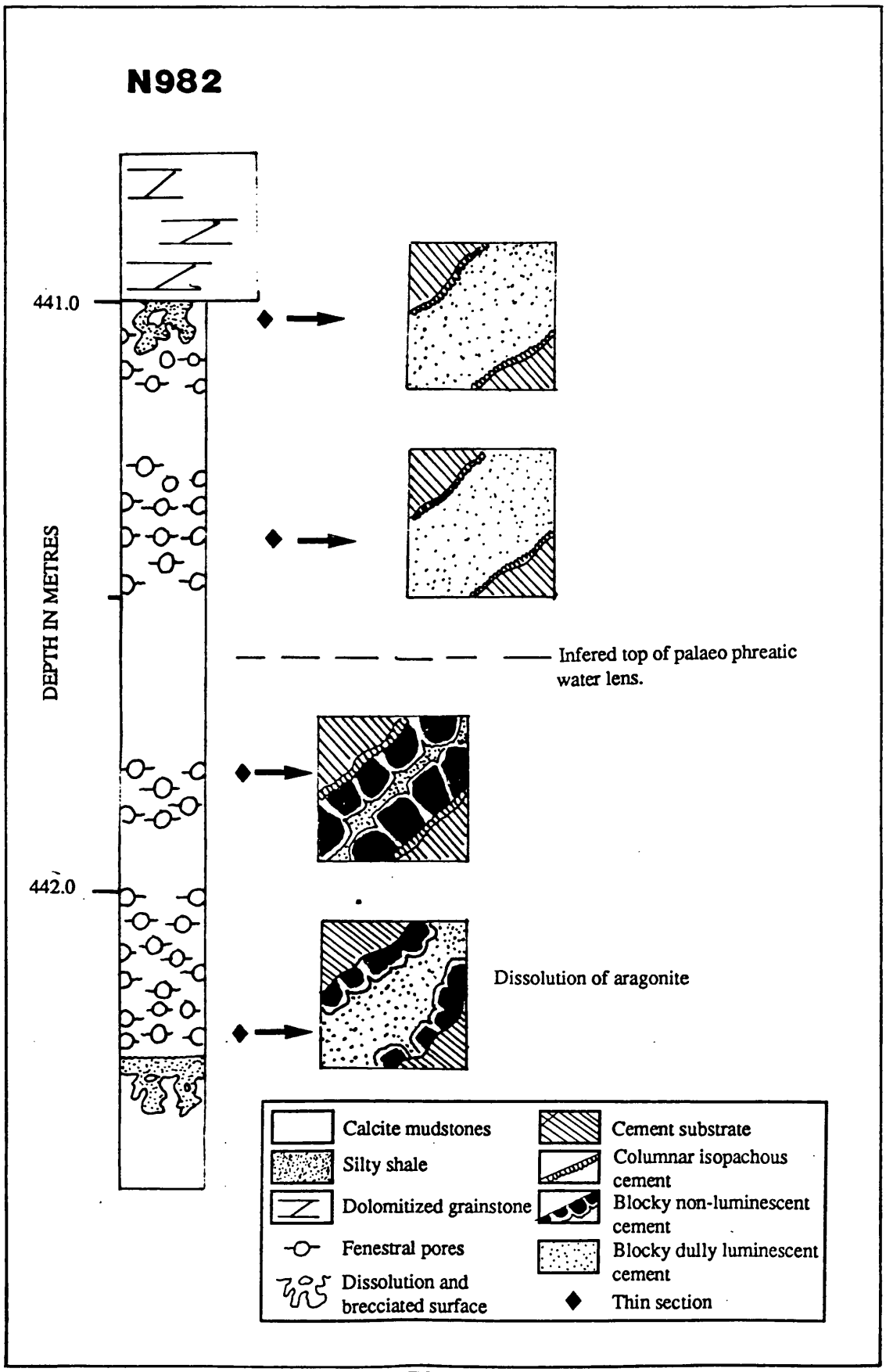

Fig. 3.35. Non-luminescent blocky calcite cement below palaeokarst surface. The cement dissappears vertically upwards, suggesting upper limint of palaeo phreatic water lens.

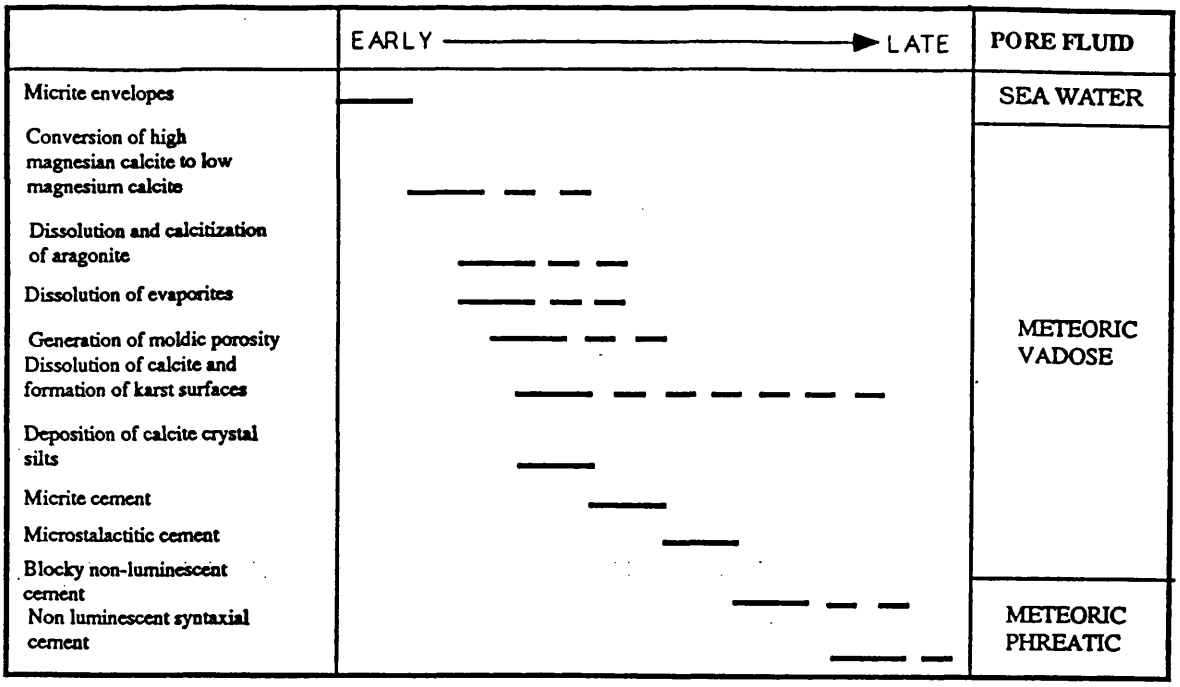

Fig. 3 .36. Summary diagram of early meteoric diagenessis in the Micrite Unit

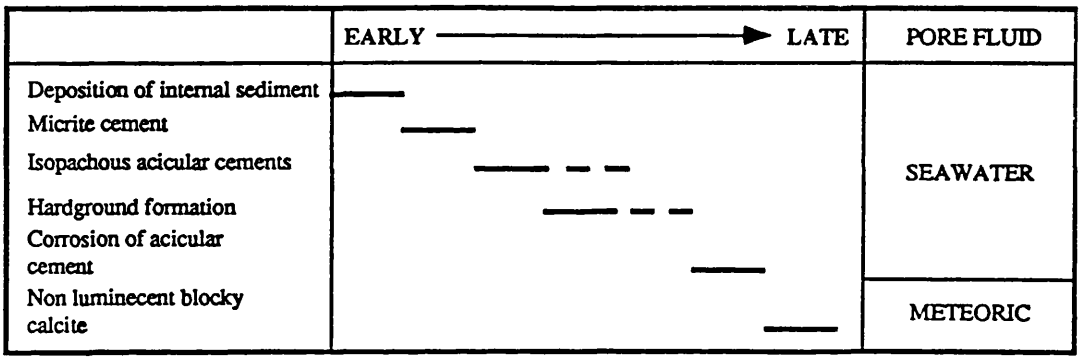

Fig. 3.37 Summary diagram of marine-meteoric diagenesis in the Micrite Unit

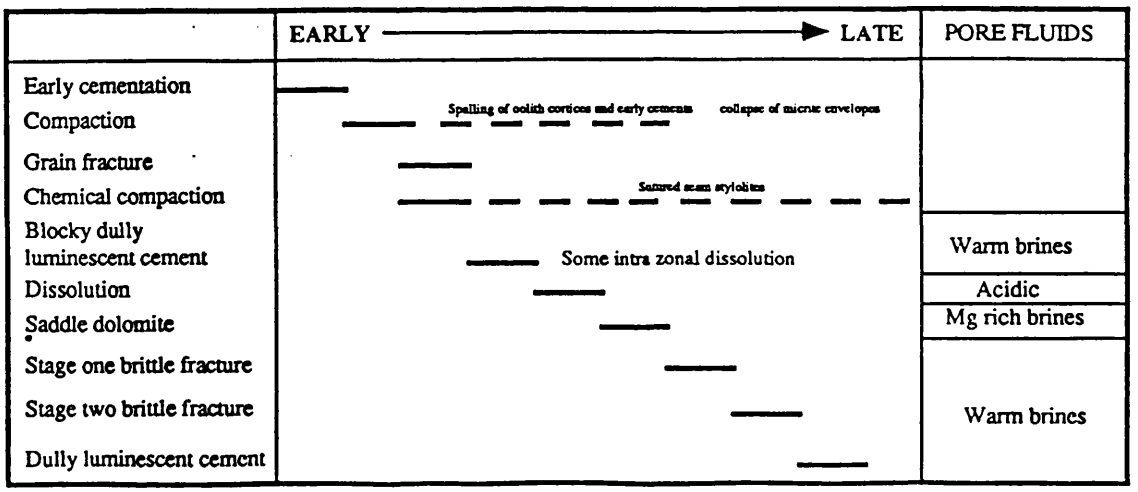

Fig. 3.38. Summary of late diagenesis in the Micrite Unit

4.1. INTRODUCTION.

The Micrite Unit is overlain by a blanket of grainstones approximately 150 m thick in the western mine area, henceforth known as the Grainstone Unit. The grainstones include oolitic, bioclastic, lithoclastic and pelloidal varieties and three siliciclastic 'marker' horizons. Characteristic sedimentary structures include plane bedding, cross-bedding and bioturbation; nodular textures also occur. The sequence is punctuated by several surfaces which carry bowl and funnel shaped depressions. A major channel system cuts into the middle to lower part of the sequence. This consists of a stacked succession of minor channels filled by a sequence of sand to granule grade grainstones with the whole assembly known collectively as the 'microconglomerate'. The sequence is shown in Fig. 4. 1. Peterographic features include columnar, syntaxial and blocky calcite cements together with features of dissolution and compaction. The succession hosts the 4, 3, 2 and 1 Ore Lenses.

4.2. GRAINSTONES.

Sixty thin sections have been used to describe the lithologies present. Replacive dolomitization sometimes prevents accurate textural classification (Chapter 5). However, twenty five samples indicate the presence of oolitic, bioclastic, pelletal and lithoclastic grainstones.

Oolitic grainstones are texturally mature and fine sand grade, ooliths are spherical to sub spherical. They consist of 20 to 30 concentric layers each a few microns thick which form dark coloured cortices (Plate 4.1.A). Each concentric shell consists of needle like crystals oriented normal to the layer surface. These alternate with laterally discontinuous layers of dark material which consist of opaque particles a few microns in diameter. This dark material is a common feature of ancient ooliths and is generally believed to have been organic (Scholle, 1978). Superimposed on the concentric structure a series of elongate dark areas approximately 10 microns wide radiate away from the nucleus.

Oolite nuclei consist of angular quartz grains, abraded bioclast fragments, lithoclasts or micritized grains. A few surficial ooliths also occur, typically developed around echinoderm plates or foraminifera. The oolitic grainstones contain an estimated 10% to 15% broken and abraded bioclasts, typically crinoid ossicles, echinoderm plates and brachiopods, with trepostome bryozoans, algal fragments and foraminifera (*?Ammodiscus*). Occassionaly bioclasts form matrix supported layers a few centimetres thick (Plate 4.1.B). Rare coated grains are also present consisting of bioclasts surrounded

by several concentric layers of dense micrite (Plate 4.1.C). One distinctive oolitic grainstone has a consistent stratigraphic position and forms a marker horizon known as the **Lower "Sandstone" Marker.** It has a sharp base and contains up to 25% siliciclastic grains (Fig. 4.2. A).

Skeletal grainstones are poorly sorted and range from fine sand to granule grade. One skeletal grainstone forms a poorly defined marker termed the **Sub Lower Sandstone Marker**, the base of this is located 6 m below the base of the Lower Sandstone Marker. The most characteristic feature of this marker is the presence of bedding parallel shale lithoclasts (Fig. 4.2.B), and, like the Lower Sandstone Marker, it may contain up to 25% siliciclastic grains. A second prominent skeletal grainstone is confined to the large channel which bounds the upper surface of the Micrite Unit (discussed in detail in section 3.6), occurring 10 m above the base (noted also by Anderson, 1990). The thickness varies from 0.7 m to 3 m and the unit is therefore lenticular. It is thinly bedded and some beds are graded. Skeletal grainstones are rich in echinoderm fragments which acount for up to 50% of the rock and include echinoid plates and spines, crinoid ossicles and crinoid arm plates. Up to 30% of fragments are of endopunctate brachiopods, the remainder consisting of trilobite cuticles and foraminifera (Plate. 4.1.D). Echinoderm fragments commonly have mud filled stereomes and some contain larger pores. Some bioclasts have two or three dark layers extending along their length and resemble phylloid blue green algae. Fusuilinid and miliolid (*Ammodiscus ?*) foraminifera are present. Gastropods, ostrocod valves and trilobite fragments also occur. Generally these have been fragmented and abraded. A few ooliths and pellets are present.

A few larger bioclasts are present in the grainstones. These are typically disarticulated spiriferid brachiopods, solitary rugose corals and crinoid ossicles. Distinctive shelly beds have formed a 'marker horizon' known as the **Brachiopod Marker** (Plate 4.1.E) located 8 m above the Lower Dark Marker (see below). This consists of 2 to 3 layers, approximately 0.5 m apart, of convex up disarticulated spiriferid brachiopod valves. Generally these are broken but a few remain intact and are filled with grainstone. Shell layers are supported by grainstones, individual valves are over 3 cm wide and up to 3 mm thick. They have no micrite coatings and internal structures appear unaltered.

A second bioclast marker, the **Lower Bryozoan Marker** occurs 15 m below the Upper Dark Marker (see below). It typically forms a bed 1.5 m thick (Ashton, pers commn, 1992) but is 2.8 m thick in hole N858. The bryozoans have more or less cylindrical stems with a number of branches up to 1 cm in diameter (Plate 4.1.F). Like the bioclasts in the brachiopod marker the bryozoan fragments are unaltered. The internal structure consisting of a central cluster of circular chambers which pass outwards into a

series of radiating parallel tubes with cross partitions. Both stems and branches may contain irregular cavities extending along their lengths and filled with grainstone. The bryozoans are disarticluated, having broken at nodal points between branches and stems. Fragments are typically 2 to 3 cm long and elongate with rectangular cross-sections, and lie parallel to bedding. The branching morphology, internal structure, dimensions and the Lower Carboniferous age of these bryozoa is consistent with the order Trepostomata genus *?Anistotrypta.*

Peloidal grainstones are of fine sand grade and well sorted. Some peloids display relic structures indicating that they were originally skeletal fragments or ooliths (Plate 4.1.G). Others consist of dense micrite. The intensity of micritization varies from surficial alteration through to patchy alteration and complete replacement (Plate 4.1.H). The environmental significance of micritization is discussed more fully in section 4.7. Pellets vary from spherical or elliptical to irregular. They are generally dark but some also contain darker particles a few microns in diameter.

Lithoclast grainstones vary from granule to fine sand grade. Individual grains are rounded but sediments are generally poorly sorted. A variety of lithoclasts are present, consisting of calcite mudstones (Plate 4.2.A), calcite mudstones which themselves contain angular fragments of calcite mudstone (Plate 4.2.B), pelletal grainstones with pellets consisting of calcite mudstones (which have been truncated against the clast margin) and fragments of *Garwoodia* oncoids. The bioclast assemblage is the same as that described from the bioclast grainstones. Other grains present include ooliths and pelloids. In one thin section from hole EP12, midway between Navan and the Clogherboy prospect, lithoclasts of oolitic packstone with a calcite mudstone matrix occur. These contain acicular calcite and micritic cements. A few composite grains also consist of 2 to 3 ooliths bound together by micrite, suggesting that they are grapestones (Plate 4.2.C). One lithoclast grainstone approximately 50 m above the base of the Grainstone Unit in the western mine area, between the Nodular and Upper Dark Marker, can be correlated over 1000 m. It is up to 4 m thick in hole N1022 but only 2 m thick in hole N1005 suggesting a lenticular geometry. It is thinly to medium bedded and contains 30 cm thick graded beds which have either sharp or gradational bases and gradational tops.

The grainstones are generally thinly to thickly bedded and internally laminated. Contacts between beds are generally planar but some have an irregular relief of a few centimetres (Plate 4.2.D). Many sedimentary layers are inclined relative to the horizontal, forming cross-bedding. This occurs in all holes logged from the base of the sequence to the upper limits of the grainstones. Cross-sets average 50 cm thick with a maximum thickness of around 1 m. In hole N975 at depth 483.6 m cross-sets are 1.5 m thick. Laminae are up to 15 mm thick and dip 20^0 to 30^0 from the horizontal but curve gently

PLATE 4.1. Lithologies and features of the Grainstone Unit.

A. Photomicrograph (plane light) of oolitic grainstone. Hole N908 at depth 369.0 m. Scale bar = 1 mm.

B. Photomicrograph (plane light) of bioclastic layer in oolitic grainstone. Hole N982 at depth 402.6 m. Scale bar = 1 mm.

C. Photomicrograph (plane light) of coated grain (c). Hole N763 at depth 440.3 m. Scale bar = 1 mm.

D. Photomicrograph (plane light) of skeletal (crinoidal) grainstone. Hole N982 at depth 402.6 m. Scale bar = 1 mm.

E. The Brachiopod Marker, the brachiopods have been disarticulated and fragmented. Shell fragments are now grain supported and convex up. Hole N710, at depth 192.2 m. Pencil for scale points to 'way up'.

F. The Lower Bryozoan Marker, bryozoan fragments have a circular cross-section. Hole N314 at depth 178.0 m. Scale in millimetres.

G. Photomicrograph (plane light) of peloidal grainstone. Hole N314 at depth 274.0 m. Scale bar = 1 mm.

H. Photomicrograph (plane light) of micritized ooliths. Hole EP12 at depth 504.7 m. Scale bar = 1mm.

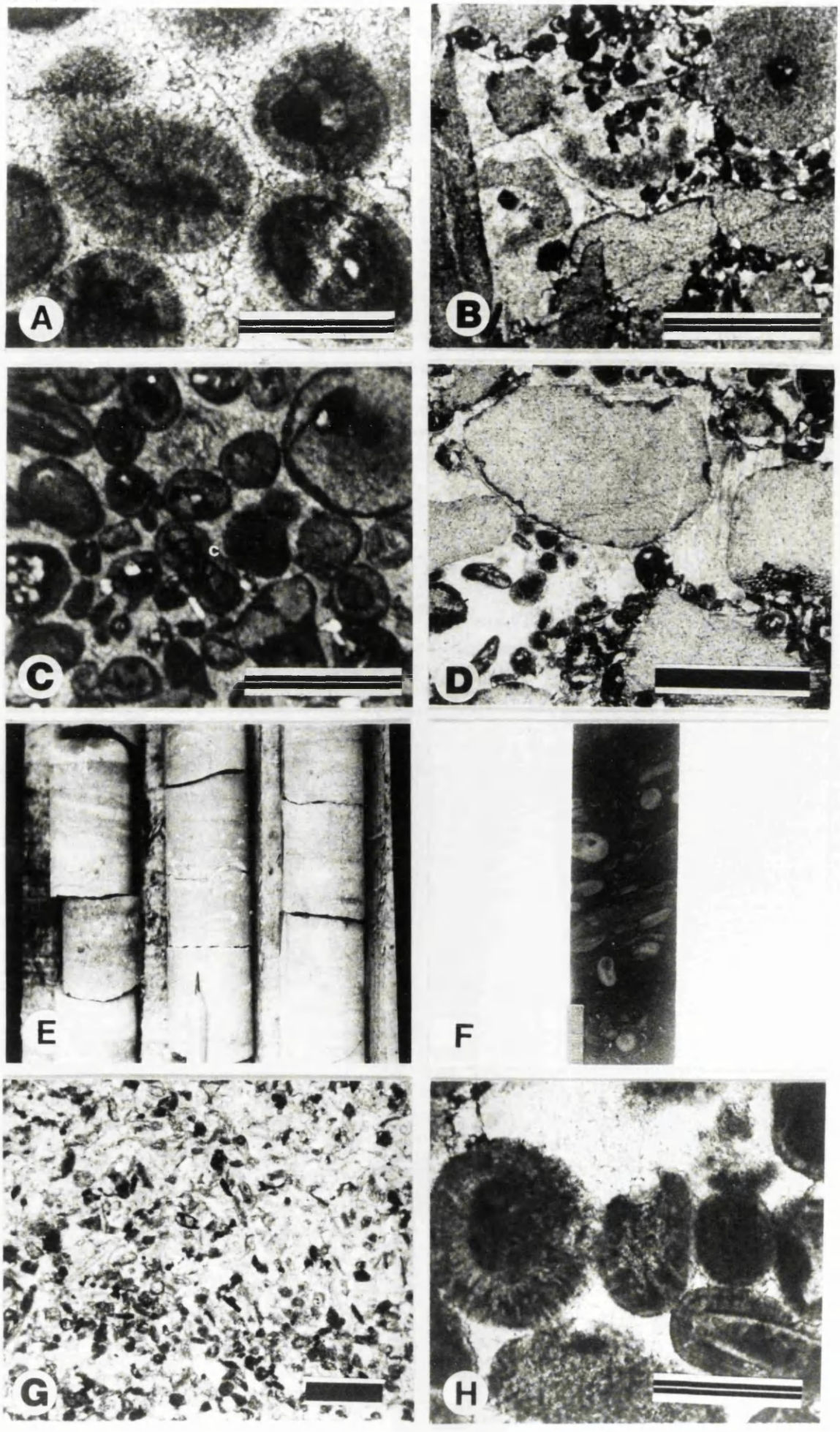
A
B
C
c
D
E
F
G
H

(Plate 4.2.E). The lower halves of some cross-laminae are rich in coarse bioclasts suggesting that they are graded (Plate 4.2.F). Cross-beds also occur in the Lower Sandstone Marker (Plate 4.2.G). Cross-beds in hole N975 at depth 421.0 m pass up into trough cross-lamination 10 cm thick (Fig. 4.3).

Occasional graded beds in the grainstones are up to 40 cm thick (average 15 to 20 cm thick). Textural relationships vary and are summarised in Fig 4.4. In hole N975 one graded bed has a sharp erosive base overlain by 5 cm of granule skeletal grainstones passing up into layered sand grade grainstones. Similar graded units in hole N982 pass up into cross-laminated grainstones. Other graded units occur in holes N272 at depth 330.0 m and N835 at depth 381.0 m. Reversly graded units occur in hole N975 at depth 416.0 m. One graded bed in hole N975 consists of a 2 cm thick bioclast lag which passes up into very fine grained cross-bedded grainstone. This can be correlated over 125 m with hole N982.

Burrows are common in the grainstones with burrowing extending over 4 m in hole N858, located between the Nodular and Lower Bryozoan Marker (depth interval 440.0 m to 436.0 m). Individual burrows are either vertical or sub-horizontal. The sub-horizontal burrows are tear- shaped, up to 2.5 cm in diameter and contain concentric laminae (Plate 4.2.H). Their dimensions and geometry are very similar to modern *Calliannassa* burrows in Bahamian and Florida lime sediments (Shinn *et al,* 1968b). Vertical 'U' shaped (cylindrical) burrows in hole N1034 at depth 502.0 m resemble *Skolithos*.

4.3. MUDDY LITHOLOGIES.

The Nodular Marker is 15 m thick in hole N862, the upper contact may be either sharp or gradational (Fig 4.5). It dies out westwards (Ashton, pers commn, 1992) and in the eastern mine area it is truncated by an Arundian submarine debris flow (see chapter 6). The marker consists of bioclastic wackestones and packstones, silty wackestone-packstones and dark shaley siltstones 2 to 3 cm thick. Bioclasts include crinoids, echinoid plates and disarticulated brachiopod fragments, a single fragment of rugose coral was noted in hole N975. Burrowing is extensive, and individual burrows are 2 cm in diameter, generally sub-horizontal and containing spreite (hole N1038). The burrowing has produced a chaotic fabric consisting of irregular patches of limestone and silty shales and coarse bioclastic lenses, with gradational or sharp interfaces (Plate. 4.3.A). Relic bedding is present in hole N1033, up to 10 cm thick (Plate 4.3.B). Beds often contain anastomosing lamination. Occasionally bedding and burrows are truncated by subvertical fissures up to 1 cm wide having a crude 'v' shaped profile, extending vertically over 10 cm (Plate 4.3. C). The **Sub Dark Marker,** 40 m above the base of the Nodular Marker, is 10 m thick in hole N1005. It resembles the Nodular Marker but is laterally

PLATE 4.2. Lithologies and features of the Grainstone Unit.

A. Photomicrograph (plane light) of lithoclast grainstone, hole N1022 at depth 522.9 m. Scale bar = 1 mm.

B. Photomicrograph (plane light) of calcite mudstone fragments. hole N1022 at depth 522.9 m. Scale bar = 1 mm.

C. Photomicrograph (plane light) of grapestone. Hole EP12 at depth 489.5 m. Scale bar = 1 mm.

D. Scour surface within grainstones, outline enhanced by pencil line for clarity. Hole N876. Scale in centimetres.

E. Cross-bedding in grainstones. Hole N975 at depth 421.0 m, width of core 3.5 cm.

F. Graded cross laminae (arrow), now extensively dolomitized. Hole N975 at depth 384.7 m. Scale bar = 1 cm.

G. Cross-bedding (C) in the Lower Sandstone Marker, Hole N998. Scale in centimetres, pencil points to 'way up'. Core saturated for clarity.

H. Burrows in grainstone (a) burrow sub-horizontal (b) vertical burrow. Both contain spreite structure. Pencil for scale.

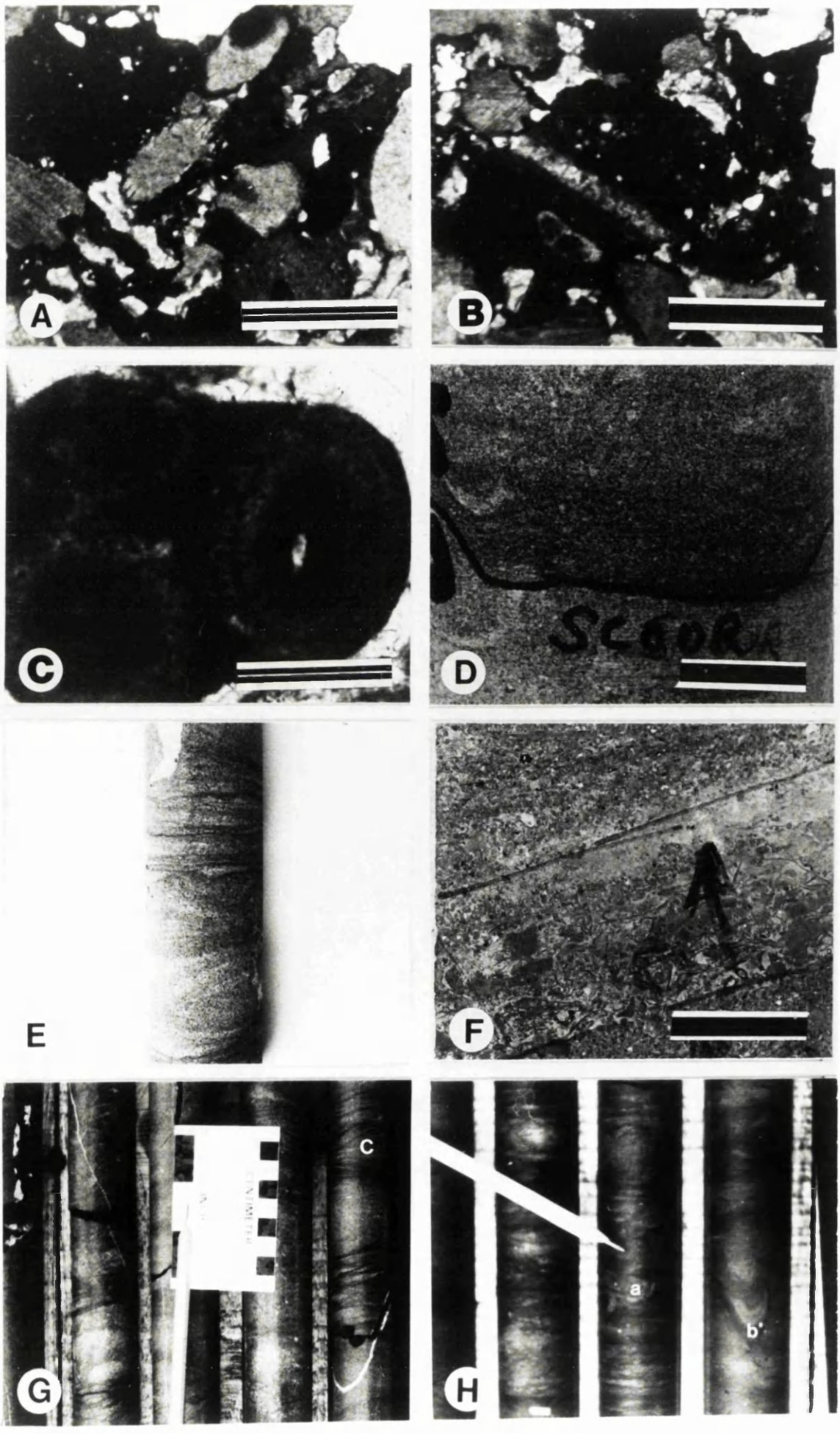
A
B
C
D
E
F
G
H
c
a
b'

discontinuous having a maximum lateral extent of 1500 m. It dies out toward the eastern mine area. Other muddy beds include a 1 m thick bioclastic wackestone in hole N351. This occurs within the channel which bounds the upper surface of the Micrite Unit shown on crossection 'E-E'. (it cannot be traced to adjacent holes). Bioclasts within this bed are irregularly distributed and a crude mottling is present, both features are interpreted as reflecting burrowing. Rare oolitic packstone textures occur in hole EP12 at depth 504.7 m forming a layer 1 cm thick with a matrix consisting of calcite mudstone.

4.4. BOWL AND FUNNEL SHAPED DISSOLUTION FEATURES.

Anderson (1990) noted that several surfaces within the Grainstone Unit carry depressions having bowl and funnel shaped profiles in elevation, resembling those in the Micrite Unit. These are important because they are filled with high grade zinc-lead ores. Like the depressions on surfaces within the Micrite Unit, they occur at consistent stratigraphical positions, notably between the Nodular and Upper Dark Markers. Bowl shaped pits are seen in 2 Zone, 1 Lens 222 west, where pits 30 cm deep and 60 cm wide are filled with dark thinly bedded shaley calcisiltite (Fig. 4.6.A). Funnel shaped depressions also occur immediately below the Nodular Marker (Fig. 4.6.B). In drill cores, depressions are represented by steeply inclined surfaces which truncate horizontal layering and cross-bedding and are overlain by shaley calcisiltites.

Funnel shaped depressions are well exposed in the 2 Zone, 3 Lens in the 1285 mine level waste storage bay 585 stope (restricted access precluded detailed examination). Here thickly bedded grainstones with extensive cross-beds have a series of depressions along 3 bedding surfaces. The depressions sharply truncate tabular and cross-bedding and are 1 to 2 m wide and up to 1 m deep, separated by blunt pinnacles. Collectively, depressions and pinnacles form a hummocky truncation type topography (Fig. 4.7). The depressions are partly connected by vertical, subvertical or sinuous shafts up to 0.5 m wide. The exact number of surfaces between each marker is currently unknown, but 3 surfaces over a vertical interval of 3 m occur in the waste storage depot, of 2 zone (refer Fig. 4.7). The underside of this system of depressions is exposed in the roof of the waste storage bay, the distribution is non random and displays a rectilinear pattern.

4.5. LINEAR EROSIVE FEATURE.

In the western mine area, between the Lower Sandstone and Nodular Markers, a linear erosive feature is present. The total relative depth of the channel system was recorded from drill core using the base of the Nodular Marker as a datum. Contours show that the erosive feature extends over an interval 30 m thick and occurs in an area over 2 km wide, striking N to S for over 2 km and extending beyond the study area (Fig. 4.8,

see also Appendix 1 for summary of data). Fig. 4.9 indicates that the feature has a profile which consists of a series of symmetrical channels up to 8 m deep and 1.5 km wide. At least thirteen channels are present, stacked on top of each other, but becoming less frequent upwards, decreasing in width and depth (Fig. 4.9). This channel system occupies roughly the same geographical position as that which truncates the Laminated Beds and is of similar length, width, depth, and orientaion (but is apparently unconnected).

4.6. MICROCONGLOMERATE.

4.6.i. Introduction.

The channel system described above is filled by generally coarse grainstones termed the 'microconglomerate' by Anderson (1990). These consist of granule and sand grade grainstones and muddy siltstones arranged in fining-upward sequences. (Fig 4.10)

4.6.ii. Lithologies.

i. Granular grainstones are a maximum of 8 m thick in hole N975. They are thinly to medium bedded and contain matrix supported small pebble grade grains (Plate 4.3.E) and a few thin sandy layers (hole N990). They have a sharp contact with the Grainstone Unit (Plate 4.3.D). The bases of coarser units are sharp and rip up clasts of the underlying lithology are present in hole N975 (Plate 4.3.F). Graded beds up to 1 m thick in hole N975, have sharp bases overlain with granule to small pebble grade grainstone passing up to fine to coarse grainstone.

ii. Sand grade grainstones are up to 3 m thick in hole N975 and contain scattered conspicuous bioclasts, typically crinoid ossicles, (a solitary rugose coral occurs in hole N975). Some of these bioclasts form shelly layers, as in hole N990. These grainstones are thinly to medium bedded and many beds are themselves laminate (Plate 4.3.G), sometimes with dark muddy interlayers as in hole N975. Graded beds up to 30 cm thick are common. In hole N975, six graded grainstone beds are stacked upon each other. Cross-bedding extends over 2 m in hole N991 with foresets are 12 to 15 mm thick dipping 20^0 to 30^0 (Fig.4.11). Sedimentary structures have been disrupted by burrows (Plate 4.3.H) with burrow influence extending over 30 cm in hole N990.

iii. Up to five shaley siltstone beds are present. The uppermost, 10 m below the Nodular Marker is up to 5 m thick in hole N991 but occurs throughout the mine area and is termed the **Sub-Nodular Marker** (Fig. 4.12). Generally the shaley siltstones are dark brown with mudstone laminae and contacts are commonly loaded. The shaley siltstones contain sandy layers, 1 to 2 cm thick (Plate 4.4.A) and fissile shales up to 10 cm thick in hole N1037. Bioclasts are common, typically crinoid ossicles and fenestrate bryozoan fronds, locally forming loosely packed matrix supported layers (up to 13 cm

PLATE 4.3. Features of the Nodular Marker and the Microconglomerate.

A. Detail of Nodular Marker. Note chaotic fabric consisting of irregular crinoidal wackestones (C) and shaley siltstones (S). Hole N975 at depth interval 370.0 m to 378.0 m. Scale in centimetres.

B. Crude bedding in Nodular Marker consisting of interbedded crinoidal wackestones (C) and silty shales (S). Scale in centimetres. Hole N998.

C. Vertical fissures (F) in Nodular Marker. Bedding can be traced across them. Note sharp basal contact (C) of Nodular Marker. Hole N1035 at depth 506.2 m. Scale in centimetres.

D. Sharp basal contact of the Microconglomerate. Hole N1034 at depth 578.7 m. Scale in centimetres.

E. Granule small-pebble grade microconglomerate displaying a variety of clast types. Hole N975. Scale in centimetres.

F. Sharp internal contact within microconglomerate facies truncating thinly laminated sand (T). Hole N975. Scale in centimetres.

G. Sand grade member of the microconglomerate. Note thinly bedded fraction on left (T) possibly inclined (?). Hole N1038 at depth 578.8 m. Core width = 3.5 cm.

H. Burrows in microconglomerate, burrows outlined in pencil for clarity. Pencil for scale points to 'way up'. Hole N1039 at depth 383.7 m.

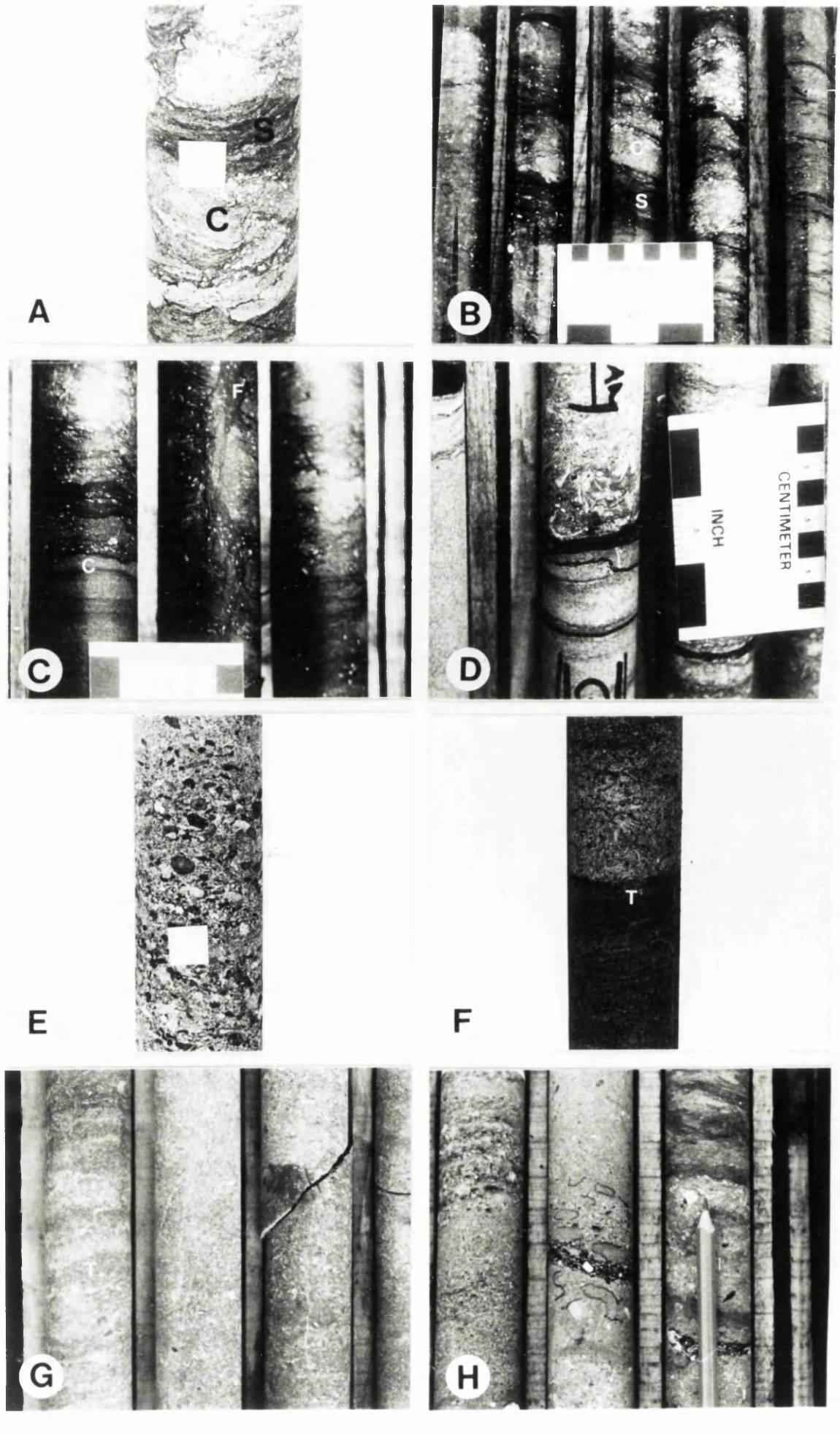
A
S
C
B
S
C
F
C
D
CENTIMETER
INCH
E
F
T
G
H

thick in hole N975). The shaley siltstone contains planar, anastomosing and cross-lamination, the last present in hole N975 at depth 394.1 m and extending over 13 cm. The contacts between shaley siltstones and grainstones are burrrowed in hole N1039. Burrowed surfaces are common. Individual burrows exposed in hole N975 at depth 391.4 m are sub-horizontal and tear-shaped (Plate 4.4.D), others are elliptical. Using Bromley's (1990) data as control they correspond to *Rhizocorallium.* In hole N975 and in hole N990 at depth 417.5 m, irregular white nodules of anhydrite up to 1 cm in diameter are present (Plate. 4.4. B-C).

4.6.iii.Grain types.

Twenty thin sections of micro-conglomerate have been examined, six from granule small pebble grade grainstones, eleven from sandstones and two from shaley siltstones. Extensive replacive dolomitzation has prevented detailed textural classification. Generally the microconglomerate is texturally and mineralogically immature. A variety of grain types are present:

1. The bioclast assemblage is varied consisting of algal grains, echinoid plates, crinoid ossicles, crinoid arm plates, echinoid spines, (two types of spine, one with radial the other with concentric structure), trepostomate bryozoans, endopunctate brachiopods, gastropods and miliolid foraminifera (*Ammodiscus?*) (Plate 4.4.E) .
2. Non skeletal grains include ooliths, micritized grains, oolitic and bioclastic lithoclasts and peloids (Plate 4.4.F). Angular fragments of calcite cement are also present. Under CL these show non-luminescent and bright orange zones of varying width (containing very faint sub zones) forming up to 10 couplets (Plate 4.4.G). These sequences differ from the indigenous cement and this, together with the truncation of couplets against clast margins, demonstrates that these are indeed fragments of cement .
3. Siliciclastic grains form up to 30% of the sediment (Plate 4.4. H)

4.6.iv. Provenence of clasts in the Microconglomerate.

The granule and sand grade grainstones include bioclasts, ooliths, fragments of calcite cement and silicate grains. The bioclast assemblge is dominated by brachiopods and echinoderms. These are stenohaline, indicating that normal marine conditions existed nearby. The gastropods are believed to reflect lagoonal environments (Walkden, 1987; Gawthorpe & Gutteridge, 1990). Shells are disarticulated, broken and abraded indicating reworking and probably a high hydraulic energy environment.

Calcite cement fragments indicate that lithified limestones were present nearby. The cement fragments contain several non luminescent and bright zones. Cements of this type are common in shallow marine limestones and are widely believed to reflect meteoric

PLATE 4.4. Features and clasts of the Microconglomerate.

A. Shaley siltstone of the Sub-Nodular Marker. Note thin sandy beds (S) and anastomosing lamination (L). Hole N975. Width of core = 3.5 cm.

B. Photomicrograph (plane light) of anhydrite nodules in shaley siltstones. Hole N990 at depth 417.5 m. Scale bar = 1 mm.

C. Photomicrograph (crossed polars) of anhydrite nodule showing radiating structure. Hole N990 at depth 417.5 m. Scale bar = 1 mm.

D. Burrow in shaley siltstone. N1036 at depth 590.5 m. Pencil for scale points to 'way up'.

E. Photomicrograph (plane light) of bioclasts. Hole N990 at depth 431.7 m. Scale bar = 1 mm.

F. Photomicrograph (plane light) of non skeletal grains. Hole N990 at depth 431.7 m. Scale bar = 1 mm.

G. Photomicrograph (CL) of cement fragment. Hole N990 at depth 433.5 m. Scale bar = 500 microns.

H. Photomicrograph (plane light) of silicate grains. Hole N990 at depth 432.4 m. Scale bar = 1 mm.

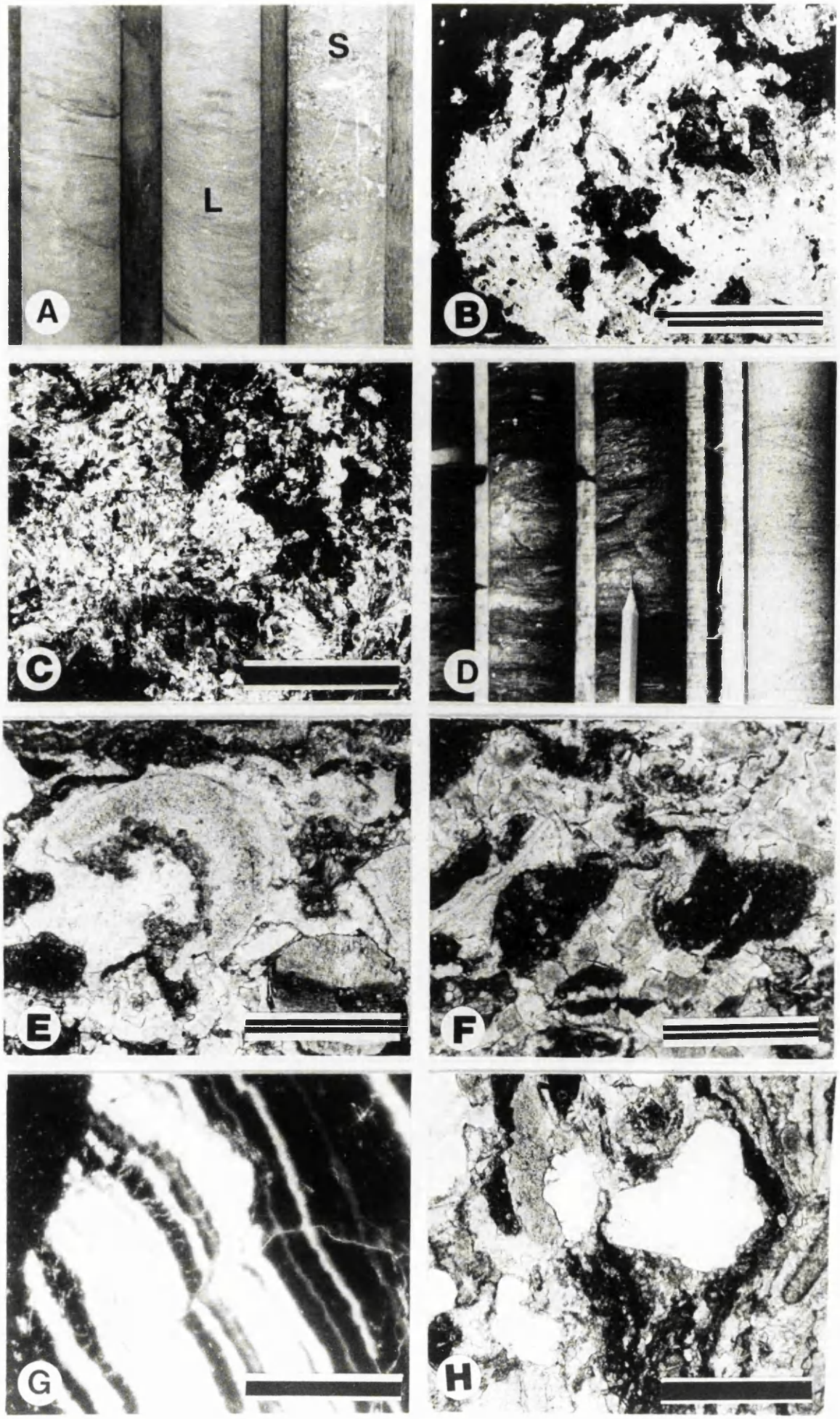
S
L
A
B
C
D
E
F
G
H

phreatic cementation (Walkden & Davies, 1983; Walkden, 1987, Horbury & Adams, 1989, Emery & Dickson, 1989; Meyers, 1991). The occurrence of these in clasts suggests derivation from limestones that had undergone meteoric phreatic cementation and thus provides indirect evidence of palaeokarst.

Siliciclastic grains include polycrystalline, polycrystalline sheared and strained quartz grains with undulose extinction and indicate derivation from igneous and high to medium grade metamorphic rocks. This suggests that crystalline basement was exposed nearby, perhaps adjacent to Lower Palaeozoic rocks.

4.7. SILICICLASTIC ROCKS.

4.7.i. Detrital grains.

Siliciclastic grains locally account for up to 25% of the grainstones and muddy lithologies (visual estimate). Where present they are generally evenly disseminated, but in the Lower Sandstone Marker siliciclastic grains form a few distinct matrix supported layers (Plate 4.5.A). In N992 silicate grains form crude circular clusters 1 to 2 mm in diameter and in hole N314 at depth 274.0 m arcuate trails. Both features are interpreted as burrow fills (Plate 4.5.B). Four different types of quartz grains are present. Monocrystalline grains have linear fluid filled vacuole trails and lath shaped solid inclusions which are not in optical continuity. With these are polycrystalline, polycrystalline sheared, and strained grains, the last with undulose extinction. Orthoclase displays Carlsbad twinning and plagioclase displays composite Carlsbad and multiple lamellar twinning. The feldspars are generally fresh but alteration is present along twin lamellae and within exsolution lamellae of perthite grains. In some grains twin lamellae have been deformed (deformation twinning). Microcline, like plagioclase, displays some alteration. The Upper Sandstone Marker (see below) contains myrmekitic or granophyric intergrowths of feldspar and irregular sub parallel rods of quartz (Plate 4.5.C). Muscovite flakes lie parallel to bedding. Other silicate grains which have been reported include tourmaline, zircon and ilmenite (Andrew & Ashton, 1985). In the lithoclast grainstone in hole N1022 granules of red jasper are present. Lithic grains are altered preventing further interpretation. Rare green grains are interpreted as detrital glauconite.

Some siliciclastic beds form distinctive 'markers'. Two dark silty shales and a sandstone are used in core correlation and account for 5% of the stratigraphic section. In stratigraphical order the shaley markers are the Lower Dark Marker and the Upper Dark Marker while the sandstone forms the Upper Sandstone Marker. The location of these is shown on cross-sections 'A-A', 'B-B', 'C-C', 'D-D', 'E-E'. Both the Nodular and Sub Dark Marker contain muddy siliclastics, but since they are predominantly calcareous they have been considered in section 4.3.

4.7.ii. Muddy siliciclastic beds.

Muddy siliciclastic beds overlie the floor of the channel which bounds the upper surface of the Micrite Unit in the eastern mine area. This lithology, on which the grainstones within the channel rest, consists of a variety of siliciclastic sediments. These are exposed in seven holes, notably N629 between 356.0 m and 353.0 m where they overlie and fill the karst modified channel floor (refer Plate 3.9, C-D and Fig 3.32). Here the lithology consists of thinly interbedded fine to medium grained light brown sandstones with occasional bioclasts, calcisiltites and black shale up to 1 cm thick. Sedimentary structures include layering 2 to 3 mm thick, cross lamination with forsets dipping 10^0 to 15^0, and graded beds (Plate 4.5.D). The bases of the graded units consist of fine to medium grade sandstone passing up to very fine grade sandstones. Other lithologies include structureless siltstones and fissile black shales containing angular fragements of calcite mudstones. Similar lithologies partially fill the bowl and funnel shaped depressions described in section 4.4 and Fig 4. 6.A.

The Lower Dark Marker (Plate 4.5.E) was first recognised by Philcox during an early drilling program (1970 to 1973). It occurs 20 m above the base of the Upper Pale Beds and is confined to the channel which bounds the Upper surface of the Micrite Unit in the eastern mine area. It is shown on cross-sections 'A-A' 'D-D', 'E-E' and is approximately 5 m thick in hole N314. Two other muddy siliciclastic beds occur within this channel one 5 m below, the other 5 m above the Lower Dark Marker. Each of these is 2 to 3 m thick.

The base of the Lower Dark Marker consists of thinly interbedded shaley siltstones and packstones up to 3 m thick. The shaley siltstones are up 3 cm thick and are delicately laminated and fissile containing bedding parallel fenestrate bryozoans and occasional crinoid rich layers. The packstone layers are up to 3 cm thick and pass gradationally up into dark silty bioclast grainstones. Both lithologies include a few large bioclasts, typically brachiopods and crinoid ossicles. Burrowed surfaces are common, individual burrows are elliptical and 15 mm wide and interpreted as *Thalassinoides*. The main features are summarised in Fig. 4.13.B.

The Upper Dark Marker has a maximum thickness of only 2.8 m (in hole EP.26). It occurs throughout the study area but is truncated to the east by an erosion surface (see chapter.6). In hole N1033 it consists of up to three black fissile calcareous shales, each about 0.7 m thick, separated by grainstones (Fig.4.13. A). The shales also contain grainstones 2 to 3 cm thick (Plate 4.5.F). Some of the thicker grainstones are cross-laminated. Burrowing is common at contacts between shales and limestones and some beds are mottled, suggesting that they have also been burrowed. Burrows in hole N1033 at depth 539.2 m contain spreite and are elliptical with a maximum diameter up to

15 mm, resembling *Thalassinoides*. *Chondrites* burrows are circular in cross-section and 1 to 2 mm in diameter, filled with grainstone. They are younger than the *Thalassinoides*. (Plate 4.5.G). A few black fissile calcareous shales within the grainstones are up to 10 cm thick. Generally their bases and tops are sharply defined. One persistent shale occurs 3 m below the base of the Lower Bryozoan Marker.

4.7.iii. Sandstones

The **Upper Sandstone Marker**, lies 12 to 15 m above the Upper Dark Marker. It is tabular with a sharp basal contact and is approximately 6 m thick (Fig.4.14). It is a very fine grained light brown micaceous sandstone containing a few silty laminae which locally give a faint dark banded appearence to the otherwise clean sandstone. In hole N1039 a 3 cm thick dark silty sandstone is present within the marker. In thin sections (holes N876 at depth 88.1 m and N710 m at depth 83.4 m) the sandstone consists of angular quartz, feldspar and mica grains similar to those described from other detrital beds, described in section 4.7.i. Visual estimation (Folk *et al.* 1970) suggests that the modal composition of the Upper Sandstone Marker is approximately 60% quartz, 30% feldspar, 5% lithic grains and 5% mica flakes. It is therefore an arkosic arenite (Pettijohn *et al.* 1973).

The Upper Sandstone Marker is thinly to medium bedded in hole N1039. Some cross-bedding is present, individual laminae are 1 mm thick, dipping 20^0 to 30^0 from the horizontal. Individual cross-sets dip in opposite directions, suggesting a 'herring-bone' arrangement (Plate 4.5.H). Some trough shaped ripples occur in hole N1039 and extend over 60 cm of drill core Burrowed surfaces are common and burrowed beds up to 1 m thick have disrupted planar and cross beds (Plate 4.6.A). In hole N876 at depth 84.5 m some burrows have been trucated by cross-bedding. A few thin clean, well sorted, fine grained sandstones occur above the Upper Sandstone Marker (Ashton, pers commn, 1992).

4.8. SEDIMENTOLOGY.

4.8.i. Introduction.

The Navan grainstones are skeletal, oolitic, peloidal and lithoclastic. Sedimentary structures include plane bedding, cross-bedding and burrowing and a few graded beds. They form lensoid banks and occupy shallow channels. The grainstones contain several siliciclastic marker beds with the whole sequence punctuated by surfaces which carry bowl and funnel shaped depressions. The environmental significance of these lithologies and their characteristic features will now be considered.

PLATE 4.5. Features of the Marker Horizons.

A. Photomicrograph (plane light) of siliciclastic sandy bed in the Lower Sandstone Marker. Hole N314 at depth 274.0 m. Scale bar = 1 mm.

B. Photomicrograph (plane light) of burrow filled with silicate grains. Hole N975 at depth 429.01 m. Scale bar = 2 mm.

C. Photomicrograph (plane light) of myrmekite grain in Lower Sandstone Marker. Hole N982 at depth 399.9 m. Scale bar = 1 mm.

D. Thinly interbedded sandstones, siltstones and silty shales overlying the karst surface at the base of the channel which bounds the upper surface of the Micrite Unit in the western mine area. Note cross-lamination (c) and load structure (s). Scale in centimetres.

E. The Lower Dark Marker. Hole N876 at depth interval 199.0 m to 203.0 m. Pencil for scale points to way up.

F. Interbedded limestones and shales of the Upper Dark Marker, note burrowed interval. Hole 1037 at depth 386.0 m. Pencil for scale points to 'way up'.

G. Burrowed contact between grainstone and black fissile shale, the Upper Dark Marker. Note *Thalassinoides* (T) burrow trucated by *Chondrites* (C). Pencil for scale points to way up.

H. Herring bone cross-bedding in the Upper Sandstone Marker. The base of the cross-beds has truncated a sub-horizontal burrow at (B). The cross-bedding is disrupted by burrows at (D). Hole N1039 at depth 314.0 m. Scale in millimetres.

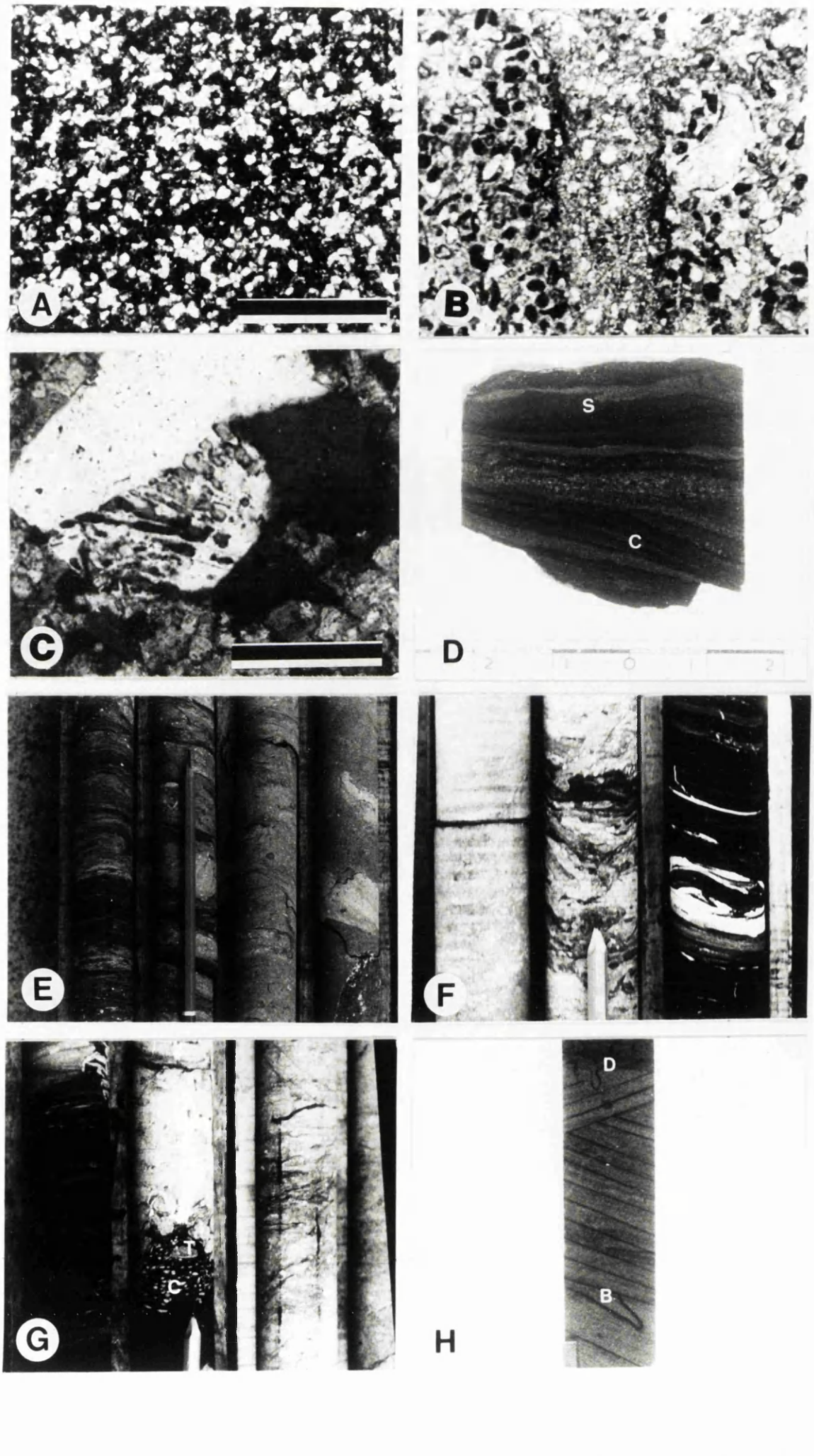
A
B
C
S
C
D
E
F
G
T
C
H
D
B

4.8.ii. Sedimentology of the grainstones

Recent carbonate sands occur most commonly in high energy shallow marine shelf environments characterised by strong tidal currents and wave activity. The bioclast assemblage at Navan is diverse and includes echinoderms, brachiopods and corals which are stenohaline and indicate normal marine conditions. The light colouration of the grainstones suggests a well oxygenated depositional environment (Enos, 1983). Bioclasts are disarticulated, broken and abraded, indicating a high energy environment with frequent reworking. Bedding parallel shell material suggests deposition from bed load transport. A high energy interpretation is also indicated by the grain supported texture and lack of matrix.

Modern skeletal sands form extensive sheets reflecting widespread and uniform deposition. Generally sand sheets extend from shelf margins to platform interiors, passing into muddy sandstones (wackestones and packstones) along their lateral and shoreward margins. Recent bioclastic sands occur on the Grand Bahamas, the coralgal facies of Purdy (1961), forming a belt 5 km wide and and 40 km long; the platform interior sand blanket (Ball, 1967). Bioclastic sands also occur landward of reefs, on the Florida shelf a sand body known as White Bank is 2 km wide and 40 km long (Enos, 1977) and sands occur landward of the Belize reef (Halley, Harris & Hine, 1983) Other notable sands occur in the Persian Gulf, Shark Bay Western Australia and leeward of the Great Barrier Reef (review by Sellwood, 1986).

Oolitic grainstones are also found in modern high energy shallow marine environments and are common in the geological record (Wilson, 1975). They are not as widespread in Recent environments as bioclastic sands (Sellwood, 1986) and are commonly located along windward (but sometimes leeward) platform margins, notably in the Bahamas where they form tidal bar belts and marine sand belts (Ball, 1967; Halley, Harris & Hine, 1983), discussed in section 3. 4.

Calcite mudstones and pelletal calcite mudstones are common lithoclasts within grainstones. In general, such sediments are interpreted as reflecting low energy environments, either lagoonal or tidal flats. Lithoclasts of these lithologies therefore indicate derivation from this type of low energy environment by erosion of the seafloor. Cements within the lithoclasts indicate that the seafloor was lithified. Calcite mudstone clasts which themselves contain clasts of calcite mudstone indicate cyclic reworking. Other grain types present in the lithoclasts which suggest low energy conditions include *Garwoodia* oncoids previously interpreted (Chapter 3) as representing a lagoonal environment. Grapestones which form a small proportion of lithoclasts, are common in Recent carbonate environments, occuring in the more protected parts of platforms and on the abandonned portions of carbonate sandbodies. In these localities sedimentation rates

are relatively low, periodic turbulence facilitates cementation at grain contacts (Winland & Mathews, 1974).

Comparison of the cross-bedding in the Navan grainstones with that in modern sand bodies indicates that the Navan grainstones formed migrating sandwaves or mega ripples with inclined surfaces reflecting former lee slopes and plane beds perhaps reflecting the more gentle back slopes, the suggested facies model for the crossbedded grainstones at Navan is shown in Fig.4.15. The blanket like distribution of the Navan grainstones indicates widespread and uniform conditions suggesting the sand sheets covering areas of more than 8 km^2. In modern sandbodies such bed forms are located along the crests of major sand bodies and are oriented according to the prevailing current regime. In hole N975, cross-bedded oolitic grainstones pass up to trough cross-lamination, suggesting that smaller scale stuctures, probably ripples, covered the surfaces of the sandwaves. Asymmetric ripples in hole N975 indicate unidirectional (tidal) current flow.

The irregular nature of some bedding planes suggests scouring of the seafloor. Further evidence of current activity is provided by coarse graded beds. In terms of physical sedimentation the graded beds represent deposition from decelerating currents. Correlation of graded units indicates these currents covered hundreds of square metres. The Navan graded beds resemble ancient storm-deposited sequences (Kresia & Bambach, 1982). Similar graded units have been recorded from the Lower Carboniferous bioclastic grainstones of South Wales and are interpreted as storm beds, with a lack of reworking reflecting deposition below fair weather wave base (Wright, 1986). The fragmental character of bioclasts forming the Brachiopod and Lower Bryozoan Markers suggest these also are storm deposits.

Burrowing is common in grainstones. *Skolithus* is believed to reflect relatively high energy environments where sedimentation rates are high, resulting in the predominance of vertical 'escape' structures (Frey & Pemberton, 1984). In modern mobile carbonate sands burrows are generally absent from the crests of sand waves and mega ripples but are common in the troughs between. Burrowed sands are common in Recent carbonate environments. They are most common in the shoreward areas of large sand shoal systems where energy is lower and on abandoned and moribund surfaces, allowing extensive burrowing and sediment churning. The maximum depth of this burrowing is around one metre (Shinn *et al,* 1968b). Some burrowed sequences at Navan extend over 1 m of drill core suggesting they represent more than one event with prolonged substrate stability and low energy conditions interspersed with more hydrodynamically active conditions. Further evidence of (contemporaneous) low energy conditions is provided by grain micritization. This is common in low energy areas with low sedimentation rates and infrequent transport. Oolitic packstones suggests deposition of calcite muds on top of

oolitic grainstones and infiltration through the grain framework to produce the packstone texture.

Two hypotheses have been suggested to explain repeated shifts between sediment mobility and sediment stability (Evans, 1984).

i. That the currents responsible for sediment movement shifted, producing abandonment of part of a sand shoal.

ii. That variations reflect changes in sealevel and the rate of sediment accumulation. When the shoal is flooded sands are mobile but when part of the shoal builds to sea-level choking of circulation occurs. The frequency of sediment mobility decreases, producing stable low energy environments.

A change from a high energy mobile sand shoal system to a low energy environment, where sands become extensively burrowed, can also be produced by passage of the sand-shoal below fairweather wave base during a relative rise in sea level (Gawthorpe & Gutteridge, 1990).

Lithoclasts within Navan grainstones suggest that these sand bodies were bordered by lagoons floored by calcite mudstones. The lateral transition was probably northerly since the palaeoshore line is believed to have lain in this direction (Phillips & Sevastoupoulo, 1986; Rees, 1987). The favoured facies model is shown in Fig 4.16 and compares with the Recent sand shoals of Joulters Key in the Bahamas, where high energy mobile sands pass shoreward into extensively burrowed sand flats (Harris, 1983, 1984). Ancient analogues include the Lower Carboniferous bioclastic sands of the Woodale Limestone of Derbyshire (Gawthorpe & Gutteridge, 1990) which are interpreted as a staked sequence of shoals which prograded basinward. In this study, all three of the proccesses described above have been proposed for the abandonment phase of the shoals. The Lower Carboniferous Llannelly Group of South Wales provides a second ancient analogue (Wright, 1986).

Between the Lower Sandstone Marker and the Nodular Marker, in the western mine area, the carbonate sands contain a major channel system. Each channel is filled by microconglomerate forming a fining up sequence. Grains present include bioclasts, lithoclasts and silicate grains, sedimentary structures include cross-bedding and graded beds. These features compare with those of modern channel fill deposits. In the Bahamas, channels cut through tidal flats (Shinn *et al,* 1969) and shallow marine sand shoals (Harris, 1983, 1984). In the Persian Gulf they truncate oolitic barrier island sands (Purser, 1973) and in Florida they truncate lagoonal and barrier island deposits and extend into the shallow marine environment (Jindrich, 1969). In Shark Bay, Western Australia, a tidal channel system cuts a sand bank which fringes the bay (Choquette & Steinen, 1980, quoting Davies, 1970). Channels within recent carbonate environments

seem to have been cut by strong tidal currents over several thousand years with their erosive bases controlled by the Pleistocene bed rock.

At Navan each channel truncates grainstones. The proposed facies model is shown in Fig. 4.17. compares, in terms of dimensions, sedimentary fill and proposed hydrodynamics to tidal channels which truncate sands in the Bahamas (Harris, 1983, 1984), Florida (Jindrich, 1969), the Persian Gulf (Purser, 1973) and Shark Bay Western Australia (Davies, 1970). Structures within the channel fill grainstones provide insight into the sedimentary proccesses during deposition. Cross-bedding suggests that the floors of the channels were covered by mega ripples or bars which most likely migrated along the channel axes in a manner similar to that of bars in modern channels (Jindrich, 1969) with graded beds indicating deposition from decelerating current flow.

Bioclasts, lithoclasts of calcite mudstone and cement fragments, and silicate grains, indicate derivation from both a shallow marine environment and a nearby land area. Such a clast assemblage is believed to reflect tidal exchange along the channel with marine sediments carried during flood tides and terrestrial clasts during ebb tides (Selley, 1967). The relationship between current velocity and diameter of quartz grains in open channels is well known. The maximum diameter of quartz in the granular grainstones is 2 mm with the diameter of lithoclasts attaining 1.5 cm indicating that the (tidal ?) current velocities in these channels were greater than 50 cm / second (Hsu, 1989, Fig.4). An ancient analogue is provided by a channel system which truncates lagoonal and barrier sands in the Miocene Sirte Basin of Libya (Selley, 1967). In this a shaley siltstone which caps the channel fill sequence indicates a period of prolonged low energy sedimentation. Abundant lithoclasts of calcite mudstone suggests that, like the Navan example, the channel dissected inner platform lagoon deposits.

Evidence for low energy sedimentation is provided by the shaley siltstones at the tops of the fining up sequences. These indicate that currents became sufficiently 'slack' to allow clays to achieve settling velocity (Hsu, 1989). The channel system is more or less bounded by the Sub-Nodular Marker in the shaley siltstones extended over a much wider area. Like the shaley siltstones below these reflect low energy depositon with *Thalassinoides* burrows indicating low rates of sedimentation. Thin laminae reflect the lowest energy conditions. Anastomosing laminae indicate some surficial current activity with cross-lamination in the shaley siltstones suggesting that the surface was rippled. These features are consistent with a lagoonal environment. Nodules of anhydrite indicate that pore waters became sufficiently saline for evaporite formation and suggest that the lagoon became restricted.

The 'muddy' marker horizons, the Nodular, Upper Dark and Lower Dark Markers, provide evidence of prolonged periods of low energy deposition which extended across

the study area. The Nodular Marker consists of bioclastic wackestone - packstones, silty wackestones-packstones with thin black silty shales and is extensively burrowed. Burrowed sequences are believed to reflect stable environments containing an abundant food supply and supporting a diverse population of suspension and deposit feeders as well as mobile carnivores (Frey & Pemberton, 1984). Abundant bioclasts within the Nodular Marker support this interpretation. Since energy conditions are low, less abrupt shifts in substrate take place, and burrows are predominantly horizontal, out pacing sediment acumulation. Shinn *et al* (1968b) demonstrated that burrowing extends vertically to depths of at least 1 m in modern carbonate sands. The Nodular Marker is 12 m thick and consists of burrowed wackestones, grainstones and argillaceous mudstones. The extensive burrowing suggests that the Nodular Marker consists of several amalgamated burrowed units, a view supported by the presence of some relic layering.

The interpretation of the Nodular Marker is problematical since the characteristic features can occur either in the outer platform environments below fairweather wave base, or within inner platform shallow lagoons. However, thinly interbedded terrigeneous sediments and carbonates containing extensive burrows are believed to indicate a lagoonal environment (Elliot, 1986 p.167; Reinson, 1984, p.129). In addition the vertical profile is comapres with the sequence from the 5 to 25 m deep lagoon of Davis reef, on the Great Barrier Reef of Australia (Tudhope, 1989 and Fig. 18). The proposed facies model is shown in Fig 4.19. It is analagous to the Miocene of the Sirte Basin where biolastic sand shoals are believed to have interfingered shorewards with muddy lagoonal shales (Selley, 1967).

The muddy siliciclastics markers, the Upper Dark and Lower Dark Markers also accumulated in low energy conditions, either within inner platform lagoons or an outer platform below fairweather wave base (see review by Selley, 1984). Both environments facilitate the accumulation of muddy siliclastic material. Wilson & Jordan (1983) suggested that the shaley beds occuring in ancient limestones reflect either climate change or uplift and distant tectonic activity. Some general comments can be made about the environmental significance of these periods. The 'markers' are enclosed within high energy grainstones interpreted as reflecting deposition on a carbonate platform. Bioclasts and grainstone layers within the silty shales indicate that normal marine conditions existed nearby or were maintained during their accumulation.

The base of the channel which bounds the upper surface of the Micrite Unit in the eastern mine area is floored with interbedded sandstones, silty shales and fissile black shales which fill the karst modified surface. Sedimentary structures include cross-lamination and thin graded units, suggesting that current activity which caused ripples to

form was followed by periods of slack water which allowed clays to settle. Such conditions could be satisfied in a tidal environment.

The Lower Dark Marker and associated silty shales are confined to the channel (Andrew & Ashton, 1985). The marker consists of interbedded silty shales and grainstones, both containing burrowed surfaces. It is likely that the Lower Dark Marker reflects low energy deposition with periodic current activity. This low energy environment was restricted to the channel and was lagoonal or estuarine (compare Andrew & Ashton, 1985). Wavy lamination in the shaley lithologies is believed to reflect episodic traction transport of sediment (Potter, Maynard & Prior, 1980) suggesting that some surficial currents were operating during deposition of these muds.

The Upper Dark Marker consists of two or three black fissile shales. Black shales commonly indicate an anoxic environment. Burrowed surfaces are present and some contain *Chondrites* which is believed to tolerate anoxia in sediments (Bromley & Ekdale, 1984). *Cruziana* is believed to reflect low energy conditions below normal wave base but within storm wave base (Frey & Pemberton, 1984). *Thalassinoides* is a burrowing trace produced by mobile deposit or suspension feeders of high diversity. Such conditions may be satisfied in either an inner platform lagoon or deep outer shelf. Burrowed surfaces and thin interbeds of limestone and shale suggests the most likely interpetation is lagoonal, though deposition below fairweather wave base cannot be ruled out.

Sandstones within the Lower Carboniferous Llanelly Formation of South Wales have been interpreted as relecting a fall in base level (Wright, 1986). The Upper Sandstone Marker is well sorted and sheet like and reflects an influx of siliclastic sand during the closing stages of grainstone deposition, perhaps due to uplift of the adjacent hinterland. It contains plane bedding, herring-bone cross-bedding and burrowed surfaces. Silty sandstones indicate periodic low energy conditions. These features suggest that it represents a siliciclastic sand body which experienced reworking in the marine environment by periodic current reversals, a common process in tidally influenced environments. Abandonment of the sandshoal is reflected in burrowed surfaces (Fig. 4.20). Sandstones have also been described from the Lower Carboniferous Moyvoughly beds 50 km SW of Navan. Here they are interpreted as the marine component of a bay fill sand, reworked by agitated marine conditions (Harwood Sulliven, 1989).
The silicate grains at Navan were derived from an area consisting of igneous and metamorphic rocks, perhaps of Moinian - Dalradian age, part of a low lying area (Andrew & Ashton, 1985). Myrmekitic textures show that some igneous rocks were granitic.

Such grains occur in modern carbonate grainstones landward of the Great Barrier Reef, landward of the Belize Reef of the Red Sea. These grains are introduced to the

shelf from rivers and redistributed by currents, travelling long distances from their source. A similar procces was proposed for the silicate grains at Navan which are believed to have been derived from a fluviatile source and transported to the Navan area by longshore drift (Strogen *et al,* 1990). However clastic grains within channel fill grainstones of the 'microconglomerate' point to some deposition of clastics directly into the study area.

4.8.iii. Significance of the Bowl and Funnel shaped depressions.

The bowl and funnel shaped depressions on surfaces below the Nodular Marker and between the Nodular and Upper Dark Marker are similar to depressions on surfaces, in the Micrite Unit, and probably also represent karren type palaeokarst (refer to section 3.10 and Appendix 2). This demonstrates that a fall in base level was followed by subaerial erosion. This interpretation is supported by comparing the morphology of the depressions with palaeokarst displayed by 'Alpine Type' Zinc-Lead deposits (Fig. 4.21). Like the Navan examples the palaeokarst is orientated along bedding planes and consists of bowl and funnel shaped depressions (Klau & Mostler, 1986). In addition, like the Navan examples, the Alpine palaeokarst depressions are partially filled with thinly bedded argillaceous sediment which contain 'floating' clasts of limestone. This lithology is believed to have been deposited while the depression was at the surface (Klau & Mostler, 1986). Palaeokarst surfaces within grainstone sequences are common in the British Lower Carboniferous. The bioclastic sand shoals of Woodale, Derbyshire contain karst surfaces (Gawthorpe & Gutteridge, 1990), the Lower Carboniferous grainstones of the Llanelly and Oolite Group of South Wales also contain palaeokarst (Wright, 1986). The reconstructed karst surface is shown in Fig. 4.22.

Since Lower Carboniferous palaeokarst surfaces represent a period of emergence of between a few thousand and several thousand years (Wright, 1982; Walkden, 1987) it is to be expected that apart from the surficial indicators of emergence the grainstones themselves should contain evidence of meteoric diagenesis. As will be shown, this is reperesented at Navan by deposition of non-luminescent syntaxial calcite cements and dissolution of presumed aragonite fossils, both of which are believed to reflect circulation of meteoric pore fluids (Walkden & Davies, 1983; Walkden, 1987, Horbury & Adams, 1989, Emery & Dickson, 1989; Meyers, 1991). Indirect evidence for palaeokarst is provided by the clasts of calcite cement in the microconglomerate which consist of bright and non-luminescent couplets which are believed to indicate emergence (Walkden & Davies, 1983; Walkden, 1987, Horbury & Adams, 1989, Emery & Dickson, 1989; Meyers, 1991).

However, vadose diagenetic features such as microstalactitic and meniscus cements and crystal silts are absent from the Navan grainstones. A similar paradox has been

described from the Lower Carboniferous palaeokarst of Anglesey, North Wales (Walkden & Davies, 1983). Here several suggestions were proposed to explain the lack of vadose cements. They may have been removed by younger episodes of subaerial erosion, overprinted by phreatic cementation, or they may not have been present in the sample population of thin sections. All three points could explain the lack of vadose features at Navan.

4.9. PETROGRAPHY OF THE GRAINSTONES.

4.9.i. Introduction.

Twenty five thin sections of grainstones have been examined. Features present include micritization, three types of calcite cement, and features indicative of dissolution, compaction and brittle fracture. Using data from Scholle (1978) the allochems forming the cement substrate consisted of calcite, represented by brachiopods and ostracods, high magnesium calcite, represented by echinodern fragments, and, probably, aragonite, now represented by shell shaped moulds outlined by micrite envelopes.

Depositional porosity in modern carbonate sands is high, 40% to 60% (Bathurst, 1986; Scholle & Halley, 1984). At Navan the pre cement porosity can be classified according to the scheme of Choquette & Pray (1970) as interparticle and intraskeletal (typically within the tests of ostracods and the tegmen of brachiopd spines). Other types of porosity included growth framework porosity, typically within the zooecia of bryozoan fronds and some shelter porosity below shell fragments. Skeletal mouldic porosity formed subsequently.

4.9.ii. Cement types.

Three calcite cement types have been identified;

1.Columnar cement crystals form isopachous crusts which line interparticle and intraparticle pores. In some thin sections this cement has filled pores and displays polygonal sutures (Plate 4.6.B). Individual crystals have a minimum length to width ratio of 1:3 and display irregular intercrystalline boundries. In sections parallel to the C-axis they generally increase in width culminating in euhedral pointed terminations (Plate 4.6.C). Each crystal contains irregular inclusions a few microns in diameter, and faint subcrystals. Inclusions are most numerous along the bases of the isopachous crusts giving the cement a cloudy appearance. Individual crystals are compositionally zoned. In hole N806 at depth 310.7 m staining reveals a reddish core which passes gradationally to a reddish-purple outer zone. Under CL the zonal sequence is difficult to interpret because of the inclusions, but in hole N908 at 369.0 m and hole N982 at 406.7 m inclusions vary from dull to dark orange while crystals are brown-orange to dark brown with a brighter

orange rim (Plate 4.6.D). The pointed terminations and lack of alteration suggest that these cements consist of low magnesium calcite, but inclusions suggest a precursor.

2. Syntaxial overgrowth cements are euhedral and commonly poikilotopic, enclosing adjacent grains. (Plate 4.6.E). The overgrowths contain numerous irregular inclusions along the contact with the host grain, decreasing outwards (Plate 4.6.F). The inner parts of overgrowths stain red, indicating that they are non ferroan. Under CL syntaxial overgrowths display a concentric zonation which can be classified according to the scheme of Walkden & Berry (1984), as either "contouring" or "pinnacle" (Plate 4.6.G-H). The earliest zones are generally brown orange with light orange inclusions, and are followed by a thinner bright orange zone. The CL characteristics compare with those of the columnar cements described by Anderson (1990). In several examples, notably in hole N982 at depth 402.6 m the earliest overgrowth cement has been corroded, with holes filled by bright orange luminescent calcite (Plate 4.7.A). In three holes, N911, N992 and EP12 the syntaxial cements are non luminescent and carry bright orange rims (Plate 4.7.B).

3. Blocky calcite cement contains few inclusions and grew syntaxially on overgrowth and columnar cements to fill remaining pore space. The contacts between adjacent blocky crystals are planar and 180^0 enfacial junctions indicate that they are compromise boundaries. Staining reveals concentric growth zones varying from purple to blue through to reddish purple, with some faint sub zones. The blue and purple stains indicate ferroan crystals, (Plate 4.7.C). Under CL blocky cements are generally dull but may carry up to 15 zones ranging from bright orange to brown orange through to dark brown (Plate 4.7.D). The interfaces between these zones are either planar or gradational and some zones are arranged in couplets.

4. Replacive quartz overgrowths have formed on detrital quartz grains, on detrital grains contained in rock fragments and on grains which acted as nuclei for ooliths. In sections normal to the C-axis the overgrowths are euhedral and hexagonal, parallel to the C-axis they are elongate (Plate 4.7.E). The overgrowths contain inclusions which are most numerous along the contact with the host grain. In some cases these are so numerous as to give the overgrowth a ragged appearence. Overgrowths also occur on polycrystalline grains with component crystals acting as a host so that several overgrowths radiate from the substrate. The overgrowths extend outward, penetrating adjacent allochems and in hole N908 at depth 369.0 m poikilotopic overgrowths preserve the original grain structure. In some allochems the internal structure has controlled the shape of the overgrowth terminations with the radial concentric structure of ooliths forming arcuate

PLATE 4.6. Diagenetic features of the Grainstone Unit.

A. General view of the Upper Sandstone Marker showing black shale and burrowed intervals (B), note cross-bedding (C). Hole 1039 at depth interval 310.0 m to 319.0 m. Pencil for scale points to 'way up'

B. Photomicrograph (plane light) of polygonal suture in columnar pore fill cement. Hole N908 at depth 869.0 m. Scale bar = 250 microns.

C. Photomicrograph (plane light) of columnar cement crystals (arrow). Hole N975 at depth 384.5 m. Scale bar = 250 microns.

D. Photomicrograph (CL) of columnar crystals (arrow) lining the inside of an ostracod. Note irregular inclusions. Hole N314 at depth 267.2 m. Scale bar = 250 microns.

E. Photomicrograph (CL) of poikilotopic syntaxial calcite cement enclosing oolith (o). Hole N982 at depth 402.6 m. Scale bar = 500 microns.

F. Photomicrograph (plane light) of inclusion rich zones (c) within syntaxial calcite cement (c). Hole N982 at depth 402.6 m. Scale bar = 250 microns.

G. Photomicrograph (CL) of contour type syntaxial overgrowth. Hole N982 at depth 407.2 m. Scale bar = 250 microns.

H. Photomicrograph (CL) of 'pinnacle' type syntaxial calcite cement. Hole N982 at depth 407.5 m. Scale bar = 250 microns.

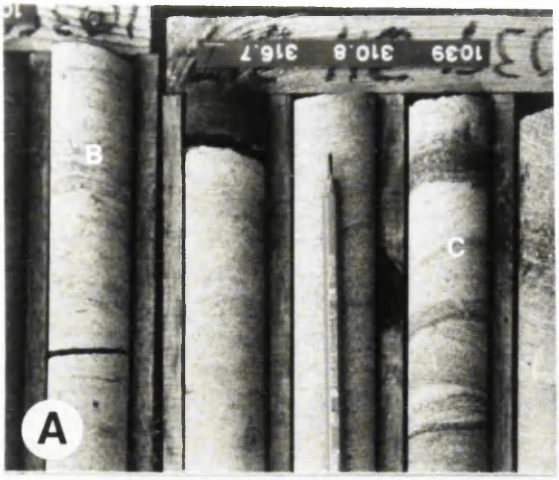
B
C
A

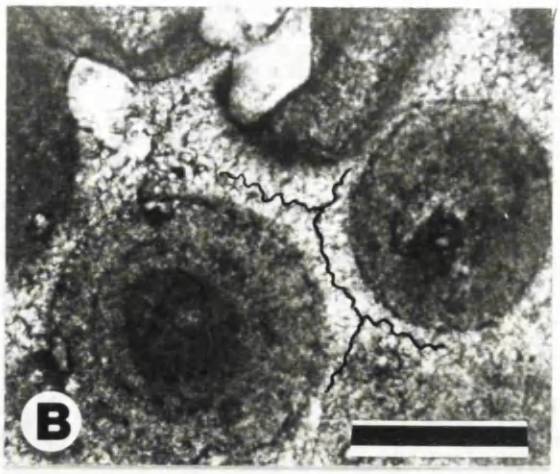
B

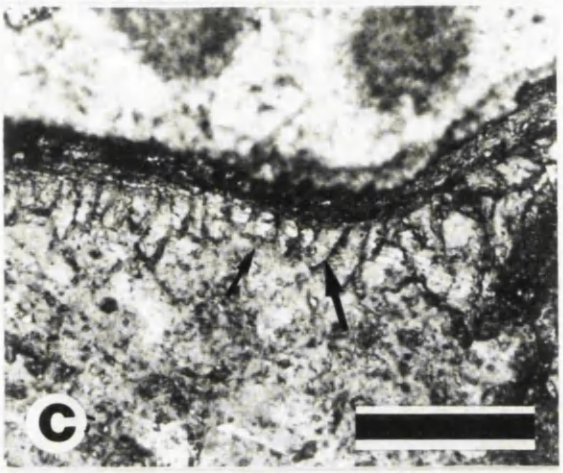
C

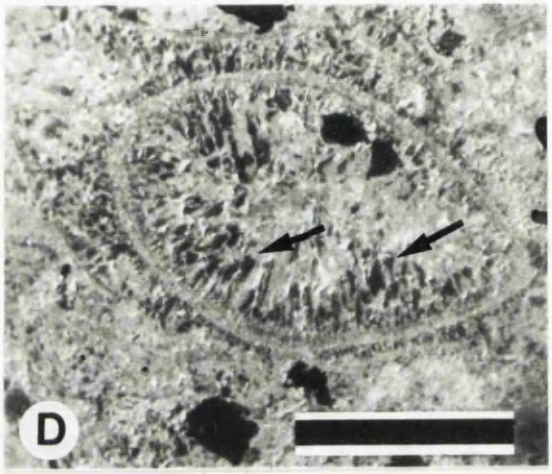
D

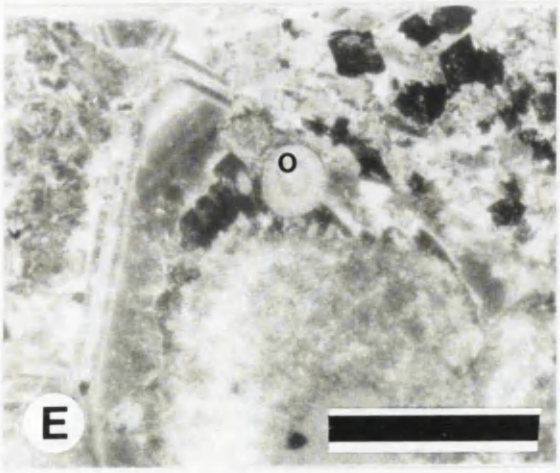
O
E

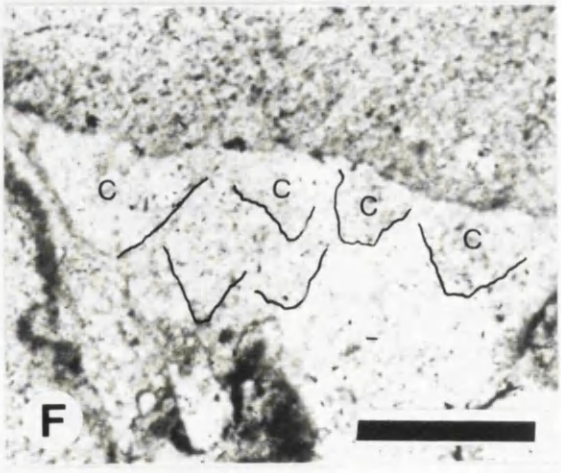
C
C
C
C
F

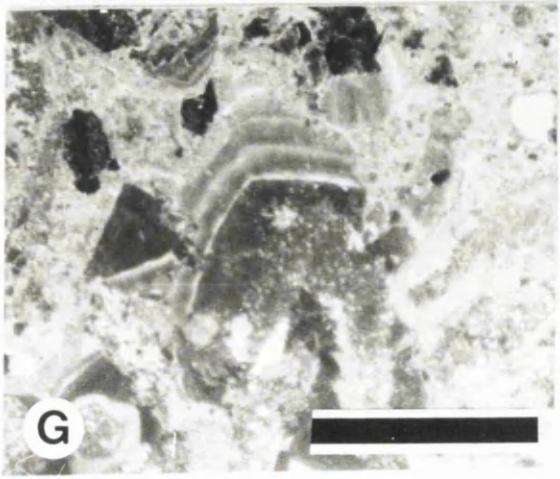
G

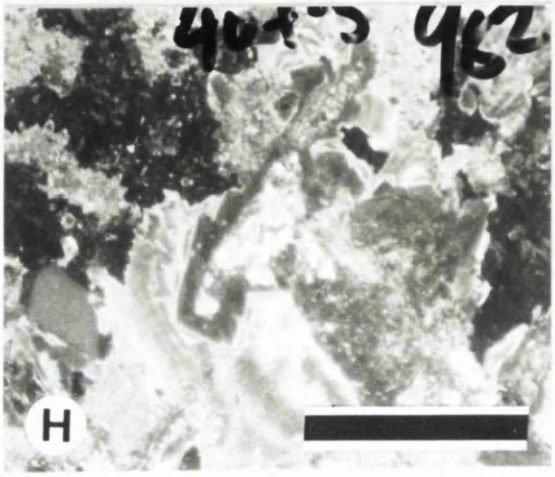
H

terminations to overgrowths. Chalcedony has replaced some grains, typically trilobites, brachiopods and adjacent cements. This usually takes the form of small radially fibrous spherules.

4.9.iii. Other features.

1. Features of Mechanical and chemical compaction;

i. Oolith cortices have spalled (Plate 4.7. F) and skeletal grains have fractured and rotated (Plate 4.7.G). Micritic envelopes have collapsed. In the Upper Sandstone Marker mica flakes have distorted and wrap around adjacent grains.

ii. Chemical compaction is represented by sutured seam stylolites which are either horizontal or vertical. The stylolites contain dark silty insoluble residue which most likely consists of clays and iron minerals (haematite, magnetite or pyrite ?) and a few quartz, feldspar and mica flakes.

iii. Contacts between some grains are sutured with some fitted fabric (Buxton & Sibley, 1981) (Plate 4.7.H). Some oolitic grainstones show interpenetration with individual grains separated by thin layers of microspar (Plate 4.8.A).

iv. Brittle fracture has occurred and has produced subvertical 'swarms' of fractures up to 1 cm wide. These generally cut across the fabric but locally refract around the interfaces of grains and cement.

2. Some skeletal grains have been bored by endolithic algae and the holes filled by micrite. Where borings have coalesced they form a laterally continuous micritic rim of irregular thickness. In hole EP12 at depth 489.5 m a few grains display laterally discontinuous micritic coatings.

3. A few ooliths (from hole EP12) contain irregular cavities penetrating cortices and truncated the internal structure.

4. Dissolution of skeletal aragonite (presumably) has taken place. This varies from partial to complete dissolution of the skeletal grains with the former grain represented only by a mold outlined by a micrite envelope. In one example (from hole EP12 at depth 489.5 m) a shell filled with internal sediment has dissolved to leave the internal sediment enclosed by shell shaped micritic envelopes.

5. Echinoderm grains contain small rhombic crystals which do not stain and which have a preferred orientation. Under CL these have dark crimson brown cores surounded by bright orange rims. They are believed to be dolomite (Plate 4.8.C).

6 In hole EP12 at depth 507.4 m the interfaces between blocky calcite crystals contain opaque interstitial material interpreted as organic.

7. Occasional finely disseminated pyrite crystals, a few microns in diameter, occur in the grainstones (Plate 4.8. D.).

8. Micrite cement forms rare discontinuous coats on some grains.

PLATE 4.7. Diagenetic features of the Grainstone Unit (continued).

A. Photomicrograph (CL) of syntaxial calcite containing internal dissolution zones (arrows). Hole N982 at depth 407.5 m. Scale bar = 250 microns.

B. Photomicrograph (CL) of non-luminescent syntaxial calcite cement. Hole EP12 at depth 504.7 m. Scale bar = 250 microns.

C. Photomicrograph (plane light) of stained blocky calcite cement displaying zones. Hole N982 at depth 402.6 m. Scale bar = 100 microns.

D. Photomicrograph (CL) of blocky calcite showing CL zones. Hole N982 at depth 402.6 m. Scale bar = 250 microns.

E. Photomicrograph (plane light) of authigenic quartz crystal note ghost of original grains (g). Scale bar = 500 microns.

F. Photomicrograph (plane light) of spalled oolith cortex (arrow). Hole N1022 at depth 522.9 m. Scale bar = 1 mm.

G. Photomicrograph (plane light) of fractured grain. Hole N1022 at depth 522.9 m. Scale bar = 1 mm.

H. Photomicrograph (plane light) of fitted fabric. Hole N1022 at depth 522.9 m. Scale bar = 1 mm.

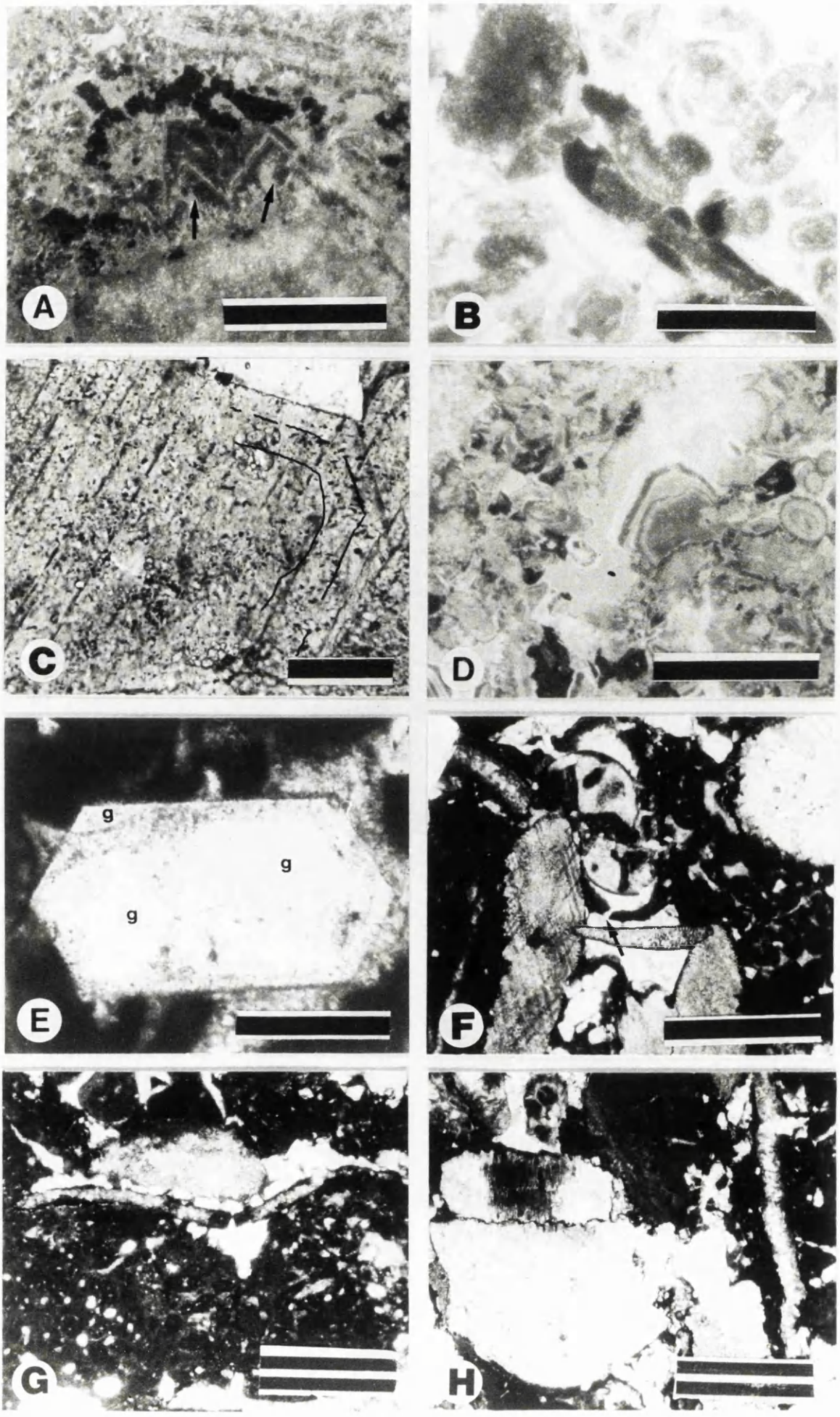
A
B
C
D
g
g
g
E
F
G
H

9. Nodular textures occur grainstones in the grainstones. Features include.
i. In hole N602 nodular textures extend over an interval of 3 m between 118.5 m and 115.5 m.and over 5 m between 123.0 m and 128.0 m. The nodularity is not continuous but forms layers with a vertical spacing of 20 cm to 1 m suggesting a control by bedding (Plate 4.8.E).
ii. Individual nodules are irregular with a maximum diameter of 15 cm in hole N1011.
iii. The nodules contain radial fibrous cement.
iv. In hole EP4A at depth 510.7 m the nodules consist of peloidal grainstone with a few skeletal grains and contain acicular and syntaxial cements. Peloids are uncompacted with no evidence of grain fracture or sutured contacts, and shelter porosity remained intact. However bioclasts have been truncated against stylolitic margins of nodules (Plate 4.8.G). Dissolution seams are generally parallel to the nodule margins and some penetrate nodules. The frequency of these seams increases towards the clast margin. These consist of an insoluble residue of clay minerals, iron minerals and a few silicate grains (Plate 4.8.F).
v.The margins of the nodules are stylolitic, they may be sharp, truncating both allochems and cement and display inter-penetration with adjacent siliciclastic grains, or they may be gradational consisting of pervasive micro-nodules surrounded by stylolites (Plate 4.8.G).
vi. The nodules have a 'fitted fabric' with nodular layers transitional with more continuous limestone beds (Plate 4.8.E).
vii. The nodules are surrounded by 'shaley' dissolution seams with layering distorted around the nodule (Plate 4.8.H). The shaley material contains spherical to elliptical micro-nodules up to 8 mm in diameter with stylolitic margins. The shaley material is rich in siliciclastic grains which are the same size and character as those in the nodules. Point counting along a series of ten traverses through nodules and adjacent matrix shows that approximately a third more clastic grains occur in the matrix.

4.10. DISTRIBUTION OF PETROGRAPHIC FEATURES.

4.10.i. Cements.

The early cements are substrate selective. Columnar cement is confined to oolitic and peloidal grainstones but rare in pelmatozoan grainstones. Syntaxial calcite is confined to the pelmatozoan grainstones and has nucleated upon echinoid grains and spines and crinoid ossicles. However, syntaxial calcite is absent where the surfaces of the grains have been altered by micritization, as in hole N982 at depth 402.6 m. Syntaxial cements occur in oolitic and shelly grainstones only where echinoiderm grains are present. Non-luminescent syntaxial calcite is rare occuring in only three thin sections from holes, N911, N992 and EP12. Over compacted grainstones indicate columnar and syntaxial

PLATE 4.8. Diagenetic features of the Grainstone Unit (continued).

A. Photomicrograph (plane light) of ooliths with concavo-convex contacts separated by relic calcite cement. Hole EP12 at depth 504.7 m. Scale bar = 1 mm.

B. Photomicrograph (plane light) of bioclast mould defined by micrite envelope. Hole N982 at depth 402.6 m. Scale bar = 1 mm.

C. Photomicrograph (plane light) of microdolomite inclusions (arrows) within echoinoderm grain. Hole N982 at depth 411. 7 m. Scale bar = 100 microns.

D. Photomicrograph (plane light) of pyrite crystals. Hole N763 at depth 440.3 m. Scale bar = 1 mm.

E. Nodular bedding in grainstones. The margins of nodules vary from sharp (s) to gradational (g).Scale in centimetres, arrow points to 'way up'.

F. Photomicrograph of dissolution seam (S) in nodule. Hole EP4A at depth 510.7 m Scale bar = 1 mm.

G. Photomicrograph of nodule margin, note truncation of allochem (arrow). Hole EP4A at depth at depth 510.7 m. Scale bar = 1mm.

H. Photomicrograph of inter nodule shaley material. Hole EP4A at depth 510.7 m.Scale bar = 1 mm.

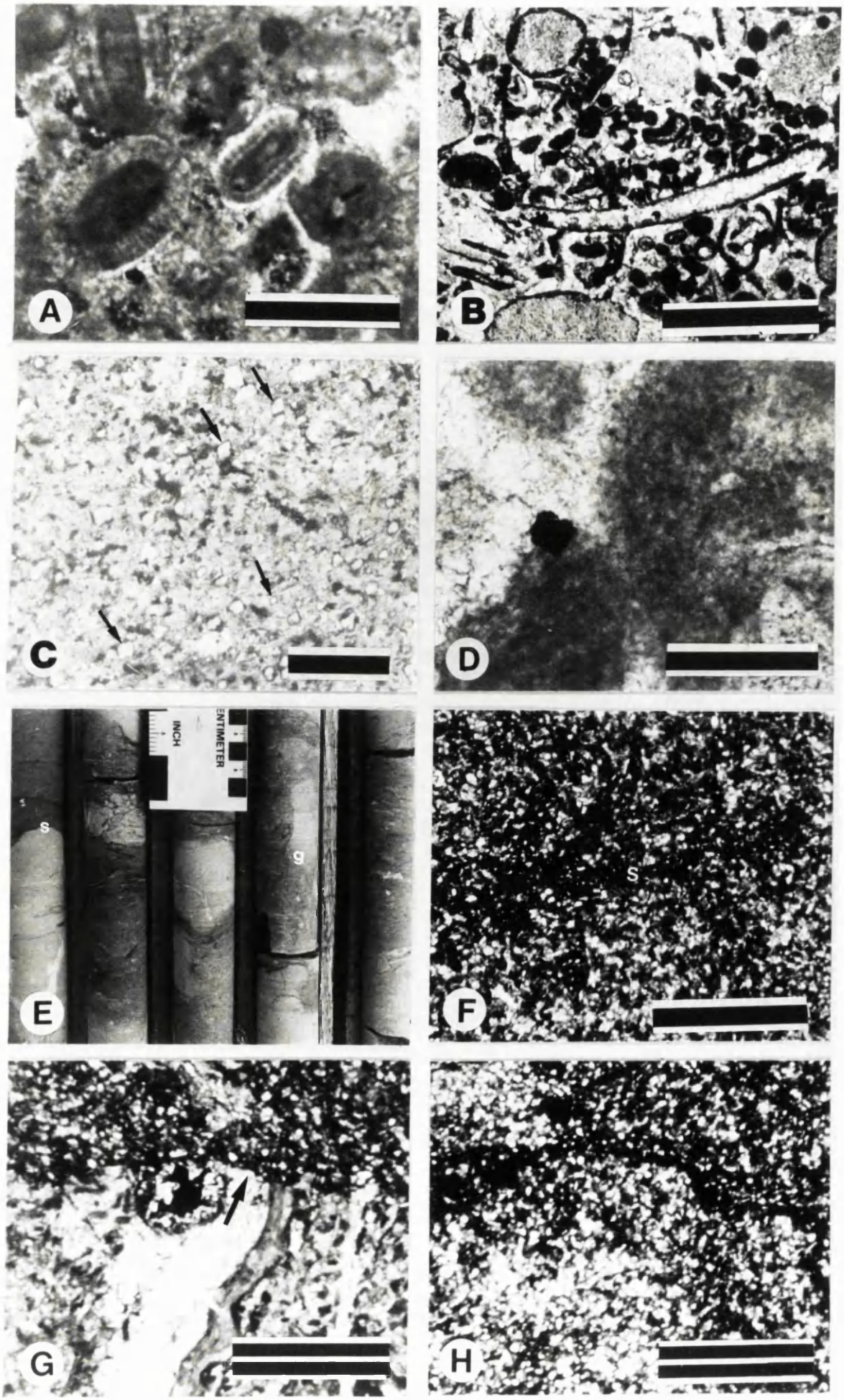
A
B
C
D
INCH
ENTIMETER
S
E
S
F
G
H

cementation was not pervasive. Syntaxial and columnar cements are absent from the Upper Sandstone Marker.

Blocky calcite is pervasive and is absent in only two thin sections where early columnar and syntaxial cements have occluded pores. Blocky cements from hole N982 at depths 407.5 m and 402.6 m contain a luminesent zonal sequence consisting of up to four dull-dark orange couplets followed by a brown orange zone, and a thin bright orange zone. Blocky calcite is present in the Upper Sandstone Marker. Authigenic quartz overgrowths occur in all thin sections containing detrial quartz including the Upper Sandstone Marker. Chalcedonic quartz is commonly associated with the quartz overgrowths.

4.10.ii. Other features.

Pyrite framboids are rare and are located around allochem surfaces. Dissolution of skeletal aragonite is confined to crinoidal grainstones, pelloidal and oolitic grainstones which contained some skeletal aragonite. Grains displaying early overgrowths and columnar cements have not been affected by grain fracture or grain interpenetration. However, three grainstones (from holes EP12 at depth 504.7 m, N982 at depth 407.5 m and N30 at depth 75 m) display grain inter-penetration which post-dates early cementation. Grainstones not containing early cements display the effects of chemical dissolution represented by grain interpenetration and fitted fabrics. Siliciclastic grain interpenetration is a common feature in the Upper Sandstone Marker. Stylolites are common through out the grainstones.

4.11. DIAGENETIC MODEL.

The Navan grainstones are dominated by either columnar cement, syntaxial cement or over compaction. All grainstones include some grain micritization and share the same later diagenetic overprint of blocky calcite cement, authigenic quartz overgrowths, stylolites and brittle fracture. It is unneccessary, therefore, to describe the petrogenesis of individual thin sections. A single diagenetic model for the grainstones together with an interpretation is presented below. The petrogenesis of the Upper Sandstone and Muddy Siliclastic markers are beyond the brief of this project.

The earliest event within the grainstones was the micritization of some ooliths and bioclasts. Pyrite framboids around the surfaces of some of these grains apparently pre date cementation. The earliest cements were columnar and syntaxial and were substrate selective. Micrite cement formed discontinuous coatings on some bioclasts. All cements reduced primary porosity. Columnar calcite formed isopachous crusts which lined pores

in oolitic and peloidal grainstones, locally filling them. Syntaxial cements developed within crinoidal grainstones but failed to nucleate on those pelmatozoan grains whose surface were altered by micritization.

Columnar and syntaxial cements display the same dark CL zones and probably nucleated at the same time, with the morphology of the cement controlled by the character of the substrate. However, Longman (1980) pointed out that syntaxial calcite cement is among the fastest growing early cements. Some support for this is seen in the grainstones where late stage syntaxial cements 'engulf' columnar cements. Deposition of columnar and syntaxial cements was followed by dissolution of skeletal aragonite and the production of molds, enhancing porosity (Fig 23.A).

Compaction followed but did not affect grainstones containing early cements. Grainstones lacking such cements were profoundly affected by grain fratutre, collapse of micritic envelopes and grain penetration with the formation of fitted fabrics. The effect of grain penetration was to further decrease porosity and produce a stable framework of interlocking particles. The relative timing of grain fracture and grain interpenetration is difficult to elucidate. However, Scholle & Halley (1984) suggest that these processes operate congruently during the early stages of burial.

Blocky calcite cement grew syntaxially upon columnar and syntaxial cements and poikilotopically enloses adjacent grains. It filled moldic pores which had remained open. This cement contains fragments of collapsed micrite envelopes, coats fractures within grains and surrounds interpenetrated grains. It thus postdates the formation of all of these features. Authigenic quartz overgrowths nucleated upon detrital quartz grains.This quartz extends outwards beyond the margins of allochems and truncates zones within columnar, syntaxial and late blocky calcites, indicating that it post dates all of them.

Sutured seam stylolites cut across the petrographic fabric truncating both cements and allochems, and indicating that chemical compaction continued during the later stages of the diagenetic cycle. Finally, subvertical fracturing post dated all previous events and fractures are filled with blocky calcite. The paragenesis is summarised in Fig. 4.23.B.

4.11.i. Interpretation.

The pre-compaction diagenetic features include:

1.Micritization.

2. Nucleation and growth of columnar and syntaxial calcite cements

3. Dissolution of skeletal aragonite.

Micritization is common in shallow marine environments but most prevalent in the stagnant marine phreatic zone (Longman, 1980; Bathurst 1964). Borings are produced by endolithic algae which chemically dissolve $CaCO_3$. It is uncertain if the micrite filling the

borings is a sediment or a cement with precipitation induced by the photosynthetic activity of the algae (review by Tucker, 1990).

Columnar cements are believed to reflect active shallow marine phreatic cementation where porewaters are constantly replenished (Kendall, 1985; and review articles by Moore 1989: Harwood, 1989; Tucker & Bathurst, 1990). In this zone, cementation is believed to begin in intraskeletal pores within bioclasts (Longman 1980). It is likely that the earliest stages of the diagenetic cycle in the Navan grainstones took place in shallow marine conditions. Comparable cements occur within other ancient limestones where they are also believed to represent shallow marine phreatic cementation (Purser, 1969; Gawthorpe & Gutteridge 1990).

Syntaxial overgrowths developed upon echinoderm grains but are absent where grain surfaces were modified by micritization. Echinoderm grains can be considered as single crystals of calcite. Cements nucleate on these 'crystals' growing parallel to their C-axes (Evamy & Shearman, 1965). This explains why syntaxial cements are absent on grains with modified surfaces. The origin of the dully luminescent syntaxial cements is problematical. However the CL character of these cements compares with that displayed by columnar cements, suggesting precipitation from pore fluids composed of sea water. Growth of syntaxial calcite cement is believed to have been accompanied by the conversion of the host grain from high magnesium to low magnesium calcite by a process of incongruent dissolution in which the Mg^{2+} is exported in the complex $MgCO_3$ while calcium is added to the available sites, preserving structutral detail. However, microdolomite inclusions present within echinoderm grains indicate that some magnesium was used to form dolomite (Leutloff & Meyers, 1984).

Occasional non-luminescent syntaxial cements present in holes N911, N992 and EP12 are believed to reflect meteoric phreatic cementation (Walkden, 1987, Emery & Dickson, 1989; review by Meyers, 1991), supporting the view that the grainstones had undergone subaerial erosion. The relative timing of the non-luminescent and dully luminescent cement is not known.

Columnar and syntaxial cements both contain inclusion rich zones. Inclusions in these types of cement have been interpreted as representing a precursor cement (Kendall & Tucker, 1973; Meyers & Lohmann, 1978). The nature of the inclusions provides a clue to the nature of the precursor. Microdolomite inclusions in syntaxial overgrowths are believed to represent a high magnesium calcite precursor. It is likely that the inclusion rich zones in the Navan cements represent a precursor but the general lack of microdolmites suggests it may not have been high magnesium calcite.

Deposition of early cements was followed by dissolution of skeletal aragonite and the production of moulds outlined by micritic evelopes. Dissolution of skeletal aragonite

is common in meteoric environments (Longman 1980; James & Choquette 1984; Walkden, 1987) again pointing to circulation of meteoric pore waters.

Within grainstones lacking early cement, compaction most likely began shortly after sediment accumulation, with rotation of some elongate grains parallel to bedding. Experimental data using uncemented equidimensional spherical grains has shown that an original depositional porosity of 40 to 60% can be reduced to a minimum threshold of 35% by mechanical reorganisation of grains at this stage. However Scholle & Halley (1984) suggested that in a natural uncemented grainstone pre cement porosity reduction by mechanical reorganisation is probably lower than 35% since allochems consist of different grain sizes and shapes, allowing closer packing (but ignoring the influence of inter-granular pores).

It is generally believed that as overburden pressure increases stress becomes concentrated at grain contacts. The results are represented at Navan by grain fracture, collapse of micrite envelopes and spalling of oolith cortices, resulting in further reduction in porosity. Fracture surfaces do not display columnar cements suggesting that fractures post dated these cements. Some chemical compaction occurred at this time, producing grain penetration and the development of a fitted fabric (Buxton & Sibley, 1981). In several oolitic grainstones grain penetration is present but the dissolution seams are separated by relic (columnar ?) cement, indicating that dissolution and grain penetration were not exclusive to uncemented grainstones, and suggesting that early cementation (perhaps underdeveloped) was not able to prevent some grain penetration. Similar relationships have been observed in the Upper Mississippian St. Genevieve Limestone of Tennesse (Scholle & Halley, 1984).

At this stage in the Navan diagenetic cycle grainstones had been micritized and received columnar and syntaxial cements. Stabilization of high magnesium calcite and dissolution of skeletal aragonite had taken place. Evidence for compaction is provided by grain fracture and grain interpenetration. These features have been overprinted by a common later paragenetic sequence. Post compaction diagenetic features include;

I. .Deposition of late blocky calcite cement.

2. Formation of authigenic quartz crystals.

4. Formation of sutured seam stylolites.

5. Brittle fracture.

The late blocky calcite cement post dates collapsed micrite envelopes, surrounds interpenetrated grains and fills moldic pores which had remained open until this time. It is interpreted as reflecting burial cementation. This view is supported by the generally blocky texture, the ferroan composition and the dull characteristics (Meyers, 1991). Authigenic quartz overgrowths are also believed to reflect burial.

Compaction was now adsorbed by a rigid framework of cemented grainstones. Instead of chemical dissolution taking place at point contacts between grains it worked along sutured seam stylolites which truncate both allochems and diagenetic fabrics. Thin sections were examined for relic interparticle, intraskeletal and moldic porosity. All pores are now filled with several generations of calcite cement. However, such tightly cemented limestones are believed to contain microscopic intercrystal porosity between columar, syntaxial and spar cement crystals (Wiggins & Harris, 1984). It is likely that such porosity is present in the Navan grainstones but is not greater than 5% .

The stylolitic character of the nodule margins within the grainstones suggests that they are a result of pressure dissolution (Appendix 2). Nodularity resulting from pressure dissolution has been disscussed by Bathurst (1984). Initiation requires a rigid body occuring within unconsolidated sediment. This situation occurs in modern carbonate environments where early seafloor cementation produces discontinuous 'hardgrounds' (Dravis, 1979). Following application of lithostatic load compaction occurs around the rigid body and is confined to the unconsolidated sediment. As the load increases pressure dissolution begins to take place and the insoluble residue accummulates as a 'shaley' matrix. The margins of the nodules consist of swarms of stylolites. This effect has been described by Jenkyns (1974) from the pelagic Ammonitico Rosso. The shale domains within nodular limestone can also be sedimentary in origin as exemplified by nodular Ordovician-Silurian shelf limestones of Norway (Moller, 1988).

In both cases clay minerals are important since they they form fluid retention sites. The fluid layers are only a few molecules thick (Weyl, 1959) but are believed to act both as solvent and conduit for the migration of calcium and carbonates ions away from the area of pressure dissolution (Weyl, 1959; Bathurst, 1984; Scholle & Halley, 1984; Moller , 1988).

The Navan nodules do not contain compacted grains and pores are filled by early columnar cement. The shaley matrix displays;

1. Silicate grains of the same diameter and character as those within the nodules.
2. The shales contain numerous sutured seam stylolites which have truncated small nodules and bioclasts. By contrast, stylolites in the nodules are confined to the margins and contain stylocumulate comparable to the shaley matrix.
3. Layering within the shaley matrix is compacted and draped around nodules.
4. Few signs of compaction occur within the nodules and pressure dissolution is confined to the nodule margins. Points 1 to 4 indicate that the shaley material compacted relative to the nodules and suggest that the latter were rigid.

4.12. SEDIMENTOLOGICAL AND PETEROGRAPHIC SYNTHESIS OF THE GRAINSTONE UNIT.

After deposition of the Micrite Unit a gentle solutional palaetopography was formed dominated by a valley 2 km wide and over 6 km long with a floor modified by karst. A relative rise in sea level flooded this channel and may initially have been confined to its channel floor. Deposits represented by a thin veneer of sandstones, shales and siltstones are confined to the channel and reflect a relatively low energy (tidal ?) environment. As sea level continued to rise, skeletal grainstones were deposited along the channel and probably migrated landwards as low sand waves swept by strong tidal currents.

The Lower Dark Marker is believed to reflect deposition within a clastic influenced low energy environment which extended along the channel. A return to higher hydraulic energies followed, with the deposition of grainstones which filled the channel and blanketed the surrounding palaeotopography. The southern Honduras shelf provides a modern analogoue. A gentle palaeotopography cut into Pleistocene limestones with up to 60 m relief is dominated by several large channels (Purdy 1974). The distribution of modern sediments during the Holocene sea level rise was influenced by this palaeotopography. Terrigenous material and lime sand were deposited along the channel floors with reefs forming on the highs. An ancient analogoue is provided by the Ordovician of the northern Appalachians where sediment distribution was controlled by palaeotopography (Knight *et al* , 1991).

At Navan the filling of the channel marked the extension of open marine conditions across the entire study area. Deposition was dominated by cross-bedded grainstones interpreted as representing open marine sand shoals. The mobile seaward portions of these passed shorewards into low energy areas characterised by extensive burrowing. Lithoclasts within the grainstones suggest that the sand shoals were bordered along their shoreward margins by muddy lagoons and intertidal deposits resembling those of the Micrite Unit below. The sand shoals were dissected by shallow tidal channels, filled by the granular sands of the microconglomerate, supplied from both adjacent shallow marine and lagoonal zones. Graded beds within grainstones suggest some storm deposition. Toward the closing stages of the Grainstone Unit, an influx of siliciclacstic sand occured, which produced the Upper Sandstone Marker, interpreted as representing a shallow marine sand shoal. Such influx of siliclastic sand perhaps reflects upliftb of the adjacent hinterland at this time. Low energy conditions extended across the study area on four significant occasions. These are represented by the Sub Nodular, Nodular, Sub Dark and Upper Dark Markers and are believed to reflect lagoonal conditions.

The surfaces of some grainstones, notably those directly below the Nodular Marker and between the Nodular and Upper Dark Marker, have been modified by palaeokarst

forming bowl and funnel shaped pits. These indicate that the grainstone, like the surfaces of the cycles in the Micrite Unit below, underwent subaerial exposure. Non-luminescent overgrowths and the dissolution of skeletal aragonite point to circulation of meteoric pore fluids and support the view that grainstones underwent subaerial erosion, but no vadose features have been recognised. The bulk of the grainstones contain columnar cements interpreted as reflecting shallow marine cementation. Some are overcompacted, indicating the distribution of these columnar cements was not pervasive and thus that some grainstones failed to undergoe shallow marine cementation. The columnar and syntaxial cements and features of grain compaction have been over printed by blocky ferroan calcite, by stylolitization and by the development of brittle fracture.

Thus, the main features of the Upper Pale Beds are:

1. A stenohaline, to normal marine salinity, bioclast assemblage.
2. Thick blankets of grainstones which contain thin shaley beds.
3. Cross-bedding, nodular bedding and extensive burrowing within the grainstones and channels.

These features are believed to be diagnostic of a middle shelf environment (Wilson & Jordan, 1983).

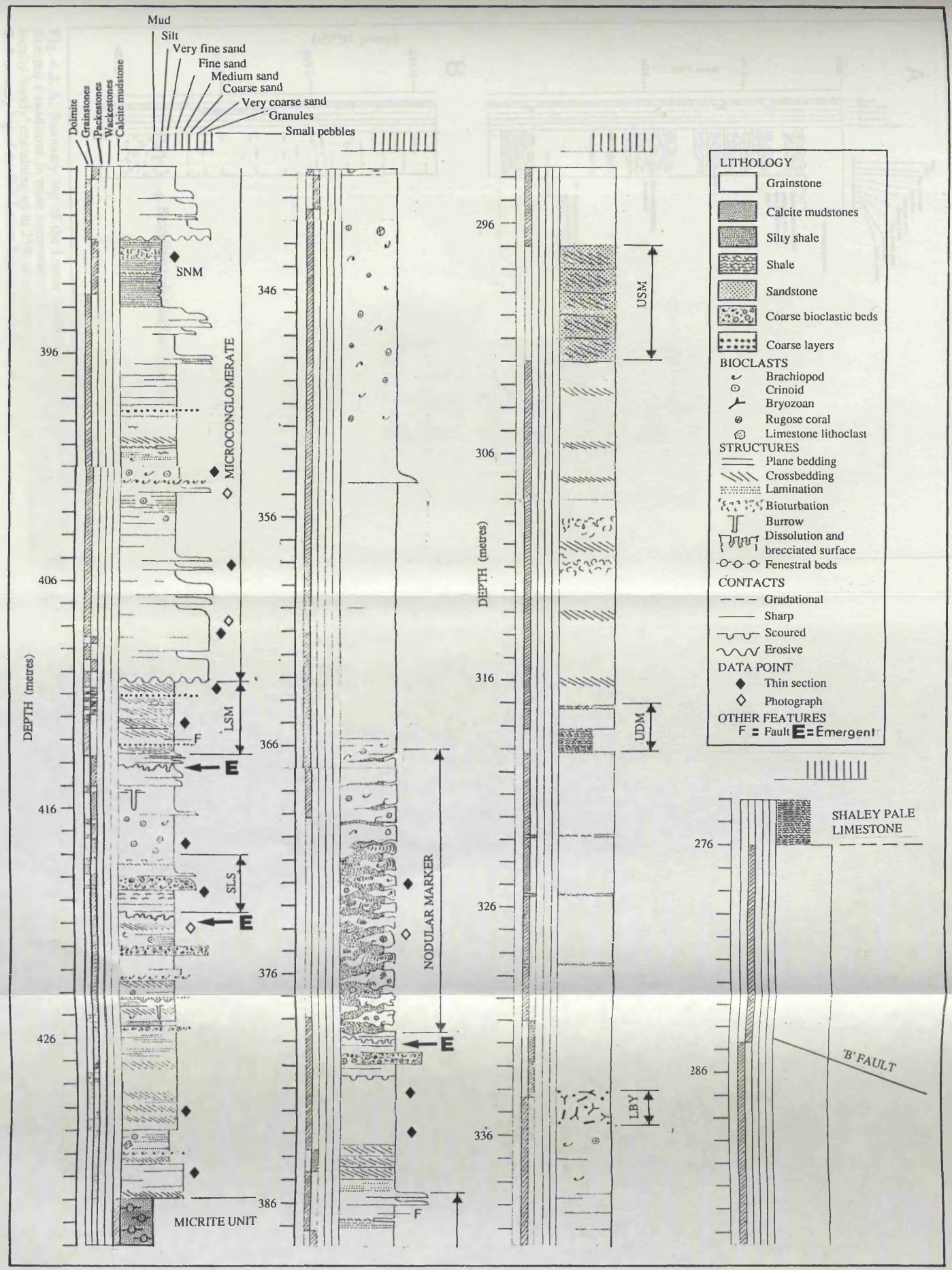

Fig. 4.1. Summary log of the Grainstone Unit, western mine area, hole N975. **SLS** = Sub Lower Sandstone Marker, **LSM** = Lower Sandstone Marker, **LBY** = Lower Bryozoan Marker, **UDM** = Upper Dark Marker, **USM** = Upper Sandstone Marker. Note extensive dolomitization of the grainstone sequence.

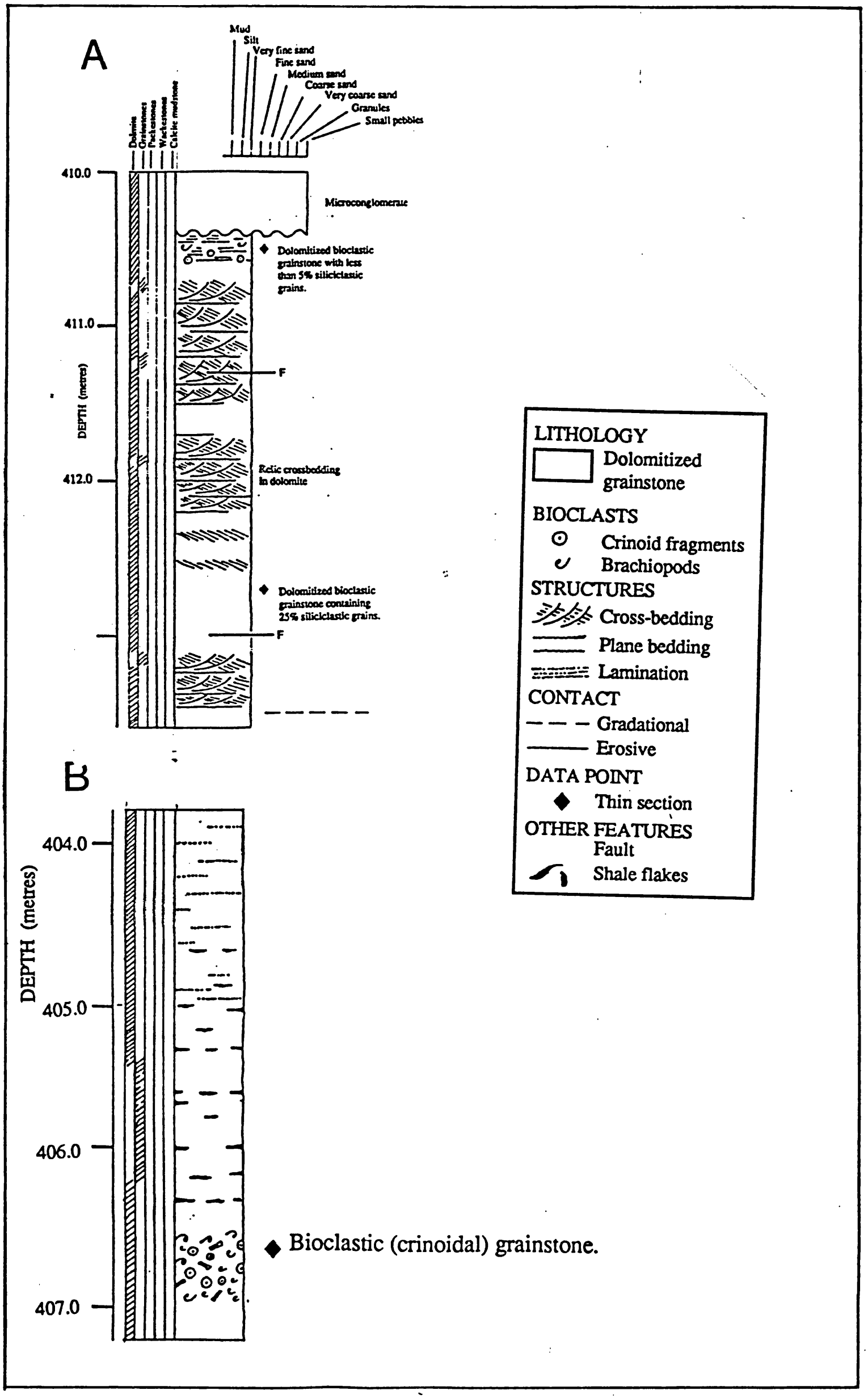

Fig. 4.2. A. Summary log of the Lower Sandstone Marker, Hole N975. Although denoted a sandstone in mine nomenclature it is in fact an oolitic grainstone which is locally 'sandy' containing up to 25% siliciclastic grains. Note extensive cross-bedding. **B.** Summary log of the Sub Lower Sandstone Marker, hole N982.

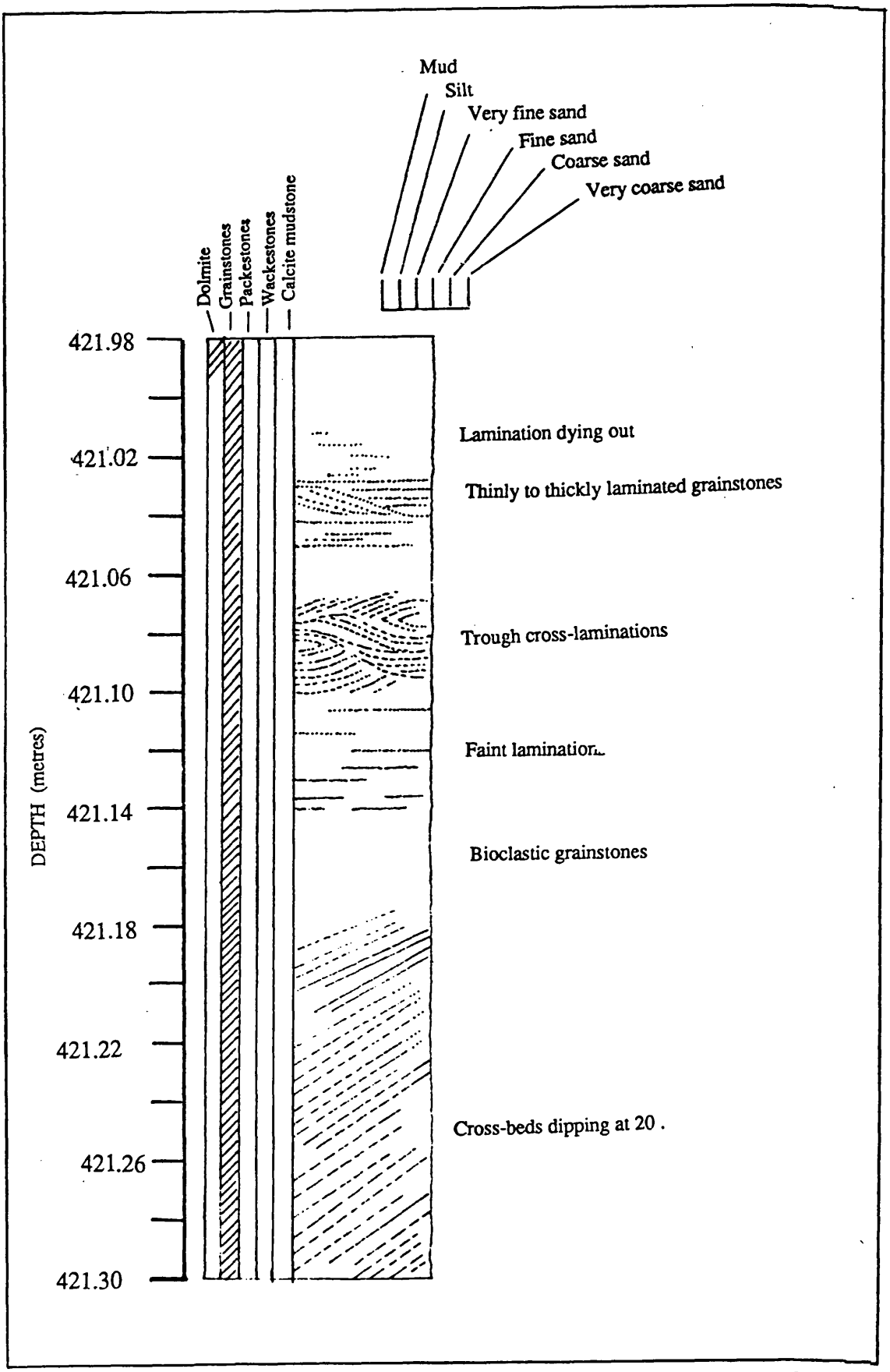

Fig. 4.3. Log showing cross-bedded grainstones passing vertically up to planar and cross-laminated grainstones. Hole N975.

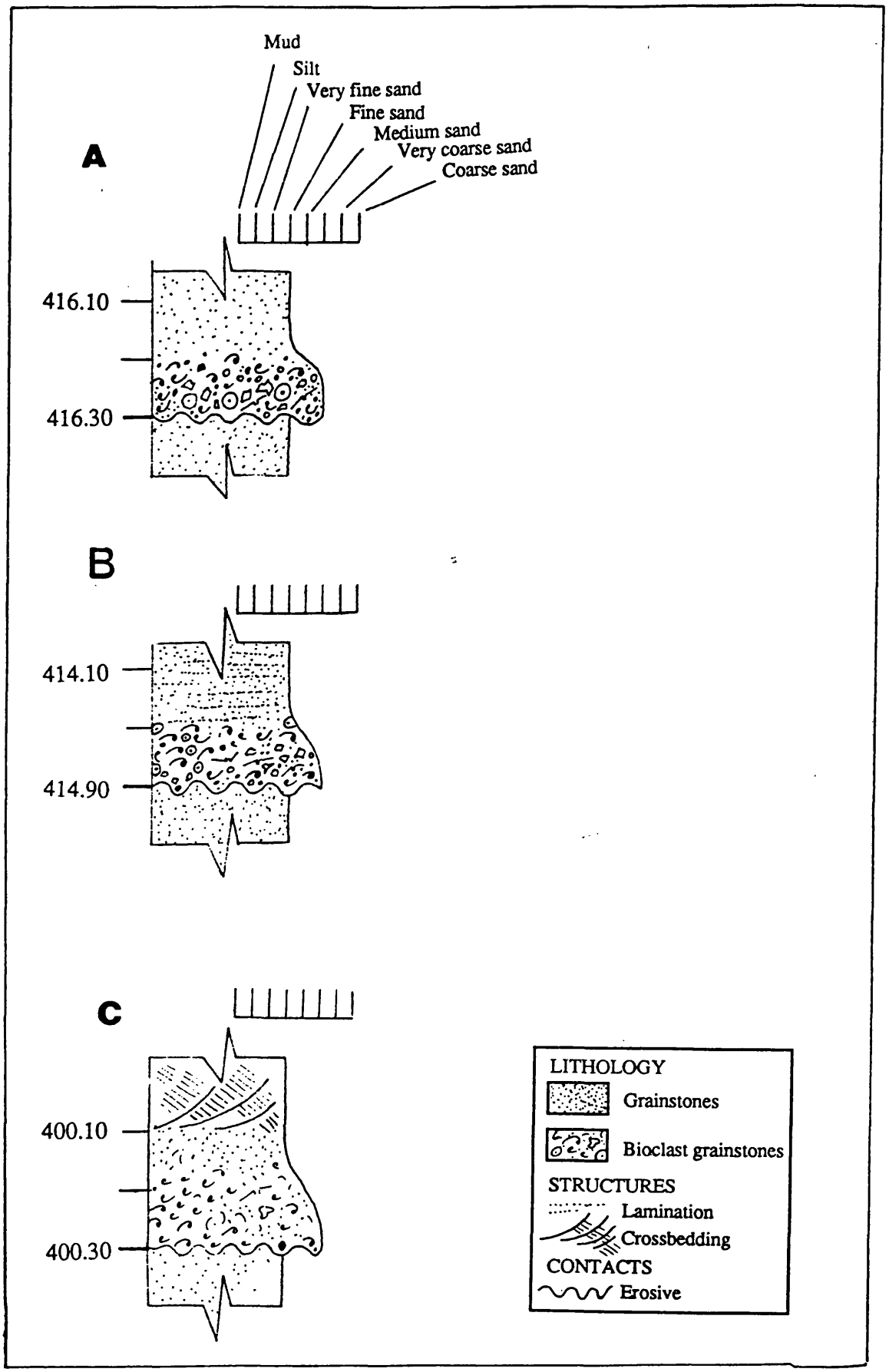

Fig. 4.4. Diagram illustrating various internal structures of graded beds within the grainstones. **'A'** Coarse bioclastic grainstone passing vertically to uniform sand grade grainstone, Hole N975. **'B'** Coarse bioclastic grainsone passing vertically into laminated sand grade grainstone Hole N975. **'C'** Coarse bioclastic grainstone passing vertically into cross-bedded sand grade grainstone, Hole N982.

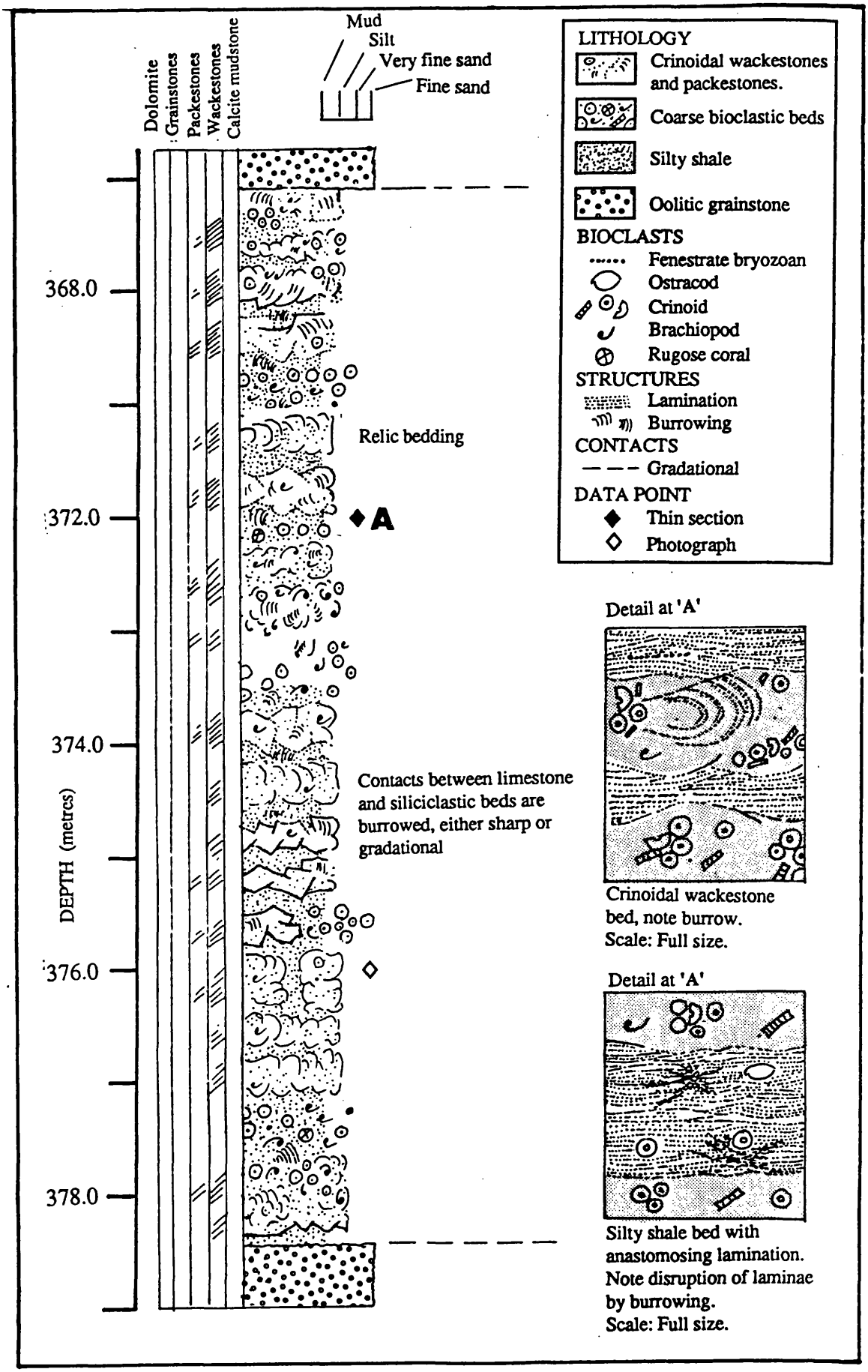

Fig. 4.5. Summary log of the Nodular Marker. The marker consists of crinoidal wackestones and packstones which contain muddy siliciclastic beds. These lithologies have been extensively burrowed to produce a chaotic fabric which contains irregular lenses of crinoid grains. Contacts between lithologies are either sharp, gradational or burrowed. Some relic layering also occurs.

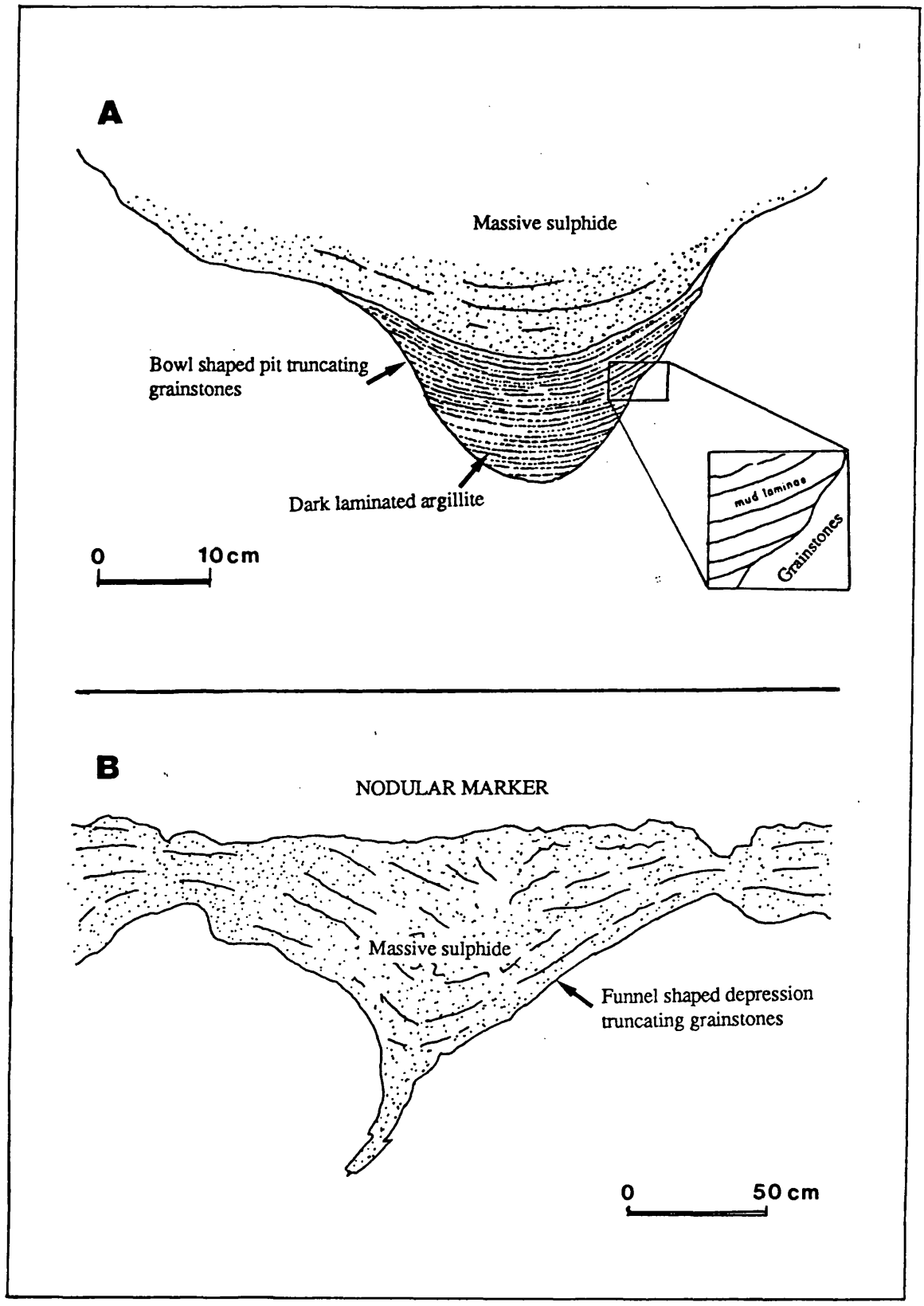

Fig. 5.6. 'A' Depression within grainstones, this has a bowl shaped profile and has been partially filled with thinly laminated muddy siliciclastics and selectively mineralized. Location 2-1 Lens 222W stope. 'B' Depression within grainstones displaying funnel shaped profile, below the Nodular Marker, modifed from Anderson (1990).

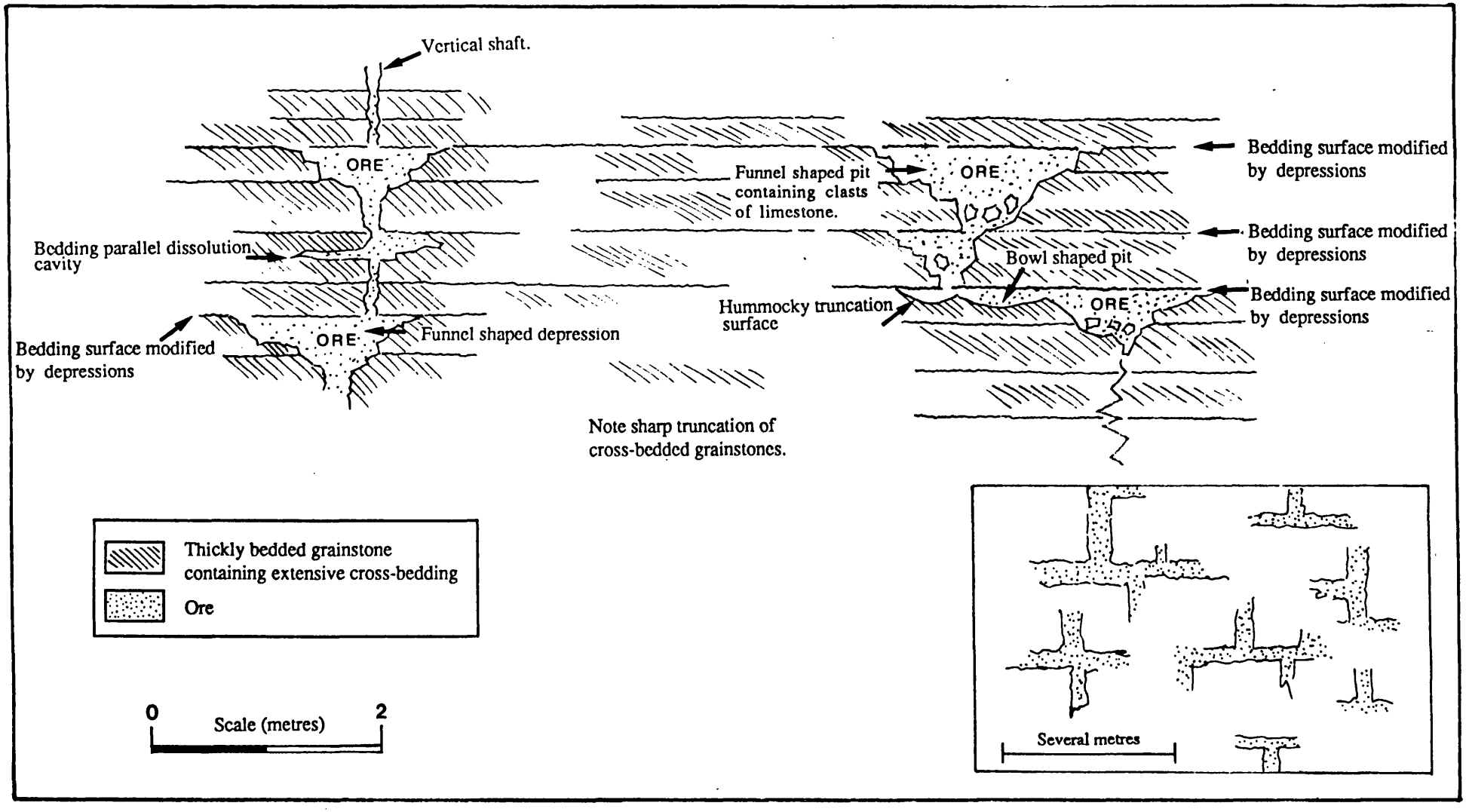

Fig. 4.7. Cross-bedded grainstones with surfaces modified by laterally linked bowl and funnel shaped depressions. The depressions are connected by subvertical shafts forming a cavity system that has been selectively mineralized. 1285 mine level Waste Storage Bay 2 Zone 3 Lens, 585 Stope. Inset rectilinier pattern of mineralization in the roof of storage bay.

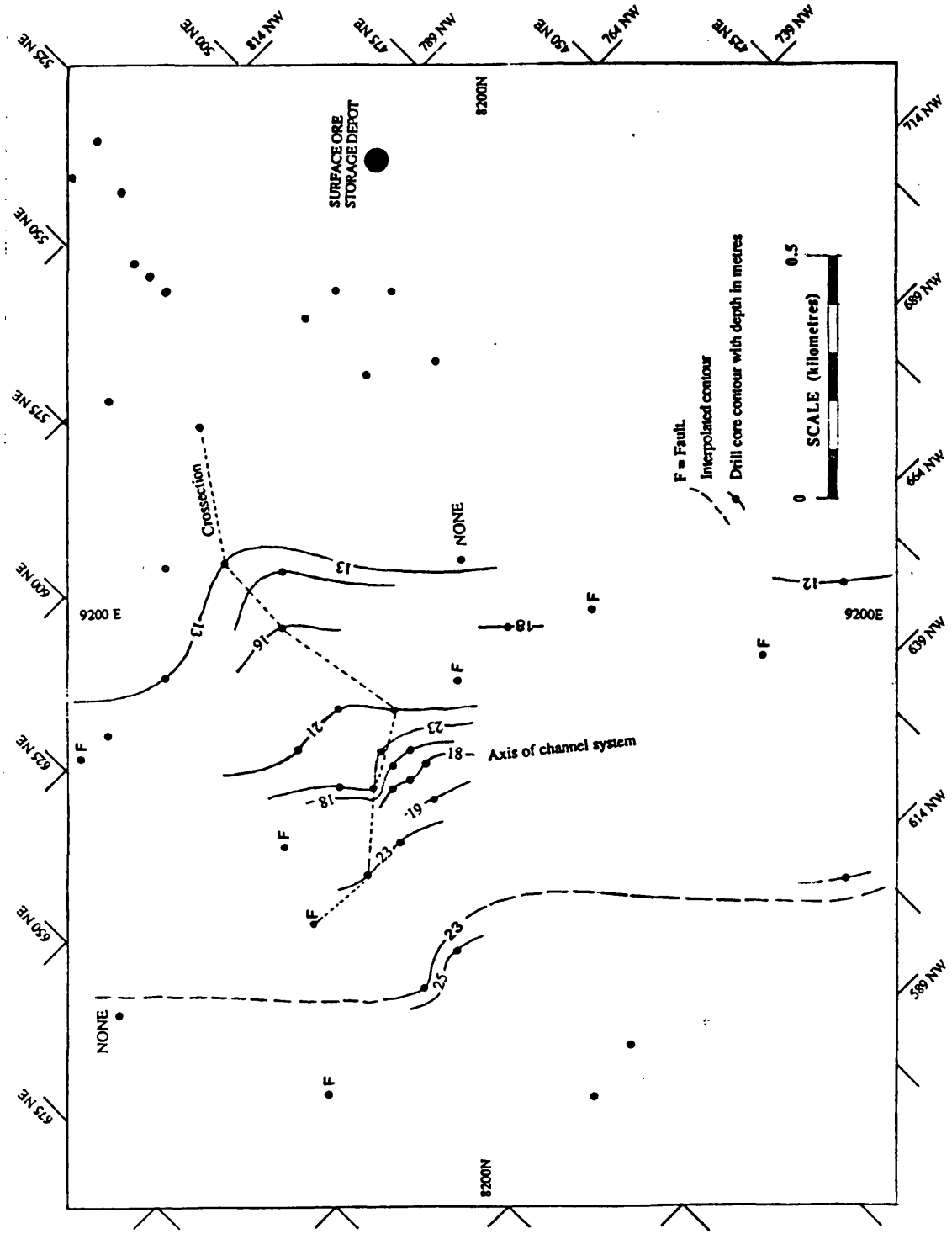

Fig. 4.8. Isopach map showing thickness and distribution of the channel interval in the western mine area.

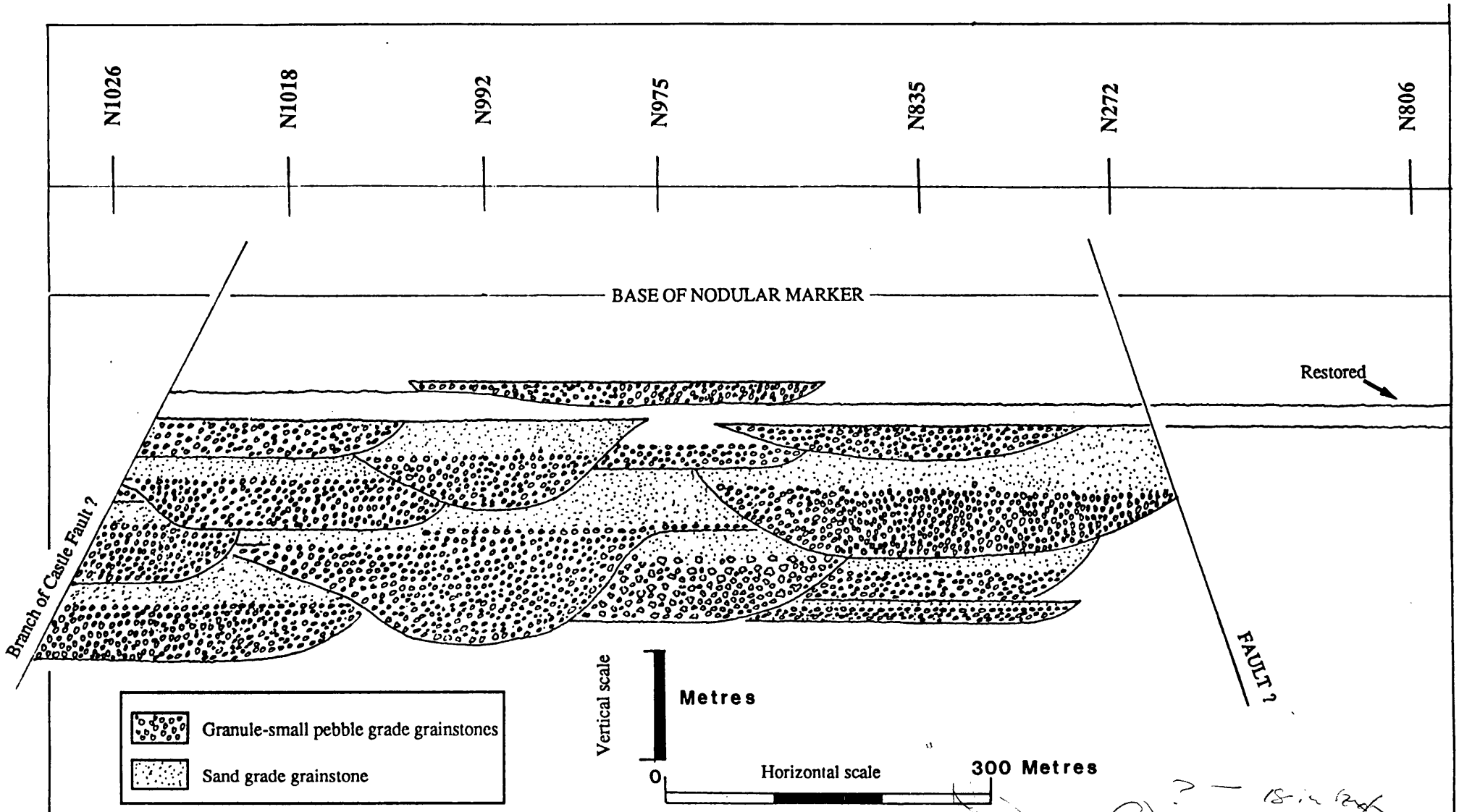

Fig. 4.9. Cross-section through the channel interval. At least 13 channels are pressent. Channels are symmetrical and appear to become shallower vertically upwards. Note erosive relationship between younger and older channels. For location of cross-section refer Fig. 4.8.

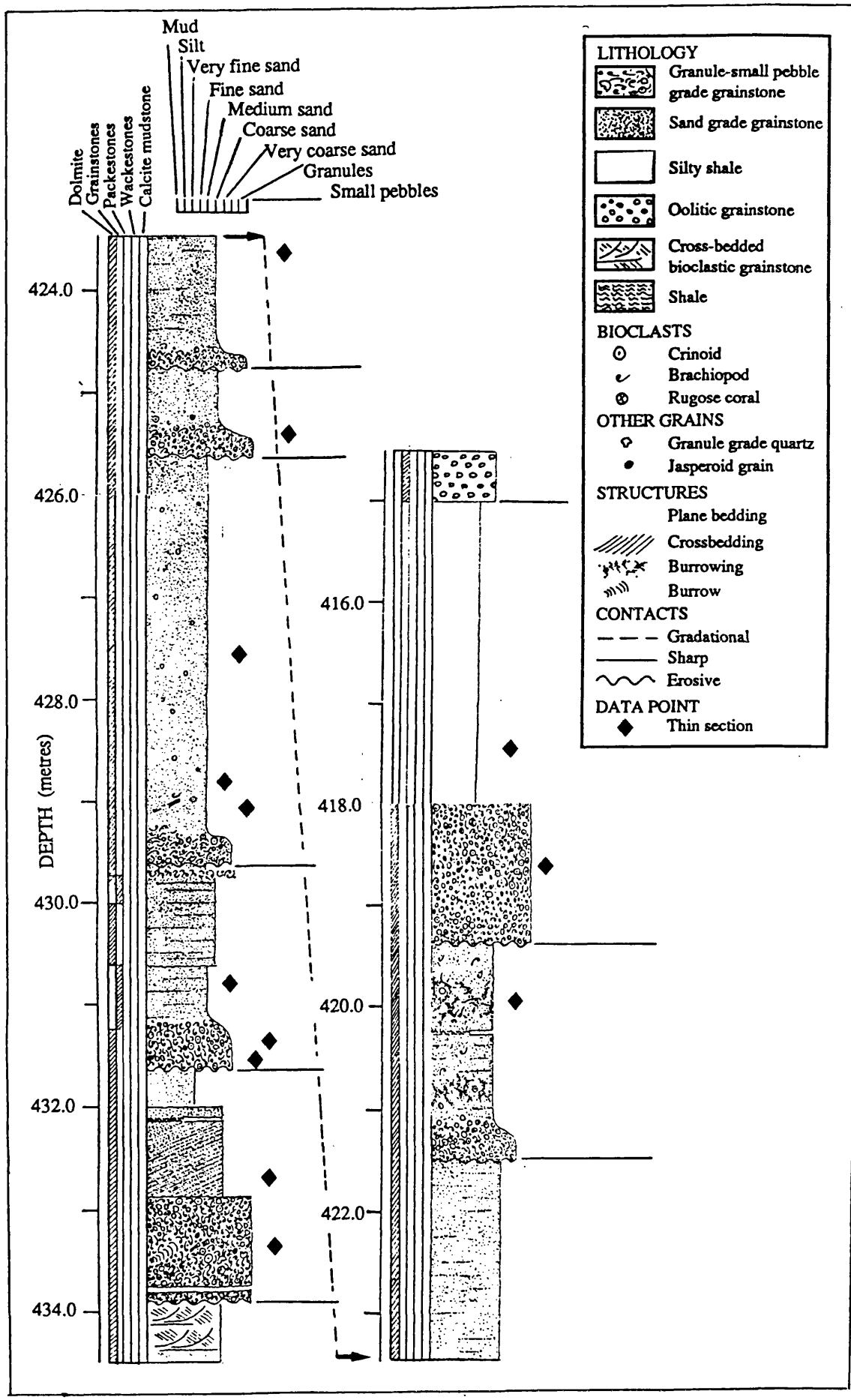

Fig. 4.10. Summary log the microconglomerate. The sequence is characterised by multiple fining upwards units. Note extensive dolomitization of this sequence Hole N990.

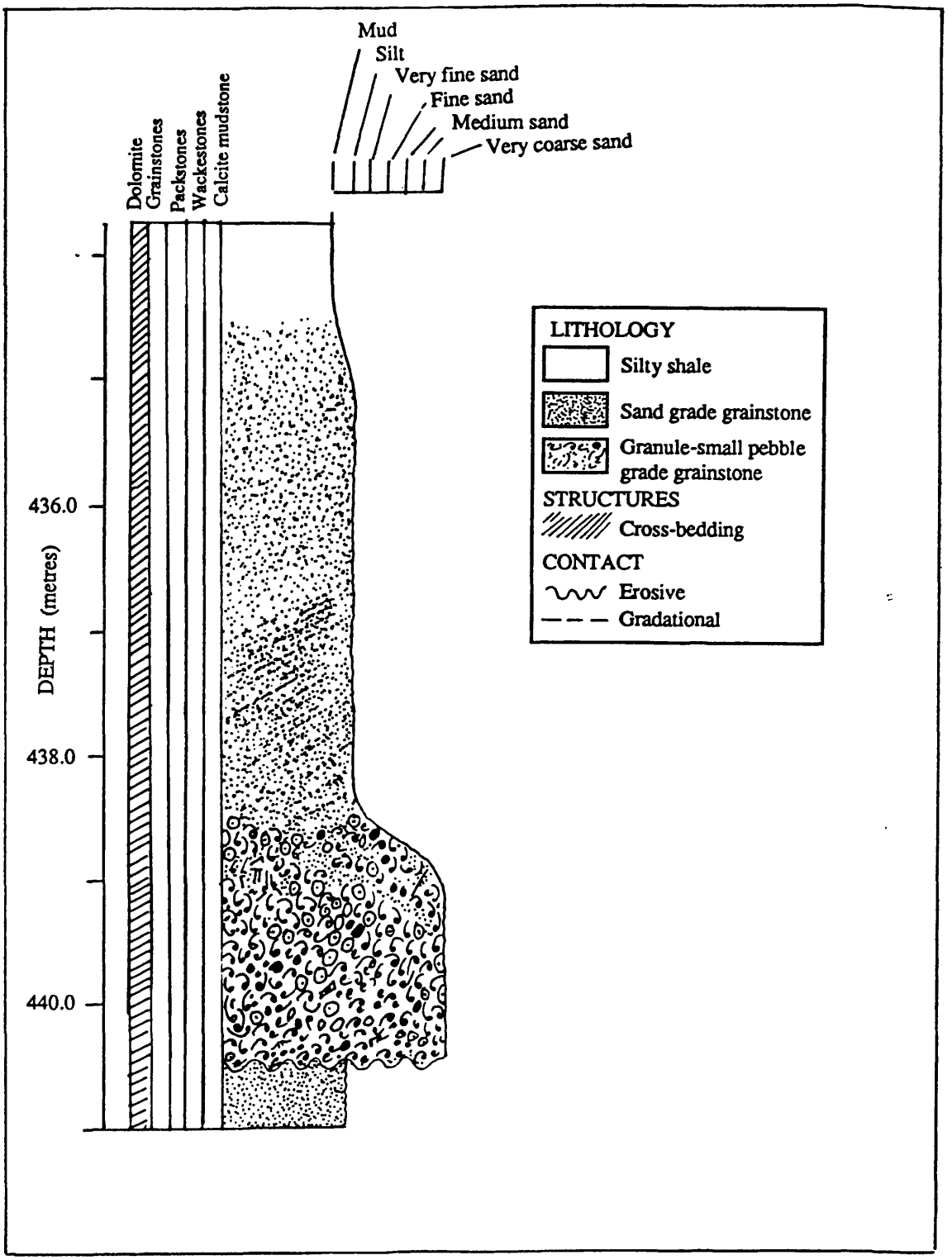

Fig. 4.11. Detailed log of fining upwards unit illustrating well developed cross-bedding, hole N991.

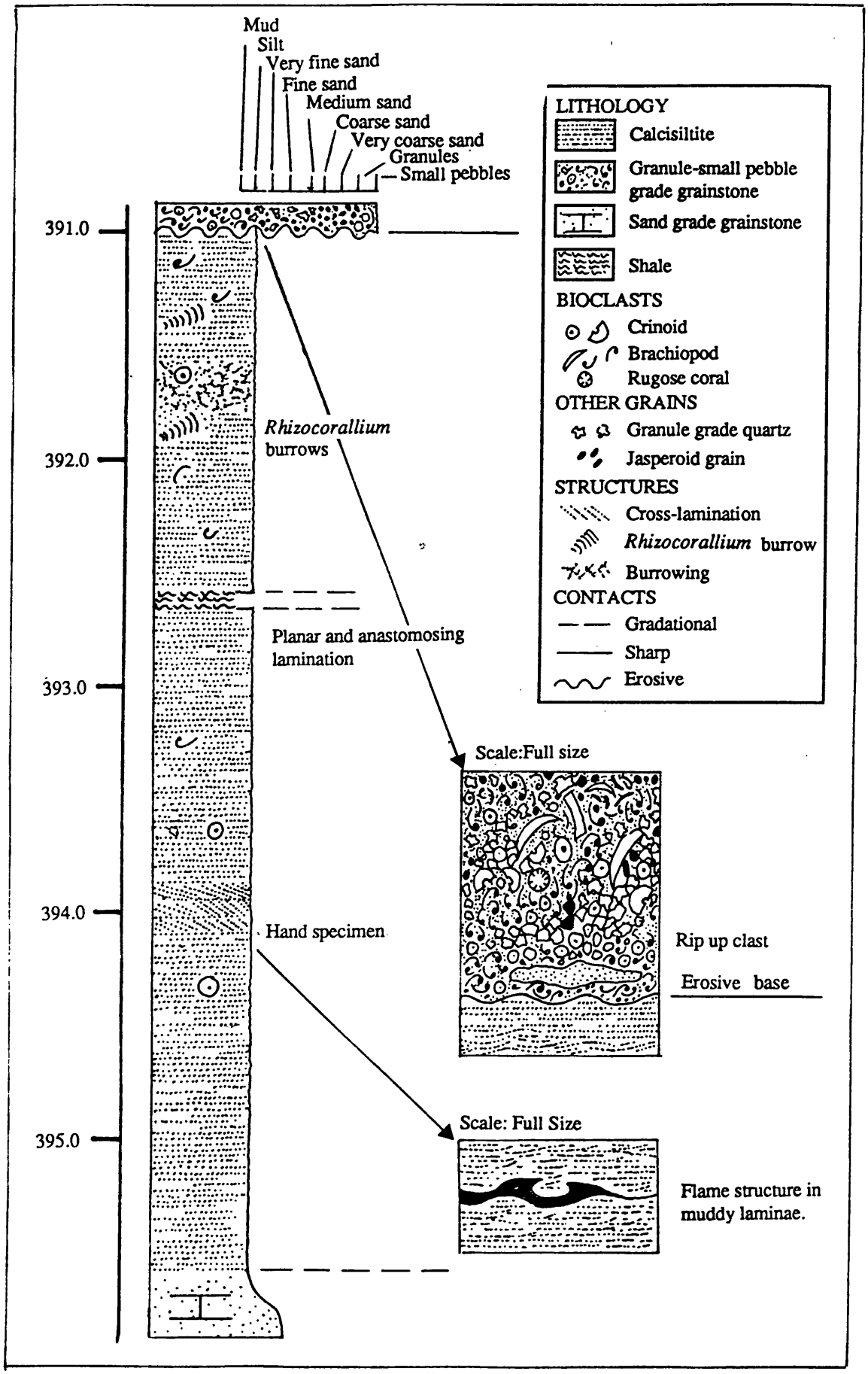

Fig. 4.12. Summary log of the Sub-Nodular Marker horizon. The markers display extensive anastomosing and planar lamination, cross-lamination is also locally developed. Hole N975.

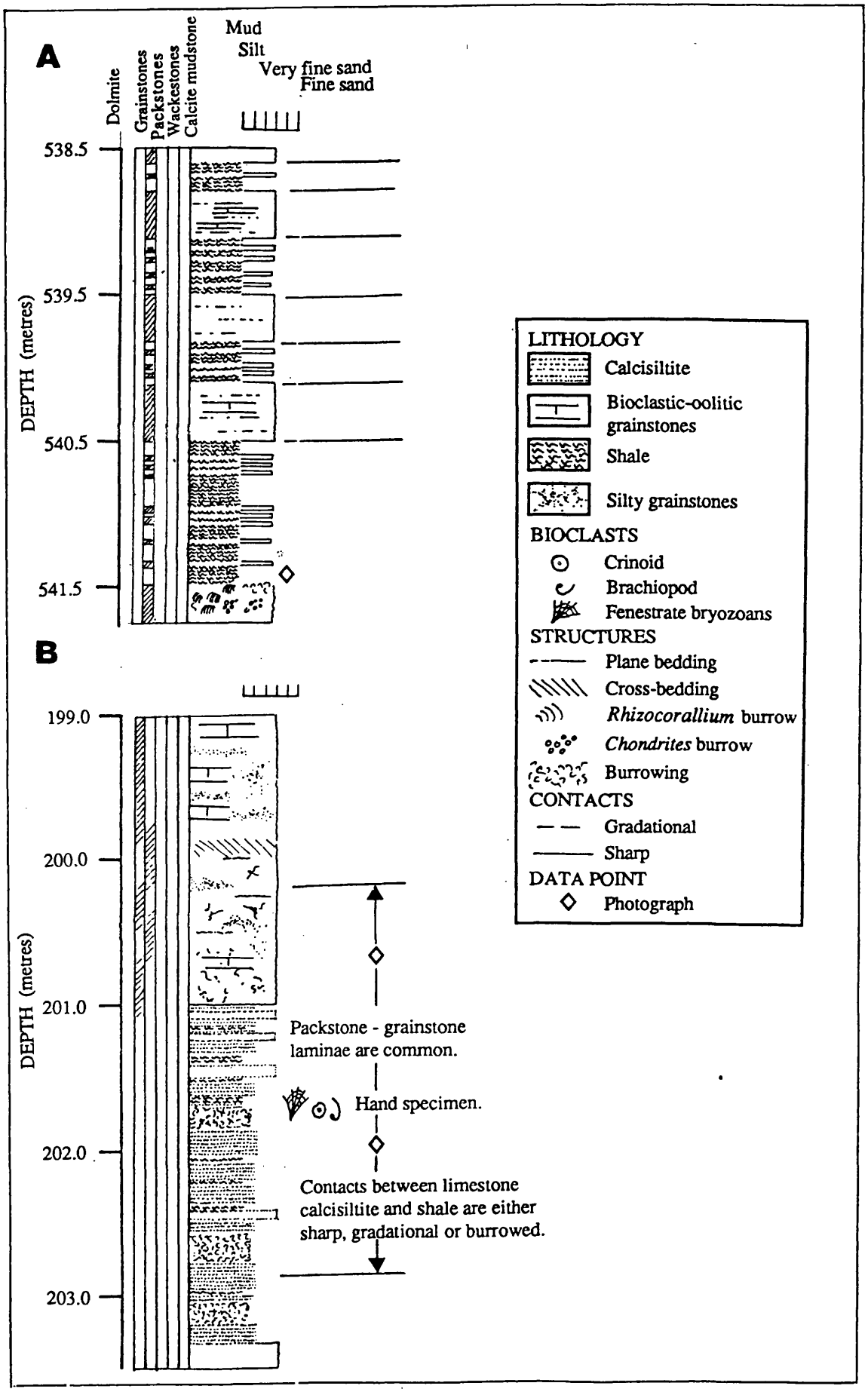

Fig. 4.13. Summary log of muddy siliciclastic marker horoizons. **'A'** The Upper Dark Marker in Hole N1033, note thin interlaminations of shales and limestones and burrowed surfaces.**'B'** The Lower Dark Marker. The lower half consists of interlaminated calcisiltite, shale and packstone-wackestones. This is overlain by silty grainstones.

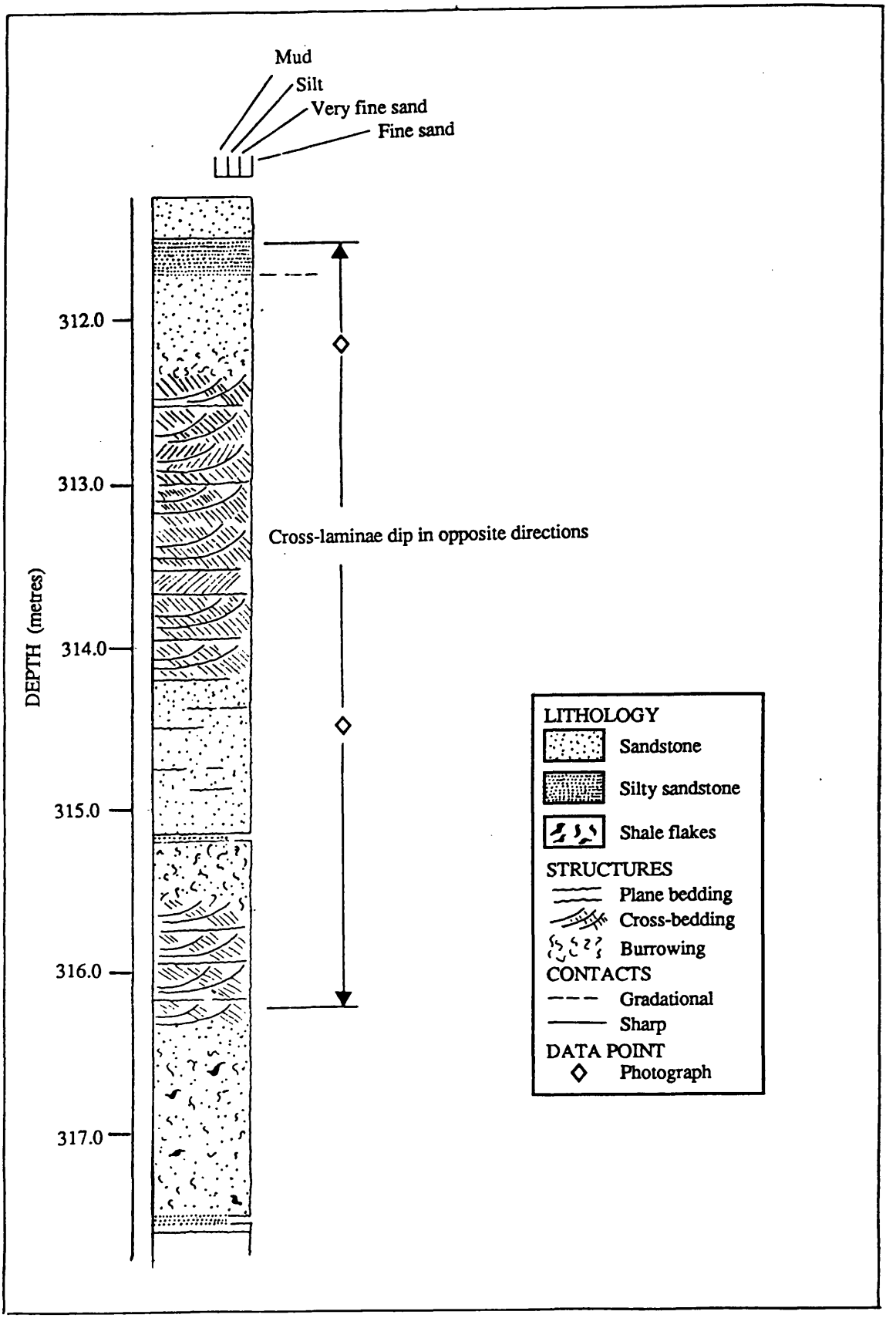

Fig. 4.14. Summary log of the Upper Sandstone Marker. The sandstone contains plane bedded, cross-bedded and burrowed intervals. Hole N1039.

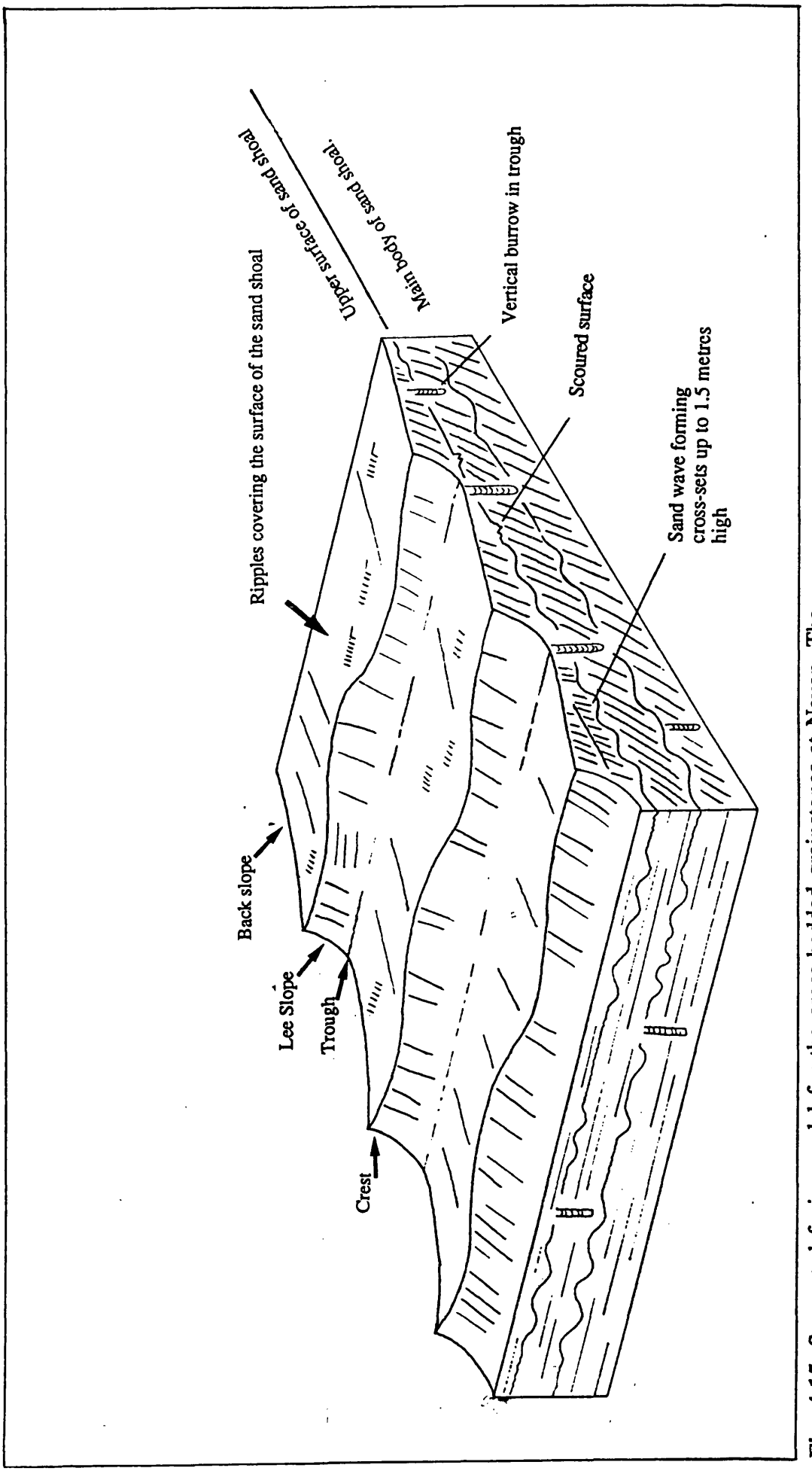

Fig. 4.15. Suggested facies model for the cross-bedded grainstones at Navan. The upper surface of the sand shoal is covered by sand waves which in turn are covered by ripples. Burrowing takes place within the troughs between the sand waves.

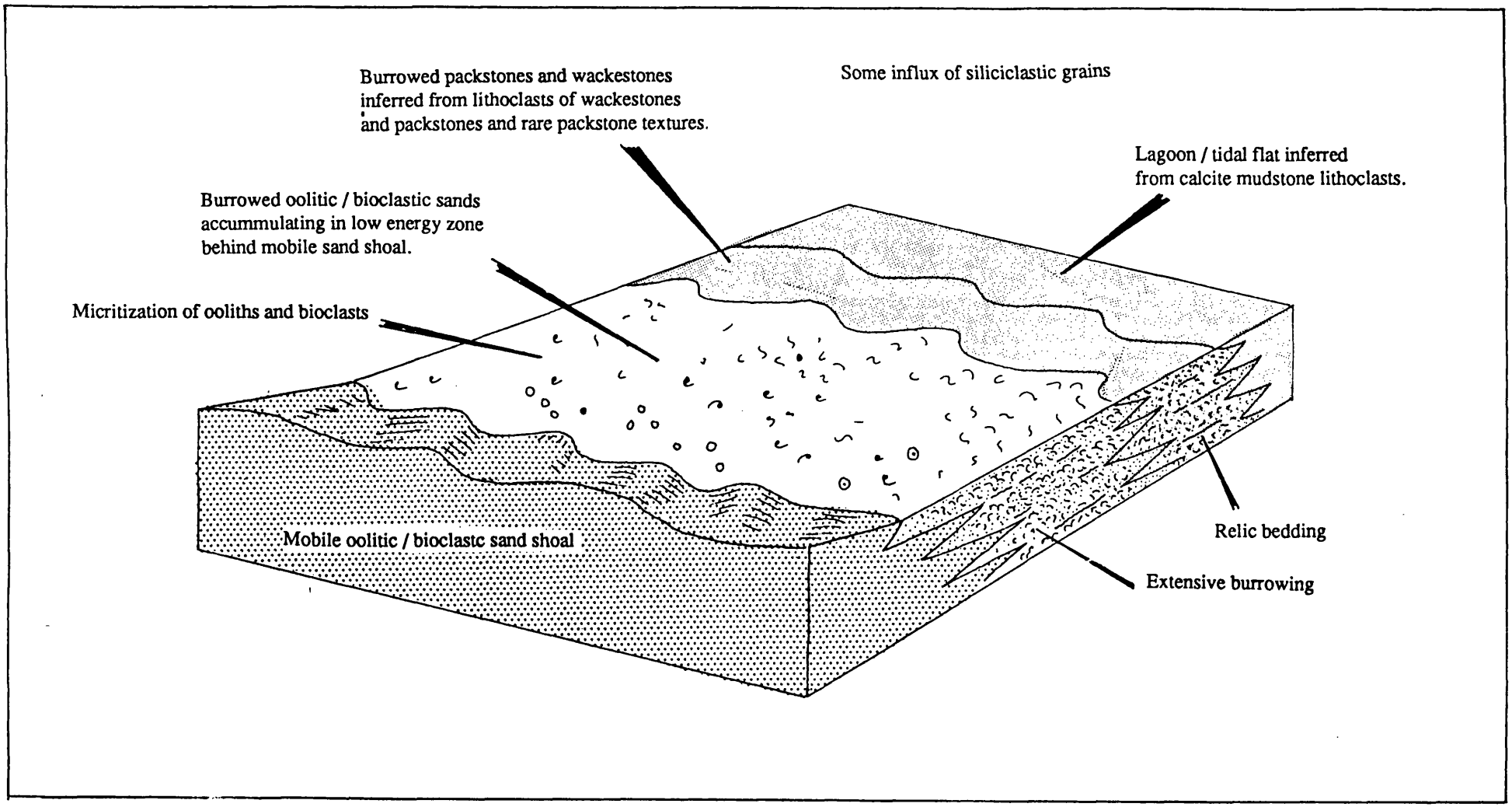

Fig. 4.16. Suggested facies model to explain the occurrence of high energy cross-bedded grainstones and low energy burrowed grainstones. An active sand shoal shallows and thus produces an area of low energy along its shoreward margin. In this zone of low energy the sands become extensively burrowed.

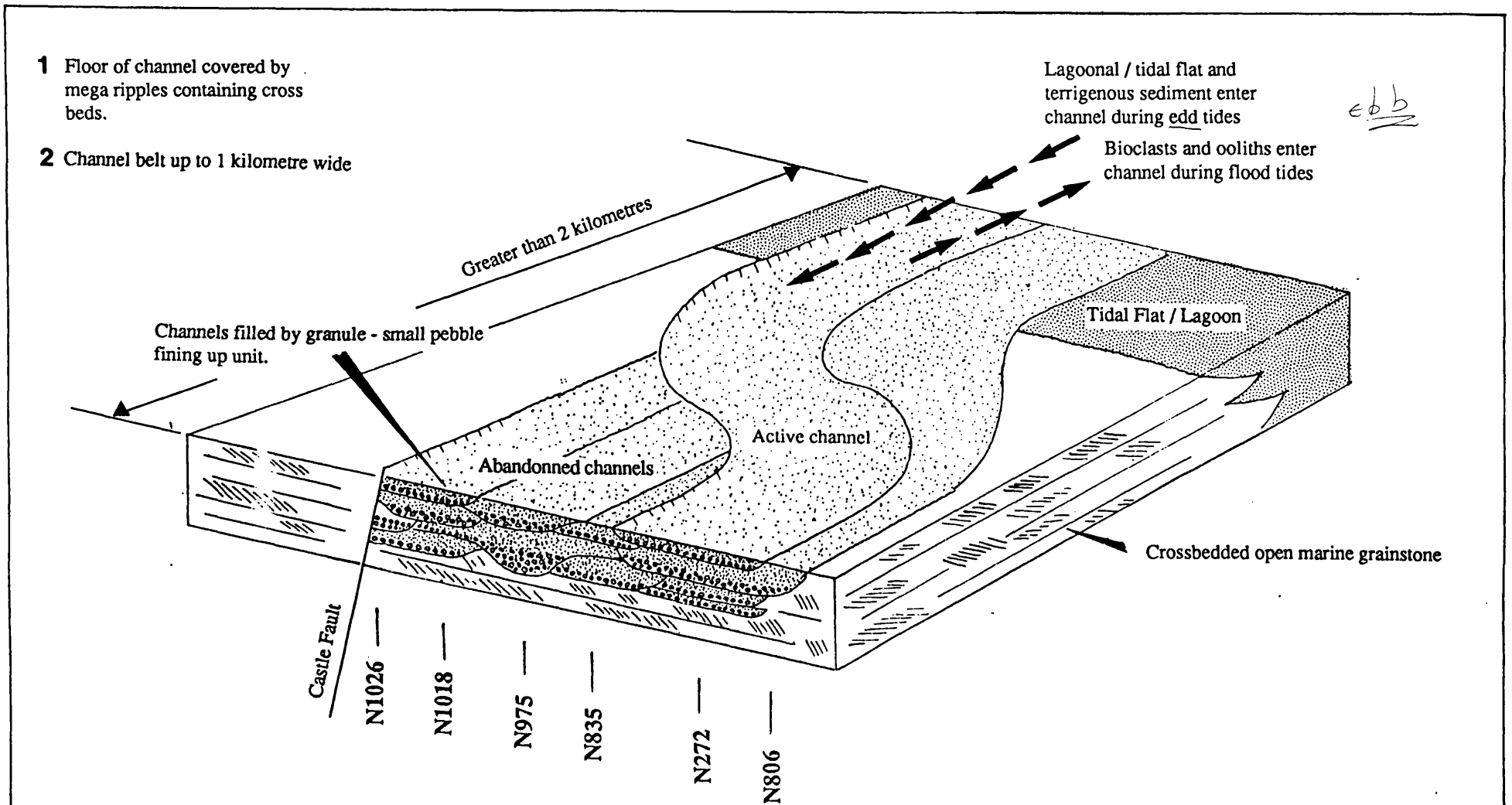

Fig. 4.17. Suggested facies model for the channel belt in the western mine area. The channels cut through lagoon and tidal flats and extend out into the shallow marine zone. During flood tides bioclasts and ooliths are washed along the channels toward the shore. During low tide, terrigeneous, tidal flat and lagoonal sediments are transported along the channel into the shallow marine zone.

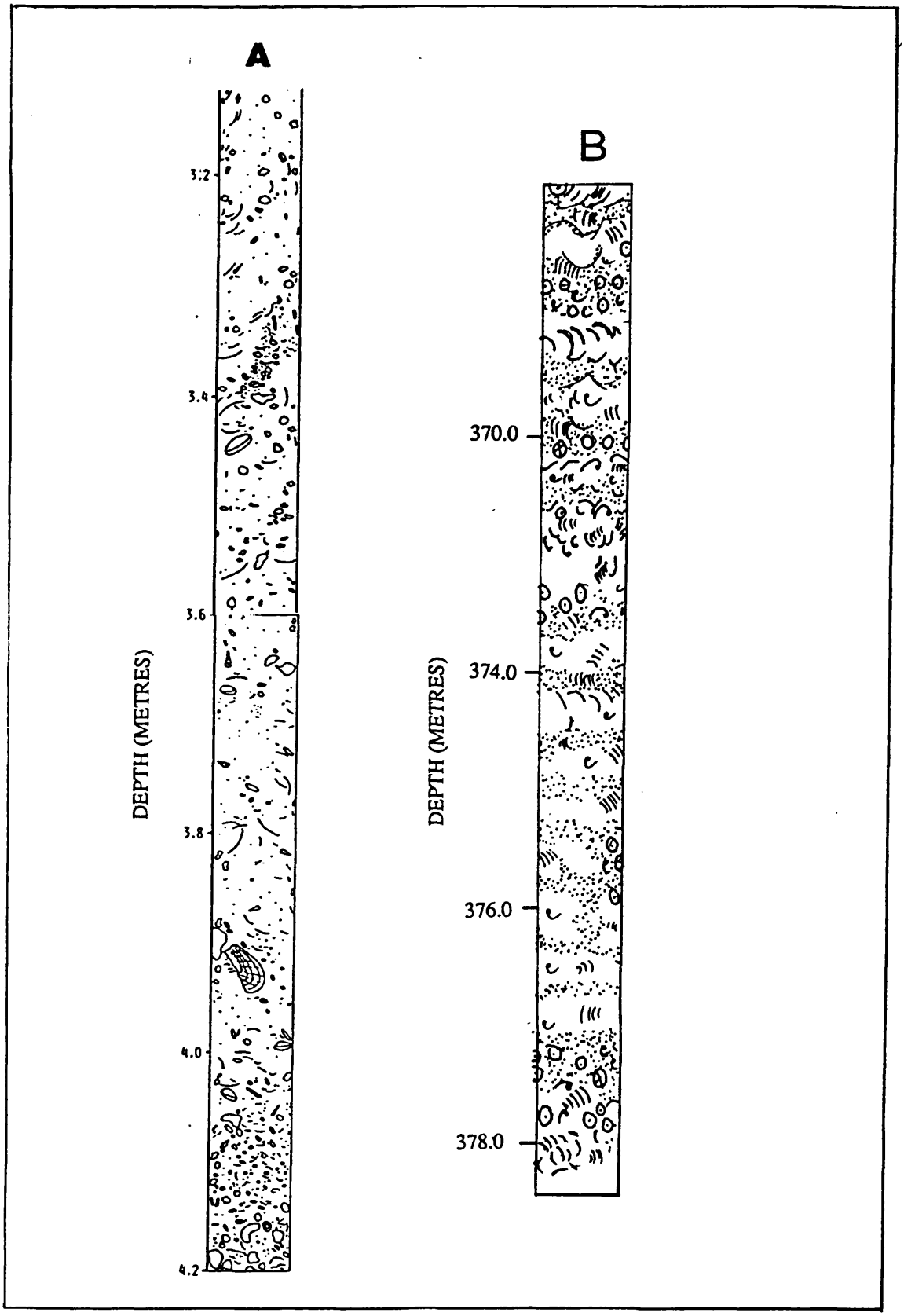

Fig. 4.18. 'A' Section of Holocence soft sediment core taken from the 5 to 25 m deep lagoon of Davis Reef, Central Great Barrier Reef, Australia. The sequence is approximately 10 m thick and consists of poorly sorted bioclastic gravels and muddy sands. The sequence has been intensively burrowed to produce a chaotic fabric. This is compared with 'B' The Nodular Marker at Navan, like the lagoonal sequence from Davis Reef the lithology consists of coarse bioclastic beds, muddy sands which have been burrowed to produce a chaotic fabric.

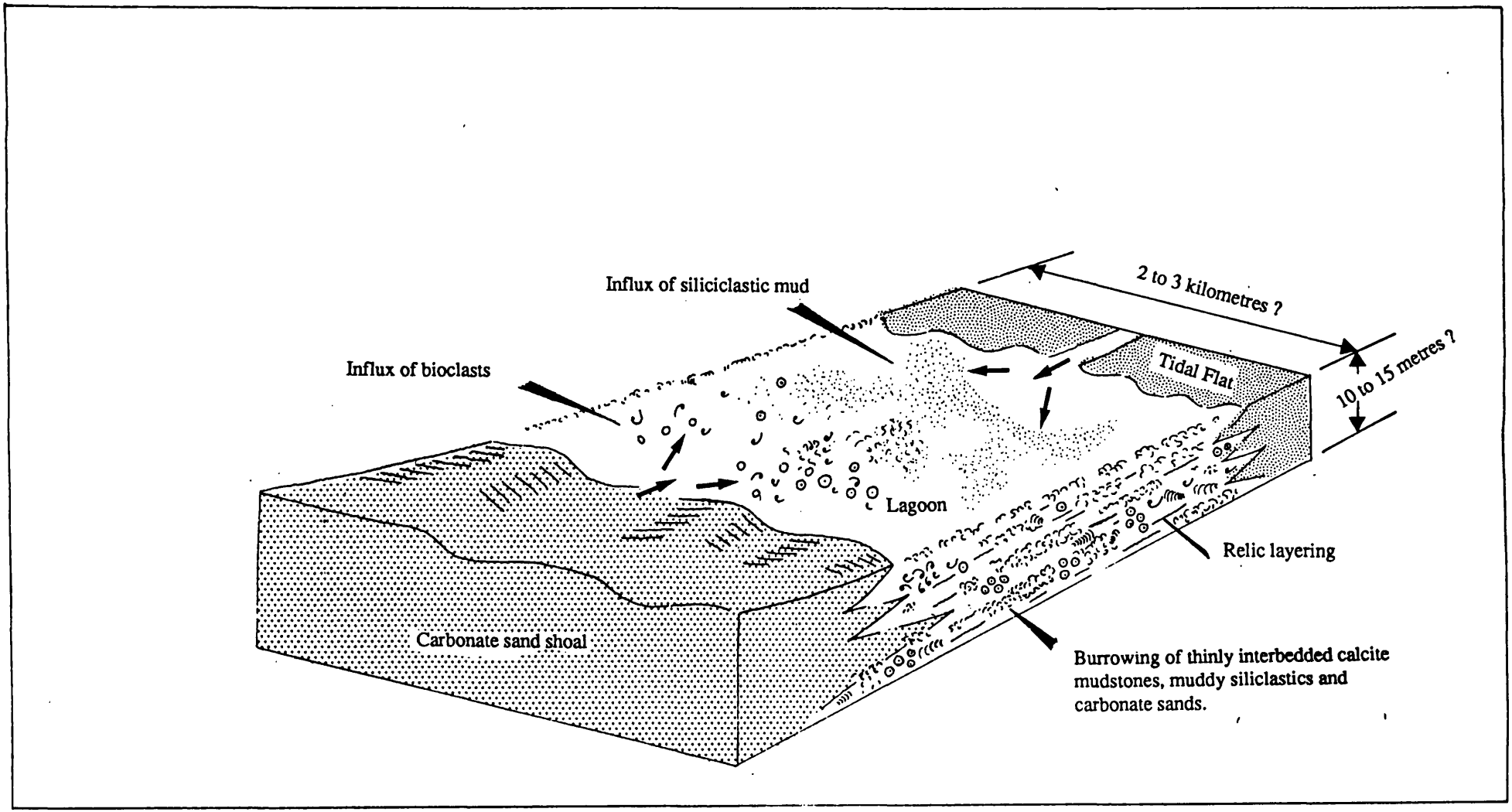

Fig. 4.19. Suggested facies model for the Nodular Marker. A low energy lagoon exists behind a carbonate sand shoal. This sand shoal supplies bioclasts from the adjacent marine environment. Muddy siliciclastics sediments are washed in from the adjacent hinterland. Both sediments are mixed by burrowing in the lagoon.

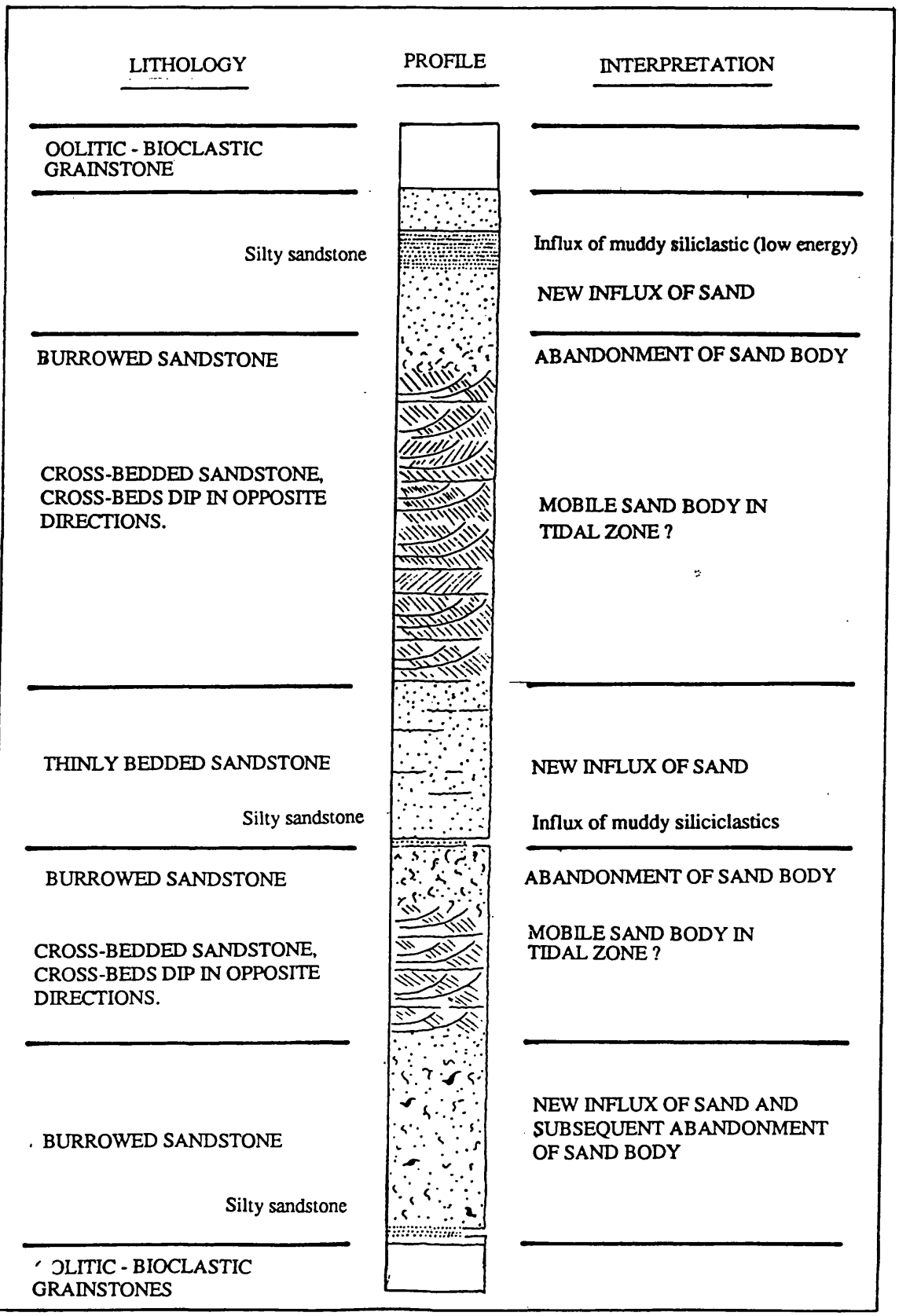

Fig. 4.20. Suggested interpretaion of the Upper Sandstone Marker The sandstone apparently consists of a several sandshoals. Each shoal, consists of thinly bedded or burrowed sandstone representing initial influx of sand. This passes upwards into cross-bedded sands, indicating that the sandshoal has become mobile; burrowed surfaces represent shoal abandonment.

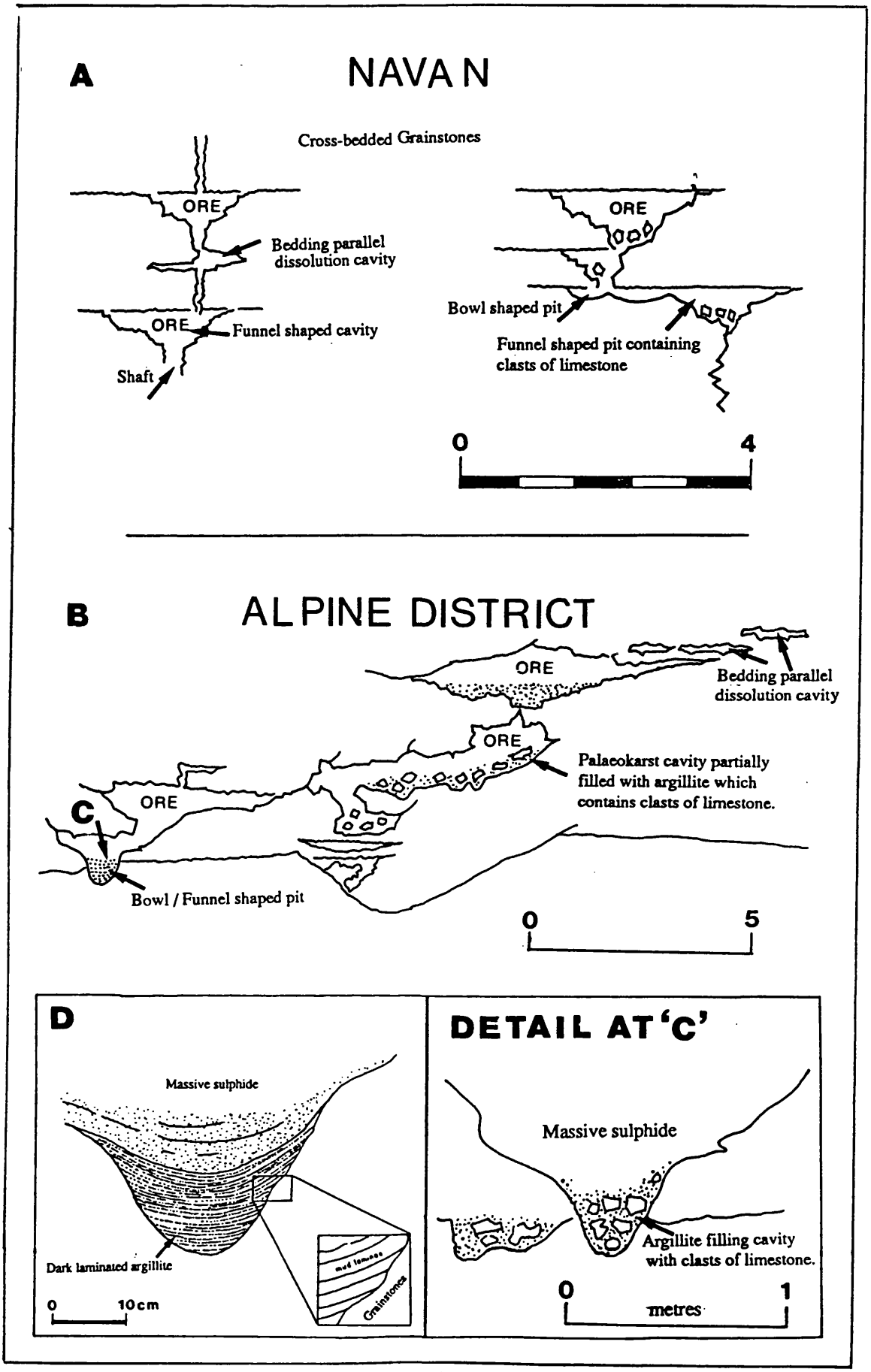

Fig. 4.21. 'A' Part of the grainstone Unit palaeokarst system present in the 1315 Waste Storage Bay , 246W stope. This is compared with 'B' palaeokarst sytems from the Alpine District, After Klau & Mostler, 1986. Like the Navan palaeokarst the Alpine examples are partly connected by vertical and crosscutting channel ways. Detail at 'C' shows individual Alpine palaeokarst depression, Compare with 'D' Palaeokarst depression at Navan.

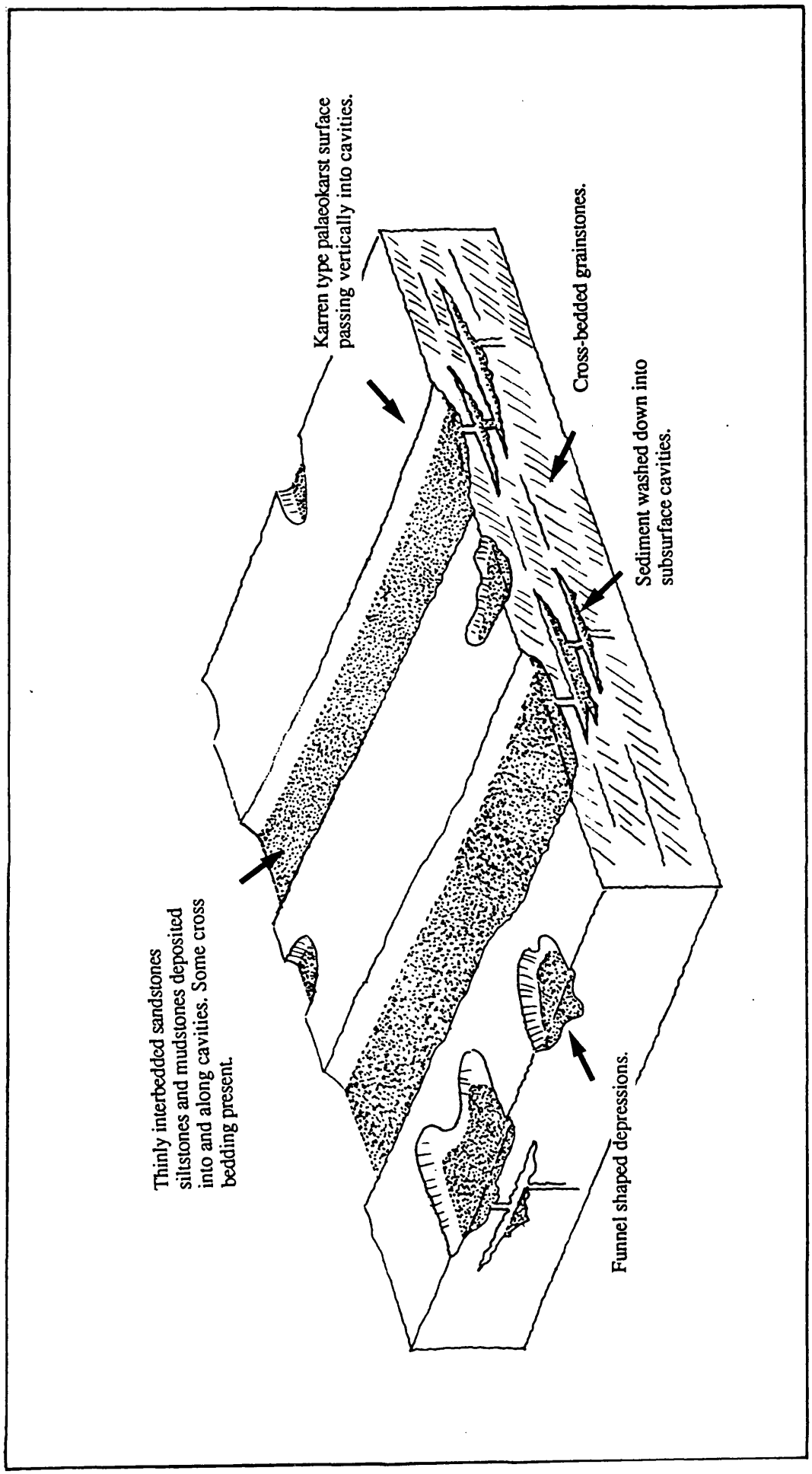

Fig. 4.22. Reconstruction of palaeokarst surface during Grainstone Unit times.

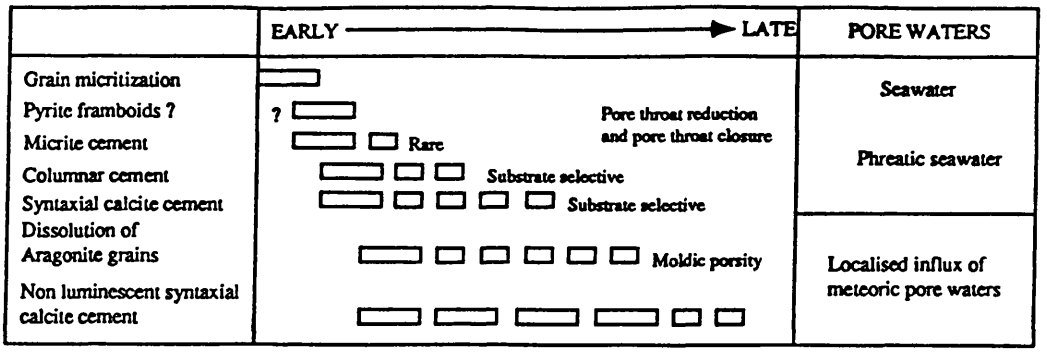

Fig. 23. A. Summary of early petrogenesis of the Grainstone Unit

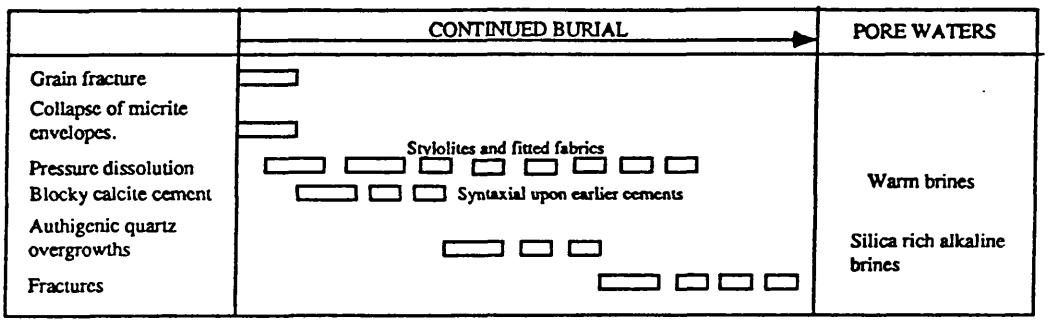

Fig. 23.B. Summary of late petrogenesis, of the Grainstone Unit.

5.1. INTRODUCTION.

Dolomitization at Navan is confined to the Pale Beds, replacing grainstones in both the Micrite and Grainstone Units. Study of the dolomite at Navan has been based on an integrated approach. Major emphasis has been placed on the distribution and geometry of dolomitization in the area. This has been backed by transmitted light microscopy, including cathodoluminescence, by isotopic analyses and by fluid inclusion microthermometry. Texturally dolomites at Navan may be unimodal or polymodal and consist of three types of crystals, each having a distinctive luminescent zonal sequence, reflecting several stages of growth. The general distribution of dolomitzation in the Pale Beds at Navan is shown in Fig. 5.1.

5.2. DISTRIBUTION OF DOLOMITE.

5.2.i. The Micrite Unit.

Oolitic grainstones within the Micrite Unit have been selectively dolomitized to form the **Five Lens Dolomite**. The distribution of dolomite within the oolitic grainstones has been determined by calculating the percentage within each unfaulted drill core (see Appendix 1) and contouring these data (Fig 5.2.). This indicates that;
1.Dolomitization is confined to a limited area (i.e. not a regional feature).
2.Dolomitization has a linear trend.

The area of dolomitization is at least 2 km wide and strkes in a NE-SW direction for over 3 km. Contours define 3 lobes which are related to major faults. Other grainstones, notably the oolitic lithoclast grainstones below the oolitic grainstone have also been dolomitzed, but are not extensive, and are not considered further. Cross-sections 'A-A', B-B', 'C-C' and 'D-D' illustrate the geometry. The vertical thickness of the Five Lens Dolomite is approximately 12 m, controlled by that of the host oolitic grainstones. Each lobe passes laterally into stratal dolomite forming layers between 6 m and 50 cm thick (holes N806 and N1017). Within the dolomite lobes at least five undolomitized areas are present. These are up to 2 m thick and extend laterally for at leats 500 m.

5.2.ii. The Grainstone Unit.

The distribution of dolomite in the Grainstone Unit has been determined by calculating the percentage of dolomite within drill cores containing little or no faulting (Appendix 1). These data were contoured at 20% intervals. The resulting isopach map is shown in Fig. 5.3, it can be seen that;
1. Dolomitization is again confined to a limited area.

2. Dolomitization has a linear trend.

The dolomite body is approximately 1.5 km wide and at least 3 km long. The contours define a NE to SW linear trend (no termination can be seen). Along the axis, in hole N990 88.7% of the grainstones are dolomitized while in hole N535 only 500 m away from the axis, this falls to only 4%. The general distribution is similar to that of the Five Lens Dolomite below.

5.3. GEOMETRY OF MASSIVE DOLOMITE.

Cross-sections 'A-A', 'B-B', 'C-C', 'D-D' and 'E-E' indicate that dolomite in the Grainstone Unit has a plume-like cross-section which is maintained along the strike of the linear dolomite trend. The maximum vertical extent of the plume is 145 m in hole N862 (section 'B-B') where dolomite extends from the base of the Lower Sandstone Marker to the base of the Shaley Pale Limestones. The plume can be divided into three components, a neck, a body of massive dolomitization and stratal dolomite 'fingers'. The simplified three dimensional geometry of this dolomite body is shown in Fig 5.4 - Fig. 5.4a. The neck is up to 400 m wide and 45 m high in section 'B-B' but only 20 m high and 200 m wide in section 'C-C'; in section 'D-D' it is 25 m high and 400 m wide and it disappears entirely in section 'E-E'. The neck passes vertically into massive dolomite up to 600 m wide in section 'C-C'. The upper contact of the massive dolomite may be gradational over several centimetres (hole N804 at depth 96.0 m) or sharp (hole N835 at depth 241.0 m). The massive dolomite passes laterally into a network of stratal dolomite with 'fingers' extending over 600 m. Individual stratal layers are up to 40 m thick at their nodal contact with the massive dolomite (section 'C-C') decreasing in thickness laterally and subdividing into layers about 1 m thick at their terminations. Some undolomitized grainstones occur within the dolomite 'plume', these are up to 30 m thick (cross-sections 'B-B' and 'C-C') and may extend laterally along stratal dolmite 'fingers' for over 400 m (cross-sections 'C-C', 'D-D').

Stratal dolomite below and adjacent to the neck of the dolomite plume forms laterally discontinuous layers 1 to 9 m thick (cross-section 'C-C'). Several of these layers have been used as crude stratigraphic markers. The **Lower Dark Marker Equivalent** (Plate 5.1.A) is 9 m thick hole (N1017) and 1 m thick (hole N806). In some areas this dolomite occurs up to 3 m above the base of the grainstones (section 'C-C'). It extends into the neck of dolomitization (cross-section 'A-A') and locally subdivides to form several layers (crossections 'C-C'). It has the same distribution as the massive dolomite and is 1.3 km wide in section 'C-C' and 700 m wide in section 'B-B', dying out in section 'D-D'. Approximately 10 m above this, a poorly represented dolomite extends along the Sub Lower Sandstone Marker and 5 m above. Dolomite also extends along the oolitic Lower Sandstone Marker. The dolomite

associated with both of these markers may increase or decease in thickness laterally and the two coalesce to form a single unit in section 'A-A'.

Locally dolomite and unaltered grainstones form alternating layers. These vary from 1 cm thick in hole N982 at depth 404.0 m to 1.2 m thick in hole N974. The sub-horizontal contacts between dolomites and grainstones may be sharp, planar or undulose (Plate 5.1.B), or gradational (hole N794 at depth 274 m). Some are stylolitic (hole N718 at depth 237.2 m).

5.4. RELATIONSHIP TO LITHOLOGIES AND FAULTS.

At Navan dolomitization is selective. This is most obvious in the Micrite Unit where the oolitic grainstones have been selectively dolomitzed to produce the Five Lens Dolomite (Fig.5.5.). In addition, this dolomitization apparently cuts across the margin of the channel which bounds the upper surface of the Micrite Unit in the eastern mine area, extending into adjacent grainstones (Fig 5.6). The dolomite 'plume' within the Grainstone Unit, also cuts across sedimentary layers, extending vertically over 100 m uninterupted and cutting across the Upper Sandstone Marker toward the upper limits of dolomitzation. Finally, it cuts across the channel filled by micro-conglomerate. The axis of massive dolomitization cuts across the strike of the microconglomerate channel sequence and across the strike of the channel which bounds the upper surface of the Micrit Unit in the eastern mine area (Fig. 5.7).

Dolomite crosses shaley lithologies; the Upper Dark Marker is completely dolomitized in hole N272 at depth 252.0 m and in hole N992 at depth 369.0 m (Fig.5.8.A). Dolomite cuts across thin black shales in hole N1000 at depth 594.0 m but locally, it has apparently been deflected beneath shales as in hole N722 at depths 272.0 m. and in hole N1018 at depth 512.0 m. (see cross-sections 'A-A', 'D-D'). The Nodular Marker has apparently acted as a barrier to dolomitization and only the basal 2.5 m are dolomitized in hole N985 at depth 381.0 m and hole N986 at depth 365.0 m. However, where the Nodular Marker is poorly developed, as in hole N1000 and N272, dolomitzation is continuous. Lateral discontinuities in other shaley lithologies have been exploited in a similar manner, notably in section 'B-B', where dolomite passes through a gap in the Sub Dark Marker. Stratal dolomite 'fingers' are contiguous with laterally extensive grainstones, but the variations in thickness along their lengths suggest that they cut across bedding. The Lower Dark Marker Equivalent occurs along the base of the grainstones. It cuts across the basal contact of the Grainstone Unit into the calcite mudstones of the Micrite Unit in holes N30 at depth 124.0 m. and hole N982 at depth 419.4 m (Fig. 5.8.B).

Evidence of pre-dolomite lithologies includes relic sedimentary structures and relic grains. Relic structures include graded beds (hole N272 at depth 224.5 m), cross

beds (hole N982 m.) and layering (Plate 5.1.C). These features are seen within adjacent undolomitized grainstones described in Chapter 4. Ghost allochems, typically ooliths and bioclasts are visible (section 5.5) and relic bioclasts are also represented by moulds filled with coarse dolomite (Plate 5.2.D). Anderson (1990) noted that the dolomite along the Lower "Sandstone" and the Sub Lower "Sandstone" Markers contain abundant siliciclastic grains, but the distribution of these varies. In hole N314 two adjacent samples from 267.2 m. and 267.1 m depth were examined; one, dolomite free, contained a few siliciclastic grains, the adjacent dolomite contained 25 to 30% siliciclastic grains. A similar relationship was noted from hole N314 at depth 274.0 m. The remaining thin sections of dolomite (4 samples) from these markers contain no siliciclastic grains, suggesting that the clastic content had only a localised lithological control. Where siliciclastic grains are present they form circular and irregular clusters suggesting redistribution by burrowing prior to dolomitization. Burrows are common in adjacent grainstones.

There are five major faults in the area, described in Chapter 1 (section 1.5). The Randlestown Fault and the Castle Fault, both strike SW-NE. The 'B' and 'T' Faults strike ENE and the 'A-C-D' fault complex strikes approximately NE (Fig 5.2 - 5.3). Recent analysis of these faults suggests that the Castle and 'B' Faults define a graben structure (Ashton pers commn, 1992). The axis of the dolomite linearment in the Grainstone Unit occurs within this graben structure. However, the axis of dolomitization intersects the 'B' Fault, cutting across it, and extends beyond the study area. Some movement on major faults post-date dolomitization. In hole N272 at depth 216.0 m a major fault zone over 30 cm wide has cut massive dolomitization.

The Five Lens Dolomite displays a series of thickness changes which extend northeastwards between and along the major faults (Fig 5.2). The dolomite in the grainstones which fill the channel adjacent to the Five Lens Dolomite lies at the same structural level as the Five Lens Dolomite and is centred upon holes N30, N941and N351 coincident with the intersection of the 'A-C-D Fault Complex', 'B' and 'T' Faults (Fig 5.2). Thus the general trend of dolomitization at all stratigraphic levels is associated with major faults.

5.5. PETROLOGY.

5.5.i. Introduction.

The weathered surfaces of the Navan dolomites vary from light brown in the Five Lens Dolomite to grey brown in the Grainstone Unit. The surficial coloration of dolomite is generally believed to reflect oxidation of Fe^{2+} within the dolomite lattice

(Gawthorpe, 1987). Both the Five Lens Dolomite and the massive dolomite stain blue with Potassium Ferricyanide, indicating that they are ferroan (Dickson, 1966) and contain more than 2 mol % $FeCO_3$ (review by Tucker, 1990c p.382). Some zones remain free of colour indicating that the Fe^{2+} concentration varies between zones.

5.5.ii. Dolomite textures.

Approximately 130 thin sections of dolomite have been examined using transmitted light microscopy, 70 from the massive dolomite in the Grainstone Unit (including 14 from the Lower Dark Marker Equivalent, 7 from the Lower "Sandstone" Marker, 4 from the Sub Lower "Sandstone" Marker) and 37 from the Five Lens Dolomite. Generally the textures in all of these are similar, consisting of hypidiotopic mosaics of crystals having cloudy cores and clear rims. These dolomites are therefore considered together; where notable diffences occur, these are described.

The dolomite is fine to medium crystalline (classification of Folk, 1962) and displays a mosaic texture typical of ancient massive dolomites (Sibley, 1980, 1982). Texture is defined as the "morphological relationships among individual rhombs" (Gregg & Sibley, 1984) and textures displayed by the Navan dolomite are classified according to the scheme of Sibley & Gregg (1987), summarised in Fig 5.9.

Approximately 70% of samples have a unimodal (Plate 5.1.E) to polymodal (Plate 5.1.F) subhedral texture with planar or irregular crystal interfaces. Dolomite from the neck of the dolomite plume are unimodal but have non planar textures and crystal interfaces are curved (Plate 5.1.G).

Polymodal fabrics occur where bioclasts have been replaced with coarser limpid crystals; these crystals occupy circular, rectangular, or shell shaped areas up to 2 mm in diameter. Textures within these areas are non planar and crystal interfaces are curved. In a few examples polymodal areas represent bioclasts which have been replaced by crystals whose diameters are smaller than the groundmass mosaics (hole N982 at depth 411.7 m, Plate 5.1.H). Where dolomite contains vugs the texture changes as the margin of the vug is approached forming a planar mosaic consisting of euhedral rhombs (Plate 5.2.A).

The unimodal and polymodal crystal mosaics are not entirely fabric destructive; ghost allochems are common. These are dark and outlined by inclusions a few microns in diameter. The margins of ghost grains are generally sharp but may be gradational and the shape varies from circular or shell shaped to irregular (Plate 5.2.B). Preservation of internal form also occurs, circular ghosts may still display concentric layers of elongate inclusions oriented normal to their margins and probably represent ooliths (Plate.5.2.C). Shell shaped ghosts may display elongate dark zones reflecting their former structure.

PLATE 5.1. Features and textures of the Navan Dolomite.

A. General view of dolomitized grainstones forming the Lower Dark Marker Equivalent. Note relic cross-bedding (B). Hole N998, scale in centimetres.

B. General view of finely crystalline dolomite containing relic grainstone (G), note the non planar gradational contacts, Hole N908, Scale bar = 1 cm..

C. General view of dolomite in the Grainstone Unit. Relic layering (L) is visible within the dolomite. Note the vuggy porosity. Hole N1021, scale in centimetres.

D. Shell shaped biomoulds (M) filled with coarse saddle dolomite crystals. These molds occur within the finely crystalline Five Lens Dolomite occuring in the Micrite Unit. Note relic porosity at (P). Hole N1033 at depth 633.2 m, scale in centimetres.

E. Photomicrograph (plane light) showing planar unimodal subhedral texture in dolomite (the Five Lens Dolomite). Hole N975 at depth 448.3 m. Scale bar = 250 microns.

F. Photomicrograph (plane light) showing polymodal subhedral texture in dolomite. Hole N975 at depth 381.3 m. Scale bar = 1 mm.

G. Photomicrograph (plane light) showing non planar texture in dolomite within Grainstone Unit. Note curved crystal interfaces. Hole N975 at depth 381.3 m. Scale bar = 250 microns.

H. Photomicrograph (CL) of rare fabric selective dolomitization in which dolomite crystals have selectively replaced a bioclast (?) grain. Dolomite rhombs are dully luminescent and carry bright terminal rims. Hole N982 at depth 379.7 m. Scale bar = 1 mm.

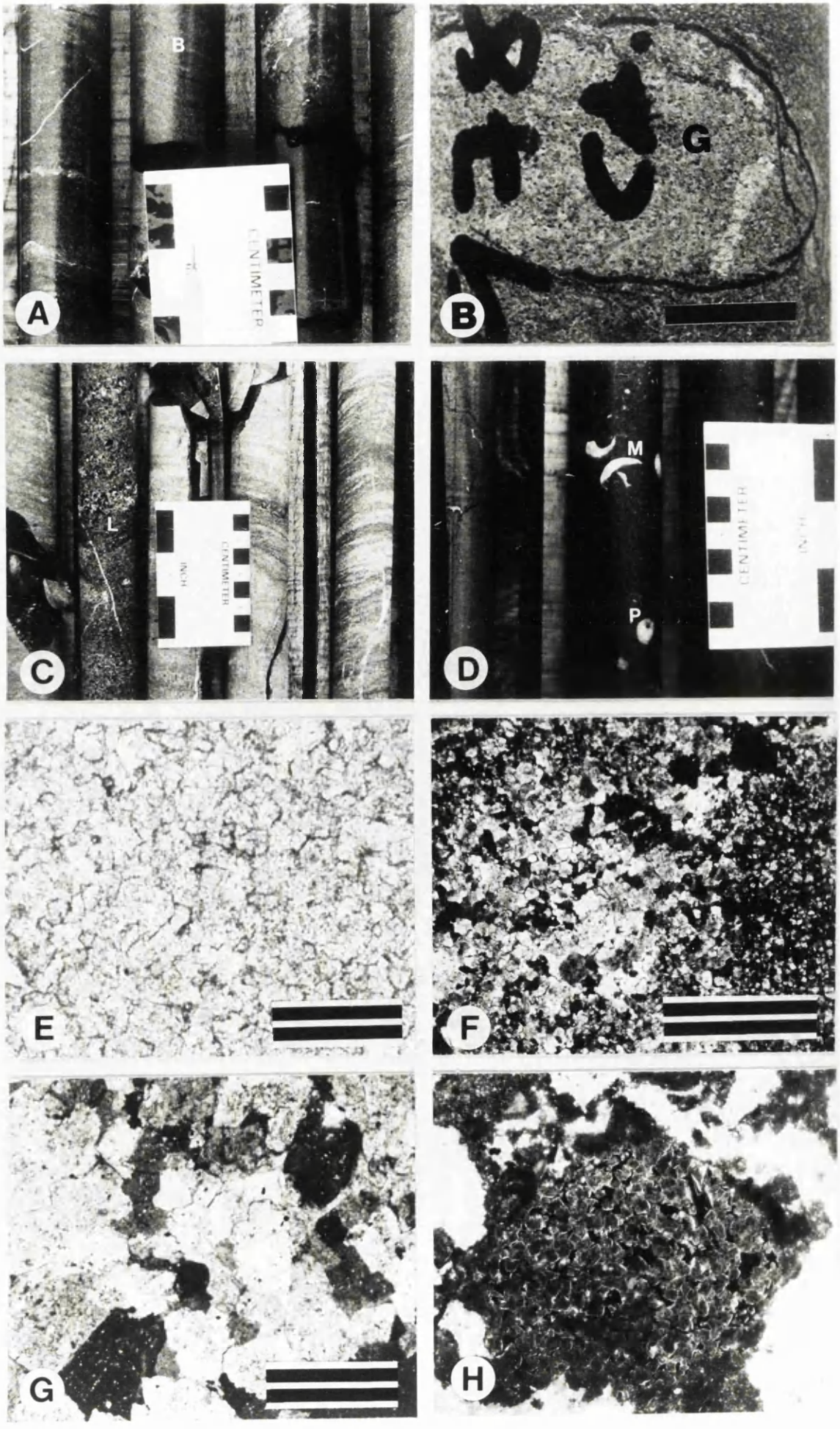
A
B
CENTIMETER
B
G
C
L
INCH
CENTIMETER
D
M
P
CENTIMETER
E
F
G
H

There is also evidence of relic diagenetic fabrics. Ghost shells may show *in situ* fractures (Plate 5.2.D) and ghost ooliths show detached cortical layers (Plate 5.2.E). Some ghost grains have inclusion rich rims containing elongate translucent inclusions a few microns wide oriented normal to the grain surfaces (Plate 5.2.F). These probably represent former fibrous cements.

Approximately 30% of the thin sections examined are dominated by fabric selective dolomitization, replacing the calcite cement between grains. Such selective dolomitization is confined to dolomite 'fronts' around the margins of the massive dolomite and extending along bases and upper surfaces of stratal dolomite 'fingers'. In drill core these dolomite 'fronts' consist of rhombs which stain blue with Potassium Ferricyanide surrounding allochems which stain red with Alizarin Red, exemplified by the Five Lens Dolomite in hole N858 at depth 497.0 m (Plate 5.2.G).

In some thin sections there may be only a few scattered dolomite crystals within an otherwise unaltered grainstone (Plate 5.2.H). Where fabric selective dolomitzation can be identified, distribution was apparently controlled by the pre-dolomite diagenetic fabric with rhombs concentrated irregularly along the interfaces between calcite cement and allochems (Plate 5.3.A). Individual dolomite crystals may penetrate part way into calcitic allochems with the original margin of the grain still visible within the rhomb as a ghost (Plate 5.3.B). With increasing dolomitization the entire cement became dolomitized, suggesting that this was more reactive than the allochems. Allochems have been partially to completely replaced by coarse dolomite crystals, this replacement is destructive (non mimetic) (Plate 5.3.C).

It appears, that the textures in the Navan dolomite are a function of the original limestone depositional and diagenetic fabrics. This is in agreement with Sibley (1980, 1982) who suggested that common textures displayed by ancient dolomites are a reflection of precursor depositional and diagenetic fabrics. Smaller crystals form mosaics and occasionally replace bioclasts. Coarser limpid crystals reflect the distribution of former bioclasts which have been replaced or dissolved and the resulting moulds occupied by dolomite cement. It has already been shown in chapters 3 and 4 that the grainstones had undergone stabilization to low magnesium calcite, suggesting that there was no mineralogical control of dolomite textures, compare Sibley (1980, 1982). However, where dolomite has preferentially replaced calcite cement, this may represent a mineralogical control, but it could also be due to the cement having a larger reactive surface area than the adjacent allochems.

5.5. iii. Dolomite crystal types.

Dolomite at Navan consists of brownish turbid rhombs filled with inclusions. Some crystals display weak undulose extinction. The crystals contain up to 6 crude

PLATE 5.2. Ghost features and textures of the Navan dolomite.

A. Photomicrograph (plane light) of planar texture in dolomite. Note sucrosic porosity (P) between rhombs defined by crystal faces. Hole N986 at depth 368.3 m. Scale bar = 1 mm.

B. Photomicrograph (plane light) of ghost bioclasts in dolomite, note shell shaped oultlines, this suggests the original protolith was a bioclastic grainstone. Hole N975 at depth 384.7 m. Scale bar = 1 mm.

C. Photomicrograph (plane light) of ghost ooliths in dolomite. Hole N992 at depth 390.0 m. Scale bar = 100 microns.

D. Photomicrograph (plane light) of ghost grain displaying a fracture, indicating dolomitzation post-dated sediment compaction and grain fracture. Hole N975 at depth 384.7 m. Scale bar = 250 microns.

E. Photomicrograph (plane light) of ghost oolith displaying spalled outer cortex. Again this suggests that dolomitzation post dated sediment compaction and grain fracture. Hole N992 at depth 390.0 m. Scale bar = 250 microns.

F. Photomicrograph (plane light) of ghost grain with elongate inclusions (arrows) extending normal to the grain surface. These inclusions are interpreted as relic columnar calcite cement, suggesting that dolomitzation post-dated early circumgranular cementation. Hole N975 at depth 384.7 m. Scale bar = 250 microns.

G. Fabric selective dolomitzation in drill core, dolomite (D) surrounds undolomitzed bioclasts (b). Note also moldic porosity (P). Hole N780 at depth 135.1 m. Scale bar = 1 cm.

H. Photomicrograph (CL) of fabric selective dolomitzation. The grainstone contains a few dolomite crystals. These cut across the contact between earliest columnar calcite cement (c) and host grains (arrows) indicting they post-date these features. Hole N1011 at depth 569.2 m. Scale bar = 100 microns.

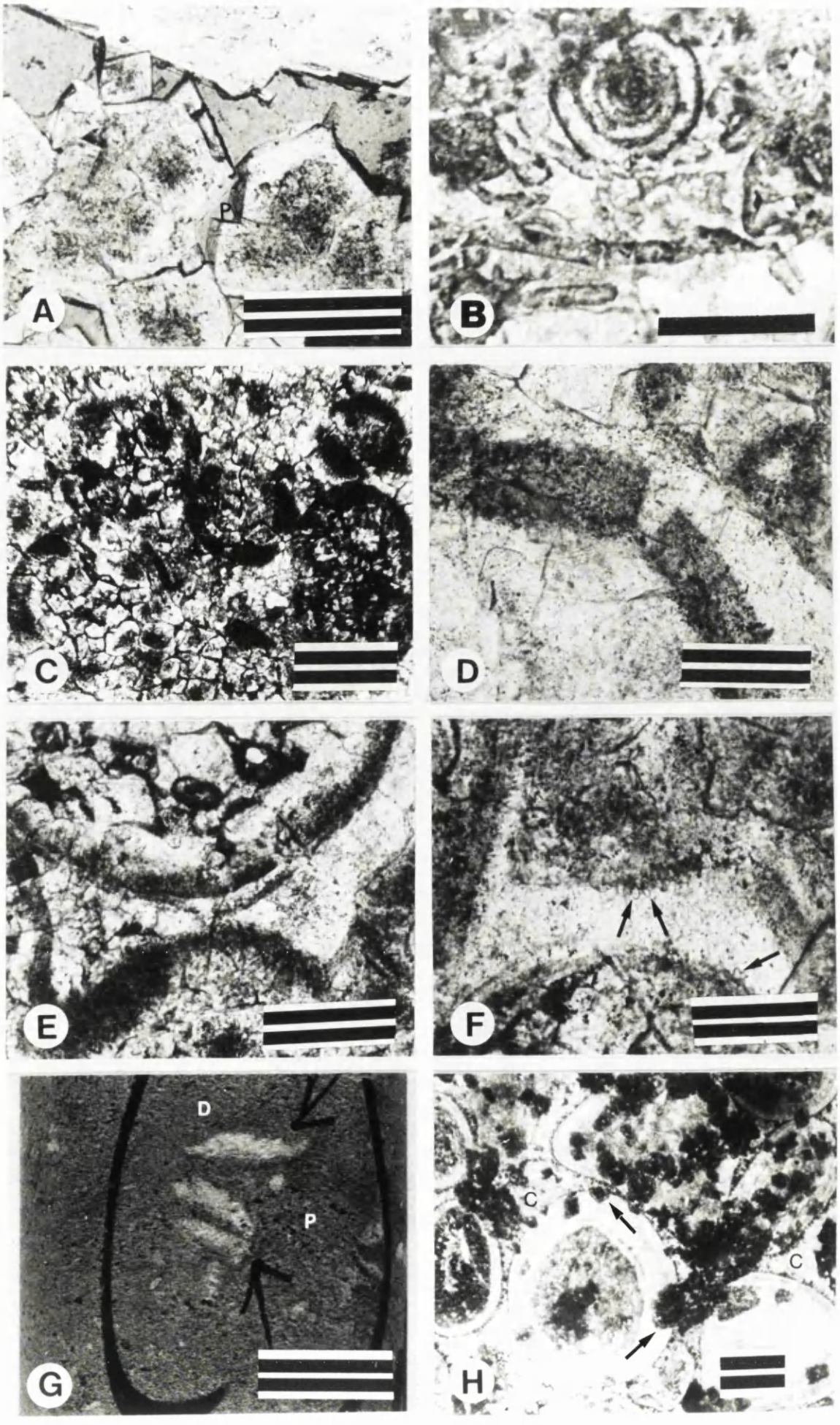
A
P
B
C
D
E
F
G
D
P
H
C
C

zones (average 3) defined by inclusion density. Some turbid cores may be surrounded by up to five clear zones which have grown syntaxially on them (Plate 5.3.D). The interface between the turbid inner rhomb and clear outer zones may be anhedral, with embayed and truncated margins, or euhedral with planar or gradational contacts. Contacts between the clear zones are planar and conformable but they vary in thickness and may display faint subzones. Generally the outer surfaces of crystals are planar but locally they have a stepped profile or display rhombic embayments, rarely the margins are ragged and irregular. Crystal apices are either pointed or rounded.

Coarser limpid crystals in polymodal fabrics also have inclusion rich cores and thick clear rims. However crystal faces and cleavage traces are curved in crossed polars and crystals display a sweeping extinction (Plate 5.3.E). The faces of many crystals are smooth but some have a stepped profile.The curved faces and sweeping extinction resemble those of the saddle dolomite of Radke & Mathis (1980).

The occurrences of single saddle dolomite crystals embedded within bioclasts (typically echinoderms) demonstrates that this type of dolomite may be replacive. However, many crystals line former moulds with apices pointing away from the substrate, suggesting that they were a cement. Thus saddle dolomite is both replacive and a cement (compare Plate 5.3.E and 5.3.F), a common feature of ancient dolomite (Sibley & Gregg, 1984).

The largest crystals are pink to white euhedral rhombs, up to 3 mm in diameter with a pearly lustre. They form crusts up to 1 cm thick lining or filling vuggy porosity (Plate 5.3.G) and fractures (see below). Such crystals again commonly display the strongly curved surfaces and cleavage traces, indicative of saddle dolomite (Radke & Mathis, 1980). The cores of such crystals are full of inclusions and a number of zones with faint subzones may be recognised. Some rhombs have stepped faces which are believed to reflect internal sub-crystals and their apices have a distinctive spear-head shape.

Inclusions are present in all three crystal types, in cores and outer zones, and along the contacts between zones. Generally they are only a few microns in diameter but some are up to 10 microns. They vary from brown to colourless. Inclusions are very common in ancient dolomites. Sibley, (1980) noted numerous inclusions in Pliocence dolomites of Curacao and suggested that they were either moulds formed by dissolution of calcite or were relic calcite. At Navan inclusions may be irregular (no definable shape), circular, elliptical or rhombic (negative crystals) in section. Some fluid filled vacuoles contain gas filled bubbles (Plate 5.3.H). These may be stationary or move erratically. Some opaque amorphous inclusions probably consist of organic material. Inclusions within crystal cores may be evenly disseminated or patchily distributed giving the cores a mottled appearance. Outside the cores some zones are rich in inclusions which may be evenly disseminated, concentrated in certain parts of

PLATE 5.3. Navan dolomite crystal types.

A. Photomicrograph (CL) of fabric selective dolomite. The dolomite appears to have exploited the interface between calcite cement (C) and host oolith (O). Note dolomite cuts across the calcite cement sequence therfore post dating it. The Five Lens Dolomite, Hole N1011 at depth 569.2 m. Scale bar = 100 microns.

B. Photomicrograph (plane light) of fabric selective dolomitzation. Dolomitization has replaced the calcite cement between grains. Individual dolomite crystals have penetrated the margin of allochems (arrow) now visible as ghosts. Hole N982 at depth 411.7 m. Stained thin section. Scale bar = 1 mm.

C. Photomicrograph (plane light) of bioclast being replaced by coarse saddle dolomite crystal. The Five Lens Dolomite, 1130 Drainage Drift. Scale bar = 1 mm.

D. Photomicrograph (plane light) of a typical dolomite crystal at Navan. The crystal displays an anhedral inclusion rich core (c) follwed by several clear zones (z). N982 at depth 439.1 m. Scale bar = 50 microns.

E. Photomicrograph (plane light) of a saddle dolomite crystal. Hole N907 at depth 356.5 m. Scale bar = 1 mm.

F. Photomicrograph (plane light) of saddle dolomite crystals (d) lining biomolds. Note geopetal sulphide (s). The Five Lens Dolomite, 1130 drainage drift. Note relic porosity (P). Scale bar = 1 mm.

G. Saddle dolomite crystal (plane light) within vuggy porosity. Crystal has a cloudy anhderal core surrounded by up to five clear zones. Note spear head termination of crystal. Hole N986 at depth 368.3 m. Scale bar = 250 microns.

H. Photomicrograph (plane light) of a two phase fluid inclusions (arrows) within Navan dolomite, note the vapour bubble. Hole N984. Scale bar = 50 microns.

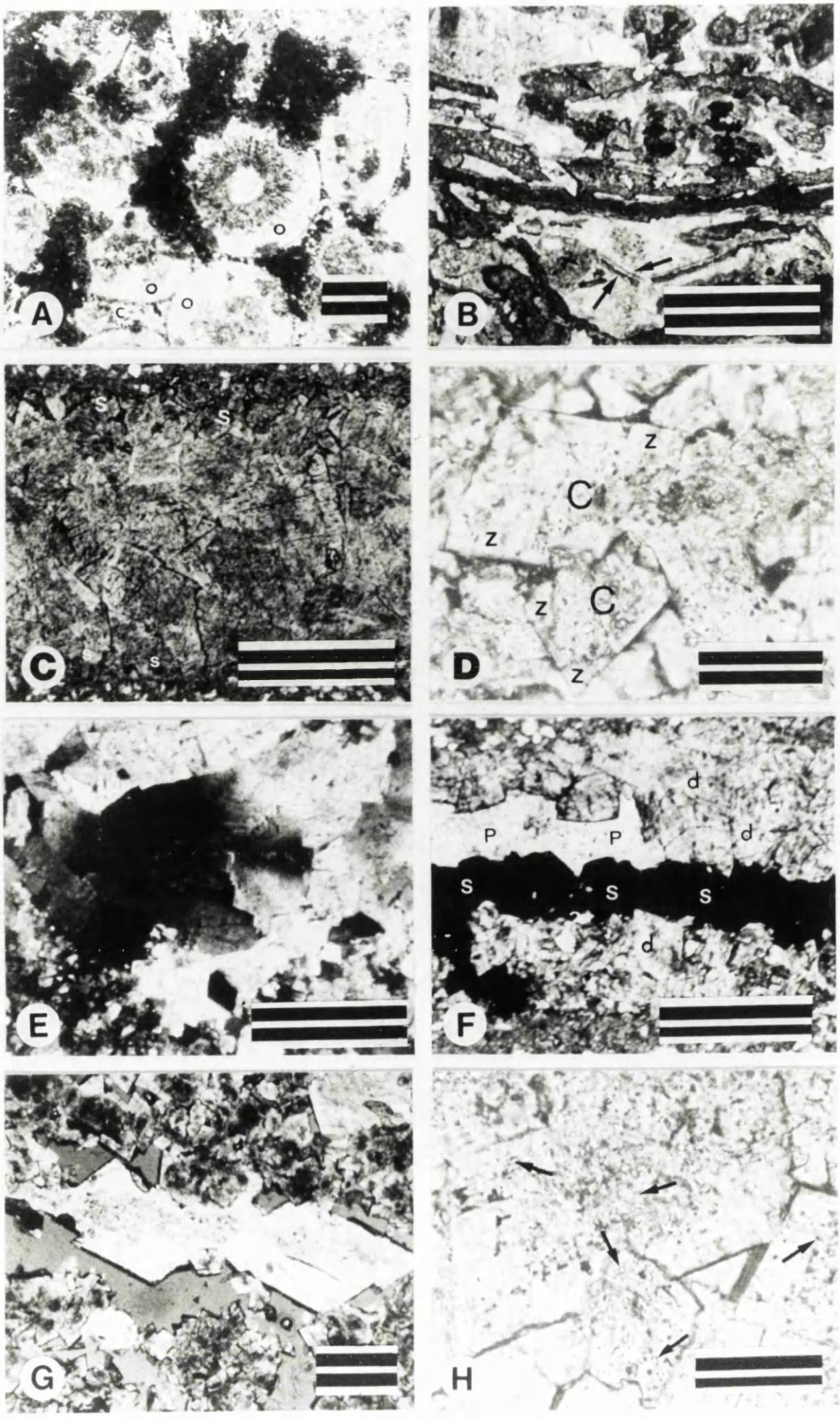
A
o
o
o
c
B
C
S
S
s
s
D
C
C
z
z
z
z
E
F
P
P
d
d
d
S
S
S
G
H

the zone, or defining faint sub zones. The pearly lustre of saddle dolomite is believed to reflect the presence of fluid inclusions (Radkhe & Mathis, 1980).

Porosity in the Navan Dolomites can be classified according to the scheme of Choquette & Pray (1970) as intercrystalline, moldic, vuggy and fracture porosity.

i). Intercrystalline pores are defined by the terminations of dolomite crystals (Plate 5.4.A). The sizes of pores vary, some are less than the diameter of the dolomite crystals and may be elongate or irregular. They may be isolated or form patches between euhedral sucrosic dolomite rhombs. Larger pores with diameters greater than the dolmite rhombs are generally polyhedral. Intercrystalline porosity may be widespread in pervasive dolomitization, reaching a maximum of 20%, or may be confined to ghost grains or areas consisting of two types of crystal and may occur in matrix selective dolomitization.

ii). Two types of mouldic porosity are present, oomoldic (Plate 5.4.B) and biomouldic Both are seen in cores but only biomoulds are large enough to be specifically identified (Plate, 5.4.C)..

iii). Irregular vugs range from a few millimetres (Plate 5.4.D) up to 10 cm diameter (hole N826 at depth 326.8 m). They may extend along former calcite filled fractures and these together with stylolites often appear corroded (Plate 5.4.E). Vugs may be of uniform diameters or more varied in size. Vuggy porosity may extend over several metres of core, or be more localized (Fig. 5.10). Some rhombs are truncated against the margins of irregular pores. Intercrystalline (sucrosic) porosity extends around the margins of some vugs (Refer Plate 5.2.A).

5.5.iv. Other features of the Navan dolomites.

1. At least 4 stages of brittle fracture have influenced the dolomites. Features vary from less than 1 mm up to 8 cm wide and may be filled by calcite, or by stage (2) (Plate 5.4.F) or stage (3) dolomite (Plate 5.4.G) (stages are defined in section 5.6.ii.). Fractures may be sub-vertical and sub-parallel or chaotic and intersecting.
2. Sutured seam stylolites may be horizontal or vertical. Some intersect and are truncated by vugs. They contain stylocumulate consisting of opaque minerals (pyrite ?, haematite ? or magnetite ?) and clays, together with a few quartz and feldspar grains and mica flakes.
3. Authigenic quartz in the dolomite resembles overgrowths in the Micrite Unit and adjacent grainstones. Crystals generally have ragged anhedral oulines and host individual dolomite rhombs. (Plate 5.4.H). Chalcedonic silica also occurs within dolomite, it is concentrated between rhombs and replacing rhomb margins. Chalcedonic silica occur in the Five Lens Dolomite in hole N975 at depth 454.7 m..
4. Opaque masses up to 1 mm in diameter fill voids between type (3) saddle dolomite crystals in hole N1021 (Plate 5.5.A). This material attracts dust and has a waxy lustre

PLATE 5.4. Porosity in the Navan dolomites.

A. Photomicrograph (plane light) of intercrystalline porosity (P). Hole N986 at depth 368.3 m. Scale bar = 250 microns.

B. Photomicrograph (plane light) of oomoldic porosity (P). Hole 1005 at depth 342.3 m. Scale bar = 1 mm.

C. Shell-shaped biomoldic pore (M) in the Five Lens Dolmite within the Micrite Unit. Hole N1036 at depth 652.4 m. Note irregular vuggy pore (V). Scale in centimetres.

D. Localised vuggy porosity in dolomite. Pencil for scale points to 'way up'.

E. Vuggy porosity in dolomite lined by saddle dolomite. Arrow shows stylolite (s) along the opposite side of vug. Here the stylolite appears to be corroded, suggesting that the vug post-dates stylolite formation. Hole N1034 at depth 401.3 m. Scale bar = 1 cm.

F. Dolomitized oolitic grainstone in the Micrite Unit, the Five Lens Dolomite. This core has been stained with Potassium Ferricyanide and Alizarin Red which has produced a deep blue colour. Dolomite filled fractures (D) have cut across earlier calcite-filled fractures (c). Hole N858 at depth 497.0 m. Scale in millimetres.

G. Fracture in dolomite filled with coarse saddle dolomite. Hole N722 at depth 294.4 m. Pencil for scale.

H. Photomicrograph (plane light) of authigenic quartz overgrowth (O) in dolomite. The outline is ragged and anhedral suggesting it has been corroded and replaced by dolomite (D). Relic overgrowth margin visible in dolomite at (R). Hole N975 at depth 384.7 m. Scale bar = 250 microns.

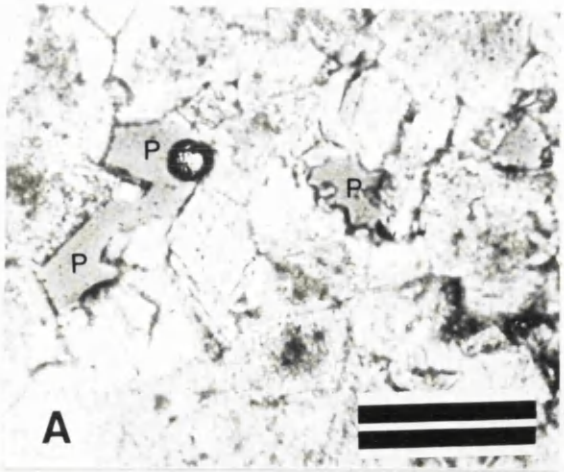
P
P
P
A

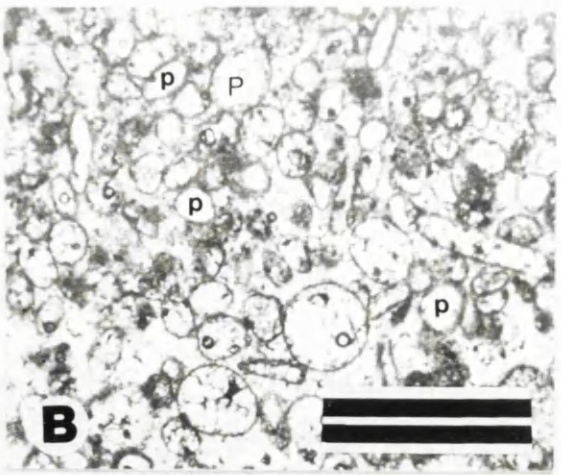
p
P
p
p
B

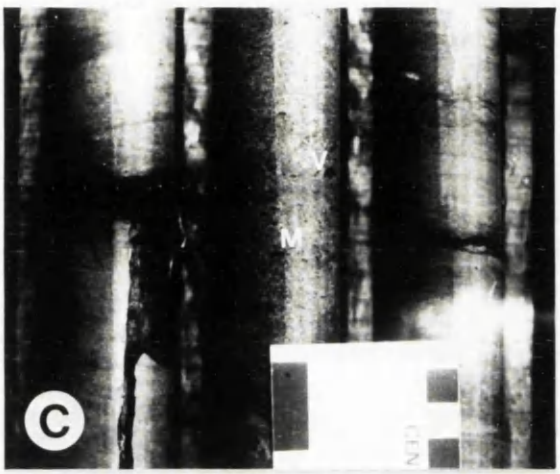
V
M
C

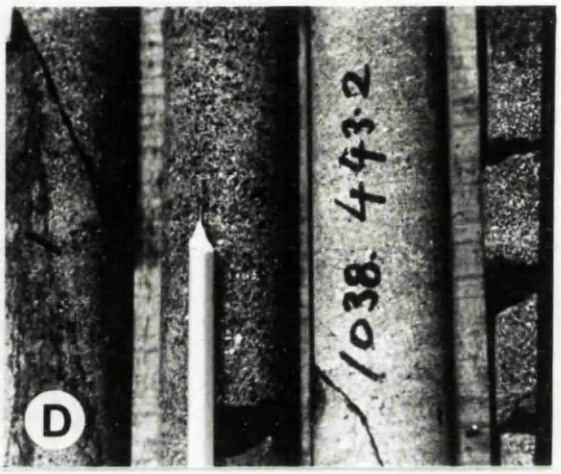
1038. 443.2
D

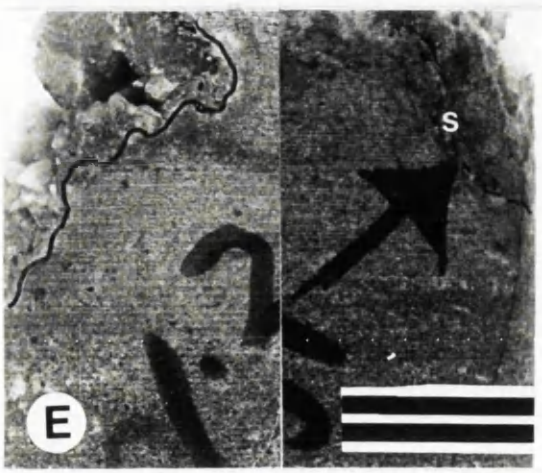
S
E

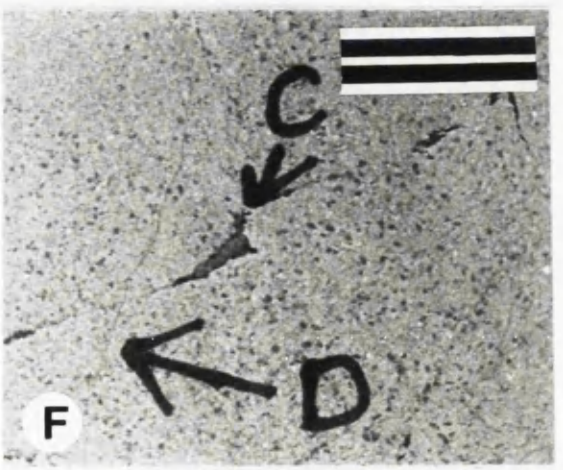
C
D
F


G

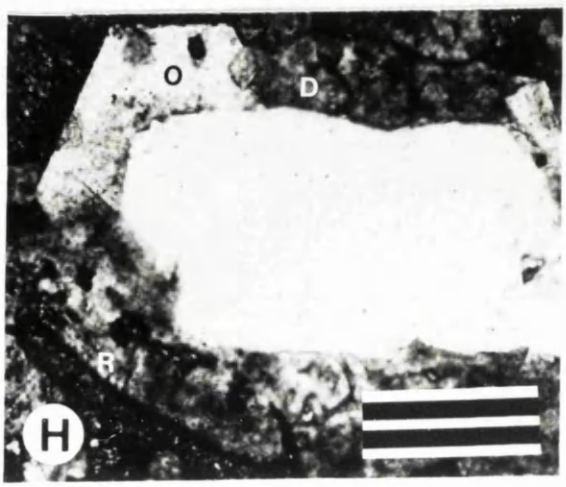
O
D
B
H

and is believed to be bitumen. Similar dark amorphous material is irregularly distributed between some rhombs.

5. Ferroan calcite cement lines some vugs and intercrystalline pores in the dolomite and overlies stage (3) dolomite crystals (Plate 5.5.B). In vugs this calcite forms crystals up to 8 mm in diameter. With Alizarin Red and Potassium Ferricyanide the cores of crystals stain deep purple while the outer margins stain deep red (Plate 5.5.C). Under CL crystals have a bright orange cores and bright yellow rims.

5. 6. CATHODOLUMINESCENCE.

5.6.i.Introduction.

Cathodoluminescence of the dolomites demonstrates complex zonal sequences within crystals with emission colours ranging from bright orange-yellow or red through to brown or non-luminescent. Zonal sequences have been divided into stages, the boundaries of which are defined by dissolution events. Brittle fracture occurred throughout dolomitzation. The general luminescence characters of the dolomite are considered here, their distribution is discussed in section 5.7. The bulk of unimodal dolomite mosaics consist of stage (1) crystals.

5.6.ii. Stage 1.

Stage (1) crystals are turbid and generally dully luminescent but may include up to six (average three) alternating dull light and dark crimson brown zones. Discrete light and dark rhombs indicate new nucleation events. The interfaces between zones may be planar or irregular with younger zones truncating earlier zones. Some crystals display up to three bright orange sub zones a few microns thick (Plate 5.5.D).

These zones may be overlain by bright, non-luminescent or dull CL zones but the younger additions are typically discordant on the inner zones (Plate 5.5.E). Therefore, by inference, dissolution appears to have modified the surfaces of the rhombs, truncating zones and forming intra crystal pores which extended along cleavage planes and the interfaces between zones (Plate. 5.5.F). Brittle fracture also took place at this time.

5.6.iii. Stage 2.

Stage two dolomite is divided into 3 substages, in chronological order these are; bright, almost non-luminescent, and dull. The bright stage consists of 2 subzones, an inner bright red zone and an outer bright orange yellow zone (Plate 5.5.G). The bright red contains faint subzones.

Where the stage (1) crystals remained free of dissolution the contact between the two is conformable. Elsewhere this bright red dolomite fills holes in stage (1), almost completely replacing some crystals, and lines fractures (Plate 5.5.H).

The bright orange-yellow zone which follows conformably contains up to seven faint subzones in hole N272 at depth 210.0 m. In a few examples a thin non-luminescent zone separates the two. In hole N272 at depth 276.0 m. the outer margins of crystals have an additional dull yellow zone. However, this is not seen elsewhere. In hole N794 at depth 213.0 m the contact between the bright red and orange-yellow zones is discordant, indicating modification by dissolution. In hole N272 at a depth of 229.0 m the bright orange yellow zone contains relic patches of bright red dolomite. A similar relationship has been described in Mississippian dolomite from the Mid continent USA (Choquette *et al,* 1992). At Navan the bright red and orange-yellow couplet lines biomoulds (Plate 5.6.A) and overgrows groups of stage (1) crystals to form the "composite crystals" (Plate 5.6.B) recently described by Choquette *et al,* (1992) from dolomite within the Burlington-Keokuk Formation, U.S. Mid Continent.

The 'non-luminescent' dolomite conformably follows the bright couplet. These crystals correspond to the saddle dolomite in polymodal fabrics. Generally non-luminescent rhombs contain up to four faint dark brown subzones and display a thin bright red rim (Plate 5.6.C). The non-luminescent dolomite also forms discreet crystals (Plate 5.6.D) indicating new nucleation and lines fractures (Plate 5.6.E). It may contain one or two non-luminescent sub zones a few microns thick. Generally the contacts between non luminescent and bright zones are conformable but occasionally they are separated by an irregular surface (hole N982 at depth 338.2 m). Finally the dully luminescent sequence consists of a light-dark-light crimson brown triplet. This conformably follows the non luminescent dolomite (Plate 5.6.F).

5.6.iv.Stage 3.

Stage (3) dolomite consists of large saddle dolomite crystals lining vugs. These are generally dull but display 7 concentric zones (Plate 5.6.G). The cores are dark crimson brown and are overlain by a thin light crimson brown zone. This is followed by dull orange, dull crimson brown and dark brown zones. The youngest zone is non-luminescent, and may carry up to 2 bright red zones. All contacts between these zones are conformable.

5.7. DISTRIBUTION OF DOLOMITE STAGES.

As noted in section 5.7 three cathodoluminescent stages each with a variety of zones have been recognised within the Navan dolomites. Generally stage (1) dolomite

PLATE 5.5. Cathodoluminescent features of the Navan dolomite.

A. Bitumen (arrow) overlying saddle dolomite. Hole N1021, scale in millimetres.

B. Blocky ferroan calcite (c) overlying saddle dolomite (d) in vug. Hole N1034 at depth 401.3 m. The core has been stained with Potassium Ferricyanide and Alizarin Red, the blocky calcite displays a purple-red colour. Scale bar = 1 cm.

C. Photomicrograph (plane light) of blocky calcite (c) in intercrystalline pores. Stained thin section. Sample from the Five Lens Dolomite, 1130 drainage drift, Mine Zone 2. Scale bar = 1 mm.

D. Photomicrograph (CL) of stage (1) dolomite. The dolomite crystals contain up to five zones. Contacts between zones are either irregular or planar, note both anhedral and euhedral cores. Hole N990 at depth 434.1 m. Scale bar = 150 microns.

E. Photomicrograph (CL) showing truncation of stage (1) dolomite zones (a). This 'solutional unconformity' has been overgrown by stage (2) dolomite (b). Hole N988 at depth 401.5 m. Scale bar = 200 microns.

F. Photomicrograph (CL) showing corrosive relationship between stage (1) dolomite (a) and stage (2) dolomite (b). The bright stage (2) dolomite extends into stage (1) crystals along linear micropores (arrows) interpreted as reflecting former cleavage surfaces. Hole N990 at depth 423.3 m. Scale bar = 200 microns.

G. Photomicrograph (CL) of stage (2) dolomite, bright substage. This shows the red inner zone and the bright orange-yellow outer zone. Hole N1005 at depth 207.3 m. Scale bar = 200 microns

H. Fracture cutting across stage (1) dolomite and lined with bright stage (2) dolomite. Hole N982 at depth 411.2 m. Scale bar = 100 microns.

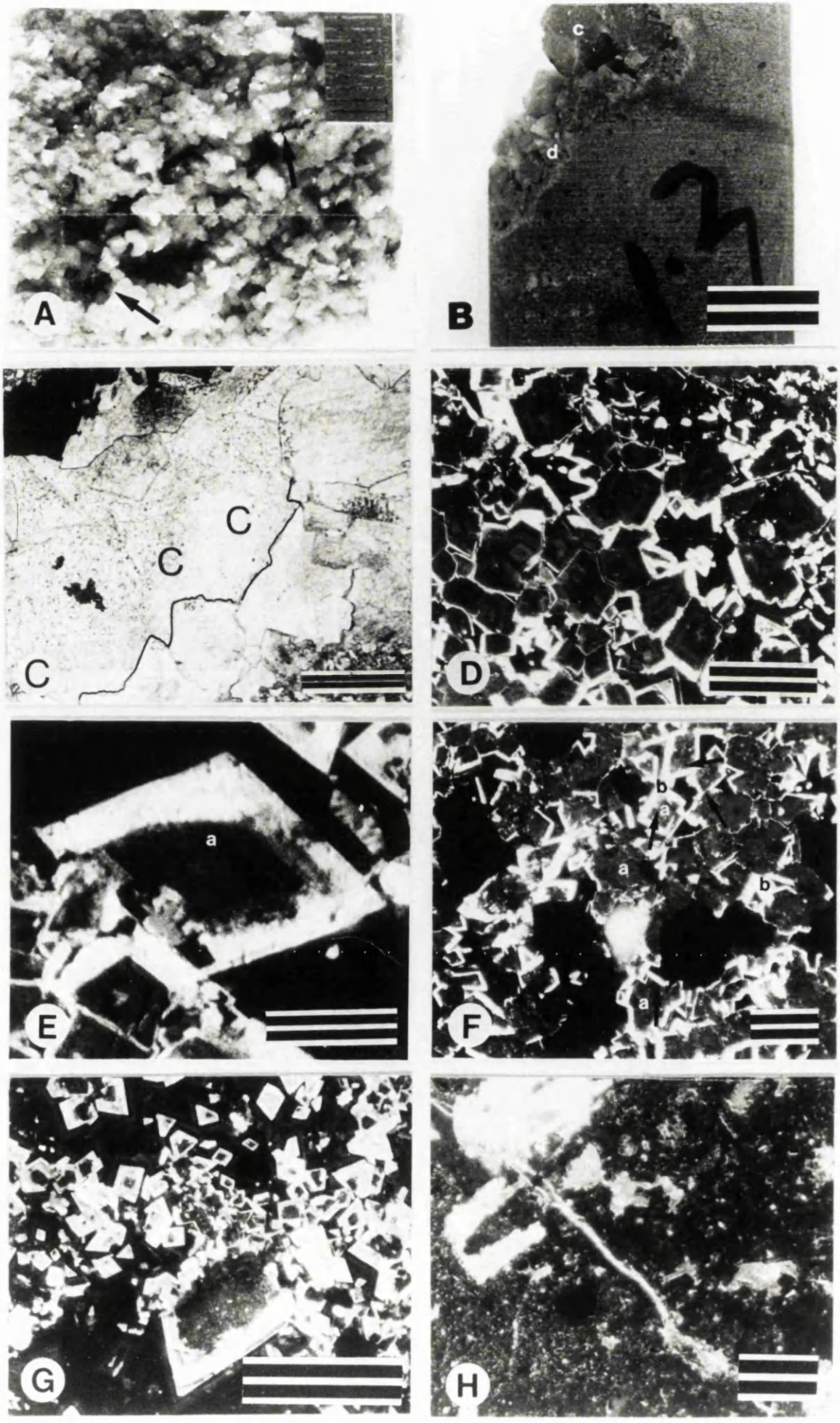
A
B
c
d
C
C
C
D
E
a
F
a
b
a
b
a
G
H

is common to all dolomite in the study. The later zones are volumetrically less significant and have a "patchy" distibution.

Stage (1) dolomite is present in every thin section from the massive dolomite, the Five Lens Dolomite and dolomite which extends along the Sub Lower and Lower Sandstone Markers. Anderson (1990) described similar pervasive dolomite. The dull crimson brown luminescent dolomite is ubiquitous but the orange subzones are rare and occur in only 20 thin sections from the massive dolomite (29 % of thin sections studied), 14 from the Marker dolomite (55% of thin sections studied), 11 from the Five Lens Dolomite (56% of thin sections)

The dissolution surface which truncates Stage (1) dolomite occurs almost throughout the Navan dolomites. It is present in 27 thin sections of massive dolomite (38% of those studied), 5 from the Five Lens Dolomite (14% of those studied) and 1 from the Marker dolomite (4% of those studied).

The overlying bright red stage (2) dolomite occurs in 25 of the thin sections examined (36% of those studied). It occurs in 3 thin sections from the Five Lens Dolomite (8% of those studied) and 2 from the Marker dolomites (8% of those studied). It is common in fractures which cut Stage (1) dolomite.

The bright orange- yellow zone which follows occurs in only 12 thin sections from the massive dolomite (17% of sections) and in only 2 from the markers (8% of sections). It is absent from the Five Lens Dolomite. The non luminescent zone which separates the bright couplet occurs in one thin section from hole N990 at depth 431.0 m. Generally this brightly luminescent couplet is most common at the core of the dolomite plume occurring in the Grainstone Unit. However, it gradually disappears along some stratal dolomite layers with increasing distance from the core (Fig. 5.11).

The non-luminescent dolomite occurs in 24 thin sections from the massive dolomite (40% of those studied), 27 thin sections from the Five Lens Dolomite (72% of those studied), and 12 from the Markers (48% of those studied). It also occurs within relic fenestral pores in the muddy cycles of the Micrite Unit and fills relic pores in grainstones. It is common in fractures.

The dully luminescent sequence of dark crimson brown and light crimson brown zones is present in only 4 thin sections from the massive dolomite (6% of thin sections), 1 from the Five Lens Dolomite (3% of thin sections), and 1 from the Marker dolomite (4% of thin sections studied).

The distribution of vuggy porosity is shown in Fig 5.12 and cross-sections 'A-A', 'B-B', 'C-C', 'D-D'. Such porosity is common in the massive dolomite, extending along the axis of dolomitization and over a vertical interval of 130.0 m

along the neck and up into the core. The vuggy zone is 350.0 m wide in sections 'B-B' and 'C-C' and is continuous along the axis for at least 500.0 m In cross-section 'B-B' a vuggy zone extends out along layers for over 400.0 m and is up to 10 m thick. The distribution in cross-section 'B-B' mimics the geometry of the dolomite body but is confined by it. In other sections ('C-C', 'D-D', and 'E-E') the distribution is patchy. The Lower Dark Marker Equivalent also displays vuggy porosity in hole N763 at depth 434.4 m and vugs are seen in the Five Lens Dolomite in hole N826 at depth 404.4 m and in hole N987 at depth 475.0 m (Plate 5.4.C). Stage (3) dolomite shows a limited distribution, lining vugs at the core of the massive dolomite and forming irregular patches along dolomite fingers.

5.8. STABLE ISOTOPES AND MICROTHERMOMETRY OF THE DOLOMITES.

5.8.i.Stable isotopes.

Twenty three stable isotope analyses of Navan dolomite have been made. Stage (1) and stage (2) and their respective zonal sequences could not be separated so bulk analyses were carried out in a manner similar to Mattes & Mountjoy, (1980); Choquette & Steinen (1980); Gawthorpe (1987) and Wilson *et al.* (1990). For techniques and procedures refer to Appendix 4. Eight samples from the Five Lens Dolomite, 8 from the stratal dolomite, 3 from massive dolomite, 2 of stage three crystals and 1 of the overlying calcite cement were analysed. The results are presented relative to the PDB standard in ‰.

The Five Lens Dolomite has $\delta^{18}O$ values which range from -6.6 to -10.4 (mean -7.55), $\delta^{13}C$ varies from +1.3 to +2.9 (mean +2.3). In the stratal dolomite $\delta^{18}O$ ranges from -7.5 to -10.1 (mean -8.7) and $\delta^{13}C$ ranges from -0.2 to +2.5 (mean +1.4). In the massive dolomite $\delta^{18}O$ values range from -7.7 to -8.4 (mean of -8.1), $\delta^{13}C$ from -0.2 to -0.8. Stage (3) crystals have a $\delta^{18}O$ of -10.0 to -6.7 with $\delta^{13}C$ ranging from +3.5 to +3.8. The calcite cement overlying stage (3) crystals has a $\delta^{18}O$ value of -8.2 with $\delta^{13}C$ of +2.5.

In addition 5 whole rock analyses of calcite grainstones within and adjacent to the dolomites gave $\delta^{18}O$ values from -6.7 to -5.4 (mean -6.3) and $\delta^{13}C$ ranging from +1.1 to +2.9 (mean +1.6).

These data are shown in Fig 5.13. All $\delta^{18}O$ values from both dolomites and grainstones are negative. However, those from dolomites are generally more negative. The range of $\delta^{18}O$ values from the Five Lens and stratal dolomite and the massive dolomite overlap considerably but $\delta^{18}O$ values from massive dolomite have a narrower range, probably reflecting the smaller number of samples. The $\delta^{13}C$ values of the dolomites are generally more varied than those of grainstones with dolomite

between vugs forming a group characterised by negative $\delta^{13}C$. The significance of these results is discussed in section 5.18.

5.8.ii.Microthermometry.

Fluid inclusions provide a valuable source of data on temperatures. The method is outlined in Appendix 4. Fluid inclusions containing vapour bubbles were heated at a rate of 10 ^{0}C per minute to establish a homogenization temperature. Six samples were examined from the Five Lens Dolomite, 8 from the massive dolomites and 2 from the stratal dolomites. The Five Lens Dolomite gave temperatures which range from 82.6 ^{0}C to 159.3 ^{0}C with an average of 123.2 ^{0}C. The massive dolomite gave temperatures ranging from 100.5^{0}C to 134.3^{0}C with an average of 114.9 ^{0}C. The stratal dolomites suggest temperatures from 59.7 ^{0}C to 102.3 ^{0}C with an averge of 81^{0}C (Fig. 5.14). These results will be disscussed in section 5.17.

5.9. THE SIGNIFICANCE OF DOLOMITE FRONT GEOMETRY.

5.9.i. Introduction.

Murray & Lucia (1967) noted that many carbonate rocks exhibit abrupt changes both vertically and laterally from limestone to dolomite. Simms (1984) suggested that dolomitization should reflect the circulation system within a platform. Braithwaite (1990) noted that there is no general correlation between a set of petrographic features and particular geological models and suggested that the most effective guides to the origin of a dolomite body are in geometry. Hardie (1987) stated "*there is a need to map in three dimensions dolomite front geometries in the hope that that their geometry will throw critical light on palaeo flow patterns*". Land (1991 pers commn.) commented that the geometry of dolomitzation should be a reflection of the fluid flow path and is therfore a key criterion in the elucidation of the dolomitization model.

This approach to the origin of massive dolomitization was recently undertaken by Wilson *et al.* (1990). Their assumption is that each dolomitization model should have its own characteristic circulation system reflected in the distribution of massive dolomite. The differences in dolomite front geometry can be used to determine which dolomite model is most appropriate. Wilson *et al.* (1990) suggested that this technique could prove useful to other massive dolomites with mappable boundaries. This hypothesis will be adopted in the following sections to help interpret dolomitization at Navan. Before this can be undertaken it is neccessary to describe the predicted geometry of dolomitzation for each model. These have been described by Wilson *et al.* (1990) and are shown in Fig 5.15. The geometries are described below and compared with examples from the geological record. For a disscussion of processes and products of each model see Appendix 3.

5.9.ii. Tidal Flat Dolomite.

Dolomitzation on tidal flats may be considered as a surficial process, produced by tidal or evaporative pumping of sea water to the surface. It produces thin laterally extensive dolomite layers. This pattern is shown by dolomite on Bahamian tidal flats (Shinn, 1983) and in the sabkha and hypersaline lagoons of the northern Arabian Gulf (Gunatilaka *et al*, 1984).

5.9.iii. Mixing zone dolomite.

In a mixing zone the interface between the fresh water lens and seawater forms a discrete concave upward lens. The geometry of dolomitization should therfore reflect this. Badiozamani (1973) suggested that dolomite bodies produced under mixing zone conditions should form either a single lens or a series of stacked lenses as a result of repeated sea level changes. This model is supported by the geometry of modern mixing zone dolomites from the Florida aquifer (Randazzo & Bloom, 1985) where drill core data indicate that the dolomite bodies form a vertical series of stacked lenses. This type of geometry has been described from ancient dolomites. The Mississpppian Ste. Genevieve limestone contains a series of dolomite lenses interpreted as reflecting mixing zones (Choquette & Steinen, 1980).

5.9.iv. Reflux dolomitzation.

Reflux of saline brines as described by Adams & Rhodes (1960) will produce a body of dolomite which consists of downwards projecting lobes with the volume of dolomite decreasing away from the source. This is supported by Simms (1984) who demonstrated the concept experimentally using a sand box. Simms was able to show that a slight increase in salinity from normal seawater of 35‰, to only 42‰, is sufficient to cause reflux.

5.9.v. Burial dolomitzation.

Dolomite produced during compaction-driven flow should form an elongate lens parallel to the platform margin flanked on the basinward side by a thick succession of shales. This geometry was described by Mattes & Mountjoy (1980) who mapped the dolomite front along the margin of the Devonian Miette build-up believed to be the result of compaction driven flow. The body consists of a massive unit which penetrates into the buildup as a series of stratal dolomite fingers interpreted as reflecting individual fluid flow paths.

5.9. vi. Hydrothermal dolomitzation.

Massive hydrothermal dolomite bodies are typically confined to limited areas. In plan they form circular or linear zones, with linear dolomitization reflecting tectonic controls. An example, from the geological record, is the dolomite at the Ruby Creek copper deposit, Alaska. This dolomite body is over 1 km wide and strikes NE for over 3 km. (Hitzman 1986a). A similar dolomite body has been described from the Lower Carboniferous Abbeytown Pb-Zn deposit of Ireland (Hitzman, 1986b).

Wilson *et al.* (1990) described the geometry of dolomite produced in a thermally driven hydrological system. Reference was initially made to the experimental work of Elder (1967,1977) in which the heating of fluid in a porous medium resulted in the formation of paired convection cells incorporating upward and outward directed flow paths. Wilson *et al.* (1990) were able to show that the theoretical geometry is supported by field mapping of dolomite fronts. A notable example is the dolomite body hosted by the Triassic Latemar build-up (Wilson *et al.* 1990). The dolomite is 800 m high and cuts across bedding. It consists of a neck 1 km in diameter and 400 m high. This passes up into massive dolomite 400 m high and over 2.5 km in diameter which consists of pods and lenses of dolomite related to fracture systems (Wilson *et al.* 1990, also personal observation of Latemar dolomite). The main dolomite body passes laterally into a stratally bound system of dolomite fingers, with the whole body having a plume-like geometry. As suggested by experiments, the core of the plume is the zone of most intense alteration represented by vuggy textures (personal observation of Latemar dolomite).

5.10. INTERPRETATION.

5.10.i. Introduction.

All available data must be utilized for the interpretation of massive dolomite (Land 1991 pers commn.). This section will consider the distribution, geometry, paragenetic sequence, timing, textures, stable isotope geochemistry and microthermometry of the Massive dolomite within the Grainstone Unit at Navan. The origin of the Five Lens Dolomite and dolomitzation which extends along the Lower Sandstone and Sub Lower Sandstone Marker will also be considered but emphasis will be placed on how these relate to the massive dolomite body in the Grainstone Unit.

5.10.ii. Geometry

Dolomite produced in a mixing zone should form a single or series of concave-up lenses. These are not present at Navan. The dolomite bodies in the mixing zone of the Florida aquifer described by Randazzo & Bloom (1985) do resemble the stratal

network at Navan. However, dolomite in mixing zones does not display the plume-like geometry seen at Navan. Other features believed to reflect mixing zone dolomitzation, include a palaeogeographic control on distribution, with dolomite extending parallel to the palaeo-shoreline. There is no evidence to suggest that the Navan dolomite occurs along an inner platform margin. It is emplaced in middle shelf grainstones and is distributed parallel to major fault systems.

The downward penetrating dolomite predicted by the reflux model with the volume of dolomite decreasing from a surficial source, is not represented at Navan. In addition, the thick sequences of evaporites expected adjacent to massive dolomite produced during seepage reflux is absent at Navan. These observations indicate that dolomitization at Navan is not the product of Seepage Refluxation.

The geometry of dolomite produced by compaction driven flow is similar to that of the Navan dolomite, since it consists of a massive body extending laterally along a stratal network (Mattes & Mounjoy, 1980). However, there are important differences; most importantly, there is no plume. There is no evidence at Navan for dolomitization from shales. There are no thick shales adjacent to the Navan dolomite and no sedimentological evidence to suggest that dolomitization occurs along a platform margin. It is reasonable to conclude that dolomitzation was not produced by compacting shales.

Experimental and field evidence have demonstrated that massive dolomitzation produced during hydrothermal circulation is;

1. Confined to a limited area.
2. Has a linear trend.
3. Has a plume shaped geometry.

These features compare with the distribution and cross-sectional geometry of massive dolomite in the Grainstone Unit at Navan. This evidence suggests, therefore, that the massive dolomite at Navan was the result of circulating hydrothermal fluids.

Wilson *et al.* (1990) quoting Freeze & Cherry (1979) described hydrothermal circulation. It is envisaged that once solutions become heated their buoyancy increases and they rise upwards and outwards along bedding producing a strata-bound network of dolomite fingers. The shape of the flow paths in a thermally driven system is governed by the Rayleigh number. The Rayleigh number is the ratio of buoyant to viscous forces (Wilson *et al.* 1990). For cool hydrothermal systems, heated fluids will rise and if vertical permeability is greater than horizontal permeability, flow will have a strong vertical component. If the horizontal permeabilty is greater the fluid will have a strong lateral component of flow, and dolomitzation will extend out along bedding.

For high Rayleigh numbers, the buoyant forces are much stronger, horizontal and vertical permeability become less influential and the fluid will form a concentrated plume. The plume circulates upwards and spreads laterally. If dolomitization occurs under these circumstances, the most intense alteration should occur along the core, where flow rates are at maximum values. This concept can be demonstrated experimentally using a sand box model. If coloured tap water is allowed to flow into thinly bedded dry sand under gravity, a massive zone of saturation is produced which then passes out along the sand layers producing a stratal network. The whole system is analogous to the geometry at Navan (Plate 5.6.H).

The gradual decrease in dolomitization toward the margin of a dolomite plume is believed to be a reflection of fluid volume flow rates; a function of temperature, hydraulic head and rock permeability, and the amount of magnesium; a function of the temperature and composition of the solution (Wilson *et al.* 1990). It is envisaged that as distance from the core of the plume increases, fluid velocity decreases, therefore rocks toward the margins of the system are exposed to less magnesium per unit time. Eventually, the capacity of a fluid to carry out dolomitzation is exhausted and a dolomite front is produced, even though fresh magnesium-bearing fluid is being continuously introduced at source.

The grainstone which hosts the Five Lens Dolomite extends throughout the study area. However, dolomitzation is not pervasive, it is confined to the mine area and has the same NE trend as the massive dolomite and, like the massive dolomite, the Five Lens Dolomite is spatially related to a major fault system. In addition fluid inclusion microthermometry from both bodies is the same.

The selective dolomitzation of these grainstones may be a reflection of the early cementation which the host grains underwent. Early calcite cementation would prevent the collapse of pores during passage into the burial environment. The estimated pre-dolomite porosity in the grainstones is believed to have been up to 10%. Thus grainstones having higher porosity than adjacent calcite mudstones were selectively dolomitzed. Dolomite extending along the Lower Sandstone and Sub Lower Sandstone Marker can be traced laterally into the neck of the dolomite plume (sections 'A-A'and 'B-B'). Such pervasive flow through the Pale Beds is also reflected in the distribution of sulphides in the Micrite Unit and overlying grainstones (Ashton *et al* 1986; Anderson 1990).

PLATE 5.6. Cathodoluminescent features of the Navan dolomite.

A. Photomicrograph (CL) showing a former biomold lined by stage (2) brightly luminescent dolomite. Note faint internal subzones in brightly luminescent dolomite. Scale bar = 250 microns.

B. Photomicrograph (CL) of stage (2) dolomite overlying groups of stage (1) crystals forming composite crystals at (A) and (B). Hole N272 at depth 210 m. Scale bar = 100 microns.

C. Photomicrograph (CL) of non-luminescent stage (2) dolomite. This conformably follows bright stage (2) dolomite and is followed by a red zone (R). Hole N908 at depth 345.8 m. Scale bar = 250 microns.

D. Photomicrograph (CL) of non-luminescent stage (2) dolomite in pore, indicating new nucleation. within oolitic grainstones in the Micrite Unit, hole N853 at depth 588.8 m. Scale bar = 250 microns.

E. Photomicrograph (CL) of stage (2) non-luminescent dolomite filling a fracture younger than stage (1) dolomite. Hole N982 at depth 411.2 m. Scale bar = 250 microns.

F. Photomicrograph (CL) of stage (2) rare dark-light-dark crimson brown dolomite (D) conformably following non-luminescent stage stage (2) dolomite. Hole N908 at depth 345.5 m. Scale bar = 250 microns.

G. Photomicrograph (CL) of stage (3) dolomite displaying internal zonal sequence. Hole N986 at depth 368.3 m. Scale bar = 250 microns.

H. Sand box analogoue for the dolomitization at Navan. Fluid flowing into dry sand under gravity produces an area of saturation. The fluid then flows laterally parallel to the layering as a series of stratal "fingers". Scale bar = 10 cm.

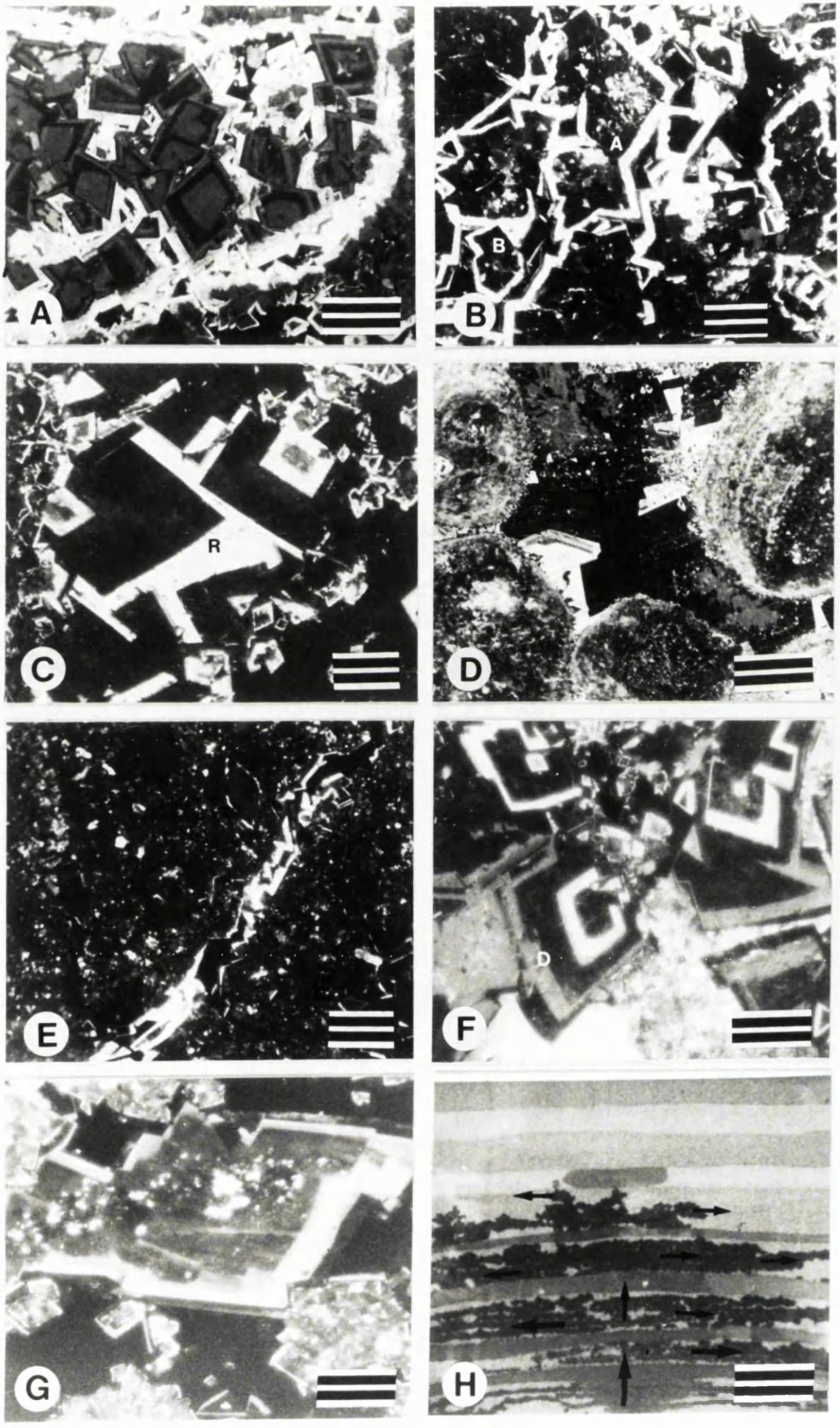
A
A
B
B
R
C
D
D
E
F
G
H

5.11. PARAGENESIS OF MASSIVE DOLOMITE.

5.11.i. Introduction.

It has been suggested that massive dolomitzation is not simply a matter of a single nucleation event, but one of several stages, with each stage defined by inter-rhomb dissolution and fracture events (ten Have & Heynen, 1985; Gawthorpe, 1987; review by Tucker, 1990c p.375). Additionally Wilson *et al.* (1990) stated that any given volume of fluid at a given temperature has a limited capacity to dolomitize and the production of massive dolomite will require repeated introductions of new volumes of fluids. Successive pulses of new fluid, reflected in several stages of crystal growth, have already been described from hydrothermal dolomite (Hitzman, 1986a, 1986b; Wilson *et al.* 1990).

5.11.ii.Paragenesis.

Pre-dolomite porosity in the grainstones is believed to have been low, perhaps up to 10%. Dolomitizing solutions may enter rocks with such low porosity and permeability via fractures, stylolites and micro-porosity (Braithwaite, 1989; Mountjoy, 1992). This has been proposed for the hydrothermal dolomite of the Triassic Latemar Build-Up, where dolomite first nucleated at the surfaces of grains and exploited linear micro-pathways (Wilson *et al.* 1990).

The stage (1) dolomite at Navan is volumetrically the most important and constitutes the main replacive stage. The dull CL emission colours suggest Fe^{2+} concentration approaching 10, 000 ppm but not exceeding 15, 000 ppm (Pierson, 1981; Fairchild, 1983). Up to five zones are present, indicating variation of iron concentration between zones. The zonal sequence within the rhombs points to differential substitution of Fe^{2+} for Ca^{2+} or Mg^{2+} which most likely reflects a fluctuating redox environment (Land 1985; review by Tucker 1990c p. 382).

Discordant relationships between zones indicate that crystal growth was punctuated by minor dissolution events which modified the surfaces of crystals. This demonstrates that the solution from which the crystals were growing became undersaturated episodically with respect to dolomite. The stylized sequence of growth is shown in Fig 5.16.

Stage (1) rhombs selectively replace calcite cement. Sibley & Gregg (1984) suggested that matrix-selective dolomitzation is produced when solutions are slightly undersaturated with respect to dolomite. The cement consisted of individual crystals which collectively would have had a greater reactive surface area (Murray, 1967: Sibley, 1980, 1982) than adjacent low magnesium calcite allochems, some of which consist of single crystals of calcite.

The discordant relationship between stage (1) crystals and later dolomite zones suggests that the precipitation of stage (1) was terminated by a dissolution event which modified the surfaces of rhombs, truncating concentric zonal sequences and producing small holes which redefined pores and increased porosity. Fracturing occurred during this event, and cut through Stage (1) rhombs. Collectively, dissolution and fracturing redefined pores and redistributed porosity.

Dissolution and fracturing were followed by nucleation of stage (2) bright red dolomite. This overgrew individual corroded rhombs and also enclosed groups of stage (1) rhombs, producing composite crystals and filling holes in stage (1) rhombs. This dolomite also fills fractures in stage (1) and replaces some bioclasts. Red emission colours are believed to reflect Fe^{2+} concentrations approaching 10, 000 ppm (Pierson , 1981). Discordant relationships between the yellow and red zones, and relic patches of red dolomite within the bright orange-yellow zone point to localised dissolution with some replacement. Bright orange-yellow emission colours are believed to reflect a decrease in Fe^{2+} concentration to less than 10, 000 ppm and an increase in Mn^{2+} concentrations from 100 to 1, 000 ppm (Pierson, 1981); however, Mn^{2+} concentrations as low as 30 to 35 ppm may cause luminescence (ten Have & Heynen, 1985).

Nucleation and growth of bright red and yellow zones modified pores and decreased porosity. This bright couplet lines mouldic pores indicating that dissolution of calcite occurred prior to crystallization of stage (2) dolomite. Faint subzones within both zones indicate minor fluctuation in bulk fluid composition during crystal growth. The dark outer rims in hole N272 at depth 276 m. (although rare) point to renewed uptake of Fe^{2+} reflecting concentrations at or just above 10, 000 ppm. Deposition of stage (2) dolomites was followed by a second phase of fracturing.

The bright red-orange yellow stage (2) couplet occurs within the massive dolomite at the core of the plume. It disappears laterally along stratal dolomite fingers and is rare in the Five Lens Dolomite and dolomite which extends along the marker horizons. The distribution of this zone suggests that the flow of pore fluids which precipitated this dolomite was concentrated in the plume core, and the occurrence of this dolomite in fractures indicates the importance of these as conduits.

The non-luminescent stage (2) dolomite overlies the red / orange-yellow zones or, where these are absent, rests directly on dull stage (1) dolomite. However, similar dolomite also forms new nuclei, filling remaining moldic pores, replacing bioclasts which had escaped dissolution, and filling fractures. The relationship between the non-luminescent overgrowths and the non-luminescent cements is unclear. Both styles

occur in the same thin section. This observation, together with more or less identical CL emmission colours, suggests they represent the same nucleation event. Non-luminescence is believed to reflect high concentrations of Fe^{2+} with total quenching equated with Fe^{2+} levels of >15, 000 ppm (Pierson, 1981; Fairchild, 1983). Faint internal subzones in both non-luminescent and bright red zones indicate minor fluctuations in pore water chemistry. A few irregular contacts between bright and non-luminescent zones point to localised dissolution. The final growths formed a dark-light-dark crimson brown triplet. Fractures which formed subsequently are filled with blocky ferroan calcite cement. The paragenetic sequence of stage (2) dolomite is shown in Fig. 5.17.

Two suggestions by ten Have & Heyenen (1985) explain the differential uptake of Fe^{2+} and Mn^{2+} during crystal growth.

1. Changes in bulk pore fluid chemistry occur (compare Meyers, 1974; Walkden, 1987; Emery & Dickson, 1989).
2. CL zones are not always a reflection of pore fluid chemistry. A change in the rate of crystal growth may be related to variations in the level of supersaturation of the solution. Where crystals grow slowly the lattice is able to sweep out impurities such as Mn^{2+} ions and thus exhibit less luminescence. During phases of rapid growth more Mn^{2+} ions incorporated producing bright emission colours.

Changes in bulk pore fluid chemistry may also be reflected in dissolution events (ten Have & Heyenen, 1985). Dissolution surfaces are common in the Navan dolomites, suggesting that changes in bulk pore fluid chemistry took place during dolomitization. However, it is not known if the variations in CL zones between stages reflect changes in the rate of crystallization or changing pore fluid chemistry. Intra stage dissolution surfaces support the latter interpretation.

5.12. EVOLUTION OF POROSITY.

Intercrystalline porosity may be generated during the following reaction;

1. $2CaCO_{3(s)} + Mg^{2+}_{(aq)} \rightarrow CaMg(CO_3)_{2\,(s)} + Ca^{2+}_{(s)}$ (after Weyl, 1960).

The pore fluids are believed to be undersaturated with respect to calcite with carbonate sourced by the indigeneous limestone. Thus as dolomite is precipitated calcite undergoes congruent dissolution. The reaction requires two moles of calcite to form one mole of dolomite. This results in volume reduction of 10% to 15% and is believed to be one way by which intercrystalline porosity is produced.

Reaction (1) could satisfactorily explain the generation of intercrystalline porosity at Navan during stage one dolomitization. However, evidence of dissolution of dolomite, the presence of dolomite cements, and the initial preservation of calcite show that pore fluids contained CO_3^{2-}, Ca^{2+}, Mg^{2+} (also Si, Fe^{2+} and Mn^{2+}). In addition, ghost allochems and relic calcite within dolomite rhombs indicate that solutions were not undersaturated with respect to calcite. This suggests that replacement of calcite by dolomite proceeded according to the reaction;

2. $CaCO_{3\,(aq)} + Mg^{2+}_{(aq)} + CO_3^{2-}{}_{(aq)} \rightarrow Ca\,Mg(CO_3)_{2(s)} + CO_3^{2-}{}_{(aq)}$
(modified from Morrow, 1982).

Isotopic evidence for this reaction is provided by the $\delta^{13}C$ values from the dolomites which are lower than $\delta^{13}C$ values from the limestones, pointing to an external supply of carbonate. In addition, dolomitization according to reaction 1 is believed to produce evenly disseminated porosity (Weyl, 1960) not observed within Navan dolomite. Such criteria were also used by Gawthorpe (1987) to elucidate the reaction process for burial dolomite in the Bowland Basin of England. If dolomitization takes place according to reaction (2) then intercrystalline porosity can be produced by dissolution of relic interstitial calcite (Braithwaite, 1990; compare Choquette *et al*, 1992).

Former biomouldic pores indicate that dissolution of calcite occurred following initial dolomitization. Corrosion of stage (1) rhombs indicates that porosity was also created by dissolution of dolomite. The timing of dolomite and calcite dissolution is problematical. However, former mouldic pores are lined by bright stage (2) dolomite, which also overlies stage (1) rhombs and may enclose groups of rhombs to produce "composite crystals". This demonstrates that both dolomite and calcite dissolution are pre-stage (2) dolomite and were probably contemporaneous. The evidence suggests that the porosity enhancement was an inherent part of the dolomitization process, produced by repeated dissolution of some calcite and dolomite. The suggested evolution of intercrystalline porosity is shown in Fig 5.18.

Further support for dolomitzation according to reaction (2) is provided by Sibley (1982). Individual crystals at Navan have cloudy cores and limpid outer zones. Sibley (1980) suggested that such crystals are produced by dolomitizing solutions which are slightly oversaturated with respect to calcite and therefore inclusions of calcite are incorporated in the centres of the rhombs. Later, as the waters become undersaturated with respect to calcite, inclusions within rhombs dissolve, with additional dissolution occurring around the rhombs and producing inclusion-free outer zones.

The truncation of zones within rhombs demonstrates that fluids episodically became undersaturated with respect to dolomite. This dissolution was finally expressed in the formation of vuggy porosity. The belief that dissolution is an inherent part of the dolomitization process is suppported by the observation that vuggy porosity only occurs within dolomite and is absent from adjacent limestones. The suggested evolution of vugs is shown in Fig 5.19. Intercrystalline and moldic pores were modified and enlarged by dissolution, linking to form irregular vugs over 10 cm in diameter.

Vugs truncate stylolites in hole N1034 at depth 401.3 m and stylolites adjacent to vugs are corroded. Vugs also extend along former calcite filled fractures, indicating that vug formation post dated fracturing, calcite cementation, and stylolite formation. Vuggy porosity is common in dolomites associated with Pb-Zn deposits. It is present in the Middle Devonian Presqu'ile dolomite of the Pine Point ore deposit (Quing & Mountjoy, 1991) and in the Middle Devonian Upper Elk Point Group (Dravis & Muir, 1991). In both examples the agents of dissolution are believed to have been hot saline acidic pore fluids. Vuggy porosity in the Lower Carboniferous burial dolomite of the Bowland Basin of northwest England was caused by acids released by degradation of organic matter by decarboxylation (Gawthorpe, 1987). This process is believed to result from the loss of -COOH group (review from Moore, 1989 p.267) which releases CO_2 and organic acids into pore fluids. Like the vugs in the Triassic Latemar dolomite, the vugs at Navan occur at the core of the dolomite body indcicating that the flow of fluid which produced the vugs was confined to this area.

Stage (3) Saddle dolomite crystals line these vugs. They provide evidence for continued passage of heated saline pore fluids, the ferroan nature of the dolomite crystals point to nucleation from anoxic pore fluids, with the zonation suggesting that anoxia fluctuated during precipitation.

5.13. TIMING OF DOLOMITIZATION.

There are several lines of evidence which point to the relative timing of dolomitzation. The features have been described from all dolomites at Navan.

1. Dolomite does not form early granular cements. As previously shown, in samples which contain only a few rhombs the dolomite is a late stage cement represented by non-luminescent bright red saddle dolomite crystals which overlie late blocky calcite cement. Such dolomite may also fill relic primary pores in grainstones and fenestral pores in mudstones. These relationships indicate that this dolomite was the last episode of pore fill cementation, as noted by Anderson (1990).

2). Where dolomitization is matrix selective scattered dully luminescent euhedral stage (1) crystals trucate the concentric zones of blocky pore fill cement (Plate 5.7.A) and

replace syntaxial calcite cements (Plate 5.7.B) and fracture fill calcite cement (Plate 5.7.C). From these observations, stage (1) dolomitization post dates blocky fracture and pore fill calcite cementation which itself post dates the remaining calcitic diagenetic sequence.

3) Pervasive dolomite contains ghost grains. It has already been shown that some shell-shaped ghosts are fractured while oolitic grains display spalled cortical layers which predated dolomitization. In dolomite which contains clastic grains, a few mica flakes wrap around adjacent grains (hole N975 at depth 429.2 m. Plate 5.7.D).

4. The surfaces of some relic grains are overlain by inclusion-rich layers. Some inclusions are elongate and orientated normal to grain surfaces. Similar inclusions from the Seroe Domi Formation of Curacao have been interpreted as relic calcite cement (Sibley, 1980 fig 3B). These features suggest that the dolomite post dates grain compaction, grain fracture and circumgranular calcitie cementation.

5. Authigenic quartz overgrowths cut across blocky calcite cement in adjacent grainstone. These quartz crystals thave been interpreted as reflecting growth under burial conditions. Within dolomite authigenic quartz has ragged anhedral outlines suggesting it has been corroded and replaced by dolomite (refer Plate 5.4.H).

6. Sutured seam stylolites are common in the Navan dolomites. These cut across stage (1) rhombs truncating internal zones and indicating that pressure dissolution post dates some dolomitzation (Plate 5.7.E). However, some stylolites contain dolomite which has the same bright orange red luminescence characteristics as the stage (2) dolomite, suggesting that some stylolite formation began after stage (1) dolomitization and during stage (2) (Plate 5.6.F).

Shinn & Halley (1984) reviewed the depths at which sylolites may form: Dunnington (1967) indicated depths of 600 m to 900 m while Buxton & Sibley (1981) suggested 1 500 m. Neugebauer (1974) suggested that dissolution is ineffective at depths less than 300 m and that significant pressure dissolution does not take place until at least 1000 m of burial. Saller (1984) using cores from Enewetak Atoll noted that pressure dissolution occurred after 800 m of burial. Meyers & Hill (1983) suggested that pressure dissolution can take place only after tens to hundreds of metres of burial. Bathurst (1975) cited numerous cases of shallow burial (a few metres) pressure dissolution.

These figures demonstrate that stylolite formation can occur during shallow or deep burial. At Navan dolomitzation postdates calcite cementation suggesting dolomitzation occurred after several hundred metres burial. Stylolites, which were produced during dolomitzation, most likey formed at a depth between 250 to 1 500 m Currently dolomite occurs at depths of 1 000 m.

PLATE 5.7. Timing of dolomitization at Navan.

A. Photomicrograph (CL) of stage (1) dolomite engulfing blocky calcite burial cement (C) and an oolith (O). The dolomite has also truncated fracture fill calcite cement (F). The Five Lens Dolomite, hole N982 at depth 433.9 m. Scale bar = 250 microns.

B. Photomicrograph (CL) of crinoid grain (C) with syntaxial calcite cement overgrowth (O). This has been truncated and replaced by Stage (1) dolomite (D). Scale bar = 250 microns.

C. Photomicrograph (plane light) of dolomite (arrow) post dating blocky fracture-fill calcite cement (C). Hole N876 at depth 162.6 m. Scale bar = 250 microns.

D. Photomicrograph (plane light) of bent mica flake (arrow) within dolomite suggesting dolomitzation has post dated compaction. N982 at depth 440.7 m. Scale bar = 250 microns.

E. Photomicrograph of sutured seam stylolite postdating dolomite (arrow). Hole N806 at depth 236 m. Scale bar = 250 microns.

F. Photomicrograph of sutured seam stylolite being occupied by bright red stage (2) dolomite (arrow). Hole N806 at depth 236 m. Scale bar = 250 microns.

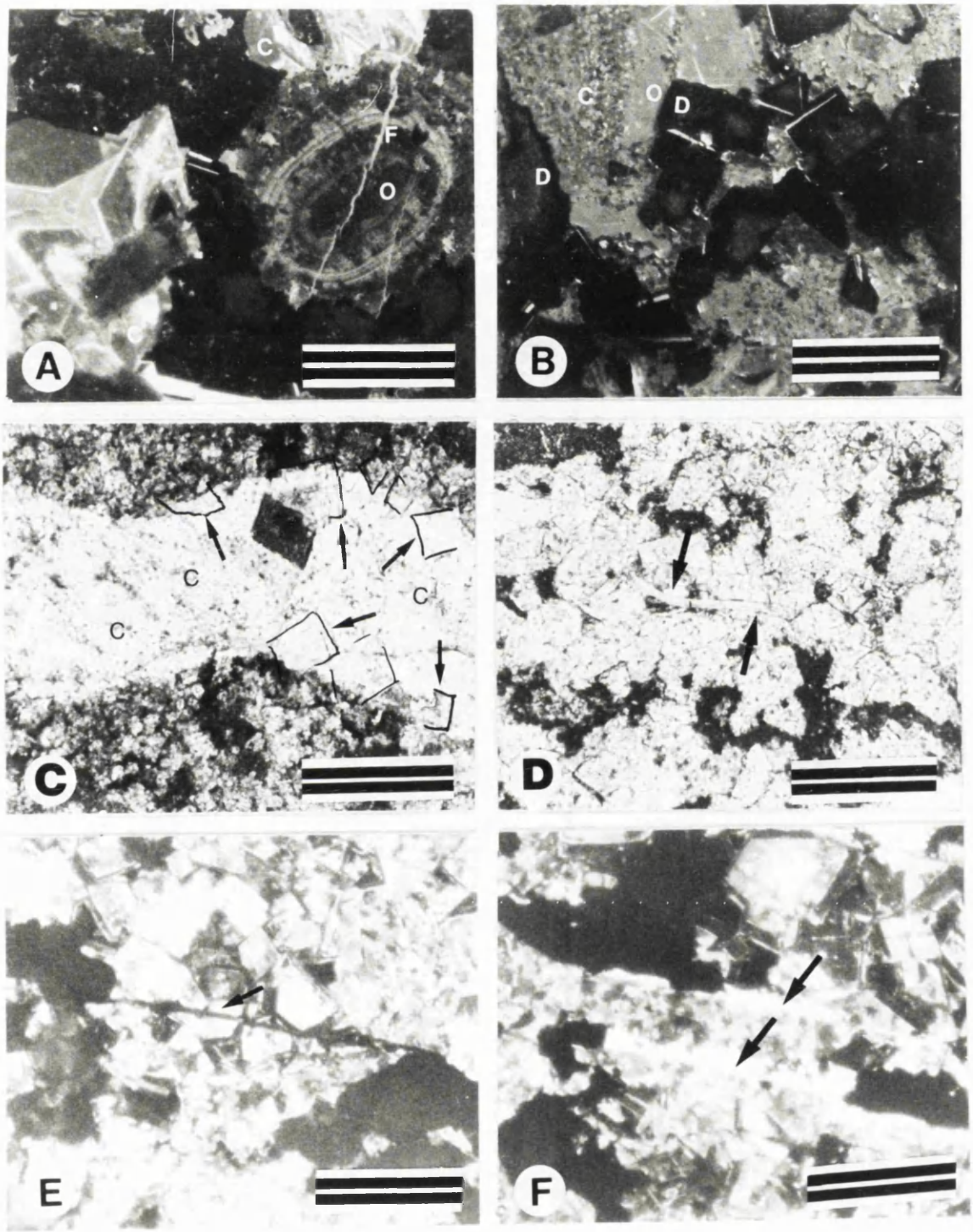
C
F
O
A
C
O
D
D
B
C
C
C
C
D
E
F

5.14. POST DOLOMITE DIAGENETIC EVENTS.

Calcite overlies stage (3) saddle dolomite and lines some intercrystalline pores. The blocky texture and ferroan composition are consistent with precipitation from pore fluids in the burial environment (Harris *et al.* 1985; Moore, 1989, Harwood, 1989). This is supported by a single $\delta^{18}O$ value of -8.2. This depleted value is most likely a reflection of fractionation between ^{18}O and ^{16}O during precipitation from heated fluids, i.e, preferential incorporation of ^{16}O into the solid as temperature increases (Fallick, pers commn. 1992). The $\delta^{13}C$ value is a typical of Carboniferous marine limestones (Dickson &Coleman, 1980). Bitumen overlies stage (3) saddle dolomite. This indicates that hydrocarbons flowed into the mine area, perhaps within the hot, saline fluids which precipitated the saddle dolomite. The bitumen is significant since it indicates that source beds in the region had passed through the oil generation 'window' of 70 ^{0}C to 100 ^{0}C which, in areas of normal geothermal gradients indicate burial depths of 2 to 3.5 km. (Tucker, 1987 p. 208). This is supported by Phillips & Sevastopulo (1986) and Jones (1992) who suggested from conodont alteration colours that the geothermal gradient was higher than normal in this region.

5.15. SIGNIFICANCE OF SADDLE DOLOMITE AND NON PLANAR TEXTURES.

Non luminescent saddle dolomite forms part of stage (2) dolomitzation and forms stage (3) dolomite and lines vuggy porosity. Radkhe & Mathis (1980) drawing upon examples from the Black Lake Field of Louisiana have documented the conditions under which saddle dolomite forms. Formation waters from the Black Lake Field, which bathe saddle dolomites, have salinities of 130 ‰ and a magnesium : calcium ratio of 1: 5. Saddle dolomite crystals are believed to reflect growth under elevated temperatures which favour the occupation of Mg^{2+} sites by Ca^{2+} producing a distorted crystal lattice. The range of temperatures under which saddle dolomite precipitates is 60 ^{0}C to 150 ^{0}C. Fluid inclusion temperatures from saddle dolomite in the Presqu'ile dolomite of the Pine Point Pb-Zn deposit suggested temperatures of 90 ^{0}C to 110 ^{0}C (Qing & Mountjoy, 1991). Gregg & Sibley (1984) produced saddle dolomite crystals experimentally over a temperature range of 250 ^{0}C to 300 ^{0}C. Non-planar fabrics occur at the core of the plume in hole N975. Such fabrics have been interpreted by Gregg & Sibley (1984) as reflecting precipitation from heated pore fluids. Gregg & Sibley (1984), drawing upon crystal growth theory, envisaged that below 50 ^{0}C crystal growth takes place by the addition of atoms layer by layer, producing smooth crystal faces. Above a certain temperature, the Critical Roughening

Temperature, atoms are added randomly to the crystal surface, the crystal surfaces produced are not planar and form an interlocking anhedral mosaic. It was suggested by Gregg & Sibley (1984) that the temperature at which the nonplanar fabrics form is between 60 ^{0}C to 100 ^{0}C. Saddle dolomite is common within stage (2) dolomitization and forms stage (3). This increase in saddle dolomite is thought to be a reflection of pore fluids becoming progressively more heated and saline.

5. 16. MICROTHERMOMETRY.

Two-phase aqueous fluid inclusions are common in dolomite produced under burial conditions (Mountjoy, 1991) and indicate a trapping temperature of greater than 50 ^{0}C (review by Moore 1989 p.71). Fluid inclusions within the Navan dolomites were selectively chosen for study. Those occuring as linear trails, or aligned along cleavage traces, or showing signs of necking were discarded. Homogenization temperatures obtained range from 59.7 ^{0}C to 159.3 ^{0}C and support the view that dolomite precipitated from hydrothermal fluids. However, the scatter of temperatures which in one sample span nearly the whole range, suggest that the homogenization temperatures must be regarded with suspicion.

Presbindowski & Larese (1987) demonstrated experimentally that fluid inclusions trapped within calcite are likely to stretch during basin subsidence. Burial heats the trapped fluid producing thermal expansion. If stress exceeds the confining strength of the mineral, stretching occurs. This change in volume resets the homogenization temperatures of the population with the final homogenization temperature recording maximum burial temperature.

However, precautions were taken: only those inclusions within crystal zones were chosen for study. In these the ability of the enclosing mineral to withstand the internal pressure exerted by thermal expansion is at its greatest. In addition, small fragments of wafer were analysed separately to avoid repeated over-heating of the whole wafer. The homogenization temperatures obtained vary from 59.7 ^{0}C to 159.3 ^{0}C and in general accord with microthermometry data from other dolomites believed to have been precipitated from heated pore fluids. Hydrothermal dolomites from the Triassic Latemar buildup have homogenisation temperatures of 75 ^{0}C to 220 ^{0}C, again comparable to the Navan data. In these inclusions there are no signs of necking. Variations are interpreted as reflecting entrapment of fluids of different temperatures (Wilson *et al.* 1990). Recently the Cambrian Boneterre Dolomite of the SE Missouri Pb-Zn district has yielded homogenization temperatures ranging from 60 ^{0}C to 187 ^{0}C. These data were interpreted as reflecting entrapment of mixed cool and heated pore fluids (Shelton *et al,* 1992). A similar range of temperatures are recorded from dolomitized Waulsortian Limestones at the Lisheen Pb-Zn deposit, County Tipperary.

The homogenization temperatures in the last, range from 105 ^{0}C to 237 ^{0}C. This range is interpreted as reflecting some stretching of inclusions during late burial but the formation temperature is believe to have been around 75 ^{0}C to 100 ^{0}C (Hitzman *et al,* 1990). Considerations of these examples suggests either:

1. Fluid inclusions at Navan have not been reset and reflect the entrapment of fluids at different temperatures.
2. Some fluid inclusions at Navan have been reset but not the entire population and thus inclusions record some primary information.

Since fluid inclusions are widely believed to be susceptible to resetting point (2) is the more prudent interpretation. The suggested likely entrapment temperature of the pore fluids around 60 ^{0}C to 100 ^{0}C.

5.17. STABLE ISOTOPES.

The oxygen isotope composition of a mineral precipitated under conditions of isotopic equilibrium, is controlled by its temperature of formation and by the oxygen isotopic composition of the water from which it formed. However, the exact relationships between the isotopic composition of dolomite, the isotopic composition of the water from which it formed, and the temperature of formation, is not known, since it has not proved possible to precipitate dolomite at sedimentary temperatures (Land 1980, 1985, Hardie 1987).

However, dolomite is relatively easy to precipitate at high temperatures (Gaines, 1980; Gregg & Sibley, 1984) and extrapolation from the $\delta^{18}0$ produced during high temperature experiments to low temperatures suggest that at 25 ^{0}C dolomite should be enriched in $^{18}0$ by +4 to +7 ‰ (Land, 1980). Some support for this fractionation value is provided by modern marine environments where dolomite is enriched with $\delta^{18}0$ relative to calcite by between 1 to 7 ‰, averaging 3 ‰ (Land, 1985). However, one problem with these data is that dolomite, although co-existing with calcite, has not been proven to be coeval with it (Land 1980).

Negative $\delta^{18}0$ values from ancient dolomites may reflect precipitation from (1) isotopically light ancient sea water (2) from meteoric water, or (3) from heated pore waters (Land, 1985). The possibility of an isotopically light Palaeozoic ocean has not been proven (Land, 1985) and it is not kown if Carboniferous seawater was isotopically light (Dickson & Coleman, 1980). Mattes & Mountjoy (1980) noted that secular variation in ^{18}O / ^{16}O bear no relationship to re-equilibrium through diagenetic reactions, therefore, secular variation is not considered further. The $\delta^{18}O$ values of the Navan dolomite are negative and are depleted relative to adjacent limestones. Machel & Anderson (1989) used a similar relationship to support the view that dolomitization

was not contemporaneous with near surface calcite cementation, ruling out a reflux or mixing zone origin for dolomite in the Nisku Formation of Alberta.

At Navan petrographic evidence and dolomite front geometry indicate that dolomitization is not the product of cool meteoric pore fluids. Thus it is unlikely that the negative $\delta^{18}0$ values are a reflection of cool pore fluids. This leaves only one alternative, that the negative $\delta^{18}O$ values of the Navan dolomite reflect precipitation from heated porewaters. This is supported petrographically by saddle dolomite which is widely believed to precipitate from hot saline pore fluids and by the microthermometry data which has yielded homogenization temperatures from 60 ^{0}C to 159 ^{0}C.

This interpretation is supported by comparison with other examples of $\delta^{18}0$ values of dolomites believed to have precipitaed from heated pore fluids.The hydrothermal dolomite within the Triassic Latemar platform has $\delta^{18}O$ values which range from -9.57 to -1.85 ‰ PDB (Wilson *et al.* 1990) while values from burial dolomite of the Bowland Basin range from -11.44 to -3.71(Gawthorpe 1987), and burial dolomites from Canada from -2.3 to -11.5 (Mattes & Mountjoy, 1980). The distribution of these fields relative to the Navan $\delta^{18}O$ values are shown in Fig 5.20. However since $\delta^{18}0$ depends not only on temperature but also on the original fluid $\delta^{18}0$, such comparisons of $\delta^{18}0$ are of limited validity unless the respective fluid $\delta^{18}O$ values are known (Fallick pers commn, 1992).

Since the Navan $\delta^{18}0$ values are whole rock values derived from both type (1) and type (2) crystals they must be considered as averages only. Crystals are zoned in a complex fashion and represent multiple nucleation events with Fe^{2+} concentration reflecting fluctuating oxygen content. Each zone probably has its own $\delta^{18}0$ value. Limestones on the Isle of Man have $\delta^{18}0$ values varying between cements (Dickson & Coleman, 1980). Intra-zonal $\delta^{18}O$ values within blocky calcite cement from the Lower Carboniferous of Wales, vary from -3.1 to -11.0 ‰ (Dickson *et al*, 1990).

It is widely believed that the $\delta^{13}C$ values of dolomite reflect the $\delta^{13}C$ values of the precursor limestone (Mattes & Mountjoy, 1980, Duham & Olson, 1980 and Choquette & Steinen, 1980). This stems from the fact that the 'reservoir' of carbon within the carbonate precursor mineral is much greater than that in the pore fluids, as a result of the relative insolubility of CO_2 (Land, 1980, 1985). The $\delta^{13}C$ of modern sea water ranges from -2 to +4 which is compatible with the $\delta^{13}C$ of ancient dolomites (Land 1980). Most Carboniferous marine carbonates have $\delta^{13}C$ values ranging from 0 to +4 PDB (Dickson & Coleman, 1980 fig. 4). These values are very common in ancient dolomite and are believed to reflect marine signatures.

Strongly negative $\delta^{13}C$ values of around -20.0, beyond the marine carbon range, are believed to reflect thermally induced decarboxylation or sulphate reduction.

Carbonates with such negative $\delta^{13}C$ values are believed to have reacted with, or precipitated from pore waters whose carbonate was supplied as a by product of such reactions (Irwin, Curtis & Coleman, 1977). The $\delta^{13}C$ values of the Navan dolomites vary from -0.85 to +3.8 and are therefore within the marine carbonate field, suggesting that the $\delta^{13}C$ values reflect those of the precursor limestone. This is supported by comparison with the $\delta^{13}C$ values of adjacent undolomitzed limestones.

It has also been suggested that marine carbon signatures recorded from late cements and massive dolomite may not be a reflection of the precursor limestone $\delta^{13}C$ values (Mattes & Mountjoy, 1980 review by Moore, 1989 p.265). It was proposed that the $\delta^{13}C$ may originally have been negative but subsequently underwent buffering by the resevoir of marine carbon during replacement reaction with the limestones.

The negative $\delta^{13}C$ values (-0.22 to -0.85 PDB) from the massive dolomite at Navan may originally have been more strongly negative, with present values reflecting buffering by the reservoir of marine carbon within the limestones during replacement reactions. However this is unproven and the negative $\delta^{13}C$ values fall within the marine carbon field.

Stage (3) saddle dolomite crystals which line vuggy porosity are not replacive. They must have precipitaed directly from solutions flowing through the vugs. The $\delta^{13}C$ values vary from +3.3 to +3.8 ‰ PDB, typical of Carboniferous marine carbonate values.

It appears that most $\delta^{13}C$ values are marine reflecting the precursor limestone and inherited during the replacement reaction. Negative $\delta^{13}C$ values may reflect originally isotopically light carbonate which has undergone buffering during replacment reactions. The yougest stage (3) saddle dolomite precipitaed directly from pore fluids, the carbon value of this is still typically marine.

5.18. SYNTHESIS.

Massive dolomitzation at Navan is confined to an elongate body which strikes NE-SW and is spatially related to the major fault system in the mine. Elevations through the dolomite reveal a plume-like geometry approximately 145 m high and 1.5 km wide. The plume is interpreted as reflecting circulation of heated pore fluids.

The dolomite post-dates calcite cementation and the replacment reaction was mole for mole. Texturally the dolomite is unimodal to polymodal with planar subhedral and occasionally non planar fabrics. Under CL a complex zonal sequence is revealed, reflecting several growth stages separated by dissolution and fracture surfaces.

Stage (1) is replacive and dully luminescent and consists of up to five zones. Stage (2) dolomite consists of up to six zones with emission colours which range

from bright orange yellow to dark brown to non-luminescent. Deposition of this was followed by the formation of vuggy porosity lined by Stage (3) saddle dolomite.

Stage (1) dolomite is pervasive and volumetrically the most significant. Stage (2) has a patchy distribution with most zones confined to the core of the dolomite plume. Vuggy porosity is also confined to the core of the dolomite plume and stage (3) dolomite lines vugs.

The original dolomitizing solution is believed to have been sea water. This sea water was modified in several ways. The occurrence of saddle dolomite suggests that it became heated and was of above average salinity. Saddle dolomite forms a significant portion of stage (2) and stage (3) dolomites. This suggests that dolomitizing solutions became heated during the final stages of dolomitzation. The $\delta^{18}0$ values and fluid inclusion microthermometry support the view that dolomitizing solutions were heated. Consideration of the CL emission colours suggests that the seawater contained Fe^{2+} and Mn^{2+} and experienced fluctuating anoxic conditions. Dissolution textures and dolomite cements indicate that the solutions carried CO_3^{2-}, Ca^{2+} and Mg^{2+}. The carbon values most likely reflect the $\delta^{13}C$ of the precursor limestone. The relationship between dolomitzation and mineralization, with respect to timing and distribution, is discussed in Chapter 7.

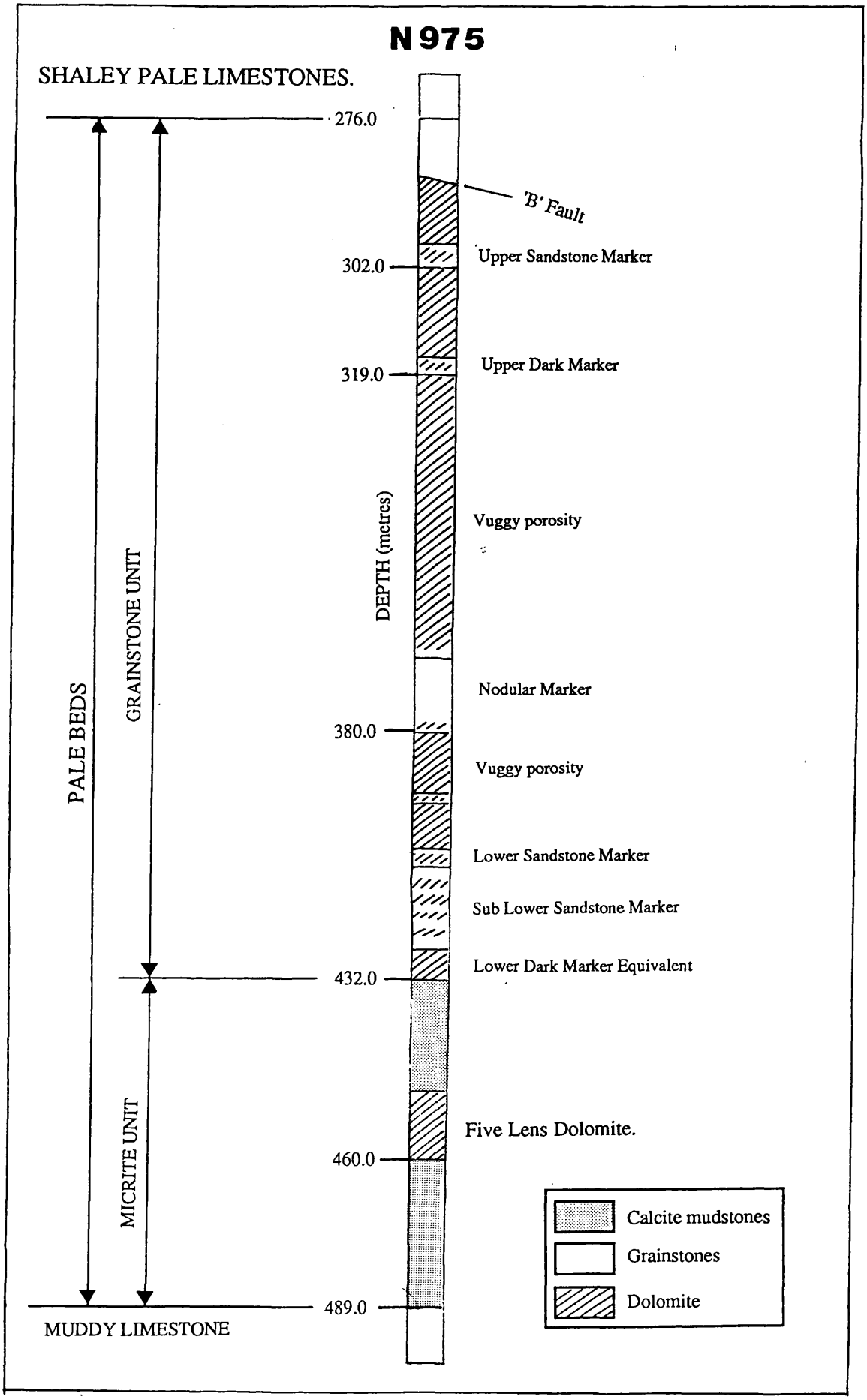

Fig. 5.1. Diagram showing generalized distribution of dolomite in the Pale Beds. Hole N975, western mine area.

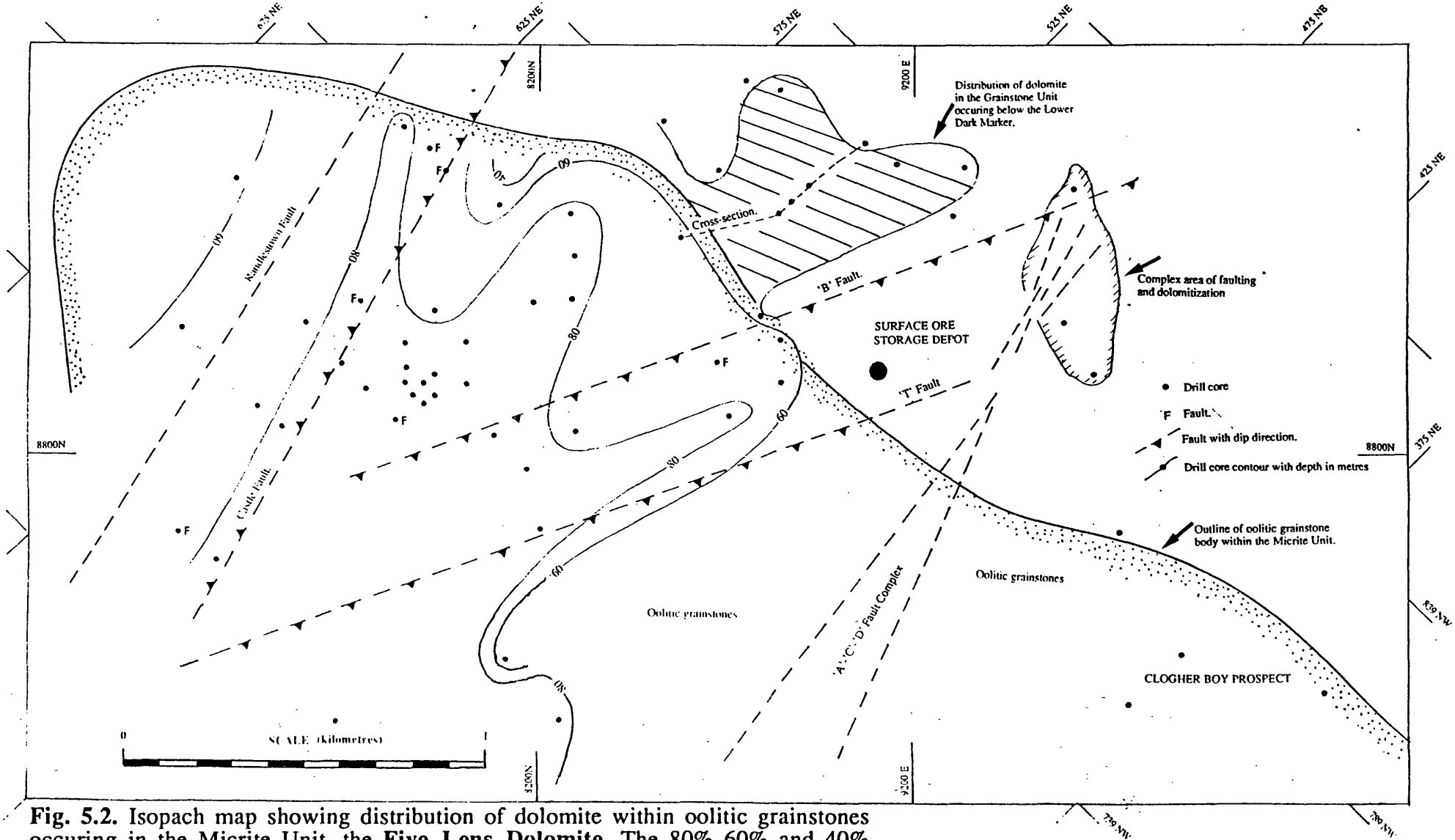

Fig. 5.2. Isopach map showing distribution of dolomite within oolitic grainstones occuring in the Micrite Unit, the **Five Lens Dolomite.** The 80% 60% and 40% contour lines define lobes which apparently extend along and between major faults. Striped zone indicates distribution of dolomite below the Lower Dark Marker. This dolomite occurs at the same stratigraphic interval as the Five Lens Dolomite. Refer to **Fig. 5.6.** for cross-section.

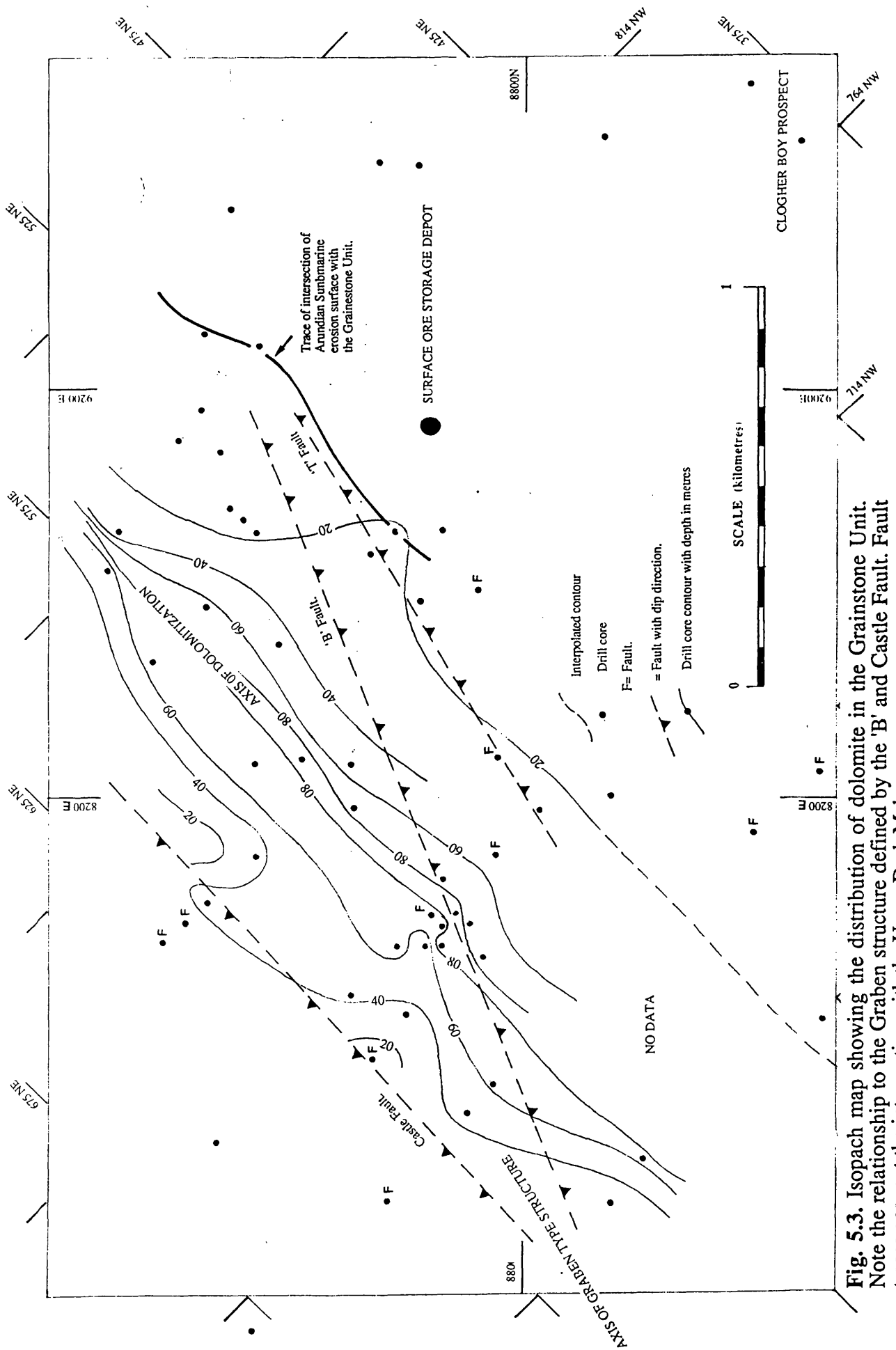

Fig. 5.3. Isopach map showing the distribution of dolomite in the Grainstone Unit. Note the relationship to the Graben structure defined by the 'B' and Castle Fault. Fault traces occur at the intersection with the Upper Dark Maker

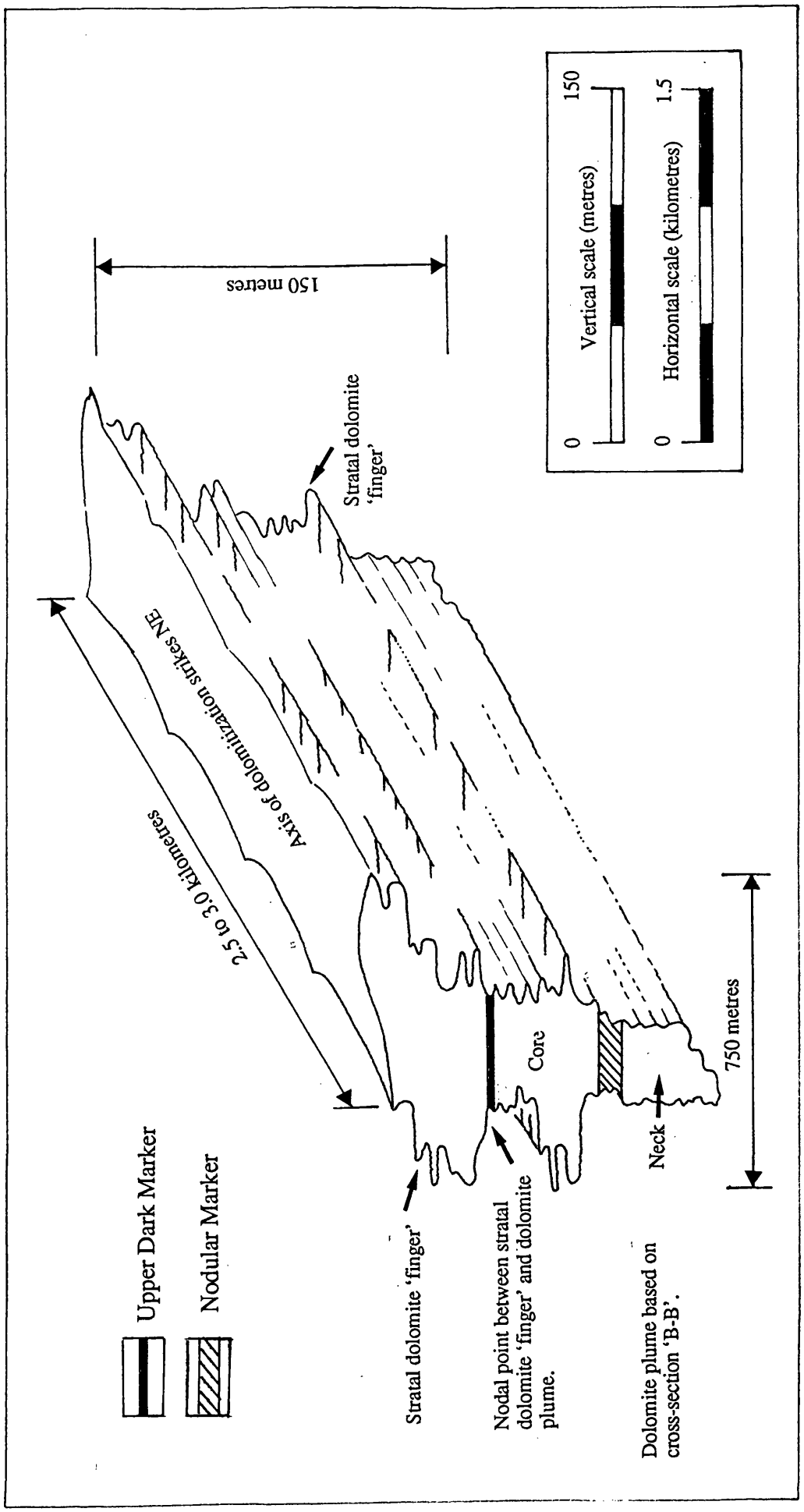

Fig. 5.4. Simplified three dimensional geometry of the Dolomite plume occuring in the Grainstone Unit. The diagram is based upon **Fig. 5.3** and cross-sections 'B-B', 'C-C', 'D-D' and 'E-E'.

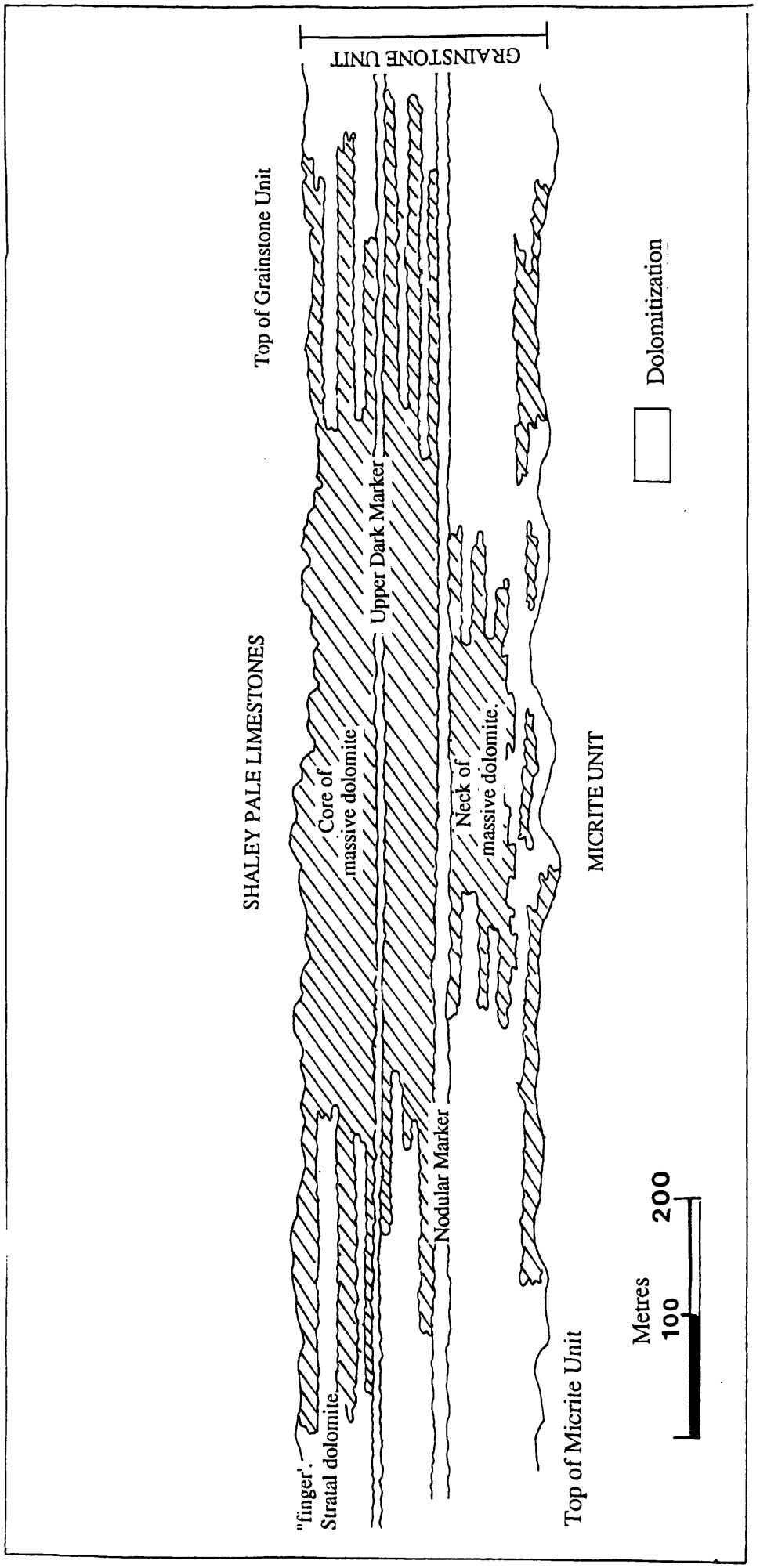

Fig. 5. 4a. Sketch of dolomite "plume " in Grainstone Unit, actual scale.

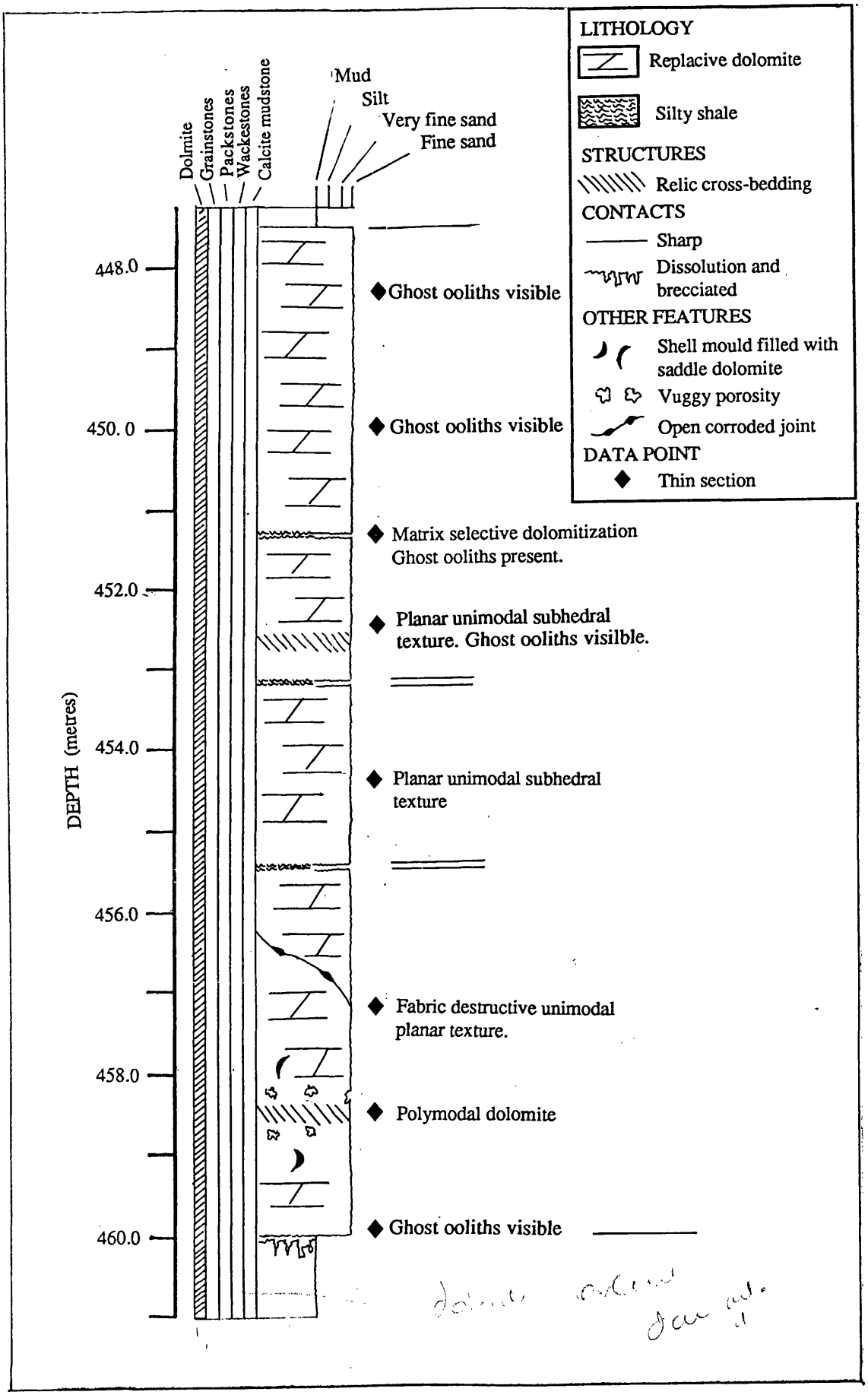

Fig. 5.5. Summary log of the Five Lens Dolomite. Thin sections contain ghost ooliths, note relic cross-bedding. Hole N975.

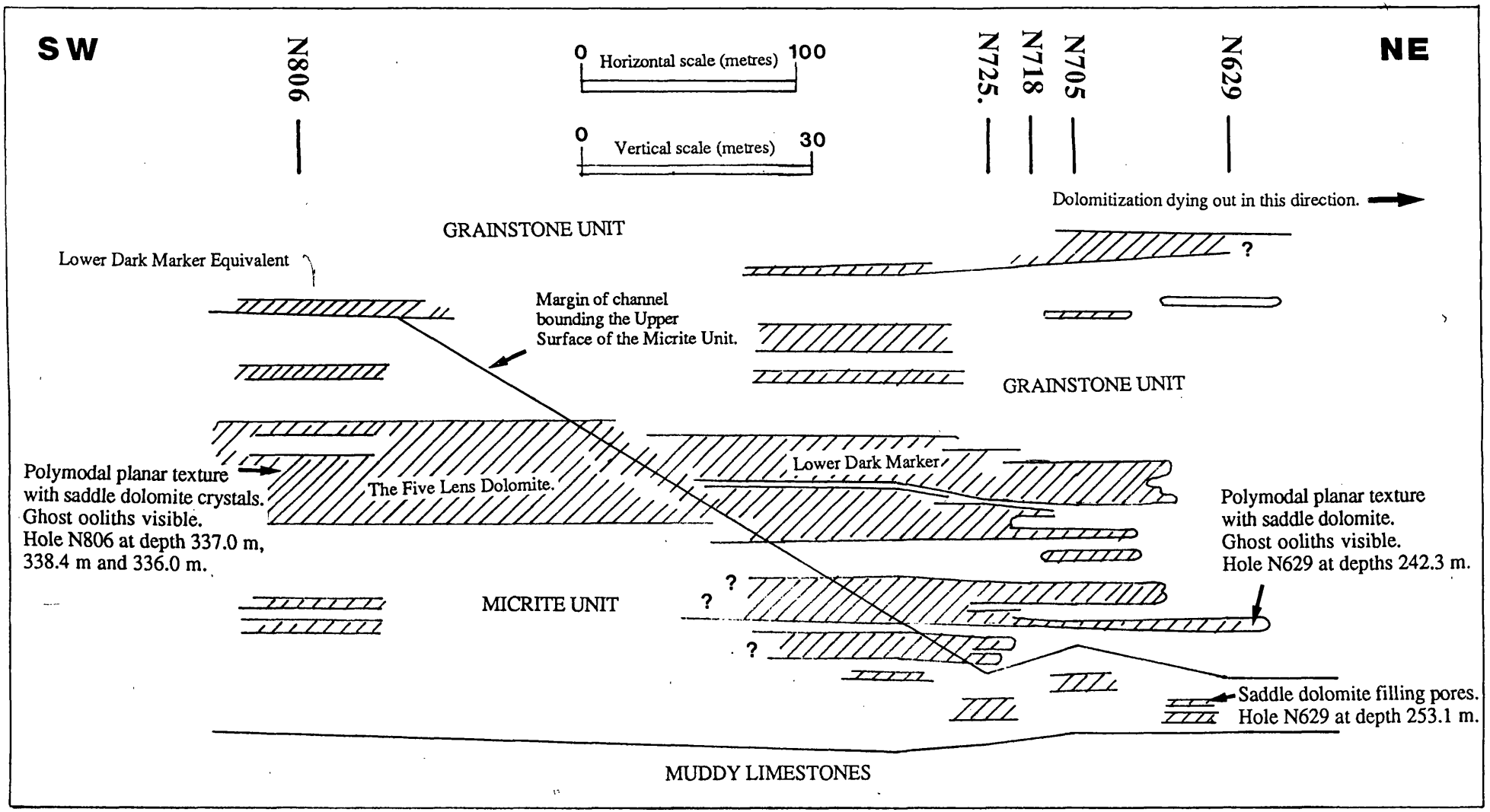

Fig. 5.6. Cross-section showing dolomitization extending from the Five Lens Dolomite and cutting across the margin of the channel which bounds the upper surface of the *Micrite Unit* in the eastern mine area. Note dolomitzation dying out toward the NE. For location of cross-section refer to **Fig. 5.2.**

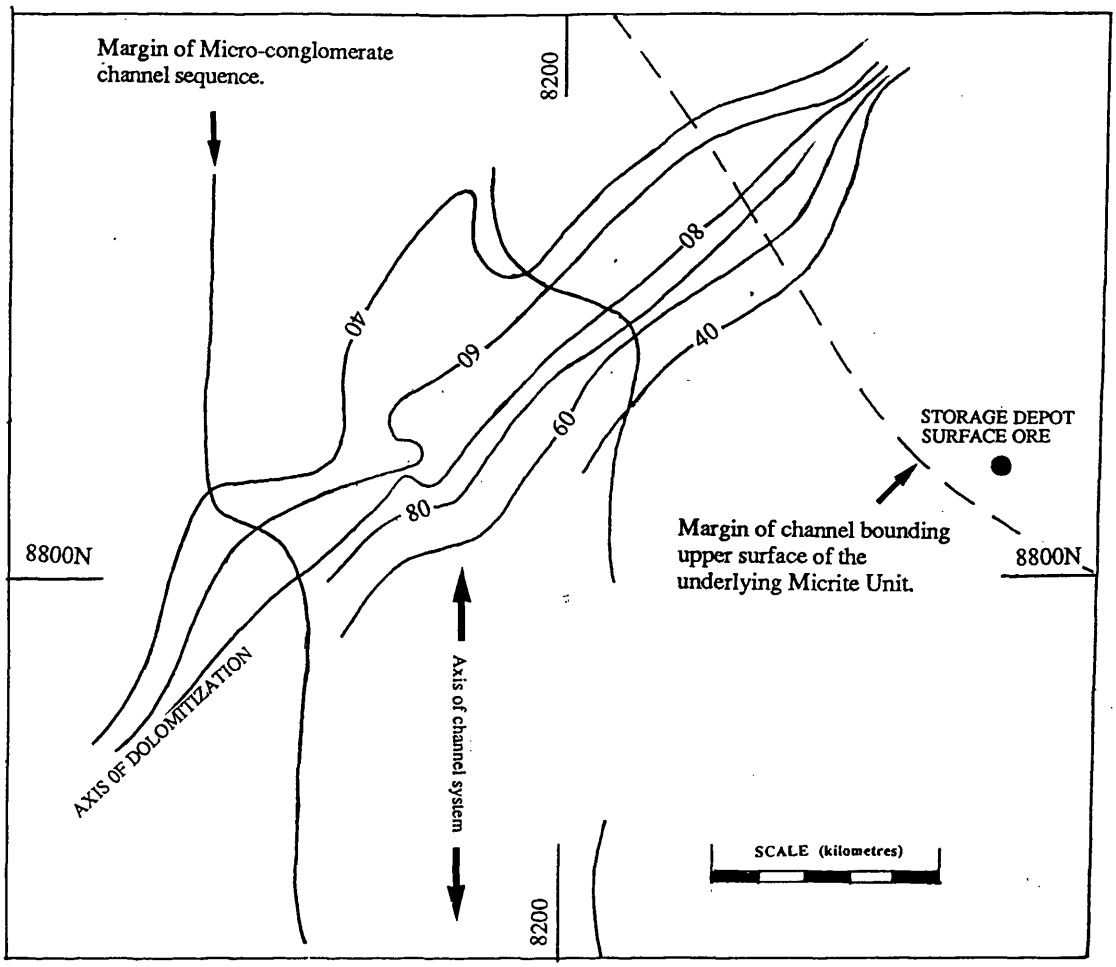

Fig.5.7. Diagram illustrating the strike of dolomitzation in the Grainstone Unit in relation to the 'Micro-conglomerate' channel sequence and the margin of the channel which bounds the upper surface of the Micrite Unit in the eastern mine area.

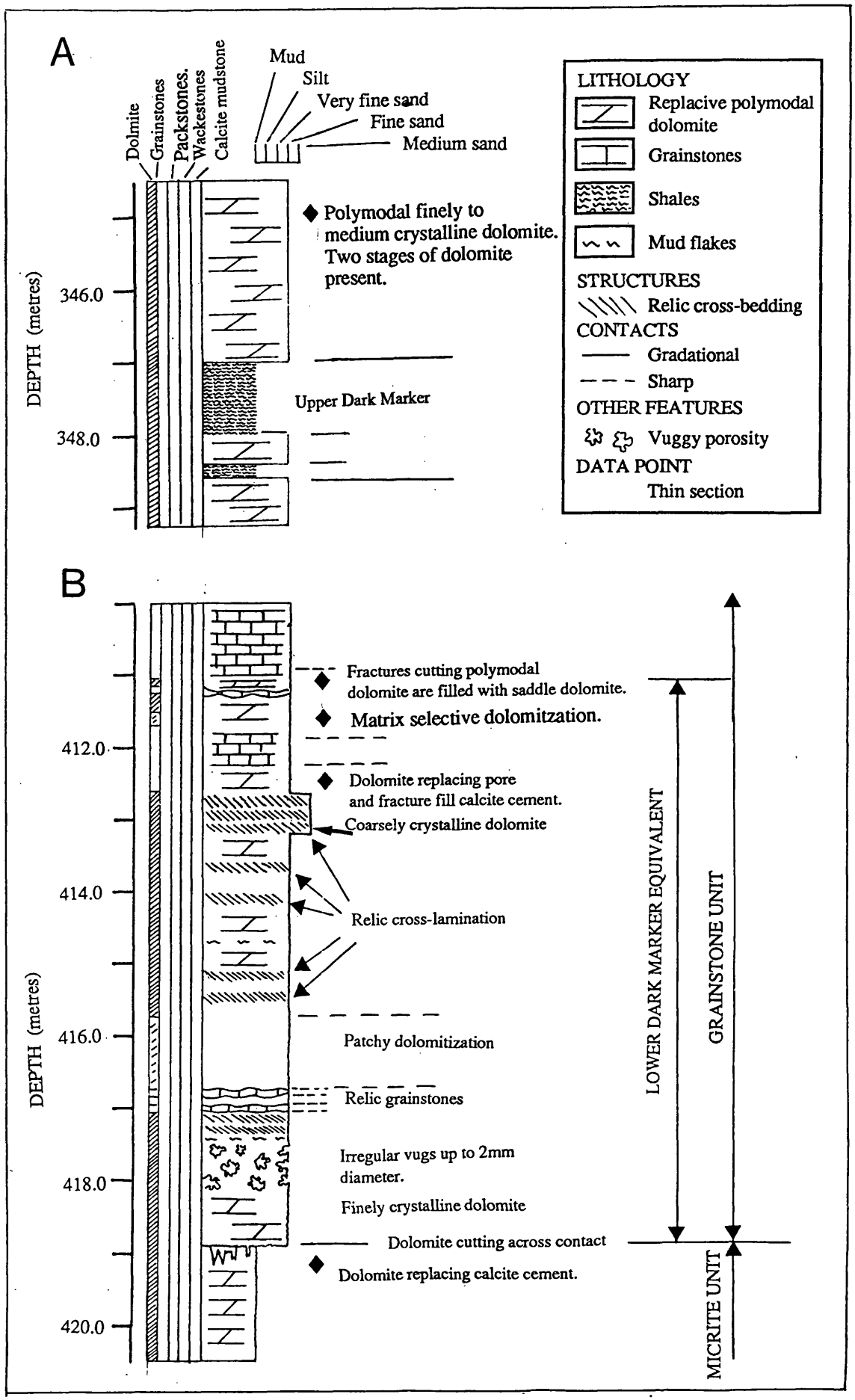

Fig. 5.8. 'A'. Summary log showing dolomitized Upper Dark Marker. Hole N992. **'B'** summary log of the Lower Dark Marker Equivalent. Dolomitization which forms this marker extends into the Micrite Unit below. Note relic cross-bedding. Hole N982.

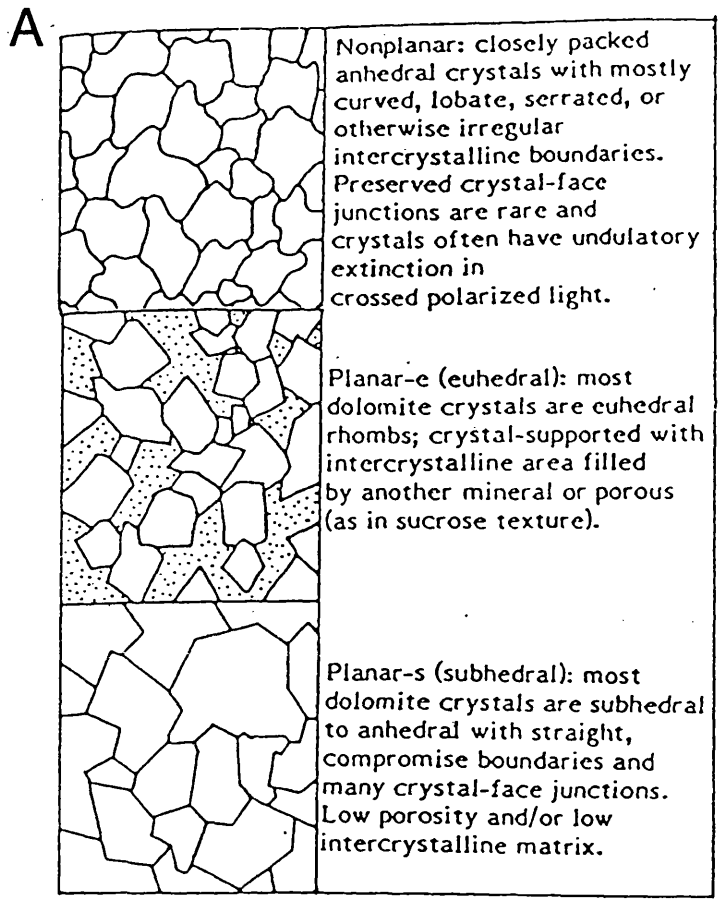

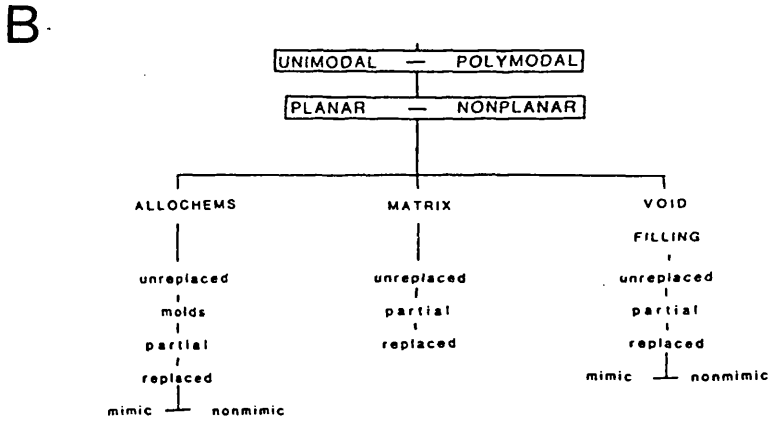

Fig. 5.9. **'A'** Planar and non planar classification of dolomite texture, from Gregg & Sibley (1984). Classification of dolomite rock textures according to the scheme of Sibley & Gregg, 1987. **'B'** All samples are classified as unimodal or polymodal and planar or non planar. Samples that have recognisable allochems, voids and matrix are then described according to the adjectives shown.

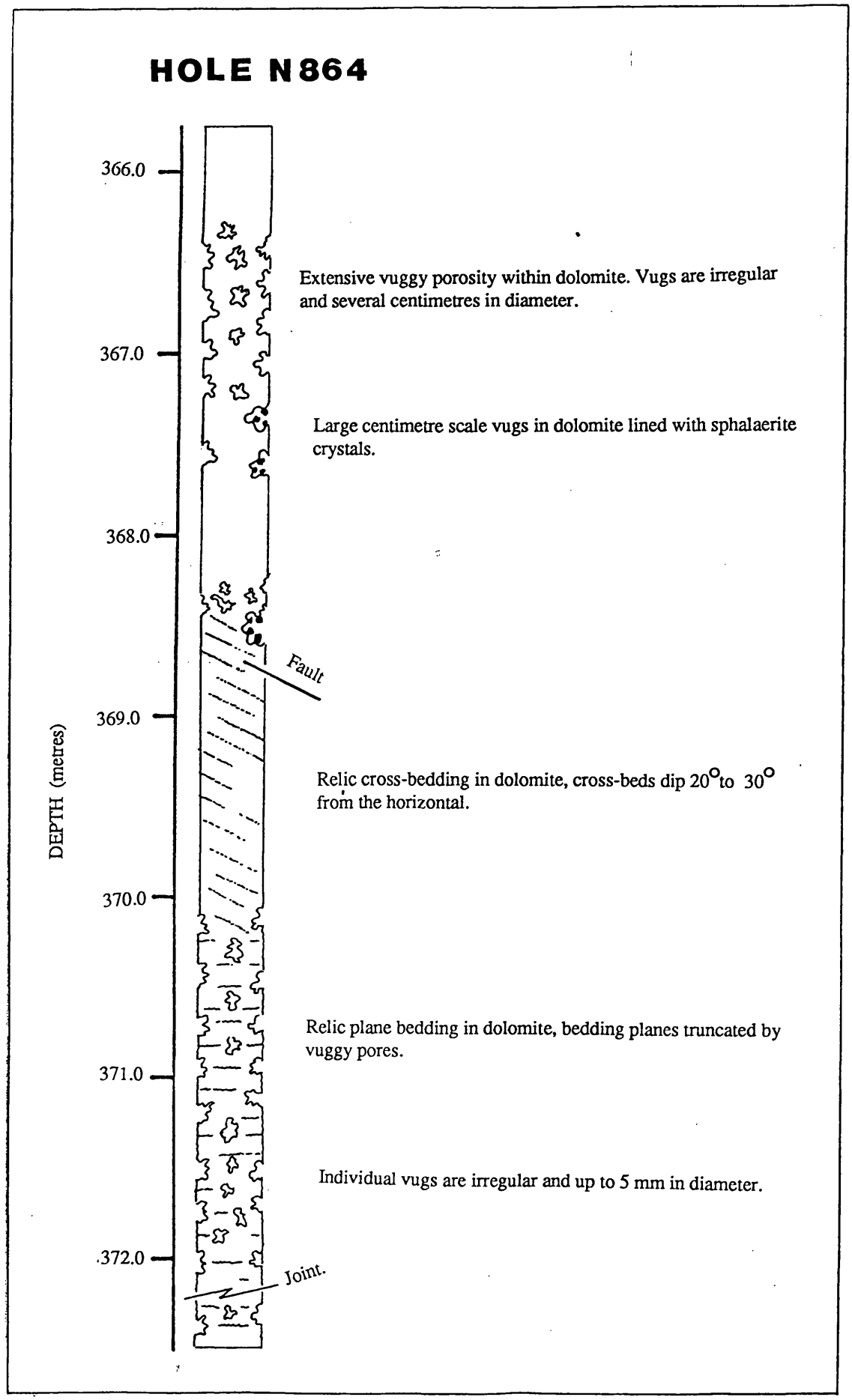

Fig. 5.10. Log showing character of vuggy porosity within dolomite occurring in the Grainstone Unit. Relic cross-bedding and layering can be seen clearly. Note sphalerite crystals lining vugs. Hole N984.

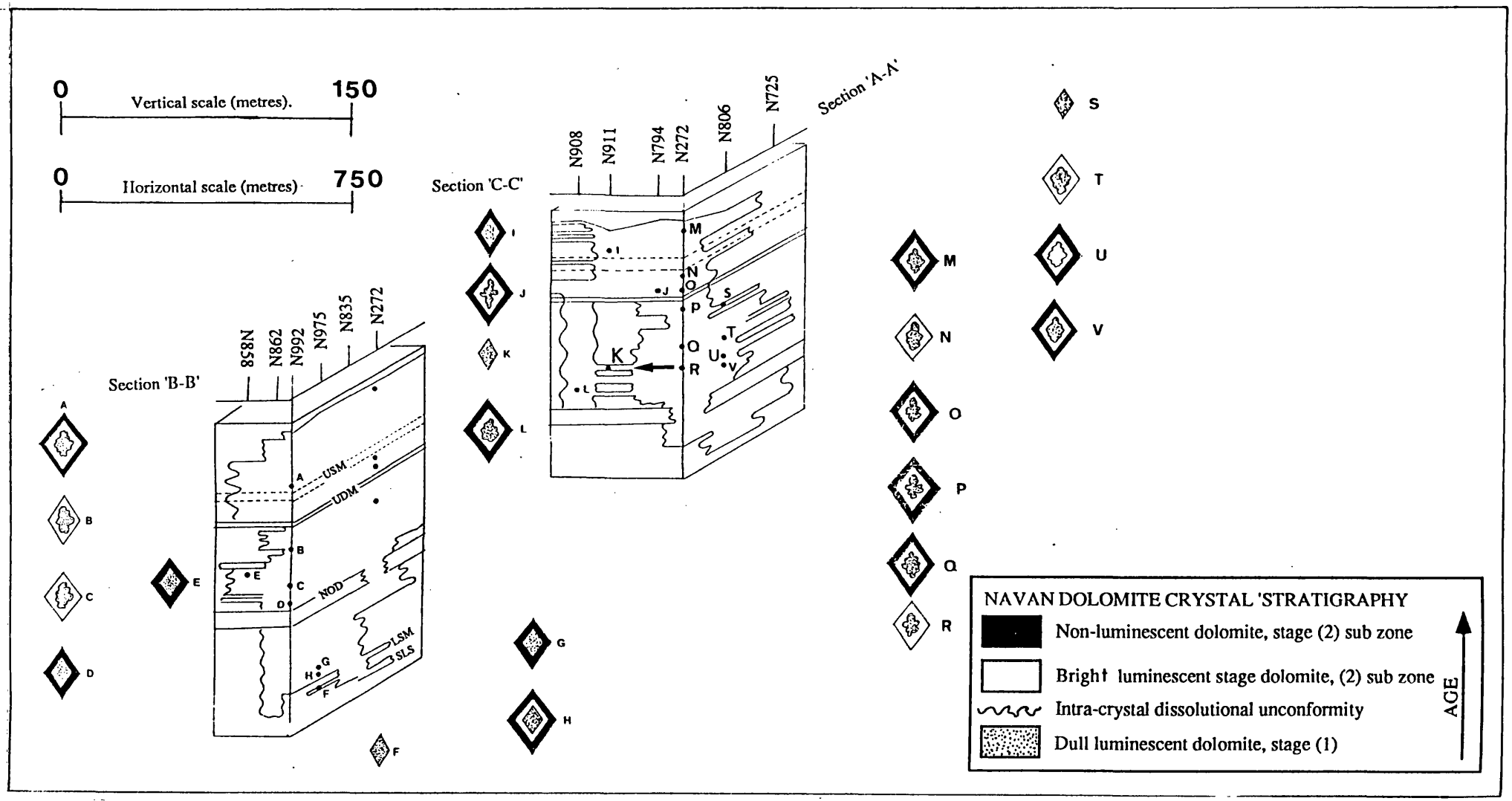

Fig. 5.11. Distribution of dolomite stages within the dolomite plume occurring in the Grainstone Unit. Stage (1) crimson brown dolomite is pervasive occurring in all thin sections. Stage (2) bright luminescent dolomite and non-luminescent dolomite is also common within the dolomite plume. However it is absent from stratal dolomite 'fingers'. Compare the position of sample 'P' with sample 'S' and the position of sample'R' with 'K'. Note also the luminesent characteristics of sample 'F'.

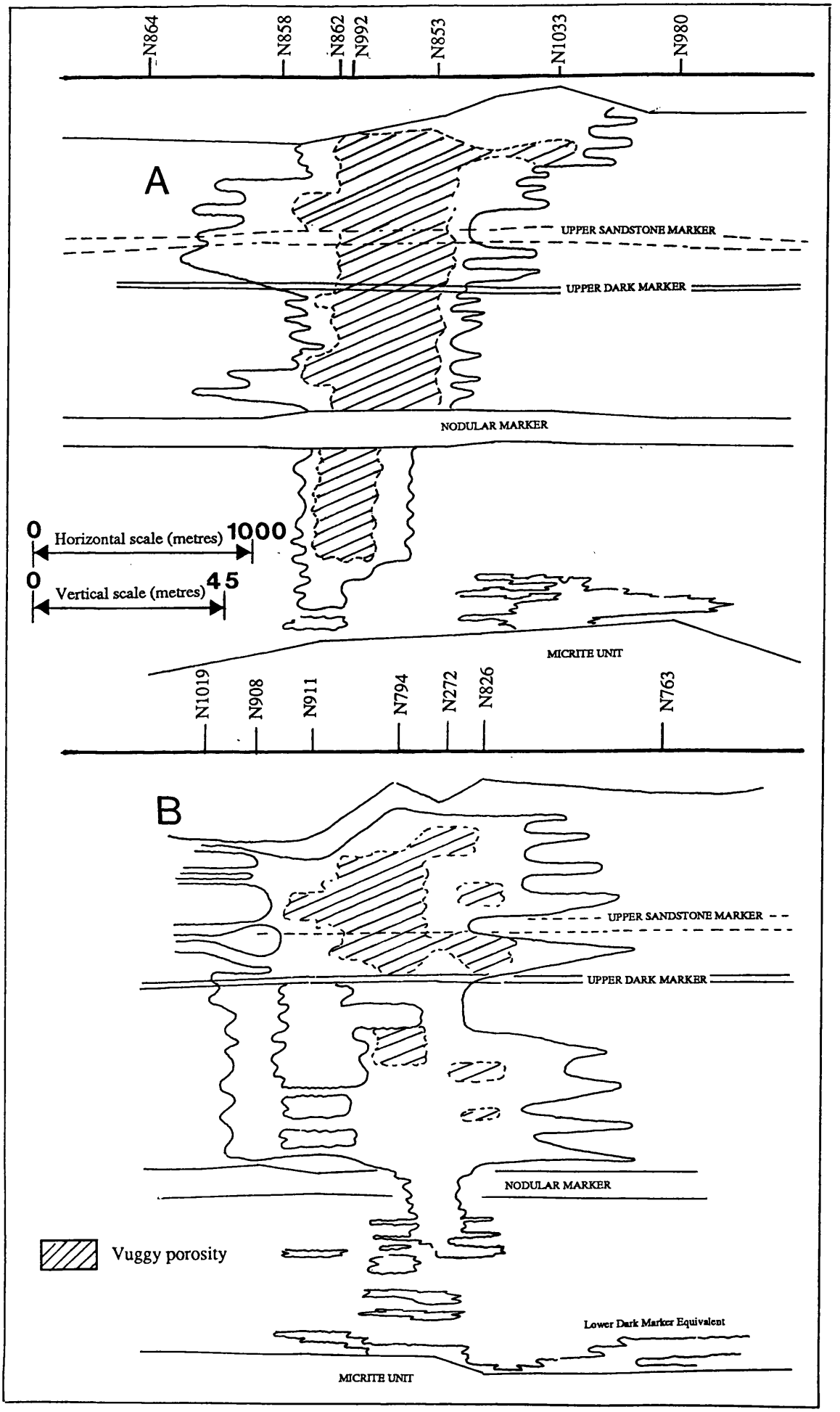

Fig. 5.12. 'A' Distribution of vuggy porosity in cross-section 'B-B'. 'B' Distribution of vuggy porosity in cross-section 'C-C'.

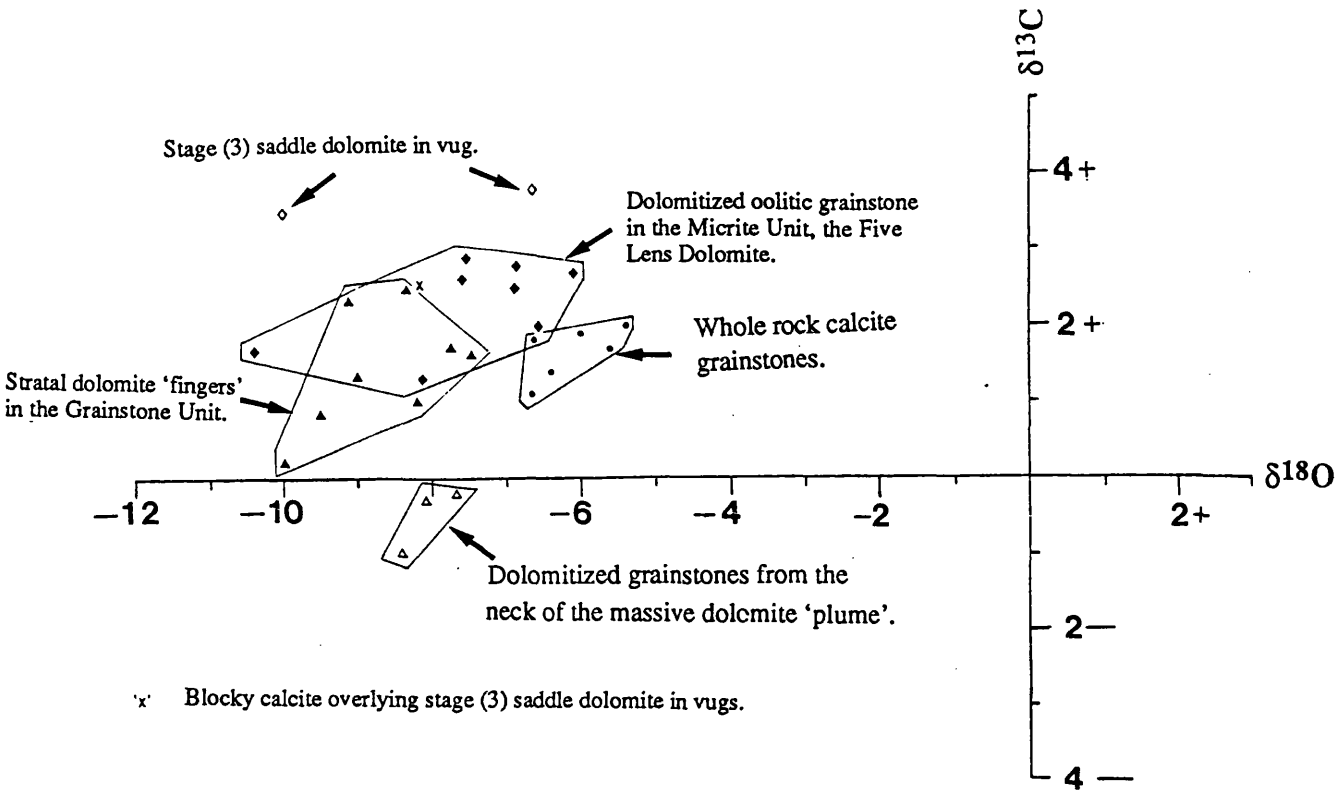

Fig. 5.13. Graph showing the relationship between $\delta^{18}O$ and $\delta^{13}C$ of Navan dolomite. Results presented relative to PDB in ‰. Stage (3) saddle dolmite in vugs and blocky calcite overlying Stage (3) saddle dolomite provided courtesey of I.K. Anderson.

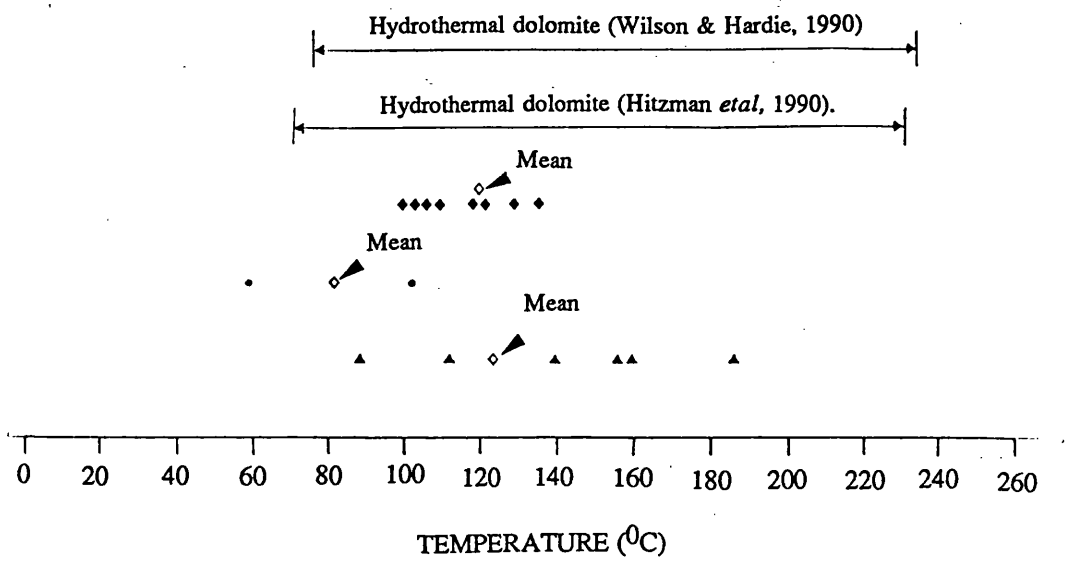

◆ Massive dolomite in the Grainstone Unit

▲ Five Lens Dolomite in the Micrite Unit

• Stratal dolomite 'fingers' in the Grainstone Unit.

Fig. 5.14. Fluid inclusion microthermometry data from Navan dolomite. This is compared with microthermometry data from other ancient dolomites believed to have precipitaetd from heated pore waters.

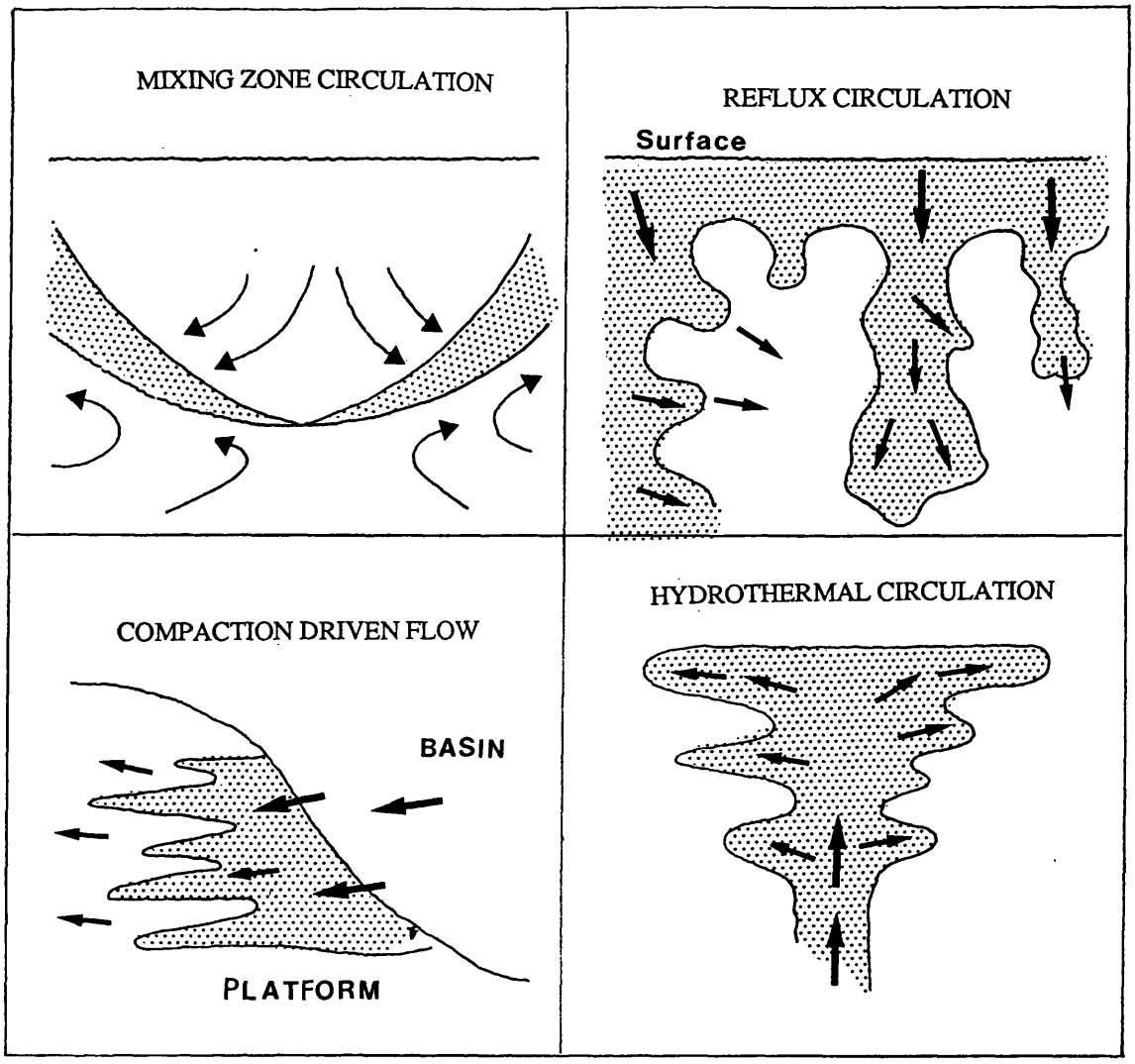

Fig. 5.15. Summary diagram showing circulation systems which could produce massive dolomite. Arrows indicate flow directions and dots indicate predicted geometry of dolomite body. Modified from Mattes & Mountjoy (1980); Simms (1984) Wilson & Hardie (1990).

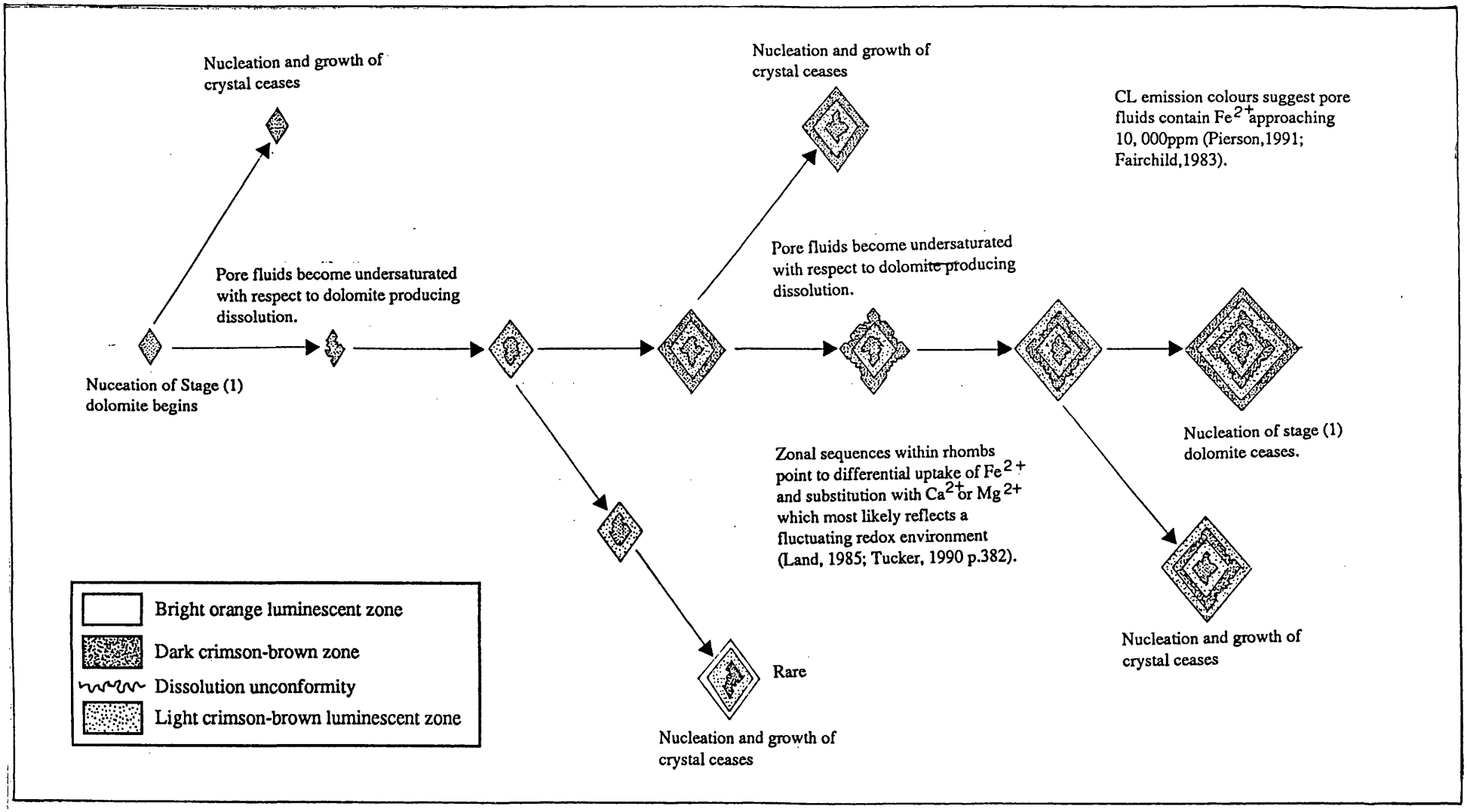

Fig. 5.16. The paragenesis of Stage (1) dolomite.

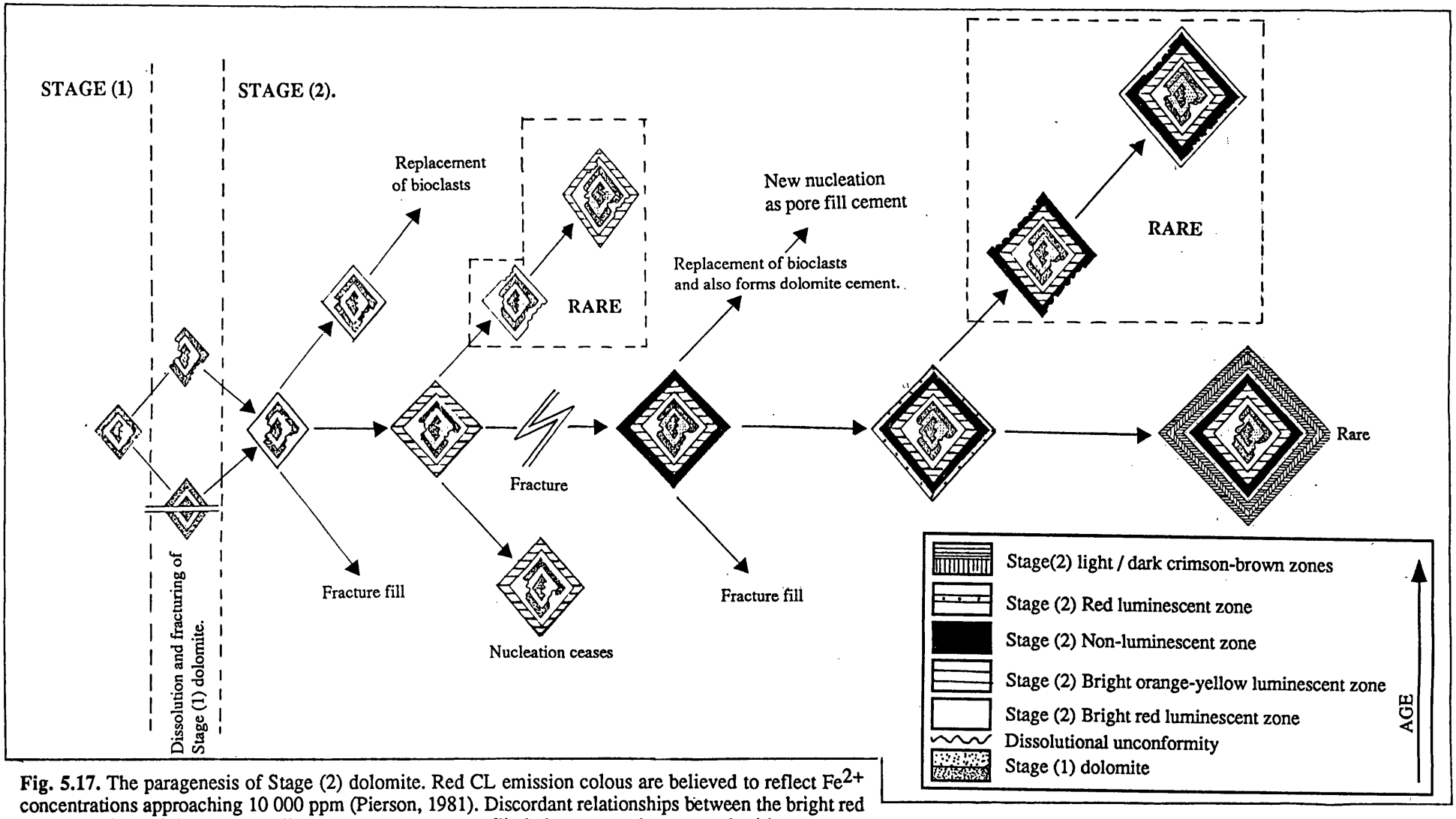

Fig. 5.17. The paragenesis of Stage (2) dolomite. Red CL emission colous are believed to reflect Fe^{2+} concentrations approaching 10 000 ppm (Pierson, 1981). Discordant relationships between the bright red and overlying bright orange-yellow zone suggests pore fliuds became undersaturated with respect to dolomite. The bright orange yellow CL emission colours reflect a decrease in Fe^{2+} concentration to less than 10 000 ppm and Mn^{2+} concentrations from 100 ppm to 1000 ppm (Pierson, 1981), perhaps as low as 30 ppm to 35 ppm (ten Have & Heyenen, 1985). Non lunminescent dolomite is believed to reflect Fe^{2+} concentrations of > 15 000 ppm.

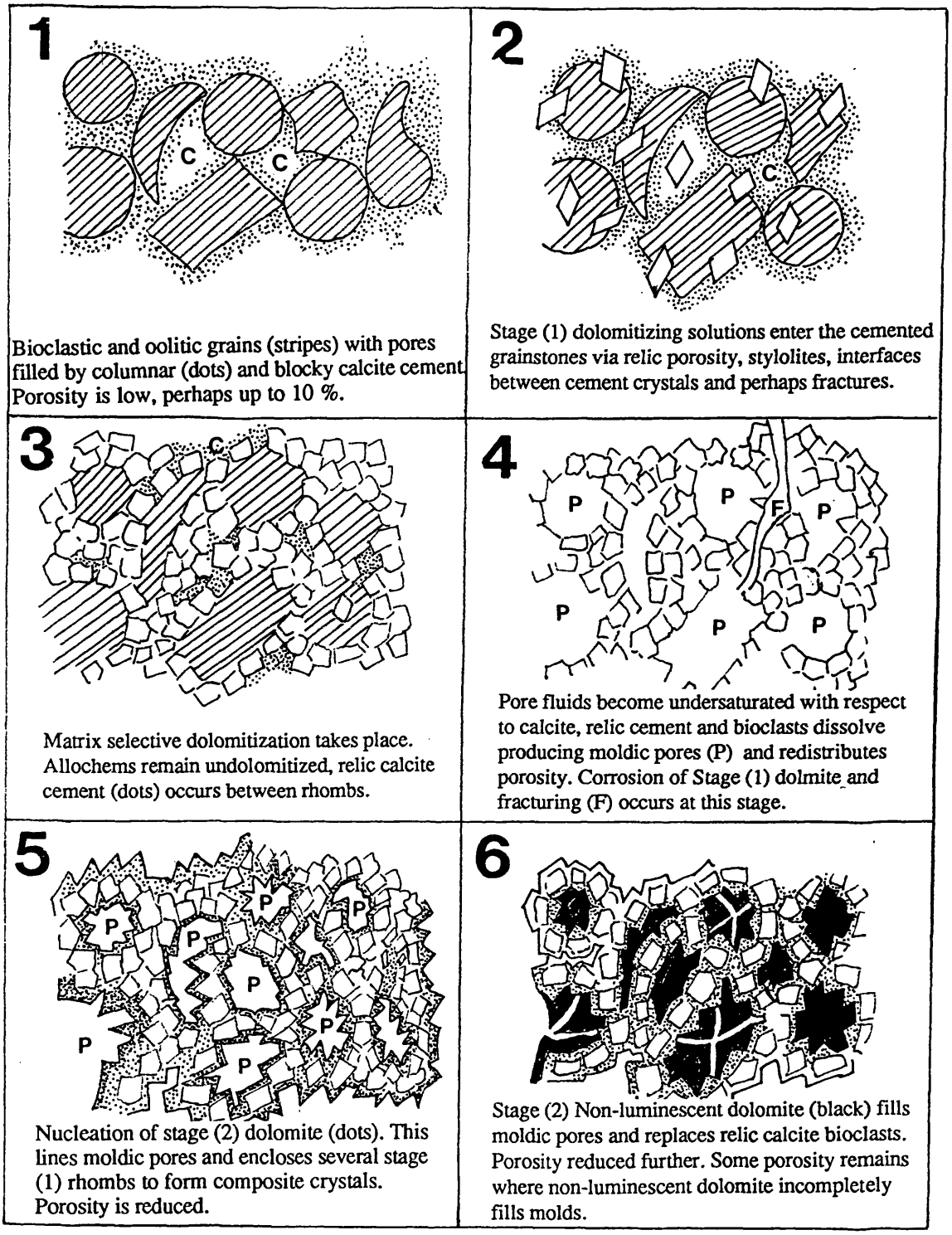

Fig. 5.18. Evolution of porosity in the Navan Dolomite. It is suggested that pores are not simply the result of volume reduction during the calcite to dolomite replacement reaction.

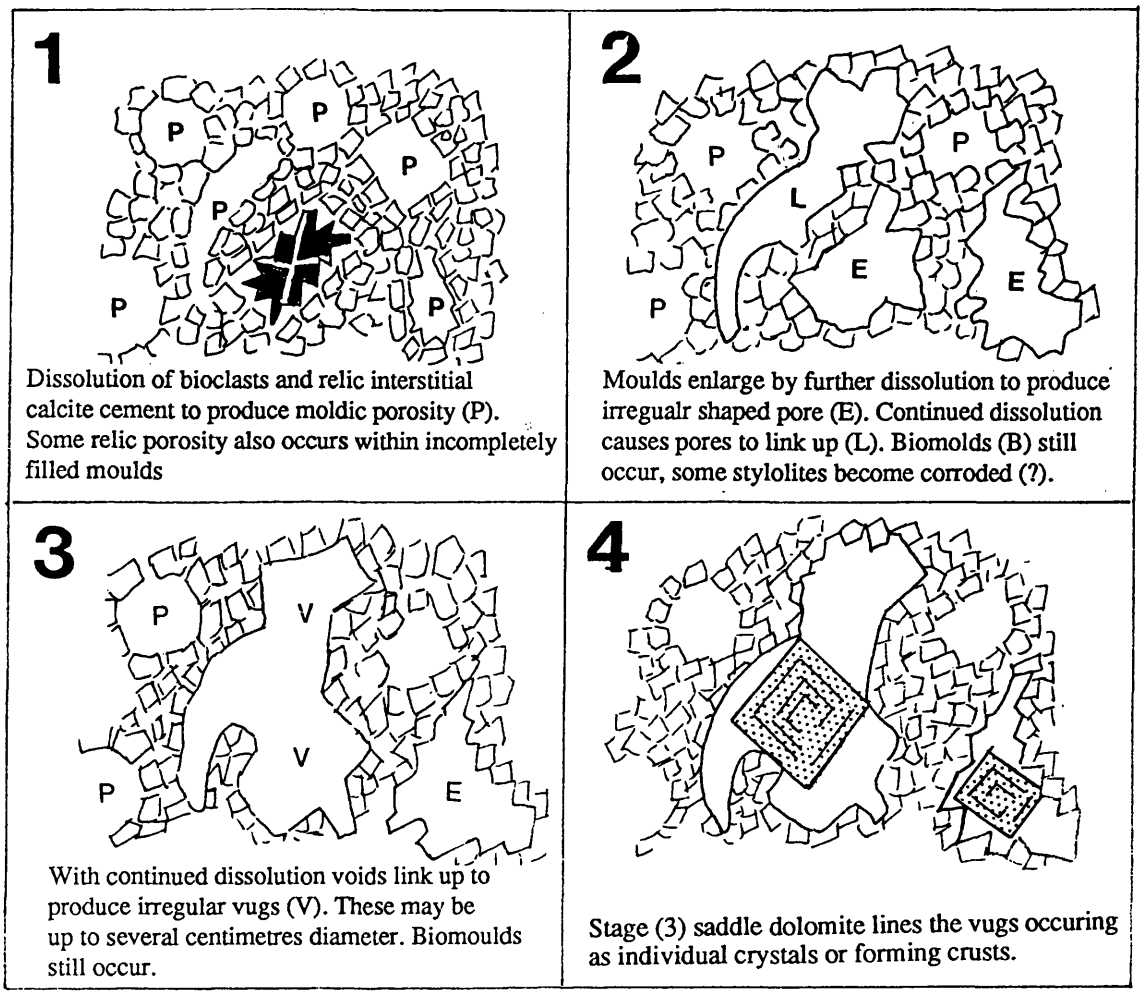

Fig. 5.19. Evolution of vuggy porosity in the Navan dolomite.

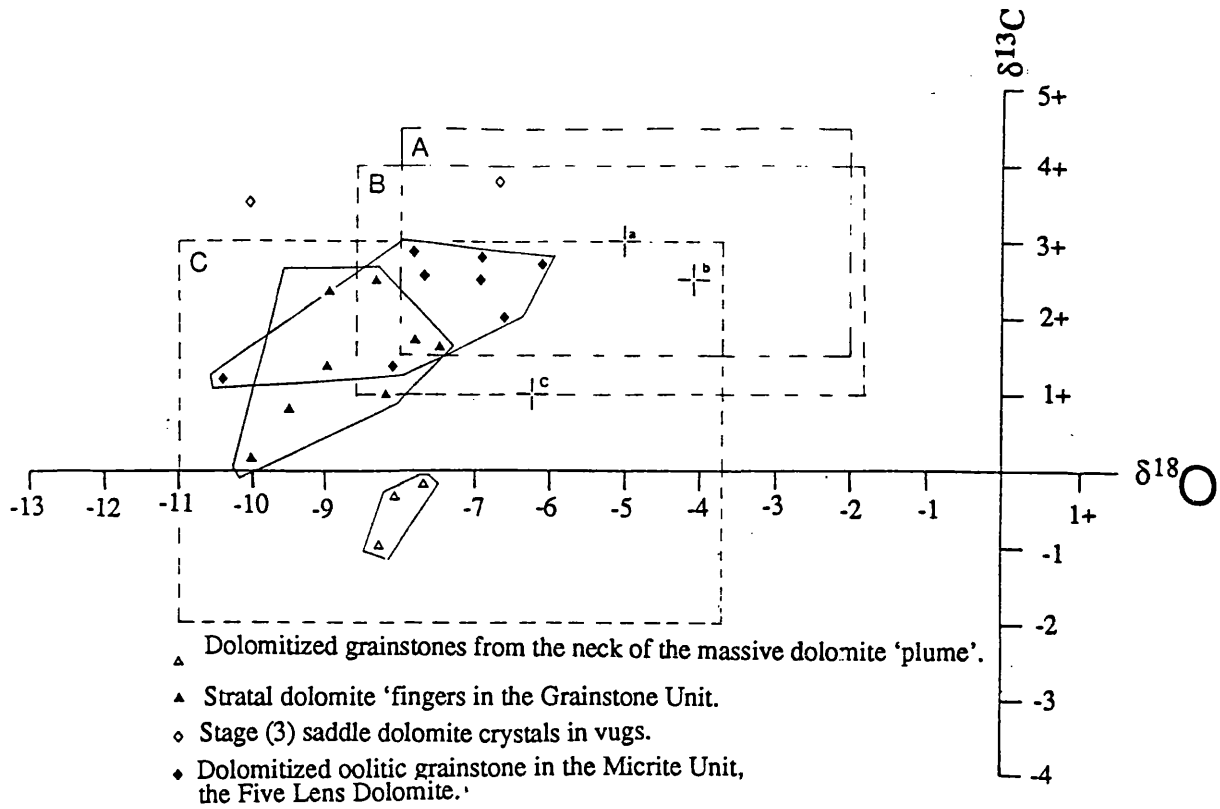

Fig. 20. Navan dolomite $\delta^{18}O$ and $\delta^{13}C$ values as compared with $\delta^{18}O$ and $\delta^{13}C$ values from ancient dolomites believed to have been precipitated from heated pore fluids. **'A'** Burial dolomite from the Devonian Miette Buildup of Aberta, Canada **'a'** = mean of isotope field (Mattes & Mountjoy, 1980) . **'B'** Hydrothermal dolomite from the Triassic Latemar Platfom **'b'** = mean of isotope field (Wilson & Hardie, 1990). **'C'** Burial dolomite from the Lower Carboniferous Bowland Basin of England **'c'** =mean of field (Gawthorpe, 1987). All results presented relative to PDB in ‰.

6.1. INTRODUCTION.

The detailed sedimentology of the sequence above the Pale Beds, including the Shaley Pale Limestones, Argillaceous Bioclastic Limestones, Waulsortian Limestones, Boulder Conglomerate and Upper Dark Limestones is beyond the brief of this project. However, it is necessary to consider it briefly to complete the disscussion of the sedimentological framework at the Navan mine. The sequence is summarised in Fig 1. 3.

6.2. i. The Shaley Pale Limestone

The Shaley Pale Limestones are a complex sequence of interbedded limestones, calcisiltites, black shales and a few sandstone beds (Plate 6. A). The conodonts *Scaliognathus anchoralis* (Andrew & Ashton, 1985) and *Polynathus mehili* (Strogen *et al,* 1990) have been recovered and indicate a Courceyan age. The limestones are generally wackestones and packstones (Strogen *et al.* 1990). Beds are irregular to planar and vary from a few centimetres up to 70 cm thick. Contacts between lithologies vary from sharp to gradational. Gradational boundaries may be interlaminated or irregular and may include slumps. Limestone beds contain crinoid fragments, shelly layers (hole N1039 at depth 364.5 m), silty layers and layers containing sub-horizontal shale flakes 2 cm long and 1 to 2 mm thick. Some beds are mottled. Shales and calcisiltites frequently contain 2 to 3 cm thick wackestones and packestones; some are rich in crinoid ossicles others are thin layers of grainstone. Common sedimentary structures include burrows (hole N1039 at depth 291 m) and cross lamination (hole N1039 at depth 284 m).

The Shaley Pale Limestones have been subdivided into Lower, Middle and Upper units by Philcox, 1990. The Lower Shaley Pale Limestones are approximately 25 m thick and contain at least 3 very fine grained calcareous sandstones, one of which is 2 m thick and contains extensive burrowed intervals. *Chondrites* was reported by Strogen *et al.* (1990). A layer of bryozoan fragments, 10 to 15 cm thick, forms a marker which defines the top of the unit. The Middle Shaley Pale Limestones are approximately 50 m thick and consist of interbedded shales and limestones and include a 2.5 m thick sandstone. The Upper Shaley Pales are 35 m thick and consist of thick shales, calcisiltites and thin beds of packstone. Thin graded packstones with erosive bases are common, other features present include soft sediment deformation and fluid escape structures and burrows (Strogen *et al.* 1990). The sequence is summarized in Fig. 6.1.

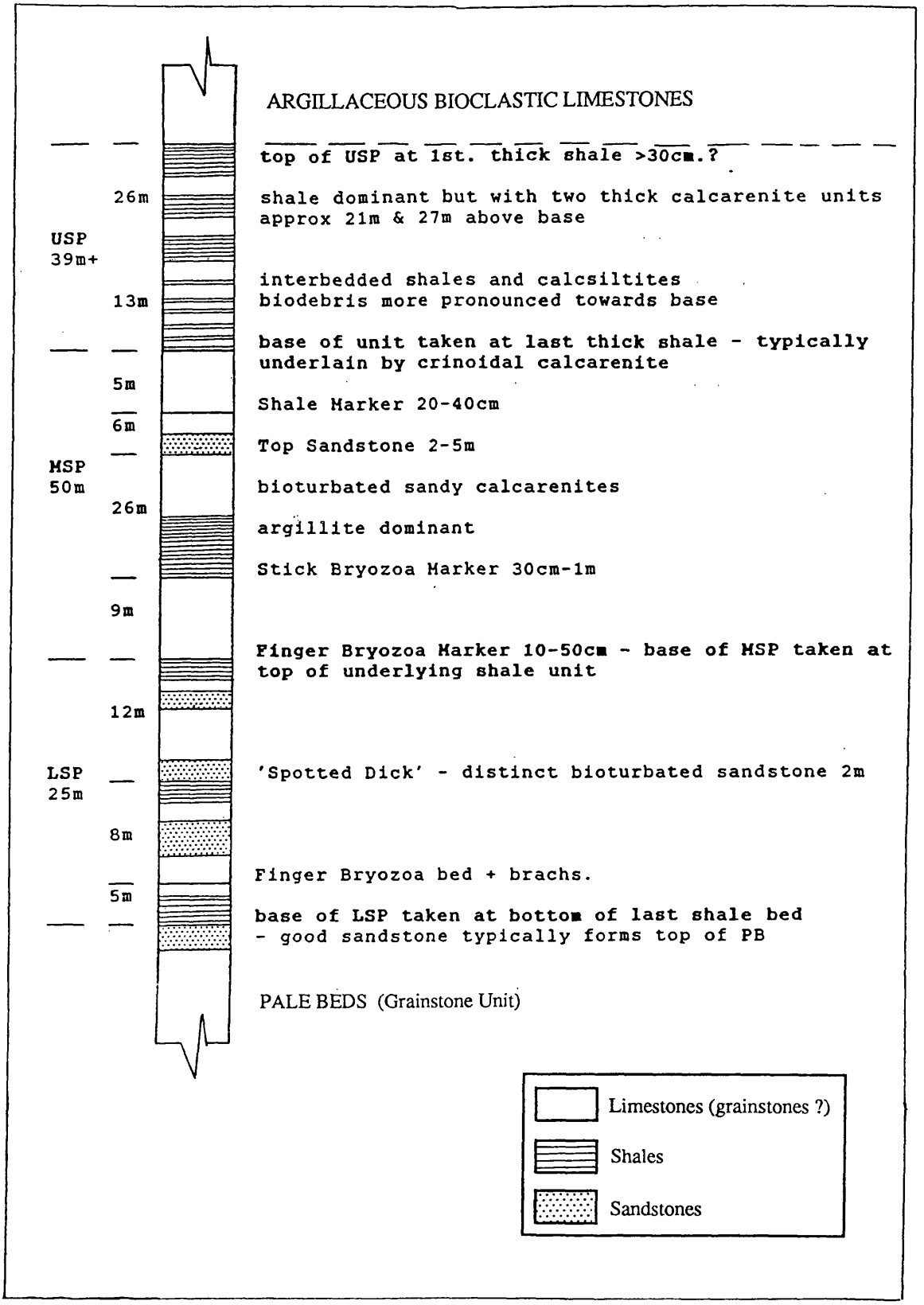

Fig. 6.1. Type section of the Shaley Pales Limestones, Hole N1022. PB = Pale Beds. LSP = Lower Shaley Pales, MSP = Middle Shaley Pales, USP = Upper Shaley Pales, ABC = Argillaceous Bioclastic Limestone, brachs = brachiopods. All thicknesses in metres. After Philcox (1990).

6.2.ii. The Argilaceous Bioclastic Limestones.

The Shaley Pale Limestones pass up into the Argillaceous Bioclastic Limestones which are at least 130 m thick. The conodont assemblage includes *Scaliognathus. anchoralis*, recovered from the lower and middle parts of the sequence, which are therefore Courceyan. They consist of thinly bedded crinoid rich shaley limestones, typically wackestones and packstones and shales which contain occasional nodular textures (Plate 6.B) (Andrew & Ashton, 1985; Strogren *et al,* 1990). The clastic component decreases vertically and the unit passes gradationally up into the Waulsortian Limestone.

Tectonic activity has affected the Shaley Pale and Argillaceous Bioclastic Limestones, producing a sequence of faulted, 'right way up' slabs. Individual fault slices are subhorizontal and up to 90 m across and 20 m thick (Philcox, 1989). These slabs form a NE to SW striking structure termed the **Shaley Pales Trough**. The trough truncates up to 250 m of stratigraphy and occurs between the 'T' and 'C' Faults. It is best developed at the NE termination of the 'T' Fault and dies out toward the SW (Philcox, 1989; pers commn, Ashton, 1992).

6.2.iii. Waulsortian Limestones.

The Waulsortian Limestones are poorly represented in the mine area, occuring only towards the western and north western limit. Andrew & Ashton (1985) suggested that the Waulsortian is entirely Chadian in age, however, the recovery of *Scaliognathus anchoralis*, suggests that the lower part of the Waulsortian is Courceyan (Philcox, 1984). A sequence exposed in hole N1024 is over 7 m thick, consisting of crudely interbedded light grey calcite mudstones and crinoid wackestones (Plate 6.C). Crinoid ossicles are disarticulated, but are not abraded, and grain surfaces do not appear to have been altered by micritization. Ossicles are up to 8 mm diameter and up to 2.5 cm long and display no preferred orientation. Locally the wackestones are grain supported. Primary pores contain three distinctive linings. Dark grey micrite is the oldest and forms layers up to 1 mm thick containing faint internal zones. This is overlain by translucent blocky calcite and clear blocky calcite, a few primary pores remain open.

Elsewhere the Waulsortian Limestones facies forms thickly to massively bedded mounds (Lees, 1962). Such mounds contain centimetre scale sparry patches (stromatactis). These features may be seen at Brae Hill quarry, County Meath 15 km to the south west of Navan where the Waulsortian is over 30 m thick. (personal observation 1990).

6.2.iv. The Erosion surface and the Boulder Conglomerate.

The sedimentary sequence has been cut by a major trucation surface which is Arundian in age. This surface strikes east to west parallel to the 'B' and 'T' Faults, extending over 3 km to the west and over 4 km to the east of the mine area. It generally slopes over 2 km toward the SE at about 20^0 (Philcox, 1989; Ashton *et al*, 1990). It truncates over 750 m of stratigraphy, cutting Waulsortian Limestones, Shaley Pale and Argillaceous Bioclastic Limestone, Pale Beds and Laminated Beds to just above the Lower Paleaozoic basement in hole EP3 and downwards into the Lower Palaeozoic basement (Ashton, pers commn. 1992) The surface varies from sharp to sheared and irregular (Ashton *et al*, 1990; Philcox, 1989).

The surface has an overall channel-like profile, best developed in the east central part of the mine. It has a local relief of several metres (Philcox, 1989; Ashton *et al*, 1990) and hosts neptunian dykes up to 1 m wide and over 10 m deep (Ashton *et al*, 1990). The surface has been displaced by the listric 'T' Fault which is believed to have produced a series of low angle fault scarps with a relief of several metres striking NNE (Ashton, *et al* 1990). Philcox (1989) also noted some fault controlled troughs cutting the erosian surface obliquely and striking NE.

The truncation surface is overlain by a poorly sorted polymict conglomerate which also fills the neptunian fissures. This conglomerate, known as the Boulder Conglomerate has a texture ranging from clast to matrix supported with clasts ranging from sand through to cobbles, boulders and blocks several metres in diameter. Clasts may be angular or rounded. The Boulder Conglomerate forms a series of lenses up to 50 m thick and extending laterally 200 to 300 m, the lenses are oriented NW to SE, and some have accumulated against fault scarps (Philcox, 1989; Ashton, *et al*, 1990).

The most common clasts within the Boulder Conglomerate consist of Waulsortian facies calcite mudstones and crinoidal wackestones, similar to the Waulsortian described in section 6. iii. Primary pores in these contain calcite cements. Other clasts present include very fine grained bioclast grainstones which contain a few conspicuous larger bioclasts, typically crinoid ossicles or rugose corals (hole U6641). Structures within clasts include 8 mm thick layering and mottled fabrics (hole U6641). In the 1285 mine level, 3 zone hanging wall, bioclast grainstone clasts contain fractures filled with calcite cement. Ashton *et al*, (1990) reported bioclast limestone clasts containing stylolites.

Rare clasts include blocks of oolite (goethitic) ironstone (Plate 6. D) and haematite seen in the 1285 mine level, 3 zone, (Ashton *et al*, 1990, personal observation 1990). Clasts of red sandstone up to 5 cm in diameter occur in hole N1011 at depths 441.0 m, 435.6 m and 436.2 m (Plate 6.E). A block of grey brown dolomite 30 cm in diameter

occurs in hole U6636 (Plate 6.F). This is finely crystalline and contains hair-width veins filled with coarser white dolomite which also fills irregular and rectangular vugs a few millimetres in diameter. Relic sedimentary structures include thin layers and mottled fabrics. Other clasts reported include blocks of Shaley Pale Limestone (Ashton *et al,* 1990), fenestral calcite mudstone (Philcox, 1989) and clasts containing sulphides (Ashton *et al.* 1990).

The matix between clasts is a black shaley mudstone, containing a few conspicuous bioclasts. Shales form layers up to several metres thick. Diagenetic features of the Boulder Conglomerate include calcite concretions up to 15 cm diameter and sutured contacts between adjacent clasts. The shales have a strong hydrocarbon odour and in the mine level 1330 / 1345 (?) mine level, 347N stope, liquid hydrocarbon flows from pores within blocks of Waulsortian Limestone

6.2.v. The Upper Dark Limestone.

The Upper Dark Limestones are believed to be Chadian in age (Philcox, 1989) with the Arundian - Chadian boundary taken at the first appearence of the Archaeodiscidae in hole N915 at Navan (Strogen *et al,* 1990). These limestones are approximately 400 m thick at Navan (Philcox, 1989). The lowest unit, the **Thin Bedded Unit**, is up to 20 m thick and rests on the Boulder Conglomerate. It consist of thin alternations of limestone and black shale which may be up to 30 cm thick (Plate 6.G). The contacts between the limestone and shale may be abrupt or gradational over several centimetres, typically represented by inter-laminations of limestone and shale. The bases of the cycles are sharp and some appear to have been inclined when deposited. Some limestones include graded units 1 to 3 cm thick with coarse bases.

The Thin Bedded Unit passes gradationally into 160 m of limestones, shales and conglomerates. The conglomerates are up to 3 m thick and generally sheet-like although, some are lenticular with a channel-like cross-section (Philcox, 1989). Typically these conglomerates form the bases of graded units. The conglomerates are poorly sorted, clasts are angular and up to 2 cm diameter, clast composition and character is the same as the Boulder Conglomerate (Philcox, 1989). Clast size is believed to decrease to the south and south west (Philcox, 1989).

Above this part of the sequence the Upper Dark Limestones are dominated by limestone shale cycles up to 1 m. thick often arranged into graded units (compare Strogen *et al,* 1989 Fig 6.e.). The limestones are wackestones and packestones and contain ooliths, lithoclasts of carbonate platform sediment, konickoporoid algae and sponge spicules (Andrew & Ashton, 1985). Many of the grains have micrite coatings (Strogen *et al,* 1989). Calcareous shales are up to 1 m thick in hole N1028. One 60 cm thick shale

has a consistent stratigraphic position and is known as the **'A-A'** marker. A similar shale 50 m above forms the **'A-C'** marker (Philcox, 1989). Occasional beds of conglomerate still occur in this part of the Upper Dark Limestone. One 20 m thick conglomerate southeast of the 'C' Fault has a consistent stratigraphic position. This contains clasts of fenestral micrite and Waulsortian Limestone and forms the Conglomerate Complex of Philcox (1989).

Locally the Upper Dark Limestones include developments of blue-grey chert. In addition nodular beds (the Boudin mudstones) up to 2 m thick are common in the lower half of the Upper Dark Limestones. Nodules are of limestone in a darker silty matrix (Plate 6.H). The shape of the nodules changes systematically. At the base of a nodular sequence, they are lenticular or rectangular in cross-section becoming 'round' vertically. 'Mature' nodules have sharp margins but others have gradational contacts. Nodules are up to 1.5 cm thick and over 3 cm in diameter. Lateral terminations are blunt, or bifurcating, or wispy. Individual layers of nodules have a constant thickness parallel to the strike of the Arundian erosion surface (Philcox, 1989). However, the nodule layers increase in thickness toward the SE, normal to the strike of the erosion surface (Philcox, 1989).

6.3. SEDIMENTOLOGY OF THE SEQUENCE.

The successions described have not been the subject of detailed study by the author. The interpretation which follows is based partly on limited observations and partly on published opinions.

6.3.i. The Shaley Pale Limestones.

The Shaley Pale Limestones are considered to be the deeper water offshore equivalent of the middle shelf oolitic and bioclastic grainstones below (Andrew & Ashton, 1985). Strogen *et al* , (1990) suggested that the sea bed was probably below fair-weather wave base and noted the absence of abraded bioclasts. The erosively based graded beds within the Upper Shaley Pale Limestones were interpreted as storm deposits (Strogen *et al.* 1990) with soft sediment deformation structures used as evidence of proximity to a shelf margin. The sandstone beds, in the Upper and Lower Shaley Pale Unit indicate episodic influx of siliciclastic detritus, perhaps as a result of storms. The Argillaceous Bioclastic Limestones have been interpreted as reflecting continuation of tranquil deep water sedimentation related to a regional deepening episode (Strogen *et al,* 1990).

PLATE 6. General views of the Late Courceyan - Arundian sequence at Navan.

A. General view of Shaley Pale Limestones. Limestones interbed with black shales, note plane and irregular contacts between lithologies. Hole N1022. Scale in centimetres.

B. General view of Argillaceous Bioclastic Limestones. Hole N1022, coin for scale.

C. General view of Waulsortian Facies crinoidal wackestones and mudstones. The crinoid rich layers form crude interbeds (C), note relic porosity (P). Hole N1024, scale in centimetres.

D. Clast of oolitic (goethitic) ironstone (O) in Boulder Conglomerate. Note clast supported fabric. Hammer for scale, 1285 Mine Level, 3 Zone (hanging wall).

E. General view of Boulder Conglomerate showing different clast types. (W) Crinoidal Waulsortian Limestone, (S) Red Sandstone, (B) Bioclastic grainstone, (M) shaley matrix. The Boulder conglomerate has both a matrix and clast supported fabric and is poorly sorted, having both angular and rounded clasts. Hole N1011. Scale in centimetres.

F. Dolomite clast from the Boulder Conglomerate. Dolomite is finely crystalline and contains fractures filled with later coarser white dolomite.Underground production drill core, Hole U6636. Scale bar = 1 cm.

G. General view of the the Thinly Bedded Unit. This consists of thin interbeds of limestone and shale. Note sharp contacts between units. Hole N1011. Scale in centimetres.

H. General view of nodules in the Upper Dark Limestones. Nodules are orientated parallel to bedding and display sharp (s) or wispy (w) terminations. Nodules occur within argillaceous layers (a). Hole N1011.

A
B
C
C
P
CENTIMETER
INCH
D
O
E
W
S
M
B
CENTIMETER
INCH
F
G
CENTIMETE
INCH
H
W
a
S
CENTIMETER
INCH

6.3.ii. The Waulsortian Limestones.

Waulsortian Limestones are believed to represent a mudbank complex consisting of mounds up to 15 m high and a few hundred metres in diameter. These mudbanks covered most of Ireland during the Courceyan (Lees, 1964). Alternating beds of crinoidal wackestone and calcite mudstone are common in the Waulsortian facies (Lees, 1964; Lees & Miller, 1985) and it was suggested by Strogen *et al*, (1989) that crinoid rich facies form the flanks of mud mounds. The mudbanks are thought to reflect a deep water outer platform environment (Lees & Miller, 1985). The lack of micritized grains is believed to indicate deposition below the photic, zone perhaps in water depths of 250 to 300 m with younger Waulsortian facies reflecting shallowing and deposition within the photic zone (Lees & Miller, 1985). The lack of abrasion indicates a local source. However, there is no correlation between calcite mudstones and the presence of crinoid grains at Navan, suggesting that crinoid 'thickets' did not act as sediment baffles. Partially intact crinoid stems indicate that slow currents flowed over the surfaces of the mounds.

6.3.iii. The truncation surface and Boulder conglomerate.

The truncation surface is believe to be a tectonic feature reflecting major extension in the Navan area (Ashton *et al,* 1990) generated during uplift during in late Couceyan to early Chadian (Philcox, 1989). The development of the truncation surface has been discussed by Philcox, (1989) who suggested that the earliest stages of development may be represented by the 'Shaley Pales Trough'. Recently, Ashton, *et al.* (1990) have proposed a model to explain the origin of this feature :

i. The onset of Late Courceyan to Chadian crustal extension produced subsidence to the south of the area along numerous southerly dipping listric faults, represented at Navan by the 'T' and 'B' Faults.

ii. Continued extension produced a series of low angle slides with decollment occuring within argillaceous beds, notably the Shaley Pale Limestones. This produced mass movement to the south, the area of maximum subsidence. It was suggested that an episode of normal faulting at this time preserved some of these slides, now represented by the Shaley Pales Trough.

iii. A combination of continued crustal extension and southward movement of hanging wall blocks resulted in catastophic low angle sliding and slumping which truncated the Shaley Pales Trough. As blocks travelled southwards they broke up and evolved into debris flows, represented by the Boulder Conglomerate.

iv. Movement of the 'T' fault displaced the truncation surface producing low angle fault scarps. These defined topographic lows which allowed the accumulation of thick sequences of Boulder Conglomerate.

The Boulder Conglomerate is believed to reflect a sequence of debris flows, each of varying density, which did not completely cover the truncation surface (Philcox, 1989). Deposition of the conglomerate was punctuated by periods of deposition from suspension, represented by shaley beds between the conglomerates.

Clasts are similar in composition to the Pale Beds and Waulsortian Limestones below, indicating that these acted as a local source. (Philcox, 1989; Ashton *et al,* 1990). The dolomite clast recorded from the Boulder Conglomerate resembles the massive dolomite in the Pale Beds. This is important since it suggests that the truncation surface postdated dolomitzation, and indicates that dolomitization was pre Arundian. The source of the goethitic ironstone and haematitic clasts is unknown.

Calcite cements, stylolites and jointing within clasts, indicate a long and complex diagenesis before clasts were incorporated into the debris flows. Liqiud hydrocarbons indicate that source rocks within or beyond the Navan area were sufficiently buried for passage through the oil generation window.

The truncation surface and Boulder Conglomerate were interpreted by Strogen *et al,* (1990) as representing the northern margin of the Dublin Basin (Fig. 6.2). The truncation surface compares with other Lower Carboniferous truncation surfaces, notably in the Dinantian Bowland Basin where they are overlain by conglomerate debris flows (Gawthorpe & Clemmy, 1985).

6.3.iv. The Upper Dark Limestones.

The Upper Dark Limestones are widely believed to be basinal. Graded beds with sharp erosive bases and diffuse tops are interpreted as reflecting deposition from turbidite flows (Marchant & Sevastoupoulo, 1980; Ashton, *et al,* 1985; Andrew & Ashton, 1986; Philcox, 1989; Ashton, *et al* 1990). Ooliths and micritized bioclasts were probably derived from an adjacent carbonate platform and transported into the basin. The turbidites flows at Navan are believed to have travelled parallel to the erosion surface from the north east (Philcox, 1989).

The conglomerates within the Upper Dark Limestones are believed to reflect submarine debris flows or high density turbidites, perhaps derived from a fault scarp or steep platform edge (Strogen *et al.* 1989). The decrease in clast size to the SW suggests that they were derived from the NE (Philcox, 1989). Like the Boulder conglomerate the clasts are believed to have been derived from the Waulsortian Limestones and Pale Beds. The accumulating turbidite sequence is believed to have onlapped the Boulder Conglomerate, filling the basin and eliminating relief to produce a level sea floor (Philcox, 1990).

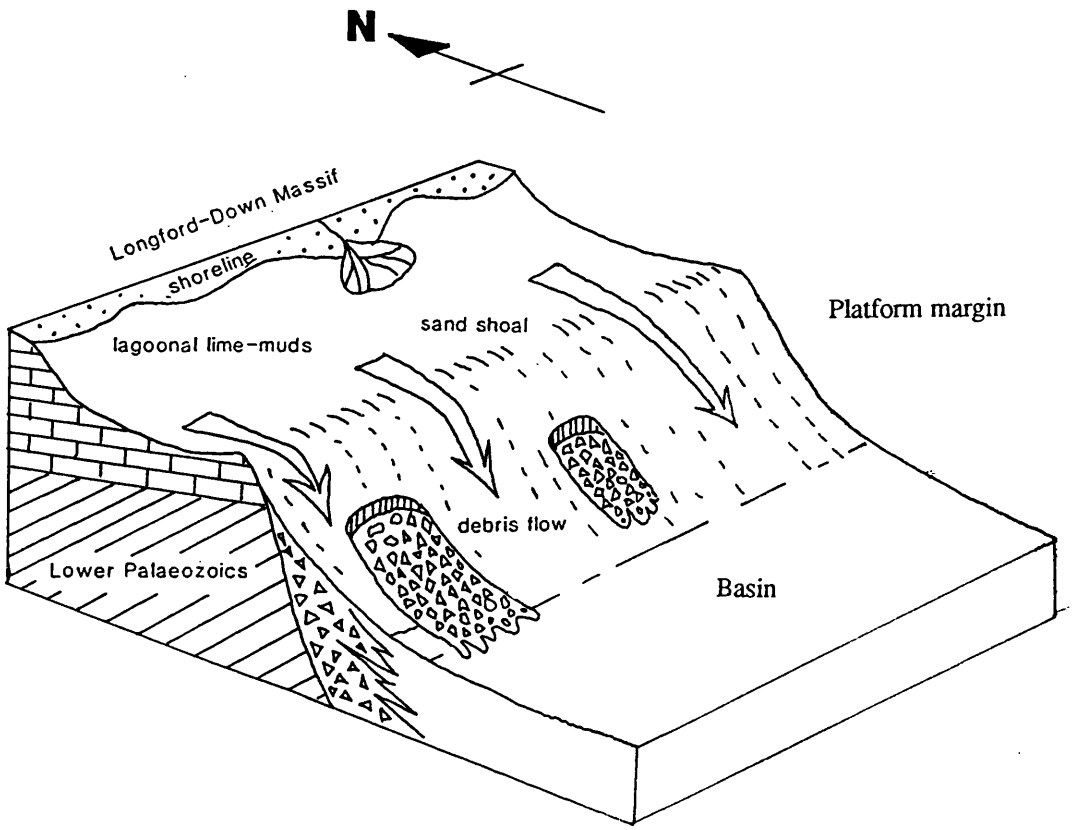

Fig. 6.2. Diagram of the northern margin of the Dublin Basin in the Navan area during Arundian times. Modified from Strogen *et al*, (1990).

6.4. SEDIMENTOLOGICAL SYNTHESIS.

The Shaley Pale Limestones are believed to reflect deep outer shelf environments, below fair weather wave base. Since they overlie middle shelf bioclastic and oolitic grainstones they indicate a relative rise in sea level. The Argillaceous Bioclastic Limestones are believed to reflect a continuation of this trend. The Waulsortian Limestones indicate that carbonate mudbanks reached the Navan area during the early Carboniferous. These mudbanks are believed to have accumulated in deep water below the photic zone.

Sedimentation was punctuated by regional tilting which produced subhorizontal sliding, now preserved in the Shaley Pales 'Trough'. This was followed by major subsidence to the south along a series of listric faults which are believed to have been related to the submarine erosion surface. This faulting also triggered a series of debris flows, the Boulder Conglomerate, which covered the erosion surface. Both the erosion surface and the Boulder Conglomerates are interpreted as reflecting a basin margin position.

Deposition of turbidites represented by the Upper Dark Limestones followed. Thin conglomerate beds within this sequence indicate that some debris flow activity was still occuring. The turbidites onlapped the margin, filling the basin and restoring a horizontal sea floor.

7.1. INTRODUCTION

The discussion is divided into 8 sections. The first, section 7.2, discusses the sedimentology of the host rocks to the Navan Ore Body and how they reflect relative sea level change. The sequence is compared with other Lower Carboniferous successions. Section 7.3 discusses the cyclicity within the host rocks, while Section 7.4 considers, the different types of early cement, the subsequent overprint by mechanical compaction and burial cementation, the timing of cementation and how these have affected porosity and permeability in the limestones. Dolomitization at Navan is discussed in Section 7.5 and is compared with dolomitzation in other Irish Zn-Pb deposits. Section 7.6 considers ground preparation within the sedimentary sequence and, the major types of porosity and permeabilty present. Section 7.7 considers the timing of mineralization with respect to calcite cementation and dolomitzation and the relationship between host rocks, dolomitization and mineralization. In section 7.8, the two genetic models proposed for the Irish ore fields; the stratal aquifer model and the crustal circulation model will be evaluated with the respect to the findings of this thesis. Finally, in section 7.9, exploration criteria are described with the aim of constraining a surface diamond drilling program.

7.2. SEDIMENTOLOGY.

The Lower Palaeozoic basement at Navan consists of thick Ordovician - Silurian black shales and tuffs which have undergone Caledonian deformation and low grade metamorphism. The sequence which follows begins with thin continental Red Beds of either late Devonian or earliest Carboniferous age and culminates in Arundian turbidites. The Dinantian succession at Navan thus reflects a gradual increase in sea level over several million years.

The Carboniferous marine transgression extended northwards over low lying continental fluviatile Red Beds. It is represented at Navan by the shaley basal member of the Laminated Beds (the 'C-G' Shale) while the remaining Laminated Beds have been interpreted as reflecting alternation of barrier sandstones, lagoonal mudstones, siltstones and tidal flat deposits. The rapid vertical facies change shown by the Laminated Beds most likely reflects alternating regressions and transgressions. The pedogenic Green Clay near the Middle of the sequence (in the 'C-E' Unit) and the nodular anhydrite, higher in the succession (the 'C-D' Unit) demonstrate that some regressions culminated in emergence.

The Laminated Beds have been cut by a channel up to 500 m wide and 20 m deep, striking NW to SE. The channel is floored with small pebble to sand grade limestone clasts. These include fragments of palaeosol, calcite cement, and lithoclasts of oolitic limestone. Other lithoclasts are shale, green clay and sandstone, and polycrystalline quartz grains. The clasts point to a hinterland consisting of lithified limestones, clastic sedimentary rocks, igneous and metamorphic rocks. The siliciclastic components were probably derived from the Longford Down Massif, but the carbonate grains point to a varied limestone landscape with lithologies (environments) which were not at this time represented in the Navan area.

The overlying Muddy Limestone consists of calcite mudstones and wackestones containing siliciclastic mud. This unit is interpreted as reflecting a clastic influenced lagoon. Like the Laminated Beds below, it contains a channel sequence. Individual channels are up to 300 m wide and 15 m deep and are again filled with Limestone Conglomerate.

The Micrite Unit consists of at least 20 metre-scale lagoon intertidal-flat shallowing up cycles. A typical cycle is up to 3 m thick and consists of pelletal and non pelletal mudstones which pass vertically upwards into fenestral and non-fenestral mudstone-wackestones, culminating in an emersion surface. The cycles indicate that the sea level changes which took place during deposition of the Laminated Beds continued during deposition of the Micrite Unit. However, it is not known if the increased cyclicity in the Micrite Unit reflects an increase in the frequency of sea level change or merely that the area was shallower and therfore more sensitive to change.

Sequences similar to the Micrite Unit at Navan occur throughout the Irish Midlands (Philcox, 1984), but sedimentary trends are poorly understood (Philcox, 1984 p. 21). Structures include fenestrae, desiccation cracks, pseudomorphs after evaporites, evaporite collapse breccias, oncoidal beds and algal laminations. Notable localities include Oldcastle (Brand & Emo, 1986), Moyvoughly (Poustie & Kucha, 1986; Harwood & Sulliven, 1990), Newtown Cashel (Crowe, 1986), Ballinallack (Jones & Brand, 1986) and finally Tatestown (Andrew & Poustie, 1986) (refer to Fig 1.2 for summary and Fig.1.3 for locations). It is not known if the Micrite Unit in other areas forms depositional cycles like those at Navan but Philcox, (1984) referred to "rhythmic fenestral micrite" at Crossakeel 50 km to west of Navan and Harwood & Sulliven (1990) referred to cycles within the Micrite Unit at Moyvoughly.

It is not known how far emersion surfaces extend beyond the Navan area. Meteoric cements and emersion surfaces have been described to the east and SE of Navan. At Tatestown 3 km to the NW of Navan, the Micrite Unit was subaerially exposed and contains phreatic cements (Andrew & Poustie, 1986 Plate 3). At Kentstown approximately 15 km ESE of Navan, oolitic grainstones within the Pale Beds (the

Proudstown Member) contain keystone vugs, meniscus cements, rhizoliths and crystal silts at several horizons. These, together with fenestral fabrics in mudstones, were interpreted as reflecting subaerial exposure (Pickard *et al,* 1992). Harwood & Sulliven (1990) reported palaeosols from from the Micrite Unit at Moyvoughly and brecciated surfaces and fenestral beds are common at Oldcastle (Holes LS20, LS59 pers. observation 1989).

The Micrite Unit has a flat base and an irregular upper surface which culminates in a NE-SW striking channel approximately 2 km wide (Andrew & Ashton, 1985; Ashton *et al,* 1986). This irregular surface and associated channel is believed to reflect a gentle palaeotopography generated during subaerial exposure. Recently Esteban (1991 p.108 - 114) elucidated the key criteria for recognition of subsurface palaeotopography. The key elements include dissolutional features along the upper surface, the prescence of fine grained siliciclastic sediments which mantle the surface, brecciated surfaces and evidence of meteoric cementation. All these have been recognised at Navan. Esteban (1991 p.99 and enclosure 3.1) also discussed the different types of palaeotopography. Acccording to his scheme of classification the Navan example appears to be similar to the 'mosaic type', consiting of non linear paleohighs which may culminate in linear palaeokarstic feature.

Andrew & Ashton (1985) and Ashton *et al* (1986) did not consider the irregular upper surface and channel together. It was suggested that the channel was sedimentary in origin and it was believed to reflect a stacked sequence of individual channel sand bodies whose margins interfingered with the adjacent calcite mudstones. However, holes N755, N722, N736 and N806 (cross-section 'D-D) were logged along the western margin of the channel to test this hypothesis. No evidence of thickly interbedded grainstones and mudstones was found. In addition three holes, N725, N718 and N705, each 40 m apart, and intersecting the channel margin at 90^0 were logged as an additional test. Once again, no evidence of interbedding of mudstones and grainstones was present. Furthermore, no evidence of channel facies such as the sequences described from the Limestone Conglomerate and the Micro-conglomerate were observed. Fig 3.31 shows that the channel margin is sharp and brecciated, supporting the view that it was subaerial and was subsequently filled by grainstones.

Anderson (1990) suggested that the linear zone of thinning of the Micrite Unit which trends NE-SW, reflected a palaeohigh in the Lower Palaeozoic basement, and indicated the position of a hypothetical north-south trending 'geofracture' (Russell & Haszeldine, 1990). Anderson (1990) suggested that the *in situ* breccia surface within the Micrite Unit consisted of lithoclasts which rolled down the flanks of the palaeohigh to accumulate in 'deep water' micrite at the toe of the palaeoslope.

The calcite mudstones are not deep water deposits, they reflect lagoonal deposition. Recent lagoon - tidal flat environments have imperceptible seaward gradients suggesting

that no virtually no paleoslope exsisted during this time. The intraclasts are *in situ* and not allocthonous. They represent a subaerial emersion surfaces. Drill core data do not furnish evidence of a palaeohigh, the Laminated Beds and Muddy Limestone are of more or less even thickness throughout the study area and show no evidence of thinning against a palaeohigh. The overlying grainstone sequence, when plotted from the Nodular and Upper Dark Marker, fill a channel (refer cross-sections 'A-A' and 'D-D').

The upper surface of the Micrite Unit At Tatestown, 3 km to the NW of Navan may represent a continuation of the Navan palaeotopography. The upper surface of the Micrite Unit here, has a concentration of quartz silt and (unspecified) organic material overlying *in situ* breciated calcite mudstone surfaces. It was suggested by Andrew & Poustie (1986) that that the material along the top of the Micrite Unit represented a 'non sequence' or a sedimentary hiatus, the precise nature of which was unspecified. Such an interpretaion is supported by different cement histories across the Micrite - Grainstone Unit contact (Andrew & Poustie, 1986). Palaeotopography also occurs in the British Lower Carboniferous. In South Wales the Lower Carboniferous Llanelly Formation has locally been completely removed during Holkerian times (Wright, 1986). The junction between Dinantian limestones and the overlying Namurian siliciclastics is believed to represent a palaeotopography (Wright, 1991 p.63). South-east of Navan, on Anglesey, a number of subaerial channels 20 m deep and 200 m wide of late Dinantian age have been recognised (Walkden & Davies, 1983).

The palaeotopography at Navan has a maximum relief of 60 m over 2 km. Thus, it is not a substantial feature. A sea-level fall of at least 60 m has been described in the British Lower Carboniferous, where sea level is believed to have fluctuated by as much as 124 m between the basal Carboniferous and Arundian stage (Wright, 1986). Recently Klein (1992) suggested that that Late Carboniferous (Pennsylvanian) sea-level fluctuated by 120 m, averaging around 90 m.

The Grainstone Unit overlying the Micrite Unit is interpreted as reflecting deposition in oolitic and bioclastic sand shoals. Lithoclasts within this sequence suggests that the contemporaneous shoreline consisted of muddy lagoons and tidal flats similar to those formed during deposition of the Micrite Unit. The thick middle shelf grainstones overlying the lagoonal and intertidal mudstones point to a relative rise in sea level. The Upper Dark and Nodular Markers, although it cannot be proved conclusively, are interpreted as reflecting lagoonal sequences. This indicates that alternate transgressions and regressions or still stands were taking place. However, the metre scale cyclicity which characterizes the Micrite Unit is absent here, suggesting that the apparent frequency of sea level change was slowing by this time, or that waters were deeper and therefore less sensitive to change.

The grainstones include several solutionally modified surfaces. These are morphologically similar to the karren type palaeokarst surfaces in the Micrite Unit and suggest that periodically regression culminated in emergence and subaerial erosion. Dissolution of skeletal aragonite and growth of non-luminescent syntaxial cements are believed to reflect meteoric phreatic cementation and support this interpretation. The grainstones also contain a channel sequence which is in the same geographical position as that in the Laminated Beds below. The channels are again filled with small pebble to sand grade clasts consisting polycrystalline quartz, lithoclasts of limestone and fragments of calcite cement. The latter consist of non-luminescent and bright luminescent couplets which are believed to reflect meteoric phreatic cementaion (Walkden, 1987; Emery & Dickson, 1989; Meyers, 1990). Such clasts provide indirect evidence for subaerial erosion during Grainstone Unit times.The origin of the carbonate grains is unknown, though the silica grains were most likely derived from the Longford Down Massif.

The grainstones are overlain by the succession of Shaley Pale Limestones, Argillaceous Bioclastic Limestones, Waulsortian Limestones, Boulder Conglomerate and Upper Dark Limestones. The Shaley Pale Limestones are belived to reflect an outer shelf environment with deposition below fair weather wavebase, suggesting sea level continued to rise. The Argillaceous Bioclastic Limestones have been interpreted as reflecting the continuation of this deepening trend. The Waulsortian Limestones are also belived to represent a deep water environment. The truncation surface which cuts through these to the Pale Beds is interpreted as resulting from fault-related erosion, reflecting proximity to the northern margin of the Dublin Basin (Strogen *et al,* 1990). The overlying Boulder Conglomerate is interpreted as a submarine debris flow deposit. The Upper Dark Limestone represents turbidites which flowed from the basin margin and the thin conglomerates within these point to continued debris flow activity.

The sequence at Navan reflects an overall increase in sea level punctuated by regressive and transgressive episodes. Philcox (1984) and Phillips & Sevastopulo (1986) proposed a similar scenario for the entire Irish Midlands. Comparable interpretation has been made for the lower Carboniferous of the Munster Basin, where the Courceyan consists of an overall transgressive sequence divided into five cycles (MacCarthy & Gardiner, 1987). In South Wales Courceyan limestones form five shoaling-up sequences with each cycle interpreted as reflecting a northward-directed transgression onto St. Georges Land. In South Wales transgressions were progressively more extensive, introducing more open marine conditions to the area, and recording an overall increase in sea level (Davies *et al* , 1991).

Carbonate platforms may be divided into two basic types; ramps with gentle slopes which lead from shallow water to deeper low energy waters without any significant break of slope, and rimmed shelves with a sharp break of slope separating the shallow water platform from the deep basinal environment (Ahr, 1973).

To determine the nature of the sequence at Navan, it is worth examining Courceyan successions beyond Ireland. Walken (1987) stated that the Early Dinantian was characterized by ramps which later evolved into rimmed shelves. This evolution is exemplified by the Dinantian sucession of the Bowland Basin which consists of lagoonal mudstones, open marine grainstones, submarine debris flows, and turbidites. The entire sequence compares with that at Navan and was interpreted as a ramp which subsequently evolved into a rimmed shelf (Gawthorpe, 1986). The basal Carboniferous (Courceyan) of South Wales is believed to represent a ramp. Like the Micrite Unit at Navan the sequence includes a peritidal muddy unit punctuated by numerous emersion surfaces, typically with palaeosols and karst. This facies is believed to have been deposited on an inner ramp with adjacent bioclast grainstones believed to represent mid ramp facies (Wright, 1986). MacCarthy & Gardiner (1987) suggested that the Courceyan succession north of the Munster Basin reflected a ramp and the Courceyan sequence at Kentsown, 15 km ESE of Navan, also represent a carbonate ramp Pickard *et al.* (1992).

7.3. ORIGIN OF CYCLICITY.

The Micrite Unit at Navan is characterised by repeated small scale shallowing up cycles, the origin of this cyclicity is considered in the following section. Recent carbonate muds accumulate at a rate of between 2 to 11 cm per 1000 years with platform margin ooid shoals having a maximum vertical accretion rate of 1 m per 1000 years. Background subsidence rates for carbonate platforms are in the order of 10 cm per 1000 years (Hardie, 1986) and thus, production of carbonate sediment can match or exceed subsidence rates, resulting in the formation of shallowing upwards cycles. Three mechanisms have been proposed to explain thick sequences of metre scale shallowing upward cycles; the Eustatic Model; the Autocyclic Model and the Tectonic Model (James, 1984; Hardie, 1991).

The **Eustatic model** has a rate of carbonate production which is constant, but the rate of subsidence or absolute sea level change is not. During periods of stability carbonate sedimentation outpaces subsidence and sediments build to sea level and prograde seaward, producing a shallowing upward cycle. A sudden rapid sea level rise

floods the the platform and the process begins again, repetition of this process produces a thick succession of shallowing-upwards cycles.

The **Autocyclic model** is not controlled by periodic changes in sea level, and background subsidence is constant. Sediment builds to sea level and progrades seaward forming a shallowing upward cycle. However, as progradation takes place the sediment source area is gradually reduced in size and is finally filled by the prograding tidal flat wedge, finally sedimentation ceases. Since sea level continues to rise the platform becomes flooded. There is, however a lag of several thousand years, during which production gradually increases until the sediment once more progrades. Repetiton of this proccess produces a sequence of metre scale shallowing upwards cycles.

Finally a **Tectonic model** has been proposed. Carbonate platforms commonly occur at divergent plate margins which are segmented by block faulting (Hardie, 1986). These blocks experience discreet pulses of subsidence up to 1 m. Following subsidence inundation of the platform takes place, allowing progradation of tidal flat shallowing upwards cycles.

Currently it is not possible to distinguish between the models since the processes produce the same result and criteria for the recogntion of the models have not been established. (Hardie, 1986, 1991 also pers commn, 1991). The small study area at Navan (3.5 km x 2 km), plus the lack of detailed sedimentological studies from adjacent areas, precludes the elucidation of the origin of the cycles. However, in order to gain insight into possible mechanisms it is worth examining regional studies of British and Irish Lower Carboniferous cyclicty. Cyclicity is ubiquitious in the late Dinantian, occuring in North Wales, Derbyshire and Cumbria (Walkden, 1987; review by Wright, 1991 p.81). Early Asbian cycles are peritidal with a grainstone base passing upward into fenestral mudstones and wackestones; palaeokarst is well developed. Late Asbian cycles are massively bedded crinoidal - pelloidal packstones and grainstones containing well developed palaeokarst. Brigantian cycles are thick and rich in terrigenous mud with subdued palaeokarst. The widespread distribution of cycles, with similar numbers of cycles occuring in different areas indicates a single dominant mechanism was responsible for the cyclicity. It was suggested by Walkden (1987) that the mechanism was eustaitc sea level change, driven by the fluctuating south-polar ice cap of Gondwanaland. The interaction of this glacio-eustatic sea level fluctuation with background subsidence was responsible for the changing styles of Asbian and Brigantian cyclicity (see Walkden for disscussion). Wright (1986) suggested that the cyclicity in the Lower Carboniferous of South Wales was the result of the interaction of eustatic sea level change, subsidence, and sediment supply.

In Ireland six cycles have been recognised in the South Munster Basin, each having a transgressive base (MacCarthy & Gardiner, 1987). Cycles 1 to 5 are Courceyan with

cycle 6 believed to be Arundian. The first, fourth , fifth and sixth cycles are regional and extend northward beyond the margin of the basin. It was suggested that these cycles were the result of eustatic sea level change coupled with periodic regional subsidence. However, cycles two and three are localized and are believed to have resulted from localized differential subsidence along the margin of the Dublin basin.

It is not known how long individual cycles at Navan took to accummulate. However, peritidal cycles are believed to be of 10 000 to 145 000 years duration (Hardie, 1986) averaging 10 000 to 100 000 years duration. (Hardie, 1991). In Britain, Walkden suggested that the avarage Asbian cycle accumulated inbetween 36 000 to 260 000 years, while the Asbian cycles of Cumbria are believed to reflect a 100 000 year sea level osscilation. (review by Wright, 1991 p.91).

7.4. PETROGRAPHY.

Cementation of lime sediment at Navan began early and much was contemporaneous with sedimentation. It took place on the sea floor in the open marine environment, within lagoons, and on tidal flats. In general, marine cements are isopachous acicular cements. Extensive meteoric cementation took place in the Micrite Unit during emergent phases. The main products included meniscus and microstalactitic cements, reflecting vadose conditions when pores were occupied by both air and water. Non-luminescent blocky and syntaxial calcite cements reflect meteoric phreatic cementation with bright internal subzones reflecting peroidic anoxic conditions. Other meteoric indicators include dissolution of aragonite grains, generation of moldic pores, and the deposition of crystal silts. The cements indicate that reduction of porosity began early at Navan, in some examples pores became filled with cement before passage into the burial environment.

Early meteoric and marine cementation was overprinted by mechancical compaction which culminated in grain fracture, spalling of oolith cortices and circumgranular cement, and collapse of micrite envelopes. This reduced porosity even further. Finally, blocky calcite overprinted the entire sequence, filling remaining pores and reducing porosity to an estimated 10% to 15%. Pressure dissolution occurred intermittantly throughout cementation, culminating in sutured seam stylolites and grain penetration. The final product was a tightly cemented limestone of low porosity and permeability.

7.5. DOLOMITIZATION.

At Navan extensive dolomitization occurs within the Micrite Unit (the Five Lens Dolomite) and in the Grainstone Unit above. In both units, it has a linear trend striking NE to SW with an overall plume shaped geometry in cross-section. Three stages of

dolomitzation are recognised separated by dissolution events. Dolomite rock textures, fluid inclusion microthermometry and $\delta^{18}O$ isotopes indicate that dolomitizing solutions were heated to around 60 °C to 100 °C. The dolomite body in the Grainstone Unit is at least 3.0 km long. The cross-sectional area of dolomitization (section 'B-B') is 84 500 m^2. If it is assumed that the cross-sectional area is more or less constant, the volume of dolomite present is at least 0.25 km^3. Land (1985) stated that dolomitization of 1 m^3 of limestone with 40% porosity at 6.3 mol % MgCO3 requires 648 pore volumes of sea water at 25 °C, assuming constant *p* CO2. Using this figure it is estimated that the volume of fluid required to produce dolomite was 54.4 km^3. The dolomite present in the Five Lens Dolomite is an additional 0.038 km^3 which would require another 9.84 km^3 of sea water. Thus the total volume of fluid required to produce dolomite at Navan is 64.24 km^3 at 40% porosity.

However, the pre dolomite porosity is believed to have been much lower than 40% due to calcite cementation, thus more $CaCO_3$ was present and therefore required a greater volume of magnesium bearing solution. In addition volumes do not consider fluids which produced the vuggy or other porosity, or dolomite precipitated as cement. ***Therefore, fluid volumes are crude estimations only.***

Several factors place constraints on the timing of dolomitzation. The crosscutting nature of the dolomite fronts and the timing of dolomitization relative to calcite cementation demonstrate that dolomitization post dates both the deposition and cementation of the youngest Pale Beds. Dolomitization has been noted in the overlying Shaley Pale Limestone (Black & Holdstock, pers commn 1990) suggesting that it may post date deposition of the Shaley Pale Limestone, but is unlikely to be extensive due to the high clastic content of this succession. The clast of dolomite observed in the debris flow (the Boulder Conglomerate) could have been derived from the Pale Beds, suggesting dolomitzation is post Courceyan but pre Chadian.

Hitzman & Large (1986) noted that extensive dolomitzation is a common feature of the Irish ore fields. However, relative to mineralization dolomitization has received little attention. Notable examples occur at Newtown Cashel (Crowe, 1986) and Abbeytown (Hitzmann, 1986b). At Abbeytown the Pb-Zn deposit is again associated with dolomitzation. This is confined to a limited area striking NE to SW and extending along a series of steeply dipping faults. In cross-section it has a crude plume-like shape approximately 100 m. high (Hitzman, 1986 and personal observation, 1988). The plume passes laterally into a sequence of stratal dolomite "fingers" (Fig. 7.1.A). One of these spreads laterally along the "Index Bed" and thus has crude stratigraphic consistency comparable to the dolomite extending along the Lower Sandstone and Sub Lower Sandstone Markers at Navan. The Abbeytown plume is divided into two zones an inner core consisting of intense dolomitzation, surrounded by an envelope of partial (matrix

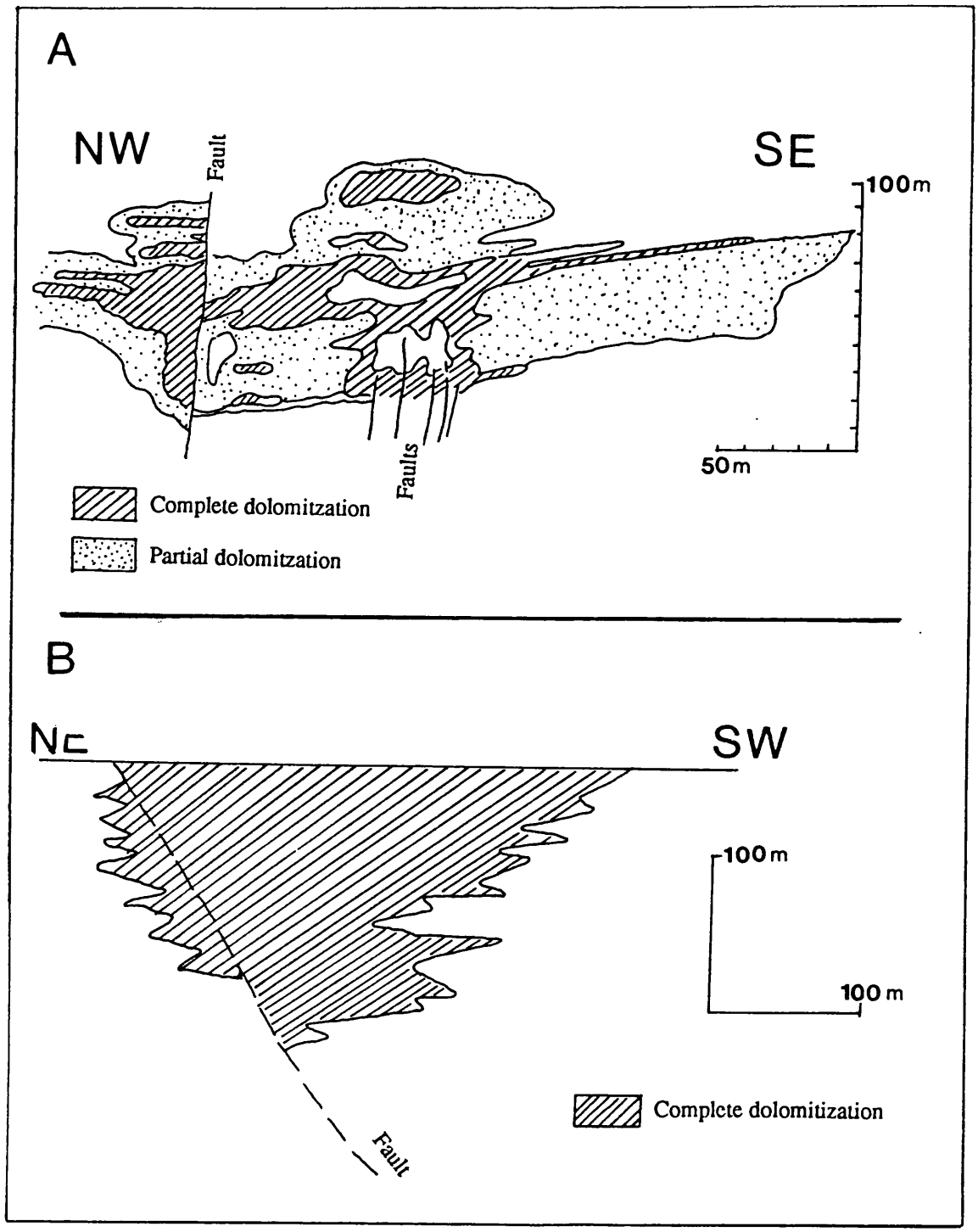

Fig. 7.1. A. Cross-section throught the hydrothermal dolomite at Abbeytown. The dolomite is plume shaped in cross-section and forms a linear body which strikes NE - SW. Modified from Hitzman (1986). **B.** Cross-section through the hydrothermal body at Newtown Cashel. The dolomitzation is related to a fault system and also extends around the margin of Lower Palaeozoic inlier at Keel, Modified from Crowe (1986).

selective) dolomitzation with vugs filled with saddle dolomite (personal observation, 1988). The dolomitizing solutions are believed to have been hydrothermal with faults and fractures acting as fluid conduits.

At Newtown Cashel two dolomite bodies are present, one pre-mineralization, the other apparently post-mineralization, separated by an unconformity. Both dolomites are described as "vuggy and intense" and cut across the stratigraphy. Both are believed to be hydrothermal. The pre- ore dolomite has pervasively altered the Micrite Unit as at Navan. The post ore dolomite occurs above the unconformity and is distributed around the western margin of the Lower Palaeozoic Keel inlier, extending along high angle faults. Like the Navan body it has a crude "plume" shaped cross-section approximately 200 m high and 400 m in wide. It apparently also passes laterally into a sequence of stratal dolomite "fingers" (Fig. 7.1.B).

The massive dolomitzation at Navan, Newtown Cashel and Abbeytown has essentially the same distribution, orientation, cross-sectional geometry, dimensions, timing and relationship with faults. It is proposed here that this style of hydrothermal alteration is characteristic of the Irish Zn-Pb ore field. Structurally controlled dolomitizaton believed to be hydrothermal occurs at Silvermines (Andrew, 1986 and personal observation 1990), Tynagh (Clifford *et al,* 1986), Harbeton bridge (Emo, 1986) and in the recently discovered Lisheen Pb-Zn deposit (Hitzmann *et al,* 1990). Extensive vuggy dolomite also occurs at Duncormick, (Carter & Wilbour, 1986) but has recieved little attention and its origin remains speculative.

7.6. GROUND PREPARATION.

The emplacement and distribution of Zn-Pb ores in the Navan area has been strongly dependent on ground conditions. Lithological variation, early cementation, the formation of karst and emersion surfaces, the late diagenetic overprint and the formation of dolomite have all prepared the framework into which the ores were emplaced. The Lower Palaeozoic sequence in holes EP3, N1014 and N1022 consists of thick black shales and tuffs. These rocks appear 'tight' and fracture porosity was not significantly developed. Some fractures are present but these were filled with blocky ferroan calcite. These rocks are considered to have been of low permeability.

The overall muddy character of the Laminated Beds and occurrence of early cements, mechanical compaction, and overprint by blocky calcite cement produced rocks of low permeability without fluid conduits. Although emergence occured several times during deposition of the Laminated Beds, the siliciclastic character of this part of the sequence precluded karst formation, and thus ground preparation is absent.

By contrast, the Micrite Unit consists of muddy cycles which contain a number of emersion surfaces. Four of these surfaces are important because they host mineralization (see below). The lowest two are breccias, the oldest overlain by a pedogenic green clay. The third is a karren type palaeokarst surface with a relief of several metres while the upper surface, the surface of the Micrite Unit itself, is bounded by a palaeotopography modifed by karren type palaeokarst. The muddy sediments between the emersion surfaces underwent both shallow marine and meteoric cementation which was subsequently overprinted by compaction and deposition of blocky calcite. In general rocks between the emersion surfaces had low porosity and permeability.

Similar palaeokarst occurs within the overlying Grainstone Unit, between the Lower Sandstone and Nodular Markers, below the Nodular Marker, and between the Nodular and Upper Dark Markers. Like surfaces in the Micrite Unit, cavities were extensively developed. These host mineralization while rocks between them were tightly cemented. The grainstones in the Pale Beds were selectively dolomitized; dissolution of dolomite and calcite produced three types of porosity, mouldic, intercrystaline and vuggy. A point was reached when dolomite became more permeable than adjacent limestones. Vuggy porosity is the most significant porosity type in the dolomite at Navan with vugs up to 8 cm diameter. Vugs are concentrated at the core of the massive dolomite body and created additional ground preparation within the grainstones. Other types of ground preparation in the Pale Beds at Navan include brecciation and fracturing (Andrew & Ashton, 1985; Ashton *et al,* 1986; Anderson 1990).

The sequence of Shaley Pales, Argillaceous Bioclastic Limestones, Waulsortian Limestones, Boulder Conglomerate and Upper Dark Limestones contains a high proportion of argillaceous sediment. It lacks emersion surfaces and was not dolomitized. Thus these rocks had low permeability and lacked fluid conduits.

In summary, the most permeable part of the the sequence at Navan lay within the Pale Beds, consisting of the Micrite Unit and overlying Grainstone Unit. Within these members, permeability was not pervasive, it was confined to emersion surfaces separated by tightly cemented limestones. The grainstones also controlled the distribution of dolomite. All significant porosity in the Pale Beds occupied by sulphides was formed in the dolomite, thus dolomitization prepared the ground into which the ores were emplaced. This porous sequence was enclosed by an envelope of low porosity and permeability which included the Laminated Beds below and the sequence overlying the Pale Beds. Anderson (1990) noted that growth of coarse blocky calcite followed deposition of the ores. He suggested by inference that mineralization did not occlude the cavities but left relic voids, estimated to represnt 20% of the cavity, subsequently filled by calcite.

7.7. MINERALIZATION.

7.7.i. Introduction.

Andrew & Ashton (1985) stated that 97% of ores at Navan are confined to the Pale Beds. Seven styles of mineralization have been described. The most important of these are massive mineralization, cavity-fill mineralization, breccia-hosted mineralization and vein-fill mineralization. Other styles include replacement of semi-lithified carbonate by sulphide, replacement mineralization and disseminated mineralization. For detailed descriptions of these styles, their paragenetic sequences and textural relationships, refer to Anderson (1990).

7.7.ii. Timing of mineralization.

Anderson (1990) considered that some mineralization was "early". In his view lime sediment was "semi lithified" and ore emplacement was "syn-diagenetic". This term referred to *"sulphide emplaced into sediment still undergoing compaction and lithification prior to complete lithification of the rocks"* (Anderson, 1990 and pers commn). The evidence he presented includes:

A). Thin layers of sulphide having bulbous bases, interpreted as load structures.
B). Buckled sulphide veins.
C). Sulphide 'rim cements'.

However Anderson (1990) believed that this early mineralization was rare. He considered much of the mineralization was late, filling fractures, veins and brecciated intervals and replacing lithified limestones. This contention is supported by several new petrographic observations.

Sulphide is present within stylolites (Plate 7.1.A), a feature also described from the Courtbrown Pb-Zn deposit (Grennen, 1986). This suggests that stylolites were acting as conduits for mineralizing fluids, supporting the view of Braithwaite (1989) who showed that stylolites may act as fluid conduits. By contrast, high amplitude sutured seam stylolites have been cut through by millimetre fractures filled with sulphide (Plate 7.1.B) indicating that some mineralization postdated stylolite formation.

A few bioclasts carry rims of galena or sphalerite. This was interpreted by Anderson (1990) as "sulphide" cement and used as evidence for early "syn-diagenetic mineralization". Present observations suggest that these rims cut across and ***replace*** calcite cement. This is best shown by sulphide rims which occur between echinoid grains and syntaxial overgrowths (Plate 7.1.C). Such rims cannot have formed before the

PLATE 7.1. Petrographic relationships between sulphides and calcite cementation.

A. Photomicrograph (plane light) of mineralization extending along a stylolite. Note fibrous calcite indicates dilation of stylolite. Hole N975 at depth 480.8 m. Scale bar = 1 mm.

B. Sutured seam stylolite (S) cut by fracture (F) filled with sulphide, scale in centimetres. The 1175 mine level 272 stope. Scale in millimetres.

C. Photomicrograph (crossed polars) of suphide rim cement. The cement (C) grew syntaxially on the echinoderm grain (E), demonstrating the cement substrate was unaltered. This indicates that the suphide rim is replacive and post dates the syntaxial calcite cement. Hole N975 at depth 504.0 m. Scale bar = 1 mm.

D. Photomicrograph (plane light) of pyrite framboids containing dolomite (d) and calcite at (c) 1375 mine level. Scale bar = 1 mm.

E. Photomicrograph (plane light) of galena crystals truncating bioclasts and cement (arrows). Hole N1020 at depth 553.6 m. Scale bar = 1 mm.

F. Photomicrograph (plane light) of pyrite truncating dolomite rhombs (arrow) in the Microconglomerate. Hole N988 at depth 401.5 m. Scale bar = 1mm.

G. Photomicrograph of former mouldic pore lined by geopetal sulphide (S) and overlain by saddle dolomite (D) suggesting sulphide emplaced during dolomitization. Sample from the 1175 mine level. Scale bar = 1 mm.

H. Photomicrograph (plane light) of sulphide (S) occuring within intergranular pore (P) in dolomite (D). Hole N763 at depth 467.0 m. Scale bar = 1 mm.

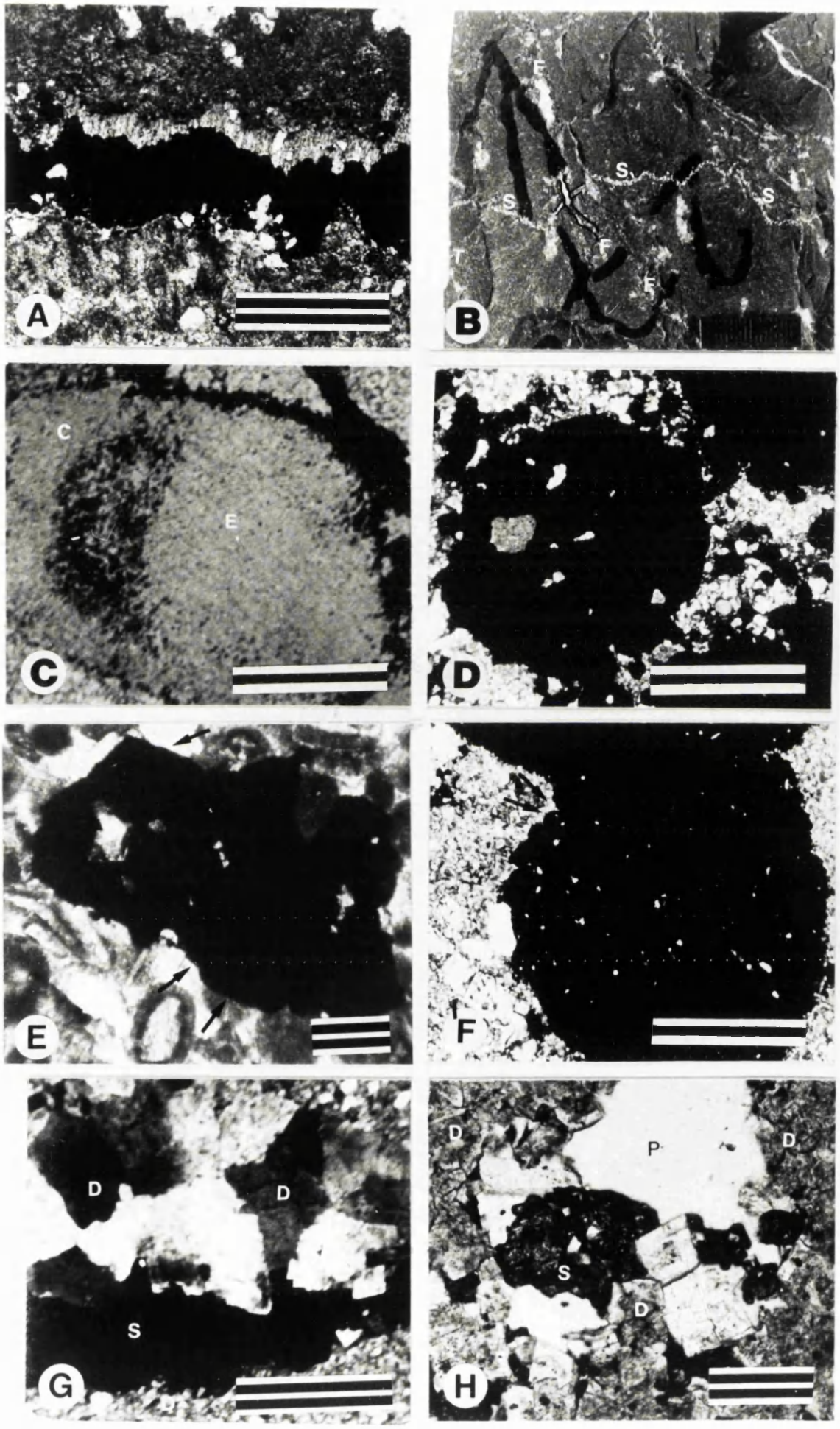
A
B
F
S
C
E
C
D
D
E
F
G
D
S
H
P

syntaxial cement because growth of the latter requires an unmodified substrate. This calls into question the findings of Kucha (1988) where similar sulphide rims were used as evidence that mineralization at the Moyvoughly prospect, County West Meath, was early 'syn-diagenetic'. Additionally Kucha (1988) was unable to distinguish between ooliths and echinoderm spines which further calls his observation into question, since it was assumed that ooliths were aragonite, which caused them to be selectively mineralized during early 'sulphidization' of the unlithified sediment.

In the Micrite Unit marcasite framboids cut across allochems, cements and floating dolomite rhombs. These framboids may contain inclusions consiting of dolomite rhombs, plagioclase and quartz grains (Plate 7.1.D). Galena crystals truncate authigenic quartz crystals which themselves post date calcite cementation. Similar relationships were noted in the overlying Grainstone Unit where pyrite has selectively replaced some allochems within the micro-conglomerate (Plate 7.1.F).
Mineralization within the Navan dolomite may be;

A). Confined to moldic and intergranular pores (Plate 7.1.G-H).
B). Confined to vugs (Plate 7.2. A).
C). Confined to fractures and brecciated dolomite (Plate 7.2.B).

Points A and B indicate that mineralization occured between dolomite stages but post dated Stage (1) dolomite when dolomitzation at Navan had established much of its present spatial and geometric character. Alteration of stage (3) saddle dolomite crystals by sulphide (Plate 7.2.C) and replacement of dolomite rhombs by sulphide (Plate 7.2.D) and sulphide filling fracures and breccia within dolomite suggest that some mineralization continued after dolomitzation. However, since the timing of mineralization with respect to dolomite paragenesis has not been the subject of a detailed study the relationship must be considered as a guidance only. The timing of mineralization relative to dolomite paragenesis is sumarised in Fig. 7.2.

7.7.iii. Relationship to host rocks.

The different styles of mineralization incorporating massive, cavity fill and breccia hosted deposits vary systematically within the Navan ore body (Anderson, 1990). In the central mine area, in the vicinity of the channel bounding the upper surface of the Micrite Unit, mineralization is dominated by two main styles, massive, (extending vertically for over 15 m) and breccia-hosted mineralization. It was shown by Anderson (1990) that these styles of mineralization change toward the west, the distribution of ores is not random, and mineralized sections have an apparent stratigraphic consistency. In the Micrite Unit mineralization occurs along the base of the Five Lens Dolomite and along the

PLATE 7.2. Dolomite - sulphide relationships.

A. Intergrown galena and sphalerite (O) filling vug in dolomite (D) margin of vug indicated by ink line. Scale in millimetres.

B. Brecciated and fractured dolomite with fractures filled by sulphide. Hole N1022, pencil for scale.

C. Photomicrograph (plane light) of saddle dolomite (D) being replaced by sulphide (S). Note alteration (A) of dolomite along the contact, with alteration extending along the cleavage (arrow). Hole N982 at depth 441.8 m. Scale bar = 200 microns.

D. Photomicrograph (plane light) of dolomite rhombs (D) being replaced by sulphides (S). Note ghosts of dolomite rhombs (G) in sulphide. Scale bar = 1 mm.

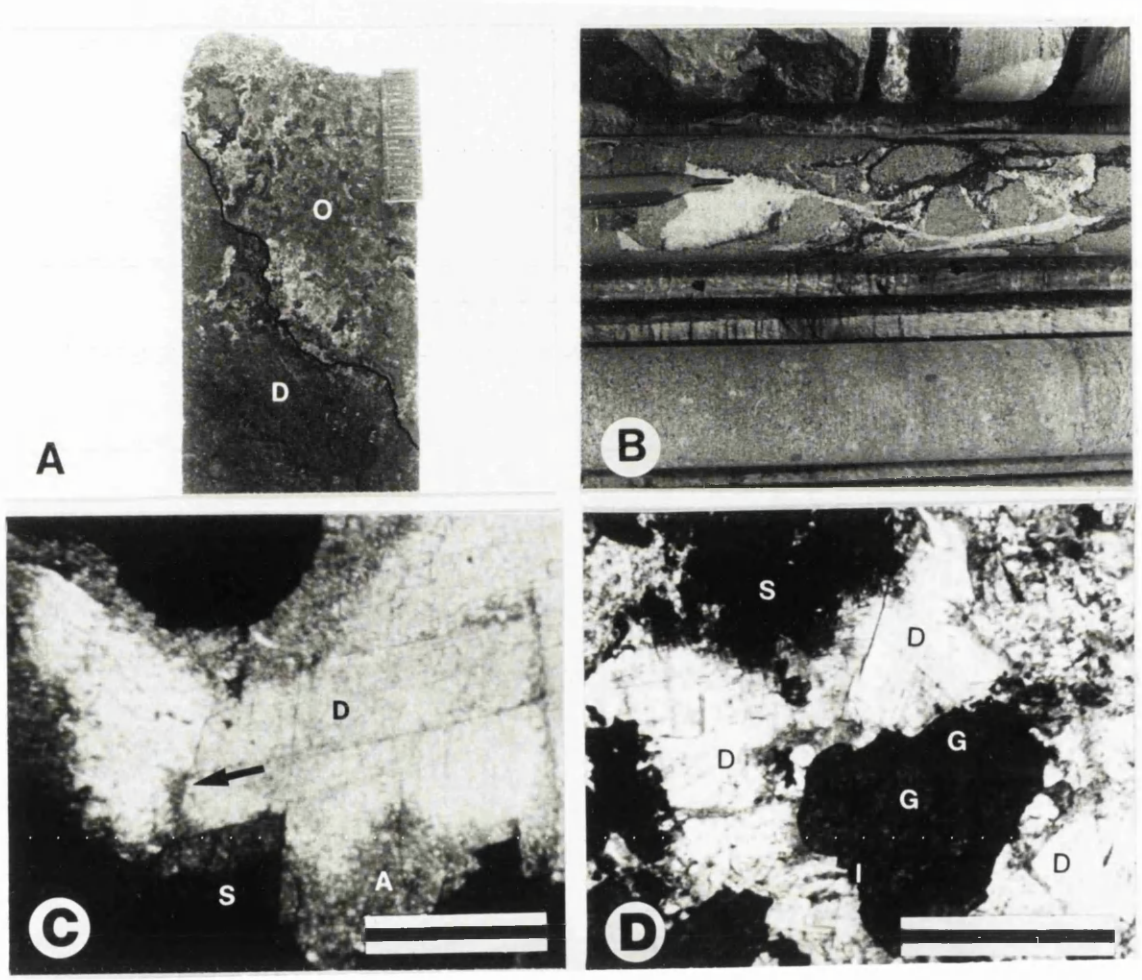
A
O
D
B
C
D
S
A
D
S
D
D
G
G
D

top of the Micrite Unit. In the overlying grainstones mineralization extends between the Lower Sandstone and Nodular Marker, below the Nodular Marker and between the Nodular Marker and the Upper Dark Marker.

Anderson (1990) described the cavities in which the ores occur. They are several metres deep and have bulbous bases, sharply truncating layering, fenestral and oncoidal beds. The cavities contain up to 0.5 m. of thinly layered sandstones, mudstones and siltstones which contain graded units. The origin of these cavities was poorly understood, but it was suggested that knowledge of their formation would be *"the key to understanding the Navan deposit"* . Anderson (1990) regarded them as dissolutional, perhaps hydrothermal in origin. A karstic origin was considered but not examined further, a reflection of the direction of the project, which concentrated upon mineralization.

It was suggested that the cavities were formed by unlithified calcite mudstone de-coupling from the base of "rigid dolomite beams" ***during*** compaction. These cavities were enlarged by hydrothermal dissolution during precipitation of sulphides. Andersons model is shown in Fig 7 .3. From a sedimentological perspective this is an unlikely scenario (also pers. commn., Gregg, 1991; Searle, 1991; Braithwaite, 1991; Bechstadt, 1991). The key criteria of modern hydrothermal karst systems consist of an extensive rectilinear network of dissolution guided by fracture systems together with exstensive silicification. In addition, such dissolution lacks evidence of near surface argillaceaous sediment (Smart & Whittaker, 1991 p.16). It was suggested that such features occurring in the geological record could reflect hydrothermal dissolution. There is no evidence of extensive silicification or of an extensive rectilinear dissoltion network at Navan and argillite is a common feature of cavities.

The cavities described by Anderson are contiguous with the karst surfaces in the Micrite Unit and the overlying grainstones; they have been considered in detail in chapters 3 and 4. The selective mineralization of these emersion surfaces was most likely a reflection of their high permeability relative to the tightly cemented limestones between. This also explains why the Pale Beds host mineralization which is not present in the underlying Laminated Beds or overlying Late Courceyan, Chadian and Arundian.

The model also explains why mineralization does not occur below the "footwall" green clay, the oldest prominant emersion surface, below which there is no evidence of significant space generating ground preparation. These controls on the distribution of ores at Navan may be compared with factors influencing ores in the Triassic Witterstein Limestone. This unit covers an area of 120 km^2 and contains several ore deposits, notably at Bleiberg. The host rocks comprise a sequence of subtidal to intertidal shallowing-up cycles termed the "cyclic facies". The cylcicity is puncuated by emersion surfaces which consist of breccia surfaces and karstic

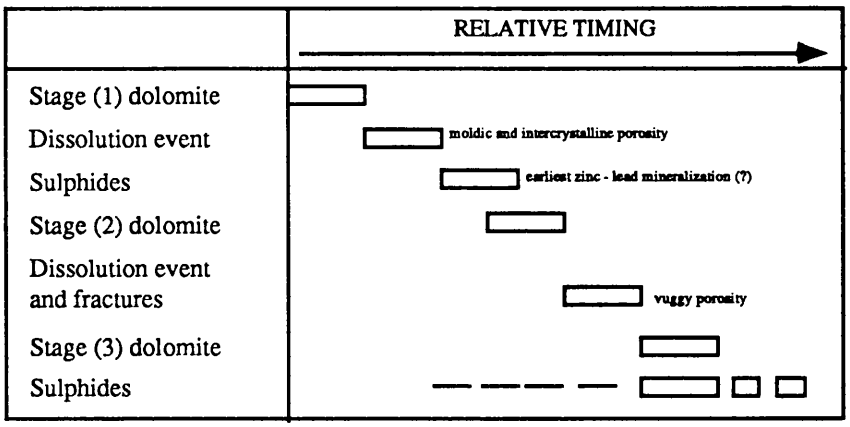

Fig. 7. 2. Timing of mineralization relative to dolomite paragenesis. For detailed disscussion of dolomite paragenesis and evolution of porosity refer to Chapter 5..

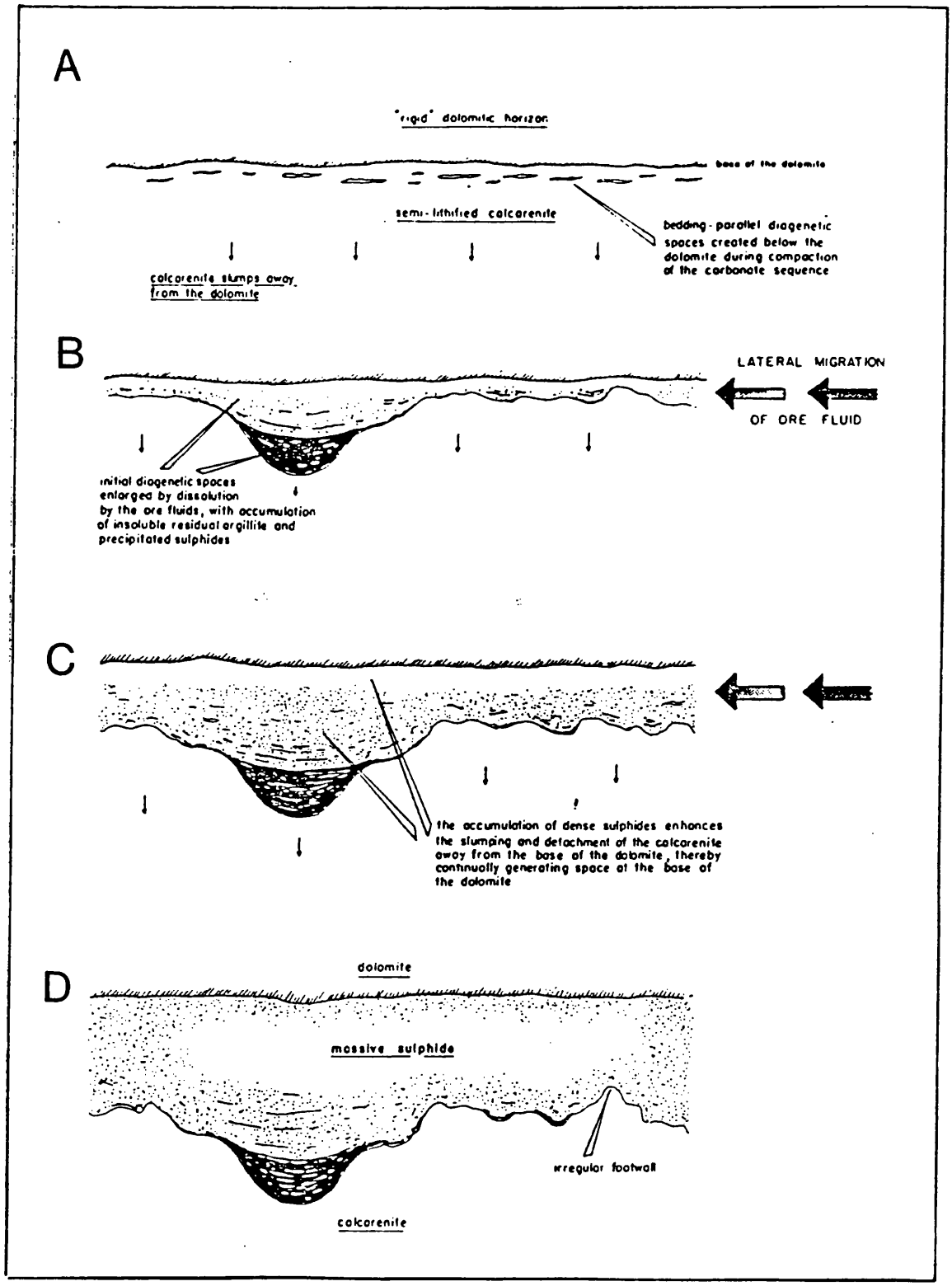

Fig. 7.3. Model of Anderson (1990) to explain the emplacement of ores in the Pale Beds at Navan. Soft sediment is believed to pull away from the base of dolomite 'crusts' during burial. This space is then enlarged by hydrothermal solutions which also precipitate sulphides. Note that the argillaceous material filling the cavity is interpreted as an insoluble residue produced during dissolution of the limestone.

cavities (Bechstadt, 1975; Bechstadt & Dohler-Hirner, 1983; Bechstadt pers. commn, 1990). The cavities are similar to those occuring at Navan (refer Fig 4.21) Like the Navan examples, the cavities have been filled by siliciclastic sediment interpreted as deposited when the cavity was on the surface (Klau & Mostler, 1986). Like the Navan deposit, the cavities in the Alpine ore district contain stalactitic sulphides, indicating that they were open at the time of mineralization (Klau & Mostler, 1986). Italian Pb-Zn deposits also relate to emersion surfaces (Assereto *et al,* 1976). Notable examples are the Cambrian Pb-Zn deposits of SW Sardinia (Boni, 1986). The host rocks here consist of lagoonal and tidal flat shallowing-up cycles containing pseudomorphs after evaporites, fenestral horizons and emersion surfaces. It is these cyclic sequences which contain the highest grade ores.

Elsewhere in the Irish Midlands the Micrite Unit hosts several other small (currently sub-economic) Pb-Zn deposits. The most important of these are at Oldcastle 30 km NW of Navan, where mineralization occurs along the top of the Micrite Unit and within fenestral horizons (Brand & Emo, 1986) and Tatestown 3 km to the NW of Navan, where mineralization also occurs along the top of the Micrite Unit (Andrew & Poustie, 1986). Other occurrences include those at Moyvoughly (Poustie & Koucha, 1986) and Ballinallack (Jones & Brand, 1986). The similarity between the Micrite Unit at these localities and its appearance at Navan suggests that mineralization may again have been controlled by palaeokarst surfaces, but this remains speculation. However, such a view is shared by Briskey *et al,* (1986) who pointed out that shelf carbonates in the British Lower Carboniferous contain numerous emersion surfaces located around the periphery of positive blocks. It was inferred from this comparison that emersion surfaces should also occur in the Lower Carboniferous shelf limestones of Ireland as they do in all other ancient shelf limestones (Briskey *et al* 1986).

The dolomite at Navan does not host mineralization except where vuggy porosity provided sufficient ground preparation. Isopach maps showing the distribution of ores define a linear NE-SW trend (Ashton *et al,* 1985) which is the same trend as the Five Lens (Fig.7.4) and Grainstone Unit dolomitzation (Fig.7.5). Both mineralization and dolomitization are spatially related to the major fault systems, but the faults are neither mineralized (Andrew & Ashton, 1985; Anderson, 1986) nor dolomitized. The close relationship between dolomitization and mineralization at Navan suggests that they are genetically related.

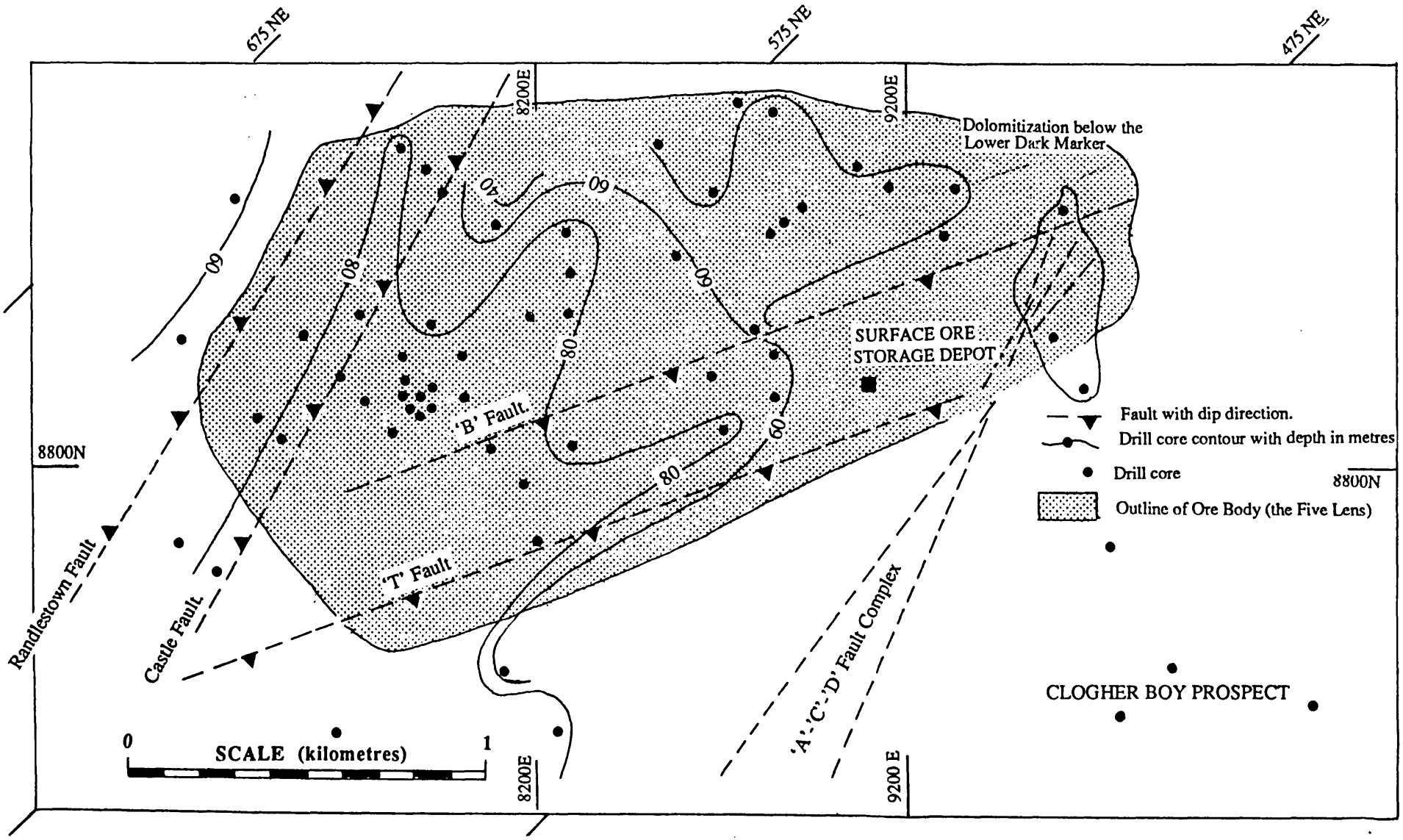

Fig. 7.4. Distribution of the Five Lens Dolomite relative to the ore body at Navan. Both the orebody and the dolomitzation are confined to a limited area and define a NE - SW trend.

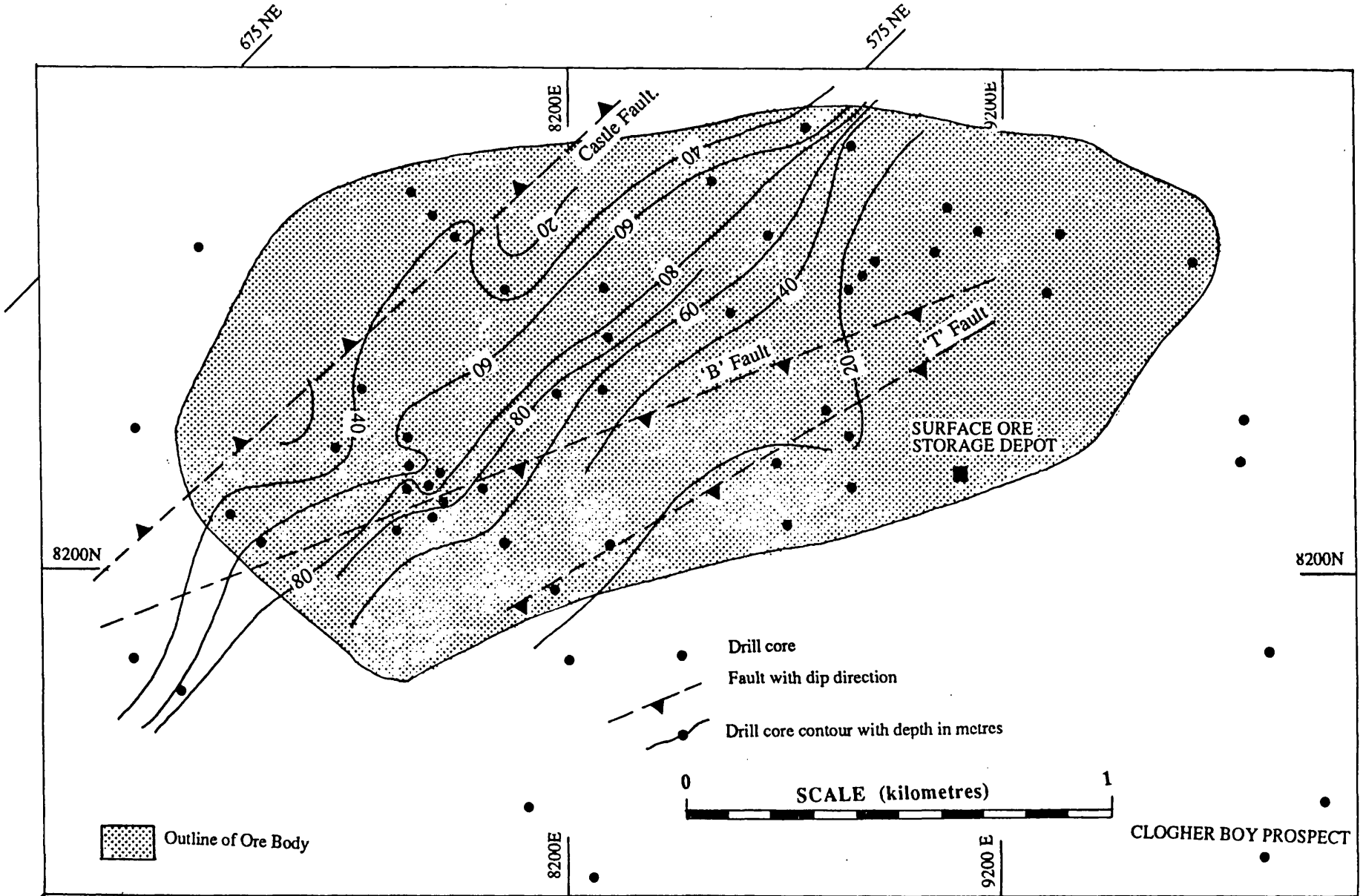

Fig. 7.5. Distribution of dolomite in the Grainstone Unit. Both the dolomite and the ore body are confined to a limited area and define a NE - SW trend.

7.8. GENETIC MODELS.

There are two main genetic models proposed to explain mineralization in the Irish ore field, the stratal aquifer model of Lydon (1986) and the deep crustal hydrothermal cell of Russell (1986). These will be described and evaluated with respect to the findings of this thesis.

Gravity and magnetric data indicate that the north Midland Region of Ireland (refer Fig. 1.9 for location) is underlain by NW trending graben and horst structures with a relief of up to 2.5 km (Brown & Williams, 1985). The basin defined by these structures contains over 350 m of Late Devonian - Early Carboniferous terrestrial Red Beds (Lydon, 1986). This is important since genetic models for SEDEX and MVT deposits envisage solutions derived from sedimentary basins; this is also a key feature of the stratal aquifer model.

The stratal aquifer model suggests that the ore solutions responsible for Irish Zn-Pb deposits were generated in structurally controlled aquifers of Red Bed facies. The aquifers were charged with sea water or brines during the Lower Carboniferous marine transgression. This transgresion deposited a blanket of muddy siliciclastic rocks across the region, burying the Red Bed facies, which was itself buried by the Pale Beds. The argillaceous beds formed both a permeability barrier and thermal insulation. Such a scenario provides the optimum conditions for large volumes of metalliferous formation water (Lydon, 1986). The pore fluid became heated to about 200 ^{0}C by a higher than average geothermal gradient (Phillips & Sevastoupulo, 1986; Jones, 1992). Metals were leached from the clay fraction, coarser grains and iron pigments within the Red Bed facies. Geopressuring developed by continued compaction on release of clay interlayer water. The geopressured water was released due to tectonism or rupturing at the basin margin, either as a single event or intermittently in accordance with the mechansim proposed by Cathles & Smith (1983) for MVT deposits.The model is sumarized in Fig. 7.6.A.

The crustal scale hydrothermal cell is specific to the Irish ore field and is shown in Fig 7.6. B. Sudden subsidence during extensional strain is believed to have sheared the upper crust which was invaded by sea water. Fluid pressure enhances brittle failure of rocks at 250 ^{0}C. Convection cells formed which involved modified saline water modified in the upper crust by hydrothermal metamorphism. These fluids became enriched in base metals. As the crust cooled by this process, the cells deepened and widened with time. Thermal "updrafts" form at temperatures of 220 ^{0}C and invaded joints and voids below the sea floor prior to exhalation into brine filled depressions. Metal sulphides were precipitated form slighlty acidic hydrothermal solutions on mixing with sea water.

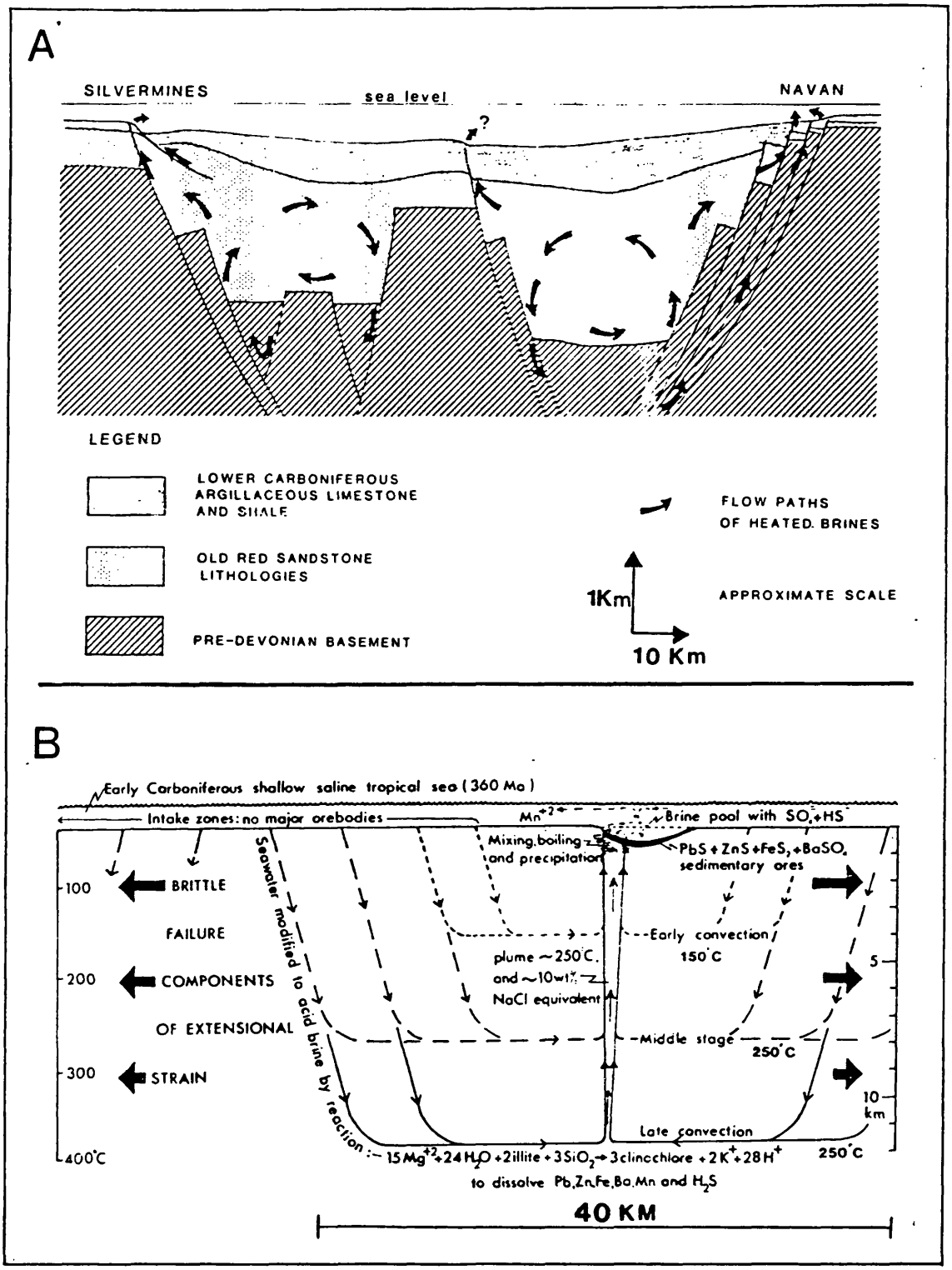

Fig. 7.6. A the stratal aquifer model, from Lydon (1986). B. The crustal scale circulation model, from Russell (1986).

At Navan the Red Beds pinch out, indicating that the deposit is located along the margin of a basin. The Red Beds have also been altered, the most intense alteration is selective, occuring along the upper surface of the Red Beds and along the sand members of fining-up cycles. This alteration demonstrates that red pigment which coats grains, and containing loosely bound hydrated metal oxides, has been removed. Petrography indicates extensive dissolution and alteration of feldspars and micas and growth of authigenic clays, feldspar and quartz, an important process in which base metals are release into pore fluids (Lydon, 1986). There is apparently no corresponding alteration of the underlying Lower Palaeozoic rocks.

The Red Beds at Navan are overlain by approximately 30 m of muddy siliciclastics which are overlain by the Pale Beds forming an effective seal. The saddle dolomite at Navan indicates circulation of saline heated pore fluids with fluid inclusion microthermometry indicating temperatures of 60 ^{0}C to 159 ^{0}C. Dissolution features within the dolomite suggests that fluids were introduced into the Navan area as 'pulses'. These features are consistent with the stratal aquifer model of Lydon (1986) which embodies the essentials of genetic models used to explain many MVT and SEDEX Zn-Pb deposits.

No evidence for a feeder zone beneath the Navan ore deposit has been described. The Lower Palaeozoic rocks are 'tight' and fracture porosity is not well developed, in addition, there is no evidence of thermal metamorphism of black shales or other lithologies at Navan. Thus, there is no geological evidence for the deep crustal circulation model of Russell (1986). This model was favoured by Anderson (1990) and radiogenic isotopes from Navan galena have been interpreted as being derived from the Lower Palaeozoic Basement (Mills *et al,* 1987). However, as Lydon (1986) pointed out, radiogenic isoptopic signatures could reflect recycled lower Palaeozoic basement, now forming Red Bed facies. In summary, the stratal aquifer of model of Lydon (1986) is in overall agreement with the findings of this thesis.

7.9. EXPLORATION IMPLICATIONS OF THE THESIS.

Drilling is the most expensive part of an exploration project, therefore the aim of this section is to outline the criteria which could help constrain a surface diamond drilling program in the Irish ore field. At Navan the location of ores has been dependent on ground preparation. The key features of this were:

1). Meteoric diagenesis which included the deposition of microstalactitic cements, dissolution of aragonite bioclasts and infiltration of crystal silts.
2). Depositional cyclicity punctuated by the formation of *in situ* breccias.

3). Formation of green pedogenic clays filling brecciated surfaces.
4). The formation of steeply inclined dissolution surfaces which truncate sedimentary layering, fenestral horizons and oncoidal beds.
5). Extensive dolomitization is related to faulting but detailed distribution was controlled by the sedimentary envelope. Both growth and dissolution (formation of vuggy porosity) of dolomite were involved.

All of these features may be recognised in diamond (BQ) drill core.

A large hydrothermal dolomite body is associated with the Navan deposit, the known distribution of ore has the same overall trend as the dolomite. Recognition of extensive dolomitzation in drill core elsewhere thus provides a focus for further exploration since mineralization may be associated.

CONCLUSIONS.

Introduction.

The aims of this thesis were:
1. To describe and interpret the sedimentology of the rocks below, above, and hosting the ore body at Navan..
2. To describe and interpret the diagenetic evolution of the host rocks and show how this evolution has affected their porosity and permeability and hence ability to transmit and trap ore bearing solutions.
3. To characterise and interpret the dolomitization present at the Navan mine.
4. To contribute to the understanding of Irish Dinantian palaeogeograhy.

Summary.

1. The Red Beds at Navan are interpreted as reflecting a meandering fluviatile system, deposition was not continuous, periodic abandonment of the flood plain led to the formation of caliche nodules. The overlying Laminated Beds reflect alternations of barrier sandstone, lagoonal mudstones and siltstones, and tidal flat sediments. At least 2 episodes of emergence punctuated the sequence, the first is represented by a pedogenic green clay, the second produced nodular anhydrite (reflecting a sabkha environment). The Muddy Limestone is believed to represent a clastic influenced lagoon.

2. The Micrite Unit consists of at least 20 metre scale lagoon tidal-flat shallowing-upwards cycles, with oolitic grainstones reflecting periodic incursions of more open

marine conditions. Cycles culminate in emergent surfaces. Three of these surfaces are important because they host high grade mineralization. The lowest is an *in situ* breccia overlain by a pedogenic green clay, the second prominent surface, 10 m above, also a breccia surface occurs . The youngest surface is a karren type palaeokarst. The upper surface of thre Micrite Unit is bounded by a palaeotopography, which includes a NW striking channel.

3. The Grainstone Unit blankets the Micrite Unit. It reflects a sequence of open marine oolitic and bioclastic sand shoals. The Lower Dark, Nodular and Upper Dark Markers are believed to represent lagoonal sediment, suggesting alternate regression and transgression. Metre-scale cyclicity is absent, suggesting that the apparent frequency of relative sea level change was slowing at this time. The grainstones contain several solutionally modified surfaces similar to the palaeokarst surfaces in the Micrite Unit below, suggesting subaerial erosion took place at this time.

4. The sequence overlying the Pale Beds consists of Shaley Pale and Argillaceous Bioclastic Limestones and Waulsortian Limestones which reflect continued deepening. The erosion surface and overlying Boulder Conglomerate are believed to reflect the northern margin of the Dublin Basin with the overlying Upper Dark Limestones reflecting basinal turbidites. The revised stratigraphic sequence at the Navan mine is shown in Fig. 7.7.

5. Cementation of lime sediment began early and was contemporaneous with sedimentation. Features of shallow marine and meteoric cementation are present, but both are overprinted by mechanical compaction which is itself over printed by blocky (burial) calcite cement. The final result was a tightly cemented limestone with low porosity and permeability

6. Dolomitzation in the Pale Beds is confined to a limited area, having a linear NE-SW trend. Three stages of dolomitization are recognised, each stage is separated by a dissolution event. The geometry and distribution of dolomitization, dolomite rock textures, fluid inclusion microthermometry and oxygen isotope data indicate that dolomitizing solutions were heated. Comparison of dolmitzation at Navan with dolomitzation in other Irish ore deposits suggests that this style of hydrothermal alteration is typical of the Irish ore field.

7. The most permeable part of the sequence at Navan is the Pale Beds, but high porosity and permeability is not pervasive, it is confined to subaerial erosion surfaces separated by

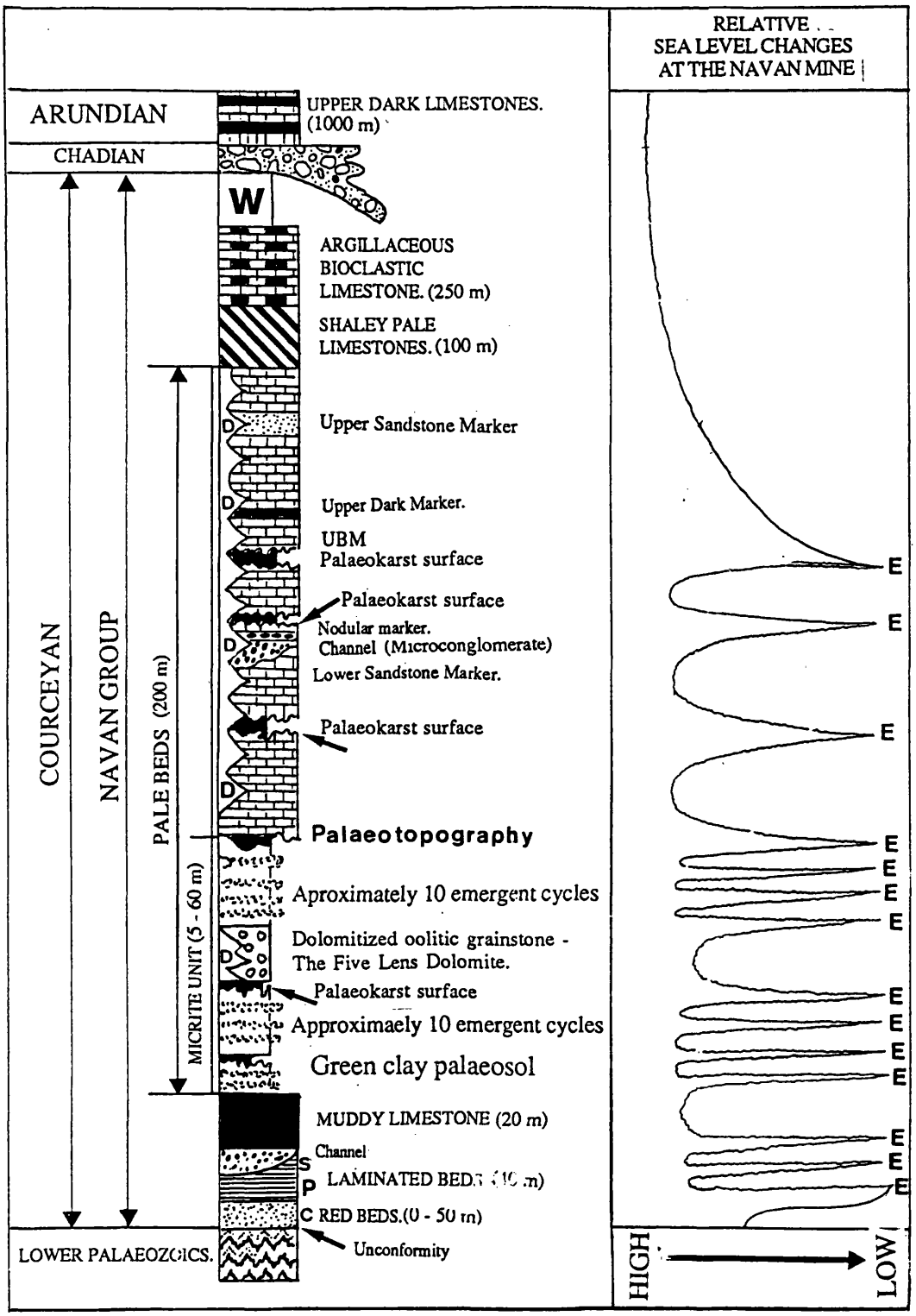

Fig. 7. 7. The revised stratigraphic sequence at the Navan mine and associated changes in relative sea level.

Boulder Conglomerate
Limestone turbidites
Sandstones
Lower Paleozoics
Shaley limestones
Crinoid rich shaley limestone
Bioclastic grainstones
Oolitic grainstones
Argillaceous lithology
Sandstones - shales - calcisiltites
Granule small pebble grade grainstone
W Waulsortian Limestone
C Caliche palaeosols
P Green clay palaeosols
S Sabkha evaporite
UBM Upper Bryozoan Marker
E Emergence
D Dolomite

tightly cemented limestones. The Pale Beds have also controlled the distribution of dolomitization, which, relative to the grainstones, has a higher porosity. The Pale Beds are enclosed in an envelope of low porosity and permeability consisting of the Laminated Beds and the sequence ovelying the Pale Beds.

8. Mineralization occured between stages of dolomitization. It post dates stage (1) dolomitzation. Alteration of dolomite by sulphide, replacement of dolomite by sulphide and the occurrence of sulphide filling fractures and brecciation within dolomite indicate that mineralization continued after dolomitization was complete.

9. The location of ores in the western mine area is strongly dependent on ground conditions and ores are located along karren type palaeokarst surfaces. This view contrasts with that of Anderson (1990) who believed that the cavities were the result of soft sediment pulling away from the base of dolomite 'crusts' during burial and compaction. The linear NE-SW trend of the dolomitization is contiguous with the outline of the orebody at Navan, suggesting the two are genetically related.

10. At Navan Red Beds pinch out and are believed to reflect a basin margin, supporting the geophysical data of Brown & Williams (1985). Feldspars and micas within the Red Beds have been altered and red pigmentation removed, indicating they have been flushed with reactive fluids. The Red Beds are overlain by a sequence of muddy siliciclastics, the Laminated Beds, which are in turn overlain by the Pale Beds. The Pale Beds contain evidence of subaerial erosion which again point to a basin margin position. These features are consistent with the stratal aquifer model of Lydon (1986).

From this summary it may be seen that the aims of the thesis have been satisfied.

Further work .

The geometry and distribution of dolomitization at Navan has been characterised and the paragenesis elucidated. This presents an ideal opportunity for a more detailed study of the trace element geochemistry of the different dolomite stages, and thus how depositing fluids evolved with time. This should be followed by a detailed fluid inclusion study involving microthermometry and salinity measurements, backed by an isotopic study of the dolomite with respect to $\delta^{18}O$ and $\delta^{13}C$.

The diagenetic evolution of the host rocks at Navan has been elucidated and dolomite paragenesis described. The timing of mineralization with respect to these event should ***now*** be the focus of a detailed study.

The Red Beds at Navan are believed to have been implicated in ore genesis. This should be pesued through a petrographic study of the Red Beds including a detailed isotopic and fluid inclusion study of the alteration products and authigenic minerals. The aim if this will be to characterise the solutions which flowed through these sediments.

APPENDIX 1.

Introduction.

Logging extended from the base of drill cores up to the base of the Shaley Pale Limestones. Drill cores are divided into two categories; those used in the construction of cross-sections, and non cross-section drill cores. The numbers of all cores are presented below.

Cross-section 'A-A'.

N509 N30 N286 N314 N629 N725 N806 N272 N835
N975 N933" N1018 N1026" N1017 N1022.

Cross-section 'B-B'.

EP27 N980' N1033 N853 N992 N862' N858 N864.

Cross-section 'C-C'.

N763 N826 N794 N911' N908' N1019'

Cross-section 'D-D'.

N755 N722 N736 N780 N804.

Cross-section 'E-E'.

EP4A N317 N351 N423 N535 N710.

Non-section logs (in numerical order).

N602 N852 N705 N718 N735 N857 N876 N907 N941"
N971* N978* N982 N984* N985 N986 N987 N988 N989
N990 N991 N993* N1000* N1000" N1004" EP3 EP12 EP20
EP21 EP26 EP27" EP30".

" indicates Tara Mine log used.
' indicates logged with department of mine geology.
* indicates selectively logged.

An example of these logs, together with logs at scales 1: 10 and 1:1 occur at the back of the thesis.

Sub-surface isopach maps have been constructed from drill core data, these data are presented below, number in brackets refers to thickness in metres.

1. Limestone Conglomerate.

Cross-section 'A-A'.

N1017 (10) N1018 (13) N933 (21) N975 (20) N835 (11) N272 (9) N806 (6)

Cross-section 'B-B'.

N1033 (20) N858 (16) N987 (19) N990 (18) N991 (21) N992 (18) N962 (17) N853 (20)

Cross-section 'C-C'.

N826 (10) N763 (12) N794 (11) N911 (18) N908 (20) N1019 (18)

Cross-section 'D-D'.

N755 (14) N722 (13) N736 (14) N806 (8) N780 (8) N804 (8)

Non section data.

N989 (20) N986 (15) N985 (17) N988 (18) N1020 (12) N1012 (11) N1015 (11) N1013 (16).

2. Oolitic grainstone body in the Micrite Unit.

Cross-section 'A-A'.

N1017 (11) N1026 (11) N1018 (11) N933 (10) N975 (12) N835 (10) N272 (11) N806 (11) N992 (9)

Cross-section 'B-B'.

EP27 (17) N980 (15) N853 (14) N990 (11) N991(11) N862 (10) N1033 (12) N858 (10) N980 (15)

Cross-section 'C-C'.

N763 (16) N826 (10) N794 (11) N911 (10) N1019 (10)

Cross-section 'D-D'.

N755 (11) N722 (9) N736 (9)

Cross-section 'E-E'.
EP4A (20) N317 (12).

Non section.
N1000 (12) N982 (11) N1001 (12) N1004 (11) N989 (10) N986 (10) N985 (10) N988 (8) N1020 (11) N1034 (13) N1013 (10.5) N987 (10.5).

3. Percent dolomite (brackets) in the oolitic grainstones (the Five Lens Dolomite).
Cross-section 'A-A'.
N806 (70) N272 (90) N835 (80) N975 (100) N992 (100) N933 (100) N1018 (95. 5) N1026 (70) N1017 (63).

Cross-section 'B-B' .
EP27 (100) N980 (75) N1033 (87) N853 (92) N991 (100) N990 (91) N862 (81) N987 (100).

Cross-section 'C-C'
N763 (87.5) N794 (100) N826 (100) N1019 (83)

Cross-section 'D-D'.
N755 (77) N722 (72).

Non cross-section.
EP26 (100) N1000 (100) N1001 (100) N982 (100) N989 (100) N986 (70) N985 (94.5) N988 (100) N1020 (75) N1013 (100)

4. Dolomitization below the Lower Dark Marker.
N535 N30 N286 N314 N629 N718 N705 N725

5. Distribution of Green shale.

Cross-section 'A-A'
N975 N992 N1017 N1026 N1018 N933 N1005

Cross-section 'B-B'
EP27 N980 N1033 N858 N862

Cross-section 'C-C'
N908 N911

Non cross-section logs
N991 N1020 N982 N985 N986 N1035 N1039 N1036 N1034 N1038 N1037 N1004 N1001 N1000 EP26.

6. Distribution of hummocky truncation surface.
Cross-section 'A-A'
N806 (1) N272 (5.5) N835 (6) N975 (0.5) N992 (4) N933 (2) N1026 (1).

Cross-section 'B-B'
N862 (1) N991 (2) N990 (2.5) N987 (2.5)

Cross-section 'C-C'
N908 (1) N763 (0.1) N794 (3.5) N826 (3) N911 (3) N1019 (0.3)

Cross-section 'D-D'
N722 (0.5) N780 (2)

Non cross-section
N982 (1.5) N985 (0.2) N986 (2) N988 (3.5) N989 (2) N1020 (1.7) N1015 (1) N1013 (1)

7. Thickness of the Micrite Unit.
Cross-section 'A-A'.
N1005 (63) N1017 (49) N1026 (50) N1018 (54) N933 (54) N975 (58) N835 (52) N272 (56) N806 (57) N725 (12) N705 (10) N718 (15) N629 (6) N314 (23) 286 (9) N30 (10) N509 (60) EP20 (18).

Cross-section 'B-B'.

EP27 (50) N980 (65) N1033 (63) N853 (63) N991 (53) N992 (53) N990 (52) N862 (50) N858 (50) N864 (30).

Cross-section 'C-C'.
N763 (55) N826 (51) N272 (56) N794 (53) N911 (59) N908 (24)

Cross-section 'D-D'.
N755 (48) N722 (48) N736 (20) N806 (52) N780 (33) N804 (18)

Cross-section 'E-E'.
N710 (13) N876 (6) N535 (20) N423 (23) N351(22) N317 (51) EP4A (50)

Non cross-section logs.
N1011 (58) EP26 (61) EP12 (33) EP21 (58) N1000 (58) N980 (63) N1001 (49) N982 (51) N1020 (60) N1034 (52) N985 (52) N986 (50) N1013 (50) N988 (50) N989 (44).

8. Thickness of the Microconglomerate.
Cross-section 'A-A'.
N272 (13.5) N835 (16) N975 (21.5) N992 (23.5) N933 (21) N1018 (23)

Cross-section 'B-B'.
EP27 (12) N853 (18) N862 (23) N991 (17) N990 (18).

Cross-section 'C-C'.
N826 (16) N911 (13)

Non-section logs.
N982 (21) N985 (23.5) N986 (21) N988 (18.5) N989 (18.5) N1013 (23) N1034 (23.5).

9. Percent dolomite (brackets) in the Grainstone Unit.
Cross-section 'A-A'.
N314 (5.3) N629 (6) N718 (10) N705 (17) N725 (19) N272 (85) N835 (80) N975 (73) N992 (53) N933 (89) N1018 (24) N1004 (8).

Crossection 'B-B'
N980 (7) N1033 (13) N853 (25) N858 (43) N862 (72) N991 (77) N990 (89)

Cross-section 'C-C'.
N908 (54) N735 (6) N794 (67) N826 (54) N911 (31)

Cross-section 'D-D'.
N755 (40.5) N722 (22) N736 (25) N780 (61) N804 (65)

Cross-section 'E-E'
N710 (36) N876 (62.5).

Non section logs
EP26 (16) EP30 (25.9) N1000 (73) N1001 (72) N1004 (74.5) N988 (73) N1020 (29.5) N1034 (45) N1013 (27).

APPENDIX. 2.

Carbonate Diagenesis, some general considerations.

Carbonate diagenesis may be subdivided into three reactive zones, meteoric, shallow marine, and burial zones, the processes of these zones will be reviewed and the diagenetic products described. For a comprehensive illustrated summary of carbonate diagenesis refer to Harris *et al.* (1985); Sellwood (1986 Fig 10.1); Moore (1989); Harwood (1989); Tucker &Wright (1990).

The Meteoric diagenetic environment.

Meteoric water has access to a large resevoir of CO_2 in the atmosphere where it is adsorbed by hydrolysis (Longman, 1980) and in soils, where CO_2 is generated by decomposition of organic matter and mixing with soil acids. Soil P CO_2 may reach 10^{-2} atmospheres, two orders of magnitude greater than P CO_2 in air (James & Choquette, 1988). This adsorption of CO_2 acidifies the water, producing undersaturation with respect to carbonate minerals. Marine carbonates consist of aragonite, high magnesian calcite and low magnesian calcite. All will dissolve in the presence of acidic meteoric water. The full sequence of reactions leading to dissolution is summarised in the equation:

$$CaCO_3 + H_2O + CO_2 \Rightarrow Ca^{2+} + 2HCO_3^-$$ (Ford & Williams, 1989).

The rate of dissolution is not uniform, aragonite is twice as soluble as high magnesium calcite which in turn is more soluble than low magnesium calcite. Magnesian calcite because of its generally greater solubility in meteoric water begins to alter to calcite

before aragonite (James & Choquette, 1984). Skeletal magnesian calcite is heterogeneous consisting of different levels of $MgCO_3$. The high magnesian calcite domains have greater solubility and dissolve first, termed incongruent dissolution (Schroeder, 1969) while Ca^{2+} is added to sites formerly occupied by the Mg^{2+} ion.

Aragonite dissolution is controlled by the micro fabric of the skeleton or cement beginning in areas of high organic content or smallest crystal size. If the water flux is large and strongly undersaturated with respect to aragonite then total dissolution will occur generating moldic porosity. If the fluid flux is slow and the water only slightly undersaturated with respect to aragonite, dissolution will take place across an intraskeletal reaction film, resulting in coarse calcite mosaics with relic internal structure. This microscale dissolution is commonly referred to as 'calcitization' (James, 1974). The most stable carbonate and therefore the last to dissolve is low magnesium calcite (Moore, 1989). Since the mineral is pervasive dissolution is comonly a bulk process affecting the whole rock.

Limestones are the most sensitive indicators of sealevel change in the geological record (Walkden, 1987; Kendall & Schlager, 1981 and review by Tucker, 1990b).
Many platforms occuring in the geological record were exposed as flat plains just above sea level with little relief (James & Choquette, 1984). These platforms were subject to subaerial erosion represented by karst. Karst is defined as "a distinct surface on land which indicates non deposition, a break in the sedimentary sequence, reflecting an interuption in sedimentation" (Esteban & Klappa, 1983).

The nature of karst is dependent on several intrinsic and extrinsic controls. The intrinsic controls include the permeability and porosity of the limestone, the mineralogical maturity of the limestone and the presence or absence of bedding planes and fractures. Extrinsic factors include the climatic regime which can be humid or arid, presence or absence of a vegetation cover and the duration and intensity of subaerial exposure (James & Choquette, 1988; James,1984; Esteban & Klappa, 1983).

Palaeokarst is defined as ancient karst which is buried by younger sediments or sedimentary rocks and thus includes both relic palaeokarst (present landscapes formed in the past) and buried palaeokarst which are karst landscapes buried by sediments. Karst is represented by a variety of geomorphological landforms ranging from whole landscapes to caves and their associated collapse breccias (Ford & Williams, 1989). Metre to centimetre scale surface dissolution features also occur, collectively known as "Karren" (Ford & Williams, 1989). Several end member karren types can be recognised, forming either on bare rock or beneath soils (Ford & Williams, 1989; James & Choquette, 1984).

The most widespread form of karren is the solution pit, this is a bowl shaped hollow up to 1m deep and circular to elliptical in plan and up to 1m in diameter. Pits occur

either singly or aligned or form clusters on bedding planes. They can form on bare rocks or can have a filling of dark siliciclastic siltstones. Their location is often controlled by "karren shafts" (see below) which they often pass downwards, producing a funnel-like profile. Solution pans have a nearly flat base which is more or less horizontal. Individual pans may attain diameters greater than several metres and are up to 1m deep. Solution runnels form on more or less horizontal surfaces and are known as "Rinnenkarren". They consist of pinnacles and flutes with overhanging walls and flat rounded bottoms and can be up to 50 cm deep. Fissure controlled karren is termed "Splitkarren". These elongate cavities form by surficial widening of joints and can range from a few centimetres to several metres wide.

The different types of karren are not mutually exclusive, centimetre scale dissolution pits and splitkarren can deepen and widen with time to form kluftkarren. These have a crude funnel like profile and are several metres deep often grading into karren shafts (See below). Eventually the gradually widening karren features link up with their nearest neighbours. This produces a humocky trucation surface or rundkarren which may be wave like (wavekarren) or consist of flat botttomed, funnel shaped and circular pits separated by blunt pinnacles and ridges (spitzkarren) with the whole surface extending laterally for several tens of metres. Solution pits and splitkarren pass vertically into "karren shafts". These are circular to elliptical in plan and may be up to 1m in diameter. In profile they can be horizontal, vertical or they can be sinuous having a meandering type profile.

The meteoric diagenetic environment is divided into the vadose zone and the phreatic zone separated by the surface of the water table. In the vadose zone pores are filled with air gases with grain surfaces coated by water films while in the phreatic zone pores are water saturated. Water percolates down throught these zones under gravity by seepage through a network of pores, or by free flow along joints and bedding parallel dissolution cavities, more common in older terrains In the upper vadose zone where soils are common, $P\ CO_2$. is high, and consequently in humid climates active dissolution of limestone takes place, generating porosity and karst. The lower vadose zone receives meteoric water over saturated with $CaCO_3$, with greatest concentration occuring in a zone termed the capilliry fringe (Moore, 1989). If CO_2 degassing takes place by evaporation or evapotranspiration, $CaCO_3$ will precipitate as cement. Cements of the vadose zone have an irregular distribution. Stalactitic cements consist of low magnesium calcite and are non ferroan and non luminescent. Cements referred to as meniscus cements also form at grain contacts. These consist of granular equant crystals which are non ferroan and non luminescent and but may contain a few bright orange zones but may also be micritic (Walkden, 1987; Emery & Dickson, 1990; Meyers, 1991; Longmann. 1980) also review

articles by Moore, (1989b), Harwood, (1989), Wright, (1990) and Harris *et al.* (1985). Thus the diagnostic features of vadose zone are dissolution of aragonite, bioclasts and deposition of stalactitic and meniscus "gravity" cements.

In the phreatic zone, below the water table, in contrast to the vadose zone, pores are filled with meteoric water. Water movement occurs by diffuse flow through the pore network or by free flow along channels bedding parallel cavities and subterranean rivers. Meteoric phreatic water is well oxygenated and forms a downward penetrating lens which may sit on an impermeable layer or, in an island setting, will float on seawater. The thickness of the phreatic lens is about forty times the height of the water table. This relationship is termed the Ghyben-Herzberg principal (Todd, 1980).

Typical products of the meteoric phreatic zone are syntaxial overgrowths and granular equidimensional cements. Both are non ferroan and are non-luminescent or containining a few bright orange zones (Longman, 1980; James & Choquette, 1984; Walkden, 1987; Emery & Dickson, 1989; Meyers, 1991).

The Marine Diagenetic environment.

Shallow marine cementation is currently taking place in many carbonate environments, on beaches, tidal flats and in reefs and carbonate sand bodies. The allochems in these environments provide suitable substrates for cement nucleation. The areas of formation provide temperature or pressure increases, especially along platform margins where cold ocean currents are forced upward into shallow waters, are sites of high wave and current activity, photosynthesis and respiration and experience high volume fluid fluxes of oxygenated marine waters through pores. Pores also provide "protective shelters" localized micro environments allowing growth of delicate cement crystals. These factors collectively promote CO_2 degassing from seawater already oversaturated with respect to $CaCO_3$ (Bathurst, 1975). This further decreases the solubility of $CaCO_3$ leading to the precipitation of cement.

Given that all calcium carbonate is available for cementation, the estimated amount of seawater required to fill one pore with calcite is 10 000 pore volumes. However, in practice, only the calcium carbonate above the saturation level is available, and therefore, to fill a pore requires an estimated 100 000 pore volumes (Scholle & Halley, 1985).

The products of modern shallow marine cementation consist of acicular crystals, typically less than 10 microns in width. These are non ferroan and non luminescent and form isopachous crusts which line pores. This seafloor cementation produces surficial crusts or "hardgrounds" on sand bodies (Dravis, 1979). Equivalent crusts on beaches are termed "beach rock". Since pores on the beach contain air gases cements here also have stalactitic morphologies.

Several explanations have been put forward to explain the acicular morphologies of modern marine cements. Folk (1974) suggested that Mg^{2+} ions in seawater poisoned the sideways growth of calcite crystals by adsorbtion of the Mg^{2+} ion for Ca^{2+}. This produces lattice distortion at the edge of the growing crystal preventing outward growth, ultimately leading to elongation of the crystal parallel to the C-axis and formation of an acicular habit. Alternatively Lahann, (1978) showed the surface charge of the calcite crystals has a net positive charge, but the highest charge density occurs on the C-axis faces. This attracts large numbers of anions relative to cations, resulting in fastest growth in the C-axis direction and formation of an acicular habit.

Seawater is supersaturated with respect to to $CaCO_3$ (Bathurst, 1975), therefore it is fair to assume that cementation should be more widespread in modern marine environments instead of being confined to surficial crusts. This implies presence of kinetic inhibitors, preventing widespread cementation. A number of candidates have been suggested, including phosphate, magnesium, sulphate and mucilaginous coatings, all may be adsorbed onto crystal surfaces and blocking nucleation and growth sites.

Modern marine cements consist of aragonite, high magnesian calcite or low magnesium calcite. It is debatable what controls whether calcite or aragonite is precipitated. It is known that magnesium ions have a retarding effect on calcite precipitation in seawater but not on aragonite precipitation, and that sulphate inhibits calcite precipitation relative to aragonite. Temperature also plays a role, with warmer temperatures favouring aragonite deposition reflected in a global decrease in aragonite secreting organisms away from the equator. A further physical control on the mineralogy of precipitation is the supply rate of CO_3^{2-} ions (Given & Wilkinson, 1985). Here it is suggested that high rates of carbonate supply favours aragonite precipitation over high magnesian calcite. Within cavities where flow rates are high aragonite forms as cementation proceeds pore throats are occluded, the supply rate is reduced and calcite cements are precipitated.

Recognition of shallow marine seafloor cements in the geological record is based on the following petrographic criteria. They are often the first generation of cements and are followed by blocky spar. Cement crystals are typically acicular, non ferroan and non luminescent. They form isopachous crusts and in marine hardgrounds they display polygonal sutures when they occlude pores (Shinn, 1969). It is difficult to determine the mineralogy of ancient acicular cements by petrographic techniques alone. Ancient aragonite, like modern aragonite, is metastable. Thus it often displays corrosion, visible under CL as holes filled with brightly luminescent calcite. Aragonite crystals commonly have a square ended termination (Folk & Assereto, 1976). Identification of high

magnesian calcite cements is more difficult since they undergo conversion to low magnesium calcite without loss of structural detail. However they may retain a "magnesium memory" represented petrographically by microdolomite inclusions (Lohmann & Meyers, 1977). Low magnesian calcite often consists of radiaxial fibrous crystals These are made up of a number of crystal which diverge away from the cement substrate and display a radially sweeping extinction.

Burial diagenetic environment.

The burial diagenetic environment occurs beneath the reach of surface related processes and cut off from chemically active atmospheric gasses (Longman, 1980; Moore, 1989; Tucker, 1990a). Pore fluids in the burial environment are under constant pressure, either hydrostatic or lithostatic. Hydrostatic pressure is pressure transmitted through the water column via pore waters. It is influenced by variables including salinity, temperature and the presence or absence of CO_2 and CH_4 (generated by organic matter degradation). Lithostatic pressure is the pressure of the overlying rock mass transmitted throught he rock framework. During burial, if pore fluid is trapped whilst the sediment is undergoing compaction, the hydrostatic pressure will increase until both hydrostatic and lithostatic pressure are equal. A further increase will lead to overpressuring, with hydrostatic pressure exceeding lithostatic pressure, and this may culminate in hydraulic fracturing. Temperature increases linearly with depth, referred to as the geothermal gradient. The average geothermal gradient is about 25 ^{0}C / km but this varies between sedimentary basins.

A number of generalisations can be made concerning the composition of burial pore waters. Generally they are saline, with salinity varying from 10 000 to 100 000 ppm (Moore, 1989). Typically they are Ca^{2+}, Cl^{2+}, Na^{2+} brines with the HCO_3^- content varying according to the salinity. They are depleted in K^+, Mg^{2+}, and SO_4^- and have high Ca:Mg ratio relative to surface pore waters (Harris *et al.* 1985; Moore, 1989; Tucker, 1990a). More saline brines are interpreted as reflecting derivation by dissolution of evaporites at the surface or subsurface, less saline brines are believed to represent mixtures of meteoric, basinal and marine waters. Pore waters may also be derived from temperature driven mineral reactions, for example illite transforms to smectite at 60^{0}C at 2000 m (Boles & Franks, 1979) and phase changes such as the conversion of gypsum to anhydrite releases molecularly bound water molecules.

The circulation of pore fluids in the burial environment is less than 1 to 10 m / y $^{-1}$ (Tucker, 1990a). It may be thermally driven, with pore fluids moving as part of large convection cells or migrating up section toward the basin margin. Vertical flow can be achieved if sufficient faults or fractures are present. All flow paths can be distorted by

aquicludes such as thin shales, which deflect flow laterally.

Deposition of cements in the subsurface is influenced by temperature and pressure which in turn influence *P* CO_2. Increasing temperature will decrease the amount of CO_2 in solution and thus lower the solubility of $CaCO_3$ ultimately leading to cement precipitation. Rapid pressure decrease will also reduce the amount of CO_2 in solution, triggering rapid and widespread cement precipitation.

The products of burial diagenesis cementation are typically equant coarsely crystalline calcite crystals. The cement is commonly ferroan and dully luminescent but is often zoned (Harris *et al,* 1985; Moore, 1989; Tucker, 1990a; Meyers, 1991). Confirmation of a burial origin is based on the following petrographic criteria. The cement post dates mechanical and chemical compaction features. It may contain fragments of collapsed micritic envelopes and overlie and fill fractures in bioclasts, or surround grains displaying concavo-convex contacts. It may contain frament of spalled oolith cortex or circumgranular cements. Burial petrographic features have been reviewed by Moore, 1989; Tucker; 1990a; Harris *et al.* 1985 and Harwood, 1989.

A number of other features are typical of the burial environment. Saddle dolomite is precipitated in temperatures of 60 ^{0}C to 150 ^{0}C from saline brine with a Ca:Mg ratio of 5:1. Syntaxial quartz overgrowths are a common feature of the burial environment (Harwood, 1989). Syntaxial overgrowths occur in the North Sea and at depths of several kilometres and at temperature of 60 ^{0}C to 100 ^{0}C. They precipitate from convectively recharging formation waters. Silica is believed to be sourced from illite-smectite transformations, from dissolution and pressure dissolution of quartz grains and feldspar alteration (McBride, 1989). Walker, (1962) suggested that replacement of carbonate by silica was a function of pH and temperature. He suggested that silica will remain in solution above pH 9, if the temperature decreases and pH falls below 9 calcite will begin to dissolve and silica will precipitae congruently.

The burial environment is a zone of chemical pressure dissolution. As burial proceeds the elastic strain between grains increases leading to an increase in the chemical potential reflected in an increase in solubility and resulting in dissolution. Away from the area of compaction stress is lower and the solubility of calcium carbonate is reduced and precipitation will occur (Weyl, 1959). The migration of calcium carbonate from areas of high to low stress is aided by a thin layer of water (Weyl, 1959). This process is reflected in sutured seam stylolites. Since stylolites are products of preferred dissolution, less soluble minerals accumulate along them. This material may consists of silt grade quartz and clay minerals termed stylocumulates (Logan & Semeniuck, 1976) or may include dolomite crystals. Pervasive dissolution is also a common diagenetic feature. The agent of dissolution is acidic pore fluid. Acidification may be brought about in a number of ways,

a commonly quoted process is decarboxylation of organic components which releases CO_2 (Moore, 1989; Tucker, 1990). The initial stages of dissolution are represented by corrosion of cement terminations (Harwood, 1989).

APPENDIX 3.

Introduction.

A brief review of dolomitization has been undertaken to better understand the processes of dolomitization at Navan. The discussion of this is divided into three sections. The first considers the major souces of magnesium bearing fluids, the second provides a summary of factors which influence nucleation and growth of dolomite. The third section considers the various models which explain the ocurrence of dolomite in the geological record. For a comprehensive account of the different dolomite models refer to Moore (1989); Tucker & Wright (1990); Braithwaite (1991).

Sources of magnesium bearing fluids.

Seawater contains 1290 ppm magnesium and 411 ppm calcium with a calcium : magnesium ratio of 3.14, it contrasts with meteoric water with an average of 15 ppm calcium and 4 ppm magnesium giving a molar ratio of 0.44 (review by Tucker 1990c p. 367). Land (1985) suggested that the only common magnesium rich fluid in the earth's crust is seawater and that therefore seawater is probably the primary agent for massive dolomitzation. Seawater may be effective as an agent of dolomitization in an unmodified state but commonly it is concentrated by evaporation, diluted by meteoric water or heated geothermally. Morrow (1982a) advocated naturally occuring alkaline ground water as an agent of dolomitzation. Such water is derived from the interaction of continental ground waters that had undergone anaerobic sulphate reduction, with weathered siliceous rocks and basalts or dissolved continental alkalic carbonate minerals

Fluids capable of dolomitzation within the deep burial environment are believed to include modified marine waters buried along with the sediment or formation waters. Formation waters may vary widely in composition and may include meteoric water which has aquired magnesium. The source of such magnesium in the burial environment is believed to be from clay mineral transformation, notably during transformation of smectite to illite. However, Morrow (1982b) suggested that such fluids are capable of only local dolomitization of limestones adjacent to shales

The factors influencing nucleation and growth of dolomite.

Lippmann (1973) has shown that seawater is supersaturated with respect to dolomite by nearly two orders of magnitude. However, dolomite rarely precipitates out of normal seawater and modern lime sediments bathed in seawater remain undolomitized. Several kinetic reasons have been proposed to explain this important paradox. None of these factors operates independently and it is difficult to separate cause from effect (Morrow, 1982a). The most important factors believed to influence dolomitzation are;

1. The ionic strength of magnesium ions.
2. Influence of carbonate ions.
3. Sulphate ions.
4. Salinity.
5. The rate of crystallisation.

Hydration of magnesium.

Each magnesium ion is surrounded by a sheath of water molecules as $[Mg(H_2O)_6]^{++}$. The strength of the electrostatic bond of the magnesium ion to the water molecule is about 20% greater than that of its calcium ion couterpart and "much greater" than that of its carbonate ion counterpart (Lippmann, 1973). It is therefore difficult to break the bonds between magnesium and water molecules allowing magnesium to be incorporated into a crystal lattice. Naturally occuring hydrous magnesium carbonates such as hydromagnesite provide evidence of the relative strength of the hydration sheath of the magnesium ion (Morrow, 1982a). In contrast calcium ions which are less strongly hydrated are more readily incorporated into a growing calcium magnesium carbonate and are able to occupy sites within the magnesium layers.

Influence of the carbonate ion

Another important kinetic effect related to the strength of the magnesium ion hydration sheath is the inability of the relatively unhydrated carbonate ion to force its way through the hydration barrier and make contact with the crystal surface. Only some of the total carbonate ions in a solution have sufficient energy to break through the hydration barrier and come into contact with the crystal surface. The low activity of the carbonate ion compared to the activities of calcium and magnesium ions in many neutral and alkaline solutions such as seawater (pH 7.8 to 8.2) is believed to be a kinetic hinderence to dolomitization (Lippmann, 1973).

An increase in the concentration of carbonate ions in solution, probably in excess

of the calcium ion, may be an important factor promoting dolomite formation (Morrow, 1982a). Increase in the carbonate ion concentration in a solution is most likely a reflection of decreasing CO_2 (review by Braithwaite, 1991). It was suggested that the greater number of carbonate ions may provide sufficent sufficient energy to shoulder aside the hydration sheath of the magnesium ions (Lippmann, 1973). This suggests that dolomitization is favoured by solution with high alkalinity where carbonate ions dominate (review by Tucker, 1990c p. 368).

Speed of crystallization.

The mineral dolomite consists of calcium and magnesium ions which occur in alternating planes separated by carbonate ions (Gaines, 1980). Rapid crystallisation influences the degree of order because ions that adhere to incorrect lattice positions of rapidly growing crystals are more likely to be entombed because the rapid crystallisation will bury the defects by continued crystal growth. Slower growth rates permit a longer period of exposure of incorrectly situated ion to the solution. This increases the likelihood that it will be displaced by the correct ion (Folk & Land, 1975).

Sulphate ions.

Sulphate ions in waters may be kinetic inhibitors to dolomitization. Experiments by Baker & Kastner (1981) carried out at 200 ^{0}C over two weeks revealed that the sulphate content of the fluids was an important control. The addition of even small amounts of sulphate, less than 5% of its seawater value, were sufficient to inhibit dolomitization, with dolomitzation of aragonite proceeding at higher sulphate levels. In addition, NH_4 produced during sulphate reduction may exchange for magnesium within the carbonate lattice releasing it for incorporation into a dolomite crystal lattice.

It was concluded, that in situations where the sulphate level is lowered, dolomitization can be expected. One effective mechanism of sulphate reduction is microbial reduction of sulphate within organic rich sediment. Such environments are found in inter and supratidal flats where cyanobacterial mats are being decomposed. The lowering of pore fluid sulphate values can also occur through the precipitation of calcium sulphate minerals, gypsum and anhydrite, in evaporitic settings. The low sulphate content of most meteoric water (mean value 12 ppm) means that dilution of sea water (2650 ppm) also lowers the sulphate content (Kastner 1984)

Hardie (1987) criticised the emphasis on sulphate concentration as a control on dolomite nucleation. He drew attention to the fact that the youngest dolomite in the Abu Dhabi sabkhas is in contact with pore fluids whose sulphate concentration is five

times that of sea water (Patterson & Kinsmann, 1982). It has also been possible to precipitate dolomite from sulphate rich solutions in the laboratory (Hardie, 1987).

Salinity.

Two parameters that affect the growth of dolomite are the magnesium : calcium ratio and salinity (Folk & Land, 1975). An increase in the magnesium : calcium ratio of the solution favours uptake of magnesium into a precipitating calcium magnesium carbonate. This is because increase in the amount of magnesium in solution provides a greater number of magnesium ions that are energetically strong enough to shed their hydration sheath and become incorporated into the crystal lattice. This view is supported by experiments on the dolomitzation of aragonitic sediment where the reaction rate at temperatures approaching 100 ^{0}C were increased by an increase in the magnesium : calcium ratio (Gaines, 1980).

The disordering effect produced by rapid precipitation may be overcome by reducing the reaction rate by dilution (Morrow, 1982a). Dilution also reduces the volume of impurities present which are able to disrupt the dolomite lattice (Folk & Land, 1975). Dilution also slows crystallization. This idea is also supported by experimental evidence where sea water with five times normal salinity was diluted, slowing the reaction rate of dolomitzation. It is believed that dilution of sea water with meteoric water produces a solution undersaturated with respect to calcite and supersaturated with respect to dolomite (Badiozamani, 1973) such a belief provides the basis for the mixed water model of dolomitization.

Other features influencing dolomitzation.

i. To date, the precipitation of dolomite at sedimentary temperatures has remained elusive. Experimental data have shown that dolomite can be precipitated with relative ease at high temperatures (see Gaines, 1980, Gregg & Sibley, 1984)). An increase in temperature during burial will reduce kinetic inhibiors to dolomitization allowing the hydration of magnesium ions to be overcome, and speed up reaction rates (Mattes & Mountjoy 1980). At low temperatures crystal growth relies upon attachment of ions to screw and step dislocations in the crystal lattice or vacancies within the lattice. However at high temperatures such preconditions are less important and nucleation occurs randomly across the crystal surface (review by Braithwaite, 1991).

ii. The mineralogy of the precursor limestone may also be a factor influencing dolomitization. Sibley (1980) suggested that the dolomitzation of aragonitic sediment proceeds considerably faster than that of calcitic sediment. Rapid conversion of aragonite to low magnesium calcite in humid climates may produce resistance to

dolomitization of Pleistocene shelf limestones. (Sibley, 1980).

iv. The presence of certain cations such as lithium and iron has a catalytic effect on dolomite formation while aspartic acid, common in natural aragonite, retards dolomitization (Gaines 1980). Finally, the length of time and supply of magnesium will govern the amount of dolomite formed (Hardie 1987).

DOLOMITE MODELS.

Evaporite dolomitization.

Most modern dolomite is evaporitic and occurs on tidal flats (Shinn 1983 and review by Tucker 1990c, p.386). The hydrological regime responsible for this style of dolomitzation has been described by McKenzie *et al.* (1980) and is based on obsevations on the Abu Dhabi sabkhas. Water is driven up onto the tidal flats during the high tides and storms, and is termed 'the recharge phase'. This water has a net downward movement through the sediment. However, since the climate is arid, the resulting evaporation of seawater from the capilliary zone above the water table and extending 15 cm to 55 cm below the surface induces a net upward flow of groundwater to the capillary fringe, a process known as evaporative pumping (Hsu & Siegenthaler, 1969). This results in dolomitization at or just below the sediment surface. In this setting the Mg:Ca ratios are high and the ground water is alkaline (pH 6.3 to 6.9). The sulphate content of the pore waters is lower than in adjacent sea water as a result of microbial reduction and sulphate precipitation, providing conditions favourable for dolomite nucleation (Patterson & Kinsman, 1982).

This mechanism has also been proposed to explain dolomitization of Bahamian tidal flats where dolomite forms crusts in the high intertidal and supratidal zones around tidal ponds, on beach ridges and on levees (Shinn, 1983). The hypersaline lagoons of the northern Arabian Gulf adjacent to the sabkhas also contain dolomite. It was suggested that in these lagoons dolomite forms as a result of partial removal of dissolved sulphate ions, moderate magnesium calcium ratios, and perhaps occasional dilution of pore waters by fresh meteoric water (Gunatilaka *et al.* 1984). The main criteria for the recognition of evaporitic dolomite have been documented by Shinn (1983) and reviewed by Tucker (1990c). Evaporitic dolomites are generally associated with;

1). Fenestral horizons.

2). Microbial laminations.

3). Pseudomorphs after evaporites.

4). Crystals in ancient tidal flat dolomites are in the size range 5 to 10 microns. Evaporites need not be present because of their low preservation potential as in the Bahamas (Shinn, 1983). Finally because dolomitzation is a near surface process, the resulting dolomite bodies will be thin and tabular similar to dolomites in the hypersaline lakes of the Northern Arabian Gulf (Gunatilaka *et al,* 1984) and on the tidal flats of Andros Island (Shinn, 1983).

Seepage Reflux.

This model was proposed by Adams & Rhodes (1960) based on observations on the Permian of west Texas. It involves a rimmed shelf behind which is a wide shallow lagoon. Seawater travelling over the rim and across the lagoon undergoes progressive evaporation and density increase. The brines are heavy and sink, migrating to the lowest part of the lagoon floor. A critical density is reached and the brine begins to flow downwards and seawards through the floor, displacing lighter marine pore fluids and dolomitizing the sediments in its flow path. If equilibrium is established between vertical barrier aggradation and relative sea level increase, a thick sequence of evaporites may form, generating huge volumes of dolomitizing fluids. The main criticism of this model is that it lacks fully documented modern examples (review by Moore, 1989). Notable ancient dolomites attributed to this model include the Presqu'ile facies of the Pine Point lead-zinc deposit (Skall, 1975). Moore, (1989) reviewed the main criteria used for the recognition of seepage reflux dolomites;
1). Close spatial relationship of dolomites to evaporites (after Beales & Hardy, 1980).
2).There is a palaeogeographic control with sedimentological and structural data interpreted as indicating a barred basin.
3). Dolomitized reflux receptor units must have had suitable porosities, permeabilities and hydrological continuity at the time of dolomitization.
4). A dolomite gradient exists with an increased volume of dolomite towards the source of the refluxing brines (after Sears & Lucia, 1980).

To this list it is possible to add the presence of collapse breccias produced by evaporite dissolution, the presence of evaporite crystals or evaporite crystal moulds, and pseudomorphs after evaporite crystals or nodules (Dunham & Olson, 1980; Beales & Hardy, 1980).

Mixing zone dolomitzation.

Dolomitization by a mixture of seawater and freshwater was first proposed by Hanshaw *et al* (1971) with magnesium supplied by sea water and active curculation of ground water acting as the pump. This is believed to provide the key elements in

the generation of massive dolomites (Land, 1985). The model was supported by Badiozamani (1973) who demonstrated that mixing of 5% to 30% seawater and fresh ground water produces a solution which is undesaturated with respect to calcite but with dolomite saturation increasing continuously, culminating in supersaturation. The mixing of seawater and fresh water maintains the high magnesium : calcium ratios, reduces the volume of sulphates present (by diluting the sea water), and reduces the high ionic strength of the solution (Folk & Land, 1975). The main criteria for recognition of mixing zone dolomitization are;

1). It is a near surface process and therefore pre dates grain fracture.

2). Forms single lenticular dolomite bodies or a succession of vertically stacked lenses as a result of relative changes in sea level (Badiozamani, 1973). This is exemplified by the Mississippian Ste. Genevieve limestones of the Illinois basin (Choquette & Steinen, 1980).

3). Limestones were porous at the time of dolomitization.

4).There is a palaeogeographic control on the distribution of dolomite which is typically confined to the landward portions of carbonate platforms (Dunhan & Olson, 1980).

5). Dolomite is not associated with evaporites.

6). Oxygen isotopes are generally positive.

7). Dolomite may be associated with vadose diagenetic fabrics.

The best modern example of mixing zone dolomitization is believed to be the partly dolomitized Hope Gate Formation. In this, dolomite replaces Pleistocene coralline algae and lime muds and fills voids as a cement (Land, 1973). This interpretation is supported by oxygen isotopes which have lower $\delta\ ^{18}O$ than those of modern sabkha dolomites. The model is also supported by experimental data, mixing of 3% to 4% seawater with Jamaican meteoric water gave a solution oversaturated with respect to dolomite and undersaturated with respect to calcite with a Ca:Mg ratio greater than 0.8, favourable to dolomite formation. The main criticism of this model is based on the rarity of abundant dolomite in modern mixing zones (Hardie 1987). Land (1985) suggested several reasons for this;

i. Few mixing zones have been studied, since coring is required.

ii. Rapid oscillations of sea-level throughout the Pleistocene have precluded the establishment of steady state coastal hydrological systems. Coastal hydrodynamics are still adjusting to a rise in sea level of about 120 m in the last 18 000 years.

iii. The saturation of dolomite in the mixing zone may be the result of changes in pCO_2, and fluctuating temperatures and pH (Hardie, 1987).

iv. Dolomite in modern mixing zones hosted by the Falmouth Formation is not

associated with calcite dissolution, could not have precipitated from waters undersaturated with respect to calcite an attribute of the mixed water model for dolomitization.

Burial dolomitization.

It has been suggested that massive dolomitization can occur in the sub-surface at depths characterised by burial diagenesis, between depths of 500 m to 2000 m (Mountjoy, 1991). This mechanism has been invoked for dolomitization along the margin of the Devonian Miette Build-ups of Jasper National Park (Mattes & Mountjoy, 1980). The criteria used for the recognition of burial dolomites have been documented by Zenger (1983) Moore (1989), Tucker (1990c) and Mountjoy (1991). These include;

1). Pervasive and fabric selective textures.

2). Secondary vuggy and intercrystalline porosity, often lined with saddle dolomite crystals.

3). Healed microfractures within the dolomite.

4). Relic stylolites within the dolomite.

5). Dolomite fronts which extend across bedding.

6). Dolomite crystals are typically ferroan.

7) Two phase fluid inclusions typically indicating temperatures in excess of 100 ^{0}C.

8). Negative $\delta\ ^{18}O$ values.

A major constraint on the burial model is the source and delivery of magnesium to the site of dolomitization Morrow (1982), Land (1985). The magnesium source is thought to be clay mineral transitions, notably the smectite to illite transition, which also releases Si and Fe^{2+} (Boles & Franks, 1979). Several problems occur with this argument.

i). Morrow (1982b) illustrated the problems of mass balance. He calculated that compaction of several hundred cubic metres of shale would be required to dolomitize 1cm^3 of adjacent limestone.

ii). Magnesium is often consumed in the production of chlorite, a common authigenic mineral.

iii). No massive release of magensium by compacting shales is documented (Land, 1985).

v). In addition to the large amounts of magnesium required for dolomitization, the pervasive flow of fluid required to resupply the magnesium becomes increasingly difficult as the permeability of the rocks becomes reduced by cementation and solution compaction. There is no continued source of basinal fluids (Land, 1985).

However, dolomitization should proceed more easily with depth. The higher temperatures mean some hinderances to dolomite formation are overcome (Gaines, 1980), the proportion of hydrated magnesium ions decreases and the reaction rate increases.

Seawater Dolomitization.

Land (1985, 1991) Braithwaite (1990) Wilson & Hardie (1990) and Tucker, (1990c p. 400) have proposed that sea water itself with little or no modification other than heating will produce dolomitization. Several models of seawater dolomitization have been proposed.

1. Cores from Enewetak atoll in the Pacific contain dolomitized Eocene coralline algae and forams at depths of 1250 m to 1400 m below sea level (Saller, 1984). The dolomite was apparently precipitated after grain fracture, which is first observed at 610 m. It was suggested that dolomitzation has taken place since the early Miocene when the Eocene strata were buried at depth. It appears that ocean water is circulating freely at depth within the atoll and is the only fluid available for dolomitization since neither fresh nor hypersaline water could have penetrated to this depth. Stable isotopes from these dolomites have positive $\delta\ ^{18}O$ values indicating precipitation in the temperature range of 15 ^0C to 18 ^0C $\delta\ ^{13}O$ values of +2.3 ‰ indicating a marine source of carbonate. The driving mechanism for dolomitization is believed to be oceanic currents and tides, which force their way into the interior of the atoll, and thermal convection generated by high heat flow through the basement of the structure.

2. Hydrothermal seawater circulation has been advocated as a dolomitization mechanism by several authors. Land (1985) stated*"I suspect that hydrothermal circulation of seawater is a vastly more important process than previously recognised"*. Kohout (1967) documented large scale circulation of sea water in the Florida platform. What has come to be called Kohout convection is driven by the horizontal density gradient between marine waters adjacent to the platform and geothermally heated groundwaters within the platform. Support for this model is provided by Fanning *et al* (1981) who documented warm submarine springs on the Floridan Platform. These springs are depleted in magnesium and depletion attributed to dolomitization. Spring waters are believed to have originated in the ocean adjacent to the Florida Platform entering it at 500 m to 1000 m depth and then percolate to the interior of the plaform where they are heated to 40 ^0C.

Kohout convection has gained much favour by workers. Land (1985) suggested the efficiency of this mechanism was multifold incorporating an efficient pump, a supply of magnesium, sufficient heat and possible interaction with meteoric waters, all

increasing the magnesium each pore volume is able to supply. The mechansim is also long lived, occurring throughout the duration of the platform (review by Tucker, 1990).

3. Dolomitization by refluxing seawater has been proposed by Simms (1984). Shallow water on a carbonate platform frequently becomes a little more saline than the ocean water adjacent to the platform due to restricted and weak circulation (reefs and sand bodies). Simms (1984) was able to show using simple sand box models that if pore water within the platform has a salinity of 35 ‰, downward reflux of only slightly hypersaline water would occur. The mechanism is supported by Whittiker & Smart (1990) who showed that sea water on the Bahamas platform with a salinity of 38 ‰ to 42 ‰ refluxed and flowed eastwards mixing with normal marine salinity of 35 ‰ at 19 ^{0}C to 20 ^{0}C derived from the Tongue of the Ocean. It was suggested that this refluxing sea water explains the pervasive secondary dolomitzation widely reported in shallow depths in this area. Geochemical evidence indicates a depletion in magnesium along the flow path from east to west (Smart 1992, pers. comm.).

Hydrothermal dolomitization.

Circulation of magnesium bearing hydrothermal solutions within the earth's crust have been advocated as an agent of dolomitization. The main features of hydrothermal dolomite bodies are;

1. Fluid inclusion microthermometry yield homogenization temperatures between 75 ^{0}C to above 200 ^{0}C (Wilson *et al.* 1990; Hitzman, 1986a, 1986b)

2. Dolomite bodies often have limited distribution and are typically elongate reflecting a structural control. The massive hydrothermal dolomite at the Ruby Creek copper deposit, Alaska, is over 1 km wide and strikes NE-SW for over 2 km along a fault (Hitzman, 1986a). A similar massive hydrothermal dolomite body has been described from the Lower Carboniferous of Ireland at the Abbeytown Mine, County Sligo. Here a dolomite body is over 200 m wide and strikes NE to SW for 0.5 km. along a fault (Hitzman, 1986b, personal observation 1988)).

3. Hydrothermal dolomite bodies are vertically extensive, contacts are sharp and cross cutting. Where it has proved possible to map dolomite fronts the dolomite body has a plume shape in cross-section, with the most intense dolomitzation occuring at the core of the plume. Exmples include the dolomite occuring in the Triassic Latemar build up of the Dolomites (Wilson *et al.* 1990), the Ruby Creek copper deposit, Alaska (Hitzman, 1986a)

4. Dolomite was believed to be the result of several fluid pulses reflected by several stages of dolomitization.

APPENDIX 4.

Isotopic analysis.

Isotope analyses of carbonates were carried out at the Scottish Universities Research and Reactor Centre at East Kilbride. Twenty eight isotope analyses were carried out on whole rock samples of dolomite and grainstones to obtain average $\delta^{18}O$ and $\delta^{13}C$ values relative to the PDB (Cretaceous PeeDee Belemnite) with dolomite samples corrected with respect to low iron concentrations. The results are presented in Fig. A. Two techniques were used to prepare samples.

1. Samples were crushed and passed through a 250 micron mesh. After flushing with distilled water to remove fines the sample was mixed with the heavy liquid tetrabromoethane diluted with acetone to a specific gravity of 2.8. This was designed to separate calcite and dolomite. However, it proved unsuccesful due to the intergrown nature of the calcite and dolomite.

2. A more succesful method proved to be the drilling of samples directly from core using a hand held hobby drill. Smear mounted samples were analysed by X-Ray diffraction using a Phillips PW 1050 - 35 vertical goniometer with a cobalt anode in conjuction with a Phillips X-Ray generator. Each sample was run between 30^0 to 40^0 2Ø interval which contains the diagnostic dolomite and calcite peaks at 36.1 and 34.2 respectively (Fig. B). Typically samples of pure dolomite were chosen for analyses but a few samples containing an estimated 2% to 3% calcite were also used. The non carbonate phases included quartz and feldspar.

Samples weighing 10 to 15 milligrams were reacted with orthophosphoric acid. Calcites were reacted at 25 ^{0}C over three hours and dolomite samples were reacted at 100 ^{0}C over three hours. It was thought that sulphide could be present in the carbonates. Phosphoric acid will react with sulphide present producing hydrogen sulphide and carbon dioxide. The Hydrogen sulphide will affect the mass spectrometer, influencing the isotopic signature of the sample. To combat this, the evolved CO_2 was passed through silver phosphate producing silver sulphide thus removing and hydrogen sulphide present.

Fluid inclusion microthermometry.

Fluid inclusion studies were carried out on polished wafers. A Leitz Dialux 20 EB petrological microscope was used with a Lin Kam TH600 heating stage, using 40x magnification . The inclusions were single and double phase, with two phase inclusions containing a small vapour bubble which commonly displayed rapid movement. Only those inclusions interpreted as primary, showing no signs of necking, and located within dolomite growth zones away from zone interfaces and cleavage were chosen for

The Five Lens Dolomite

Hole	Depth	Line Number	$\delta^{18}O$	$\delta^{13}C$
N975	451.2		-6.6	2.0
N975	452.2		-6.9	2.5
N975	457.2		-6.9	2.8
N975	454.7	C5883	-6.1	2.7
N975	450.2	C5394	-7.8	2.8
N975	448.2	C5422	-10.4	1.7
1130 DD Bed 5		C5880	-8.1	1.3
1130 DD Bed 7		C5881	-6.1	2.6

Stratal dolomite 'fingers'

Hole	Depth	Line Number	$\delta^{18}O$	$\delta^{13}C$
N982	406.1		-9.0	1.3
U5885			-7.5	1.6
N982	418.5		-9.1	2.3
N975	415.2	C5911	-8.2	1.0
N982	418.7	C5913	-8.3	2.5
N975	414.0	C5914	-9.5	0.89
N982	399.9	C5882	-7.8	1.7
N314	274.0	C5888	-10.1	0.2

Grainstones

Hole	Depth	Line Number	$\delta^{18}O$	$\delta^{13}C$
N314	274.9	C5872	-5.6	1.7
N982	408.2		-6.7	1.1
N975	431.9		-5.4	2.0
N982	408.9	C5929	-6.4	1.4
N314	267.2	C5924	-6.7	1.8
N995	500.6		-6.0	1.9

Massive dolomite

Hole	Depth	Line Number	$\delta^{18}O$	$\delta^{13}C$
N975	381.3	C5436	-8.1	-0.3
N986	368.3	C5435	-8.3	-1.0
N984		C5430	-7.7	-0.22

*Stage (3) crystals

Hole	Depth	Line Number	$\delta^{18}O$	$\delta^{13}C$
B(2)		C2615	-10.0	-3.5
B(3)		C2616	-6.7	3.8

*Calcite overlying stage (3) dolomite crystals

Hole	Depth	Line Number	$\delta^{18}O$	$\delta^{13}C$
B(3)			-8.2	3.5

Fig. A. Summary of isotope results. All depths in metres. * sample courtesy I.K. Anderson.

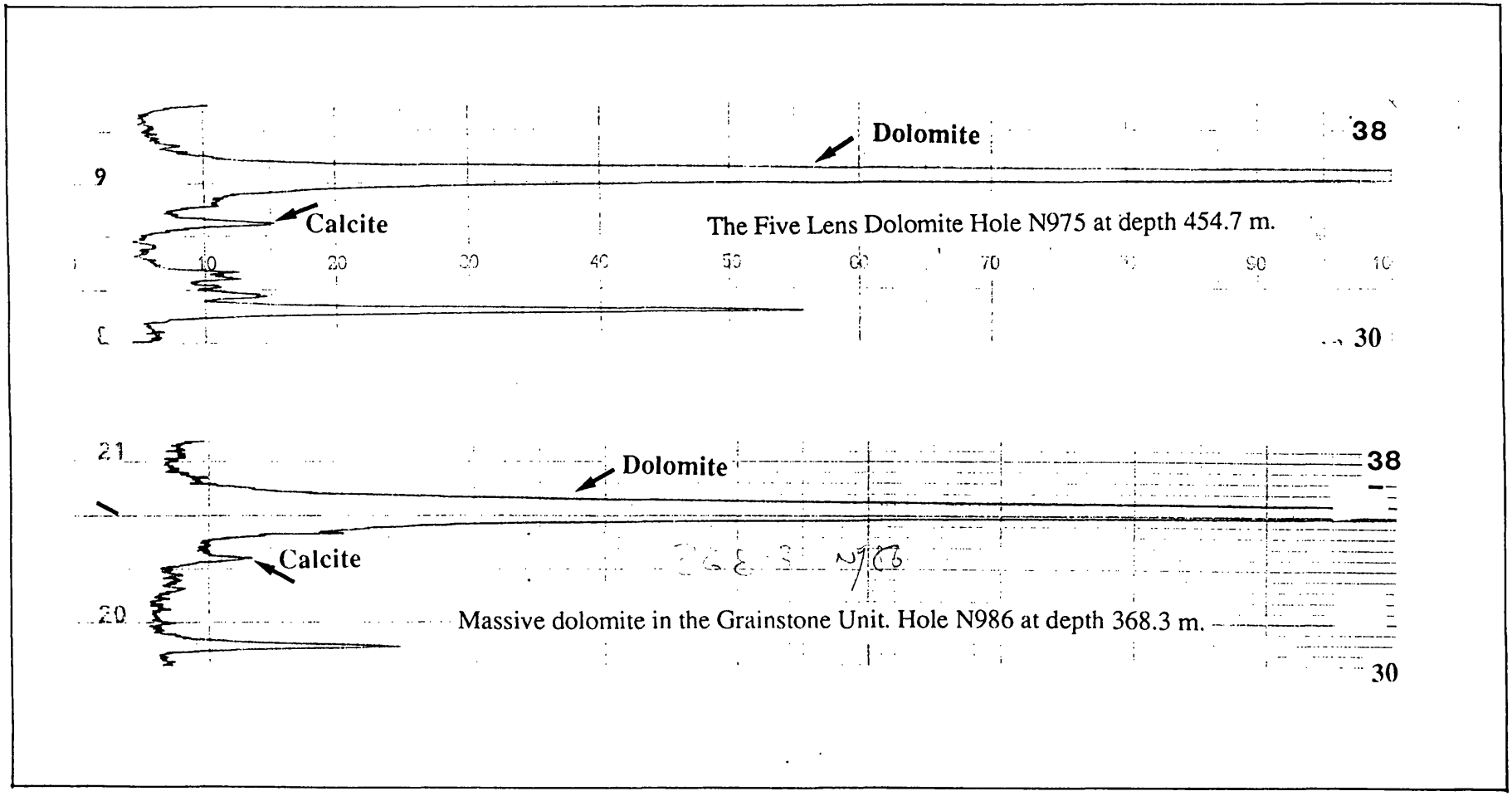

Fig. B. Examples of Navan dolomite diffractograms enclosing diagnostic calcite and dolomite peaks. Note strong dolomite peak at 36.1 and weak calcite peak at 34.2.

measurement.

To avoid overheating, stretching and decrepitation of the whole wafer, 2 to 3 mm. pieces were analysed individually. Each was heated at a rate of 10 ^{0}C per minute until the vapour bubble disappeared. Up to 8 measurements were carried out on each inclusion to check for reproduceability and the average computed, the results are presented in Fig. C. The mineralogy of the footwall 'Green Shale' was determined by a semi sedimentaion and X-Ray diffraction. This entailed crushing of sample to a powder and mixing with de-ionised water, the solution was left for three hours allowing the non clay fraction to settle out of suspension. The remaining liquid was smear mounted and left to dry. The residue was analysed by a Phillips PW 1050 X-Ray Diffraction machine an Co K α radiation. The diffractogram is shown in Fig. D.

Cathodoluminescene was carried out on both limestones and dolomites. The technique is standard and it is therefore unnecessary to review the technique here. For a comprehensive review of the procedure, refer to Miller (1989).

Masive dolomite in the Grainstone Unit

Inclusion number	Number of measurements	Maximum temperature	Minimum temperature	Mean temperature
1	3	140	130	134.3
2	4	122	118	120.6
3	8	120	88	102.5
4	6	130	127	128.8
5	6	122	117	118.6
6	6	103	94	100.5
7	6	108	107	108.1
8	6	108	105	106.5

The Five Lens Dolomite

Inclusion number	Number of measurements	Maximum temperature	Minimum temperature	Mean temperature
1	3	90	87	88
2	3	84	82	82.6
3	6	152	133	139.5
4	4	115	108	111.5
5	3	160	158	159.3
6	3	160	157	158.3

Statal dolomite fingers

Inclusion number	Number of measurements	Maximum temperature	Minimum temperature	Mean temperature
1	6	103	101	102.3
2	7	60	59	59.7

Fig. C. Navan dolomite fluid inclusion data, all temperatures in ^{0}C.

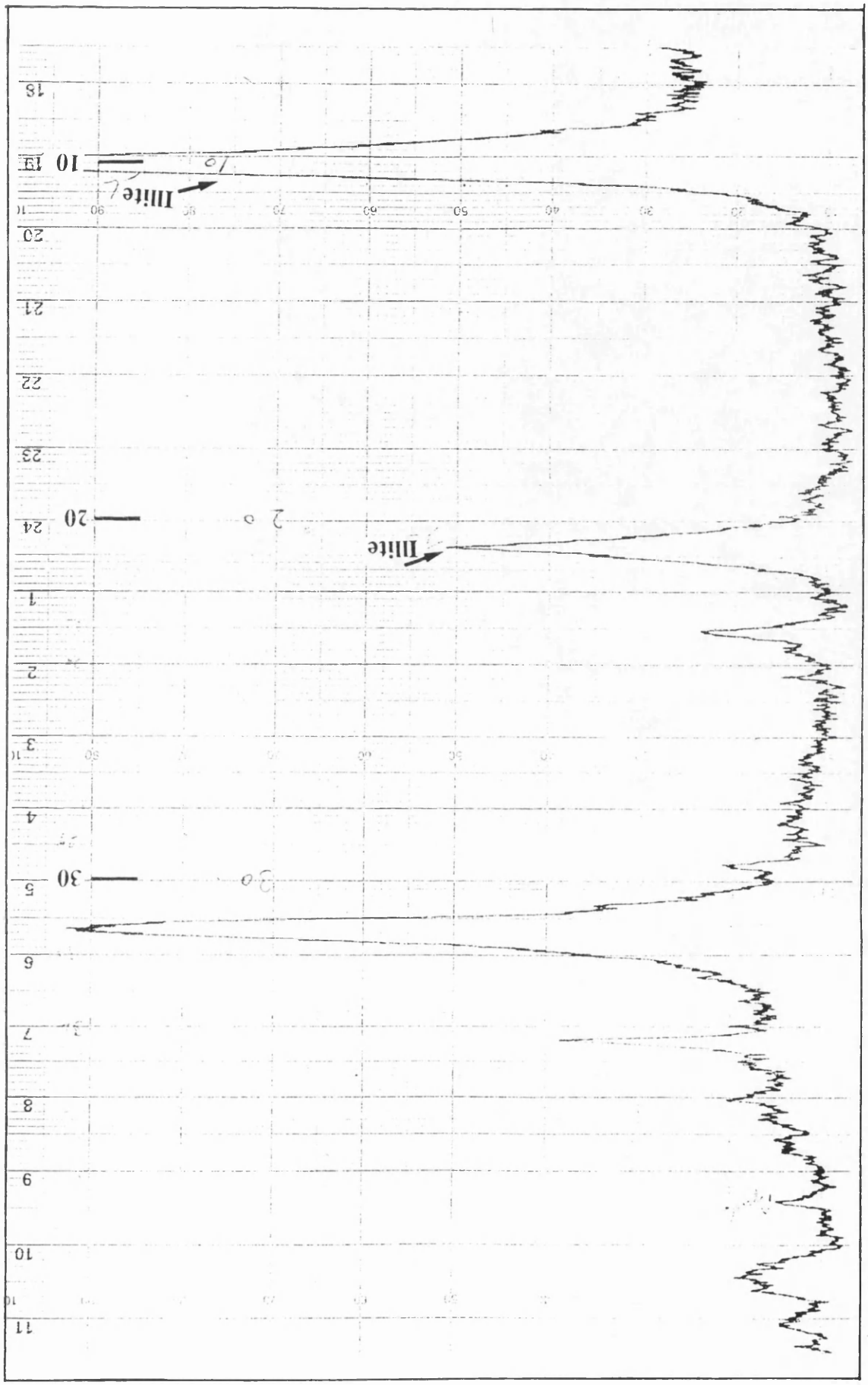

Fig. D. Diffractogram of Footwall Green Clay. Hole N1036 at depth 656.7 m.

Adams, J. E. and Rhodes, M. L. (1960). Dolomitization by Seepage Refluxion. *Bulletin of the American Association of Petroleum Geologists.* **v.44** p.1912-1920.

Ahr, W. M. (1973). The carbonate ramp: an alternative to the shelf model. *Transactions of the Gulf Coast Association of Geological Societies* **v.23** p.221-225.

Aitken J. D. (1967). Classification and environmental significnce of cryptalgal limestones and dolomites, with illustrations from the Cambrian and Ordovician of S.W. Alberta. *Journal of Sedimentary Petrology.* **v.37** p.1163-1178.

Allen, J. R. L (1970). Studues in fluviatile sedimentation: a comparison of fining upward cyclothems, with special reference to coarse member composition and interpretation. *Journal of Sedimentary Petrology* **v.40** p. 298-323.

Allen, J. R. L. (1974) Sedimentology of the Old Red Sandstone (Silurian-Devonian) in the Clee Hills area, Shropshire England. *Sedimentary Geology.* **v.12** p.73-167.

Allen, J. R. L. (1986). Pedogenic calcretes in the Old Red Sandstone facies (late Silurian-Early Carboniferous) of the Anglo Welsh area, southern Britain. In: *Palaeosols their recognition and interpreteation* (ed. V. P. Wright) p.58-82. Blackwell Scientific Publications.

Anderson, I. K. (1990). Ore depositional proccesses in the formation of the Navan Zinc - Lead deposit, Ireland. *Unpublished Ph. D Thesis,* University of Strathclyde.

Anderton, R., Bridges, P. H., Leeder, M. R. and Sellwood, B. W. (1985). *A dynamic stratigraphy of the British Isles, a study of crustal evolution.* George, Allen and Unwin London.

Andrew, C. J. (1986). The tectonic-stratigraphic controls to mineralization in the Silvermines area, County Tipperary, Ireland. In: *The geology and genesis of mineral deposits in Ireland.* Andrew, C. J., Crow, R. W. A., Finlay, S., Pennell, W. M., and Pyne, J. F. (eds). Special Publication of the Irish Association for Economic Geology, Dublin. p. 377-418.

Andrew, C. J. and Ashton, J. H. (1985). Regional setting, geology and metal distribution patterns of the Navan Orebody. *Transactions of the Institution of Mining and Metallurgy, Section B: Applied Earth Science* . **v.94.** B66 - B93.

Andrew, C. J. and Poustie, A. (1986). Syndiagenetic or epigenetic mineralization - the evidence from the Tatestown zinc-lead prospect, Co Meath. In: *The geology and genesis of mineral deposits in Ireland.* Andrew, C. J., Crow, R. W. A., Finlay, S., Pennell, W. M., and Pyne, J. F. (eds). Special Publication of the Irish Association for Economic Geology, Dublin. p.281-296.

Arnaud-Vanneau, A. and Arnaud, H. (1990). Hauterivian to Lower Aptian carbonate shelf sedimentation and sequence stratigraphy in the Jura and Northern sub-alpine chains (southeastern France and Swiss Jura). In: *Carbonate platforms, Facies sequences and evolution.* Eds. M. E. Tucker, J. L., Wilson., P. D. Crevello, J. R. Sarg. J. F. Read. *Special Publication of the International Association of Sedimentologists.* Blackwell Scientific Publications

Ashton, J. H., Black, A., Geraghty, J., Holdstock, M. and Hyland, E. In press. The geological setting and metal distribution patterns of Zn-Pb-Fe mineralization in the Navan Boulder Conglomerate. *The Irish minerals industry, a review of the decade, 1980 to 1990,* Irish Association for Economic Geology .

Ashton, J. H., Downing, D. T., and Finlay, S. (1986). The geology of the Navan Zn-Pb orebody. In: *The geology and genesis of mineral deposits in Ireland.* Andrew, C. J., Crow, R. W. A., Finlay, S., Pennell, W. M. and Pyne, J. F. (eds). Special Publication of the Irish Association for Economic Geology, Dublin. p. 243-280.

Assereto, R., Brig, O. L., Brusca, C., Omenetto, P., Zuffardi, P. (1976). Italian ore-mineral deposits related to emersion surfaces, a summary. *Mineralium Deposita* (BERL) **v.11** p.170-179.

Badiozamani, K. (1973). Dorag Dolomitzation model: Application to the middle Ordovician of Wisconsin. *Journal of Sedimentary Petrology.* **v.43.** p. 969-984.

Baker, P. A. and Kastner, M. (1981). Constraints on the formation of sedimentary dolomite. *Science* . **v.213** p.214-216.

Ball, M. M. (1967). Carbonate sand bodies of Florida and the Bahamas. *Journal of Sedimentary Petrology.* **v.37** p.556-591.

Bathurst, R. G. C. (1958). Diagenetic fabric in some British Dinantian Limestones. *Liverpool and Manchester Geological Journal* **v.2** p.11-36.

Bathurst, R. G. C. (1964). The replacement of aragonite by calcite in the molluscan shell wall. In: *Approaches to palaeoecology.* (eds. Imbrie J and Newell N.D). p.357-376 . New York Wiley.

Bathurst, R. G. C. (1975). *Carbonate sediments and their diagenesis.* Elsevier Scientific Publishing Co. pp.658.

Bathurst, R. G. C. (1984). The integration of pressure solution with mechanical compaction. In: *Stylolites and related phenomenon relevence to hydrocarbon resevoirs.* Special Publication of the Abhu Dhabi National Resevoir Research Foundation. p.41-55.

Bathurst. R. G. C. (1986) Carbonate diagenesis and resevoir development; Conservation, destruction and creation of pores. *Quarterly Journal of the Colorado School of Mines.* p.1-25

Beales, F. W. and Hardy, J. W. (1980). Criteria for the recognition of diverse dolomite types with an emphasis on studies of host rocks for Mississippi Valey-Type ore deposits. In: *Concepts and models of dolomitzation* (ed. by D. H. Zenger, J. B. Dunham and R. L. Ethington). Special Publication number 28 of the Society of Economic Palaeontologists and Mineralogists) p. 259-297.

Bechstadt, T (1975). Lead Zinc ores dependent on cyclic sedimentation, Witterstein Limestone of Bleiberg-Kreuth Carinthia, Austria. *Mineralium Deposita.* Berl **v.10** p.234-248.

Bechstadt, T. and Dohler-Hirner, B. (1983). Lead-Zinc deposits of Bleiberg-Kreuth. In: *Carbonate Depositional Environments.* (eds. P. A. Scholle, D. G. Bebout, and C. H. Moore) American Association of Petroleum Geologists, Memoir 33. p.73-92.

Berner, R. A. (1969). Migration of iron and sulphur within anaerobic sediments during early diagenesis. *American Journal of Science.* **v.267** p.19-42.

Berner, R. A. (1984). Sedimentary pyrite formation - an update. *Geochemica et Cosmochima Acta* **v.48** p.605-615.

Bjorlykke, K. (1985). Formation of secondary porosity: How important is it ?. In: *Clastic diagenesis.* (eds. D.A. McDonald and R. C. Surdam) American Association of Petroleum Geologists Memoir 37. Tulsa Oaklahoma.

Blackbourn, G. A. (1987). Sedimentary environments and stratigraphy of the late Devonian-early Carboniferous Clair Basin, west of Shetland. In: *European Dinantian environments.* (eds. J. Miller, A. E. Adams and V. P. Wright). Geological Journal Special Issue No.12. p.75-92. John Wiley and Sons Ltd.

Bocacz, K., Dzuulynski. S., Haranczyk, C., and Subczynski, P. (1975). Origin of ore bearing dolomite in the Triassic of the Cracow-Silesian region Pb-Zn ore district. *Rocznik Polskiego Towarzystwa Geoilogicznego Annales de la societe de Pologne.* **Vol XLV 2** p.139-155.

Boles, J. R. and Franks, S. G. (1979). Clay diagenesis in Wilcox Sandstones of SW Texas: Implications of smectite diagenesis on sandstone cementation. *Journal of Sedimentary Petrology* **v.49** p.55-70.

Boni, M. (1986). Pb-Zn deposits in the Sardinian Cambrian: A comparison with the Irish Carboniferous . In: *The geology and genesis of mineral deposits in Ireland.* Andrew, C. J., Crow, R. W. A., Finlay, S. Pennell, W. M. and Pyne, J. F. (eds). Special Publication of the Irish Association for Economic Geology, Dublin. p.667-684

Boyce, A. J., Anderton, R., and Russell, M. J. (1983). Rapid subsidence and base metal mineralization in Ireland. *Transactions of the Institute of Mining and Metallurgy. Section B: Applied Earth Science, 92.*

Braithwaite, C. J. R. (1984). Depositional history of the late Pleistocene limestones of the Kenya coast. *Journal of the Geological Society, London.* **v.141.** p.685-699.

Braithwaite, C. J. R. (1989). Stylolites as open fluid conduits. *Marine and Petroleum Geology.* **v.6** p.93-96.

Braithwaite, C. J. R. (1991) Dolomites a review of origins, geometry and textures. *Transactions of the Royal Society of Edinburgh* . **v.82.** p.99-112.

Brand, S. F. and Emo, G. T. (1986). A note on Zn-Pb-Ba mineralization near Oldcastle Co. Meath. In: *The geology and genesis of mineral deposits in Ireland.* Andrew, C. J., Crow, R. W. A., Finlay, S. Pennell, W. M. and Pyne, J. F. (eds). Special Publication of the Irish Association for Economic Geology, Dublin. p.297-304.

Brewer, R. (1964). *Fabric and mineral analysis of soils.* Kreiger Publishers New York, Wiley New York.

Briskey, J. A., Dingess, P. R., Smith, F., Gilbert, R. C., Augustus, K. A. and Cole, G. P. (1986). Localization and source of Mississippi Valley-Type zinc deposits in Tennessee, USA, and comparisons with Lower Carboniferous rocks of Ireland.. In: *The geology and genesis of mineral deposits in Ireland.* Andrew, C. J., Crow, R. W. A., Finlay, S. Pennell, W. M. and Pyne, J. F. (eds). Special Publication of the Irish Association for Economic Geology, Dublin. p.635-661

Bromley, R. G. (1990). *Trace Fossils biology and taphonomy.* Special Topics in Palaeontology. Unwin Hyman London.

Bromley, R. G. and Ekdale, A. A. (1984). Chondrites: A trace fossil indicator of anoxia in sediments. *Science.* **v.224** p872-874.

Brown, C. and Williams, B. (1985). A gravity and magnetic interpretation of the structure of the Irish Midlands and its relation to ore genesis. *Journal of the Geological Society of London.* **v.142** p.1059-1076.

Buxton T. M. and Sibley, D. F. (1981). Pressure solution features in a shallow buried limestone. *Journal of Sedimentary Petrology* . **v.51** p.19-26.

Carter, J. S. and Wibur, D. G. (1986) The geological setting of Zn mineralization near Duncormick in the Wexford Permo-Carboniferous outlier. In: *The geology and genesis of mineral deposits in Ireland.* Andrew, C. J., Crow, R. W. A., Finlay, S. Pennell, W. M. and Pyne, J. F. (eds). Special Publication of the Irish Association for Economic Geology, Dublin. p. 471-474

Cathles, L. M and Smith, A. T. (1983). Thermal constraints on the formation of MVT deposits their implications for episodic basin dewatering and deposit genesis. *Economic Geology.* **v.78** p.983-1002.

Choquette, P. W., Cox, A. and Meyers, W. J. (1992). Characteristics, distribution and origins of porosity in shelf dolostones: Burlington-Keokuk Formation (Mississippian), US Mid Continent. *Journal of Sedimentary Petrology.* **v.62** No.2 p.167-189.

Choquette P. W. and Pray L. C. (1970) Geological nomenclature and classification of porosity in sedimentary carbonates. In: *Carbonates II: Porosity and classification of reservoir rocks.* American Association of Petroleum Geologists. Reprint series number 5 1972. Tulsa Oaklahoma.

Choquette P. W. and Steinen, R. P (1980). Mississppian non supra tidal dolomite, St. Genevieve Limestone, Illinois Basin: Evidence for mixed water dolomitization. In: *Concepts and models of dolomitzation* (ed. by D. H. Zenger, J. B. Dunham and R. L.Ethington). Special Publication of the Society of Economic Palaeontologists and Mineralogists **28** p163-197.

Chowns, T. M. and Elkins, J. E. (1974). The origin of quartz geodes and cauliflower cherts through silicification of anhydrite nodules. *Journal of Sedimentary Petrology.* **v.44** p.885-903.

Clayton, G., Graham, J. R., Higgs, Holland, C. H. Naylor, D. (1980). Devonian rocks in Ireland. *Journal of Earth Sciences Royal Dublin Society* . **v.2** p.161-185.

Clayton G. and Higgs, K. (1978). The Tournasian marine transgression in Ireland. *Journal of Earth Sciences Royal Dublin Society.* **v.2** p.1-10.

Clifford, J. A., Ryan, P., Kucha, H. (1986). A review of the geological setting of the Tynagh orebody, Co Galway. In: *The geology and genesis of mineral deposits in Ireland.* Andrew, C. J., Crow, R. W. A., Finlay, S., Pennell, W. M., and Pyne, J. F. (eds). Special Publication of the Irish Association for Economic Geology, Dublin. p. 419-440.

Collinson, J. D. (1986). Alluvial sediments. In: *Sedimentary environments and facies.* 2nd Edition (ed. H. G. Reading). Blackwell Scientific Publications. p.20-54.

Colthurst, J. R. J. (1978). Old Red Sandstone rocks surrounding the Slievenamon inlier, Counties Tipperary and Kilkenny. *Journal of Earth Sciences Royal Dublin Society.* **v.11.** p.77-103.

Craig, D. H. (1988). Caves and other features of the Permian karst in the San Andreas Dolomite, Yates Field Reservoir west Texas. In: *Palaeokarst* (Eds. N. P. James and P. W. Choquette) Spinger Verlag New York.

Crowe, R. W. A (1986). The stratigraphy and structural setting of Zn-Ba-Pb mineralization at Newtown Cashel, Co. Longford. In: *The geology and genesis of mineral deposits in Ireland.* Andrew, C. J., Crow, R. W. A., Finlay, S. Pennell, W. M. and Pyne, J. F. (eds). Special Publication of the Irish Association for Economic Geology, Dublin. p.331-340.

Davies, G. R. (1970). Carbonate Bank Sedimentation, eastern Shark Bay western Australia. *American Association of Petroleum Geologists.* Memoir 13 p.85 -168.

Davies J. R. (1991). Karstification and pedogenesis on late Dinantian carbonate platform, Anglesey north Wales. *Proceedings of the Yorkshire Geological Society.* **v.48.** part 3 p. 297-321.

Davies, J. R. McNestry, A. and Waters, R. A. (1991). Palaeoenvironments and palynofacies of a pulsed transgression: The late Devonian and early Dinantian (Lower Carboniferous) rocks of south east Wales. *Geological Magazine.* **v.128** (4) p. 355-380.

Dickson, J. A. D. (1966). Carbonate idenification and genesis as revealed by staining. *Journal of Sedimentary Petrology.* **v.36** p.491 -505.

Dickson, J. A. D. (1991). Disequilibrium carbon and oxygen isotope variations in natural calcite. *Nature.* **v.353** p.842-844.

Dickson J. A. D. and Coleman, M. L. (1980). Changes in carbon and oxygen isotope composition during limestone diagenesis. *Sedimentology.* **v.27** p.107 to 118.

Dorobrek, S. L.(1987). Petrography, geochemistry and origin of burial diagenetic fabrics, Silurian-Devonian Helderberg Group (carbonate rocks) central Appalchians. *American Association of Petroleum Geologists.* **v.71.** p.492-514.

Downing D. T. Ashton, J. H. (1985). The Geology of the Navan orebody. In: *The Tara Mines story.* Libby, D. J, Downing D. T. Ashton, J. H., Oram, R. A, Murchu, D. O. Dallas, W. G, Maybury, M. *Transactions of the Institute of Mining and Metallurgy. Section A: Mining Industry.* **v.94** A1 - A41.

Dravis, G. (1979). Rapid and widespread generation of oolitic hardgrounds on a high energy Bahamian platform, Eleuthera Bank, Bahamas. *Journal of Sedimentary Petrology.* **v.49** p.195-208.

Dravis, J. J. and Muir, I. D. (1991). Controls on widespresd dissolution of burial dolomites, middle Devonian Upper Elk Point Group, Western Canada,. *Dolomieu Conference on Carbonate Platforms and Dolomitization Abstracts.* Eds. A. Bosellini, R. Brander, E. Flugel, B. Purser, W.Schlager, M. Tucker, D. Zenger. p.64.

Dunham, R. J. (1962). Classsification of carbonate rocks according to depositional texture. In: *Classification of carbonate rocks* (ed. W. E. Ham). Memoir of the American Association of Petroleum Geologists 1 p.108-121.

Dunham R. J. (1969) Early vadose silt in Townsend mound (reef) New Mexico. In: *Depositional environments in carbonate rocks.* (ed. G. M Freidman.) Special Publication Number 14 of the Society of Economic Paleontologists and Mineralogists.

Dunham, J. B and Olson, E. R. (1980). Shallow subsurface dolomitzation in the Hanson Creek Formation (Ordovician-Silurian) of central Nevada. In: *Concepts and models of dolomitzation* (ed. by D. H. Zenger, J. B. Dunham and R. L. Ethington). Special Publication of the Society of Economic Palaeontologists and Mineralogists **28** p 139-162.

Dunnington, H. V. (1967). Aspects of diagenesis and shape change in stylolitic limestone Reservoirs. *7th world Petroleum Congress Proceedings. Mexico.* **v.2** p.339-317.

Elder. J. W. (1967). Steady free convection in a porous medium heated from below. *Journal of Fluid mechanics.* **v.27.** p.29-40.

Elder, J. W. (1977). Thermal convection. *Journal of the Geological Society of London.* **v.133** p.293-309.

Elliot, T. (1986). Siliciclastic shorelines. In: *Sedimentary environments and facies.* 2nd edition (ed. H. G. Reading). Blackwell Scientific Publications. p.155-187

Emery, D. and Dickson, J. A. D. (1989). A syndepositional meteoric phreatic lens in the Middle Jurassic Lincolnshire limestone, England, UK. *Sedimentary Geology.* **v.65** p. 273-284.

Emo, G. T. (1986) Some considerations regarding the styles of mineralization at Harberton Bridge, Co Kildare in: *The geology and genesis of mineral deposits in Ireland.* Andrew, C. J., Crow, R. W. A., Finlay, S., Pennell, W. M. and Pyne, J. F. (eds). Special Publication of the Irish Association for Economic Geology, Dublin.p. 461-470.

Enos, P. (1977). Holocene sediment accumulations of the south Florida shelf margin. In *Quaternary sedimentation in south Florida* (Eds. Enos, P and Perkins R. D.) Memoir of the Geological Society of America **147** p.1-130

Enos, P. (1983). Shelf. In: *Carbonate depositional environments* (eds. P. A. Scholle, D. G. Bebout, and C. H. Moore). Memoir 33 of the American Association of Petroleum Geologists. p.267-296. Tulsa Oaklahoma.

Esteban, M. (1991). Palaeokarst: Practical applications. In: *Paleokarsts and Palaeokarstic resevoirs* (Ed. by V. P. Wright, M. Esteban; P. L. Smart). P.R.I.S. Occasional Publication Series 2 p.89-119. University of Reading.

Esteban, M. and Klappa, C. (1983). Subaerial exposure. In: *Carbonate depositional environments.* American Association of Petroleum Geologists, Memoir 33. Scholle, P. A., Bebout, D. G., Moore, C. H. (eds). Tulsa Oaklahoma. p.1-55.

Evamy, B. D. and Shearman, D. J. (1965). The development of overgrowths from echinoderm fragments. *Sedimentology.* **v.5** p. 211-233.

Evan, C. C. (1984). Development of an ooid shoal complex: The importance of antecedant and syndepositional topography. In: *Carbonate sands: a core workshop* (ed. P. M. Harris). Society for Economic Palaeontologists and Mineralogists p. 392-428. Tulsa Oaklahoma.

Fairchild, I. J. (1983). Chemical controls of cathodoluminescene of natural dolomites and calcite: New data and review. *Sedimentology.* **v.30** p.579-583.

Fanning, K. A., Byrne, R. H., Breland, J. A., Moore, W. S., Elsinger, R. J. and Pyle, T. E. (1981). Geothermal springs of west Florida continental shelf evidence for dolomitzation and radionucleide enrichment. *Earth and Planetry Science Letters* **v.52.** p.345-354.

Flugel, E. (1982). *Microfacies analysis of limestones.* Springer-Verlag, Berlin.

Folk, R. L. (1962). Spectral subdivisions of limestone types. In: *Classification of carbonate rocks* (Ed. W. E. Ham) Memoir of the American Association of Petroleum Geologists 1 p. 62-84.

Folk, R. L. (1974). The natural history of crystalline calcium carbonate: effect of magnesium content and salinity. *Journal of Sedimentary Petrology.* **v.44.** p.40-53.

Folk, R. L and Andrews, P. B. and Lewis, P. W. (1970). Detrital sedimentary rock classification and nomenclature for use in New Zealand. *New Zealand Journal of Geology and Geophysics.* **v.13** p.937-968.

Folk, R. L. and Assereto, R. (1976). Comparitive fabrics of length slow and length fast calcite and calcitized aragonite in a Holocene speleothem, Carlsbad Caverns, New mexico. *Journal of Sedimentary Petrology.* **v.46** p.486-496.

Folk, R. L. and Land, L. S. (1975). Mg : Ca ratio and salinity, two controls over crystallization of dolomite. *Bulletin of the American Association of Petroleum Geologists* **v.59** p.60-68.

Ford, D. and Williams, P. (1989). *Karst Geomorphology and Hydrogeology.* Unwin Hyman London.

Francis, F. E. (1986). The calcareous palaeosols of the basal Purbeck Formation (Upper Jurassic) southern England In: *Palaeosols their recognition and interpreteation* (ed. V.P. Wright) p.112-134. Blackwell Scientific Publications.

Freeze, R. A. and Cherry, A. (1979). *Groundwater.* New Jeresey, Prentice Hall. pp 640.

Frey, R. W. and Pemberton, S. G. (1984). Trace fossil facies models. In: *Facies Models.* 2nd Edition (Ed. R.G. Walker) p.189-211. Geoscience Canada reprint series 1.

Gaines, A. M. (1980). Dolomitzation kinetics: Recent experimental results. In: *Concepts and models of dolomitzation* (ed. by D. H. Zenger, J. B. Dunham and R. L.Ethington). Special Publication of the Society of Economic Palaeontologists and Mineralogists **28** p. 81-86.

Garwood, E. J. (1931). The Tuedian beds of northern Cumberland and Roxburghshire east of Liddel Water. *Quarterly Journal of the Geological Society of London.* **v.87** p.97-159.

Gawthorpe, R. L. (1986). Sedimentation during carbonate ramp-to-slope evolution in a tectonically active area: Bowland Basin (Dinantian), northern England. *Sedimentology.* **v.33** p.185-206.

Gawthorpe, R. L (1987). Burial dolomitzation and porosity development in a mixed carbonate-clastic sequence: an example from the Bowland Basin, Northern England. *Sedimentology.* **v.34** p.533-558.

Gawthorpe, R. L and Clemmey, H. (1985). Geometry of submarine slides in the Bowland Basin (Dinantian) and their relation to debris flows. *Journal of the Geological Society of London.* **v.142** p.555-565.

Gawthorpe, R. L. and Gutteridge, P. (1990). Geometry and Evolution of platform-margin bioclastic shoals, Late Dinantian (Mississippian), Derbyshire, UK. In: *Carbonbate platforms, facies sequences and evolution* (Eds. M. E Tucker, J. L. Wilson P. D Crevello and R. J Sarg. J. F. Read). Special Publication of the International Association of Sedimentologists. Blackwell Scientific Publications.

Ginsburg, R. N., Hardie, L. A., Bricker O. P., and Wanless, H. R. (1977). Exposure index: A quantitative approach to defining position within the tidal zone. In: *Sedimentation on modern carbonate tidal flats of north west Andros Island Bahamas* (Ed. L.A Hardie), p.7-11 John Hopkins University press Baltimore.

Given, R. K and Wilkinson, B. H. (1985). Kinetic control of morphology, composition and mineralogy of abiotic sedimentary carbonates. *Journal of Sedimentary Petrology.* **v.55** p.109-119.

Goldstein, R. H. (1988). Cement stratigraphy of Pennsylvanian Holder Formation, Sacramento Mountains. *American Association of Petroleum Geologists Bulletin.* **v.72** p.425-438.

Gregg J. M. and Sibley, J. M. (1984) Epigenetic dolomitzation and the origin of xenotopic dolomite texture. *Journal of Sedimentary Petrology.* **v.54** p.908-931.

Grennan, E.F. (1986). Geology and genesis of the Courtbrown Pb-Zn-Ag deposit. In: *The geology and genesis of mineral deposits in Ireland.* Andrew, C. J., Crow, R. W. A., Finlay, S., Pennell, W. M., and Pyne, J. F. (eds). Special Publication of the Irish Association for Economic Geology, Dublin.p.449-458.

Grover, G. and Read, J. F. (1983). Palaeoaquifer and deep burial related cements defined by regional cathodoluminescent patterns, Middle Ordovician carbonates virginia. *American Association of Petroleum Geologists.* **v.67** No8 p.1275-1303.

Gunatilaka, A. Saleh, A., Al Temeemi, A., Nasser N. (1984). Occurrence of subtidal dolomite in a hypersaline lagoon, Kuwait. *Nature.* **v.31** p.450-452.

Gustafson, L. B. and Williams, N. (1981). Sediment-hosted stratiform deposits of copper, Lead, and Zinc. *Economic Geology 75th Anniversary Volume* p.139-178.

Hagni, R. D. (1976). Tri-state ore deposit: The character of their host rocks and their genesis. In: *Handbook of stratbound and stratiform ore deposits*: K. H. Wolf (ed) Amsterdam Elsevier Scientific Publications **v.6.** p.457-494.

Halley, R. B., Harris, P. M. Hine A. C. (1983). Bank Margin. In: *Carbonate depositional environments.* American Association of Petroleum Geologists, Memoir 33. p.463-507. Scholle, P. A., Bebout, D. G., Moore, C. H. (eds). Tulsa Oaklahoma.

Handshaw, B. C. Back, W., and Deike, R.G. (1971). A geochemical hypothesis for dolomitization by groundwater. *Economic Geology.* **v.66** p.710-724.

Hardie L. A. (1977). Sedimentation on modern carbonate tidal flats of north west Andros Island Bahamas. John Hopkins University Press Baltimore.

Hardie, L. A. (1986). Stratigraphic models for carbonate tidal flat deposition. *Quarterly Journal of the Colorado School of Mines* . p.59-76.

Hardie, L. A. (1987). Dolomitzation: A critical review of some current views. *Journal of Sedimentary Petrology.* **v.57** p.166-183.

Hardie, L. A. (1991). On the origin and significance of high frequency depositional cycles in shallow carbonate platforms. In: *Dolomieu confernence on carbonate platforms and dolomitzation, confernence, Abstracts.* Eds. A. Bossellini, R. Brander, E. Flugel, B. Purser, W. Schlager, M. Tucker, D. Zenger. p.102.

Harris. P. M. (1983). The Joulters ooid shoal, great Bahamas Bank. In: *Coated Grains* (Ed. T. M. Peyrt) Springer verlag Heidelberg.

Harris, P.M. (1984). Cores from a modern carbonate sand body, the Joulters oolite shoal, Great Bahama Bank. In: *Carbonate sands - A core workshop* (ed. P.M. Harris). Society of Economic Paleontologists and Mineralogists Core Workshop. 5. pp.463.

Harris, P. M., Kendall, C. St. G., Lerche, I. (1985). Carbonate cementation a brief review. In: *Carbonate cements* (Eds.Schneidermann, N., Harris P. M). Society of Economic Paleontologists and Mineralogists. Special Publication **36.** p.79-85.

Harwood, G. M. (1989). Microscopic techniques II. Principles of sedimentary petrography. In: *Techniques in Sedimentology* (ed. M. E. Tucker). Blackwell Scientific Publications. p.108-173.

Harwood, G. M and Sulliven, M. (1990). Sedimentary history of the Moyvougly area, county Westmeath: evidence for synsedimentary fault movements in a mixed carbonate siliciclastic system of Courceyan age. *Society of Economic Paleontologists and Mineralogists Core Work Shop.*

Hayes, M. O. (1979). Barrier Island morphology as a function of tidal wave regime. In: *Barrier islands - from the Gulf of St Lawrence to the Gulf of Mexico.* Ed. Leatherman, S. P. Academic Press New York.

Hine, A. C. (1977). Lilybank Bahamas: History of an active oolite sand shoal. *Journal of Sedimentary Petrology.* **v.47.** p.1554-1581.

Hitzman, M.W. (1986a). The Geology of the Ruby Creek Copper Deposit, southwestern Brooks Range, Alaska. *Economic Gelogy.* **v.81** p.1644-1674.

Hitzman, M. W. (1986b). Geology of the Abbeytown Mine, Co Sligo, Ireland. In: *The geology and genesis of mineral deposits in Ireland.* Andrew, C. J., Crow, R. W. A., Finlay, S. Pennell, W. M. and Pyne, J. F. (eds). Special Publication of the Irish Association for Economic Geology, Dublin. p.341-354.

Hitzman, M. W, and Large, D. (1986). A review and classification of Irish carbonate hosted base metal deposits. In: *The geology and genesis of mineral deposits in Ireland.* Andrew, C. J., Crow, R. W. A., Finlay, S. Pennell, W. M. and Pyne, J. F. (eds). Special Publication of the Irish Association for Economic Geology, Dublin. p.341-354.

Hitzman, M. W., O'Connor, P. G., Shearly, E., Shaffalitzky, C., Thompson, T. (1990). Discovery and geology of the Lisheen Zn-Pb-Ag Prospect Co Tipperary Ireland. *The Irish minerals Industry, a review of the decade.* Irish Association for Economic Geology.

Hjulstrom (1939). In: Hsu, K. J. (1989). *Physical principals of sedimentology, Fig. 4.8.* Springer Velag Berlin. p.65.

Holdstock. M. P. (1982). Breccia hosted Zinc-Lead mineralization in Tournasian and Lower Visean carbonates at Harberton Bridge, County Kildare. In: *Mineral exploration in Ireland progress and developments 1971-1981* (eds. A. G. Brown, and J. F. Pyne) Irish Association for Economic Geology. Dublin. p.83-91.

Horbury, A. D. and Adams, A. E. (1989). Meteoric phreatic diagenesis in cyclic late Dinantian carbonates, north west England. *Sedimentary Geology.* **v.65** p.319-344.

Howard, J. D. and Reineck, H. E. (1979). Sedimentary structures of "high energy" beach to offshore sequences; Ventura port Hueneme area, California (abs). *Bulletin of the American Assocaition of Petroleum Geologists.* **v.63.** p.468-469.

Hsu, K. J. (1989). *Physical principals of sedimntology.* Springer Verlag Berlin.

Hsu, K. J. and Siegenthaler, C. (1969). Preliminary experiments on hydrodynamic movement induced by evaporation and their bearing on the dolomite problem, *Sedimentology.* **v.12** p.11-25.

Irwin, H., Curtis, C. D. and Coleman, M. (1977). Isotopic evidence for source of diagenetic carbonates formed during burial of organic rich sediments. *Nature* **v.269** p.209-213.

James, N. P. (1974). Diagenesis of scleractinian corals in the subaerial vadose environment. *Journal of Paleontology.* **v.48** p.785-799.

James, N. P. (1984). Shallowing-upward sequences in carbonates. In: *Facies Models* 2nd Edition (Ed. R.G. Walker). Geoscience Canada, reprint series 1. p.213-229.

James N. P. and Choquette, P. W. (1984). Diagenesis 9 Limestones - The meteoric diagenetic environment . *Geoscience Canada* **v.11** p.161-194.

James, N. P. and Choquette, P. W. (1988). Introduction. In: *Palaeokarst* (Eds. N. P. James and P. W. Choquette). Spinger Verlag New York.

Jenkyns, H. C. (1974). Origin of Red Nodular Limestones (Ammonitico Rosso, Knollenkalke) in the Mediterranean Jurassic, a diagenetic model. In: *Pelagic environments; on land and under the sea* (eds. K. J. Hsu and H. C. Jenkyn). International Association of Sedimentologists Special Publication. Number 1. p.249-271.

Jindrich, V. V. (1969). Recent carbonate sedimetation by tidal channels in the Florida keys. *Journal of Sedimentary Petrology.* **v.39** p.531-53.

Jones, G. L. In press. Irish Carboniferous conodonts record maturation levels and their influence of tectonism, igneous activity and mineralization. *Terra Nova* .

Jones, G. V. and Brand, S. F. (1986). The setting, styles of mineralization and mode of origin of the Ballinallack Zn-Pb deposit in: *The geology and genesis of mineral deposits in Ireland.* Andrew, C. J ., Crow, R. W. A., Finlay, S., Pennell, W. M. and Pyne, J. F. (eds). Special Publication of the Irish Association for Economic Geology, Dublin. p.355-376.

Kastner, M. (1984). Control of dolomite formation. *Nature.* **v.311** p.410-411.

Kaufman, J. and Cander, H. S. Daniels L. D. Meyers, W. J. (1988). Calcite cement stratigraphy and cementation history of the Burlington Keokuk formation (Mississippian), Illinois and Missouri. *Journal of Sedimentary Petrology.* **v. 58** p.312-326.

Kegan, J. R. (1981). Stratigraphic palynology of the early Carboniferous sediments in two bore hole cores from Moate, Co Westmeath, Ireland. Unpublished M.Sc. Thesis. University of Dublin.

Kendall, A. C. (1984). Evaporites. In: *Facies Models.* 2nd Edition. (ed. R. G. Walker) Geoscience of Canada Reprint Series 1. p.259-296.

Kendall, A. C. (1985). Radiaxial fibrous calcite: a reappraisal. In: *Carbonate cements* (Eds. Schneidermann, N. and Harris, P.M). Society of Economic Paleontologists and Economic Mineralogists. Special Publication **36.** p. 59-77.

Kendall, A. C. and Tucker, M. E. (1973). Radiaxial fibrous calcite: A replacement after acicular carbonate. *Sedimentology.* **v.20** p. 365-389.

Kendall, C. G. st C. and Skipwith, P. A. d'E. (1968). Recent algal mats of a Persian Gulf lagoon. *Journal of Sedimentary Petrology.* **v.38** p.1040-1058.

Kendall, C. G. st C. and Schlager, W. (1981). Carbonates and relative changes of sealevel. *Marine Geology.* **v.44** p.181-212.

Kinsmann D. J. J. and Holland H. D. (1969). The co-precipitaion of cations with $CaCO_3$ IV,. The Co precipitation of Sr^{2+} with aragonite between 16^0 - 96 ^{0}C. *Gecochemica Cosmochima Acta.* **v.33.** p.1-17.

Kinsman, D. J. J and Park, R. K. (1976). Algal belt and coastal sabkha evolution, Trucial coast, Persian Gulf. In: *Stromatolites* (ed M.R. Walker). p.421-433. Elsevier Amsterdam.

Klau, W. and Mostler, H. (1986). On the formation of Alpine Middle and Upper Triassic Pb-Zn deposits, with some remaks on Irish carbonate hosted base metal deposits. In: *The geology and genesis of Mineral deposits in Ireland.* Andrew, C. J., Crow, R. W. A., Finlay, S. Pennell, W. M. and Pyne, J. F. (eds). Special Publication of the Irish Association for Economic Geology, Dublin.

Klein, G. (1992). Climatic and teconic sea level gauge for mid-continent Pennsylvanian cyclothems. *Geology.* **v.20** p.363-366.

Knight I., James, N. P., Lane, T. E. (1991). The Ordovician St George Unconformity, Northern Appalachians: The relationship of plate convergence at the St. Lawrence promotory to the Sauk / Tippcanoe sequence boundry. *Geological Society of America Bulletin.* **v.103** p.1205-1225.

Kohout, F. A. (1967). Groundwater flow and geothermal regime of the Florida Plateau. *Transactions of the Gulf Coast Association of Geological Societies.* **v.17** p.339-354.

Kreisia, R. D. and Bambach, R. K. (1982). The role of storm processes in generating shell beds on Palaeozoic shelf environments. In: *Cyclic event stratification* (eds. G.Einselle and A. Seillacher). Springer verlag Berlin. p.200-207.

Kucha, H. (1988). Sulphides as rim cements, filling cements and replacemnet of carbonate sediments, Moyvoughly Ireland, a product of two convection cells. *Transactctions of the Institute of Mining and Metallurgy, Section B.* **v.97** B64.

Kyle, R.J. (1983). Economic aspects of subaerial carbonates. In: *Carbonate depositional environments.* American Association of Petroleum Geologists, Memoir 33. Scholle, P. A., Bebout, D. G., Moore, C. H. (eds). Tulsa 0aklahoma. p.73-92

Lahann, R. W. (1978). A chemical model for calcite growth and morphology control. *Journal of Sedimentary Petrology.* **v.48** p.337-344.

Land, L. S. (1967). Diagenesis of skeletal carbonates. *Journal of Sedimentary Petrology.* **v.37** p.914-930.

Land, L. S. (1970) Phreatic versus meteoric diagenesis of limestone: evidence from a fossil water table. *Sedimentology.* **v.14** p.175-185

Land, L. S. (1973). Contemporaneous dolomitzation of Middle Pleistocene reefs by meteoric water, north Jamaica. *Bulletin of Marine Sciences.* **v.23.** p.64-92.

Land, L. S. (1980). The isotopic and trace element geochemistry of dolomite; The state of the art. In *Concepts and models of dolomitzation* (ed by D. H. Zenger, J. B. Dunham and R. L.Ethington). Special Publication of the Society of Economic Palaeontologists and Mineralogists 28 p. 97-110.

Land, L. S. (1985) The origin of Massive dolomite. *Journal of Geological Education.* **v.33** p.112-125.

Land. L. S., Mackenzie, F. T, and Gould, S. J. (1967). Pleistocene history of Bermuda. *Geological Society of America Bulletin.* **v.78** p.993-1006.

Larsonneur, C. Bouyssee, P. and Auffre, J. (1982). The surficial sediments of the English Channel and its western approaches. *Sedimentology.* **v.29** p.851-864.

Leeder, M. R. (1973). Sedimentology and palaeogeography of the Upper Old Red Sandstone in the Scottish Border Basin. *Scottish Journal of Geology.* **v.9** p.117 - 44.

Leeder, M. R. (1975). Pedogenic carbonate and flood sediment accretion rates: a quantative model for alluvial arid zone lithofacies. *Geological Magazine.* **v.112** p.257-270.

Leeder, M.R. (1987) Tectonic and palaeogeographic models for Lower Carboniferous Europe. In: *European Dinatian environments* (eds. J. Miller, A. E. Adams, and V.P. Wright). John Willey and Sons Chichester, Publisher. p.1-20.

Lees, A. (1961). The Waulsortian reefs of Eire, a carbonate mudmound complex of Lower Carboniferous age. *Journal of Geology.* **v.69** p.101-109.

Lees, A. (1964). The structure and origin of the Waulsortian (Lower Carboniferous) reefs of west central Eire. *Philosophical Transactions of the Royal Society of London.* **B247** p. 483- 531.

Lees, A. and Miller, J. (1985). Facies variation in Waulsortian buildups, mid Dinantian builds ups from Europe and North America. *Geological Journal.* **v.20** p.159 to 180.

Leutloff, A. H. and Meyers, W. J. (1984). Regional distribution of microdolomite inclusions in Mississippian echinoderms from southwest New Mexico. *Journal of Sedimentary Petrology* **v.54** p. 432-446.

Lippmann, F. (1973). *Sedimentary carbonate minerals.* pp.228 Springer Verlag Berlin.

Logan , B. W. (1974) Inventory of diagenesis in Holocene - Recent carbonate sediments, Shark Bay western Australia. In: *Evolution and diagenesis of Quaternary carbonate sequences, Shark Bay Western Australia* (eds. B. W. Logan, J. F. Read, G. M. Hagan, P. Hoffman, R. G. Brown, P. J. Woods, C. D. Gebelein). Amerciacan Association of Petroleum Geologists Memoir 22 Tulsa Oaklahoma, p.195-249.

Logan, B. W. and Semeniuck, V. (1976). Dynamic metamorphism; processes and products in Devonian carbonate rocks, Canning Basin, Western Australia. *Special Publication of the Geological Society of Australia.* **16** p.1-18.

Lohmann, K. C. and Meyers, W. J. (1977). Microdolomite inclusions in cloudy prismatic calcites - a proposed criterion for former high magnesioum calcites. *Journal of Sedimentary Petrology.* **v.47** p.1078-1088.

Longmann, M. W. (1980). Carbonate diagenetic textures from near surface diagenetic environments. *American Association of Petroleum Geologists Bulletin.* **v.63** p.461-487.

Loreau, J. P. (1982). Sediments aragoitieques et leur genese. *Memoir au Museum d' hitoire Naturelle serie C.* **v.47.**

Lydon, W. J. (1986) Models for the generation of metaliferous hydrothermal systems within sedimentary rocks and their applicability to the Irish carboniferous Zn-Pb deposits. In: *The geology and genesis of mineral deposits in Ireland.* Andrew, C. J., Crow, R. W .A., Finlay, S. Pennell, W. M. and Pyne, J. F. (eds). Special Publication of the Irish Association for Economic Geology, Dublin. p.555-577.

MacCarthy, I. A. J. and Gardiner , P. R. R. (1987). Dinantian cyclicity: a case study from the Munster Basin of Southern Ireland. In: *European Dinatian environments* (eds. J. Miller, A. E. Adams, and V. P Wright). John Willey and Sons Chichester. p.199-238.

Machel, H. and Anderson J. H. (1989). Pervasive subsurface dolomitzation of the Nisku Formation in central Alberta. *Journal of Sedimentary Petrology.* **v.59** p.891-911.

Machel, H. and Mountjoy, E. W. (1987). General constraints on extensive pervasive dolomitzation and their application to the Devonian carbonates of Western Canada. *Bulletin of the Canadian Petroleum Geology.* **v.25** p.143-158.

Marchant, T. R. and Sevastoupoulo, G.D. (1980). The Calp of the Dublin district. *Irish Journal of Earth Science.* **v.3** p.195-3203.

Mattes, B. W. and Mountjoy, E. W. (1980). Burial dolomitzation of the Upper Devionian Miette Build Up, Jasper National Park, Alberta. In: *Concepts and models of dolomitzation* (ed by D.H. Zenger, J. B. Dunham and R. L.Ethington). Special Publication **28** of the Society of Economic Palaeontologists and Mineralogists) p. 259-297.

McBride, E. (1989). Quartz cement in sandstones a review. *Earth Science Reviews.* **v.26** p.69-112.

McCubbin, D. G. (1982). Barrier-Island strand plain facies: In: *Sandstone depositional environments.* (eds. P.A. Scholle and D. Spearing). Memoir **31** of the American Association of Petroleum Geologists. Tulsa Oaklahoma. p. 247-280.

McKenzie, J. A. Hsu, K. J. and Schneider J. F. (1980). Movement of subsurface waters under the sabkha, Abu Dhabi, UEA, and its realation to evaporite dolomite genesis. In: *Concepts and models of dolomitzation* (ed by D. H. Zenger, J. B. Dunham and R. L.Ethington). Special Publication **28** of the Society of Economic Palaeontologists and Mineralogists. p.11-30.

Meyers, W. J. (1974). Carbonate cement stratigraphy of the Lake Valley Formation (Mississipian) Sacramento Mountains, New Mexico. *Journal of Sedimentary Petrology.* **v.44** p.837-861.

Meyers, W. J. (1978). Carbonate cements, their regional distribution and interprteation in Mississippian Limestones of SW New Mexico. *Sedimentology.* **v.25** p.371-400.

Meyers, W. J. (1988). Palaeokarstic features in Mississipian limestones, New Mexico. In: *Palaeokarst* (Eds. James, N.P. and Choquette P.W). Springer Verlag Berlin. p.306-228

Meyers. W. J. (1991). Calcite cement stratigraphy: An overview. In: *Luminescencence microscopy and spectroscopy* (eds. C. E. Barker, and O. C. Kopp). Society for Economic Paleontology and Mineralogy, short course 25, Dallas Texas. p.133-148.

Meyers, W. J. and Hill, B. E. (1983). Quantitative studies of compaction in Mississippian skeletal limestones New Mexico. *Journal of Sedimentary Petrology.* **v.53** p.231-242.

Meyers, W. J. and Lohmann K. C. (1978). Microdolomite rich syntaxial cements: Proposed meteoric - marine mixing zone phreatic cements from Mississippian Limestones, New Mexico. *Journal of Sedimentary Petrology.* **v.48** p.475-488.

Miller, J. (1989). Cathodoluminescence microscopy. In: *Techniques in sedimentology.* (ed. M. E. Tucker). Blackwell Scientific Publications. p.174-190.

Milliken, K. L. (1979). The silicified evaporite syndrome-two aspects of silicificatiuon history of former evaporite nodules from south kentucky and north Tennesee. *Journal of Sedimentary Petrology.* **v.49** p.245-256.

Mills, H., Halliday, A. N., Ashton, J. H., Anderson, I. K. and Russell, M. J. (1987). Origin of a giant orebody at Navan, Ireland. *Nature.* **v.327** p.223-226.

Minero, C, (1988). Sedimentaion and diagenesis along an island sheltered platform, El Abra Formation Cretaceous of Mexico. In: *Palaeokarst* (eds. N.P. James and P.W Choquette) Spinger Verlag New York. p.385-405.

Moller, N. K and Kvingan K. (1988). The genesis of nodular limestones in the Ordovician and Silurian of the Oslo Region. *Sedimentology.* **v.35** No3 p.405-420.

Monty, C. L. V. (1981). Spongiostromate vs Porostromate stromatolites and oncolites. In: *Phanaerozoic stromatolites* (ed. C. L. V. Monty) p.1-14. Springer Verlag, Berlin.

Moore, C. H. (1989). *Carbonate diagenesis and porosity.* Developments in sedimentology 46. Publishers Elsevier.

Morrow, D. W. (1982a). Diagenesis 1 Dolomite - Part 1. The chemistry of dolomitzation and dolomite precipitation. *Geoscience Canada.* **v.9** p.5-13.

Morrow, D. W. (1982b). Diagenesis 2. Dolomite part 2. Dolomitization models and ancient dolostones. *Geoscience Canada.* **v.9** p.95-107.

Mountjoy E. W. (1991). Has Burial dolomitzation come of age ?. *Dolomieu conference on carbonate platforms and dolomitzation. Abstracts.* Eds. A. Bossellini; R. Brander, E. Flugel; B. Purser, W. Schlager, M. Tucker, D. Zenger. p.177.

Mountjoy, E. W. (1992). Dolomitization in resevoirs. In: Quantitative diagenesis: recent developments and applications to resevoir geology. NATO Advanced Study Institute for postdoctoral scientists and advanced students. University of Reading Short Course.

Murray, R. C. and Lucia, F. J. (1967). Cause and control of dolomite distribution and rock selectivity. *Geological Society of America Bulletin.* **v.78** p.21-35.

Mussman W. J. Montanez, I. P. and Read, F. J. (1988). Ordovician Knox Palaeokarst Unconformity, Appalacians. In: *Palaeokarst* (Eds N. P. James and P. W Choquette) Spinger Verlag New York. p.211-228

Neugebauer, J. (1974). Some aspects of cementation in chalk. In: *Pelagic sediments on land and under the sea* (eds K. J. Hsu and H. C. Jenkyns). Internaional Assocaition of Sedimentologists Special Publication 1 p.149-176.

Ori, G. G. and Penney S. R. (1982). The stratigraphy and sedimentology of the Old Red Sandstone sequence at Dunmore East, County Waterford. *Jounal of Earth Science Royal Dublin Society.* p.37-42.

Park, R. K. (1977). The preservation potential of some stromatolites. *Sedimentology.* **v.24** p.485-506.

Patterson, R. J. and Kinsman, D. J. J. (1982). Formation of diagenetic dolomite in coastal sabkhas along the Arabian (Persian) Gulf. *Bulletin of the American Association of Petroleum Geologists.* **v.66** p.28-43.

Pettijohn, F. J., Potter, P. E., Siever, R. 1972. *Sand and sandstone.* Springer New York.

Philcox, M. E, (1980). *Unpublished internal report for Tara mines.*

Philcox, M. E. (1984). Lower Carboniferous Lithostratigraphy of the Irish Midlands. *Special Publication of the Irish Association for Economic Geology.*

Philcox. M. E. (1989). The Mid Dinantian unconformity at Navan, Ireland. In: *The role of tectonics in Devonian and Carboniferous sedimentation in the British Isles* (eds. R. S. Arthurton, P. Gutteridge and S. C. Nolan) Yorkshire Geological Society Occasional Publication **6.** p.67-81.

Philcox, M. E. (1990). *Unpublished internal report for Tara Mines.*

Phillips, W. E. and Sevastopulo, G. D. (1986). The Stratigraphic and structural setting of Irish Mineral deposits. In: *The geology and genesis of mineral deposits in Ireland.* Andrew, C. J., Crow, R. W. A., Finlay, S. Pennell, W. M. and Pyne, J. F. (eds). Special Publication of the Irish Association for Economic Geology, Dublin. p.1-30.

Pickard, N. A. H. Jones, L. J. Rees, J. G. Somerville I. D; Strogen, P. (1992). Lower Carboniferous (Dinantian) stratigraphy and structutre of the Walterstown-Kentstown area, Co. Meath Ireland. *Geological Journal.* **v.27** p.35-38.

Pierson, B. J. (1981). The control of cathodoluminescene in dolomite by Fe and Mn. *Sedimentology.* **v.28,** p.601-610.

Pilkey, D. H., Bush, D. M. and Rodriguez, R. W. (1988). Carbonate terrigenous sedimentation on the northern Puerto Rico shelf. In: *Carbonate-clastic transitions.* (eds. L. J. Doyle and H. H. Roberts). Developments in Sedimentology **42** Elsevier.

Pomar, L. (1991). Reef geometries, erosion surfaces and high frequency sealevel changes, Upper Miocene Reef Complex Mallorca Spain. *Sedimentology.* **v.38** No. 2 p.243-270.

Potter, P. E., Maynard, J.B. and Prior W. A. (1980). *Sedimentology of shale.* Springer Verlag.

Poustie, A, and Kucha, H. (1986). The geological setting, style and petrology of zinc-lead mineralization in the Moyvoughly area Co. Westmeath. In: *The geology and genesis of mineral deposits in Ireland.* Andrew, C. J., Crow, R. W. A., Finlay, S. Pennell, W. M. and Pyne, J. F. (eds). Special Publication of the Irish Association for Economic Geology, Dublin.p.305-318.

Presbindowski, D. R. and Larese, R. E. (1987). Experimental stretching of fluid inclusion in calcite - implications for diagenetic studies. *Geology.* **v.15** p.333-336.

Purdy, E. G. (1961). Bahamian oolite shoals. *American Association of Petroleum Geologists Bulletin.* **v.45.** p.53-62.

Purdy E. G. (1974). Karst determines facies patterns British Honduras, Holocene carbonate sedimentation model. *Bulletin of the American Associaton of Petroleum Geologists.* **v.58** p.825-855.

Purser, B. H. (1969). Synsedimentary lithification of middle Jurassic limestones in the Paris Basin. *Sedimentology.* **v.12** p.205-230.

Purser, B. H. (1973). *The Persian Gulf: Holocene carbonate sedimentation and diagenesis in a shallow epicontinental sea.* Springer Verlag Berlin.

Quing, H. and Mountjoy, E. (1991). Presqu'ile dolomite at Pine Point and adjacent subsurface: Evidence for hydrothermal dissolution and a late Cretaceous maximum burial origin for saddle dolomite and mineralization. *Dolomieu Conference on Carbonate Platforms and Dolomitization, Abstracts.* Eds. A. Bosellini, R. Brander, E. Flugel, B. Purser, W. Schlager, M. Tucker, D.Zenger p.220.

Radkhe, B. H. and Mathis, R. L. (1980). On the formation and occurrence of saddle dolomite. *Journal of Sedimentary Petrology.* **v.50** p.1149-1168.

Raiswell, R. (1982). Pyrite texture, isotopic composition and availabilty of iron. *American Journal of Science.* **v.282** p.1244-1263.

Randazzo, A. F. and Bloom, J. J. (1985). Mineralogical changes along the freshwater / saltwater interface of a modern aquifer. *Sedimentary Geology.* **v.43** p.219-239.

Rees, J.G. (1987). The Carboniferous geology of the Boyne Valley area Ireland. *Unpublished PhD thesis* . University of Dublin.

Reineck, H. E. and Wunderlich, F. (1968). Classification and origin of flaser and lenticular bedding. *Sedimentology.* **v.11** p.99-104.

Reinson, G.E. (1984). Barrier island and associated strand Plain systems. In: *Facies Models.* 2nd edition (ed. R. G. Walker). Geoscience Canada Reprint Series 1.

Riding, R. and Wright, V. P. (1981). Palaeosols and tidal flat / lagoonal sequences on Carboniferous carbonate shelf: Sedimentary associatiuons of triple disconformities. *Journal of Sedimentary Petrology.* **v. 51** p1323-1339.

Romano, M. (1980). The stratigraphy of the Ordovicain rocks between Slane and Collon, eastern Ireland. *Journal of Earth Science, Royal Dublin Society.* **v.3.** p.53-79.

Russell, M. J. (1986). Extension and convection: A genetic model for the Irish Carboniferous base metal and barite deposits. In: *The geology and genesis of mineral deposits in Ireland.* Andrew, C. J., Crow, R. W. A., Finlay, S. Pennell, W. M. and Pyne, J. F. (eds). Special Publication of the Irish Association for Economic Geology, Dublin.p.545-554.

Russell, M. J. and Haszeldine, R. S. (1990). Accounting for geofractures. *The Irish Minerals industry - A review of the decade, abstracts volume.* Irish Association for Economic Geology.

Saller, A. H. (1984). Petrographic and geochemical constraints on the origin of subsurface dolomite Enewetak atoll an example of dolomitzation by normal seawater. *Geology.* **v.12** p.217-220.

Sangster, D. F. (1976). Carbonate hosted Lead-Zinc deposits. In: *Handbook of stratabound and stratiform ore deposits*: K. H. Wolf (ed) Amsterdam Elsevier Scientific Publications **v.6** p.447-465.

Sangster, D. F. (1990). Mississippi Valley-Type and SEDEX Lead-Zinc deposts: a comparative examination. *Transactions of the Institute of Mining and Metallurgy (Section B, Applied Earth Science)* **v.99** B21.

Scholle, P. A. (1978). *A colour illustrated guide to carbonate rock constituents, textures cements and porosities.* American Association of Petroleum Geologists Memoir 27 Tulsa Oaklahoma.

Scholle, P. A. and Halley, R. B. (1984). Burial diagenesis out of sight, out of mind. In: Stylolites and related phenomenon relavence to hydrocarbon resevoirs. *Special publication of the Abhu Dhabi National Resevoir Research Foundation.*

Scholle, P. A. and Halley, R. B. (1985). Burial diagenesis: out of sight, out of mind. In: *Carbonate cements* (eds. N. Schneiderman and P. M. Harris). Special Publication of the Society of Economic Palaeontologists and Mineralogists **36** p.309-334.

Scholle, P. A. and Kling S. A. (1972) Southern British Honduras: Lagoonal Coccolith ooze. *Journal of Sedimentary Petrology.* **v.42.** p.195-204.

Schreiber, B. C. Tucker M. E. and Till, R. (1986). Arid shorelines and evaporites. In: *Sedimentary environments and facies* (ed. H.G. Reading). Blackwell Scientific Publications. p.189-228.

Schroeder, J. H. (1969). Experimental dissolution of calcium, magnesium and strontium from Recent biogenic carbonates. *Journal of Sedimentary Petrology.* **v.39** p.1057-1073.

Schwarzacher, W. (1975). *Sedimentology and quantitative stratigraphy.* Developments in Sedimentology. **19** Elsevier Amsterdam pp.382.

Sears, S. O. and Lucia, F. J. (1980). Dolomitization of the nothern Michigan Niagara Reefs by brine refluxion and freshwater / seawater mixing. In: *Concepts and models of dolomitzation* (eds. D. H. Zenger, J. B. Dunham and R. L.Ethington). Special Publication of the Society of Economic Palaeontologists and Mineralogists. **28** p.215-237.

Seilacher, A. (1967) Bathymetry of trace fossils. *Marine Geology.* **v.5** p.413-428.

Selley R. C. (1967). Palaeocurrents and sediment transport in the Sirte Basin, Libya. *Journal of Geology.* **v.75** p.214-223.

Selley, R. C. (1968). Nearshore marine and continental sediments of the Sirte Basin, Libya. *Quarterly Journal of the Geological society of London* . **v.124** p.419-60.

Selley, R. C. (1985). *Ancient sedimentary environments.* 3rd edition, Chapman and Hall London.

Sellwood, B. W. (1986) Shallow marine carbonate environments. In: *Sedimentary environments and facies* (ed. H. G. Reading). p.283-341. Blackwell Scientific Publications.

Shearman, D. J. (1978). Evaporites of coastal sabkhas. In: *Marine Evaporites.* (Eds. W. E. Dean and B. C. Schreiber). Society for Economic Palaeontologists and Mineralogists short course 4. Tulsa Oaklahoma. p.6-42.

Shelton, K. L. and Bauer, R. M., Gregg J. M. (1992). Fluid inclusion studies of regionally extensive epigenetic dolomites, Bonettere Dolomites (Cambrian), southeast Missourri: Evidence of multiple fluids during dolomitzation and Lead-Zinc minearalization. *Geological Society of America Bulletin.* **v.104** p.675 -683.

Shinn, E. A. (1968a). The practical significance of birdseye structures in carbonate rocks. *Journal of Sedimentary Petrology.* **v.38** p.215-223.

Shinn, E. A. (1968b). Burrowing in recent lime sediments of Florida and Bahamas. *Journal of Paleontology.* **v.42** p.879-894.

Shinn, E. A. (1969). Submarine lithification of Holocene carbonate sediments in the Persian Gulf. *Sedimentology.* **v.12** p.109-144.

Shinn, E. A. (1973). Carbonate coastal accretion in an area of longshore transport, NE Qatar, Persian Gulf. In: *The Persian Gulf-Holocence carbonate sedimentation and diagenesis in a shallow epicontinental sea* (ed. B. H. Purser). Springer-Verlag Berlin. p.179-191.

Shinn, E. A. (1983). Tidal flat. In: *Carbonate depositional environments.* American Association of Petroleum Geologists, Memoir 33. Scholle, P. A., Bebout, D. G., Moore, C. H. (eds). Tulsa Oaklahoma. p.171-210

Shinn, E. A., Lloyd, R. M., Ginsburg, R. N. (1969). Anatomy of a modern carbonate tidal flat, Andros Island, Bahamas. *Journal of Sedimentary Petrology.* **v.39** p. 1202-1228.

Sibley. D.F. (1980). Climatic control of dolomitzation Seroe Domi Formation (Pliocene) Bonaire. In: *Concepts and models of dolomitzation* (eds. D. H. Zenger, J. B. Dunham and R. L.Ethington). Special Publication of the Society of Economic Paleontologists and Mineralogists. **28.** p.247-258.

Sibley, D. F. (1982). The origin of common dolomite fabrics. *Journal of Sedimentary Petrology.* **v.52** p1987-1100.

Sibley, D. F. and Gregg, J. M. (1987). Classification of dolomite rock textures. *Journal of Sediemtary Petrology.* **v.57.** p.967-975.

Simms, M. (1984). Dolomitzation by groundwater flow systems in carbonate platforms. *Transactions of Gulf Coast Association of Geological Societies.* **v.34** p.411-420.

Simon, J. B. (1984). Sedimentation of a small complex alluvial fan of possible Upper Old Red sandstone age, northeast County Antrim. *Irish Journal of Earth Science.* **v.6.** p.109-119.

Skall, H. (1975). The palaeoenvironment of the Pine Point Lead-Zinc District. *Economic Geology.* **v.70** p.22-47.

Smart, P. L., Palmer, R. J., Whitiker, F. and Wright, V. P. (1988). Neptunian dikes and fissure fills: An overview and account of some modern examples In: *Palaeokarst* (eds. N. P. James and P. W. Choquette) Springer-Verlag. p.149-163.

Smart, P. L and Whittiker, F. F. (1991). Karst processes, hydrology and porosity evolution. In: *Palaeokarst and Palaeokarstic Resevoirs* (Eds. V. P. Wright, M. Esteban and P. L. Smart) P.R.I.S. Occasional Publication Series 2 p.1-55. University of Reading.

Sommerville, I. D. (1979). Minor cyclicty in the Asbian (Upper D_1) limestones in the Llangollen district of North Wales. *Proccedings of the Yorkshire Geological Society.* **v.42** p.317-337.

Stockman, K. W. H., Ginsburg, R. N. and Shinn E. A. (1967). The production of lime mud by algae in south Florida. *Journal of sedimentary Petrology.* **v.37** p. 633-648.

Strogen, P, Jones, G. L. Somerville, I. D. (1990). The stratigraphy and sedimentology of Lower Carboniferous (Dinanian) boreholes fron West County Meath, Ireland. Geological journal **v.25** p. 103 - 137.

Tebbut, G. E., Conley, C. D., Boyd, D. W. (1965). Lithogenesis of a distinctive carbonate rock fabric, In: *Contributions to geology* (ed. R. B. Park). Larimie University of Wyoming. p.1-13.

ten Have, T. and Heijenen, W. (1985). Cathodoluminescence activation and zonation in carbonates rocks. *Geol Mijn.* **v.64** p.297-310.

Todd, D. K. (1980). *Groundwater hyrology.* pp.535. John Wiley and Sons London.

Tucker, M. E. (1987). *Sedimetary petrology: An introduction.* Geoscience Text. Volume 3. Blackwell Scientific Publications.

Tucker, M. E. (1990a). Diagenesis in the burial environment. In *Carbonate Sedimentology.* M. E. Tucker and V. P. Wright. Blackwell Scientific Publications. p.348-362

Tucker, M. E. (1990b). Geological background to carbonate sedimentation. In: *Carbonate sedimentology.* M. E. Tucker and V. P. Wright. Blackwell Scientific Publications. p.28-67

Tucker, M. E. (1990c). Dolomites and dolomitzation models. In: *Carbonate sedimentology.* M.E. Tucker and V. P. Wright. Blackwell Scientific Publications. p.365-396.

Tucker, M. E. and Bathurst, R. G. C. (1990). Marine Diagenesis; Modern and ancient. In: *Carbonate diagenesis* (eds M. E. Tucker and R. G. C. Bathurst). Reprint series volume 1 of the International Association of Sedimentologists. Blackwell Scientific Publications. p.1-9.

Tucker, M. E. and Wright, V. P. (1990) *Carbonate sedimentology.* Blackwell Scientific Publications.

Tudope, A. W. (1989). Shallowing upwards sedimentation in a coral reef lagoon, Great Barrier Reef of Australia. *Journal of Sedimentary Petrology.* **v.59** p.1036-1051.

Turner, J. S, Hornung, G. Rex, D. C. (1972). Tertiary igneous activity at Navan County Meath. *Irish Naturalists Journal.* **v.11** p.262-64..

Varker, W. J. and Sevastopulo, C. D. (1985) The Carboniferous system part 1- Conodonts of the Dinantian subsystem from Great Britain and Ireland. In: *A stratigraphical index of British conodonts* (eds. R. L. Austin and A. C. Higgins) Ellis Hotwood Ltd. Chichester. p.167-209.

Walkden, G. M. (1974). Palaeokarst surfaces in Upper Visean (Carboniferous) limestones of the Derbyshire Block, England. *Journal of Sedimentary Petrology.* **v.44** No.4 p.1232-1248.

Walkden, G. M. (1987). Sedimentary and diagenetic styles in late Dinatian carbonates of Britain. In: *European Dinatian environments* (eds. J. Miller, A. E. Adams and V. P. Wright). John Willey and Sons Chichester. p.131-158.

Walkden, G. M. and Berry, J. R. (1984). Natural calcites in cathodoluminescence: crystal growth during diagenesis. *Nature.* **v.308** p.525-527.

Walkden , G. M. and Davies, J. (1983). Polyphase erosian of subaerial omission surfaces in the Late Dinantion of Anglesey, north Wales. *Sedimentology.* **v.30** p.861-878.

Walker, R. G. (1984). General introduction: Facies, facies sequences and facies models. In: *Facies Models* 2nd edition (ed. R. G. Walker). Geoscience Canada, reprint series 1. p.1-11.

Walker, R. G. (1984). Sandy fluvial systems. In: *Facies models* .(ed. R. G. Walker) 2nd Edition. Geoscience Canada reprint series 1, p. 71-90.

Walker, T. R. (1962). The reversible nature of the chert carbonate replacement reaction in sedimentary rocks. *Geological Society of America Bulletin.* **v.73** p.237-242.

Walker, T. R. (1967). Formation of red beds in moist tropical climates. *Bulletin of the Geological Society of America.* **v.85** p. 633 - 638.

Walker, T. R., Wagh, B., Crone, A. J. (1978). Diagenesis in first cycle desert alluvium of Cenozoic age, southwestern United States and northwestern Mexico. *Bulletin of the Geological Society of America.* **v.89** p.19-32.

Wanless, H. R. (1979). Limestone response to stress: pressure solution and dolomitization. *Journal of Sedimentary Petrology.* **v.49** p.437-462.

Wanless H .R. (1981). Finning upwards sedimentary sequences generated in seagrass beds. *Journal of Sedimentary Petrology.* **v.51.** No.2 p.445-454.

Weyl, P. K. (1959). Pressure-solution and the force of crystallization phenomenological theory *Journal of Geophysical Reseach.* **v.64.** p.2001-2025.

Weyl, P. K. (1960). Porosity through dolomitzation conservation of mass requirements. *Journal of Sedimentary Petrology*. **v.30**. p.85-90.

Whittiker, F. F. and Smart, P. L. (1990). Active circulation of saline groundwater in carbonate platforms: evidence from the Great Bahamas Bank. *Geology*. **v.18** p.200-203.

Wiggins, W. D. and Harris, P. M. (1984). Cementation and porosimetry of shoaling sequences in the subsurface Pettit Limestone, Cretaceous of east Texas. In: *Carbonate sands: a core workshop* (ed. P.M. Harris). Society for Economic Palaeontologists and Mineralogists p. 263-305. Tulsa Oaklahoma.

Wilson, E. N. and Hardie, L. A. and Phillips O. W. (1990). Dolomitization front Geometry, Fluid Flow Patterns and the origin of massive dolomite: The Triassic Latemar Build Up. northern Italy *American Journal of Science*. **v.290** p.741-769.

Wilson, J. L. (1975). *Carbonate facies in geological history*. Springer-Verlag Berlin.

Wilson, J. L. and Jordan, C. (1983). Middle Shelf. In: *Carbonate depositional environments*. American Association of Petroleum Geologists, Memoir 33. Scholle, P. A., Bebout, D. G., Moore, C. H. (eds). Tulsa Oaklahoma. p.297-444.

Winland, H. D. and Mathews R. K. (1974). Origin and significance of grapestones Bahamas Islands. *Journal of Sedimentary Petrology*. **v.44** No3 p.932-927.

Wright, V.P. (1982). The recognition and interpretation of palaeokarsts; Two examples from the lower Carboniferous of south Wales. *Journal of Sedimentary Petrology*. **v.52** p.83-94.

Wright, V. P. (1983). Morphogenesis of oncoids in the Lower Carboniferous Llanelly Formation of South Wales. In: *Coated grains* (Ed. T. M. P. Peyrt) p.424-434. Spinger-Verlag Berlin.

Wright, V.P. (1986). Facies sequence on a carbonate ramp, the Carboniferous of south Wales. *Sedimentology*. **v.33** p.221-241.

Wright, V. P. (1988). Palaeokarst and palaeosols as indicators of palaeoclimate and porosity evolution: A case study from the Carboniferous of south Wales. In: *Palaeokarst* (Eds N.P. James and P.W Choquette) Spinger Verlag New York. p.329-341.

Wright V. P. (1990a). Peritidal carbonates. In: *Carbonate sedimentology*. Tucker, M. E. and Wright, V. P. Blackwell Scientific Publications. p.137-164.

Wright, V. P. (1990b). Meteoric diagenesis. In: *Carbonate sedimentology*. M. E. Tucker and V. P. Wright. Blackwell Scientific Publications. p.336-348.

Wright, V. P. (1991) Palaeokarst: Types, recognition. controls and associations. In: *Palaeokarsts and Palaeokarstic Resevoirs* (Ed by V. P. Wright; M. Esteban; P. L. Smart). P.R.I.S. Occasional Publication Series 2. p.1-55. University of Reading.

Zenger, D.H. (1983). Burial dolomitization in the Lost Burrow Formation (Devonian), east central California and the significance of late diagenetic dolomitization. *Geology*. **v.11** p.519-522.

CROSS-SECTION 'B-B'

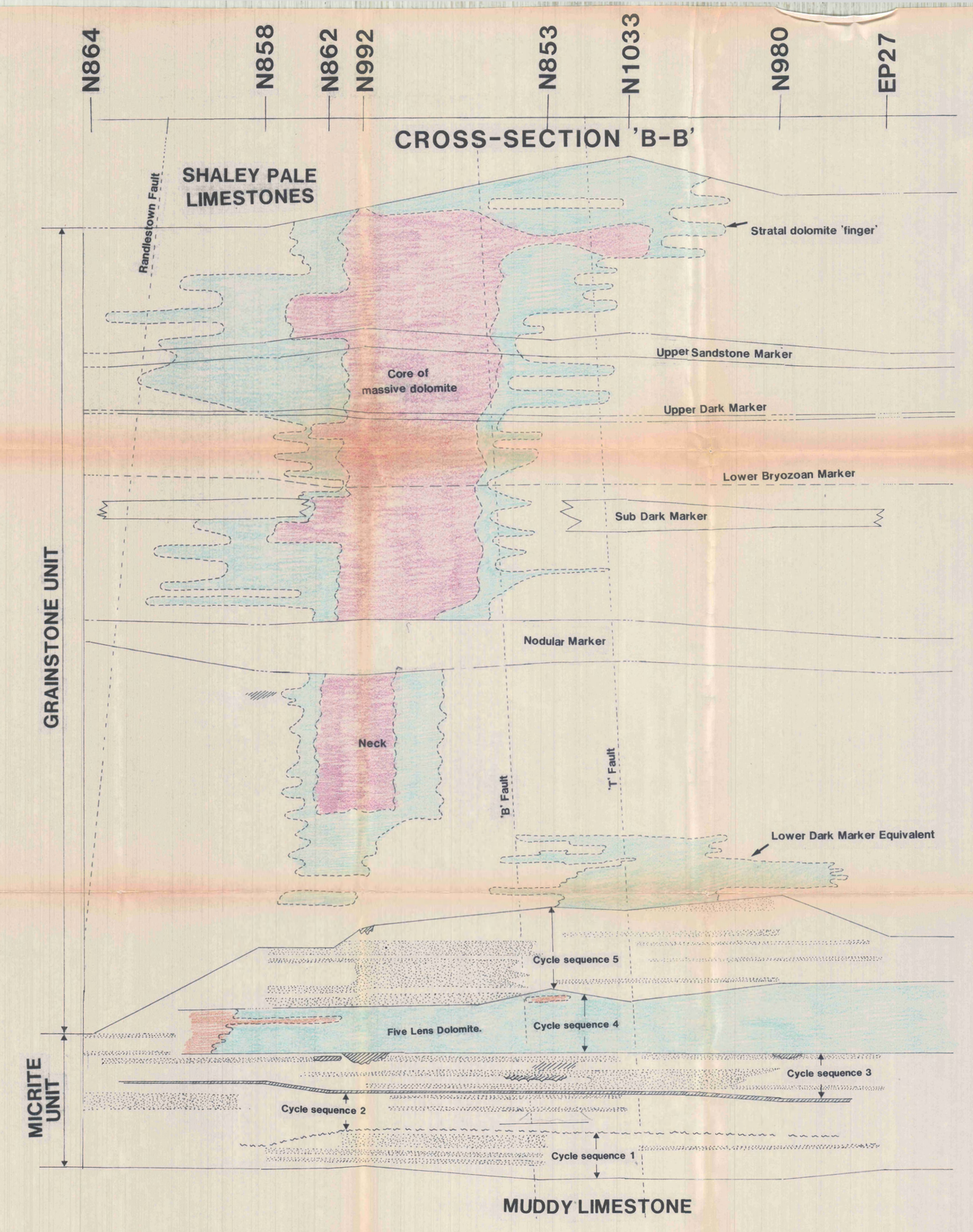

MUDDY LIMESTONE

CROSS-SECTION 'C-C'

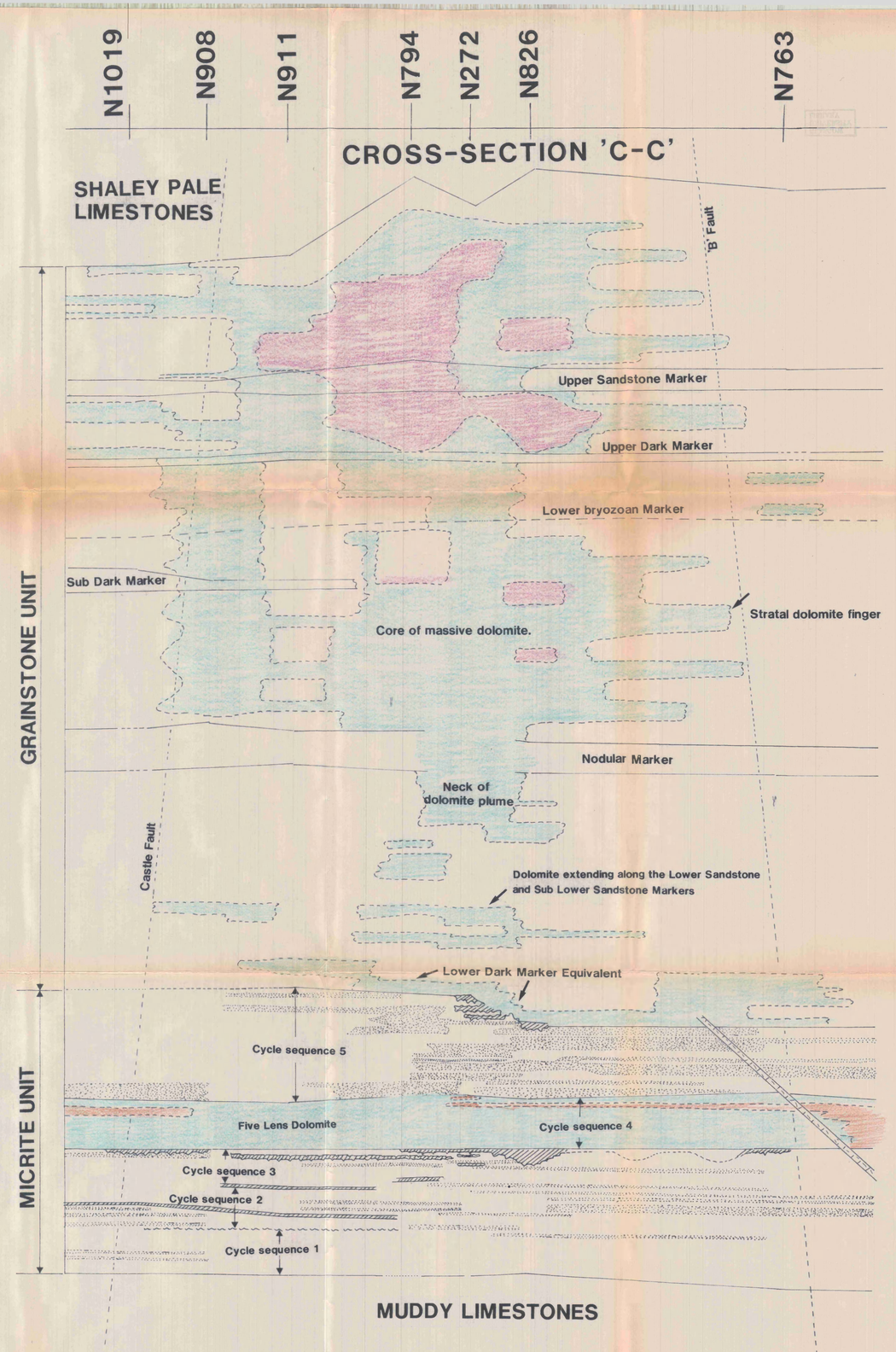

MUDDY LIMESTONES

CROSS-SECTION 'D-D'

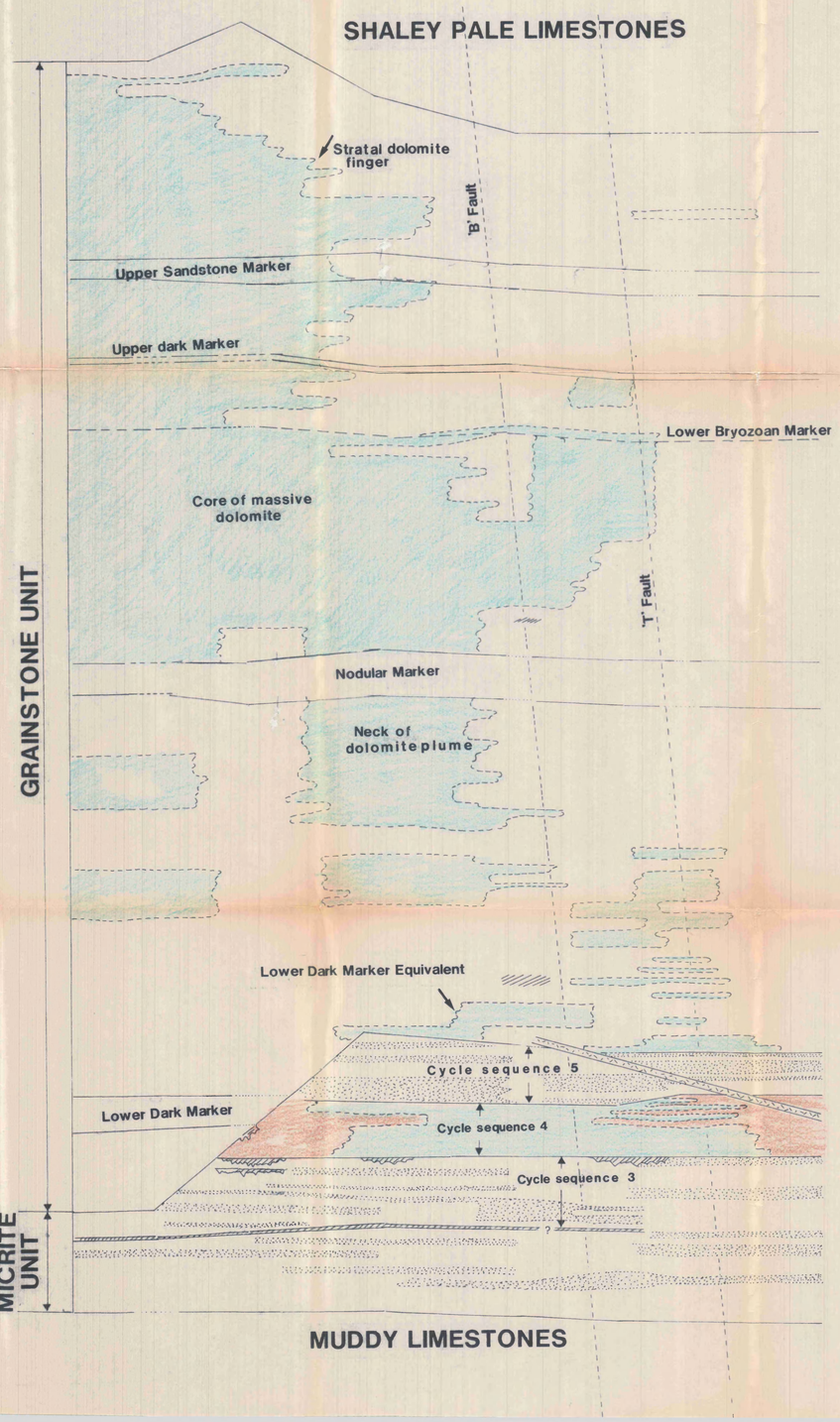

MUDDY LIMESTONES

CROSS-SECTION 'E-E'

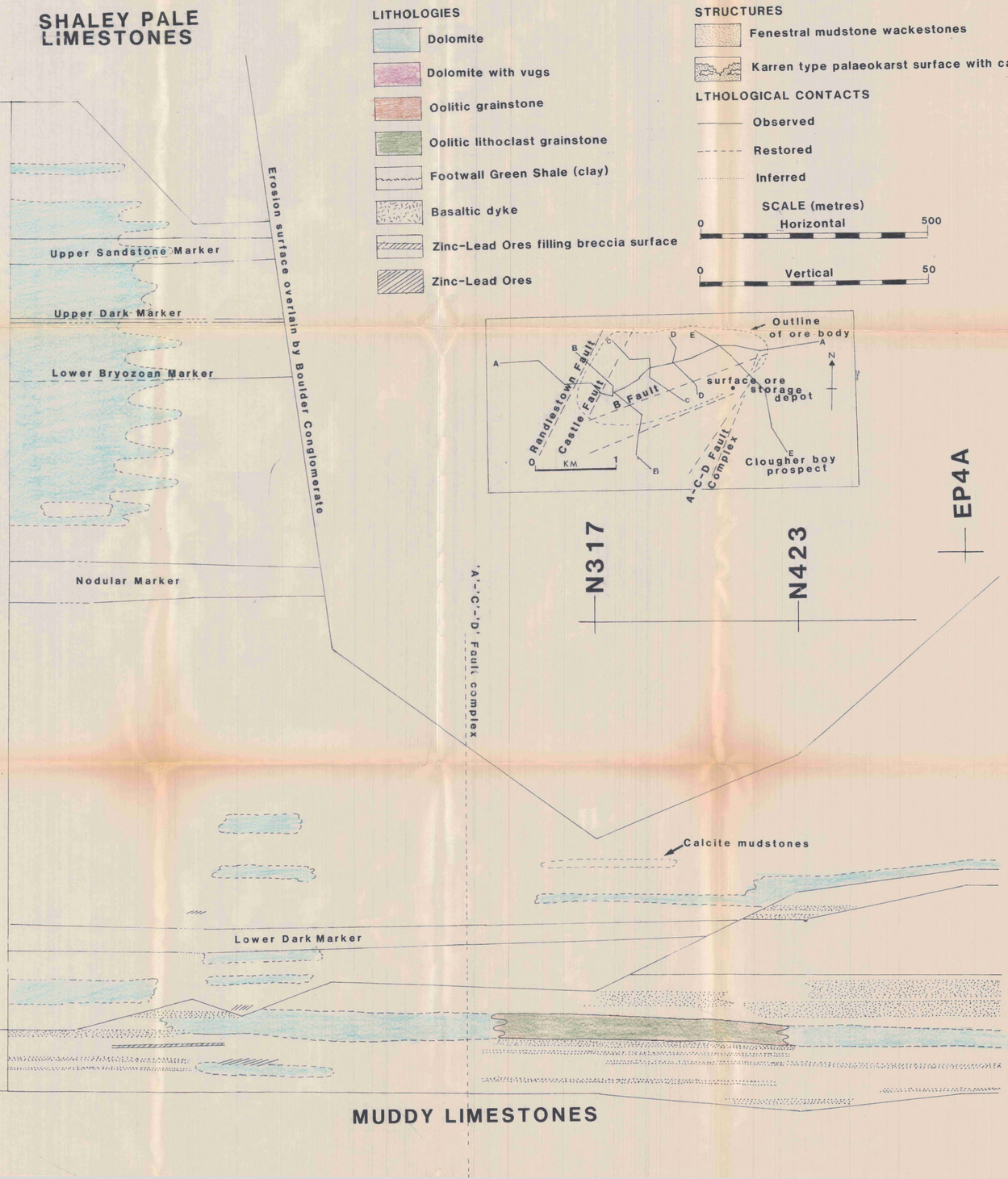

MUDDY LIMESTONES

LITHOLOGIES

- Dolomite
- Dolomite with vugs
- Oolitic grainstone
- Oolitic lithoclast grainstone
- Footwall Green Shale (clay)
- Basaltic dyke
- Zinc-Lead Ores filling breccia surface
- Zinc-Lead Ores

STRUCTURES

- Fenestral mudstone wackestones
- Karren type palaeokarst surface with cavities

LTHOLOGICAL CONTACTS

- Observed
- Restored
- Inferred

SCALE (metres)

Horizontal 0 — 500

Vertical 0 — 50

CROSS-SECTION 'A-A'

N1022 N1005 N1017 N1026 N1018 N933 N992 N975 N835 N272 N806 N725 N314 N629 N286

N30 N509

Randlestown Fault

Castle Fault

SHALEY PALE LIMESTONES

GRAINSTONE UNIT

MICRITE UNIT

Upper Sandstone Marker

Upper Dark Marker

Lower Bryozoan Marker

Sub Dark Marker

Nodular Marker

Erosion Surface overlain by Boulder Conglomerate

Dolomite extending along the Sub Lower Sandstone Marker

Dolomite extending along Lower Sandstone and Sub Lower Sandstone Markers

Lower Dark Marker Equivalent

Cycle sequence 5

Cycle sequence 4

Cycle sequence 3

Cycle sequence 2

Cycle sequence 1

the Five Lens Dolomite

Lower Dark Marker

MUDDY LIMESTONE

LITHOLOGIES

- Dolomite
- Dolomite with vugs
- Oolitic grainstone
- Oolitic lithoclast grainstone
- Footwall Green shale (clay)
- Zinc-Lead ores
- Zinc-Lead ores filling breccia surface

(Microconglomerate not shown for clarity refer Fig 4.9)

STRUCTURES

- Fenestral mudstone-wackestones
- Karren type palaeokarst surface with cavities

LITHOLOGICAL CONTACTS

- Observed
- Restored
- Inferred

SCALE (metres)

0 Horizontal 500

0 Vertical 50

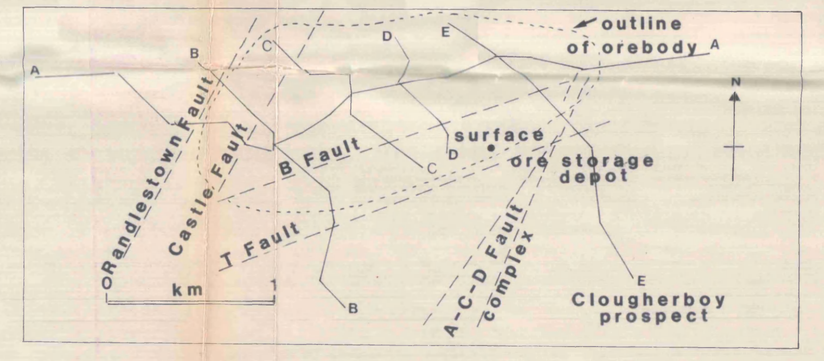

LITHOLOGY

- MICRITE
- (WAULSORTIAN) 'REEF'
- CALCSILTITE
- CALCARENITE
- CALCIRUDITE
- BOULDER / CONGLOMERATE
- BRECCIA
- ARGILLITE OR MUD
- SHALE (OR SHALE WISPS)
- SILT OR SILTSTONE
- SAND OR SANDSTONE
- DOLOMITE
- CALCAREOUS
- SPARRY
- INTERBEDS
- ------- TRANSITION

BEDDING FEATURES

- L LAMINATED (<0.01m)
- t THIN (0.01-0.1m)
- m MEDIUM (0.1-0.3m)
- T THICK (0.3-1.0m)
- M MASSIVE (>1.0m)
- FINING DOWN
- FINING UP
- X CROSSBEDDED

TEXTURAL FEATURES

- STYLOLITES
- BIOTURBATION
- SOFT-SEDIMENT DEFORMATION
- BOUDINAGE
- NODULAR
- MUD WISPS
- NEPTUNEAN DYKE
- GEOPETAL
- STROMATACTIS
- BIRDSEYE
- INTRACLASTS
- OOLITES & PELLETS
- ONCOLITIC
- VUGGY

FOSSILS

- CRINOIDS
- SOLITARY CORALS
- SYRINGOPORA
- BRACHIOPODS
- BIODEBRIS

BRYOZOA

- FENESTELLIDAE
- FINGER
- ENCRUSTING
- STICK

ALTERATION AND OTHER FEATURES

- DOLOMITIZATION
- CALCIFICATION
- LEACHING
- BL BLEACHING
- HE HEMATITIZATION
- S SILICIFICATION
- Rn REDUCTION (RED BEDS TURNED GREEN)
- Py PYRITIZATION
- CT CHERT (NODULAR OR BEDDED, FOUND IN UDL)
- HYC HYDROCARBON
- CHA COLOUR CHANGE

IGNEOUS

- MINOR INTRUSIVE
- MAJOR INTRUSIVE
- TUFF
- VOLCANICS

STRUCTURE

- -- U -- UNCONFORMITY
- FAULT
- FOLDING

BRECCIAS

- BX GENERAL
- BXT TECTONIC
- BXS SLUMP

GRAIN OR CLAST SIZE

< 0.06mm	SILTITE
0.06 - 2.0mm	ARENITE
> 2.0mm	MICROCONGLOMERATE OR RUDITE

MINERALISATION

- BEDDING-PARALLEL
- CROSS-CUTTING
- FRACTURE-FILL
- DISSEMINATED

TARA DIAMOND DRILL LOG

SHEET NO: 5

LOGGED BY: _____ HOLE NO: 80c

DATE: 4/4/90 DR GOES 10 726-3 - LOM. PAGE 3 OF 5

LITHOLOGICAL AND MINERALIZATION LOG | STRUCTURAL LOG

LOG SUMMARY	DEPTH	LITHOLOGY MAJOR	LITHOLOGY MINOR	FEATURES	BEDDING	ALTERATION	MINZ BP	MINZ FF	COMMENTS	BEDDING B- 1 2 3 4 <	JOINTING J- 1 2 3 4 <	FAULTING F- 1 2 3 4 <	FEATURE	FROM	TO
	240								Dolomite Lens Pitsuugs.						
	243														
	246														
	249														
NODULE MARKER.	252														
	255								weakly dol Calc Arenite.						
	258								dolomitic Original sed texture visible also some disseminated pyr. + laminated layers.						
	261														
	264								10cm fissile to block shale, > blk laml dolomitised calc Arenite silt.						
	267								dolomite Calc Arenite.			—	highly carbonaceous vertical fault with shale		
	270								dolomitic Calc Arenite bioturbated dolomitized calc Arenite						
	273													138	
	276													255	
	279								muddy dolomitic calc Arenite. dolomitized calc Arenite					15	
	282														
	285														
	288														
	291														
	294														
	297														
	300														

TARA DIAMOND DRILL LOG

SHEET NO: 5

LOGGED BY: GRIZZ

HOLE NO: 806

DATE: 4/4/90

NOTE DDR CONTINUES TO 2263 EOH

PAGE 5 OF 5

LITHOLOGICAL AND MINERALIZATION LOG / STRUCTURAL LOG

LOG SUMMARY	DEPTH	LITHOLOGY MAJOR	LITHOLOGY MINOR	FEATURES	BEDDING	ALTERATION	MINZ BP	MINZ FF	COMMENTS	BEDDING B- 1 2 3 4 <	JOINTING J- 1 2 3 4 <	FAULTING F- 1 2 3 4 <	FEATURE	FROM	TO
MICRITE UNIT.	3 240								very finely xtalline dm.						
	3 243			Bx, Bx					20cm Bx below. 20cm.						
									very weak fen. 20cm Massive lam sulph. ec.						
	3 246								cavities - holes mm scale 30cm. very weakly fen.						
									very weakley fenestral.						
	3 249								very weakley fenestra. ~~pm~~ pels and holes.						
	3 252														
	353			Bx					Brecciated mc filled with sulphide						
	3 255														
									0.5 weak fen.						
	3 258														
	3 261								30cm birdseyes fenestrae. Stylonodular						
	362								20cm very uniform ~~muddy~~ mic.						
MUDDY LIMESTONE	3 264			F Shale					Fault or cavity filled with silty material nodular or clastic. Thinly bedded.						
									micritic calc arenite probably pelletal mic						
	267														
									nodular oncolitic? strange brown material in between.						
	3 270														
	3 273														
LAMINATED BEDS.	3 276	CB													
		CC													
	3 279	CD													
	3 282														
E.O.H.	285														
	288														
	291														
	294														
	297														
	300														

TARA DIAMOND DRILL LOG

SHEET NO: 4

LOGGED BY: G. Rizzi

HOLE NO: 80C

DATE: 4 / 4 / 90

PAGE 4 OF 5

LITHOLOGICAL AND MINERALIZATION LOG — STRUCTURAL LOG

Log summary: [illegible] of GRAINSTONE UNIT. (180–221); MICRITE UNIT (221–240)

DEPTH	FEATURES	COMMENTS
2 180		
		dolomite
		very gradational [illegible] dol calc Arenite
2 183		
2 186		not dolomite crinoid rich calc Arenite [illegible]
2 189		ripple cross lam calc Arenite
2 192		dolomite plus patches of calc Arenite.
2 195		
2 198		2?'
3 201		
3 204		
3 207		Banded calc Arenite light grey- light brown calc Arenite bands
3 210	(S)	
3 213		nodular calc Arenite with some fracture fill mineralization.
3 216		202
3 219	3?	
		> very finely dissem ZnS. pelletal [illegible]
3 222		very weak fen
3 225		very weak fenestrae
		very finely crystalline dolomite light brown
3 228		fenestral
		cavitied zone with fenestrae [illegible] possibly some [illegible] [illegible]
3 231		0.7 cavity zone
		> gradational up
3 234		weakly dolomitized very uniform [illegible] calc Arenite.
3 237		gradational relationship
		uniform very finely crystalline dol
3 240		

FROM / TO (margin notes): 321 / 308 ; 308 / 1 / 04 ; 308 / 221 / 04 ; 25 / 287 / 253 / 30

TARA DIAMOND DRILL LOG

SHEET NO: 4

LOGGED BY: GIAN

HOLE NO: N806

DATE: 16/9/90 S.N.

PAGE 2 OF 5

LITHOLOGICAL AND MINERALIZATION LOG

STRUCTURAL LOG

LOG SUMMARY	DEPTH	LITHOLOGY MAJOR	LITHOLOGY MINOR	FEATUREB	BEDDING	ALTERATION	MINZ	COMMENTS	BEDDING B- 1 2 3 4 <	JOINTING J- 1 2 3 4 <	FAULTING F- 1 2 3 4 <	FEATURE	FROM	TO
	180							155 SP						
	183													
	186													
	189													
3MC	192													
	195													
	198													
	201													
	204													
	207													
	210													
LBY	213			LBY										
	216							gradational contact						
GRAINSTONE UNIT	219													
	222													
	225			S										
	228													
	231													
	234			S										
	237			S										
	240													

TARA DIAMOND DRILL LOG

SHEET NO: 3

LOGGED BY: G.RIZZI

HOLE NO: N806

DATE: 16 / 9 / 90

PAGE 1 OF 5

LITHOLOGICAL AND MINERALIZATION LOG | STRUCTURAL LOG

LOG SUMMARY	DEPTH	LITHOLOGY MAJOR	LITHOLOGY MINOR	FEATURES	BEDDING	ALTERATION	MINZ BP	MINZ FF	COMMENTS	BEDDING B- 1 2 3 4 <	JOINTING J- 1 2 3 4 <	FAULTING F- 1 2 3 4 <	FEATURE	FROM	TO
	120														
	123														
	126														
	129														
	132														
	135														
	138														
	141														
	144														
	147														
SHALEY PALES	150														
	153								1m BLACK CHT						
GRAINSTONE UNIT	156														
	159														
	162														
	165														
	168														
	171														
	174														
	177														
	180														

phi scale											DOLOMITE				MINERALS				FOSSILS	SPECIFIC FEATURE, SAMPLE, PHOTO.
Silt	V.f Sand	Fine Sand	Med Sand	Coarse Sand	V Coarse Sand	Granules	Sm Pebbles	Med Pebbles	Large Pebbles		ENTIRE	PATCHY/IRREG	CLAST ONLY	MATRIX ONLY	SPHALERITE	GALENA	PYRITE	OTHER		
4	3	2	1	0	-1	-2	-3	-4												

DATE 9 11 88 | HOLE Nº 975 | BOX: 497.5 - 503.5

LOG Nº 4 | SECTION 18. | Fm/MARKER LCS.

REMARKS | 1:1

LIMESTONE CONGLOMERATE.

SCALE 1:1.

Muddy limestone LCS-TRANSITION CONTACT gradational. The lower unit grades up into the ML. At contact bioclastic debris dies out

bioclastic debris dies out.

contact gradational.

Crudely banded layer unit very fine 2.5 phi sand grade with gradational to indistinct boundaries. Bands undulose possibly distorted by compaction

lighter areas are fine to medium sand. Generally the rock appears to have a nodular texture.

PHOTO 1

quite sharp probably erosive contact present ripping up layer of silty shale.

ripped up and bent laminae

Zone of discontinuous ~~light~~ fine sandy laminae. Possibly due to deplanktering. May be algal laminite. Silty Material is very organic rich. Some of the laminae have pyramid shapes in the upper laminae. Possible Some of the laminae appear to have been ripped up and bent.

unusual laminae (Specimen)

GR 88.

DATE: | HOLE Nº: | BOX: 3836 389.6.

LOG Nº: 23? | SECTION: | Fm/MARKER: MC

REMARKS 1:10

MICRO CONGLOMERATE

SCALE 1:10.

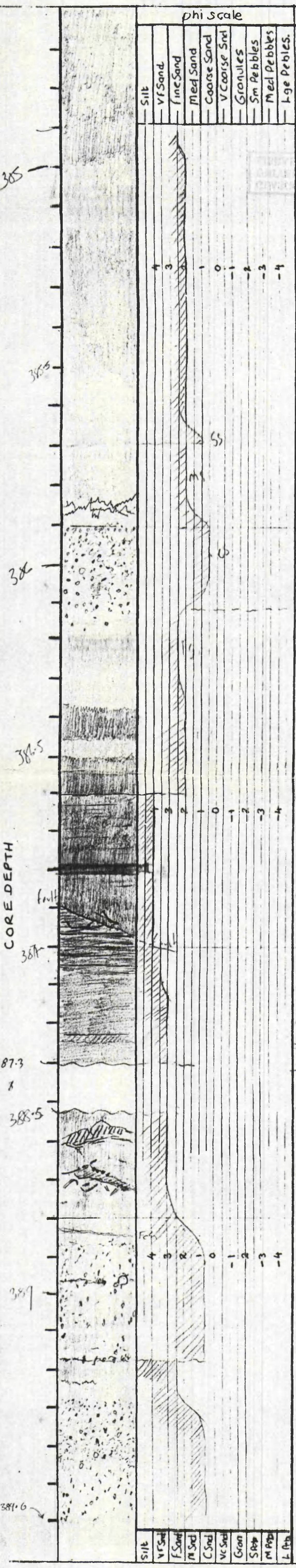

DOLOMITE: ENTIRE	PATCHY	CLAST ONLY	MATRIX	MINERALN: SPHALERITE.	GALENA.	PYRITE.	OTHER.	FOSSILS	SPECIFIC FEATURE, SAMPLE PHOTO	SEDIMENTARY TRENDS
									SEE NOTE BOOK FOR CONTINUATION.	FINES UP
								coral	stylolites	FINES UP.
								Infilled erosive base!	SAMPLE oolitic	FINES UP
									dolomite/pyrite in matrix.	
									Two cm shale	FINES UP
									1-3 fault	
									irregular cavity as below layered sulphide bound	
								CONTINUATION — UNIFORM DOL STYLOTIC IN PLACES BX F-1 387.5m		
									NOTE BOOK.	FINES UP.
								crinoid ossicles / in clst	trace [illegible] FeS2 [illegible]	
										FINES UP.

Remarks:

uniform dolomite upper 30cm [illegible] fine to fine scale laminations [illegible] up to fine sand. Gradational contact [illegible] lithology

basal [illegible] granule [illegible]

Coarse sand plus pellets non-dolomitic

No contact visible possibly obscured by dolomitization

[illegible] very fine laminations.

[illegible] 2.5 phi sand ooids visible [illegible] dolomite.

very finely bedded 2 phi sand. Beds 6-10cm thick emphasised by slight variation in [illegible]

laminations more [illegible]

small silty splays [illegible] of fault giving [illegible] a brecciated appearance to some clasts.

finely laminated laminations [illegible] to [illegible] [illegible] Gradational [illegible]

lots of cracks [illegible] suggest it may be a [illegible] brittle [illegible] effect. [illegible] BX [illegible] below. Opening infilled by calcite [illegible] also the breccia [illegible] mineralized [illegible] with the [illegible] disseminated ZnS [illegible] also below FeS2 [illegible] horizontal.

[illegible] highly irregular gypsum/calcite [illegible] lined with FeS2. Highly irregular [illegible] in [illegible] whole [illegible]. Trace ZnS [illegible] plus [illegible] brecciated FeS2 lamina. The brecciated layers of FeS2 [illegible] ZnS and PbS. Some just below [illegible]. PbS also present. [illegible] also clasts of [illegible] in the calcite/gypsum [illegible] just below [illegible] calcite/gypsum. The [illegible] clasts [illegible] brecciated dolomite [illegible]

grades [illegible] very finely crystalline homogeneous dolomite.

SEE NOTE BOOK.

[illegible] lined with FeS2.

0.5 phi sand plus granules and small pebble [illegible] very [illegible] lamination

gradational contact

The conglomerate grades [illegible] 7.5 phi sand [illegible] [illegible] are [illegible] Ophi

[illegible] sand
granule [illegible] occasional [illegible] pebble generally well sorted plus occasional granules

Continuation of last box.

NOTE WIDTH NOT TO SC[ALE]